



UNSW
SYDNEY

ONLINE
6–10 DECEMBER 2021

INTERNATIONAL FUTURE MINING CONFERENCE 2021

Conference Proceedings



ADDIN PRANOWO

GLENCORE TECH

5TH INTERNATIONAL FUTURE MINING CONFERENCE

Future Mining, Building Tomorrow

**6–10 DECEMBER 2021
ONLINE**

The Australasian Institute of Mining and Metallurgy
Publication Series No 7/2021



Published by:
The Australasian Institute of Mining and Metallurgy
Ground Floor, 204 Lygon Street, Carlton Victoria 3053, Australia

© The Australasian Institute of Mining and Metallurgy 2021

No part of this publication may be reproduced, stored in a retrieval system or transmitted in any form by any means without permission in writing from the publisher.

All papers published in this volume were peer reviewed before publication.

The AusIMM is not responsible as a body for the facts and opinions advanced in any of its publications.

ISBN 978-1-922395-02-3

ORGANISING COMMITTEE

Serkan Saydam FAusIMM
Conference Organising Committee Chair

Gavin Gillett

Peter Knights
MAusIMM

Phoebe McAuliffe
SAusIMM

Rudrajit Mitra
MAusIMM

Peter Moser

Rithin Payyanadan

Dion Pastars

Steven Schafrik

Russell Seib
MAusIMM(CP)

Chengguo Zhang
MAusIMM

AUSIMM

AusIMM Event Management Team

REVIEWERS

We would like to thank the following people for their contribution towards enhancing the quality of the papers included in this volume:

Seher Ata

George Barakos

Andrew Dempster

David Evans

Peter Knights

Hamed Lamei Ramandi

Binghao Li

Boge Liu

Rudrajit Mitra

Harmony Musiyarira

Joung Oh

Simit Raval

Oscar Jamie Restrepo Baena

Serkan Saydam

Sarp Saydam

Steven Schafrik

Russell Seib

Carlito Tabelin

Carlos Tapia Cortez

Nguyen Thi Hoai Nga

Berk Tulu

Ronny Webber-Youngman

Chennguo Zhang

FOREWORD

The Fifth International Future Mining Conference 2021 follows on from the successful previous four conferences held in Sydney in 2008, 2011, 2015 and 2019. The Future Mining Conference series has really become a unique key event in the mining calendar and the conference will continue to be held every three to four years.

The Future Mining Conference series have been a forum for communication between current and future industry leaders, technologists, scientists and engineers, mine executives, investors, government representatives, academics and all the other stakeholders. The conference aims to address innovations and opportunities to transfer scientific and technological developments from other disciplines into the minerals industry. It also intends to examine the human factors and skill needs for the future operations, identify possible blue-sky scenarios of 'Mining in the Future', strategies of mining education and research, novel mining systems and future commodities and directions.

The main themes of the conference include automation; mine internet of things; mineral processing and beneficiation frontiers; sustainability; the future demands of critical and digital minerals, future skills; and new mining frontiers including space resources engineering.

The conference has seven distinguished keynote speakers: Cam McCuaig (Head of Geoscience Excellence, Resource Centre of Excellence, BHP), James Davison (General Manager Surface Mining and Technology, Rio Tinto), Adrian Beer (CEO, METS Ignited), Gustavo Pilger (World Wide GEOVIA R&D Strategy & Management Director, Dassault Systemes), Rose Amal (Scientia Professor and a Co-Director of ARC Training Centre for the Global Hydrogen Economy, UNSW), Peter Johnson (Chairman, Maptek), and Kris Zacny (VP and Senior Research Scientist, Honeybee Robotics) who between them, will cover different aspects of 'Mining in the Future'.

All extended abstracts and papers in this conference proceedings have been independently peer reviewed and edited to ensure the highest relevance and quality.

We appreciate all those who have contributed in many ways to the event and would like to thank all authors and presenters for their valuable contribution, the organising committee for their hard work and the sponsors and exhibitors for making this Conference a successful event.

Organising a conference such as this requires considerable experience, effort and enthusiasm. We wish to thank The Australasian Institute of Mining and Metallurgy (the AusIMM) team who worked tirelessly and professionally.

On behalf of the organising committee, The University of New South Wales (UNSW Sydney) and the AusIMM, we welcome you to the Fifth International Future Mining Conference 2021, held virtually.

Yours faithfully,

Serkan Saydam FAusIMM

5th International Future Mining Conference Organising Committee Chair

SPONSORS

Major Conference Sponsor



Technology Commercialisation Sponsor



Gold Sponsors



Premier Content Supporter



Technical Session Sponsor



Conference Supporters



CONTENTS

Artificial intelligence

Overcoming the challenges of machine learning at scale <i>H Bridgwater</i>	2
Methane concentration forward prediction using machine learning from measurements in underground mines <i>T Dias, B Belle and G L Danko</i>	4
Artificial-intelligence based geotechnical hazard detection for autonomous mining <i>E Isleyen and H Ş Duzgun</i>	24
Bad data – does it really kill off AI and machine learning? <i>Z Pokrajcic and P Stewart</i>	28
Automatic magnetite identification at Placer deposit using multi-spectral camera mounted on UAV and machine learning <i>B B Sinaice, Y Takanohashi, N Owada, S Utsuki, J Hyongdoo, Z B Bagai, E Shemang and Y Kawamura</i>	33
Data driven geology – adopting a data driven culture and reaping the benefits of machine learning <i>S Sullivan</i>	43

Automation in mining

Enhanced orebody knowledge through scanning technologies and workflows <i>H C Grobler and M Pienaar</i>	46
Using machine learning and novel algorithms to predict muck pile shape and engineer a perfect blast <i>O Radzhabov and B Gyngell</i>	69

Autonomous vehicles

Autonomous dozers – technical challenges and the benefits to mine operation <i>E Abbo and D Poller</i>	77
Automation considerations for underground shuttle car haulage <i>V Androulakis, J Sottile, Z Agioutantis and S Schafrik</i>	81
Assessment of excavation technologies for a small-scale mining robot and development of future concepts <i>M Berner and N A Sifferlinger</i>	98
Intelligent characteristics and technical path of fully mechanised mining <i>H M Li, Z G Wang, S R Wang and W Wang</i>	101
Development of spilling judgment system for dump truck loading using digital twin technology <i>T Sato, K Yoshino, H Toriya, M Saadat, H Kuroki, Y Goto, I Kitahara and Y Kawamura</i>	112
Application of use case modelling to achieve safe, efficient mining equipment automation <i>W X Tong, P Knights, T Phillips, M S Kizil and M Nehring</i>	121

Roof bolting module automation for enhancing miner safety <i>A Xenaki, H Zhang, S Schafrik, Z Agioutantis and S Nikolaidis</i>	128
---	-----

Digital transformation

Integrated operations for complex resources <i>P A Dowd</i>	140
Creating the modern mine – beyond 2025 at Prominent Hill Operations <i>G Iwanow, K Mant and K Hobbs</i>	145
Developing a foundation of a framework for evaluating the impact of mining technological innovation on a company's market value <i>P Mugebe, M S Kizil, M Yahyaei and R Low</i>	149
Digital twins meet virtual reality in the Australian mining industry <i>J Qu, M S Kizil, M Yahyaei and P Knights</i>	153
Global digitalisation trends in mining and their impact on aspects of sustainability <i>A Sørensen, F Uth, R Mitra, F Lehnen, B Schwarze and E Clausen</i>	156
The breakthrough technology for digital transformation of mining business <i>B Vorobyov, S Reznichenko and V Monastyrrov</i>	159

Energy systems and sustainability

Hydrogen power for the mining industry <i>F Aguey-Zinsou</i>	162
Safety culture survey in coal-fired powerplant (PT X) at South Kalimantan, Indonesia <i>M Ashifa</i>	165
A simulation based feasibility evaluation of renewable power generation on an off-grid mine (Jundee Gold Mine) <i>S Bacich</i>	179
Hydro-electrical power potentials in the Peruvian mining industry <i>Y Feldmann, G Blauermel, M Roth, B Alapfy, T Hillig and B G Lottermoser</i>	205
Sustainable power generation for mining operations with natural ester technology <i>K Y Lam, A Sbravati, P Reilly and J Tan</i>	207
Carbon footprint reduction with continuous mining equipment <i>M Schmid, A Heiertz and S Blunck</i>	211
Do we have enough copper to decarbonise society? An overview of resources/production from porphyry ores/E-wastes <i>C B Tabelin, I Park, T Phengsaart, S Jeon, M Villacorte-Tabelin, D Alonzo, K Yoo, M Ito and N Hiroyoshi</i>	223

Future skills

Mine training for future skills <i>S Bowes</i>	226
Aligning competency orientated work integrated learning models for mining engineers and mine surveyors <i>H C Grobler</i>	230

Miners of the future – ensuring good working conditions in the future digital mine <i>J Johansson, L Abrahamsson and J Lööw</i>	238
Human performance variability and responsiveness to training in traditional and autonomous haulage operations <i>G K Karadjian</i>	241
Unlocking human creativity – people, technology and the changing role of organisations <i>B Kubat</i>	244
Highly sought-after mine managers – what qualifications, responsibilities and duties are of great importance to mining companies? <i>W E Oching and G Bonci</i>	248
An AI-based personalised evaluation and training system for displaced workers in mining industry <i>H Soydan, H Ş Duzgun, J Brune and X Zhang</i>	254

IoT

Optimising blast hole loading with MWD and 3D image analysis <i>B Gyngell, T Buschjost, T Worsey and G Diehr</i>	259
Enabling the digital mine of the future through autonomous underground data capture <i>S Hrabar and J Gray</i>	267
Optically powered monitoring networks <i>F Ladouceur, Y Chen and L Silvestri</i>	271
The potential of a mine-wide digital rock mass condition monitoring system <i>M Nöger, T Ladinig, P Hartlieb, D Dendl, P Moser and T Griesser</i>	274
Optical light microscopy – a novel tool for near real time coalmine dust monitoring <i>N Santa, E Sarver, C Keles and J R Saylor</i>	276
Underground rock bolt identification from 3D LiDAR scanning data <i>S Saydam, B Liu, B Li and W Zhang</i>	279
Mobile laser scanning for automated point cloud registration, object detection and structural mapping in mining <i>S K Singh, S Raval and B P Banerjee</i>	282
Improving interpretation of seismic data using deep generative networks <i>R Xu, V Puzyrev, C Elders, E F Salmi and E J Sellers</i>	286

Mineral processing frontiers

Challenges and approaches to flotation of sea floor massive sulfide ores <i>K Aikawa, I Park, N Hiroyoshi and M Ito</i>	296
Comparative study on rougher copper recovery prediction using selected predictive algorithms <i>B Amankwaa-Kyeremeh, W Skinner and R K Asamoah</i>	300
Correlating process mineralogy and pulp chemistry for quick ore variability diagnosis <i>B Amankwaa-Kyeremeh, C J Greet, W Skinner and R K Asamoah</i>	308
High density gravity separation circuits – a pathway to sustainable minerals beneficiation <i>M T Gill, R M G MacHunter and E Raffailac</i>	315

Mechano-activation and acid leaching of lithium from spodumene <i>N C Lim, R D Alorro, M Aylmore, L G Dyer and H E Lim</i>	323
Technospheric mining of cobalt from nickel slag – a study on complexation leaching <i>B Lim, M Aylmore, D Grimsey and R D Alorro</i>	326
Differentiation of AG/SAG mill feed particle size variations in batch milling process using acoustic emissions <i>K B Owusu, W Skinner and R K Asamoah</i>	328
Influence of lifter height on mill acoustics and performance <i>K B Owusu, C J Greet, W Skinner and R K Asamoah</i>	338
Direct leaching of rare earth elements from circulating fluidised bed combustion coal fly ash by hydrochloric acid <i>M C Pacaña, A E Dahan, C B Tabelin, V T Resabal, R D Alorro, L S Silva and R M Baute</i>	349
Measuring charge motion from inside an operating SAG mill <i>P Shelley, E Davies, J Olivier and I Einav</i>	353

Mining system innovations

Mine floor material recovery must become part of life-of-mine plan <i>K Biegaj and S C Dominy</i>	358
Research progress towards the unlocking of <i>in situ</i> recovery <i>L L Kuhar</i>	366
Raise caving – a new cave mining method for mining at great depths <i>T Ladinig, H Wagner, J Bergström, M Koivisto and M Wimmer</i>	368
Sleep/wake up system for underground mines <i>J Peiris, K Zhao, B Li, H Gong and A Seneviratne</i>	385
BHP WAIO Mine Planning Integration from 5YP to execution <i>L Talavera</i>	389
Image-based recognition of withdrawn coal and automatic control of drawing opening in longwall top-coal caving faces <i>J Wang, L Li, S Yang and W Pan</i>	398

New mining frontiers

Leveraging virtual reality for mine accident investigations <i>H C Grobler, H Thomas and J van Dalen</i>	405
---	-----

Space mining

Picturing the future – assessment of mining systems needed for lunar volatiles excavation <i>M Bates, A Williams, P Siribalamurali, J M Chua, Z Li and C Zhang</i>	419
Off Earth mining? Watch this space... <i>N J Bennett and A G Dempster</i>	422
Regulating space mining – use a system that works <i>A J Cannon</i>	429
Development of a Martian water resource project management system <i>S Casanova, R C Anderson and S Saydam</i>	440

Integrating the approaches to space and mining project life cycles <i>A G Dempster</i>	442
Facilitating commercial lunar water ice extraction – a terrestrial mining perspective on governance <i>B McKeown, S Saydam and A G Dempster</i>	456
Determination of the stability of microtunnel opening in lunar regolith and low gravity conditions <i>T Pelech, M Dello-Iacovo, N Barnett, J Oh and S Saydam</i>	459
High vacuum metallurgy – opportunities in lunar resource processing <i>M G Shaw, G A Brooks, M A Rhamdhani, A R Duffy and M I Pownceby</i>	463
Design and application of swarm robotics system using ABCO method for off-Earth mining <i>J Tan, N Melkounian, R Akmeiawati and D Harvey</i>	474
Author Index	486

Artificial intelligence

Overcoming the challenges of machine learning at scale

H Bridgwater¹

1. Principal Industry Engagement, Unearthed, Perth WA 6000. Email: holly@unearthed.solutions

INTRODUCTION

Data science – machine learning and AI – offers incredible potential for transforming industrial businesses. While the understanding of how to apply data science to particular use cases is increasing, scaling data science across organisations has been challenging for the mining industry. This is a challenge that is being experienced by many industrial sectors. Much of the cost and time to value comes from deploying and operationalising machine learning models. For many companies, deploying ML models is slower and more expensive than expected. To realise the value from data science, businesses are looking to employ scalable processes, tools and systems that can take experimental machine learning models into a production system. The recently developed field to address this: MLOps (a set of practices that aims to deploy and maintain machine learning models in production reliably and efficiently) is still in its infancy. The tools and systems are relatively new, and few people have expertise in this space. We also face the challenges of limited internal resources, which reduces the opportunity to trial new approaches. Ultimately, this combination of issues results in data science not yet being an accessible tool for most technical professionals within the mining industry.

This paper explores the different approaches, learnings, strategies, tools and processes that are being used to address this challenge. In the conference presentation we will share, findings and learnings from work across the mining industry, as well as specific use cases. Learnings can be captured across three key themes; tools and platforms, processes, and people and culture.

Tools and Platforms: There is a relatively limited number of enterprise software providers that offer a full suite of ML tooling. Examples include Microsoft Azure and AWS. These tools, however, are not ‘plug and play’ and typically require significant costs and effort to build and integrate with existing systems. Companies will also likely need to seek additional skillsets in MLOps to support using these tools internally. We observe a broad range of adoption from fully integrated ML tooling to no internal IT infrastructure for ML.

Processes: In general, data science activities are approached as ‘projects’, and are typically run via standard project management processes. More sophisticated organisations are shifting this thinking towards data science ‘products’, that follow a product life cycle. This is typically more appropriate when models are in deployment and are consistently delivering a service or ‘product’ to the organisation that needs to be managed over time. In either case, a typical data science approach consists of four key phases;

1. **Business Understanding:** Identifying a problem, reviewing prior work, calculating potential value and understanding the feasibility of approaching it with data science.
2. **Data acquisition and understanding:** Understanding what data sources are available and where, wrangling and cleaning the data sets, identifying signals in the data sets to justify continuing with the project.
3. **Model development:** Transforming the data, generating features, selecting and training models, retraining and validating performance.
4. **Deployment:** Packaging and validating the model, monitoring the performance of the model over time, connecting to applications for use by operations.

People and culture: While there is increasing interest from technical professionals to apply machine learning in their roles, there is generally limited capacity available in operations to run data science projects. Organisations have gained learnings from trialling centralised and decentralised (asset based) data science functions. Understanding has been built on the range of skills required for scaling data science, which includes; data engineers, MLOps/DevOps engineers, as well as data scientists. Concerns over ‘black box’ solutions are still a considerable barrier to adopting machine

learning approaches. This has resulted in an increased focus on explainability, and closer alignment to how the predictions or outputs generated, will be used in operations.

CONCLUSION

There is a broad range of 'readiness level' for scaling machine learning in the resources sector. Significant gains have been made in understanding the skills requirements and appropriate organisational structures. We observe a positive trend towards and growing understanding of MLOps, but recognition that the current tooling available on the market is not sufficient to enable data science as an accessible tool for most technical professionals in operational roles.

ACKNOWLEDGEMENTS

We would like to acknowledge contributions from individuals within OZ Minerals, Newcrest Mining, Roy Hill and Western Power in supporting developing a shared understanding of the status quo of machine learning operations in resources and energy companies.

Methane concentration forward prediction using machine learning from measurements in underground mines

T Dias¹, B Belle² and G L Danko³

1. Graduate Research Assistant, University of Nevada, Reno NV 89502, USA.
Email: tdiasdealmeida@unr.edu
2. Lead Ventilation and Gas Manager, Anglo American Coal, Australia; Adjunct Professor of Mining, University of NSW, Australia; Adjunct Professor of Mining University Queensland, Australia.
3. Professor, University of Nevada, Reno NV 89502, USA. Email: danko@unr.edu

ABSTRACT

Unmanaged gases inside the mine airways are hazards to health and explosions, especially methane (CH₄) in coalmines. Temperature rise caused by heat release from the strata and machinery is another factor that may harm the health and safety of workers in underground mines. Control of methane and other gas components as well as high temperature near a working face requires overall and localised ventilation management and adequate mine cooling systems. Continuously monitoring the *in situ*, atmospheric conditions as well as the amount of contaminant gases, especially methane, are important factors for predicting the necessary actions for keeping the mine a safe and healthy place for workers. Studies are reported for predicting ahead of time methane concentration variations inside underground mines using long-short-term memory (LSTM) artificial recurrent neural network, time-series regression predictor (time series filter), as well as transport model-based methods. Different combinations of the variables and techniques are tested in the LSTM model to find best results for accuracy and applicability. Forward time step variations are tested in time-series regression models to explore the best prediction outcome. The results show that the LSTM and time-series techniques perform similarly and both are sensitive to sliding window sizes and the number of forward-step predictions. The time series filter showed to be extremely faster than the LSTM model and presented a higher accuracy using the first order fitting, especially when the filtered data is used for training and predicting. The transport model used to back-calculate the line source responsible for the increase in methane concentration in different locations inside the mine provides an output that is slightly better than the original data for the time series filter to make the predictions, which gives basically the same relative error compared to the predictions using the original CH₄ concentration using both the time series filter and the LSTM. Recommendations are discussed for transport model-based solutions for forward predictions combining their parameter identification with those used for NN model training. For the case studied in this paper, the predictions are acceptable, but more tests are needed to increase the accuracy and reliability of the predictions from the models and to verify the applicability to the mining industry.

INTRODUCTION

The intake air of underground mines has a composition of 78 per cent nitrogen, 21 per cent oxygen and 1 per cent of other gases (McPherson, 2009). The composition changes as they are mixed with gases from strata (eg methane and carbon dioxide) and also gases from chemical reactions, oxidation, burning of fuels and the use of explosives. Common toxic gases encountered in underground mines are reviewed by Osunmakinde (2013), emphasizing the problem that mine's gases are not easily detected by human sense. The presence of these gases, especially methane in mine openings (Eltischlager *et al*, 2001) may cause serious hazards (explosion hazards from methane emissions related to geologic features in coalmines), especially due to gas outbursts. Another harmful factor for health and safety in underground mines is heat release, accompanied by a rise in temperature (Nie *et al*, 2018).

Altogether, the atmospheric conditions in the mine workings need careful ventilation design and operation under continuous monitoring to check compliance with safety and health limitations in both gas component concentrations as well as temperature and humidity. Continuous AMS (Atmospheric Monitoring Systems) are commonly used in metal and coalmines, assisting the mines in maintaining operations within safety and health limitations. A modern mine may employ an AMS network of

thousands of various gas, pressure, temperature, humidity and air flow rate sensors, collecting samples in every minute during mining operation.

The amount of atmospheric data from the AMS sensors are usually evaluated against dangerous threshold crossings to assure compliance with target values for compliance. However, the data is far too rich in information to be used only for spot-like threshold or set-value evaluation. Trend analysis and deep learning from the variations of the AMS signals may allow to use the investment value for AMS operation for early-warning safety and health assurance not only in the present, but in future time and not only in the monitored locations, but everywhere in the mine airways. Such an AMS data evaluation system (Danko *et al*, 2019) is under development and the present paper details a study in AMS signal analysis for trend detection.

An artificial neural network, as described by Haykin (1999) and Gurney (1997) is a machine that performs pattern recognition and perception, enhanced through 'experience'. All of this is done by artificial 'neurons' or 'processing units' that when connected are called synaptic weights and are used for store knowledge acquired from the surroundings. The 'processing units', also called nodes by Gurney (1997) are connected to each other and when there is a large connection of nodes, it is referred to as a net. According to Rojas (1996) each neuron receives a certain number of signals (x_i) which depends on the number of inputs. These signals are then multiplied by their respective weights (w_i) and then all the different signals are added and integrated into the neuron and the primitive function (f) is evaluated at these points, as shown in Figure 1.

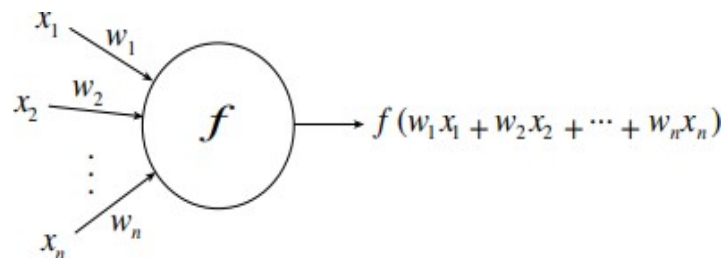


FIG 1 – A general neuron at work.

A network architecture is defined depending on how the neurons are disposed. There are three kinds of architecture: recurrent networks, single-layer networks and multi-layer networks (Mas and Flores, 2007). A layer is a group of neurons working together in a network (Kriesel, nd). The single-layer network, sometimes also called single-layer perceptron, is the simplest form of an artificial neural network. This kind of network is most used in classification patterns and it consists only of a certain number of input neurons and some output neurons (output layer).

Multi-layer feed-forward networks usually has more than one hidden layer. When combined with back-propagation algorithm they are the most used and useful type of neural network (Svozil, Kvasnicka and Pospichal, 1997; Blum and Socha, 2005). One problem with this type of network is that it results in a large amount of calculations, therefore gradient loss and overfitting may occur (Li, Zhang and Chen, 2019). If the error is not small enough so the predictions from the network do not match the target, an interactive process of gradient descent is applied for trying to adjust the weights and, therefore, minimising the error.

There are many techniques for training a neural network, but the two most used are supervised learning and unsupervised learning. Supervised learning is the case where the correct response (target) is already known. The input and target data are entered into the network and it tries to find some relationship between these data, comparing input and output. Differently, Unsupervised learning only uses input data and the network itself tries to classify this data into categories, target information is not provided (Gurney, 1997).

For using a multi-layer feedforward network, it needs to be trained and tested. The training process, as described by Svozil, Kvasnicka and Pospichal (1997) requires several steps: First, some random numbers are chosen for the weights. After that, the iteration process starts and passes all the information through all the nodes in the layers and the result is compared with the desired target. Each complete iteration is called an epoch. If the predictions from the network are not satisfactory, the network uses backpropagation and tries to adjust the weights and, hence, minimise the error.

This error can be used as a measure of the performance of the network's predictions. When a network is well trained, it is said to generalise. Generalisation is when the trained network gives perfect or nearly perfect predictions for a new set of data that has never been used in the training set. However, if the network is trained too many times, overfitting may occur. Overfitting is when the network 'memorises' the training set and consequently gives perfect predictions for the data that has been trained, but fails to give good predictions for a new data set. To overcome this problem, a sufficiently large training set must be used.

However, for doing multi-step ahead predictions, it is better to use a time series neural network, because they do not have the problem of long-time dependencies that feedforward networks have, caused by vanishing or exploded gradient (Diaconescu, nd; Tsungnan *et al*, 1996). Some authors, such as Tsungnan *et al* (1996) and Connor and Atlas (1991). have used an architectural approach to deal with long-term dependencies called Nonlinear Autoregressive models with exogenous inputs (NARX models). This model is recognised for being well suited for modelling non-linear systems such as biological wastewater treatment and catalytic reformer in petroleum refinery (Su, McAvoy and Werbos, 1992) and time series (Connor and Atlas, 1991). In this type of network, outputs from the model are used as new inputs, as shown in Figure 2, where output at time instant $y(k+1)$ is fed back into the network along with the input $u(k)$.

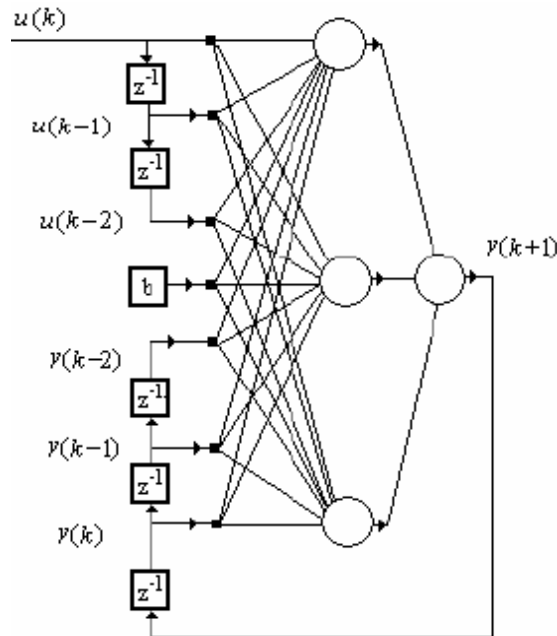


FIG 2 – Schematic of a NARX neural network (Diaconescu, nd).

It was observed for this type of neural network that the more inputs it has, the better the prediction is (Diaconescu, nd). One variant of the common NN is the recurrent neural network (RNN) (Liang and Cai, 2020). The difference from RNN to the conventional NN is that there are connections between layers and also connections between neurons within layers. One type of RNN is the long-short-term memory (LSTM). It is a powerful version of the conventional NN and RNN in the sense that it has the ability of dealing with the explosion gradient in training process (Sangiorgio and Dercole, 2020). because it has four main components: input gate (i_g) forget gate (f_g) output gate (o_t) and a cell (c_t). These gates help the LSTM remember just useful information across the time series data. These four parameters can be mathematically described as:

$$i_t = \sigma(W^i)H + b_i \quad (1)$$

$$f_t = \sigma(W^f)H_f + b_f \quad (2)$$

$$o_t = \sigma(W^o)H_o + b_o \quad (3)$$

$$C' = \tanh(W^{(c)})H_c + b_c \quad (4)$$

$$C_t = f_t * C_{t-1} + i_t * C'_{t-1} \quad (5)$$

$$h_t = o_t * \tanh(C_t) \quad (6)$$

In this definition, σ is the sigmoid function, W^i, W^f, W^o and W^c are the weights of the input gate, forget gate, output gate and cell state, respectively. The output is represented by h_t . According to Miao *et al* (2020), the input gate and forget gate are responsible for updating the cell state, because these are the gates that control which information the LSTM keeps or discards. The LSTM can be trained in two ways, as stated by Sangiorgio and Dercole (2020) with teacher forcing (TF) or without TF. Training with teacher forcing is the case where the predictions from the LSTM are not fed back into it, so new predictions cannot be made based on past predictions. The schematic is shown in Figure 3.

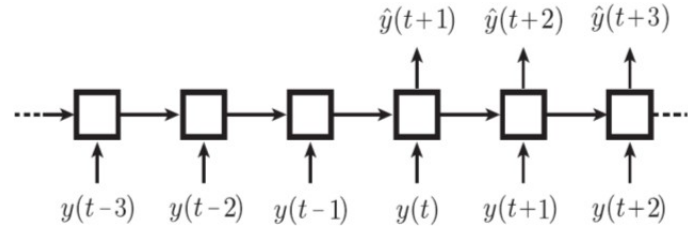


FIG 3 – Training with TF.

It is observed from Figure 3 that even if more than one step ahead is to be predicted, the data provided for predicting is always real data, not the own predictions from the LSTM. This type of predicting is good because it does not propagate error in time.

On the other hand, training without TF is the case where the LSTM uses its own predictions as new inputs and make new predictions based on previous ones, shown in Figure 4.

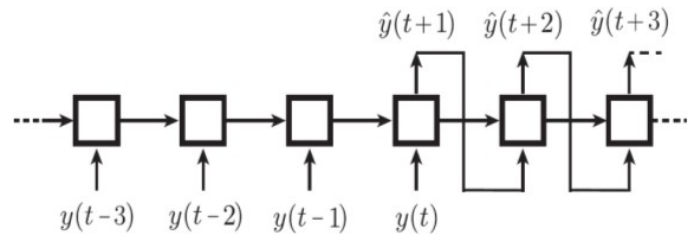


FIG 4 – Training without TF.

This training technique allows for multi-step ahead predictions using past predicted values from the LSTM. In this case, the propagation of error in time is greater and the value predicted at a certain time step affects future predicted values.

Besides the teaching method, the parameters used for tuning the LSTM are very important. According to Sarkar and De Bruyn (2020), the so called hyperparameters can increase or decrease a LSTM's performance. Some of the parameters are the number of hidden units, the learning rate and the batch size.

The hidden units are related to ability of the LSTM recognise relationship in the data. If there are too few, the LSTM may not capture the relationship. Conversely, too many increases the chance of overfitting. The learning rate is responsible for algorithm to 'learn' and it is considered the most important parameter by Greff *et al* (2017) and Bengio (2012). If it is too low, the training process is very slow and may never converge. If it is too high, instability in the training part may occur. The mini-batch size, according to Bengio (2012), can vary between one and few hundreds and it is said to impact the speed of the computation. Besides hyperparameters, Bengio (2012) emphasizes that pre-processing the data before passing it to the LSTM is also a good practice.

The goal of this research is to be able to predict ahead the methane concentration of an underground mine and study the possibility of creating a 'smart system' that can detect any sign of health danger so the due precautions can be taken before the problem even happens. As a first approach, the LSTM method will use a combination of the available variables (airflow, barometric pressure and methane concentration from different locations inside the mine) for training and later use the trained LSTM to try to predict ahead data that can match with the monitored data.

Different combinations of the variables will be tested and the one that gives the best result will be chosen to verify its accuracy and applicability. The accuracy of the LSTM model will be further compared to a transport model based on the energy balance inside the mine and also a time series filter model so conclusions can be drawn regarding the strengths and weaknesses of each model.

METHODOLOGY

The methane versus time shown in this study represents an example of a time series that potentially could be predicted. The approach presented in this paper should be a selection guide to help choosing the right methodology that someone can use to do predications and how to determine how well a methodology works with someone's own data series. That being said, below is a procedure that can be applied to a data set, starting from data pre-processing until the final predictions. The data used for performing the tasks presented in this paper comes from four different locations inside an underground mine. Figure 5 shows the schematic of these locations along the mine.

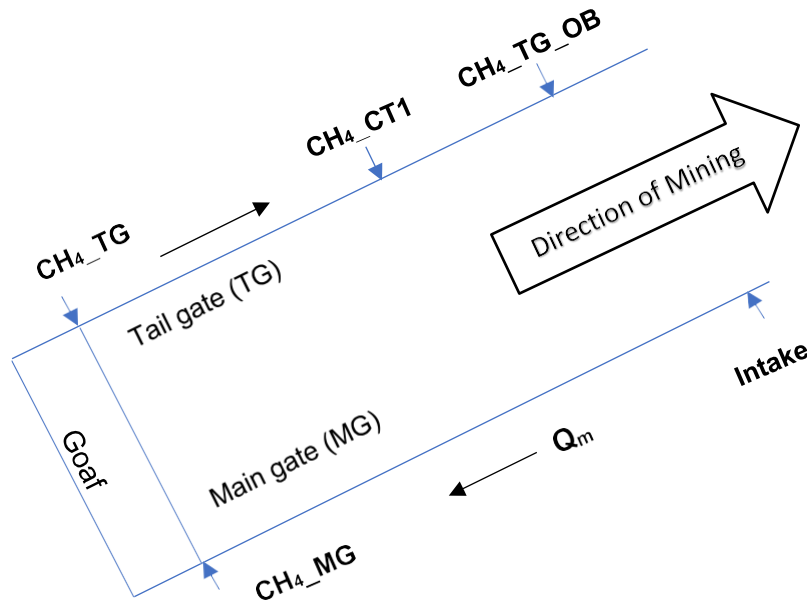


FIG 5 – Schematic layout of AMS sensor locations inside the mine.

The MG location is the intake airway path and the TG is the return airway. As discussed in section 1, the LSTM model and neural networks in general perform better if the data is as smooth as possible, thus the data above was filtered so a comparison can be done later regarding the results from the raw data and the filtered data.

Data filtering

Filtering is an important part of signal processing. According to Marlin (2000) the so called 'noise', which is a high frequency component generated by factors such as electrical interference and mechanical vibration, among others, can damage the quality of the real signal on (Horowitz and Hill, 2018). Therefore, the goal of filtering is to smooth the signal and remove incorporated noise by reducing its amplitude to zero (Marlin, 2000; Kordestani, Xiang and Ye, 2018). In order to deal with noisy data, a digital or an analogue filter can be used (Smith, 1997). These types of filters are used for signal separation and signal restoration. Digital filters can be separated into two categories: finite impulse response (FIR) and infinite impulse response (IIR). One of the most common and simple types of filter used in the industry is the moving average filter (MAF) because of its simplicity and capability of attenuate the noise (Kordestani, Xiang and Ye, 2018; Smith, 1997). The drawback of this filter is that it is not suitable for frequency domain signals, because it has poor capability of separating band of frequencies. It is a FIR and its mathematical formulation is:

$$Y_i = \frac{1}{M} \sum_{j=0}^{M-1} X(i+j) \quad (7)$$

Where Y_i is the signal output at the i th step, $X(i + j)$ is the signal input from the i th step to the j th step and M is the number of points in the average. Several other IIR and FIR filters are investigated by Smith (1997).

In this section, a novel FIR low pass filter is used. In summary, what this particular filter does is, for a set of data, for example:

$$S = \{p_1, p_2, p_3, p_4, p_n\} \quad (8)$$

It applies the least square fitting technique to a subset T of the data set S . The length l of this subset is user defined and it consists of a moving window. For instance, if l is defined as three, then the first subset would be:

$$T_1 = \{p_1, p_2, p_3\} \quad (9)$$

The second subset would be:

$$T_2 = \{p_2, p_3, p_4\} \quad (10)$$

And so on, until the last element of S . For each subset, the least square fitting is applied in the form of a linear model using the 'polyfit' function from the software MATLAB R2019a-academic use.

$$y = a * x + b \quad (11)$$

After the 'polyfit' function finds the best coefficients for the equation, the 'polyval' function is used to evaluate the polynomial at the points going from zero to l . The result of y is stored in a matrix M for instance, if S is equal six and l is equal two, matrix M would have the following format:

$$M = \begin{pmatrix} y_{1,1} & 0 & 0 & 0 & 0 \\ y_{2,1} & y_{2,2} & 0 & 0 & 0 \\ 0 & y_{3,2} & y_{3,3} & 0 & 0 \\ 0 & 0 & y_{4,3} & y_{4,4} & 0 \\ 0 & 0 & 0 & y_{5,4} & y_{5,6} \\ 0 & 0 & 0 & 0 & y_{6,6} \end{pmatrix} \quad (12)$$

Where each column of M contains l points. Zeros are placed where the following conditions are true:

$$M_{ij} = 0, \text{ if } j > i \text{ or if } j + l > i \quad (13)$$

Once matrix M is completed, each row is averaged by l generating the filter output with the reduced frequency component, that is, the daily variation. Besides filtering the data, this same filter will be also used to do predictions. The difference is that for predicting one point ahead the best fitted points (for example $y_{3,1}$), the 'polyval' function evaluates the generated polynomial curve at the point $l + 1$.

The example shows in Figure 6 the lines generated by the filter with length l equal three along a section of the original curve for the methane concentration at location MG.

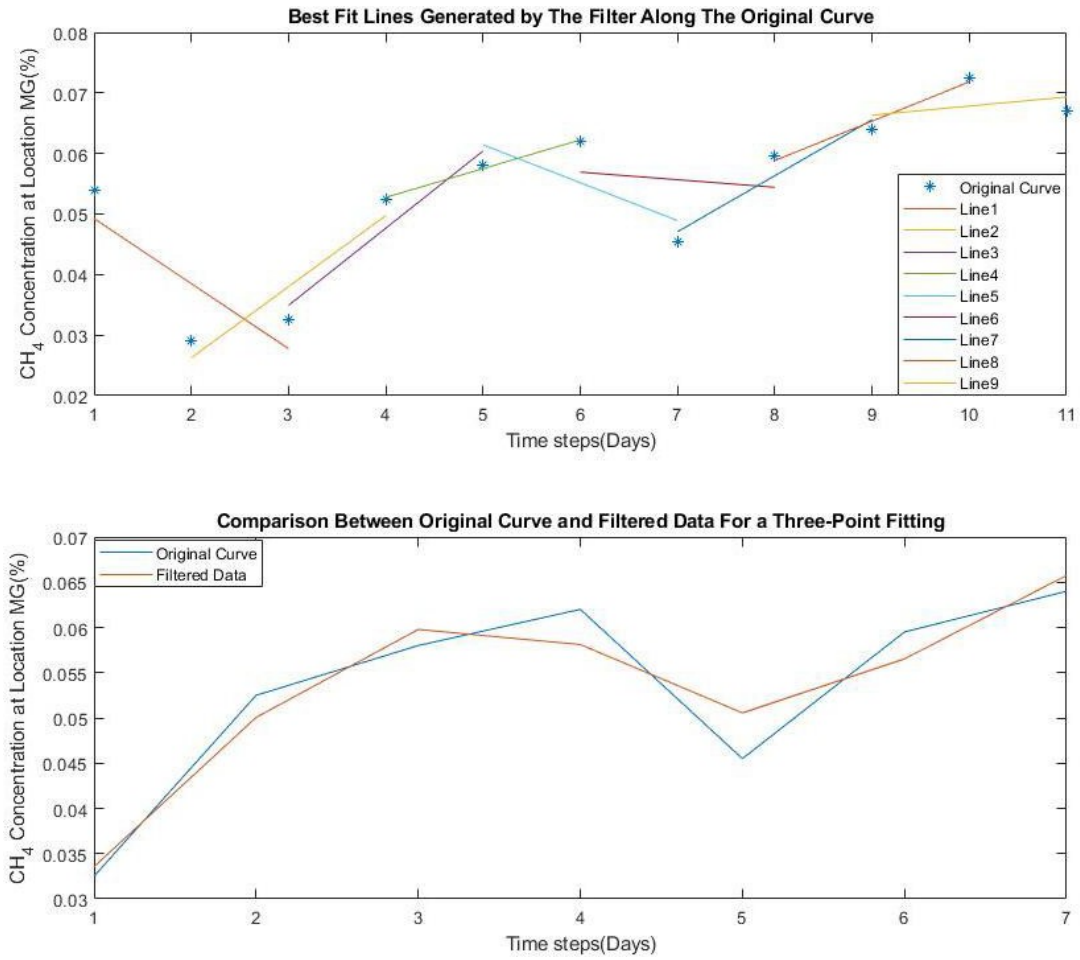


FIG 6 – Section of a curve showing the lines generated by the filter for a three-point fitting (top); smoothed curve generated by the filter (bottom).

After averaging each line by the filter length, the smoother curve is generated as shown on the bottom of Figure 6. The smaller the size of the ‘filter length’, the better is the fit values found by the filter because the high frequency component is not being filtered so strongly. If l is equal to two, the best fit lines generated by the filter would match exactly each point of the original curve. However, this filter configuration with l equal two cannot be used because it would not smooth the original curve, once the high frequency components would not be eliminated because the averaged values generated by the ‘polyval’ function would coincide exactly with the original values of the curve.

Figure 7 (top) shows a complete example comparing the filtered (filter length equal three) and original daily average CH₄ concentration at locations MG in Figure 5. The two subsequent figures (middle and bottom) show the absolute and relative errors between the original and filtered data. The absolute error is defined as:

$$E_{ai} = v_{oi} - v_{fi} \quad (14)$$

Where E_{ai} is the absolute error for each time step, v_{oi} is the original measured value and v_{fi} is the filtered value. The relative error is defined as:

$$E_{ri} = \frac{E_{ai}}{v_{oi}} * 100$$

Where E_{ri} is the relative error for each time step.

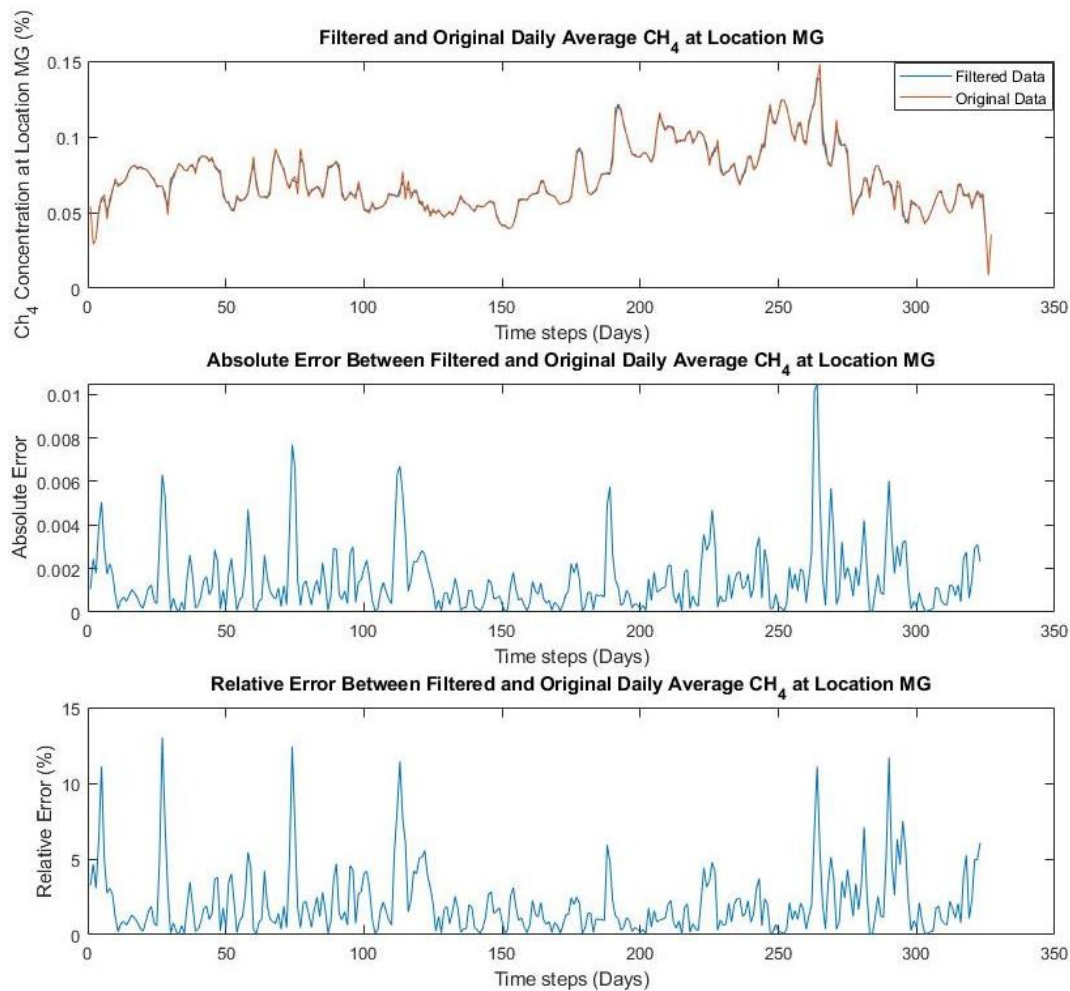


FIG 7 – Comparison between filtered and original curve at location MG.

The filter was applied to smooth all the data in the different locations in Figure 5. The goal of the filter is to make the data smoother, however, depending on the number of points that are used as the 'filter length' (points that are used to find the best fit), the outcome may be a distortion of the original data causing an increase in both relative and absolute errors. A comparison will be made between the original data and the filtered data. The goal is to verify if filtering the data is improving the predictions or if it is destroying the daily variation component, if the latter is true, filtering will not be used because it is against the goal of accurate hazard evaluation for every day.

Tasks

The data above will be used as training variables and also as target for training a LSTM and a time-series filter model. In order to better understand the behaviour of the LSTM and the filter model and its usefulness, a set of tasks are tested in this paper.

Direct forward-prediction of methane concentrations with (a) time-series filter model and (b) LSTM model

The goal is to see how well the daily average data can be predicted for the next day. Task (a) is based on a 'polyfit' function from MATLAB and it will be used for the last two (filtered or original) data points. The goal is to fit a 1st-order function and forward predict the next new point(s) with this 1st-order predictor (it is possible to predict 1, 2, 3 days ahead, to see how far it is acceptable, but the real interest is only 1 day ahead). This scheme will be used from day 2 through day 324 and forward predict consecutive days (3, 4, 5), (4, 5, 6) and so on, through days (325, 326, 327). Next, the predicted curves will be compared with the real measured curves. As an additional step, it will be checked if the forward prediction is better when using the original or the filtered curves.

Next, the same time-series filter will be used for the last three (filtered or original) points, but now fitting a 2nd-order function and forward predicting the next new point(s) with this 2nd-order predictor. This scheme will be applied from day 3 through day 323 and forward predict consecutive days (4, 5, 6), (5, 6, 7) and so on through days (325, 326, 327) and compare the curves with the measured curves.

1. The 1st null-hypothesis to prove is that this simple 'polyfit' forward prediction scheme is as good or better than the LSTM prediction (for at least the 1st next day).
2. The 2nd null-hypothesis is that the 1st-order prediction is better than the 2nd-order forward prediction if the filtered input curve is used.
3. The 3rd null-hypothesis is that the 2nd order prediction is better than the 1st order forward prediction if the un-filtered input curve is used.

The LSTM model in use is the one available in MATLAB. The LSTM configuration parameters is shown in Table 1.

TABLE 1
LSTM configuration.

Max epochs	Gradient threshold	Initial learning rate	Learning rate drop period	Learning rate drop factor	Mini Batch size	Number of hidden units
500	1	0.005	250	0.01	2	3

This LSTM model will be trained in a sliding window fashion, where data from 1 to 5-time steps are used for training and the sixth data point is predicted, for example. Continuing with this training, time steps from 2 to 6 are trained and the seventh point is predicted. The goal is to see how well the LSTM can predict at least one step ahead in addition to verify how sensitive it is to the training window size.

Forward-prediction of root-cause CH₄ sources with (a) time-series filter model and (b) LSTM model

The transport model used in this section has a complex structure and a full description can be found in the book 'Model Elements and Network Solutions of Heat, Mass and Momentum Transport Processes' written by George Danko (Danko, 2017).

In this step, the CH₄ line source that is responsible for CH₄ increase in each section will be back-calculated (1: Intake to MG; 2: MG to TG; 3 TG to Panel End; 4: MG to Cross-cut). The concentration of the intake is 0.05 per cent constant (mass fraction:0.0005 kg of CH₄/kg air). This exercise will include two influencing factors: the CH₄ differences between in and out and the Q_m flow rate of the air. The same exercises as in (1) will be done, showing the QCH₄ sources back-calculated from the measurements and the predicted values from methods (a) and (b).

RESULTS AND DISCUSSION

Forward prediction using the time series filter

The goal of this section is described in task 1a. Firstly, the predictions will be made using the original data and, later, the filtered data. Conclusions will be drawn regarding which set of data give better results. The time series filter uses two data points for finding the best line equation using a 1st-order function and it predicts one point ahead. It also uses a moving window style as previously explained. For each prediction, the absolute and relative errors will be calculated so comparisons can be done against the other predictors. The first predictions are made for the methane concentration at location MG as shown in Figure 8.

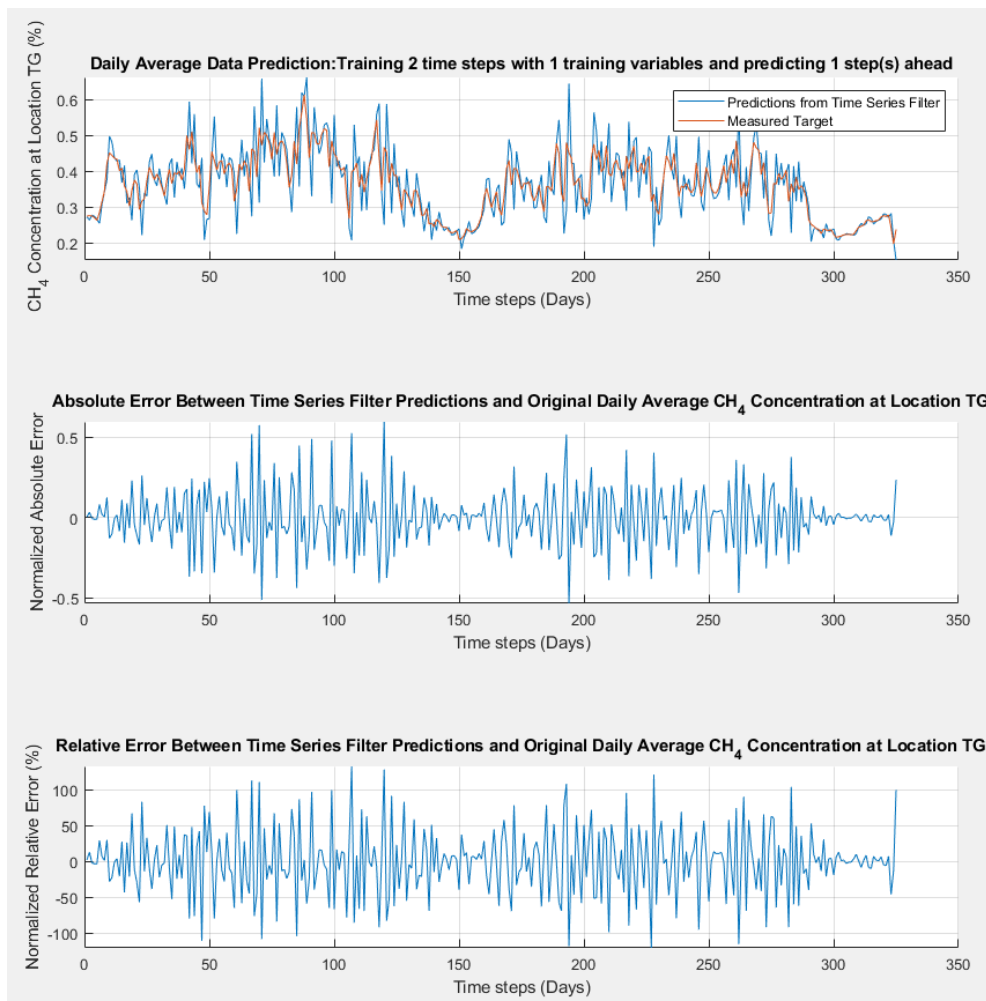


FIG 8 – Time series filter predictions and error calculation for a first order polynomial fitting at location TG using unfiltered data.

The time taken to perform these predictions was 0.17 seconds. The same variable was used however, this time, with the filtered data. The predictions are shown in Figure 9.

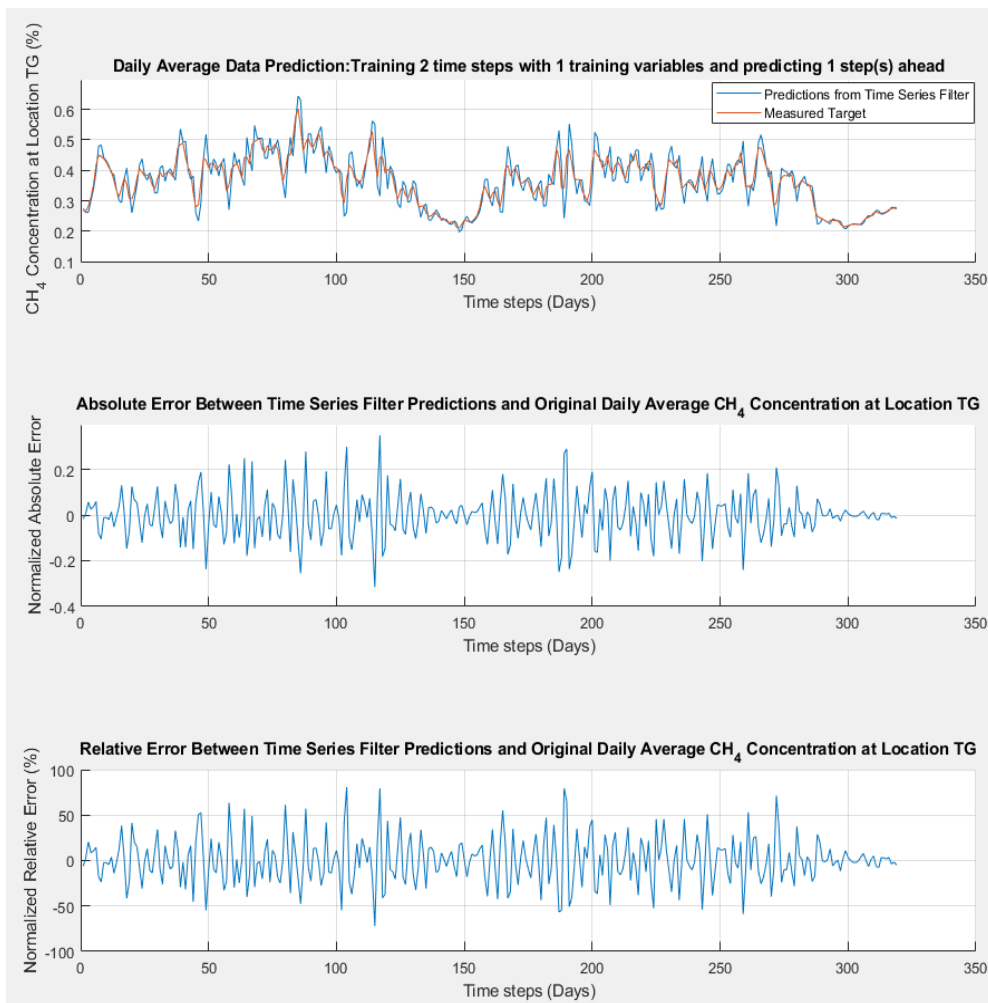


FIG 9 – Time series filter predictions and error calculation for a first order polynomial fitting at location TG using filtered data.

The time taken to do these predictions was 0.15 seconds. Comparing Figures 8 and 9 it is observed that predictions from Figure 9 are better. The picks are not as high as those in Figure 8 and their occurrence is lower. Comparing the absolute errors, it is cleared observed that the predictions from the filtered data are giving the lowest errors. The highest error pick in Figure 9 is around 0.3 (CH₄ concentration units), while in Figure 8 is around 0.5, showing that filtering the data has the potential to give better results.

The same set of data was used however, this time, the times series filter will use a second order polynomial fit. The filter predictor uses three data points, instead of two as previously used, to find the points that best fit the original curve. Firstly, the predictions are made for the unfiltered data and then for the filtered data, shown in Figures 10 and 11.

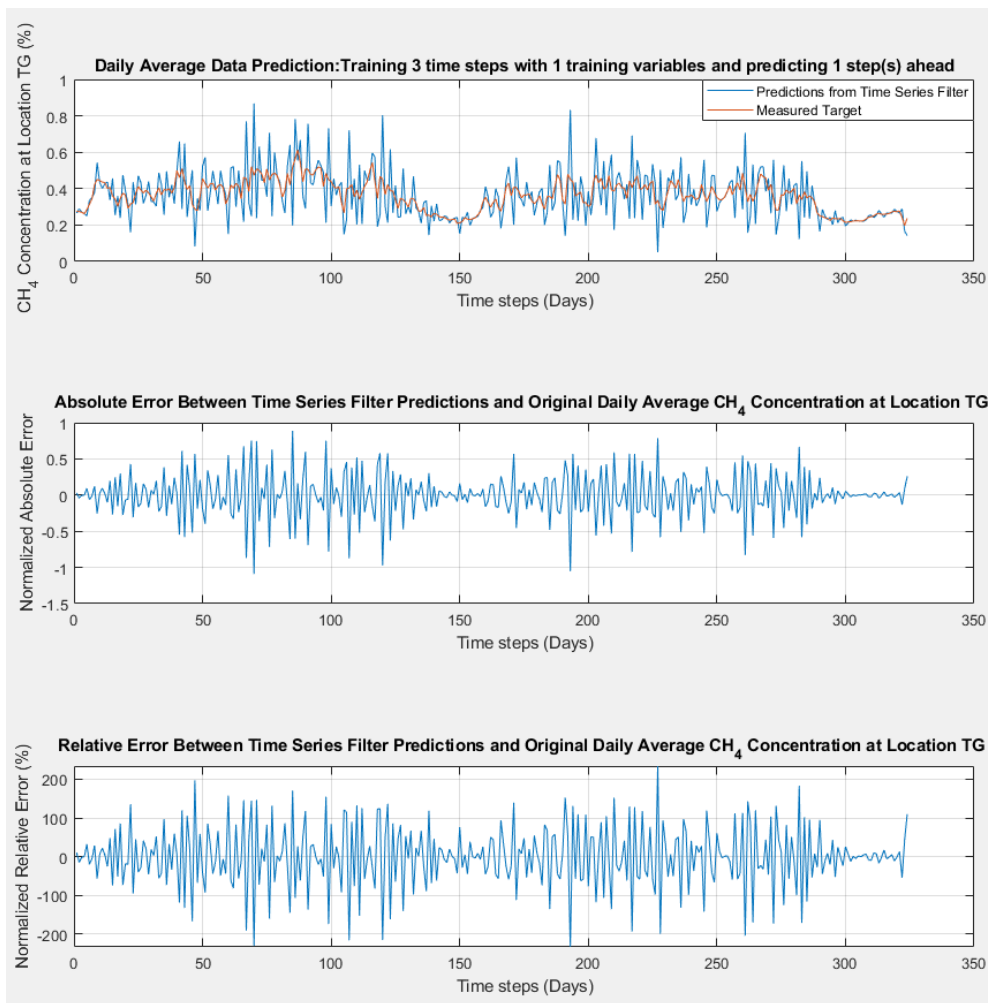


FIG 10 – Time series filter predictions and error calculation for a second order polynomial fitting using the unfiltered data.

The same filter configuration was used, but this time the predictions were made for the filtered data.

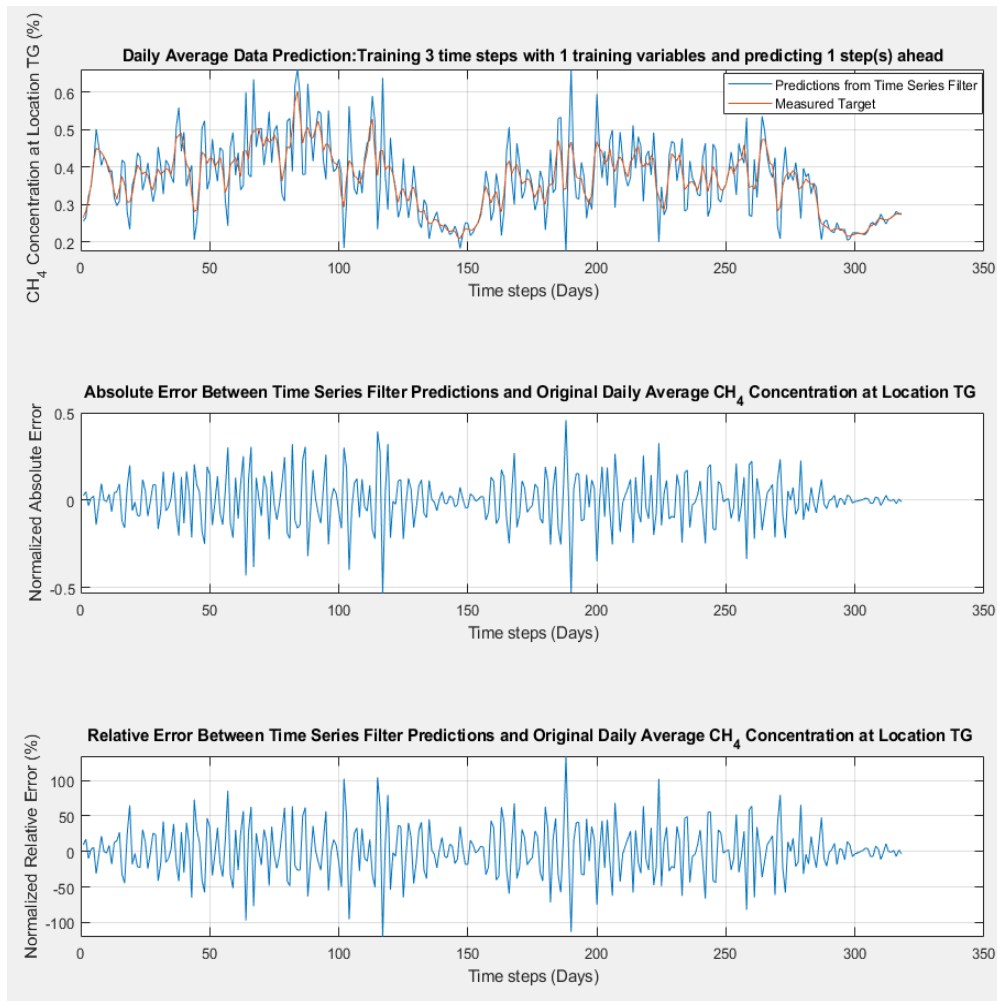


FIG 11 – Time series filter predictions and error calculation for a second order polynomial fitting using the filtered data.

The time taken to perform the predictions was 0.16 seconds. Observing the predictions using the second order polynomial fitting for the unfiltered and filtered data (Figures 10 and 11) it is clearly observed that the unfiltered data shows much more high overshoot picks over the original curve. The absolute error comparing Figures 10 and 11 shows that the predictions using the filtered data are better than the ones using the unfiltered data. The highest absolute error for the filtered data is around 0.4 while for the unfiltered data it almost reaches 1. Comparing the absolute error plots, the concentration of high picks for the filtered data are all almost around 0.2 whereas for the unfiltered data it happens around 0.3 and over. Furthermore, comparing the relative error plots, the filtered data presents fewer points going over 50 per cent while the unfiltered data predictions have several error points over 50 per cent. This shows that the predictions using the second order polynomial fitting are better if the filtered data is used.

Comparing the predictions from the first order fitting with those from the second order fitting for the unfiltered data (Figures 8 and 10). it is clearly observed that the first order fitting is better than the second order fitting. It is visible in Figure 8 that the highest absolute error is around 0.5. Conversely, the absolute error calculation based for Figure 10 shows several picks going over 0.5. If the comparisons are made for the filtered data (Figures 9 and 11) it is visible that the high overshooting picks for the second order fitting are much more noticeable than in the first order fitting. The absolute error show that for the first order fitting, almost all high picks but one is below 0.2 whereas for the second order fitting there are several high picks that go over 0.02. Comparing the relative error, the highest pick for the first order fitting happens around 70 per cent while for the second order fitting there are several points going over 100 per cent, showing that the first order fitting has higher performance.

Forward prediction using the LSTM

In this section, the predictions for the methane concentration at location TG is made using the LSTM with the configurations displayed in Table 1. Five data points are used for training the LSTM and it has to predict one step ahead. The training variables used are the methane concentration at locations MG and the airflow rate. Firstly, the predictions are made using the unfiltered data and then the filtered data is used. Conclusions are drawn regarding which set of data give the best predictions. Figure 12 shows the predictions.

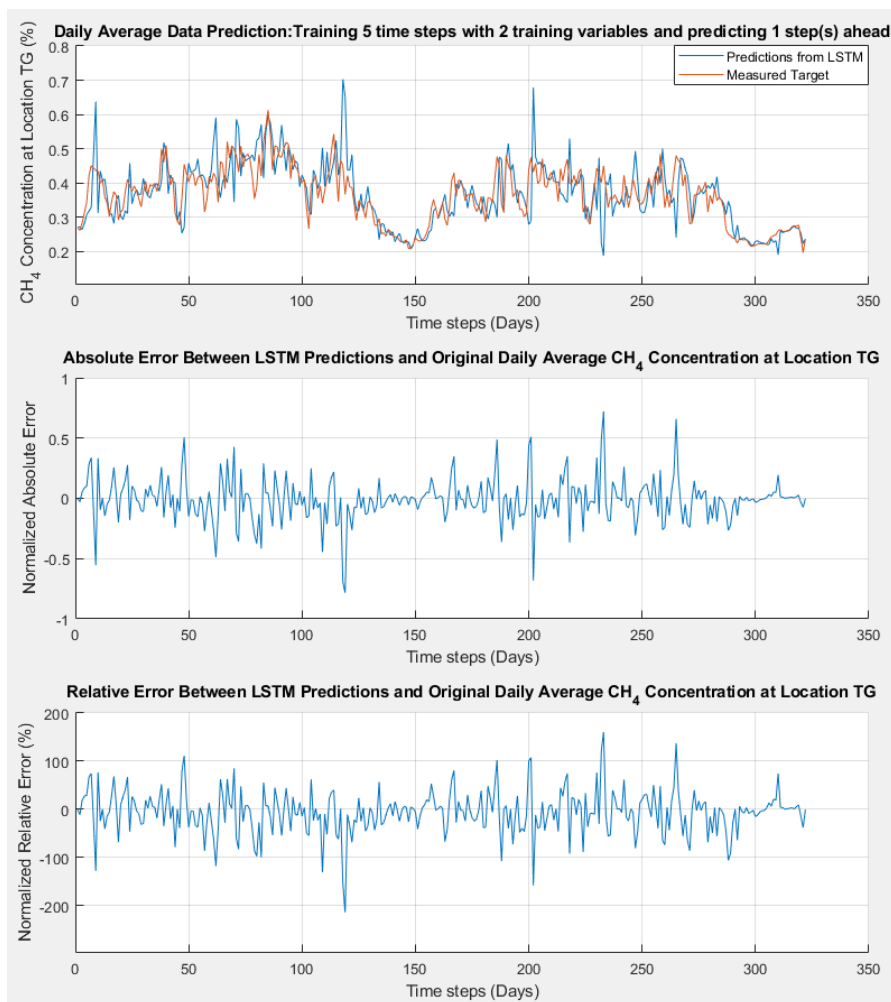


FIG 12 – LSTM predictions and error calculation for the unfiltered data at location TG.

The time taken to make the predictions was 21 minutes. The predictions were made once again however, this time, using the filtered data (Figure 13).

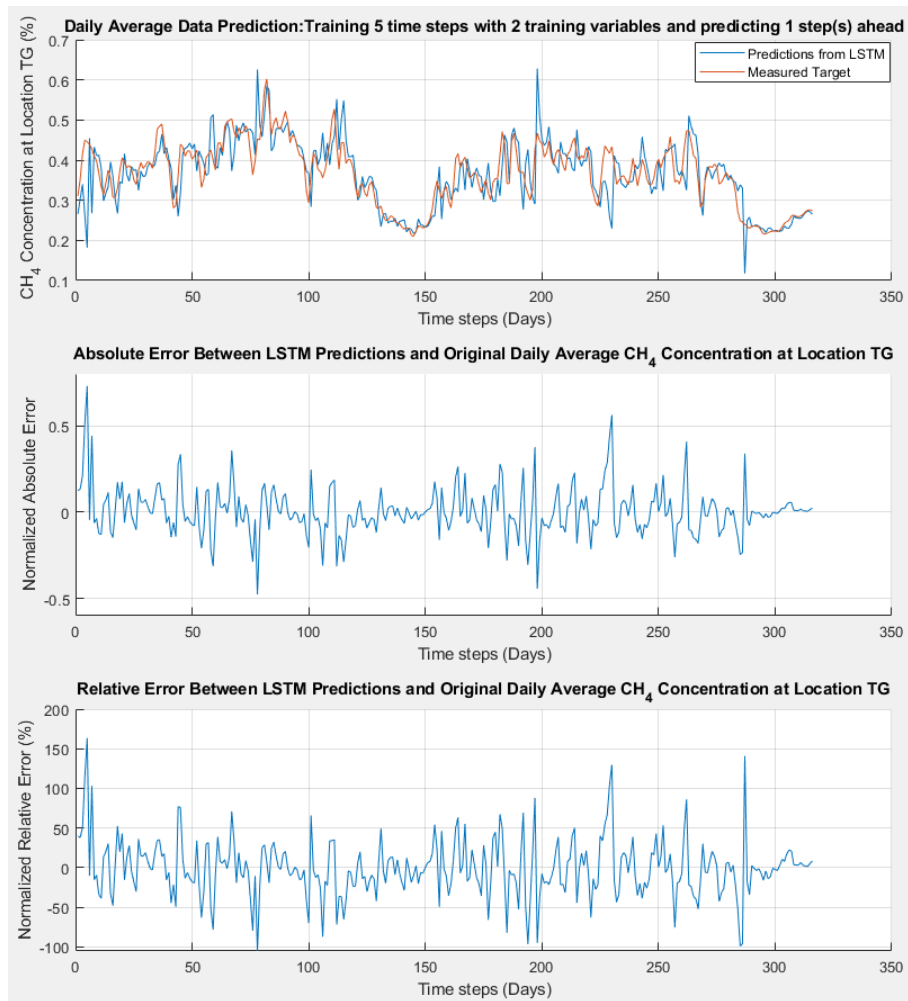


FIG 13 – LSTM predictions and error calculation for the filtered data at location TG.

The time spent for predicting was 19 minutes. Comparing the absolute error plots in Figures 12 and 13 it is observed that the absolute error for the LSTM predictions using the filtered data are about the same as those using the unfiltered data. Comparing the relative errors, it is seen that the errors are smaller for the filtered data.

Comparing the filtering data effect on the time series filter and the LSTM it is clear that the effect is greater for the time series filter, once it gives better predictions for the filtered data (comparing its own predictions, not the LSTM predictions). Comparing the predictions from the times series filter with those from the LSTM for the unfiltered data (Figures 8 and 12), it is visible that the predictions from the filter have more high picks than those from the LSTM. However, the LSTM predictions seem to be shifted along the original curve, characteristic that doesn't happen in Figure 8. Comparing the absolute errors (Figures 8 and 12), the predictions from the LSTM present high picks that go over 0.5, while the error from the time series filter stay within the range of 0.5. Comparing the predictions for the filtered data (Figures 9 and 13), it is clearly visible that the predictions from the filter have more high picks again and the shift-look is still present in the LSTM predictions. Comparing the absolute error plots (Figures 9 and 13), the filter predictions are better. The highest pick in Figure 9 is around 0.3 while in Figure 13 is close to 0.5. Furthermore, the high picks in Figure 9 are almost all below 0.2.

Comparisons between the LSTM and the second order time series fitting for the unfiltered data show that the LSTM predictions are better (Figures 10 and 12), what is proven by the absolute error plots and it is even more clear comparing the relative errors.

Comparing the predictions for the filtered data (Figures 11 and 13), the predictions from the filter show more overshooting high picks. However, the absolute error plots show that predictions from the LSTM are just slightly better than those from the filter, characteristic that is also shown in the relative error plots. One possible explanation is that despite the predictions from the filter have more

high overshooting picks, what increases the error, the LSTM predictions are somehow shifted, so one error compensates the other.

The error is not significantly different comparing the filter predictions to the LSTM predictions, however the time taken to perform the predictions has a huge difference. For industry applications, using the filtered data and making the predictions with the time series filter has clear advantages over the LSTM model, especially regarding time and computational power. Another very important factor is the LSTM tuning parameters. The LSTM predictions can be greatly affected by the configuration displayed in Table 1 (at least theoretically). However, finding the right parameters is a trial and error procedure that can consume a lot of time.

Evaluating the null-hypothesis developed in section 2, the first one is true: a simple 'polyfit' forward prediction scheme is as good or better than the LSTM prediction (for at least the 1st next day). The second null-hypothesis is also true: a 1st-order prediction is better than the 2nd-order forward prediction if the filtered input curve is used. Finally, the third null-hypothesis was not true: the 2nd order prediction is not better than the 1st order forward prediction if the unfiltered input curve is used. So far, filtering the data has shown to be advantageous when it comes to do predictions, both using the LSTM and the time series filter.

Further tests with the LSTM showed that the increasing the number of time steps trained did not have a positive effect on the accuracy of the predictions, in fact, it made the shift-look increase even more and, consequently, the errors, both absolute and relative. Keeping the number of time steps trained at five and increasing the number of points predicted ahead (two points, for example) also had a negative impact in the accuracy of the predictions. The shift-look style is even more noticeable and the error is greater than for a single step ahead prediction. In summary, the errors, both absolute and relative, are greater if the number of time steps ahead to be predicted are increased.

Forward-prediction of root-cause CH₄ sources

The methodology used in this section is described in section 2.2. The idea is to see if the line source variation with time is easier to forward-predict one-time step ahead (meaning with less error) using the LSTM or time-series filter than the next methane concentration directly. The rationale of this idea is that the transport model includes two influencing factors in the CH₄ concentration change simultaneously: the time-variable CH₄ source and the changing air flow rate. On the other hand, the other two methods use only CH₄ concentration change alone to predict a future outcome. Figure 14 (top) shows the back calculated line source responsible for the increase in methane concentration at location TG. The time series filter was used to do a one step ahead prediction for this line source and, after that, this line source was converted back to the methane concentration at location TG. The result, along with the predictions from the time series filter, is shown in Figure 14 (middle). The results in Figure 14 show that the predictions from the time series filter using the line source is about the same as the predictions using the original methane concentration, which is proven by seen the relative error plot.

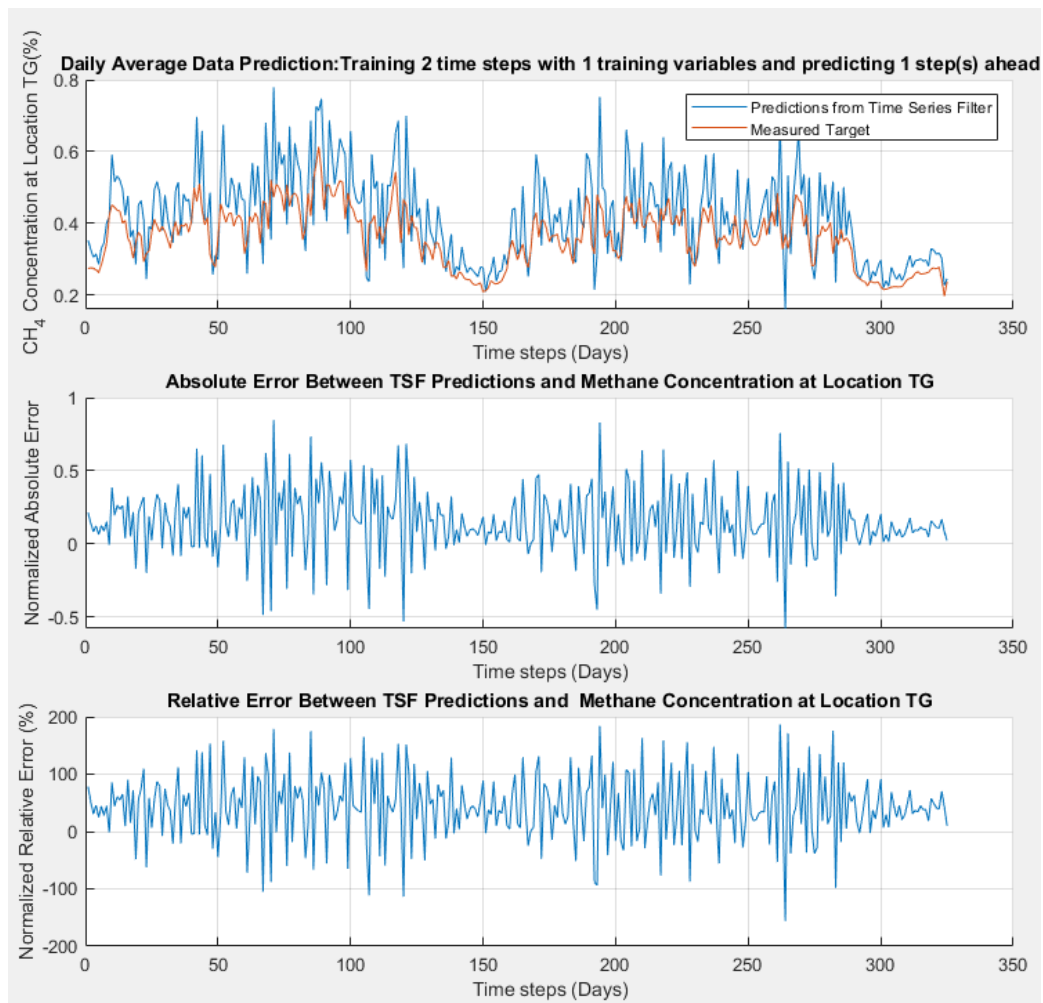


FIG 14 – Back-calculated line source for CH₄ concentration at location TG showing the predictions from the time series filter using unfiltered data.

Comparing the relative error of Figure 14 with Figure 11 is observed that the predictions using directly the filtered original methane concentration present a higher number of picks, suggesting that the time series filter performs better if the predictions are made from the direct CH₄ concentration. Figure 15 shows the predictions for the LSTM. The time taken to do the predictions was 20 minutes.

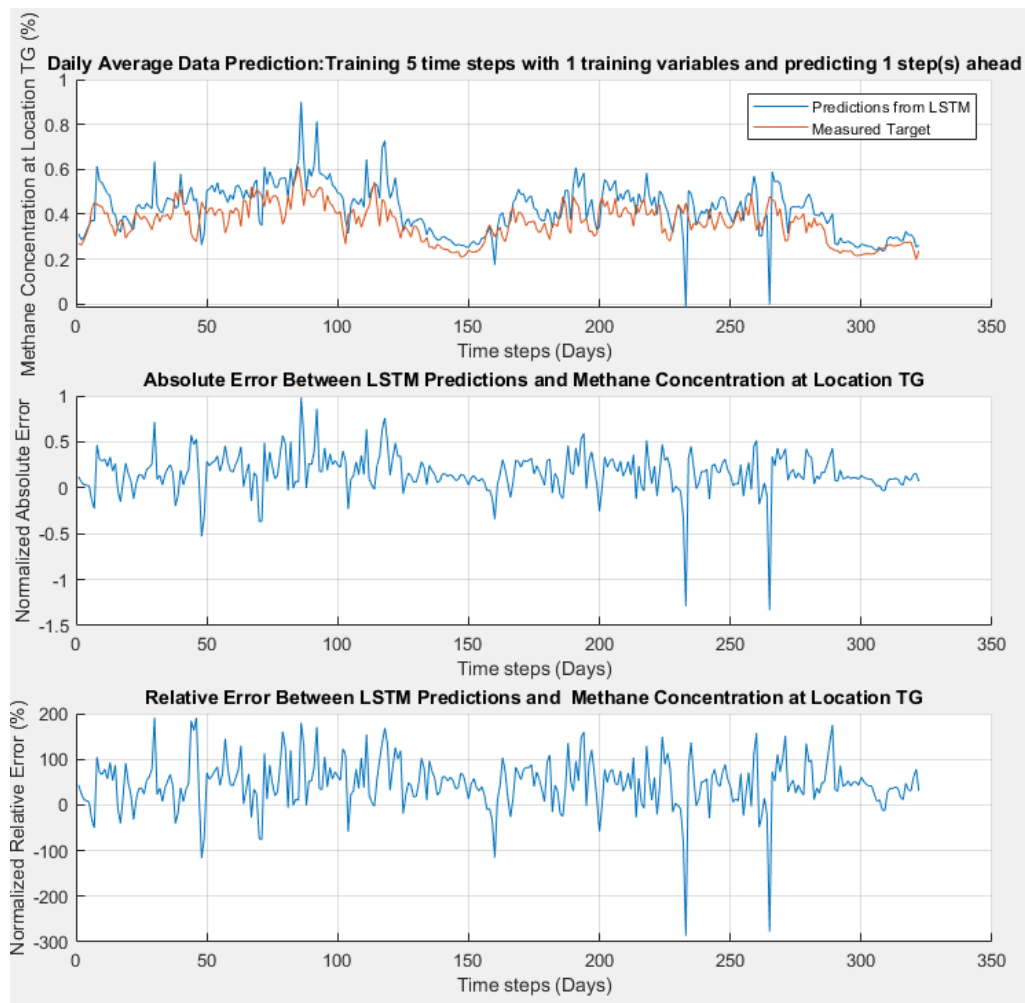


FIG 15 – Transport model back calculated line source for CH₄ concentration at location MG showing the predictions from the LSTM using unfiltered data.

Comparing the error plots from Figures 14 and 15, it is observed that the predictions from the time series filter model are slightly better than the LSTM predictions. If the comparisons are made with the relative error in Figure 13, the predictions in Figure 13 look much better. In summary, the tests carried out in this section show that using the direct CH₄ gives better predictions both from the time series filter and the LSTM models.

The time series data used in the study don't vary solely by natural processes with time. The variables may be actively controlled by the mine during production. However, all changes in the monitored signal variations are reflected in the input data used to train the evaluation models. Active adjustments in ventilation parameters are routinely used for controlling the methane emissions variations by air dilutions inside a mine. Analysing these methods is not in the scope of the present study. The goal is to analyse machine learning algorithms applicable to finding a relationship between variables that are related to the methane concentration for forward prediction. As shown, a simple method can be more accurate and faster than a complex NN model. Based on the results, the method should depend on the quality of the data available, the accuracy required from the model and the computational power available. In fact, to know if the methodology used works for the case studied, it really depends on the required accuracy. The two methodologies presented in this paper show high errors during the predictions. However, it does not mean that if the error is high, the prediction is not useful. For example, if the threshold limit for the methane concentration is 1 per cent and the LSTM predicts a point that is 50 per cent relative error from the original data, the error seems to be high, but if the original point is well below the threshold limit value, the prediction is still acceptable.

CONCLUSION

So far, the tests have shown that the LSTM predictions are as good as the time series filter predictions. The LSTM tests showed that increasing the number of time steps trained did not increase the accuracy of the predictions, on the contrary, made them even worse. Likewise, increasing the number of time steps predicted ahead increased the error between predictions and original target and made the shift-look behaviour even more noticeable. Maybe with a different configuration the LSTM would perform better. One action that can be done is to decrease the mini batch size; the drawback is that the time for training the LSTM increases.

The tests with the time series filter showed that it is much faster than the LSTM and it is easier to be implemented. The first order polynomial fitting gives the best results compared with the second order fitting and the LSTM. Filtering the data makes the predictions better for both LSTM and the time series filter.

The time series filter is preferred for continuous, real-time application because it is much faster than the LSTM and it requires less computational power.

The tests showed that the predictions using the direct CH₄ gives better predictions than both from the time series filter or the LSTM model.

For the cases studied in this paper, the predictions are acceptable, but more tests are warranted to try to increase the accuracy of the predictions from the line-source transport model.

ACKNOWLEDGEMENTS

The study is part of a research project thankfully sponsored by the Alpha Foundation for the Improvement of Mine Safety and Health, Inc (ALPHA FOUNDATION). The views, opinions and recommendations expressed herein are solely those of the authors and do not imply any endorsement by the ALPHA FOUNDATION, its Directors and staff.

REFERENCES

- Bengio, Y, 2012. Practical Recommendations for Gradient-Based Training of Deep Architectures. Lecture Notes in Computer Science, [online] pp 437–478. Available at: https://link.springer.com/chapter/10.1007%2F978-3-642-35289-8_26 [Accessed 22 Nov. 2019].
- Blum, C and Socha, K, 2005. Training feed-forward neural networks with ant colony optimization: an application to pattern classification. *Fifth International Conference on Hybrid Intelligent Systems (HIS'05)*.
- Connor, J and Atlas, L, 1991. Recurrent neural networks and time series prediction. *IJCNN-91-Seattle International Joint Conference on Neural Networks*. <https://doi.org/10.1109/ijcnn.1991.155194>
- Danko, G, Asante, W K, Bahrami, D and Stewart, C, 2019. Dynamic Models in Atmospheric Monitoring Signal Evaluation for Safety, Health and Cost Benefits, *Mining, Metallurgy and Exploration*, 36(6), ISSN: 2524–3462 (Print) 2524–3470 (Online). pp 1235–1252. Open Access Springer publication).
- Danko, G L, 2017. *Model elements and network solutions of heat, mass and momentum transport processes*. Springer-Verlag GmbH Berlin, Germany Springer.
- Diaconescu, E, nd. The use of NARX Neural Networks to predict Chaotic Time Series. [online]. Available at: <http://www.wseas.us/e-library/transactions/research/2008/27-464.pdf> [Accessed 24 Jun. 2021].
- Eltschlager, K, Hawkins, J, Ehler, W, Baldassare, F and Dep, P, 2001. Technical measures for the investigation and mitigation of fugitive methane hazards in areas of coal mining, *Office of Surface Mining Reclamation and Enforcement*. [online]. Available at: <https://www.osmre.gov/resources/blasting/docs/MineGasesDust/Methane.pdf> [Accessed 24 Jun. 2021].
- Greff, K, Srivastava, R K, Koutnik, J, Steunebrink, B R and Schmidhuber, J, 2017. LSTM: A Search Space Odyssey. *IEEE Transactions on Neural Networks and Learning Systems*, [online] 28(10): 2222–2232. Available at: <https://arxiv.org/pdf/1503.04069.pdf>.
- Gurney, K, 1997. *An introduction to neural networks*. Taylor and Francis.
- Haykin, S, 1999. *Neural networks: a comprehensive foundation*. Delhi: Pearson Education.
- Horowitz, P and Hill, W, 2018. *The art of electronics*. New York: Cambridge University Press.
- Kordestani, H, Xiang, Y-Q and Ye, X-W, 2018. Output-Only Damage Detection of Steel Beam Using Moving Average Filter. *Shock and Vibration*, 2018, pp 1–13.

- Kriesel, D, nd. A Brief Introduction to Neural Networks. [online] Available at: https://www.dkriesel.com/_media/science/neuronale-netze-en-zeta2-2col-dkrieselcom.pdf [Accessed 24 Jun. 2021].
- Li, T, Zhang, Z and Chen, H, 2019. Predicting the combustion state of rotary kilns using a Convolutional Recurrent Neural Network. *Journal of Process Control*, 84, pp 207–214.
- Liang, L and Cai, X, 2020. Forecasting Peer-to-Peer Platform Default Rate with LSTM Neural Network. *Electronic Commerce Research and Applications*, p. 100997.
- Marlin, T E, 2000. *Process control: designing processes and control systems for dynamic performance*. Boston: McGraw-Hill.
- Mas, J F and Flores, J J, 2007. The application of artificial neural networks to the analysis of remotely sensed data. *International Journal of Remote Sensing*, 29(3): 617–663.
- Mcpherson, M J, 2009. *Subsurface ventilation and environmental engineering*. London; New York: Chapman and Hall.
- Miao, K, Han, T, Yao, Y, Lu, H, Chen, P, Wang, B and Zhang, J, 2020. Application of LSTM for short term fog forecasting based on meteorological elements. *Neurocomputing*, 408, pp 285–291.
- Nie, X, Wei, X, Li, X and Lu, C, 2018. Heat Treatment and Ventilation Optimization in a Deep Mine. *Advances in Civil Engineering*, 2018, pp 1–12.
- Osunmakinde, I O, 2013. Towards Safety from Toxic Gases in Underground Mines Using Wireless Sensor Networks and Ambient Intelligence. *International Journal of Distributed Sensor Networks*, 9(2), 159273.
- Rojas, R, 1996. *Neural Networks*. Springer Berlin Heidelberg.
- Sangiorgio, M and Dercole, F, 2020. Robustness of LSTM neural networks for multi-step forecasting of chaotic time series. *Chaos, Solitons and Fractals*, 139, p 110045.
- Sarkar, M and De Bruyn, A, 2020. LSTM Response Models for Direct Marketing Analytics: Replacing Feature Engineering with Deep Learning. *SSRN Electronic Journal*.
- Smith, S W, 1997. *The scientist and engineer's guide to digital signal processing*. California Technical Pub.
- Su, H T, McAvoy, T J and Werbos, P, 1992. Long-term predictions of chemical processes using recurrent neural networks: a parallel training approach. *Industrial and Engineering Chemistry Research*, 31(5), 1338–1352.
- Svozil, D, Kvasnicka, V and Pospichal, J, 1997. Introduction to multi-layer feed-forward neural networks. *Chemometrics and Intelligent Laboratory Systems*, [online] 39(1): 43–62. Available at: <https://www.sciencedirect.com/science/article/pii/S0169743997000610> [Accessed 20 Jan. 2020].
- Tsungnan, L, Horne, B G, Tino, P and Giles, C L, 1996. Learning long-term dependencies in NARX recurrent neural networks. *IEEE Transactions on Neural Networks*, 7(6): 1329–1338.

Artificial-intelligence based geotechnical hazard detection for autonomous mining

E Isleyen¹ and H Ş Duzgun²

1. Postdoctoral researcher, Colorado School of Mines, Golden CO 80403.
Email: isleyen@mines.edu
2. Professor, Colorado School of Mines, Golden CO 80403 Email: duzgun@mines.edu

INTRODUCTION

An AI-based roof fall hazard detection system is developed for the future of mine autonomy. Subtropolis Underground Limestone Mine (SULM) is used as a case study. SULM experiences routine roof falls caused by high horizontal stresses. High horizontal stresses produce visual clues in the form of roof beams since the roof beams subjected to horizontal stresses deform or sag more than those only subjected to gravity. The ground control personnel in the SULM have been able to associate areas of high horizontal stress with roof beams. They have identified the depth and the frequency as the most important characteristics of the stress-induced roof beams. The association between the characteristics of roof beams with roof fall hazards is also verified by a statistical analysis of past roof falls and the frequency–depth measurement of roof beams. Since the roof beams are visual clues, the researchers decided to work with images, and chose convolutional neural networks (CNN) as the AI approach. Therefore, based on the recommendations of ground control personnel, images depicting hazardous and non-hazardous roof conditions are collected.

METHODOLOGY

Images were collected under two roof condition classes: hazardous and non-hazardous. These images were used to train and validate the convolutional neural network algorithm. The hazard level difference between locations suggested by the mine personnel is demonstrated by statistical analysis. Images were obtained using a Nikon D5000 camera, from locations labelled by human experts as hazardous and non-hazardous (Figure 1). To increase the number of available training and validation images, and to bring the images down to standard input size for the CNN. The images obtained after tiling goes through a data augmentation stage before used in CNN.



FIG 1 – Images for hazardous (left) and non-hazardous (right) roof conditions.

CNNs are a particular deep learning architecture designed to learn to recognise recurring features. They capably process data that is in the form of multiple arrays, eg an image with three colour channels. The number of images is insufficient to train a CNN from scratch. Therefore, a transfer learning approach is implemented to decrease the number of images required to train a network. In transfer learning, a network trained with a large data set is used as a starting point to train another network with a smaller data set. In this study, a network trained on ImageNet data set is utilised. This study used a 152 layered ResNet network pre-trained on the ImageNet data set. The last layer of the network is trained with the images collected for this study.

A synthetic hazardous roof image data set is created by rendering images from a 3D model of a hazardous roof condition developed with close-range digital photogrammetry (Figure 2). The rendered images are used to improve the size of the data set.

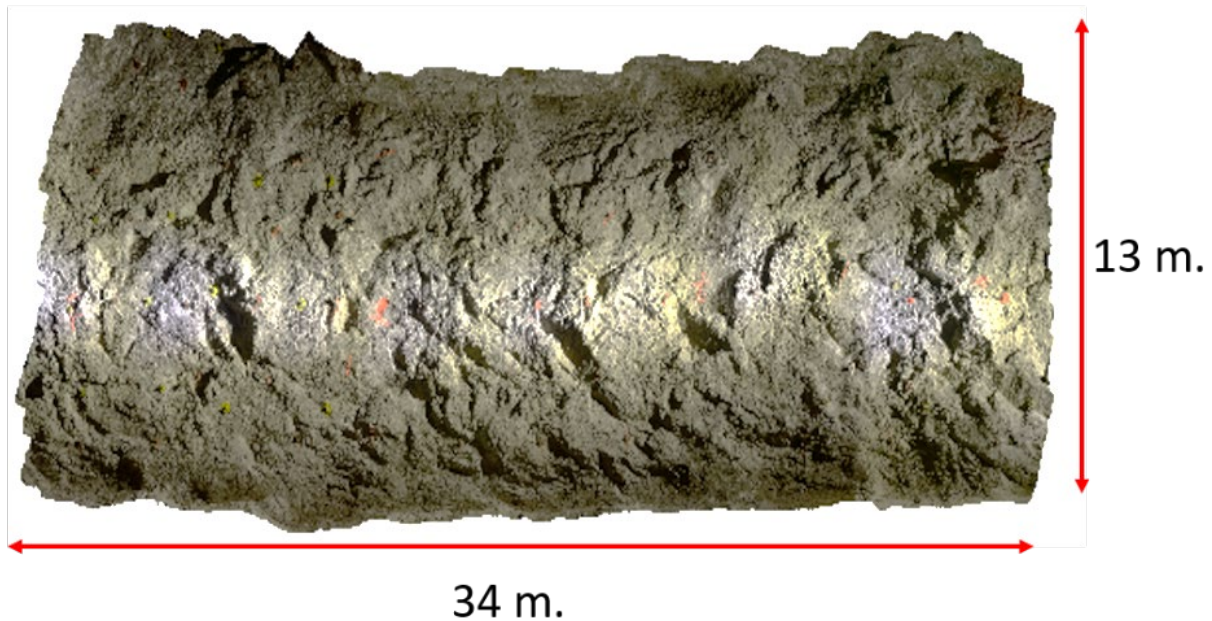


FIG 2 – 3D Model of a hazardous roof condition.

A simple and easy-to-implement data sampling algorithm based on image features is developed. The objective of this data sampling algorithm is to improve classification performance by rejecting non-informative training images. Investigation of Gabor magnitude responses revealed that it is plausible to design a data sampling technique based on Gabor magnitude variances (Figure 3).

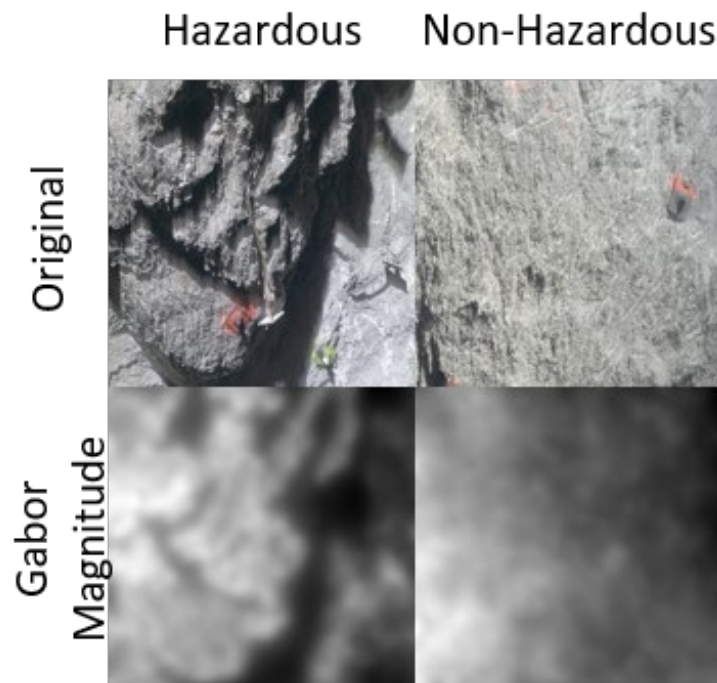


FIG 3 – Gabor magnitude responses for a hazardous and non-hazardous roof conditions.

RESULTS

CNNs are trained after each step and their performances are compared in terms of true positive rate and false positive rate (Figure 4). The aim is to increase the true positive rate and decrease the false positive rate.

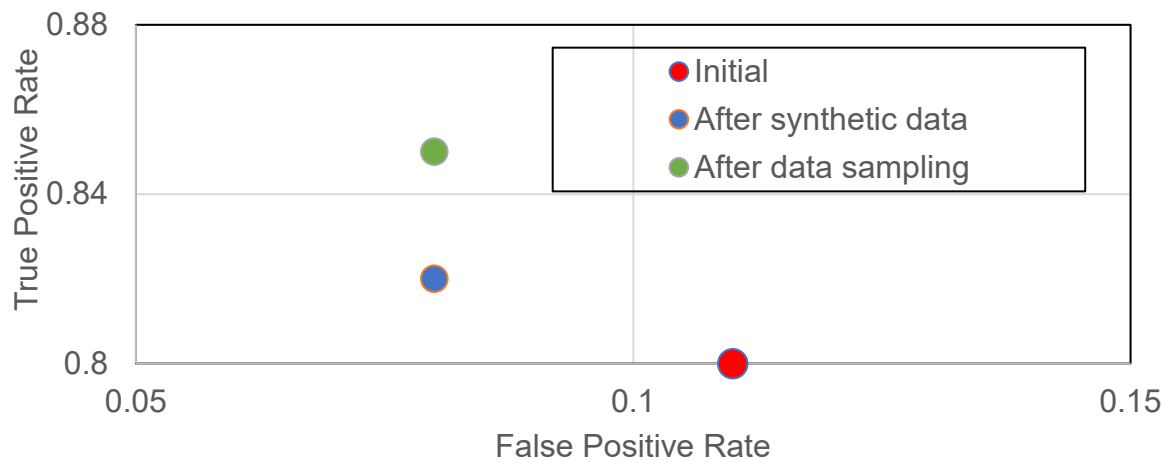


FIG 4 – Comparison of network performances.

The figure shows that after synthetic data generation, the true positive rate was increased, and the false positive rate was decreased. Then, after data sampling step, the true positive rate was further increased while the false positive rate remained the same.

The final network is tested on an independent sample to verify the proposed methodology. The test images are collected from areas reserved for test image data collection and no training, validation, or photogrammetry image was collected in those areas. The test data set includes 80 hazardous and 160 non-hazardous roof images. The confusion matrix of the test results is given in Table 1.

TABLE 1

Confusion matrix for the test data set.

		Predicted	
		Hazard	Non-hazard
Actual	Hazard	79	1
	Non-hazard	24	136

The confusion matrix shows that the network is very successful in the classification of hazardous roof images. The test accuracy is 90 per cent. However, accuracy alone is not a good measure of the CNN's success. Confidence of the users are improved significantly when the image features used by the network are understood. Deep learning interpretation techniques are developed to provide users an understanding of network predictions. These techniques highlight image regions that contribute most to the network predictions at the pixel level. The technique used in this study is called integrated gradients. The example results of the integrated gradients are given in Figure 5.

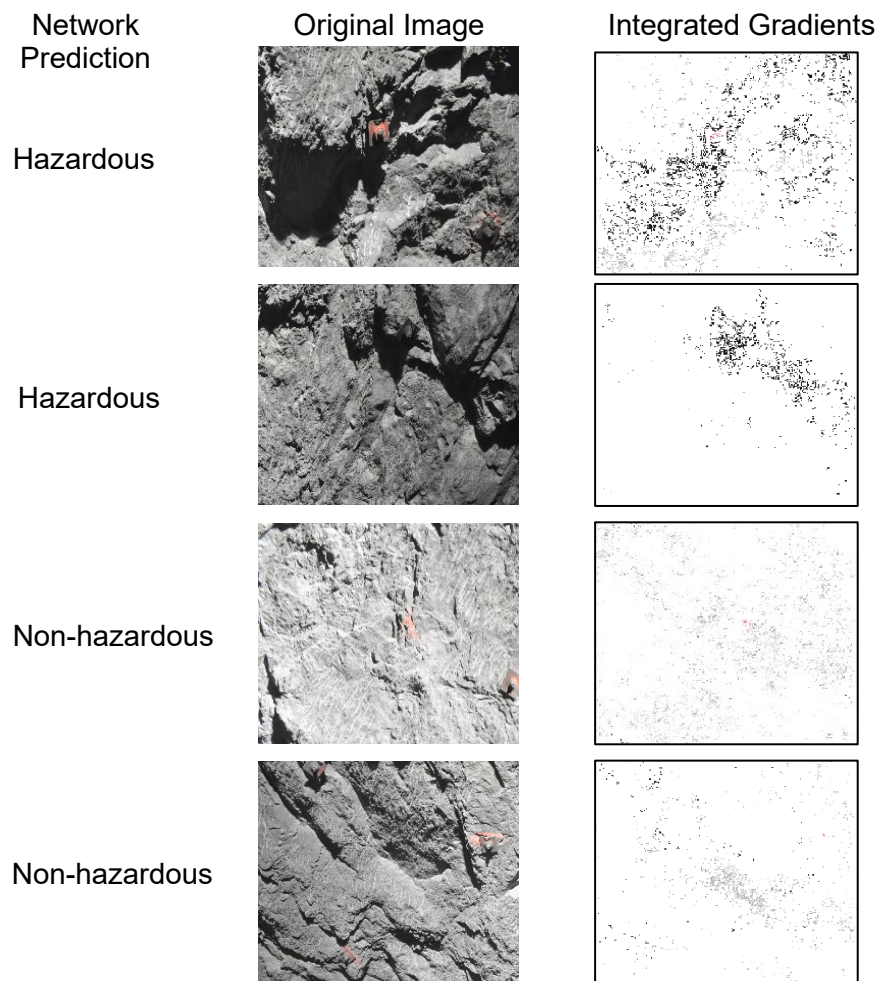


FIG 5 – Integrated gradients results.

The integrated gradients results show that the CNN uses the same geological features that the ground control personnel use during roof fall hazard inspections. The hazardous roof condition predictions are based on where the roof beams are in the images. The non-hazardous roof condition predictions are based on where the smooth roof conditions are observed in the images.

CONCLUSION

In this study, a CNN-based, autonomous roof-fall-hazard detection system was developed for the Subtropolis case. Mining industry expects an increased use of autonomous systems. Identifying geological hazards without human involvement is an important milestone to achieve fully autonomous underground operations. This study presents the first step toward autonomous geotechnical hazard detection in the mining and underground construction industry. Combining the network developed in this study with robotic systems or autonomous vehicles can provide real-time hazard detection.

Bad data – does it really kill off AI and machine learning?

Z Pokrajcic¹ and P Stewart²

1. Technical Director, Petra Data Science, Brisbane Qld 4000.
Email: zpokrajcic@petradatascience.com
2. CEO, Petra Data Science, Brisbane, Qld 4000. Email: pstewart@petradatascience.com

INTRODUCTION

Machine learning is a branch of AI (artificial intelligence) that consists of deep learning, supervised and unsupervised learning. It is the convergence of computer science and mathematical branches of statistics and calculus. It can be described as the automatic application of mathematical techniques on a massive scale using volumes of data enabled by extremely fast computing speeds. Some circles consider this to be machines imitating intelligent behaviour.

With the availability of large volumes of data and extremely fast computing capability together with easy access to latest digital techniques using open source libraries, digital approaches to plant optimisation and orebody understanding using AI and machine learning are becoming commonplace. However, there is a persistent perception in industry that mining data is lacking and of low quality therefore will generate ineffective and bad prediction models.

The concerns include insufficient data (missing data), data of poor quality (erroneous fields and strings) or data that is just wrong (values are not accurate). This is compounded by the fact that data is located and stored in many disparate systems and databases.

AUTOMATED METHODS TO ADDRESS DATA QUALITY CONCERNS

Experience gleaned by undertaking many digital optimisation and prediction programs using volumes of mine operating data in the application of machine learning has shown that operating data is almost never considered accurate, reliable or complete.

Fortunately, purpose built automated mathematical algorithms have been deployed across numerous applications to address these issues in near real-time so that machine learning models can run on perceived below par operating data to produce valid predictions and recommendations.

Outlined below are some data cleaning and correction functions commonly applied to mine operating data.

1. Data cleaning.

Software that automatically stores and filters data including buffering data from selected time frame, convert data format and filter invalid data (IEEE SA, 2021). It also automatically removes erroneous entries such as #NA or blank fields and has the ability to forward fill blank fields with mean values from most recent entries, if deemed valid.

2. Calibration and autocorrection.

Key online sensors such as those coming from on stream analyses (OSAs) and particle size indicators (PSIs) can be automatically corrected using truth data. Truth data is typically laboratory analytical results from daily composite samples.

Figure 1 shows commonly depicted drift and inaccuracies in OSA data, shown in the discrepancy between Amdel (OSA) and Lab composite (laboratory analytical results) trends around 28/1 to 3/2.

During model development, the OSA input data is corrected to better reflect corresponding laboratory results so that model inputs reflect actual trends rather than equipment and instrument error.

3. Anomaly detection and sensor health.

Often, truth data to be used for auto-correction is not available. Hence, the more practised method of monitoring online sensors and instruments for anomalies to trigger real-time alerts and sensor health information for model inputs is used.

Figure 2 shows an example of the anomalies detected from single process variable linked to an online instrument. These reports are generated automatically for regular review by maintenance personnel.

The information is most valuable to trigger real-time alerts on instrument health to prompt physical investigation of the probe or equipment. If the instrument output is an important input to a machine learning model, real-time removal or switching of the input for a correlated variable are options, discussed in point 4.

4. Automated real-time model switching contingent upon sensor health of model inputs.

The nature of machine learning models means that hundreds of variables can contribute to the model output. The inputs and internal interactions of model are visible and can be investigated and interpreted. This is particularly true for supervised machine learning where predictions are derived using actual observations, that is, the target variable exists.

SHAP (SHapley Additive exPlanations) values are a method to explain individual predictions. SHAP is based on the game theory where each variable is a "player" in a game where the prediction is the 'payout'. Shapley values tell us how to fairly distribute the payout among the variables or players.

SHAP are available as free open source libraries that produce interpretable plots and charts, below are a couple used extensively to interpret models.

These models include machine learning techniques such as decision trees and neural networks, including gradient boosted decision tree based regression models (lightGBM, CatBoost etc) and neural networks. The process is semi-automated selecting the best performing model based on metrics such as error and correlation coefficients. The metrics reflect model performance on unseen data, data not used in model training/building.

- Variable Importance Plot.

This chart lists the most significant variables in descending order. The top variables contribute more to the model than the bottom ones and thus have high predictive power.

- SHAP Value Plot.

The plot shows the positive and negative relationships of input variables with the target variable. It is made of all the datum in the training data. The variables are ranked in descending order. The horizontal location shows whether the effect of that value is associated with a higher or lower prediction. Colour shows whether that variable is high (in red) or low (in blue) for that observation.

Given the large number of input variables to a machine learning model, as shown in Figure 3, it is possible to remove a variable as a model input if anomaly detection suggests a critical error in its output. If the variable has a high predictor importance, substitution with another highly correlated variable is an option.

Software is also available to guarantee the integrity of the inputs to a machine learning model, to ensure the inputs are not corrupted or values tampered with.

5. Re-training of machine learning models at regular intervals.

The ability to ingest new, more recent data and information and automatically re-run the model building process to generate a re-trained model helps to eliminate the issue caused by covariate shift (Babic *et al*, 2021) where model inputs (including their statistical properties and distributions) used in building the model differ to those presented when the model is deployed.

Software ensures that the machine learning model can be easily updated, maintained, and automatically re-trained with new data at regular intervals.

Regular model re-training ensures the machine learning models are up to date and reflect most recent operation and performance.

6. Real-time display of model output in the control system for continuous visibility of model performance.

The simplest way to monitor and ensure model output performance and validity is to display the machine learning model prediction on the direct control system (DCS), as shown in Figure 4.

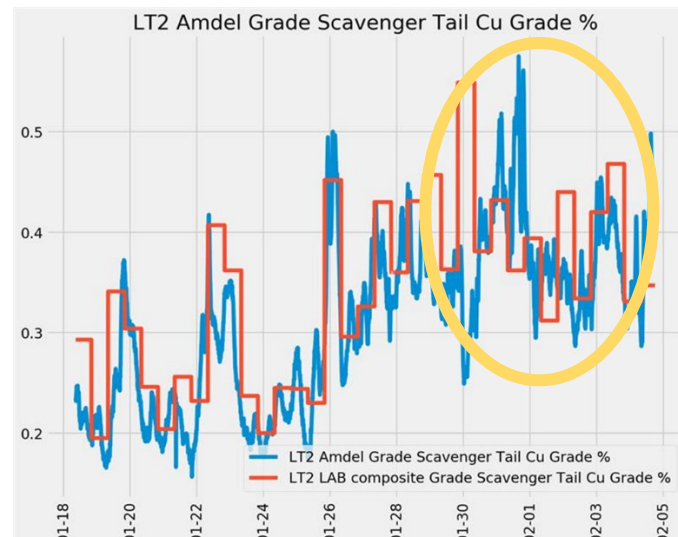


FIG 1 – Example (between 28/1 to 3/2) where autocorrection of online sensors and instruments is required.

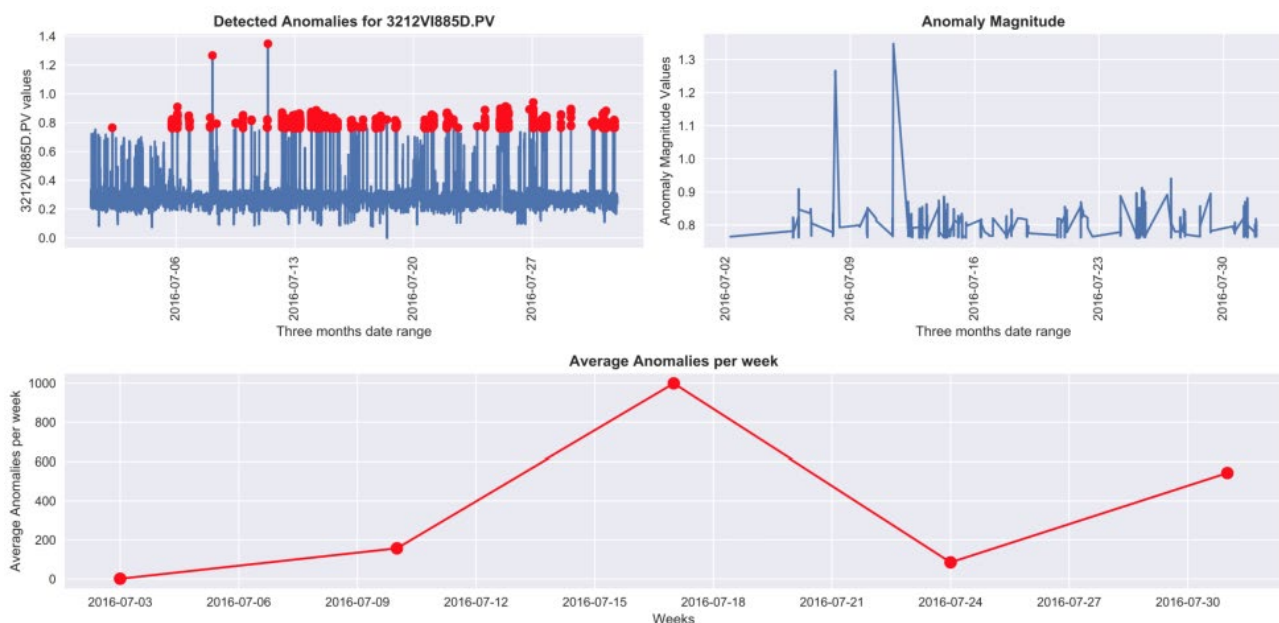


FIG 2 – Example of anomaly detection for sensor and instrument health alerts and model input substitution.

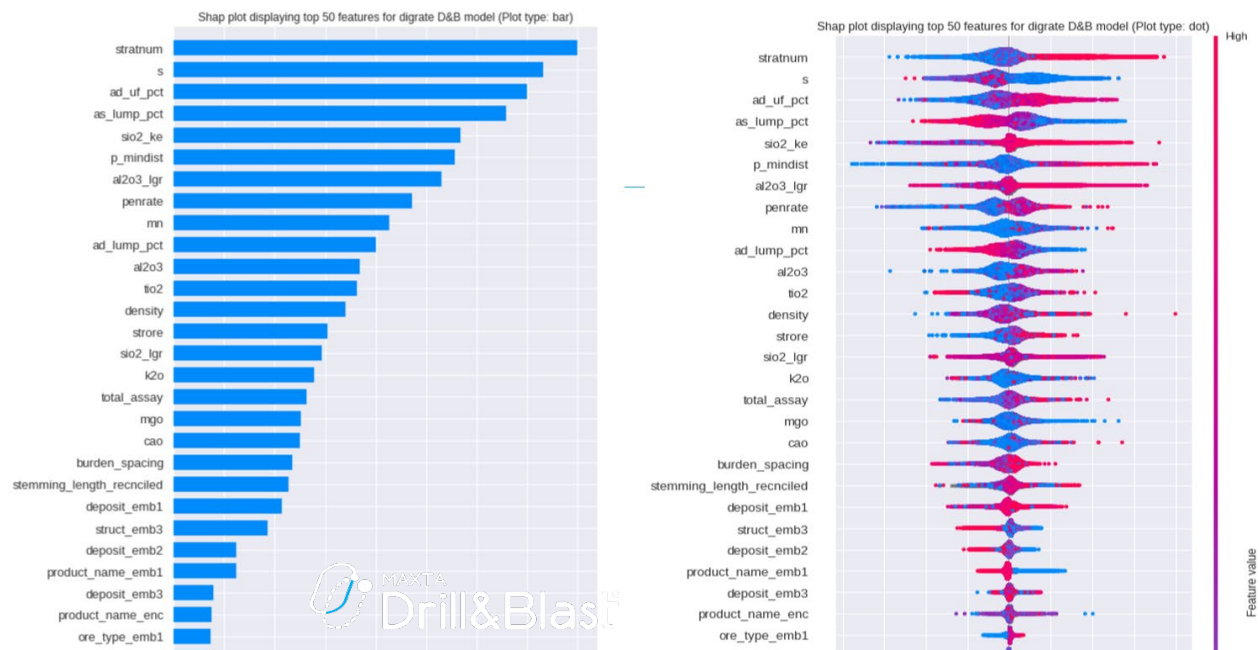


FIG 3 – SHAP (SHapley Additive exPlanations) used to interpret machine learning model inputs and highlight options for variable removal and substitution should anomalies be detected.

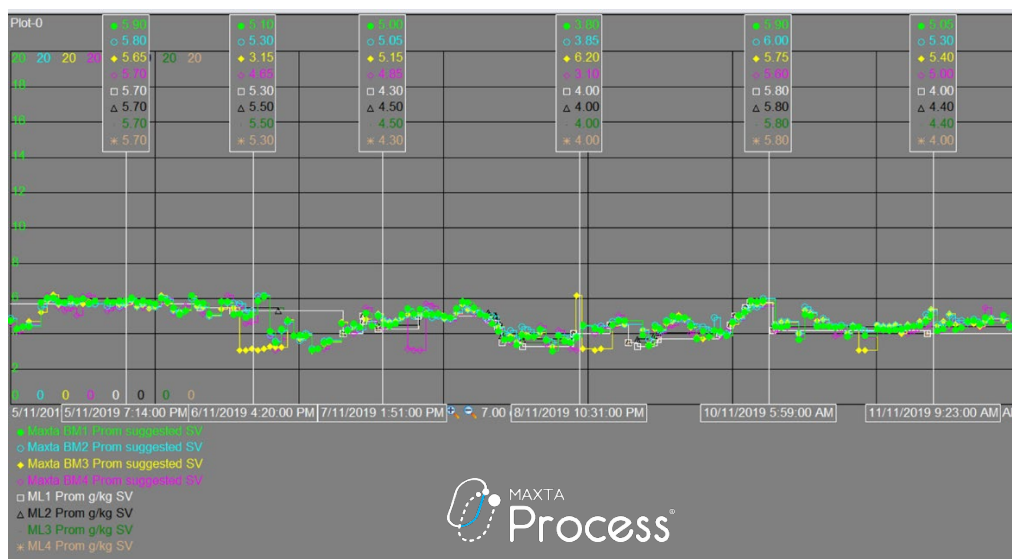


FIG 4 – Machine learning model output displayed in DCS for straightforward monitoring of performance.

Finally, modifying or altering input data in order to generate a better prediction model can be ineffective when the model is deployed to operations, as it is then exposed to poor quality data. A study is currently underway to assess the impact of cleaning training data off-line on model accuracy and performance when deployed to operations. It is expected that cleaning data off-line for the purpose of building superior models is of limited value because when deployed, the model needs to be able to run on live data sources that may consist of poor quality and erroneous data.

Data cleaning and correction functions, such as those outlined here, are inbuilt in the software and are purpose designed to handle raw data feeds in near real-time.

CONCLUSION

Raw mining data can be of poor quality but there are proven methods currently operational where these data issues are corrected and addressed in near-real-time to ensure AI and machine learning integrity.

REFERENCES

- Babic, B. Cohen, I G, Evgeniou, T and Gerke, S, 2021. When Machine Learning Goes Off the Rails – A guide to managing the risks, HBR. <https://hbr.org/2021/01/when-machine-learning-goes-off-the-rails>
- IEEE SA, 2021. P2805.2 – Data acquisition, Filtering and buffering Protocols for Edge Computing Node, IEEE Standards Association (Institute of Electrical and Electronics Engineers). https://standards.ieee.org/project/2805_2.html

Automatic magnetite identification at Placer deposit using multi-spectral camera mounted on UAV and machine learning

B B Sinaice¹, Y Takanohashi², N Owada³, S Utsuki⁴, J Hyongdoo⁵, Z B Baga⁶, E Shemang⁷ and Y Kawamura⁸

1. PhD student, Graduate school of International Resource Sciences, Akita University; 1–1 Tegatagakuen-machi, Akita, Akita Prefecture 010–8502, Japan. Email: bsinaice@rocketmail.com
2. Masters student, Graduate school of International Resource Sciences, Akita University; 1–1 Tegatagakuen-machi, Akita, Akita Prefecture 010–8502, Japan. Email: deil0157sp@gmail.com
3. Technician, Faculty of International Resource Sciences, Akita University; 1–1 Tegatagakuen-machi, Akita, Akita Prefecture 010–8502, Japan. Email: jixidahetian@gmail.com
4. Consultant, UGS-Utsuki Geo Solution, 1–18–2-304 Nishikicho Tachikawa Tokyo Japan. Email: utsuki.shinji.77@gmail.com
5. Professor, Western Australian School of Mines Minerals, Energy and Chemical Engineering, Curtin University; Kalgoorlie WA 6430. Email: hyongdoo.jang@curtin.edu.au
6. Professor, Department of Geology, University of Botswana. Email: bagaizb16@gmail.com
7. Professor, Department of Earth and Environmental Science, Botswana International University of Science and Technology, Palapye, Botswana. Email: shemange@biust.ac.bw
8. Professor, Faculty of Engineering, Division of Sustainable Resources Engineering, Hokkaido University; Kita 13, Nishi 8, Kita-ku, Sapporo 060–8628, Japan. Email: kawamura@eng.hokudai.ac.jp

ABSTRACT

As safety, accuracy and overall system optimisation requirements evolve, the world is rapidly moving into a computer age where equipment automation makes the most sense in every industry. The use of drones in mining environments is one way in which data pertaining to the state of a site can be remotely collected. Though capable of visualising what a miner would be able to see without the need for their physical presence, most production drones are incapable of classifying rocks or minerals with their traditional visible light camera sensors. To counter this, this paper proposes the employment of a multispectral image capturing camera mounted on a drone. Depth possessing imagery data from within the visible near-infrared range (VNIR) was captured via the Unmanned Automatic Vehicle (UAV) drone with multispectral image gathering capabilities at different flight elevations. This was an attempt to remotely identify magnetite iron sands via the UAV drone specialised in collecting five band spectral information at a minimum accuracy of ± 16 nm. Having accumulated the data, visual imagery is fed into a Spectral Angle Mapper (SAM) and a machine learning (ML) algorithm specialised in classifying spectral imagery data. This algorithm is trained and tested in order to classify the magnetite deposits, hence deducing the amount of iron present from within each image corresponding with the site capture point. With the algorithm, a high global classification accuracy of 85.7 per cent was attained. Thus, deeming the system highly viable in mining environments that are constantly aiming for risk potential elimination, by increasing the physical distance between miners and the site. This paper, therefore, confirms the initial hypothesis aimed at achieving overall system optimisation within a mine site by means of the integrated system composed of a UAV drone, multispectral imaging, SAM analysis and ML.

INTRODUCTION

Safety, cost efficiency and overall system optimisation via artificially intelligent (AI) machine learning (ML) algorithms are goals set by modern day industries that invest heavily in output maximisation. The mining industry has been no stranger to this as the introduction of automated haul trucks in the attempt to improve safety and ore tracking abilities (Erbe *et al*, 2004) has been seen. 3D laser scanning of mines in order to assess the current state of a mine so as to enable better planning for the future has also been a common occurrence (Mohajane *et al*, 2017). With regards to rocks and minerals, the introduction of hyperspectral imaging in the detection of their spectral characteristics has received positive feedback (Fox *et al*, 2017).

Though this is the case, the employment of hyperspectral imaging has not been without flaws. These include the time (Ganesh and Kannan, 2017), monetary (Zhang and Li, 2014) and computational requirements (Fox *et al*, 2017) necessary to process this large data. Part of this reason being the multitudes of redundant bands, deemed unnecessary to perform classifications of a specific rock as their inclusivity does not improve the overall nature of the data (van der Meer *et al*, 2012). With such high requirements, it is difficult to perform rapid field spectral imaging as it takes time to acquire the hundreds of spectral bands. Coupled with the weight constraint, it is even more difficult to employ this technology in aerial assessments of a site at considerable spatial areas and resolutions due to the time it requires to capture a single hundred bands deep image (Ganesh and Kannan, 2017).

In order to address this, research has been done, that is aimed at employing unmanned automated vehicles (UAVs) such as drones to identify certain rocks or minerals in mine sites. Despite this, it is difficult to perform a thorough mine site rock or mineral assessment via a visible light camera mounted drone. This is due to the fact that such cameras do not collect the intrinsic characteristics of rocks and minerals beyond the visible light spectrum. With further investigations, it was found that Mohajane *et al* (2017) employed a method which incorporated remote collection of vegetation data via a multispectral camera mounted UAV done in their attempt to identify certain vegetation species. With modifications and improvements of this methodology, a novel method by which rocks and/or minerals can be identified in rapid, large area and detailed field assessments was born. This proposed method combines multispectral UAV drone technology with SAM, and ML algorithms in an attempt to automatically identify magnetite iron sands.

This combined system has the potential to optimise several aspects of the mining chain, hence the motivation for this study. The main objective of this study was to assess an efficient approach for the automatic identification of magnetite iron sands at the Kamaiso placer deposit, located in Yamagata prefecture, Japan. For this purpose, investigations on the viability of a multispectral camera mounted UAV drone will be discussed. Positive results of this research, assessed via SAM and several ML models would aid in ascertaining feasibility for field applications.

METHODOLOGICAL STRATEGIES

The study area

The study area, Kamaiso, is located along the west coast of Yamagata prefecture bounded to the left by the Japan sea. This site, is a magnetite iron sand placer deposit which is said to have been a result of volcanic activity by Mt Chokai estimated to have taken place 600 000 years ago (Kobayashi *et al*, 2019). With ore grades declining worldwide, it makes sense to explore the possibility of mining easily accessible placer deposits such as those in Kamaiso (Nguyen *et al*, 2018). These present an opportunity to maximise profit margins depending on the amount of resources present. These deposits are on the coast and rather difficult to quantify due to the close proximity with the sea. Aerial methods such as the employment of UAV drones present an alternative way of exploring and quantifying target resources within this area effectively. Figure 1 is a map showing a 30 m × 90 m area from which experiments were conducted in an attempt to apply drone technology in identifying magnetite iron sands.

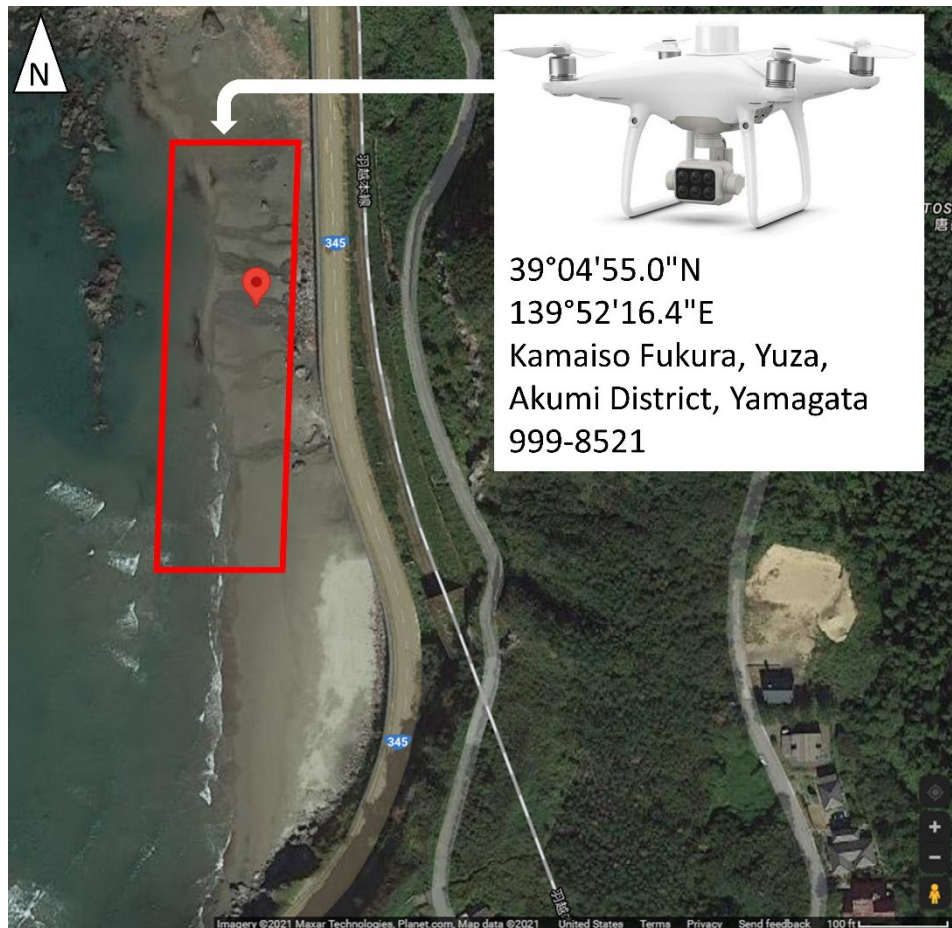


FIG 1 – Map showing Kamaiso magnetite iron sand placer deposits. Red polygon represents the study area within which the UAV drone shown was flown. Map acquired from: Google maps.

UAV drone mounted multispectral camera

Drone technology has evolved over the years, with recent developments catering to specialised industrial applications. One of the advantages of UAV drones is the protection of human life as sites can be assessed from a remote area (Erbe *et al*, 2004). In addition, camera mounted drones aid in real time assessments of sites via visual feed. This feed can be in the form of real, false or manipulated colours which are preprogramed to represent a certain phenomenon understood by the operator (Mohajane *et al*, 2017).

It is said that hyperspectral imaging is arguably one of the best methods by which rocks and minerals can be identified through their spectral characteristics (Fox *et al*, 2017). However, van der Meer *et al* (2012) have been able to attain high classification accuracy outputs in similar rock identification problems via multispectral imaging. Motivated by the demonstrated multispectral capabilities, this paper employed a multispectral camera mounted drone (Figure 1). The spectral sensor specifications were as follows: Blue: 450 nm \pm 16 nm, Green: 560 nm \pm 16 nm, Red: 650 nm \pm 16 nm, Red Edge: 730 nm \pm 16 nm, Near Infrared: 840 nm \pm 26 nm. The drone moreover boasts a 62.7° field of view. In addition to multispectral abilities, the device is coupled with a visible light camera. This aids in facilitating the extraction of magnetite iron sands spectral information in true visible light colours as well as multispectral bands. This, consequently makes the system effective in a wide range of electromagnetic spectra within the visible-near-infrared range (VNIR).

The drone flight height plan was set to three different elevations so as to investigate the effect of ground resolution, proximity to the subject, and the ease of flying. From investigating these attributes, it would be easier to find the optimum height at which rock identification can be performed effectively. The three flight heights measured from the camera sensor to the subject were 2 m, 10 m and 20 m. The drone was moreover set such that aerial multispectral imaging procedure was automatically performed at intervals that ensured an equal amount of area was captured by the end of the flight mission. In principle, this meant that more multispectral images were to be captured at 2 m, followed

by 10 m, with the least number being at 20 m. As a test flight, the drone was flown over the area in order to pre-program the flight plan and ensure the drone flies within the desired area, direction and height before allowing it perform all these manoeuvres autonomously from a remote area.

A breakdown of SAM analysis

Mohajane *et al* (2017) have employed several indexes in the attempt to perform rapid field vegetation classification based on a number of criteria. Such included the intensity of certain vegetation colours and moisture content via SAM. Using the same principle, Zhang and Li (2014) have employed SAM as an index in the attempt to classify lithology. SAM is a physically-based spectral classification that uses an n-dimensional angle to match pixels to reference spectra (Weyermann *et al*, 2009). The algorithm determines the spectral similarity between two spectra by calculating the angle between the spectra, treating them as vectors in a space with dimensionality equal to the number of bands (Shafri, Suhaili and Mansor, 2007). This technique, when used on calibrated reflectance data, is relatively insensitive to illumination and albedo effects (Girouard *et al*, 2004). This makes SAM highly applicable in multitudes of real life field observations. In short, SAM compares the angle between the endmember spectrum vector and each pixel vector in n-dimensional space. Smaller angles represent closer matches to the reference spectrum. Pixels further away than the specified maximum angle threshold in radians are not classified as the reference spectrum of what is sought after. Figure 2 illustrates the principle SAM analysis.

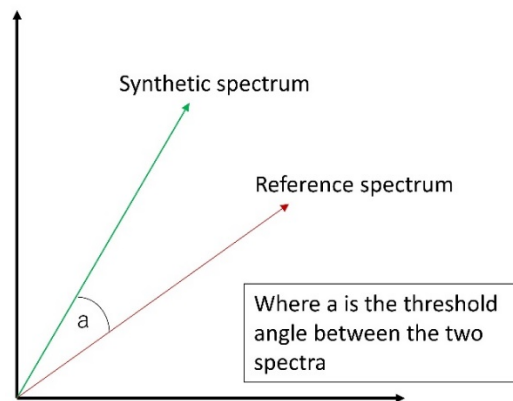


FIG 2 – Schematic diagram showing the principle of SAM. Reference spectrum is usually what is sought after.

On ground, the drone is linked to a tablet which receives captured data allowing for on-site SAM analysis, aiding in the identification of magnetite iron sands. To perform SAM, multispectral images are imported into a SAM operation algorithm such as python. Thereafter, the user pinpoints the area of importance, which in this case was any area within the multispectral image scene known to be occupied by iron-sand. The algorithm then performs a cosine similarity computation for every pixel in the image scene to determine whether or not there are similarities between the reference and subsequent subjects (Weyermann *et al*, 2009). To determine the threshold from the resolution of whether or not new subjects are similar or related to the reference, equation 1 is used.

$$a = \cos^{-1} \left(\frac{t \cdot t_0}{\|t\| \cdot \|t_0\|} \right) \quad (1)$$

Where a is the threshold for variables related to the reference, t_0 is the reference spectra, and t is the subject's spectra.

Why employ machine learning

In order to determine the viability of the SAM analysis, ML models are an upheld method by which this task can be performed (Saha and Annamalai, 2021). To achieve this, the multispectral images are converted into quantitative data sets, thereafter, the SAM mask is extracted so as to act as the ground truth. The feature mask is used as a reference or target. These target pixels' spectral variables are assigned labels so as to take advantage of supervised ML models. Whilst (ground truth) pixels within the mask are labelled as target, the rest of the unmasked pixels from the image

scene are labelled as noise. Labelled data sets allow the model to take advantage of both the global and local structures of the data (Sharma *et al*, 2021). Several ML models are trained with regards to the ground truth or target pixel variables. Thereafter, the top performing models are compared in terms of classification performance for all three flight elevations. From these classification performances, determining the best UAV flight elevation to identify magnetite iron sand post SAM is made possible.

EXPERIMENTAL AND ANALYTICAL RESULTS

In the field UAV drone applications

Based on the flight history logs at the different flight elevation heights, 80, 32 and eight multispectral images at 2 m, 10 m and 20 m respectively (Table 1) were captured. These variables were measured from the time the mission started; to the time it ended. Again, based on these post flight logs, it has been demonstrated that greater elevations allow for a wider area to be captured at a given time, hence disregarding the need to operate the UAV drone at close proximities to the subject. This is a great advantage as it saves time, and computational requirements to process numerous data sets. Though Table 1 demonstrates the implications of flying at three different elevations, it does not communicate outputs pertaining to the actual identification of magnetite. This is a task meant for the SAM analysis.

TABLE 1

Multispectral UAV drone post flight logs for three different flight elevations.

UAV drone flight elevation	Number of Images captured	Flight time (minutes: seconds)	Battery power consumed during mission (%)
2 metres	80	21:32	69
10 metres	32	8:23	29
20 metres	8	2:08	7

Outputs pertaining to SAM analysis

Multispectral images were analysed for the three flight heights and the results show that by altering the reference value threshold, an accurate mapping of the area can be achieved. This is in agreement with Shafri, Suhaili and Mansor (2007) where altering of their threshold values ensured them better subject separation. From the visual analysis of Figure 3, it is clear to see that the SAM analysis seems to have performed well across all the three flight heights. The smaller the threshold, the smaller the mask, meaning less of the targeted magnetite iron sands are identified, resulting in none of the non-magnetite pixels being misidentified. On the other hand, the larger the threshold, the more magnetite iron sand pixels are identified. This however means non-magnetite pixels are likely to be identified as magnetite. To resolve this, one would have to alter the threshold such that the mask perfectly overlays the magnetite pixels only.

For this study, the best SAM threshold values from visual interpretation are 0.12, 0.13 and 0.17 for 2 m, 10 m and 20 m flight elevation heights respectively (Figure 3). As this is the case, it can therefore be said that distance from the sensor to the subject affects the nature of the results as the SAM value needed to be altered for each planned flight height. The lower the UAV drone, the lower the threshold required to identify magnetite iron sands, whilst the opposite was true at higher UAV drone flights. It should be noted that since the multispectral sensors are located at different positions of the multispectral camera (see Figure 1), parallax error needed to be accounted for. In order to correct for parallax error, an edge detection method was used. This method calculates the centre of gravity for all five multispectral bands and automatically nullifies the differences in position of the captured multispectral band images. The result is a perfect overlay of all five multispectral images

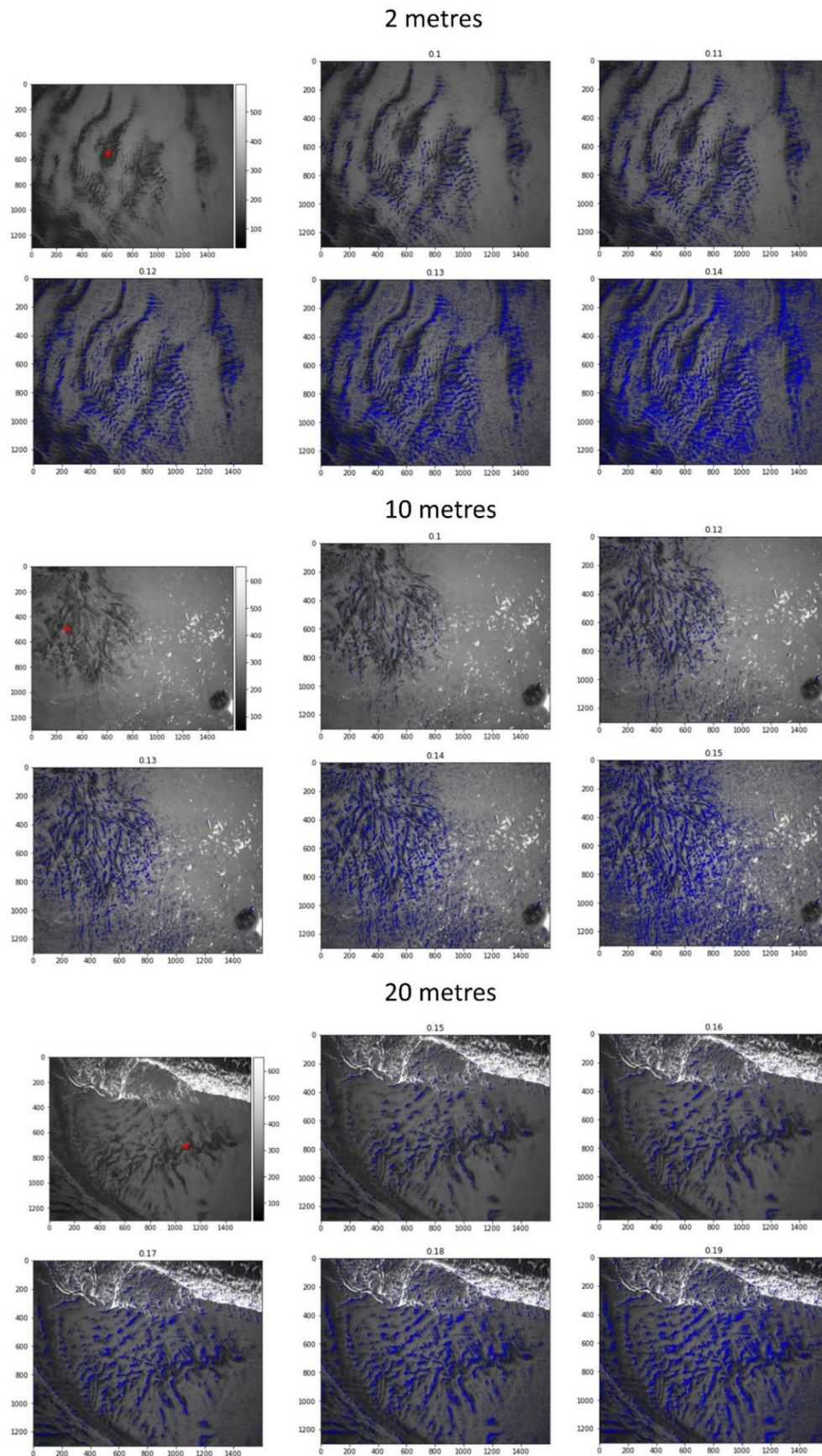


FIG 3 – SAM analysis for 2 metres, 10 metres and 20 metres UAV drone heights at different reference spectral thresholds. The red points represent the user selected reference point (pre-SAM), whilst the blue overlay represent areas within the threshold limit (post SAM). The best threshold cosine similarities are 0.12, 0.13 and 0.17 at 2 m, 10 m and 20 m respectively.

Another assessment that can be made is, the more the threshold values, the more noise was introduced (Girouard *et al*, 2004). Such noise may be due to the presence of mini-ripples. These trick the SAM into assuming there is similarity in image pixel characteristics between the actual reference subject and those exhibited by ripples and shadows. Though a visual assessment of the SAM mask illustrations seems rather subjective, it can still be argued that this method provides a great amount of information pertaining to the location of a specific subject such as the magnetite iron sands. Application of this drone coupled SAM analysis has the potential to be employed in a plethora of applications within the mining industry. These include resource mapping, resource estimation, mine site monitoring, and ore processing amongst others where quick and accurate separation of rocks and/or minerals are constantly performed.

Classification via machine learning

To eliminate subjectivity pertaining to the visual interpretation of SAM analysis masks, ML algorithms are a trusted way in which human error can be eliminated in an objective analysis of data (Saha and Annamalai, 2021). The mask data from the 0.12, 0.13 and 0.17 SAM threshold for 2 m, 10 m and 20 m flight elevation heights respectively (labelled as target), is mixed with the rest of the non-masked pixel data (labelled as noise) so as to build input data. This input data is automatically separated into training and testing data sets. The output variable is predicted or classified from the training database (Sharma *et al*, 2021). Meaning, algorithms try to learn some patterns in the data during training, so as to implement these learnt patterns to the testing data set. Hence, providing results in relation to the learnt patterns.

The spectral data was pre-processed in the following ratios: 80 per cent designated to training and the remainder to testing. The total number of training and testing variables stood at 5000 for each of the three flight elevation heights. Moreover, a five-fold-cross-validation was used at all times in order to ensure that every observation from the original data set has the chance of appearing in training and test sets. Therefore, this method generally results in a less biased model compared to other validation methods (Sharma *et al*, 2021).

Using *MATLAB R2020b classification learner Machine Learning toolbox*, multiple ML algorithms were evaluated. Classification performance was presented in terms of global accuracy, average per class precision, and time taken to train the algorithm. These attributes are said to be amongst the most important classification evaluation criteria (Saha and Annamalai, 2021). These said attributes moreover govern industrial applicability, and the overall viability of the algorithm in solving the task at hand. Table 2 is a compilation of the top three performing ML algorithms for the three multispectral UAV drone flight heights post SAM mask overlays. It quantitatively demonstrates the differences in classification based on differences in flight elevation. In definition, global accuracy refers to the validation accuracy acquired during training. Average per-class precision refers to the individual magnetite iron sands (target) and the environment (noise) classification averages in testing the models. Lastly, training time refers to elapsed time in training the models to classify the data sets based on the presence of magnetite iron sand. These are important performance variables in comparing different ML algorithms given their intended application.

Results from the ML models in Table 2 show that the best performing model was Ensemble (RUS Boosted Trees) for 2 m flight elevation. This model acquired the best outputs in terms of global accuracy (85.7 per cent), per-class precision (84.5 per cent), and training time (5.8 seconds). On the other hand, the Tree (Course-tree) model performed the best for 10 m flight elevation. This model acquired the best outputs in terms of global accuracy (78.7 per cent), per-class precision (83.4 per cent), and training time (1 second). Lastly, the Tree (Course-tree) model performed the best for 20 m flight elevation. This model acquired the best outputs in terms of global accuracy (85.7 per cent), per-class precision (88.9 per cent), and training time (1 second).

From the results compiled in Table 2, the differences in accuracies acquired and elapsed times when training the ML models for the three flight heights can moreover be appreciated. This confirms the hypothesis which stated that with the automatic magnetite iron sand identification system, rapid run times and good accuracies will be attained. This is of course without compromise to the fundamental differences in the multispectral characteristics of magnetite iron sands and the surrounding environment.

TABLE 2

Top three machine learning classification comparisons based on post SAM feature masks for three different multispectral UAV drone flight elevations.

UAV drone flight elevation	Machine learning model	Global accuracy (%)	Average per-class precision (%)	Training time (seconds)
2 metres	Ensemble (Bagged Trees)	78.6	83.4	8.4
	Ensemble (Subspace KNN)	71.4	77.8	8.1
	Ensemble (RUS Boosted Trees)	85.7	84.5	5.8
0 metres	Tree (Fine-tree)	78.6	83.4	1.5
	Tree (Medium-tree)	78.6	83.4	1.0
	Tree (Course-tree)	78.6	83.4	0.9
20 metres	Tree (Fine-tree)	85.7	88.9	1.9
	Tree (Medium-tree)	85.7	88.9	1.2
	Tree (Course-tree)	85.7	88.9	1.0

To further assess the viability of the best performing ML models for the three flight elevation heights, Figure 4 presents two performance metrics. The first is True Positive Rates (TPR), defined as the probability that an actual positive will test positive (equation 1). The second is False Negative Rates (FNR), defined as the probability that a true positive will be missed by the test (equation 2). Both variables are highly viable in assessing the capability of the ML models in classifying magnetite iron sands. At 2 m, the ML model has an 80 per cent TPR, which is not satisfactory as the masked (target) pixel data should have had a 100 per cent target return. This means 20 per cent of the masked pixels were thought to have been noise, suggesting the SAM mask at 2 m did not perform well at discriminating magnetite iron sand pixels from the rest of the non-target pixels. This in essence means flying and collecting data at this elevation is not the best practice. At 10 m, the SAM mask has a 100 per cent target TPR, meaning the masked pixels were undisturbed, suggesting the mask did not include any noise. The same can be said for the 20 m flight elevation, making these flight elevations the most viable. At 20 m, the model has a higher noise TRP of 77.8 per cent compared to the 67.7 per cent at 10 m. This suggests the SAM mask performed better at discriminating the targeted magnetite iron sand pixels from the rest of the pixels in the image scene.

2m :Ensemble (RUS booted trees)

Noise	88.9%	11.1%	88.9%	11.1%
Target	20.0%	80.0%	80.0%	20.0%
	Noise	Target	TPR	FNR

10m: Tree (Course trees)

Noise	66.7%	33.3%	67.7%	33.3%
Target		100%	100%	
	Noise	Target	TPR	FNR

20m: Trees (Course trees)

Noise	77.8%	22.2%	77.8%	22.2%
Target		100.0%	100%	
	Noise	Target	TPR	FNR

FIG 4 – Confusion matrices from Ensemble (RUS Boosted Trees) at 2 m UAV drone elevation, Tree (Course-tree) at 10 m UAV drone elevation, and Tree (Course-tree) at 20 m UAV drone.

True Positive Rates (TPR):

$$TPR = 100 \left(\frac{TP}{TP + FN} \right) \quad (2)$$

False Negative Rates (FNR):

$$FNR = 100 \left(\frac{FN}{TP + FN} \right) \quad (3)$$

Where FN is false negatives and TP is true positives.

Another assessment that can be drawn from Figure 4 confusion matrix are the average per-class precisions of 84.5 per cent, 83.4 per cent and 88.9 per cent at 2 m, 10 m and 20 m flight elevations respectively; at 20 m, the model is still seen to perform better. It can consequently be said that the best classification model for this magnetite iron sands identification problem is Tree (Course tree) at 20 m. Therefore, it has been proven that at 20 m flight elevation, more is achieved in terms of power consumption, area coverage, time, and most importantly, viability in rapid field applications. All this made possible from having employed a multispectral UAV drone mounted camera.

CONCLUSIONS

This paper proposed the employment of a multispectral UAV drone mounted camera in the automatic identification of magnetite iron sands at a placer deposit. First, the UAV drone was flown at three different flight elevations of 2 m, 10 m, and 20 m so as to find the optimum magnetite iron sand identification flight height. Based on flight times, power consumption and number of spectral images captured, 20 m flight height was the most viable. The paper goes on to investigate the SAM analysis at these three flight elevations and found that the SAM mask covered the targeted areas better at 10 m and 20 m possessing cosine similarity threshold values of 0.13 and 0.17 respectively. This was however a subjective observation, hence, the paper continued to address the viability of SAM analysis masked pixels via different ML models. It was found that the SAM masks indeed performed better at higher elevations of 10 m and 20 m with the Tree (Course-tree) models, resulting in global accuracies of 78.6 per cent and 85.7 per cent respectively. A closer look into the per-class classification capabilities of the ML model shows that at 20 m, the model is more superior with a per-class average of 88.9 per cent. In conclusion, the recommended optimum flight elevation in the automatic identification of magnetite iron sands was 20 m for this study.

The study has demonstrated system capabilities with the potential for applicability in the mining industry/sphere. These applications include rock and mineral exploration from a remote location; mapping of mine sites via UAV drone technology; the ability to identify rocks and minerals based on their cosine similarities (SAM analysis) to a reference or known spectrum; the ability to take advantage of multispectral imaging from an elevation and distance of one's choosing, and lastly, the flexibility of applying objective ML models in the classification of rocks and minerals.

ACKNOWLEDGEMENTS

This Work Was Supported by JSPS 'Establishment of Research and Education Hub on Smart Mining for Sustainable Resource Development in Southern African Countries'. Grant number: JPJSCCB2018005. We express our sincere gratitude to Ms Segofalang Annah Modisenyane for her expertise in relation to linguistic editing.

REFERENCES

- Erbe, H-H, Udd, J E and Sasiadek, J, 2004. Mining Automation. IFAC Proceedings, Volume 37, Issue 5, June 2004, Pages 299–304. [https://doi.org/10.1016/S1474-6670\(17\)32384-4](https://doi.org/10.1016/S1474-6670(17)32384-4)
- Fox, N, Parbhakar-Fox, A, Moltzen, J, Feig, S, Goemann, K and Huntington, J, 2017. Applications of hyperspectral mineralogy for geoenvironmental characterisation. *Minerals Engineering*, 107, 63–77. <https://doi.org/10.1016/j.mineng.2016.11.008>.
- Ganesh, U K and Kannan, S T, 2017. Creation of hyper spectral library and lithological discrimination of granite rocks using SVCHR -1024: Lab based approach. *Journal of Hyperspectral Remote Sensing*, 10.
- Girouard, G, Bannari, A, Harti, A E and Desrochers, A, 2004. Validated Spectral Angle Mapper Algorithm for Geological Mapping: Comparative Study between Quickbird and Landsat-TM, 6.

- Kobayashi, S, Ikuta, K, Sugimoto, R, Honda, H, Yamada, M, Tominaga, O, Shoji, J and Taniguchi, M, 2019. Estimation of submarine groundwater discharge and its impact on the nutrient environment at Kamaiso beach, Yamagata, Japan. *NIPPON SUISAN GAKKAISHI*, 85(1), 30–39. <https://doi.org/10.2331/suisan.18-00020>
- Mohajane, M, Essahlaoui, A, Oudija, F, El Hafyani, M and Cláudia Teodoro, A, 2017. Mapping Forest Species in the Central Middle Atlas of Morocco (Azrou Forest) through Remote Sensing Techniques. *ISPRS International Journal of Geo-Information*, 6(9), 275. <https://doi.org/10.3390/ijgi6090275>.
- Nguyen, H H, Carter, A, Hoang, L V and Vu, S T, 2018. Provenance, routing and weathering history of heavy minerals from coastal placer deposits of southern Vietnam. *Sedimentary Geology*, 373, 228–238. <https://doi.org/10.1016/j.sedgeo.2018.06.008>
- Saha, D and Annamalai, M, 2021. Machine learning techniques for analysis of hyperspectral images to determine quality of food products: A review. *Current Research in Food Science*, S2665927121000034. <https://doi.org/10.1016/j.crfs.2021.01.002>.
- Shafri, H Z M, Suhaili, A and Mansor, S, 2007. The Performance of Maximum Likelihood, Spectral Angle Mapper, Neural Network and Decision Tree Classifiers in Hyperspectral Image Analysis. *Journal of Computer Science*, 3(6), 419–423. <https://doi.org/10.3844/jcssp.2007.419.423>.
- Sharma, N, Sharma, R and Jindal, N, 2021. Machine Learning and Deep Learning Applications-A Vision. *Global Transitions Proceedings*, S2666285X21000042. <https://doi.org/10.1016/j.gltp.2021.01.004>.
- van der Meer, F D, van der Werff, H M A, van Ruitenbeek, F J A, Hecker, C A, Bakker, W H, Noomen, M F, van der Meijde, M, Carranza, E J M, Smeth, J B de and Woldai, T, 2012. Multi – and hyperspectral geologic remote sensing: A review. *International Journal of Applied Earth Observation and Geoinformation*, 14(1), 112–128. <https://doi.org/10.1016/j.jag.2011.08.002>.
- Weyermann, J, Schläpfer, D, Hueni, A, Kneubühler, M and Schaepman, M, 2009. Spectral Angle Mapper (SAM) for anisotropy class indexing in imaging spectrometry data, S S Shen and P E Lewis, Eds.; p. 74570B, <https://doi.org/10.1117/12.825991>.
- Zhang, X and Li, P, 2014. Lithological mapping from hyperspectral data by improved use of spectral angle mapper. *International Journal of Applied Earth Observation and Geoinformation*, 31, 95–109. <https://doi.org/10.1016/j.jag.2014.03.007>.

Data driven geology – adopting a data driven culture and reaping the benefits of machine learning

S Sullivan¹

1. FAusIMM, Senior Technical Sales Specialist, Maptek, Adelaide South Australia 5065.
Email: steve.sullivan@maptek.com.au

INTRODUCTION

Geological models are the cornerstone of every mining operation. Understanding the interplay of lithology, alteration, gangue and economic mineral distribution, weathering and structure are important in delivering a model which best reflects the underlying geology and can then be used as the fundamental basis from which mine planning and evaluation studies are developed.

The geology itself is unchanging. It is our perception of the geology that changes as we get more information. Therefore geological models cannot be static. As new data is collected and validated, models must be continuously refreshed to provide the latest knowledge to consumers of the resource model. Geologists hold the keys to the most valuable data and are accountable for its timely provision.

Current resource modelling practices are being challenged as upfront performance comes into question. The timeliness of model generation is important with respect to improving accuracy and mine productivity. Taking days, weeks or even months to refresh resource models is no longer sustainable.

Artificial intelligence and cloud computing herald significant increases in the speed and repeatability of modelling, with the promise of streamlining daily workflows for geologists and engineers. This approach is supported by machine learning and delivers the best of both worlds – removing the need for mining professionals to spend time on mundane processing tasks while freeing them up to apply their professional expertise to interpretation and evaluation.

Technological innovation can already, or will soon be able to, emulate and improve on many tasks which were once the sole responsibility of the mine geologist. Enhanced sensors can scan and characterise rock types and alteration, and others can interpret frequency and orientation of structures. Machine learning services can take this input data and create interpreted 3D models within minutes, generating block models for grade estimation and reporting.

Digital transformation requires data analytics. To drive your operation from these analytics, you need to adopt a data driven culture. Not just you, your team or your site, but the entire company needs to embrace change to benefit from transition to digital systems.

A data driven culture embraces systems which are robust, repeatable and user-independent, meeting the needs of a mobile, shift-based and geographically dispersed workforce. A data driven approach requires thoughtful examination and documentation of data inputs and processes. It requires moving away from a traditional hierarchical way of working to a more distributed model. From a data point of view this can be termed the democratisation of data.

Digitalisation is the pathway to the democratisation of data, allowing organisations to realise the benefits of a continuously updated single source of truth. Cloud computing has also made this approach more practical as there is no need for capital outlay or maintenance costs – companies can just pay for computer time. A data driven approach also removes much of the personal geological bias and makes for a consistent, repeatable and auditable process.

With the complete adoption of a data driven workflow, the corporate geologist analyses information on screen as it passes through the system, with signoff points at critical stages. Data imports are fully connected, data is validated, processes are automatically triggered on preset thresholds, and results are collated and displayed with alerts to users when ready for analysis and signoff. The geological dashboard provides an analogue to what already exists in the mine processing environment, where data flows and key criteria are observed as material steps through the system.

To put this into perspective, in an open pit production environment a data driven system provides fully automated:

- input of new data from core scanning, laboratory analysis and geophysical sensors
- data validation against predetermined rules
- integration of all sources of data into standardised and accepted units
- prediction of missing data from neighbouring sample data
- derivation of classification codes based on lithology, chemistry or other measured criteria
- construction of 3D domain models
- estimation of numeric and categorical variables
- generation and optimisation of grade control dig outlines
- reporting of grades and volumes of each material type
- upload of dig outlines to the production management system for deployment.

This data driven process runs in minutes, ensuring that mine production is always using the latest and most relevant data. A dashboard allows tracking and management by the ore production manager with alerts triggered when data driven processes detect data or results outside preset thresholds. Otherwise, no manual interaction is necessary. The data drives the process.

With interest in mining related studies waning at universities, there are not the number of graduates available to fulfil the workload demanded by current work practices. A data driven approach supplements this diminished pool of labour and mentors these fledglings into a professional and accountable workforce. This is the future of mining.

Committing to this change in workplace operations requires a cultural shift which may not come easily. The technical side of a data driven approach can be achieved with emerging technologies. Managing the human side of data driven systems requires clear communication and support from management, as well as personnel who are adaptive to the benefits of an improved and more efficient means of delivering outcomes.

Automation in mining

Enhanced orebody knowledge through scanning technologies and workflows

H C Grobler¹ and M Pienaar²

1. Head of Department, University of Johannesburg, Gauteng, South Africa.
Email: hgrobler@uj.ac.za
2. Project Leader, Mandela Mining Precinct

ABSTRACT

The paper evaluates the application of integrated scanning technologies for reef identification and mapping in the underground environment. The scanning technologies evaluated includes Light Detection and Ranging (LIDAR), multispectral, ground penetrating radar and thermal scanning technologies to scan a gold reef exposure and platinum reef exposure with the related structural features and geological intrusions. The identification of geological features can facilitate more accurate and detailed mapping of the orebody and provide additional information regarding geological structures and the identification of potential geological hazards. A literature review of current mapping technologies for geology and current scanning technologies including LIDAR, Multispectral and Thermal scanning was conducted. Various scanning technologies were tested on the same baseline and a comparison of efficiency and visibility versus cost and time requirements was made. Studies concluded that geology can be mapped effectively under specific circumstances and can add value in the mapping, inspection and supervision of working underground faces in a narrow tabular mineral deposit.

INTRODUCTION

Geological structures are routinely mapped in development ends and stopes to provide a map of the stratigraphy, lithology, structure and sedimentology of the reef where any exposures are intersected. The thickness of the reef, faults and dykes are recorded and plotted on mineplans. The Mine Health and Safety Act Chapter 17 (22) prescribes a Geological Plan ‘... drawn to a legible scale, depicting geological features that could affect mining, or these features may be shown on the plan(s) referred to in regulation 17(23)’, plans of the workings showing ‘...outlines and dips of the workings; ...faults; dykes and water plugs’ (DMR, 2011).

The Geologist, Geotechnical Engineer, Surveyor and Sampling crews will map reef width, waste channels, over and underbreak and any possible reef in foot or reef in hanging wall for various purposes. In some cases, work is duplicated but not compared and reconciled into a single model. The information gathered by the geologist and sampler is combined in a structure and facies plan that provides a geological model for the calculation of Mineral reserves and resources. LIDAR technology may provide a complete data set that can be used for multiple applications. One scan can provide the data to update mine plans, geology, stratigraphy for geotechnical purposes and documenting the installation of support and services in a working end.

Underground mapping requires the location and mapping of geological structures in a three-dimensional space referenced to the mine survey network. To map accurately, it is best to map as soon as possible after as structure has been exposed to reduce the structure from being obscured by dust, mud, paint or cement and where possible have the face washed down before mapping commences. In most cases, the geologist will offset the excavation using standard tape surveying and where possible capture additional detail with a camera. Although this method is effective and has been used for decades, there is a potential of detail being lost due to observer and environmental constraints further complicated by the short amount of time available to make these observations.

Sedimentological features that are mapped can include grain size, distribution, pebble size (gold bearing rock), bedding features, rock colours and visible minerals in the exposure. ‘Structural interpretation is dependent on the quality of the mapping done’ (Pienaar, nd) and is therefore subjective based on the observer’s experience and the knowledge available at the time of the observations. In this paper, laserscanning techniques to map geology including the collection of

pointcloud information, HDMI photogrammetry and thermal scanning was evaluated to inform the following research questions:

- Can laserscanning be used to map geology?
- Can multi-spectral imagery indicate reef horizons?
- Can mapping out of a pointcloud be automated?
- Can a pointcloud provide information that can be used for 'non-survey' purposes?

STANDARD GEOLOGICAL MAPPING METHODS

Strike can be defined as the 'line of intersection of the plane of the reef with any horizontal plane' (Jackson, 1946). Dip can be defined as the 'inclination of the reef pane to the horizontal' (Jackson, 1946). The mapping of dip and strike using a clinorules and tapes for standard sampling and mapping purposes are described by Jackson (1946) and Storrar (1987). In most cases, strike and dip are still measured using conventional tapes and clinorules. Strike can be measured by stretching a horizontal string between two points on the same level (contact) of the feature to be measured and relating it to a reference direction obtained from survey stations, major dip will be at 90° to the strike line (Storrar, 1987). Reef width (RW) must be measured at right angles to the plane of the reef using (Jackson, 1946) measured using two clinorules, with one ruler one held at right angles to the plane of the reef (Strike and Dip) and the other used to measure at right angles to the first ruler (Jackson, 1946). The application of the Brunton Pocket Transit with Clinometer is described in detail the 'Manual of Field Geology', and in detail in a manual developed by the manufacturer (Brunton, 2017). Several site-specific guidelines on the mapping of structures have been generated through the years and are still in circulation.

Graphical methods of plotting geological features

Various methods exist to graphically plot structure (Lurie, 2013; Storrar, 1987; Berkman, 2001; Brunton, 2017; Jackson, 1946; Metcalfe, 1951; Pienaar, nd) and to plot structures from photography (Rutland, 1969; Baffoe, Boah and Afam, 2018; Benton *et al*, 2016; Fraštia, Chlepková and Bartoš, 2008; Lurie, 2013).

- Dip isogons, tables to determine apparent dip not perpendicular to strike and a nomogram for estimating apparent dip (Berkman, 2001). This nomogram seems to still be used in some mining operations (Pienaar, nd).
- Bramel's chart nomogram (Metcalfe, 1951) as a form of stereonet to determine true dip from apparent dip measurements.
- 'Cotangent semi-graphic method' (Pienaar, nd; Lurie, 2013)
- Graphic 'circle' method (Lurie, 2013)
- Tangent vectors and a graphical solution of the three-point problem using the position and elevation of three points on a reef horizon (Berkman, 2001).
- The use of the 'Orthographic'-, 'Wulff' – and 'Schmidt' stereonets to plot features are supplied but not discussed in the Australian Field Geologist monograph (Berkman, 2001). The stereonet provides a graphic method of representing the relationship between intersecting planes. The dip and strike of a feature can be plotted as a 'great circle' or arc representing a plane of a specific feature providing a method of representing and analysing structural features. The plotting of the pole of a plane can be used when more than one discontinuity is present, when the poles of multiple discontinuities plot close together (pole density), joint sets can be identified (Strauss, 2019).
- The 'Douglas protractor' can be used to plot vectors of apparent dip to determine the strike and true dip of a plane.
- Davies, William and Shillito (2018) describes a graphic method of plotting structural data in outcrops from photographic information.

Mathematical solutions to determine strike and dip

When the deflection angle is measured on the horizontal plane (van Zyl, 1984; Berkman, 2001; Ritson, 1989) the apparent dip can be calculated using the following formula:

$$\tan(d^\circ) = \tan(D^\circ) * \sin H^\circ \quad (1)$$

When the deflection angle is measured in the plane of the reef (van Zyl, 1984; Ritson, 1989) the apparent dip can be calculated using the following formula:

$$\sin d^\circ = \sin D^\circ * \cos \theta \quad (2)$$

where:

d°	Minor Dip
D°	True (Major) Dip
H°	Deflection Angle between Strike and Minor Dip
θ	Deflection Angle between True Dip and line of Minor Dip

The calculation of Minor dips, three borehole problems, reef dislocations and lines of intersections (LOI) by mathematical methods can be mathematically solved using the methods described by (van Zyl, 1984; Ritson, 1989) and graphically by orthographic methods as described by Lurie (2013) and Strauss (2019). Ritson (1989) describes a formula to calculate the major dip and direction of strike from two measured minor dips using:

$$\tan \frac{A - B}{2} = \frac{\sin(d_1 - d_2)}{\sin(d_1 + d_2)} * \cot \frac{C}{2} \quad (3)$$

Photogrammetrical methods to map geology

Although the use of basic photography to record underground conditions, geological features and sampling procedures at the West Rand Consolidated Mines was described by Coetzee, the full application of the recorded photographs (still on film) (Coetzee, 1984) was limited to serve only to enhance standard reporting. The photographs could not be geo-referenced accurately and it was not possible to digitise the data. Coetzee described the application of photography for underground grade control at a gold mine and commented positively on the use of photographs to substantiate sampling reports and resolving disputes. The selective use of photographs may also create bias and areas of concern may be 'ignored' in order to create a biased report in isolated cases (Coetzee, 1984).

Close range terrestrial photogrammetry up to ranges of 300 m have diversified into non-topographic applications including geology (Wolf, Dewitt and Wilkinson, 2014) as it makes it possible to study objects that may be inaccessible to direct measurement. In a Mining application, photogrammetry can enable the observer to remain at a safe distance from the working face, thereby reducing the time of exposure to risk. Benton *et al* (2016) compared the use of close-range photogrammetry and compared it with conventional rock mass monitoring instrumentation, the results support the argument that photogrammetry may provide a safe alternative to conventional geotechnical instrumentation in hazardous areas. Baffoe, Boah and Afam (2018) describes the mapping of geological structures with a standard SLR camera and using 'Sirojoint' software to map structures on a stereonet to predict failures. The use of 'False colour' infrared photogrammetry is described by Davies (1991) to produce a permanent record of geological features. Lurie (2013) discussed the mapping and identification of structures from photography through:

- Shape and form such as contacts, displacements, faults and dykes, the tone and texture
- Tone and texture of material caused by weathering or the inherent characteristics of the material seen
- Drainage characteristics of the rock that may indicate specific structures or horizons (Lurie, 2013).

THE DEVELOPMENT OF A 3D GROUND MODEL

Williams (1967) described a simplified computer equation for the determination of strike and dip for photogrammetric applications in engineering geology, stating that 'all detailed information for the determination of dips and strike directions of major bedding planes would be obtainable from the three-space coordinates measured in the spatial models'. Chmelina *et al* (2010) describes the development of a geological and geotechnical model containing precise geo-referenced geometry and attribute data to support design, construction and operation in the tunnelling environment. Real-time geological mapping of the front face (Moulin and Vallon, 2010) through the monitoring of the disk cutters of the tunnel boring machine. Sensors providing information on the load force of the cutters, tool wear and operating parameters can be used to develop an understanding of the geology directly ahead of the cutting head.

Laser scanning, a literature review

The 3D nature of geology is best represented in a 3D environment. A TLS system allows 3D detail to be captured on location allowing the 'effects of structure on sedimentology' to be modelled and be visualised in a 3D CAD environment. Geological layers detection and characterisation using high resolution point clouds acquired from Terrestrial Laser Scanning (TLS) and Photogrammetry can be used to identify the geometry of the geological layers and semi-automatically segment the different lithologies. The semi-automatic segmentation was based on intensity information for each lithological class and filtering and clustering classes out of the point cloud (Humair *et al*, 2015). Verifying existing geological cross-section of coal lithology with laser scanning at the AGH experimental mine and a case study of a Vietnamese mine was described by Buczek, Paszek and Szafarczyk (2018). Monsalve discussed the application of laser scanning for rock mass characterisation and discrete fracture network generation in an underground limestone mine describes the use of 'I-site' software to edit and process laser scans to define discrete fracture networks and the ability to integrate different software packages in a clearly defined workflow (Monsalve *et al*, 2019).

Russell and Stacey (2019) described the use of a Terrestrial Laser Scanner (TLS) to map faces in an opencast iron-ore mine to improve geotechnical data. The authors referenced the use of 'semi-automated techniques' that rely on user structural interpretations of specific features of mapping a mine face Feng and Röshoff (2015) and Slob *et al* (2007) based on digital photogrammetry techniques. The advantages of using a laserscan for mapping includes accurate 'discontinuity orientation measurements' and oblique planes of strata being easier to be observed. The application of texture or 'roughness' for analysis to extract discontinuities, joint spacing measurements and stereonet plotting in a CAD environment to assist semi-automated environment. Slob *et al* (2007) discussed the process of automated processing of fracture mapping using 3D laser scanning techniques through surface reconstruction or direct segmentation. Feng and Röshoff (2015) provides a survey of 3D Laser Scanning techniques in the field of rock mechanics. Terrestrial photogrammetry to monitor the stability of rock slopes augmented by laser scanning to obtain a point cloud to create a digital elevation model of the rock face that can enable the automation of image processing and DEM creation (Fraštia, Chlepková and Bartoš, 2008).

Structural geology can in some cases be mapped through semi-automated processing a RGB value colourised plot can be used to identify structures visually. 'Semi-automated process using open-source software DSE (Discontinuity Set Extractor) are able to derive segments from normal vectors which in turn can be used to generate a 'pole plot' in order to generate discontinuity sets. From the discontinuity sets dip directions and joint planes can be identified (Buyer and Schubert, 2017). Bell (2006) described how potential hazards can be mapped, identified and compiled as a site hazard map. Joint mapping for the prediction of rockfalls was described in an iron ore mine case study (Gumede and Stacey, 2007). Riquelme, Abellán and Roberto (2015) proposed a new method of mapping discontinuities such as roughness, spacing, infilling, weathering and the presence of water in a rock mass using a LIDAR generated pointcloud using 'Discontinuity Set Extractor' (DSE) opensource software.

SITE TESTS

Light Detection and Ranging (LIDAR), multispectral and thermal scanning technologies were used to scan a test site consisting of a pillar of Merensky reef in the test mine in the Rustenburg area of

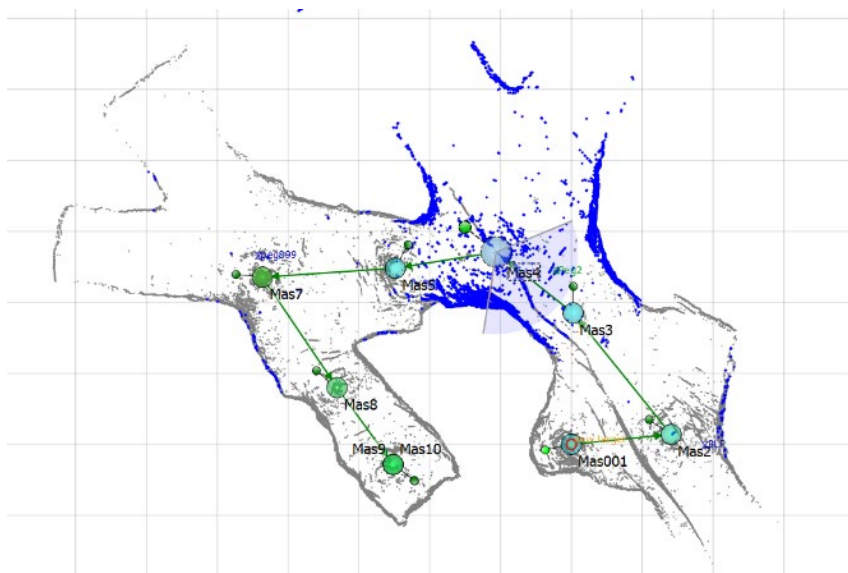
the Pilanesberg Complex. The testing aimed to prove that the identification of geological features from a LIDAR scan may facilitate more accurate and detailed mapping of the orebody and provide additional information regarding geological structures and the identification of potential geological hazards that can in turn improve the accuracy of production planning and orebody knowledge.

Visual observation of the pillar and immediate surrounding excavations indicated a dyke of approximately 30 cm wide cutting NW SE in the Main Belt North drive near survey station M0949. In the working panel (Main Bord1 NW the Merensky reef with a pronounced roll from East to West with a small, suspected Iron-rich ultramafic pegmatite (IRUP) in the corner of the pillar, jointing structures in the NW SE orientation and some form of reef displacement in the form of either a fault or a roll in the reef. In the Main Belt drive the geology on the face of the pillar could not be observed clearly due to dust and mud accumulation and whitewash used to indicate the grade line. The pillar was mapped conventionally using tapes, clinorules and compass to provide the baseline of information available for the specific pillar.

Laser Scan of the pillar

A laser scan of the working place and surrounding pillars was made using the Zoller and Fröhlich (Z&F) 5010X Terrestrial Laser Scanner to create a point cloud. The scan was started at the opposite side of the pillar to provide the geologist sufficient time to map the panel conventionally.

The Z&F 5010X scanner can take a 'maximum measurement rate of 1 016 027 pixel/sec' in a '320°x 360° field-of-view' up to a distance of a 'maximum range of 187 m' (Zoller and Fröhlich GmbH, nda). The scanner was set at medium resolution and high quality, that translates to a coverage of a lidar point every 6.3 mm at a distance of 10 metres. The time per scan including setting up, scanning, photographing and moving to a new set-up position was in the order of 12–15 minutes per scan. A total of 10 scans, numbered Mas1 to Mas10, including a full HDMI photograph at each set-up was made. Three survey stations were observed for orientation and included in the scan. The scan was made on a local survey system but can be geo-referenced once the survey station coordinates have been made available. An outline of the laserscan coverage can be seen in Figure 1.



The 3D Laser Scanner is equipped with High Dynamic Range (HDR) camera that takes a series of photographs that can be linked to create a panoramic 360-degree image at each set-up. The scanner completes a rotation to generate the point cloud and then based on the camera selected, proceeds to take 42 individual photographs to construct a 80 Mega Pixel panorama 'bubble view'. The duration of the full panoramic photograph is approximately 3.5 minutes. The colour pixels of the panoramic image can then be assigned to the correlated point in the point cloud to produce a true to life 3D colour point cloud. High Dynamic Range imaging (HDRi) is commonly known as bracketing in Single Lens Reflex (SLR) cameras. Combining this technology with an LED lighting (Z+F SmartLight) system (Zoller and Fröhlich, ndb) has revolutionised capturing images in dark spaces. The Z&F

smartlight orientates the strong LED light source in the same orientation as the camera and illuminates the centre point of each individual photograph separately. Before the introduction of this latest camera technology in scanners, Reflective index images were preferred due to over and under exposed images.

In some cases the level of detail in a stringer below the reef horizon could be measured to 25 mm as indicated in Figure 2 based on a laserscan made in the footwall drive of a platinum mine.



FIG 2 – Stringers indicated in the pointcloud.

Thermal scan, accuracy, properties

During a previous investigation the results from a thermal – and laserscan of a wide gold reef exposed in a trackless gold mine (Figure 3), temperature differentials could be observed within the scan data. These results prompted the hypothesis that thermal images could possibly be used to map geology if the thermal signature of the reef is known. The question was formulated if the Pilanesberg complex stratigraphy would have unique thermal signature due to the higher thermal signature of the bushveld complex.

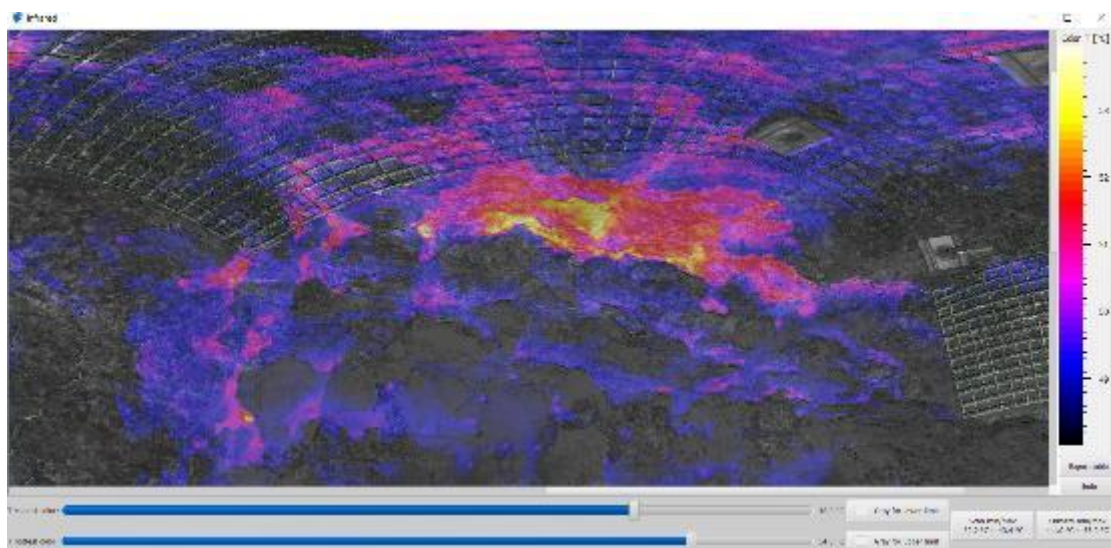


FIG 3 – Thermal scan results of a VCR gold stope.

A thermal scan was undertaken at the same time as the LIDAR data collection at the Merensky test mine. The Zoller and Fröhlich T-Cam thermal camera can be attached to the top of the scanner (Zoller and Fröhlich, ndc), providing a 360° thermal panorama scan of the area, linked to a point cloud scan made at the same position. This allows for an additional spectrum beyond visible spectra, with specific reference to heat sensing in imaging that can be mapped onto the point cloud.

The thermal camera was tested and calibrated off-site before the scanning campaign. The Thermal camera connection and data transfer was successful and data could be obtained. Unfortunately, it appears that the thermal conditions in the panels has stabilised and as a result almost no thermal variance could be obtained. It is proposed that the long time between the face being mined and the scanning campaign has caused the 'rock skin' to equalise with the ambient temperature. An example of the results is shown below. The verification of the thermal images can be checked by the second image that shows two persons in the scan. The thermal image indicates thermal variances on the persons at a higher temperature than that of the surrounding area. Persons standing 30 m away from the scanner could be identified through their thermal signature.

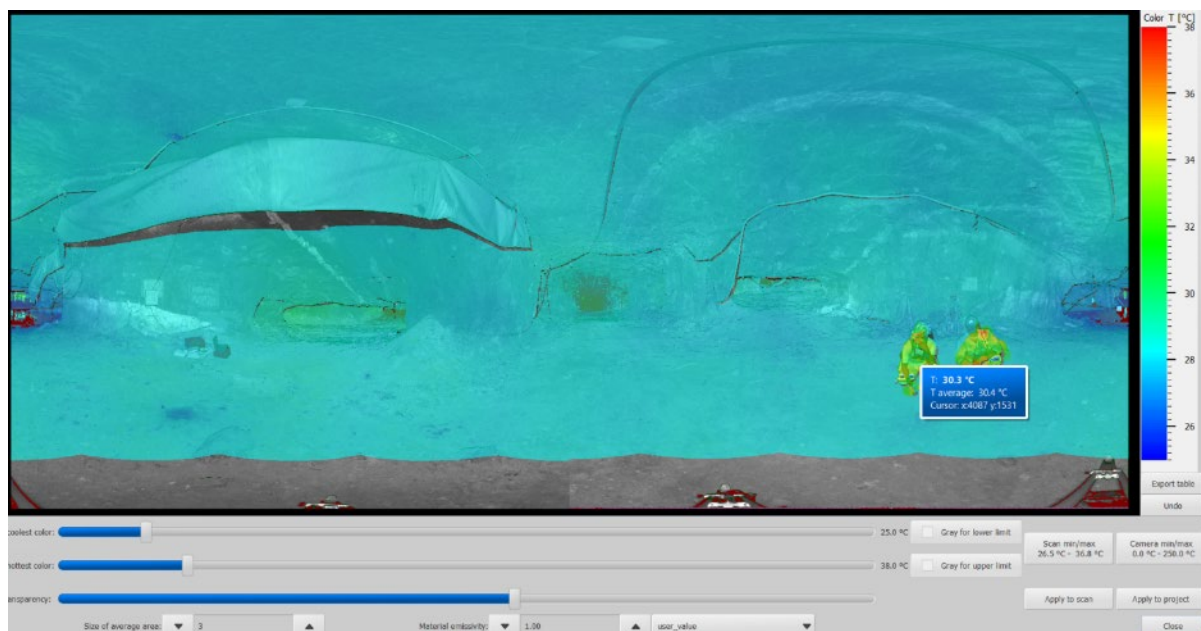


FIG 4 – A thermal plot of a stope and two miners.

The dyke intersection in the Belt Road was measured and it was attempted to identify the dyke and Merensky refractive index in the figure below. As is apparent from the figure below, the dyke could not be identified from refractive index. The thermal scan appears to indicate a slight temperature variation between the dyke exposure and the host rock.

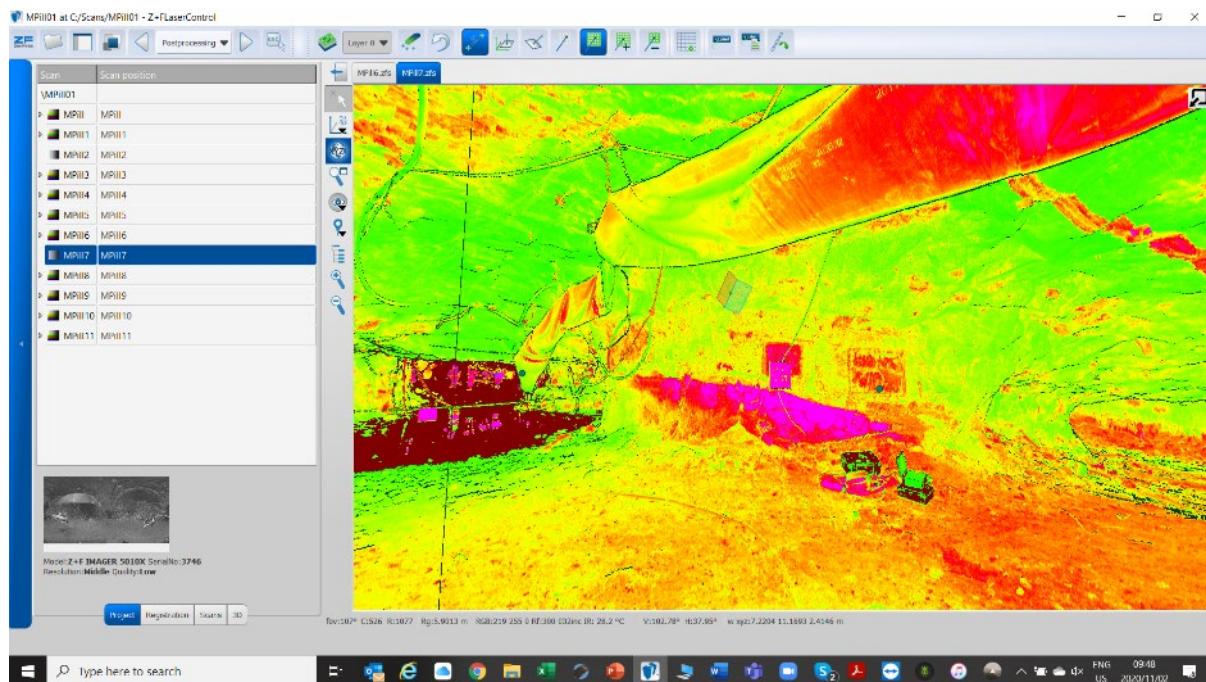


FIG 5 – Dyke intersection in the beltroad from pointcloud and photograph, Z+F Scout software (Source Grobler, 2020).

Davis, Wilson and van der Merwe (2007) described the determination and mapping of densities in PGM reef to monitor lithological differences as a ‘rapid and effective tool’. The knowledge of the thermal properties of rock can assist in understanding the resource better and assist in the planning process (Jones, 2015). Jones experimented with the correlation between density and thermal conductivity to determine the characteristics of various rock types and was able to develop a database of thermal properties. For the purpose of this project it was proposed that a thermal camera may be able to differentiate different rock types by thermal signature which in turn could be used in an Artificial Intelligence algorithm to perform mapping of geological features in a working mine based on a thermal scan cross-referenced to a potential database of thermal properties. Jones determined that the ‘heat flux’ indicates a steep drop within the first 5 days and then stabilises after 10–20 days (Jones, 2015), this may inform the results that was obtained by the scan and is discussed in this report.

Two scan campaigns at the test mine identified short comings in the ability of a thermal scanner to positively identify geological structures. It was suggested that the age of the faces scanned at the test site has allowed the face and geological features to cool down to the ambient temperature of the entire excavation. In some instances, a slight signature of the dyke intersection could be detected but the quality of differentiation was insufficient to provide a convincing argument.

It was decided to scan a ‘freshly blasted’ face to determine if better results may be obtained. An exposed reef intersection of a gold mine that was blasted within the past 24 hours was identified as the best possible option. The exposed test area of Ventersdorp contact reef (VCR) in the gold mine at a depth of 3400 m below surface was developed as a reef-drive from a cross-cut. The hanging wall conditions were not ideal and a lack of ventilation made the working end extremely humid and uncomfortable. The instruments could not acclimatise in the humidity and the temperature differential caused malfunctions in both instruments. One scanner was able to operate but the data was corrupted. It is suspected that the continuous fogging of the receiving mirror in the scanner caused a fatal malfunction. A second scanner took 20–30 minutes to acclimatise fully after which it performed flawlessly. The pointcloud obtained from this instrument provided the only useable data. The thermal scan from the first scanner provided an image but the high temperature in the working place provided little evidence of differentiation in reflectivity based on a thermal signature of the VCR reef.

The second scanner was able to provide grey scale images but does not have the lighting adaptor that the first scanner has. The images provided by the second scanner is of an extremely high quality.



FIG 6 – A grey scale pointcloud of the reef drive exposing VCR reef.

A total of eight scanning set-ups was made and linked with a cloud-to-cloud registration. The accuracy of registration was 7 mm. From the results of the three thermal scanning campaigns it would appear that full colour HDMI images may provide more value than images obtained from refractive index – and thermographic scan results.

SCAN RESULTS

A visual comparison between the mine plan and raw point cloud using an overlay but not to scale is represented in the figure below. It appears that the mine plan does not reflect the final face positions very accurately. This is as a result of the mine using tapes for measuring versus the high-density point cloud.

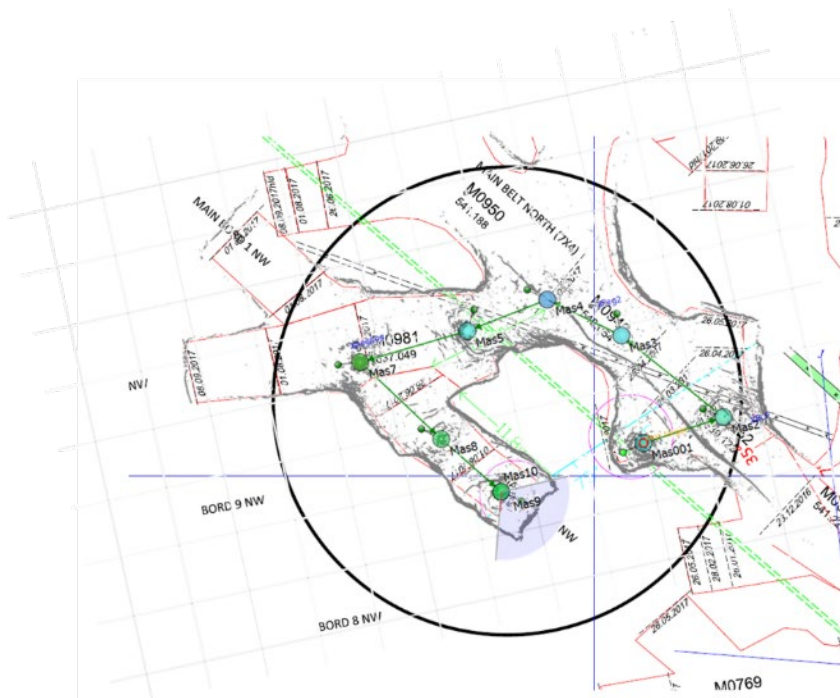


FIG 7 – Comparison of the mine plan to the point cloud.

The dyke intersection in the Belt Road was measured at 0.39 m wide and indicated with the two red lines in the figure below.

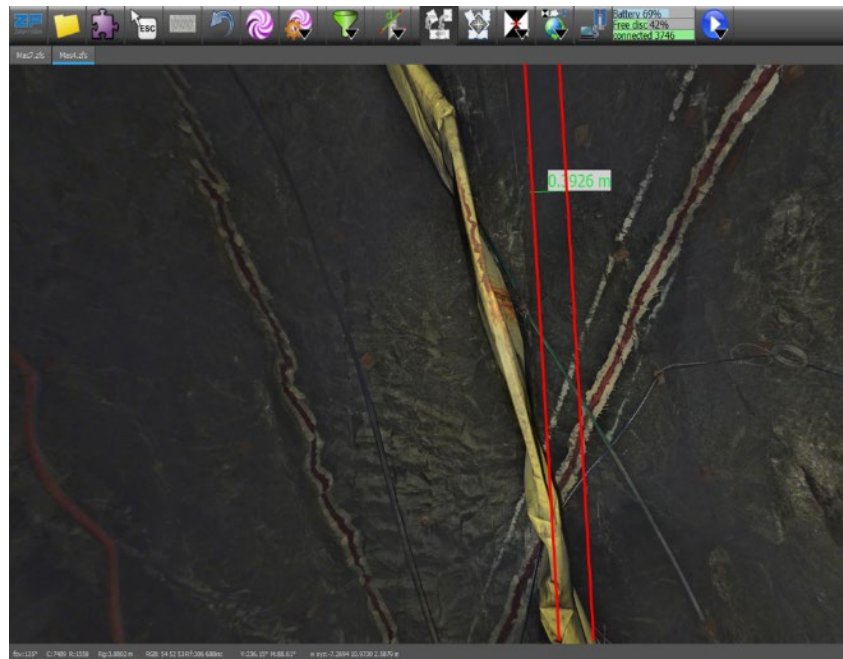


FIG 8 – Dyke intersection in the belt road from pointcloud and photograph, Z+F Scout software (Source Grobler, 2020).

The pillar was well lit and a good Merensky exposure could be measured and scanned. It is indicated in the figure below. Note the mud and dust obscuring the footwall contact.

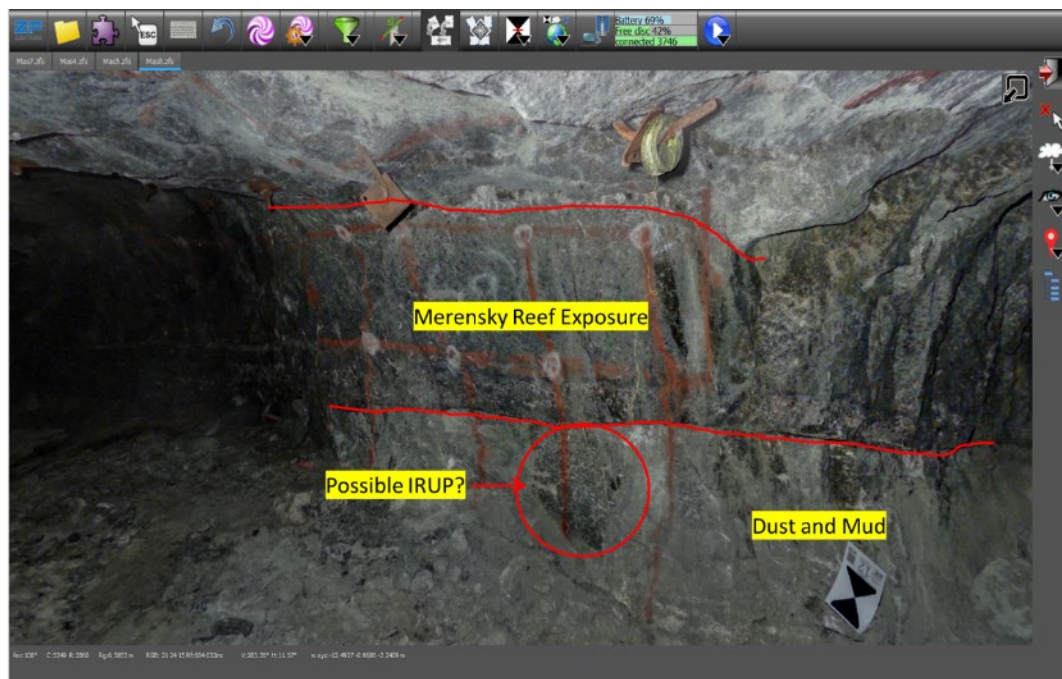


FIG 9 – Merensky exposure on Pillar with potential IRUP Z+F Scout software (Source Grobler, 2020).

A scan of the Eastern side of the pillar and the face of the Main Board NW1 Panel indicated a reef displacement through faulting and associated jointing or a succession of joints as indicated in the figure below.

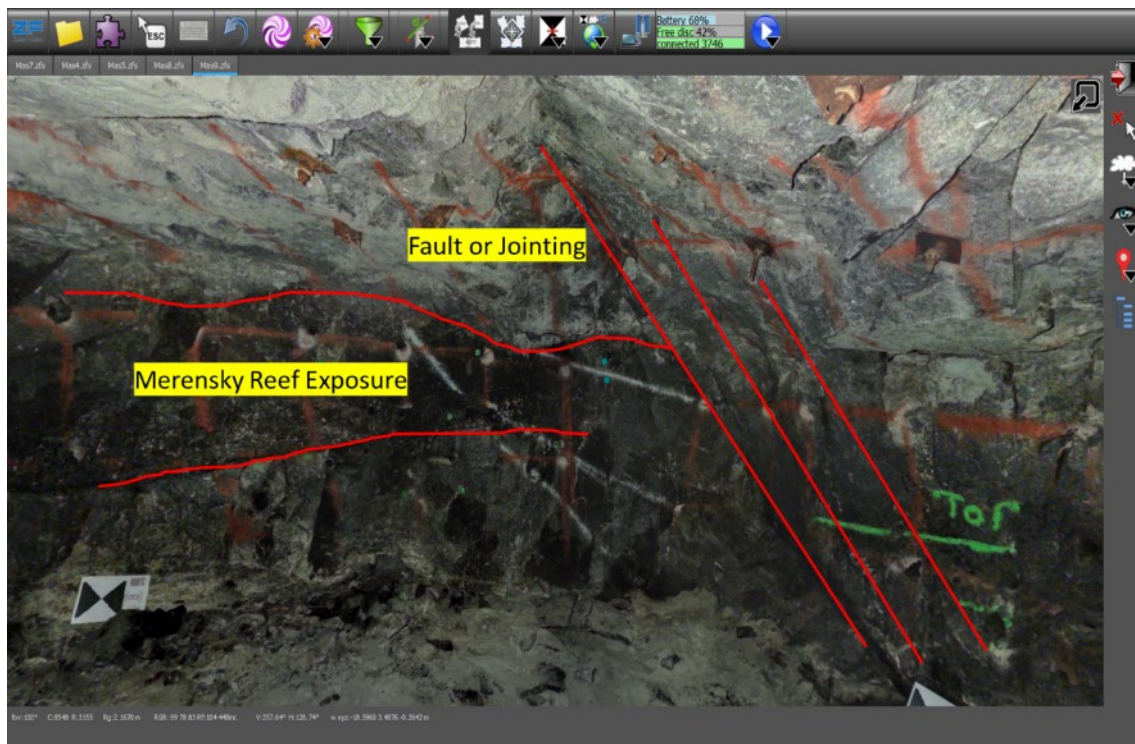


FIG 10 – The Eastern side of the pillar indicating a series of joints and possible fault. Z+F Scout software (Source Grobler, 2020).

The Main Board NW1 Panel face exposure of the panel could not clearly identify the Merensky exposure. The jointing structures can be clearly seen in the scan below:

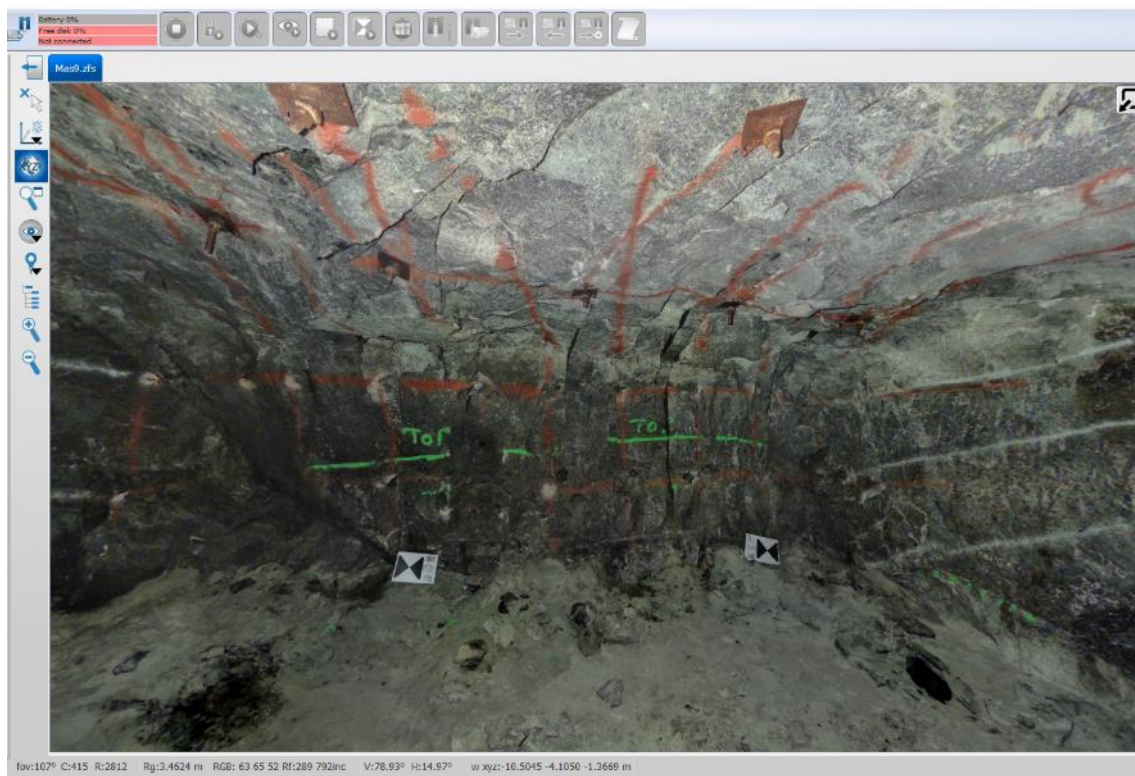


FIG 11 – Main Board NW1 Panel face exposure. Z+F Scout software (Source Grobler, 2020).

The scanning campaign at the gold mine allowed a visual comparison between the mine plan and raw point cloud using an overlay but not to scale is represented in the figure below. The accumulation

of broken ore on the footwall partially obscured the VCR exposure that was barely visible on the righthand side of the reef-drive as indicated in this section of the scan.



FIG 12 – VCR exposed in the footwall of the excavation.

The fault intersection can be seen and measured; the orientation shows the ‘outside skin’ of the point cloud looking into the reef drive. It is often found that data becomes easier distinguishable when looking ‘into the point cloud’.

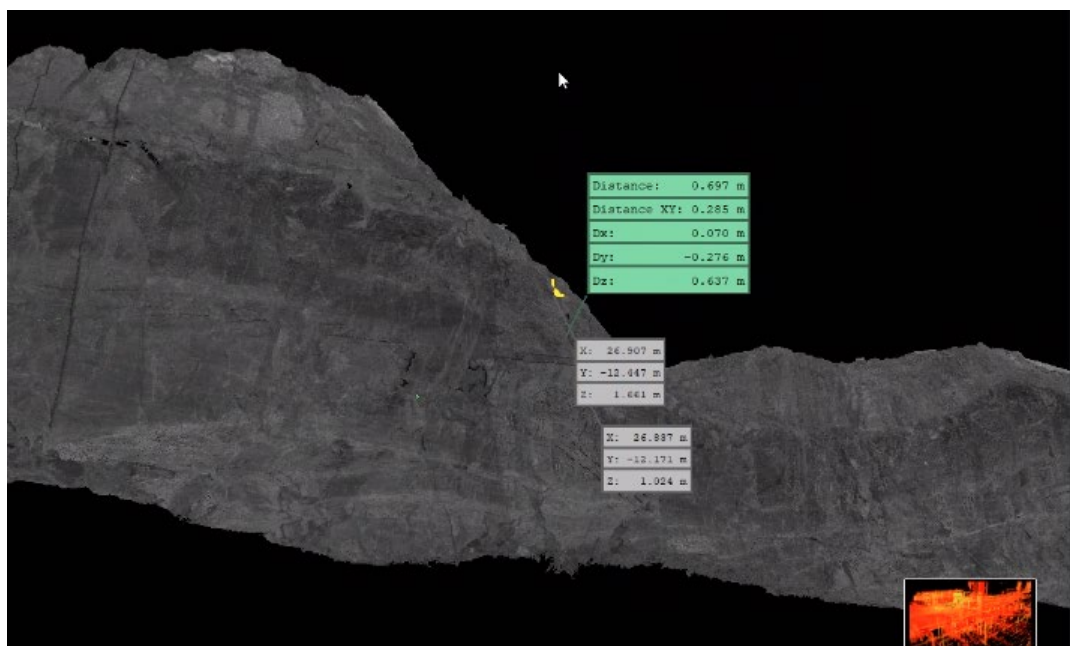


FIG 13 – External view of the pointcloud identifying a fault in the reef.

The mapping done by the geologist using conventional photography can identify the fault clearly but the photograph cannot be used for measurements or digitising the data.

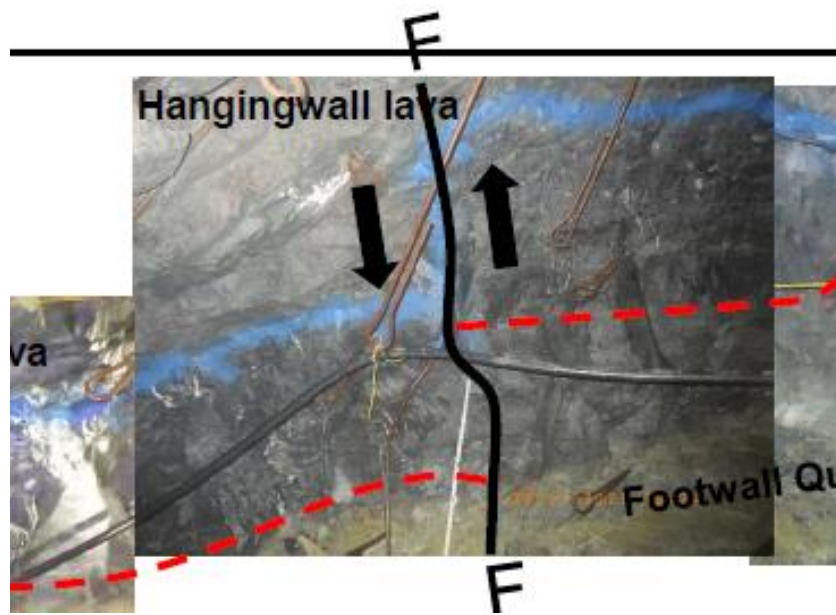


FIG 14 – Geologists photograph of the fault.

The reef could be digitised and tracked using CAD software. The two lines indicate the Top Reef contact of the VCR and the bottom line represents the lower mineralised zone contact.

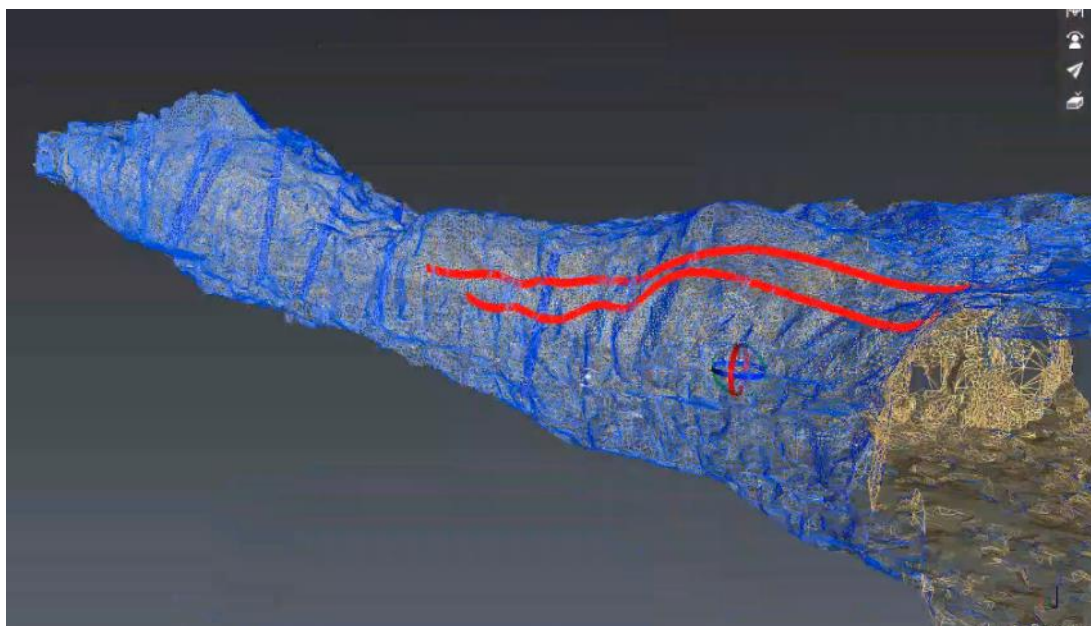


FIG 15 – A CAD digitised reef contact line from the pointcloud.

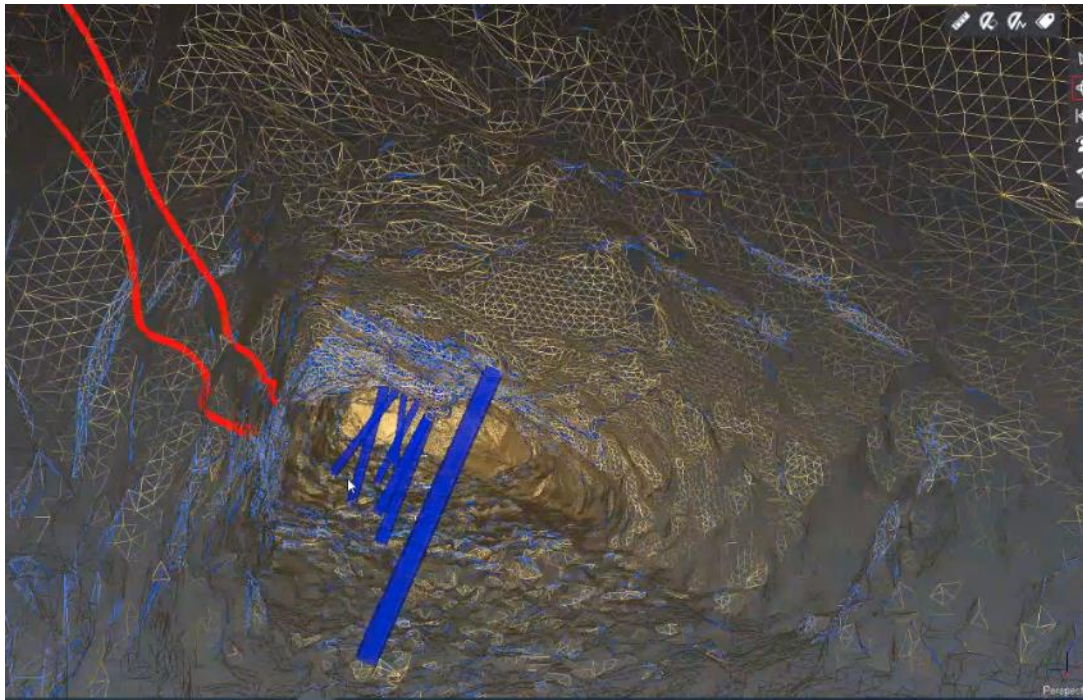


FIG 16 – Extruded support from the pointcloud.

The support could be modelled and extracted both to indicate the actual position and orientation of the support and to extrude the actual shape of the support which can potentially be compared for deformation. Similarly, the excavation dimensions can be used to determine over-and underbreak as well as determining scaling, cleaning of accumulations and adherence to the mine layout.

From the results it was concluded that it was not possible to distinguish a definite residual thermal signature of the rock strata from the scans generated.

The final test was to use a portable SLAM technology LIDAR scanner. Two different OEM's were approached to conduct a scan of the same pillar. The SLAM technology linked the scans seamlessly and presented a great scan of the void. The detail in the scan, based on the method of scanning and the lighting conditions was not acceptable for geological scanning. It is assumed that the scanning method used in these portable slam scanners are limited, at the moment, to surface applications where lighting and atmospheric conditions have a reduced effect on the scan results

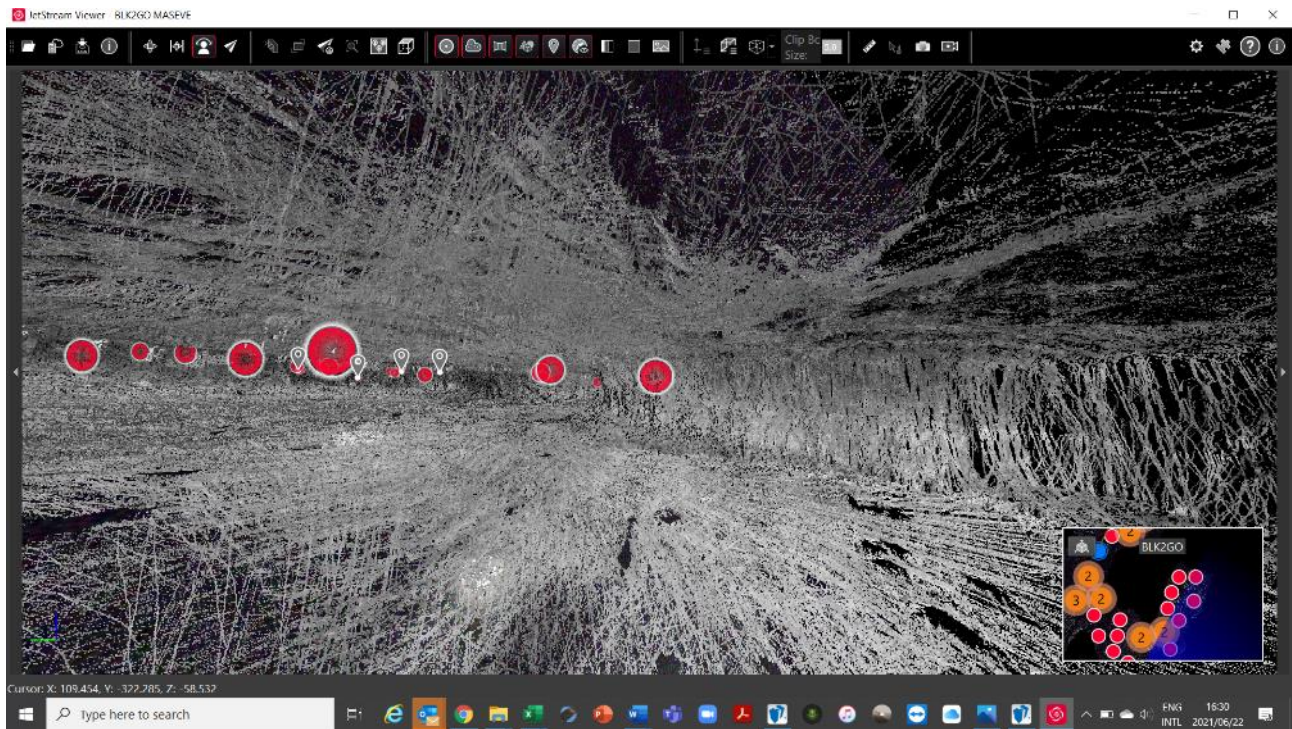


FIG 17 – SLAM technology generated pointcloud.

The ability of these scanners to 'geotag' features by adding a photograph and comments to certain positions in the scan can be used to mark points of interest but it is uncertain if these geotags can be used to digitise features from the geotag.

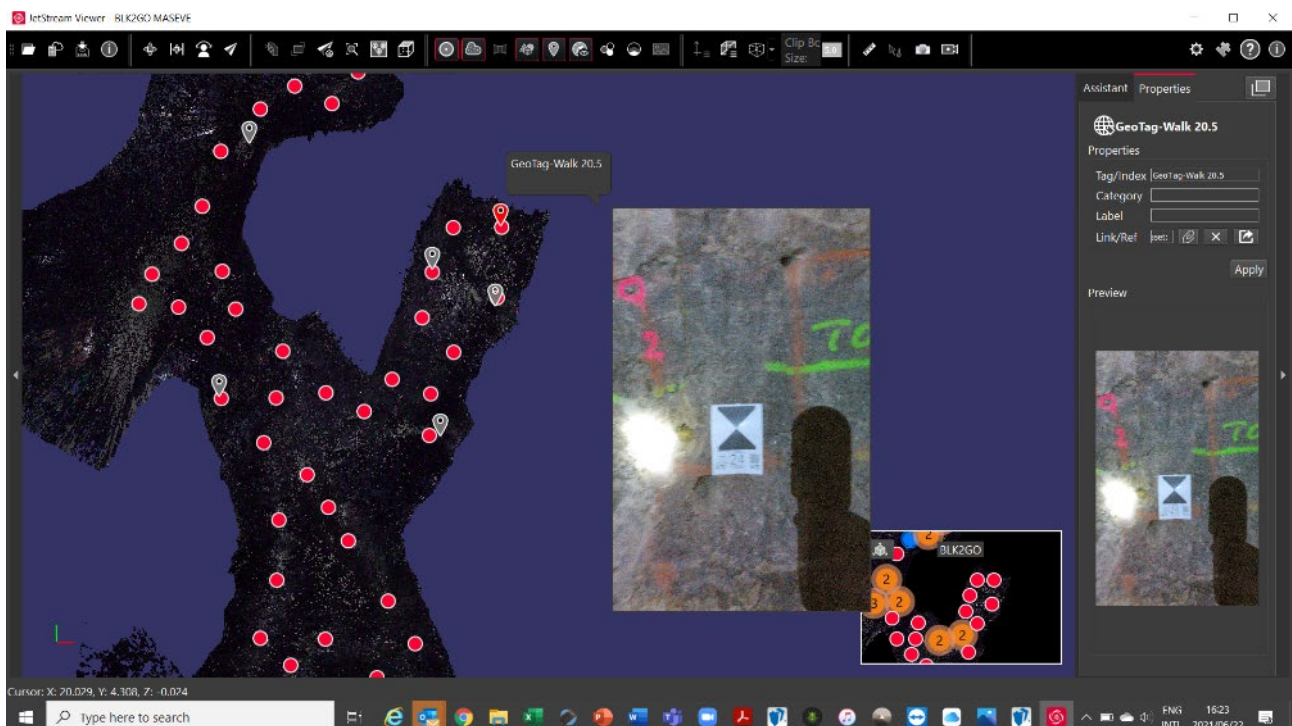


FIG 18 – Georeferenced photograph points in the plan view of the pointcloud.

CALCULATION OF LINES OF INTERSECTION AND REEF PLANES

The visual identification of reef exposures was facilitated by the HDS images captured with the laser scan. From the point cloud scan, points of tope reef intersection was identified and coordinates (y,x,z) could be obtained. This was done for multiple reef exposures in the panels as well as positions where the fault and dyke could be observed.

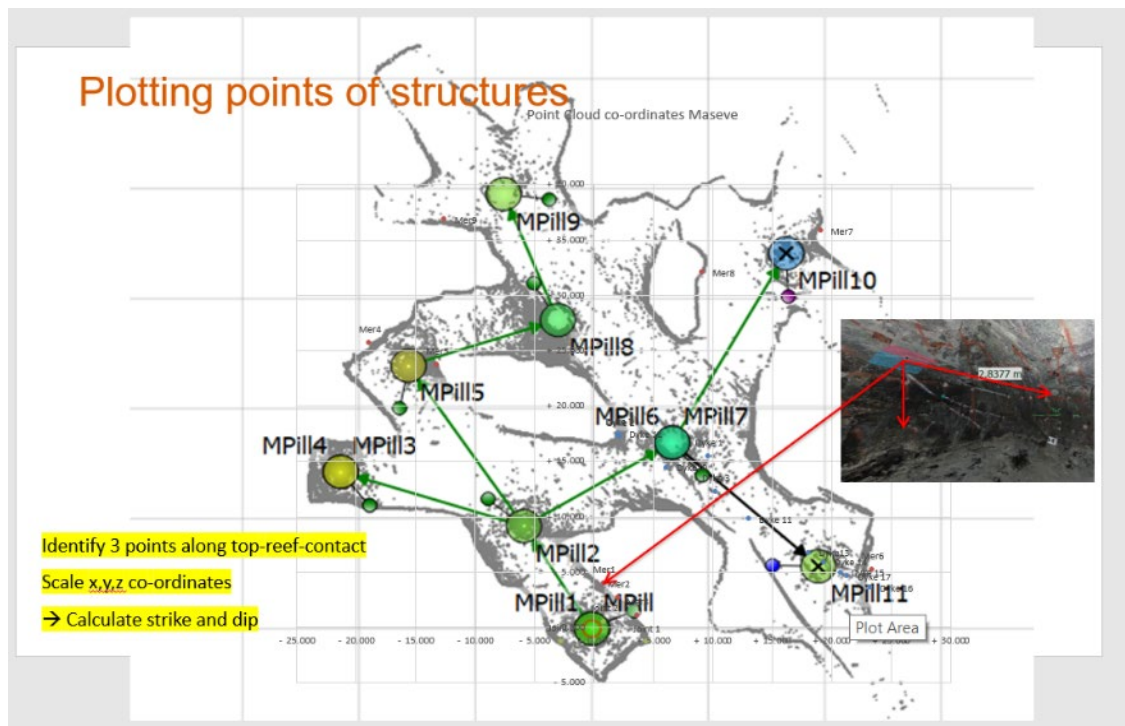


FIG 19 – Manually identified points of reef intersection for strike and dip calculation.

In order to perform a Strike and Dip calculation, three points on the top reef contact has to be selected. Using a basic ‘three-pointer’ calculation, the strike and dip of the structure can be calculated directly from the laser pointcloud.

TABLE 1

Tabulation of scaled coordinates from the pointcloud.

Scaled	Y Co-ordinates	X Co-ordinates	Z Co-ordinate
Joint 1	+ 4.420	- 1.367	- 0.963
Joint 2	+ 0.889	+ 0.457	+ 1.138
Joint 3	- 2.752	- 1.309	- 0.371
Mer1	+ 0.827	+ 3.897	- 0.518
Mer2	+ 2.064	+ 2.634	- 0.466
Mer3	+ 3.639	+ 1.027	- 0.258
Mer4	- 18.864	+ 25.607	- 1.564
Mer5	- 13.198	+ 23.650	- 1.116
Mer6	+ 23.412	+ 5.132	- 0.531
Mer7	+ 19.072	+ 35.769	+ 2.205
Mer8	+ 9.112	+ 32.002	+ 1.227
Mer9	- 12.567	+ 36.824	- 0.538
Dyke 1	+ 9.653	+ 15.428	+ 3.682
Dyke 2	+ 2.217	+ 17.208	+ 1.823
Dyke 3	+ 10.243	+ 12.182	+ 3.479
Dyke 4	+ 20.796	- 6.801	- 0.597
Dyke 5	+ 23.363	- 8.280	+ 2.393
Dyke 6	+ 25.742	- 9.788	+ 2.602
Dyke 7	+ 2.113	+ 17.246	+ 1.520
Dyke10	+ 6.101	+ 14.391	+ 3.724
Dyke 11	+ 13.036	+ 9.741	+ 2.632
Dyke 12	+ 2.133	+ 17.436	+ 0.713
Dyke13	+ 18.068	+ 6.708	+ 1.485
Dyke 14	+ 19.347	+ 5.867	+ 1.213
Dyke 15	+ 20.802	+ 4.909	+ 1.341
Dyke 16	+ 23.201	+ 3.537	- 1.769
Dyke 17	+ 21.338	+ 4.563	+ 1.395

The method used required the identification of three geometrically spaced points to perform the calculation. The method of calculation of strike and dip requires the following steps (Ritson, 1989, pp 234–298; van Zyl, 1984, pp 150–186):

1. Determine the highest elevated point of the three identified points and determine the shallowest and deepest reef elevations.
2. Construct a triangle between the three borehole positions.
3. Calculate a Join to determine the directions (α_1 and α_2) and horizontal distances (HD1 and HD2) from the highest point to the two lower points.
4. Calculate the elevation difference between the highest point and the two lower points.
5. Using the Vertical distances (VD1 and VD2) and horizontal distances (HD1 and HD2) between the highest point and the two lower points, calculate the two minor dips (d°_1 and d°_2).
6. By constructing a line from the middle point to intersect the triangle at a point on the same elevation as the second highest elevation point on the longer side, a strike line (of same elevation) can be constructed.
7. The Major dip (D°) direction is perpendicular to strike direction.
8. Calculate the Major Dip (D°) using the formula:

$$\sin H^{\circ} = \frac{\tan d^{\circ}}{\tan D^{\circ}}$$

$$\cos x^{\circ} = \frac{\tan d^{\circ}}{\tan D^{\circ}}$$

where:

d° is the Minor dip

D° is the Major dip

H° is angle between STRIKE and Minor dip on PLAN

x° is angle between the MAJOR DIP and Minor dip on PLAN

and Strike direction of an inclined plane is the direction of a horizontal line between two points of the same elevation on that plane (Storror, 1987).

A total of 26 calculations was performed from the scaled positions. The Merensky reef exposure calculations indicated a Major Dip D° of 5.5 degrees with a standard deviation of 6 minutes, when compared to the accuracy achieved by compass and clinorules, the order of achievable accuracy is significantly improved.

TABLE 2

Tabulation of results of Merensky strike and dip from pointcloud.

Merensky Intersections	Major Dip (D°)	Strike Bearing
734	005:29:29.4	341:34:55.8
725	005:30:11.4	339:04:04.7
715	005:30:11.0	339:28:12.6
154	005:32:56.0	339:20:38.5
453	005:19:18.6	342:24:18.9
843	005:35:05.8	341:09:08.4
839	005:23:12.6	339:58:35.8
958	005:37:32.4	336:19:30.8
Average Merensky	005:29:44.6	339:54:55.7
St Dev	000:05:59.7	001:52:34.7

The Dyke exposure calculations indicated a Major Dip D° of 84 degrees with a standard deviation of 2 degrees. This is a high standard deviation but when compared with the accuracy achieved by compass and clinorules (± 5 degrees). The strike direction of the dyke could be determined within a 40'.

TABLE 3

Tabulation of dyke strike and dip from pointcloud.

Dyke Intersections	Major Dip (D°)	Strike Bearing
Dyke 654	087:24:48.8	302:33:43.0
Dyke101112	085:01:11.7	304:29:43.1
Dyke131716	086:59:15.4	303:19:58.1
Dyke 654	087:24:48.8	302:33:43.0
Dyke101217	083:37:25.0	303:38:41.4
Dyke 3715	082:55:24.6	303:22:22.0
Dyke 11216	082:35:07.3	304:09:13.0
Dyke 13717	081:32:00.7	303:27:35.0
Average Dyke	084:41:15.3	303:26:52.3
St Dev	002:21:23.6	000:40:42.7

This method of calculation, although seemingly onerous is easily converted to code which will enable the user to 'automatically' calculate strike and dip. If this calculation can be automated, it can be included in an image recognition software package which will enable an artificial intelligence routine to automatically determine the strike and dip of a feature from a pointcloud.

ADDITIONAL INFORMATION PROVIDED FROM A LIDAR SCAN

The platinum study area was barred and cleaned again to prepare for the installation of electrodes drilled into the pillar for the study of electric resistivity mapping of the pillar. As a result of the cleaning, the geological features could be defined with greater ease. It was therefore decided to scan the area again to update the pointcloud and imagery with the most up to date information and at the same time provide spatially referenced coordinates for the electrode positions. Future studies will attempt to combine pointcloud data with resistivity maps and Ground Penetrating Radar data to provide a representation of geological conditions ahead of the panel.

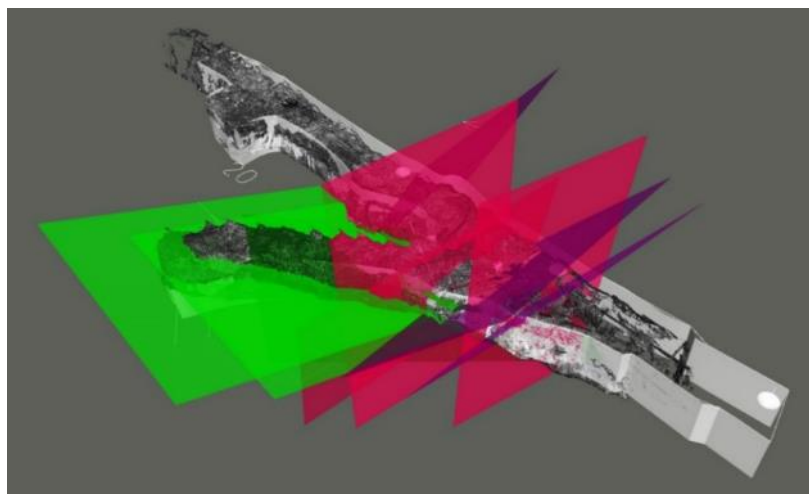


FIG 20 – Structures identified from a pointcloud (Webber-Youngman *et al.*, 2019).

A total of 32 Electrode positions could be identified and coordinated from the point-cloud, refer to Figure 1. A plan of the pillar and electrode positions from the pointcloud. A number of electrodes were marked off but not installed. From the point-cloud it was possible to identify if the electrode was installed or not. It appears that electrodes 12, 24, 25, 26, 27, 28 and 29 was not installed. The electrodes can be identified on the 3D photo and a position established in 3D from the point cloud. A clear distinction between an electrode position and point where the electrode was not installed.

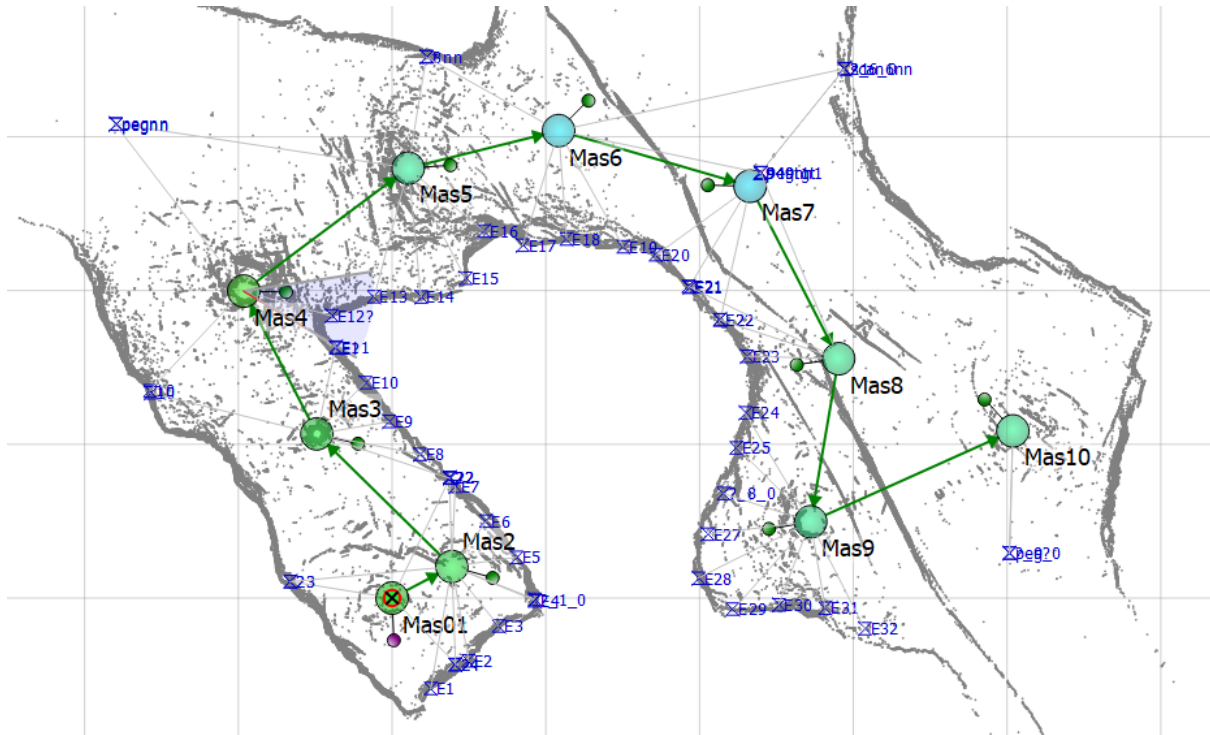


FIG 21 – A plan of the pillar and electrode positions from the pointcloud.

An example of a position where no electrode appears to have been placed, the image on the left is the pointcloud that can be manipulated on a 3D axis to find the exact centre of a target.

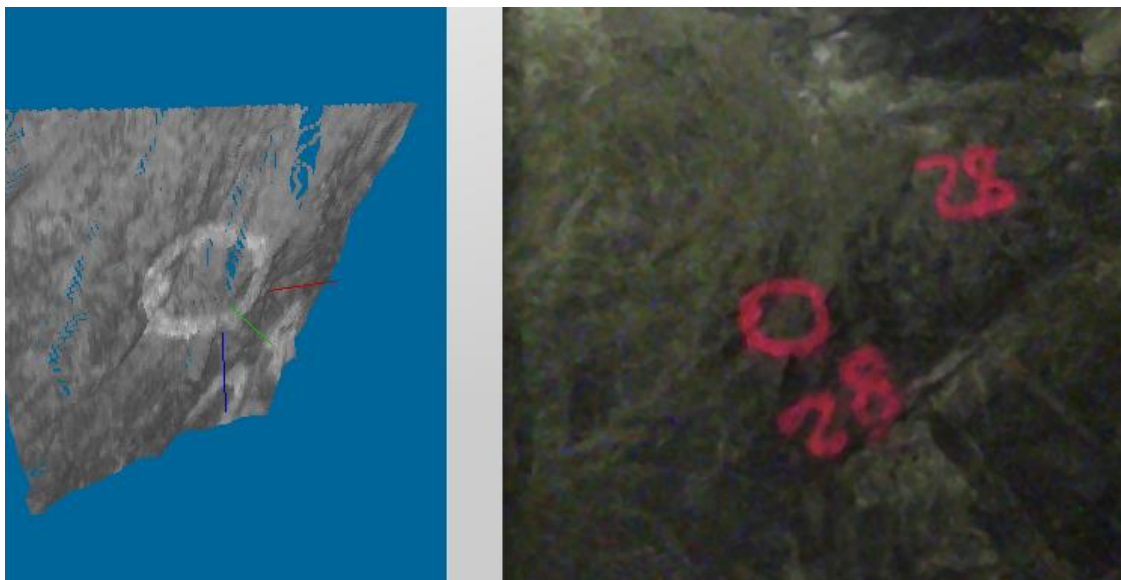


FIG 22 – 3D plot of position where no electrode was placed.

An example of a position where an electrode was placed indicates the extended bolt head of the electrode in the pointcloud.

In previous forensic scans it was possible to identify blast damage from the pointcloud data. In both site investigations it was possible to observe the blast damage 'from the outside' of the excavation. In both cases using different scanners, it is possible to observe 'sockets', blast damage and drill holes from the pointcloud.

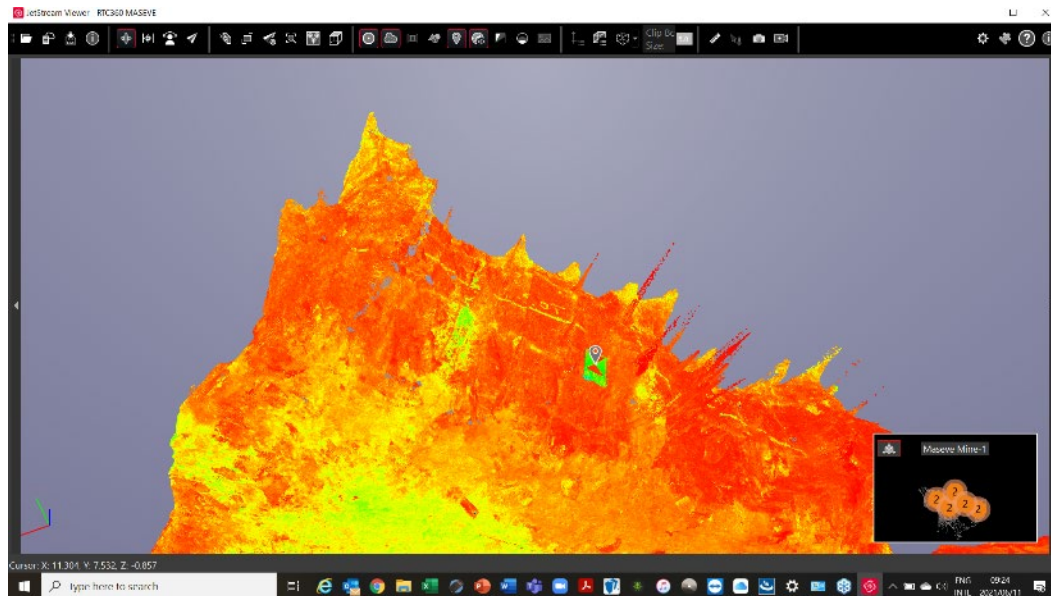


FIG 23 – Pointcloud indicating sockets and blast damage.

LIDAR WORKFLOW

A geological LIDAR workflow requires a survey planning, data collection, post-processing and Interpretation that will inform the geological model. Auto-tracking or the tracing of geological features are common in seismic data sets. In order to determine dip and strike of a reef horizon can be determined if two apparent dips are visible in the data. If three points can be identified the dip and azimuth can be calculated. TLS will produce a pointcloud, these points can be connected to form a triangulated irregular network (TIN) or 'mesh' that can be texture mapped using the photographs taken by the system. Using a mesh, the data can be filtered and simplified, making the data easier to work with (Hodgetts, 2009).

LIDAR scans are normally completed in a localised survey system with a random point of origin. These scans once completed can be geo-referenced and orientated to the mine survey system through identifying survey stations with known coordinates in the scan. A basic coordinate transformation is available in the software but a simple Helmert coordinate transformation can be made for individual points of interest such as electrode positions.

A Helmert transformation was performed on the local coordinates obtained from the lidar scan. A Helmert transformation is a seven-parameter transformation using rotation, scaling and translation to convert coordinates from a local system to the WGS84 Local Origin system of the mine (Watson, 2006).

$$"new" \Delta y = \lambda * [(old \Delta y * \cos(Swing)) + (old \Delta x * \sin(Swing))]$$

$$"new" \Delta x = \lambda * [(old \Delta x * \cos(Swing)) - (old \Delta y * \sin(Swing))]$$

where λ is the scale factor calculated from the horizontal distance between known points on the old and the new system.

CONCLUSIONS

Geological mapping of structures is important to the development of a detailed orebody model. Major geological features are required to be measured and plotted on prescribed plans. Standard geological mapping of structures has not changed much and still makes use of basic measuring equipment such as clinorules, tapes and compasses.

The use of LIDAR and photogrammetry to map structure has been adopted in surface structural mapping and monitoring and is seeing more acceptance in surface mining operations. In some instances, lithology can be mapped through image recognition and semi-automated processes. The generation of a coloured point-cloud can capture a high-definition data set that can add value to a number of technical service workflows. Although TLS methods are becoming widely acceptable the workflow and automisation of mapping from a point cloud has not reached its full potential. From the literature search it has become evident that little to no underground application of geological mapping and structure recognition has been developed to a commercial application. The ease of laser scanning and the reduction in cost of these systems have made it possible for most mining operations to purchase a system. The increased complexity of pointcloud registration and data manipulation from the TLS to a CAD system is still a challenge. It is estimated that data verification and completion require 3 times as much time as the time taken to perform the scan. The benefit and detail of data captured offsets these challenges and makes the adoption of laserscanning for non-topographical applications a feasible alternative to conventional geological mapping.

Some advantages of Laser Scanning for geological mapping

- The laserscan does not require light to perform the mapping and the addition of the LED light provides more light on the underground mine face than can be provided by a standard mining cap-lamp and handheld illumination.
- TLS can scan in zero-light conditions and map based on 'reflectivity' of material. With a LED light attachment, high definition (HD) photographs can supplement the imagery.
- The TLS distance range enables the remote scanning and photography of features that are too high or inaccessible to an observer to map accurately. Safety implication for working at heights.
- Remote scanning removes the observer from contact with the face. Some mine standards require the observer (geologist) to remain within 0.5 m of the last support. This feature has safety implications by removing the observer from high-risk areas.
- Laserscan and HD image records the entire face including detail that may at the time have been missed by the observer.
- The laser pointcloud provides a credible, measurable and repeatable record or 'snapshot' of the face created at the time of the scan.
- Thermal imaging provides a thermal map of *in situ* rock temperatures with a potential application in identifying stress fractures and loose rocks.
- The 'thermal radiation emitted' by structures and minerals in the rock may be able to be detected and mapped. This feature has the potential to be correlated to specific lithology or structures.
- Laser Scanning technology provides potential in mapping and measuring dimensions of sedimentological aspects of the reef for deposition studies and provides the potential for image recognition to identify reef bands from pebble size and distribution.
- Laser scanning can map faces with sufficient detail to free the geologist and rock-engineer up to concentrate on faces with structures and non-conformal geology for detailed investigation.
- Laser scanning provides a visual record of the geology in areas where mud, dust, services (pipes and cables), support, permanent mesh or concrete support obscures the geology.
- Laser scanning technology can be used to scan core in core trays to provide a high quality colour record that can be measured for logging purposes.

From the results it was concluded that it was not possible to distinguish a definite residual thermal signature of the rock strata from the scans generated. The field tests under extreme environmental conditions highlighted the need for sufficient 'acclimatisation' of lidar equipment to the ambient conditions before starting scanning operations. Some instruments may not indicate that conditions are not ideal and as a result can corrupt scanning data completely.

The selection of LIDAR equipment will depend on individual site requirements and user requirements. The outcomes and intended end-user application must be weighed against the range of the instrument and accuracy that is currently entering the market. The time taken for a scan and the weight of the instrument will play a bigger role for underground applications whereas range and accuracy will have a higher priority than weight for surface mining applications. All the equipment tested was robust enough to handle standard underground conditions. It is critical to understand the difference between survey grade lidar applications and less accurate systems. For mining applications it is strongly recommended that only survey grade lidar systems be used.

REFERENCES

- Baffoe, P, Boah, F N and Afam, M, 2018. Mapping 3D Geological Structures and Predicting the Kinematics of the Pitwalls Using Photogrammetric Techniques: A Case Study, *American Journal of Engineering Research (AJER) Volume-7, Issue-7*, pp. 64–76.
- Bell, F G, 2006. *Engineering Geology, 2nd Edition*. Butterworth-Heinemann.
- Benton, D, Chambers, A, Raffaldi, M, Finley, S and Powers, M, 2016. Close-Range Photogrammetry in Underground Mining Ground Control. *Remote Sensing System Engineering VI*.
- Berkman, D A, 2001. *Field Geologists' Manual*, Monograph 9, Fourth Edition (The Australasian Institute of Mining and Metallurgy: Melbourne).
- Brunton, 2017. *The ABC's of Compass and Map*, Brunton.
- Buczek, M, Paszek, M and Szafarczyk, A, 2018. Application of Laser Scanning for Creating Geological Documentation. *E3S Web of Conferences 35, 04001*.
- Buyer, A and Schubert, W, 2017. *Calculation the Spacing of Discontinuities from 3D Point Clouds*. s.l, s.n, pp 270–278.
- Chmelina, K, Molina, C A, Contreras Delgado, J and Zobl, F, 2010. UCIS Underground Construction Information System. In: *Technology innovation in underground construction*. Balkema, pp 9–30.
- Coetzee, B C, 1984. The use of photography in controlling grade at the West Rand Consolidated Mines. *Journal of the Institute of Mine Surveyors of South Africa Vol 22 No 8Dec 1984*, pp 113–118.
- Davies, N S, William, J M and Shillito, A P, 2018. A Graphic Method For Depicting Horizontal Direction Data On Vertical Outcrop Photographs, *Journal of Sedimentary Research, 2018, v. 88v. 88*, pp 516–521.
- Davies, R M, 1991. A review of some mining orientated applications of small format photography. *Journal of the Institute of Mine Surveyors of South Africa Mar 1991 Vol 26 No 1*.
- Davis, M D, Wilson, A H and van der Merwe, A J, 2007. The use of density as a stratigraphic and correlative tool for the Bushveld complex, South Africa. *Fifth decennial international conference on mineral exploration*, pp 1193–1197.
- DMR, 2011. *Mine Health and Safety Act No 29 of 1996 Government Gazette 27 May 2011*. Pretoria: The Department of Mineral Resources of South Africa.
- Feng, Q and Röshoff, K, 2015. A Survey of 3D Laser Scanning Techniques for Application to Rock Mechanics and Rock Engineering. In: *The ISRM Suggested Methods for Rock Characterization, Testing and Monitoring: 2007–2014*.
- Fraštia, M, Chlepková, M and Bartoš, P, 2008. Photogrammetric Monitoring of the Stability of Rock Environment. *Journal of the Institute of Mine Surveyors of South Africa Jun 2008, Vol 32 No 10*, pp 742–752.
- Gumede, H and Stacey, T, 2007. Measurement of typical joint characteristics in South African gold mines and the use of these characteristics in the prediction of rock falls. *The Journal of The Southern African Institute of Mining and Metallurgy VOLUME 107*, pp 337.
- Hodgetts, D, 2009. Lidar in the Environmental Sciences: Geological Applications. In: G L Heritage and A R G Large, eds. *Laser Scanning for the Environmental Sciences*. s.l.:Wiley Blackwell, pp 165–177.
- Humair, F, Abellan, A, Carrea, D, Mtasci, B, Epard, J-L and Jaboyedoff, M, 2015. 3D point clouds: Example of a box-fold in the Swiss Jura Mountains, November 2015. *European Journal of Remote Sensing 48*., DOI: 10.5721/EuJRS20154831, pp 541–568.
- Jackson, J O, 1946. *Mine Valuation (Rand Practice)*. Johannesburg: Louis Gordon.
- Jones, M, 2015. Thermophysical properties of rocks from the bushveld complex. *The Journal of the South African Institute of Mining and Metallurgy, Vol 115*, pp 153–160.
- Lurie, J, 2013. *South African Geology for Mining, Metallurgical, Hydrological and Civil Engineering, 11th Revised Edition*. s.l.:Lupon Publishing.
- Metcalfe, J E, 1951. *A Mining Engineer's Survey manual*. London: Electrical Press.

- Monsalve, J J, Baggett, J, Bishop, R and Ripepi, N, 2019. Application of laser scanning for rock mass characterization and discrete fracture network generation in an underground limestone mine. *International Journal of Mining Science and Technology*.
- Moulin, P and Vallon, F, 2010. Real-time geological mapping of the front face. In: *Technology innovation in underground construction*. s.l.:Balkema, pp 225–237.
- Pienaar, M, nd. *Underground Structural Mapping*, s.l.: s.n.
- Riquelme, A, Abellán, A and Roberto, T, 2015. Discontinuity spacing analysis in rock masses using 3D point clouds, *Engineering Geology* (2015), doi: 10.1016/j.enggeo.2015.06.00.
- Ritson, T P, 1989. *Surveying for Mine Surveyors*. Johannesburg: Institute of Mine Surveyors of South Africa.
- Russell, T and Stacey, T, 2019. Using laser scanner face mapping to improve geotechnical data confidence at Sishen mine. *Journal of South African Institute of Mining and Metallurgy Vol.119 n.1*.
- Rutland, R, 1969. Graphic determination of slope and of Dip and strike. *Photogrammetric Engineering*, pp 178–184.
- Slob, S, Hack, H, Feng, Q, Roshoff, K and Turner, A 2007. Fracture mapping using 3D laser scanning techniques. *11th Congress of the International Society for Rock Mechanics*; The second half century of rock mechanics, Volume: 1.
- Storrar, C D, 1987. *South African Mine Valuation*. Johannesburg: Institute of Mine Surveyors of South Africa.
- Strauss, H, 2019. *Stereographic analysis, Mining Technical Services IVB* s.l.:University of Johannesburg, Department of Mining Engineering and Mine Surveying.
- van Zyl, J T, 1984. *Problems and Solutions for Mine Surveyors*. Johannesburg: Institute of Mine Surveyors of South Africa.
- Watson, G A, 2006. Computing Helmert transformations. *Journal of Computational and Applied Mathematics* 197 (2006), Elsevier Science direct, pp 387–394.
- Webber-Youngman, R, Grobler, H, Gazi, T, Stroh, F and van der Vyver, A, 2019. The impact of forensic laser scanning technology on incident investigations in the mining industry. *The Journal of the South African Institute of Mining and Metallurgy (SAIMM)*, SAIMM Journal Volume 119 No. 10, pp 817–824.
- Williams, H S, 1967. Spatial methods and photogrammetric applications in engineering geology. *Journal of the Institute of Mine Surveyors of South Africa, Dec 1967, Vol 14 No 8*, pp 237–243.
- Wolf, P R, Dewitt, B A and Wilkinson, B E, 2014. *Elements of photogrammetry with applications in GIS 4th Edition*. s.l.:McGraw Hill.
- Zoller and Fröhlich GmbH, nda. Z+F IMAGER® 5010X https://www.zf-laser.com/fileadmin/editor/Datenblaetter/Z_F_IMAGER_5010X_System_Requirements_E_FINAL.pdf.
- Zoller and Fröhlich, ndb. Zoller + Fröhlich GmbH Z+F T-Cam https://www.zf-laser.com/fileadmin/editor/Datenblaetter/Datasheet_TCam_e.pdf.
- Zoller and Fröhlich, ndc. Zoller + Fröhlich GmbH Z+F SmartLight https://www.zf-laser.com/fileadmin/editor/Datenblaetter/DataSheet_SmartLight_E.pdf.

Using machine learning and novel algorithms to predict muck pile shape and engineer a perfect blast

O Radzhabov¹ and B Gyngell²

1. Senior Computer Vision Engineer, Strayos Inc. Email: oradzhabov@strayos.com

2. COO, Strayos Inc. Email: brad.gyngell@strayos.com

ABSTRACT

Predicting the distribution of the volume of blasted rock mass in the surface prior to blasting itself is an extremely important and difficult task in surface mining, including the features of the interaction of various properties of rock mass and explosives materials, local geology, the initial distribution of explosive mass, time intervals between explosions, etc. Because the speed of the processes during the explosion is quite high, it is extremely difficult to control the explosion process in the real time. At the moment, the most effective approach is to simulate physics processes and determine all the initial parameters until the time of blasting. It is hard to overestimate the value of predicting the movement of blown up volume and includes saving on the further stages of mining operations, as well as minimising the cost of preparatory operations before an explosion.

Based on previous experience from the strength of materials and mechanics, as well as utilising statistics and an engineering approach, a numerical model was developed for simulating the volume distribution of blasted rock mass over the surface and caused by a series of explosions located in different space areas occurred at different time moments.

Using the strength of materials allowed to take into account the strength characteristics of destructible material of rock mass. Mechanics equations made it possible to establish the relationship between the geometric and energy characteristics of the discrete system, thereby determining the initial particle velocities after the destruction of the whole mass during a single explosion, as well as the trajectory of these particles.

The implemented model combines the simplicity of direct methods to depriving of time-consuming iterative algorithms with a time step and contains the necessary equations that satisfy the conservation of energy requirements to provide the natural results. Thus, we were able to implement an extremely fast approach for obtaining the physical modelling results of the blasted volume distribution. The high simulation speed allows to use this approach not only to predict the results of the explosion, but also opens up the possibility of using it in more complex algorithms where thousands or millions of numerical experiments are needed to perform reverse engineering tasks.

One of the priority areas for the further development of this model can be using of machine learning methods to tune empirical parameters for an additional improvement the accuracy, as well as using of multi-criteria optimisation to implement an automatic solution for searching the optimal source parameter values based on given results.

INTRODUCTION

The numerical simulation algorithm presented in this work makes it possible to obtain the volume distribution of the blasted material along the vertical plane directed toward from the blasting site. The algorithm makes it possible to take into account the basic physical properties of the destructible material, the energy characteristics of the explosive, the geometric and mass-volume characteristics, as well as the time intervals between individual explosions.

The algorithm is iterative, each iteration of which takes into account a separate new explosion. So if the initial data includes five drill holes located backward from the blasting site, with four timing delays set between corresponding blasts, the algorithm will perform five iterations.

The structure of a separate iteration of the algorithm includes two main components:

1. explosion impact
2. ballistics.

Which allow one to take into account the mechanics of fracture of a solid body and the kinematics of motion of individual particles in a gravitational field.

The specified algorithm components are direct-method in closed form, and do not contain iterations for individual particles. This feature makes the algorithm very efficient in terms of speed of numerical simulation.

SINGLE EXPLOSION SIMULATION DESCRIPTION

To simulate single explosion algorithm uses one iteration, which includes explosion impact and particles flight kinematic (ballistics).

Single explosion algorithm consists of two structural parts that separate the logic for the purpose of transparency of its understanding and simplicity for possible further improvement.

Below is the general order of the steps of the algorithm:

1. Taking into account the mass-energy characteristics of the explosive, the amount of energy released by the mass of the explosive material is determined.
2. Taking into account the geometric and physical characteristics of the breaking material, the amount of energy required for its destruction is determined.
3. Taking into account the geometric configuration and physical properties of the material, the energy remaining immediately after the destruction of the material is distributed throughout the volume and forms the field of the initial velocities of the particles obtained after the destruction.
4. Taking into account the given field of the initial velocities, the kinematic equations are integrated. As a result, the profile of the final volume distribution of the blasted material is determined.

The first three steps from the list above corresponds to the explosion impact stage. The remaining step refers to the ballistics stage.

The indicated steps of the algorithm are presented in linear closed form, without any iterations and that ultimately allows them to be executed as quickly as possible.

Explosion impact

To simplify simulation, Explosion Impact stage – is only step where explosion could take effect to simulation. Here applied energy distributes over crushed mass and put extra velocity to the velocity profile at specific timestamp. Since the speed of sound in the rock mass is much greater than the ballistic velocity here was assumed that shock waves after explosion distributed instantly (Needham, 2018).

The explosion impact uses an energetic approach to determine the amount of energy remained immediately after breaking a mass of material into individual particles and uses the geometric approach to obtain a field of distribution of an additional velocities (Maienschein, 2002).

Explosion energy E_e could be represented as:

$$E_e = m_e \cdot \hat{E}_e$$

where:

m_e = Explosive material mass, kg

\hat{E}_e = Explosive energy per kg, calculated as explosive energy per kg for TNT ($4.184 \cdot 10^6 J$) multiplied by TNT equivalent for particular explosive material

For Ammonium Nitrate/Fuel Oil (ANFO) TNT equivalent equal to 0.74 (Dewey, 2020), and explosive energy per kg will be:

$$\hat{E}_e = 4.184 \cdot 10^6 \cdot 0.74 = 3.1 \cdot 10^6 J$$

Energy E_c required for crashing an entire volume of solid material with specific isotropic properties could be represented as:

$$E_c = \sigma_t \cdot V \cdot C_e$$

where:

σ_t = Solid material Tensile Strength. Values range $3 \cdot 10^6 \dots 22 \cdot 10^6 Pa$

V = Crushing mass volume, m^3

C_e = Empiric Coefficient = 0.15; can take in account undefined effects like viscosity, dissipation, uncertain structure of solid material

Finally to take in account the friction dissipation, which extends the description of used material, remained energy E_r could be represented as:

$$E_r = (E_e - E_c) \cdot (1 - C_d)$$

where:

C_d = Dissipation Coefficient, equal to friction coefficient between materials. For material pair concrete-concrete it equal to 0.8

During obtaining the profile of extra velocity, reflection shock waves effect was utilised to improve the representative capacity of the algorithm as well as simulate the solid wall impermeability.

Figure 1 shows how the reflection waves were utilised to obtain the velocity profile raised by point-explosion impact.

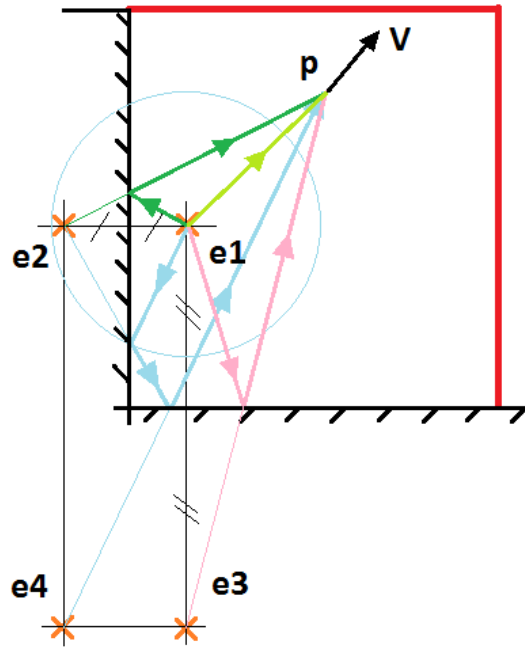


FIG 1 – Shock waves impact to the velocity profile. e_1 – point instance of explosion location. e_2, e_3, e_4 – reflections of explosion locations. p – entire particle.

Summary extra/impact velocity profile v_{imp} integrated wrt applied remained energy E_r which was defined in previous steps could be derived from kinetic energy E_k from following equation:

$$E_r = E_k = \frac{m \cdot v_{imp}^2}{2}$$

where:

m = Crushing mass = $V \cdot \rho$, kg

V = Crushing mass volume, m^3

ρ = Crushing mass density. Values range 2000...6000 $\left[\frac{kg}{m^3}\right]$

Ballistics

Based on the results of explosion impact, where we obtained the profile of extra velocities v_{imp} we can update the current state of the kinematic system represented by following derivative equation:

$$x = x_0 + \dot{x} \cdot t + \frac{\ddot{x} \cdot t^2}{2}$$

where:

x_0 = initial position profile, m

\dot{x} = initial velocity profile v_0 , m/s

\ddot{x} = acceleration $[0.0, -9.81]$, m/s^2

Update includes following steps:

1. Initialise the velocity profile by latest velocity profile from previous explosion and impact of current explosion as:

$$v_0 = v_{-1} + v_{imp}$$

2. Find the time profile as minimum between ballistics purpose and timestamp of the next explosion.

After kinematic system has been updated it should be integrated to obtain the end of state of current iteration.

RESULTS

After the described algorithm has been implemented it was tested on real data sets. For testing purposes pre- and post-blasting terrains from open pit mines have been reconstructed to 3D models. Data was kindly provided by OSP Group.

Exported 3D models of reconstructed models as well as cut-fill elevation analysis allow to obtain real terrain's modification after blasting work.

At the same time existed shot-plan and blasting parameters allow to apply described algorithm to pre-blasting terrain and predict the post-blasting mass distribution by explosion simulation.

Table 1 provides common parameters used in explosion simulation.

TABLE 1
Simulation blasting parameters.

Parameter name	Value
Material density	2300 (kg/m ³)
Tensile strength	2 (MPa)
Explosive energy per mass unit	3.7 (MJ/kg)
Powder factor	0.24 (kg/m ³)
Timing delay between rows	7 (ms)
Stemming in holes	6.5 (m)

By tensile strength it could be assumed that crushed material most probably is soft sandstone or shale. From value of explosive energy per mass unit the relative effectiveness factor can be found which corresponds to ANMAL or Ammonite. Relatively low value of powder factor as well as

minimum timing delay between explosions in drill hole rows allow to assume that explosion's aims are just to crush and not distributing the material over terrain.

Figure 2 shows a 3D models of reconstructed pre/post blasting terrains. Here we can see how rock mass moved after blasting. In this case the blast produced only a small amount of muck pile movement.

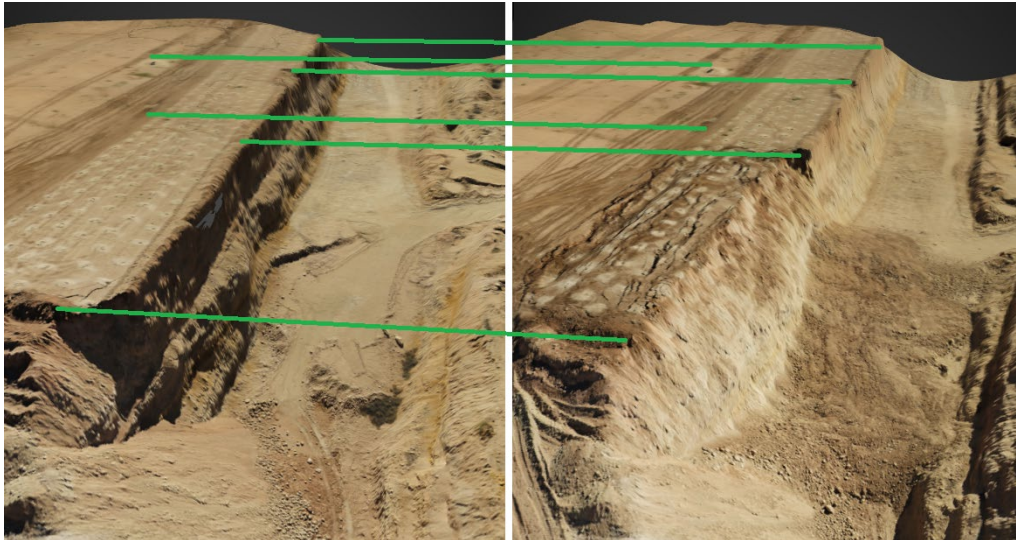


FIG 2 – Reconstructed pre/post blasting terrains. Green lines show matched areas to better find similarities and blasting volume.

Figure 3 shows the results of cut-fill comparison between pre- and post-blasting results. It could be noticed how bench's face lost the volume (blue and green areas) and muck pile (yellow, orange, red) added the material.

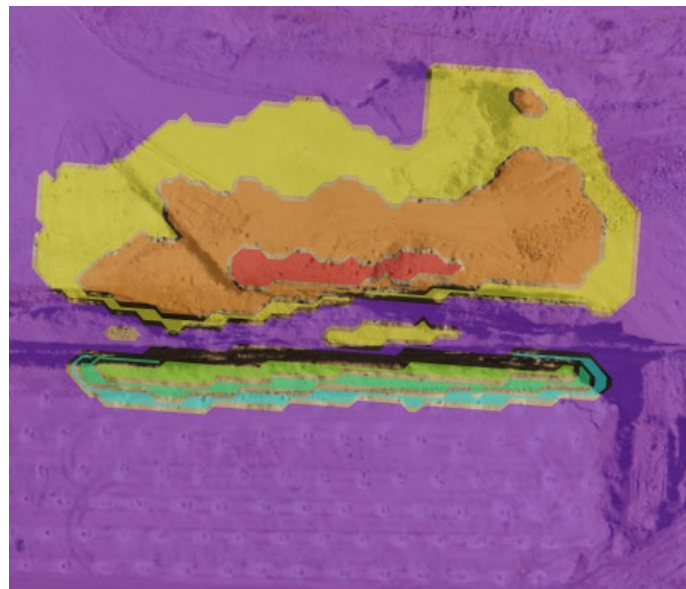


FIG 3 – Orthographic view of elevation comparison between pre- and post-blasting reconstructed models.

Figure 4 shows comparison of real reconstructed post-blasting model and predicted mass distribution on the pre-blasting model. Blue lines correspond to six rows of drill holes.

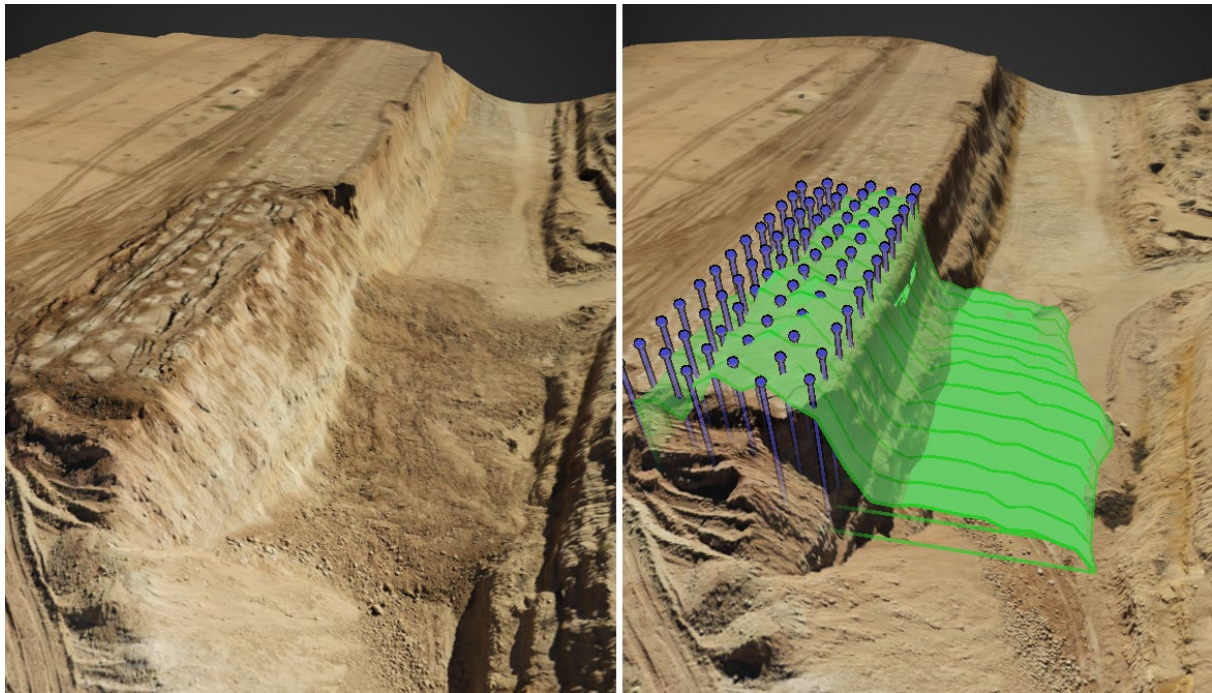


FIG 4 – Comparison of real post-blasting (left image) and explosion simulation results (green surface) on the pre-blast terrain (right image).

It could be noticed that as well as on the post-blast reconstruction the simulation results shows slight whole material moving and matching of the lateral muck pile spread (maximum muck pile distribution distance from the bench's face).

To see the influence of timing delay of explosions between rows of drill holes we simulated the same task but with timing delay increased to 200 (ms).

Figure 5 shows results of two simulation corresponded to original seven (ms) (green surface) and timing delay increased to 200 (ms) (purple surface).

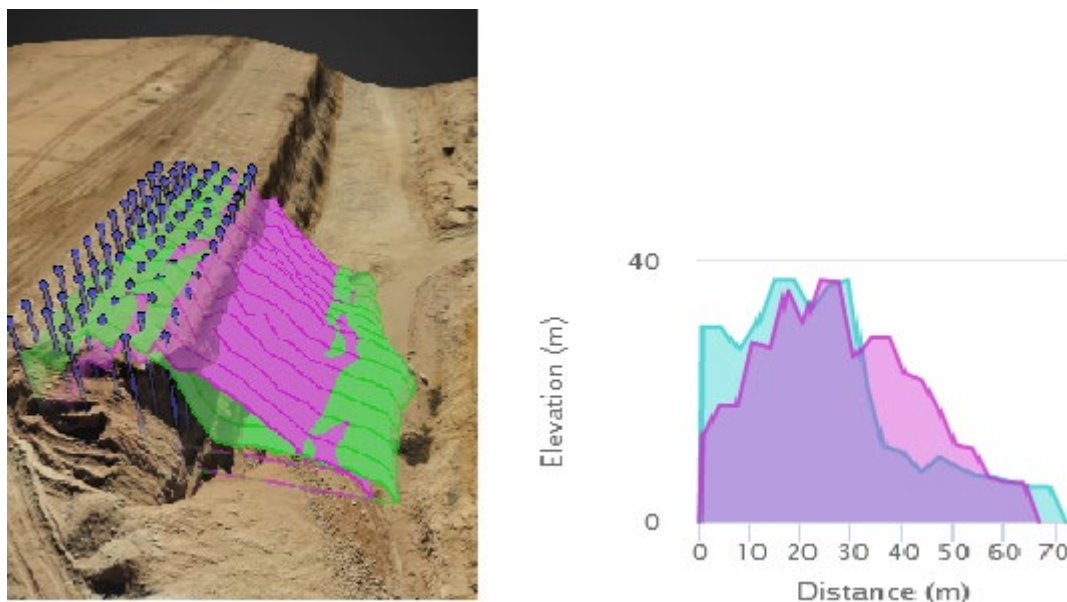


FIG 5 – Influence of timing delay to simulation results.

It could be noticed that increasing the timing delay leads to movement the whole material toward from the front (increasing the throw value) and decreased the lateral muck pile spread (maximum distribution distance from the bench's face).

CONCLUSIONS

In this paper, a numerical simulation algorithm is presented that makes it possible to estimate the distribution of the volume of the exploded material along the vertical plane from the place of the explosion. The algorithm takes into account the basic physical properties of the destructible material, the energy characteristics of the explosive, the geometric and mass-volume characteristics, as well as the time intervals between individual explosions.

The key feature of the algorithm is the fact that it is presented in a closed form and allows calculations to be performed very quickly.

The list of algorithm parameters includes empirical parameters, the value of which is established empirically. In order to improve the accuracy of the results of this algorithm, the values of these parameters can be refined using training data and machine learning technologies.

The main advantage of the developed model is its simplicity. Each element of the model is presented in a linear form, which makes it easy to understand its logic, make adjustments or further enhancements.

The time for execution of the algorithm makes it possible to use it in complex processes of searching for the optimal design of blasting operations and to determine the optimal geometric configuration of the mass and spatial arrangement of explosives, the time between separate explosions.

The disadvantages of the model include the lack of accounting for nonlinear relationships and, as a consequence, the limited accuracy of modelling some processes.

Implementation of this algorithm uses in Strayos platform for predicting of the muck pile contour based on blasting simulation.

ACKNOWLEDGEMENTS

Thanks to Nabil Ratbi from OCP Group (<https://ocpgroup.ma>) for providing materials which allowed us to test the described methods.

REFERENCES

- Dewey, J M, 2020. Studies of the TNT equivalence of propane, propane/oxygen and ANFO. *Shock Waves*, 30, 483–489. <https://doi.org/10.1007/s00193-020-00949-w>
- Maienschein, J L, 2002. Estimating equivalency of explosives through a thermochemical approach, *12th International Detonation Symposium*, 11–16 August 2002.
- Needham, C E, 2018. *Blast Waves*. Shock Wave and High Pressure Phenomena. doi: 10.1007/978-3-319-65382-2

Autonomous vehicles

Autonomous dozers – technical challenges and the benefits to mine operation

E Abbo¹ and D Poller²

1. VP Product and Strategy, Auto-mate, Osborne Park WA 6017.
Email: elad.abbo@auto-mate.net
2. CEO, Auto-mate, Osborne Park WA 6017. Email: daniel.poller@auto-mate.net

INTRODUCTION

Autonomous vehicle solutions are no longer ‘futuristic technologies’. Autonomous technologies have evolved rapidly in different arenas and domains, such as: defence, agriculture, on-road automotive and the mining industry.

The utilisation and benefits of remote-control and tele-remote dozer systems are well recognised in the mining industry and have been operational for a long time. The objective of remote-control and tele-remote operation is to increase safety by removing the human operator from the area of risk and control the operation of the dozer remotely, away from the dozer by line-of-sight or from a control room beyond line-of-sight.

The use of autonomous dozers in operational environments adds new challenges to the technology developers. The autonomous dozer actions require the development of specific autonomous functionality to control the blade and the ripper in addition to the principal requirement of controlling the platform motion.

Working with soil, together with the relationship with the terrain surface, requires a deep understanding of the complex dynamic forces that impact the dozer’s performance during operation. The artificial intelligence driver is required to identify the nature and layout of the terrain surface, to detect positive and negative obstacles, and to plan and manage the platform and its tools accordingly in order to achieve the desired outcome.

In order to perform autonomous dozer work, efficiently, it is a requirement of the autonomous system to meet edge performances in different technical aspects of the system, inter alia:

- Dozer position and angles – Based on a global positioning system, such as DGPS, RTK or simultaneous localisation and mapping algorithm, the autonomous system is required to use an accurate positioning solution. Due to the unique physical structure and dynamic motion of the dozer, it is extremely important to include, in addition, accurate inertial measurement units to measure the precise rates and six degrees of freedom of the dozer’s body.
- Blade relative position – As the blade has its own independent freedom of degrees, it is mandatory to include precise sensors and indicators to measure the accurate rates and angles of the blade position in Pitch, Tilt and Height axes as shown in Figure 1. The measurement technique depends on the dozer type and can be calculated by either integrated sensors in the dozer’s cylinders or by external measurement units.
- Terrain mapping – In order to autonomously plan the dozer’s platform and blade commands in real time, it is required that the autonomous system generates real-time accurate perception mapping around the dozer, and more specifically, in front of the blade. This requirement creates a technical challenge due to the harsh and dusty environment in front of the dozer during operation and the inability to install the sensors on the blade itself. The installation of sensors on the top of the dozer or even of the upper level of the front cylinders creates a visual ‘dead-zone’ in front of the blade because of the lack of line-of-site vision between the sensors and the terrain especially when the blade is in its high position. A possible solution to the real-time perception requirement is to create ‘semi real-time’ mapping by using accumulate mapping. While using an accumulate map technique, the autonomous system saves the real-time mapping in front of the blade and casts it on the ‘dead zone’ area. As presented in Figure 2, this allows the autonomous system to plan the dozer, and blade controls and commands, based on the stored ‘semi real-time’ map.

- Mission plan – Based on the real-time global and relative position of the dozer and the blade, and the precise terrain mapping, the autonomous system calculates the deviation between the actual and desired position of the dozer and blade. The deviation analysis is been calculated in all dimensions and generates motion and blade commands which are transferred to the dozer actuators.
- Real-time control – Given the impact of the terrain, dozer and blade on each other during the dozing work, the autonomous system is required to analyse, calculate and command the dozer and blade motions at frequent rates in order to compensate the gap. For example, if the level of the dozer at the Z axis reduces (due to ground fall), the autonomous system will calculate the opposite corrective action to correct the error.

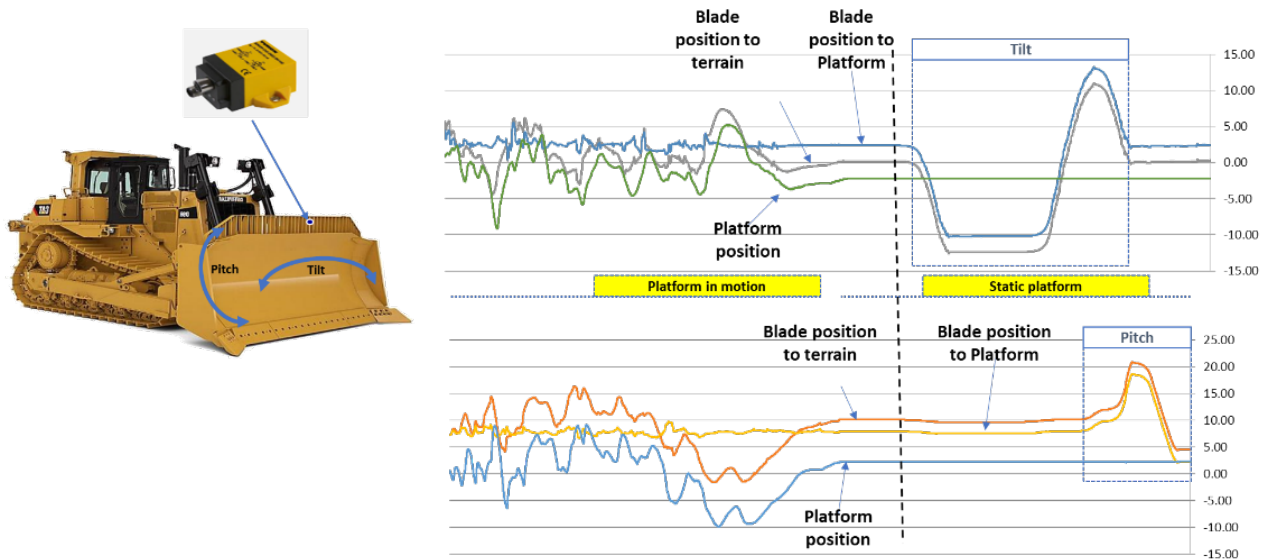


FIG 1 – Actual versus required position analysis.

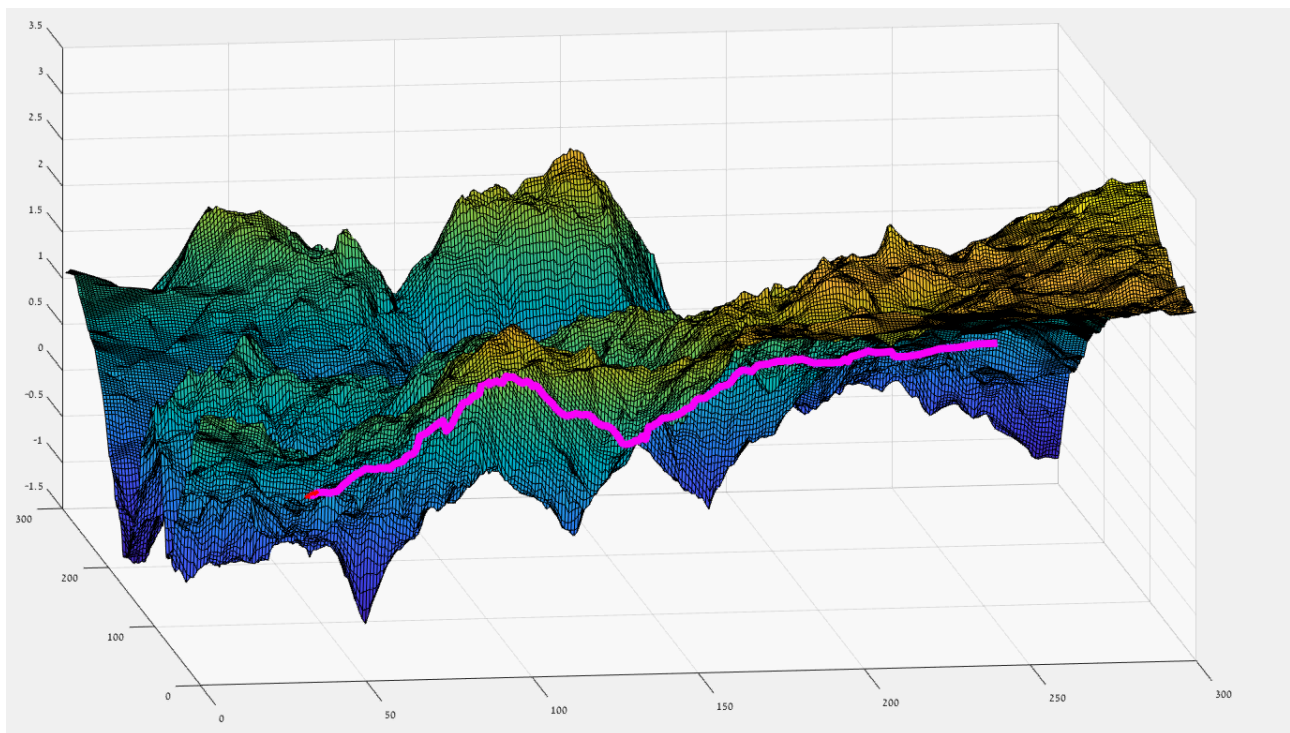


FIG 2 – Blade edge position in reference to Blade trajectory.

The advantages and expected benefits of the autonomous dozer work are varied. In addition to removing drivers from areas of risk, the 360-degree sensor cover also enables the artificial

intelligence driver to detect obstacles that would be in the blind spots of a human driver. It also allows the identification of these objects in harsh environmental conditions. Figures 3 to 5 present the use of simulation for the development, testing and evaluation processes of the autonomous system functionalities in a simulated environment while performing operational dozing activities, such as terrain leveling and bulk push.

Current autonomous technologies enable various dozing activities in the mining environment such as: route clearing, bulk push, stockpile management and rehabilitation. Challenges do exist, but the solution is achievable. The current challenges relate to the ability of the dozers to work very closely to edges and voids that require more accurate position solutions, enhance mapping coverage and faster response times.

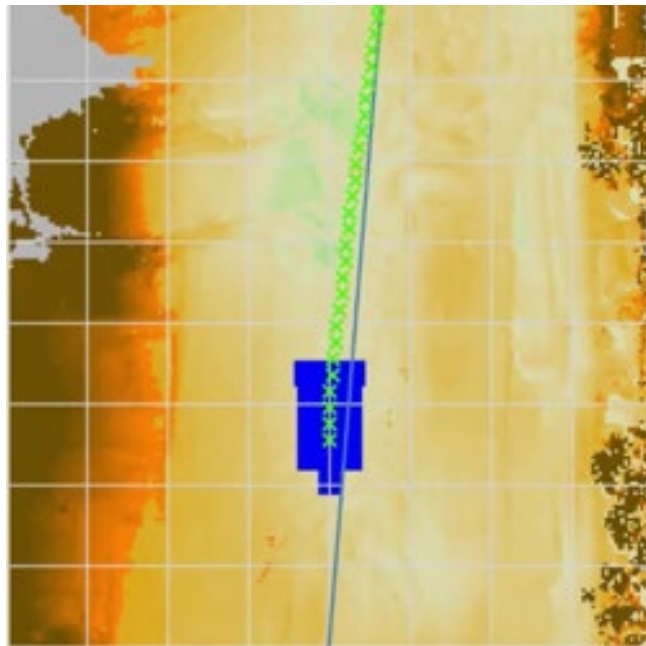


FIG 3 – Autonomous terrain leveling.

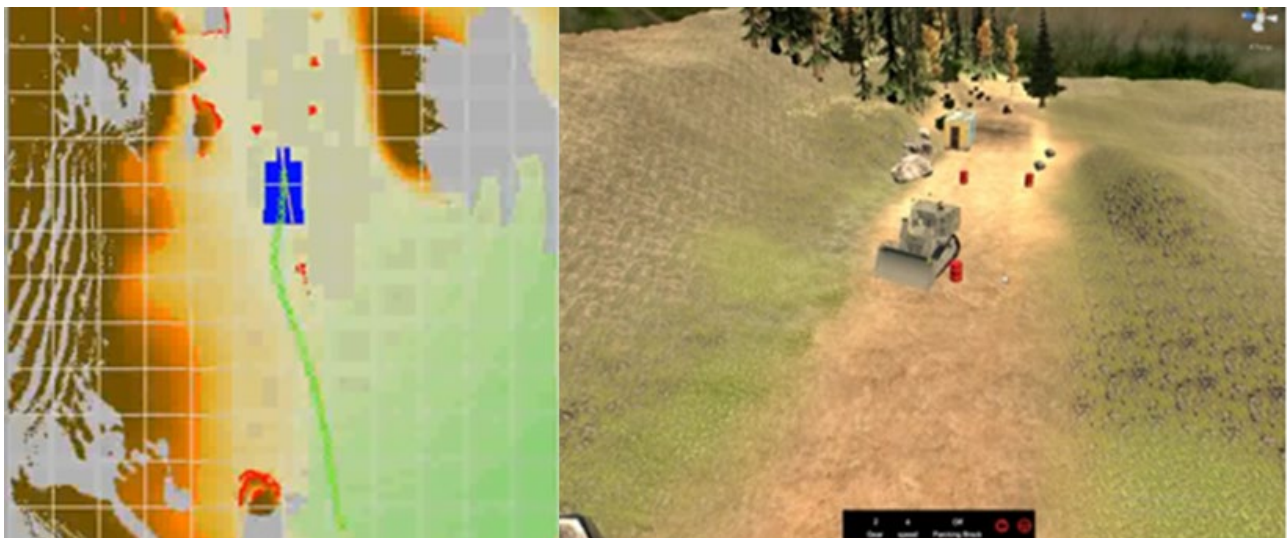


FIG 4 – Obstacle detection and avoidance in simulation.

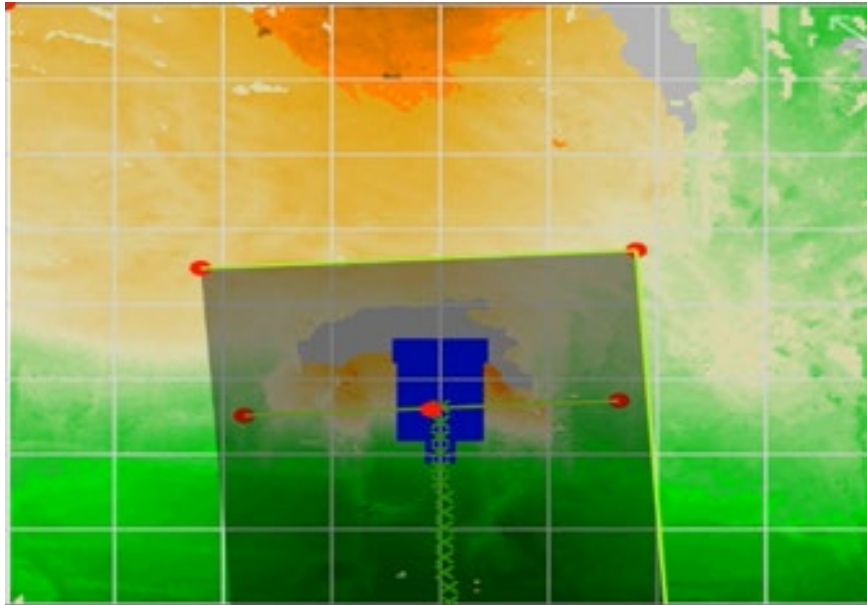


FIG 5 – Autonomous dozer performs Bulk push.

As time progresses the hardware prices will become more accessible to most mining players and consequently, by converting existing dozer fleets, the autonomous dozers' work becomes a reality.

ACKNOWLEDGEMENT

Dror Mizrahi, System engineer, Elta system.

Automation considerations for underground shuttle car haulage

V Androulakis¹, J Sottile², Z Agioutantis³ and S Schafrik⁴

1. PhD, Department of Mining Engineering, University of Kentucky, Lexington KY 40506.
Email: vandroulakis@uky.edu
2. Professor, Department of Mining Engineering, University of Kentucky, Lexington KY 40506.
Email: joseph.sottile@uky.edu
3. Professor and Department Chair, Department of Mining Engineering, University of Kentucky, Lexington KY 40506. Email: zach.agioutantis@uky.edu
4. Associate Professor, Department of Mining Engineering, University of Kentucky, Lexington KY 40506. Email: steven.schafrik@uky.edu

ABSTRACT

As the currently economically viable resources continue to be exploited, the mining industry needs to plan for deeper orebodies and more-challenging mining environments. In the endeavour of the mining operators and equipment manufacturers to prepare for the future, mining technology embraces new advancements in robotics, autonomous vehicles, smart mining systems and other high-tech options. Delegating tasks from humans to autonomous vehicles offers a means to optimise two critical factors in every mine: safety and productivity. The relocation of the operators from the active face to a safer location, such as a control room, can effectively reduce accidents and exposure to unhealthy conditions. The shift to self-driving machines can, not only increase the health and safety of the workforce, but also optimise certain aspects of operations that machines can sometimes negotiate better than humans can, such as productivity, efficiency, and speed. This paper presents technical considerations for introducing an autonomous shuttle car in room and pillar underground coalmines with respect to a process workflow. A laboratory-scale shuttle car prototype that can navigate a scaled room and pillar section was built and deployed in a laboratory environment. Sensor selection, data management, as well as the developed navigation system are discussed in the framework of the developed workflow. The lab-scale shuttle car is currently being tested in a lab-scale mock mine. Although the laboratory simulations are based on a number of simplifying assumptions, they are sufficient for this pilot project. Systematic investigation is being conducted to determine possible inefficiencies and achieve sufficient navigation around the pillars. Additionally, plans to equip a full-size shuttle car with the proposed system and test it in a real environment have been laid out in collaboration with industrial partners.

INTRODUCTION

In recent years, mining technology has embraced new advancements in robotics, autonomous vehicles, smart mining systems and other high-tech approaches in an effort to prepare for the mines of the future. Deeper orebodies and increasingly challenging mining environments will be encountered, as the currently economically viable resources cannot fulfill the increasing demands of society on mineral resources. Integration of autonomous vehicles and smart mining solutions into the mining cycle is one of the most popular trends towards achieving that goal (Sahu, 2018).

Delegating tasks from humans to autonomous vehicles offers a means to optimise two critical factors in every mine: safety and productivity. The relocation of the operators from the active face to a safer location, such as a control room, can effectively reduce accidents and exposure to unhealthy conditions. The shift to self-driving machines can thus, not only increase the health and safety of the workforce, but also optimise certain aspects of operations that machines can sometimes negotiate better than humans can, such as productivity, efficiency, and speed. In some cases, autonomous solutions can enable mining to continue even when health risks would normally prohibit personnel from working, such as shortly after a blast before noxious gases have been diluted by the ventilation system. Optimising energy and fuel consumption, regulating flow of traffic with efficient fleet management, reducing damage to equipment are a few additional advantages that the autonomous solutions can offer, leading to uninterrupted mining operations, as well as reduced production and maintenance costs.

This paper presents technical considerations for introducing an autonomous shuttle car in underground room and pillar coalmines with respect to a process workflow. A 1/6th scale shuttle car prototype was built and deployed in the laboratory to navigate a 1/6th scale room and pillar operation. Sensor selection, data management, as well as the developed navigation system are discussed in the framework of the proposed workflow.

The next section discusses common sensors integrated into autonomous vehicles, as well as the current trends of commercial implementation of autonomous solutions within mining operations. Then, over two sections, we present a brief description of the constructed lab-scale shuttle car and the data management approach, respectively. Next, we describe the framework of the proposed navigation system. This leads us into discussions on various considerations and observations from the work done so far. Finally, we present the conclusion and describe the plans for the proposed system.

AUTONOMOUS VEHICLES FOR MINING APPLICATIONS

The existing literature and commercial sources provide several examples of smart solutions implemented in both surface and underground mines. Several mining companies around the world have begun concentrating efforts towards automating equipment used for cutting, drilling, loading, and materials haulage. Haulage equipment such as haul trucks, wheel loaders, and load-haul-dump (LHD) vehicles are the most common targets of such automation projects. Automating drilling and cutting equipment for both surface and underground environments presents great interest for mining companies, as well. Naturally, these projects have raised the need for the mining industry to develop appropriate data management systems, mining performance monitoring systems, and big data analytics solutions (Sammurco *et al*, 2018).

Teleoperated LHD equipment has also attracted great interest for research and experimentation in various mines around the world (Mäkelä, 2001; Paraszczak, Gustafson and Schunnesson, 2015; Schunnesson, Gustafson and Kumar, 2009; Paraszczak, 2014). Autonomous fleet management systems controlling wheel trucks and wheel loaders have been developed and implemented commercially by leading companies including Komatsu, Hitachi, and Caterpillar (Gleason, 2018; Hamada and Saito, 2018; Caterpillar, 2020). Drilling systems, roof bolters, and continuous miners are other types of equipment that can be converted into autonomous operation (Kempenaars, 2019; King, Hicks and Signer, 1993; Mansouri, Andreasson and Pecora, 2016; Ralston *et al*, 2010). To support the operation of the envisioned autonomous equipment, the smart solutions have to encompass aspects from multiple disciplines, such as artificial intelligence, data management, network efficiency, and human factors (Bodin *et al*, 2015; Hyder, Siau and Nah, 2019; Magnusson, Lilienthal and Duckett, 2007).

The commercially implemented haulage systems (AHS) (eg Komatsu FrontRunner AHS, Cat® MineStar™ Command, Sandvik AutoMine® umbrella, Hitachi AHS etc) are commonly accompanied by an appropriate data management suite. These suites provide tools that collect, analyse, and visualise data from various sensors, allowing for a real-time monitoring of the mining operations. Such tools and features are used for:

1. mine development, production, and maintenance scheduling
2. equipment and personnel tracking in the mine
3. mapping and visualisation
4. real-time equipment health monitoring and productivity information.

A reliable data management design comprises the backbone of an autonomous system of the above-described size and complexity. The speed and reliability of the data management system directly affects reliability of the collected and interpreted information. As a result, the production management of the entire mining cycle is defined by the data management system. The data management strategies associated with each commercial system described above are highly customised, and at the same time, are continuously enhanced based on the performance of the systems in the field.

On the other hand, the prevalent material haulage equipment used in underground room-and-pillar (R&P) coalmines, the shuttle car, has not been a popular choice for conversion to autonomous

operation. The operator of the shuttle car, which transports coal from the working face to the feeder-breaker, has to repeatedly traverse a nearly identical route in an open cab (with a protective canopy). This results in the continuous exposure of the operator to numerous occupational hazards. Exposure to noise, gases, dust, vibration, thermal stress, and slips, trips and falls from climbing on and off equipment, crushing by heavy equipment, and roof and rib falls place the operator at risk for soft tissue injuries, respiratory disease, occupational hearing loss, physical strain, severe injuries, and even fatalities. The high-risk environment of the underground mine due to the poor visibility, the blind intersections, the confined space, and the mobile equipment congestion can lead to human-machine or machine-machine collisions. Additionally, the operator fatigue, boredom, and complacency add more risk factors. Nearly 800 miners have been injured and 16 fatalities have occurred in underground powered haulage incidents involving shuttle cars and scoops from January 2001 to September 2010, and another 277 injuries and four fatalities between 2014 and 2016 (Mine Safety and Health Administration, 2010, 2014, 2015, 2016).

Although the above-mentioned statistics make it clear that the automation of shuttle cars could significantly improve the safety of the equipment operators and the other miners at the working section, and potentially increase the productivity of the mining cycle, the existing literature on automating the shuttle car is scarce. The small market size and the lack of industrial and academic research published on this topic are possible reasons for that scarcity. The complexity and various limitations of the implementation of autonomous equipment in underground mines may discourage such projects, as well. These complexities and limitations can be derived by the study of the few published endeavours of implementing autonomous mining equipment in the underground environment. For example, it is a GPS-denied environment and there is a lack of wireless communications infrastructure in the environment. Although the room and pillar geometry is regular and repeatable, it is also in a state of change as mining advances. The restricted space for vehicle manoeuvring, the multiple human-machine and machine-machine interactions, the presence of power cables and ventilation controls, and the noise introduced into the collected sensor data due to suspended dust and ventilation curtains are additional obstacles to autonomous navigation (Androulakis *et al*, 2020).

In an effort to provide some insightful considerations and possible solutions for the described problem, the authors present an approach that consists of the design of a laboratory scaled experimental set-up and a custom data management system that will allow a shuttle car to efficiently navigate around the room and pillar mine. The objective of this endeavour is to examine the feasibility of such a system.

SET-UP OF SIMULATIONS AND TESTING

To test and develop the software that controls and monitors the autonomous navigation of the shuttle car around the pillars, a simulated environment was constructed with off-the-shelf components. This environment is comprised of: i) a 1/6th scale mock mine; and ii) a 1/6th scale shuttle car prototype.

Mock mine

The mock mine represents a portion of a room and pillar mine with square pillars having a width of 15.2 m and entries having a width of 6.0 m. A plan view and the dimensions of the scaled mock mine are shown in Figure 1, whereas Figure 2 presents a view of the constructed mock mine.

Currently, the development of the navigation system takes into account only the geometry of the entries and cross-cuts of the mine, without taking into account any data with respect to the roof, and thus the absence of a roof in the mock mine does not affect the development and testing of the algorithms. Additionally, the floor of the mock mine does not replicate the conditions of the floor in an actual mine (eg friction coefficient, floor inclination, possible muddy conditions). These assumptions were made to reduce the complexity of the problem and allow for focusing on the problem of traversing around the pillars. However, the performance of the navigation system is deemed sufficient for the scope of this research, namely, to examine the feasibility of the integration of an autonomous shuttle car into the underground room and pillar mining cycle.

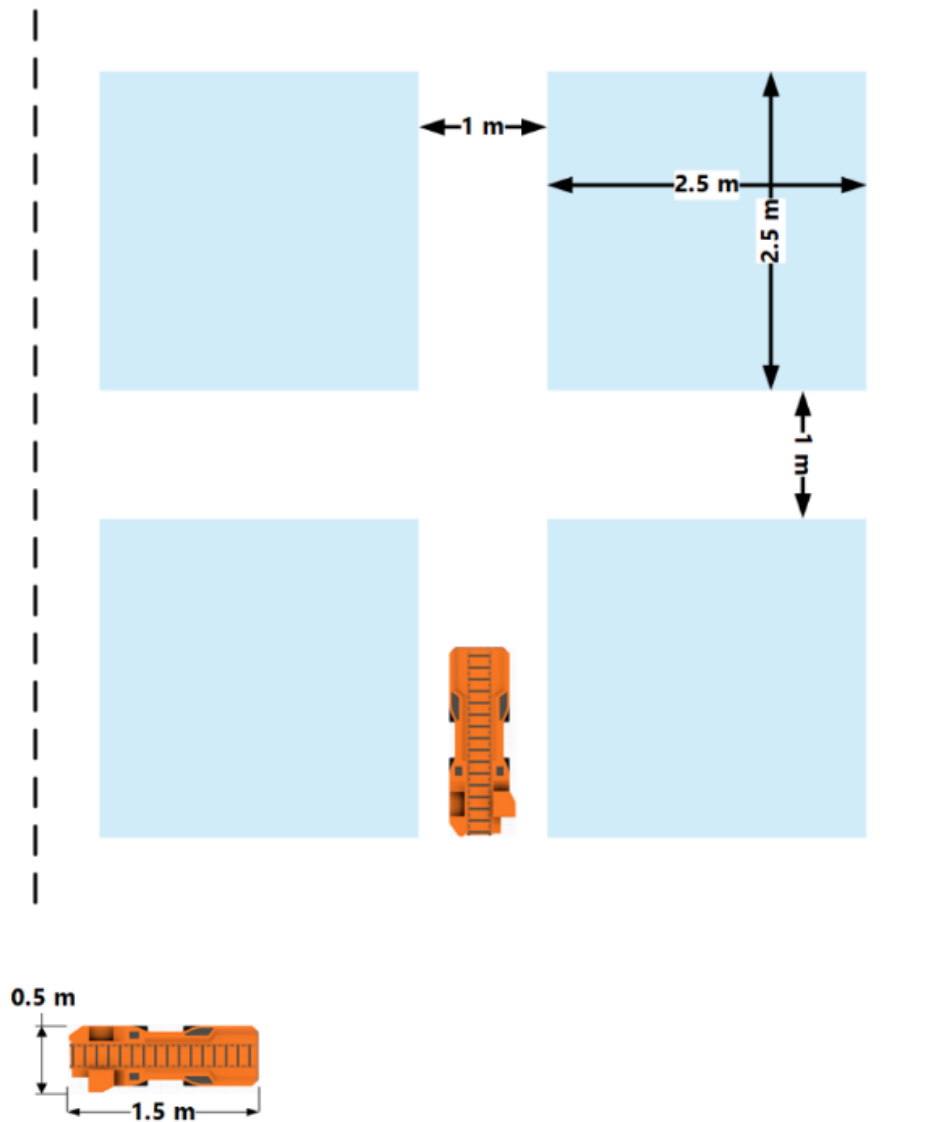


FIG 1 – Plan view of simulated room and pillar layout.

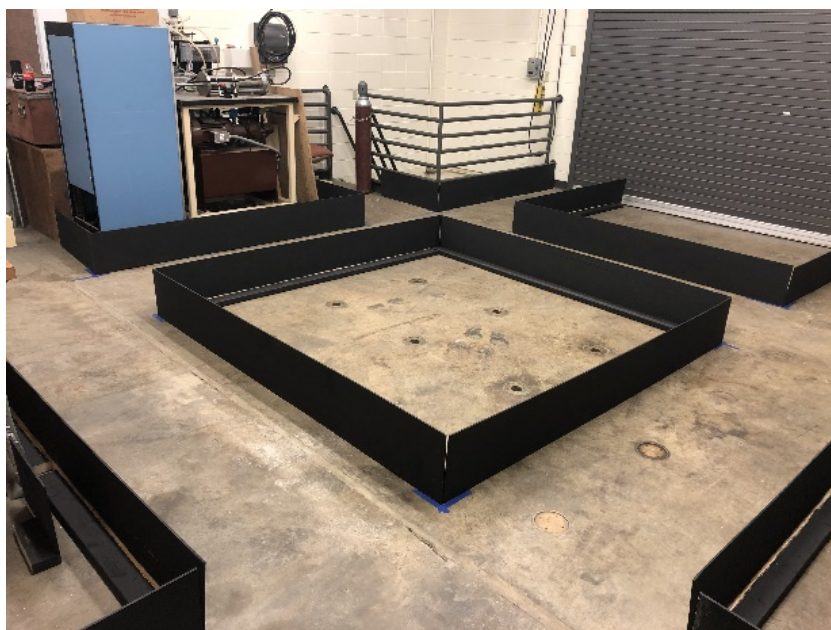


FIG 2 – Mock mine (Androulakis *et al*, 2020).

Laboratory-scale shuttle car

The body of the laboratory-scale shuttle car is based on a Joy 10SC32B shuttle car. A 3D data file, provided by Komatsu Mining Corp., was used to design scaled stereo lithography (STL) files for a 3D printer to print the body in several parts (because the available equipment could not print the entire body in one part). A Gigabot 3+ 3D printer and a Makerbot Replicator Z18 3D printer were used for that purpose.

The chassis of the prototype includes two identical axles from an off-the-shelf remote control (RC) vehicle. The axles are connected with aluminium frame rails. A wooden bin mounted between the rails holds the electronic parts, while the frame rails provide a means to mount the shuttle car body to the chassis. The locomotive system includes four servomotors for steering and two brushless dc (BLDC) planetary gear motors for trammig (Figure 3). The two BLDC traction motors are controlled by a BLDC motor controller, which reads the pulse-width-modulation (PWM) signals sent from an RC transmitter to the RC receiver. The four steering servomotors are controlled directly from the RC receiver. Additional details on the shuttle car can be found in Androulakis *et al* (2020).

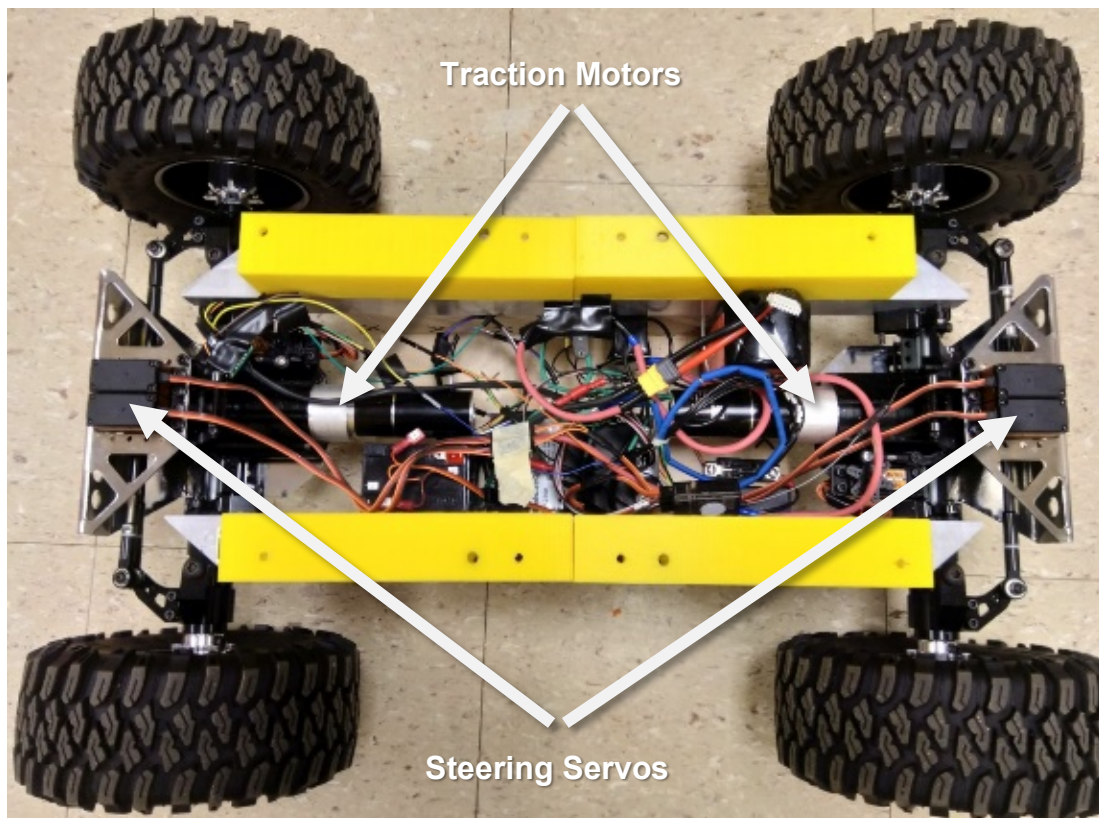


FIG 3 – 1/6th-scale shuttle car locomotive system.

Sensors

The prototype collects information about its surroundings and its movement through two different sensor modalities (Figure 4):

- **Four 2D LiDAR scanners:** The 2D LiDAR scanners used for the lab-scale shuttle car are the off-the-shelf RPLiDAR A1M8 scanners and are used for mapping, navigation, and obstacle detection. A housing assembly was designed and 3D printed to facilitate mounting the sensors on the lab-scale shuttle car. The RPLiDAR A1M8 scanner, developed by SLAMTEC, is a low-cost 360° laser scanner with a working range between 0.15 m and 12 m. The angular resolution is one degree, ie the scanner can ideally take 360 measurements per scan. The maximum update rate of the RPLiDAR scanner is 10 Hz or 100 ms per scan. However, the measured update rates of the 2D LiDAR scanners are lower than the maximum rates reported in the specifications. The operating frequency of the 2D LiDAR scanners is between 5 and 10 Hz per scan, with the typical frequency reported by SLAMTEC to be 5.5 Hz (under the condition that the LiDAR scanner retrieves 360 range measurements per scan). However, the

average update rate measured in the laboratory is between 7–8 Hz per scan. Because of the higher frequency compared with the typical operating frequency, the number of range measurements collected during one scan are less than 360. The average observed value is 160–175 measurements per scan. Despite that the decreased number of measurements reduces the resolution of the maps created, the information provided is sufficient for the navigation algorithms and the decision-making processes.

- **Four ultrasonic sensors:** The ultrasonic sensors are used for proximity safety to compensate for the inability of the LiDAR scanners to detect objects located closer than 15 cm. The ultrasonic sensors selected are the off-the-shelf Sonar Phidget DST1200_0 sensors. The sensor has a working range between 40.0 mm and 10.0 m. Preliminary testing with the DST1200_0 has shown that it has sufficient accuracy to determine distance to the simulated coal ribs when the shuttle car is positioned approximately parallel to the rib (ie within $\pm 30^\circ$) and the sensor is mounted perpendicular to the direction of travel. The maximum update rate is 10 Hz (100 ms per measurement). The average update rate measured in the laboratory coincides with the above-mentioned rate.



FIG 4 – Prototype equipped with LiDAR units and ultrasonic sensors.

DATA MANAGEMENT

The general data workflow that regulates the collection, storage, and processing of the sensor data, as well as the autonomous decision-making for the laboratory scale shuttle car is depicted in Figure 5. The system (described in detail in Androulakis *et al*, (2020)) is divided into three subsystems, namely data collection, data storage, and autonomous logic controller (ALC).

Data collection

The data collection subsystem, depicted by the upper-left (orange) solid box of the schematic in Figure 5, includes the onboard hardware that collects the ultrasonic and LiDAR sensor data. The

sensors are cable-connected to a number of microcontrollers (Raspberry Pi 3 Model B+), which control the continuous acquisition of the latest sensor data, as well as the data's registration to the custom data storage medium through wireless LAN networking. The microcontrollers are programmed to collect new data from the sensors and post the data into the data storage medium in a continuous loop.

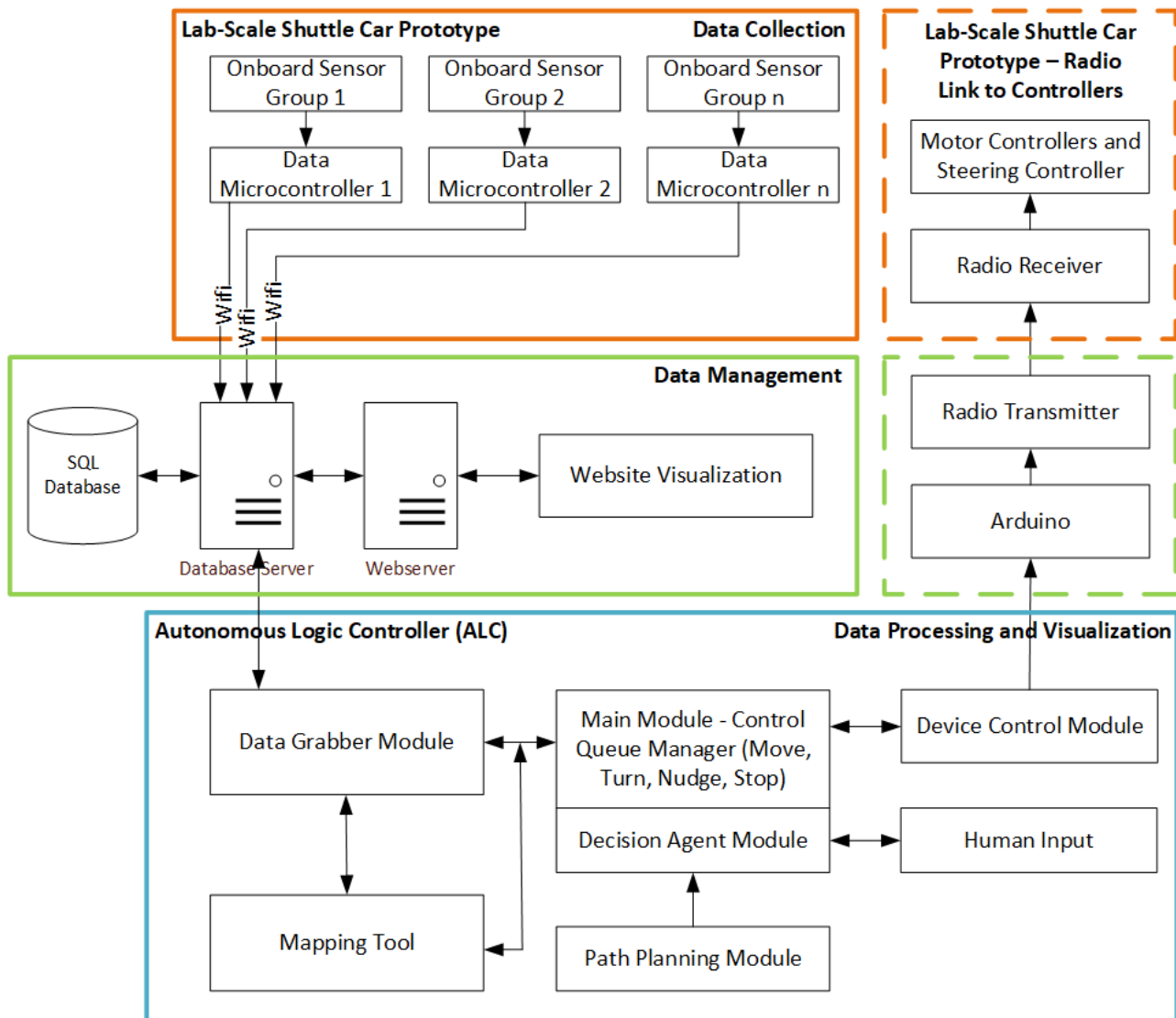


FIG 5 – Schematic of data flow and management.

Data storage

The data storage subsystem is comprised of an SQL database server and a Webserver that store and distribute the sensor data to the ALC subsystem. This part is represented by the middle (green) solid box of the schematic.

The custom SQL database developed is the storage medium of the data collected from the Raspberry Pi microcontrollers. The microcontrollers populate the database in real-time in an asynchronous manner. At the same time, the database server handles the requests for data reporting from the ALC, as well as the webserver.

In order to store each data stream into the database, the following naming convention for the sensors has been utilised:

- the sensor names are 6–8 characters long
- characters 1–2 denote the type of sensor: *US* for ultrasonic or *LR* for the LiDAR scanner

- characters 3–4 denote the longitudinal position of the sensor on the prototype: *DS* for discharge end or *LD* for loading end
- characters 5–6 denote the lateral position of the sensor on the prototype: *OP* for operator side or *OF* for off-side
- characters 7–8 denote the pointing direction of the point sensors (only for ultrasonic sensors): *OP* for operator side, *OF* for off-side, *IB* for inby direction or *OB* for outby direction.

Figure 6 depicts a labelled schematic of the shuttle car parts, which illustrates the naming convention. Note that in underground coalmines, movement towards the face is referred to as *inby*, while the movement away from the face is referred to as *outby*.

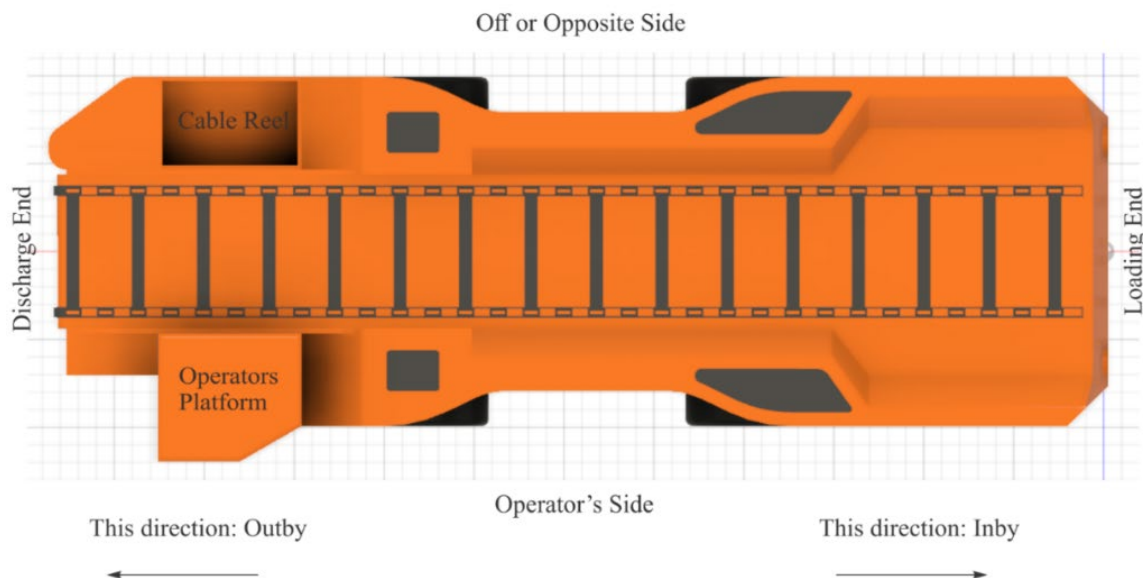


FIG 6 – Indexed top view of shuttle car schematic.

Each time the microcontrollers post a new record to the server, the arrival time of that record is created (current timestamp) and attached to the information of the recording. These times are used to calculate the effective update rate for each sensor. The update rates for the different sensors using this procedure are shown in Table 1. These rates coincide with the operating frequencies of the sensors used. This means that there are negligible latencies during the communication of the collected data to the SQL database. Specifically, the average update rate for the LiDAR scanners is 136.15 ms, which corresponds to an update frequency of 7.35 Hz, while the average update rate of the ultrasonic sensors is 100.63 ms or 9.94 Hz.

TABLE 1

Effective update rates of onboard sensors (calculated on the database server).

Sensor	Sensor type	Longitudinal position	Transverse position	Pointing direction	Update rate (ms)
LRLDOP	LiDAR	Loading end	Operator side	Omnidir.	139.53
LRLDOF	LiDAR	Loading end	Opposite/off side	Omnidir.	127.90
LRDSOP	LiDAR	Discharge end	Operator side	Omnidir.	136.35
LRDSOF	LiDAR	Discharge end	Opposite/off side	Omnidir.	140.80
USLDOPIB	Ultrasonic	Loading end	Operator side	Inby	101.45
USLDOFIB	Ultrasonic	Loading end	Opposite/off side	Inby	100.86
USDSOPOB	Ultrasonic	Discharge end	Operator side	Outby	99.75
USDSOFOB	Ultrasonic	Discharge end	Opposite/off side	Outby	100.44

Autonomous logic controller

The ALC is the front-end interface that is responsible for the data processing and visualisation, as well as providing the operator the means to monitor and control the shuttle car during the execution of the given mission. This part is represented by the lower (blue) solid box of the schematic in Figure 5. The ALC is a Windows application developed under the .NET framework using C# programming language. This multimodular interface has been developed for decision-making and for communication to the shuttle car traction motors and steering servomotors. Human input is also required for setting parameters and assigning missions. The main input of this subsystem is the collected sensor data retrieved from the data storage subsystem, while the main output is a series of PWM signals that control the movement of the shuttle car in real-time.

The most important modules that comprise the interface are the following:

- **Main Module:** Allows the shuttle car supervisor to control and monitor the starting, pausing, resuming, and termination of the execution of the given mission. At the same time, it enables the remote monitoring of the shuttle car movement and the controlling of the speed and steering angle of the vehicle in real-time.
- **Data Grabber Module:** Enables the front-end application to retrieve the latest updated sensor data from the SQL database in real-time.
- **Path Planning Module:** Provides the means to the shuttle car supervisor to create a mission for the shuttle car, either in a semi-autonomous manner through creating a small number of abstract commands or in a fully autonomous way through utilisation of graph theory.
- **Mapping Tool:** Processes and visualises the data collected from the LiDAR scanners into a map of the surroundings in real-time. Additionally, the tool compresses the information from that map into a few meaningful parameters that are used as input for the decision agent module. The real-time maps of the current surroundings of the vehicle are extended up to 12 m (the range of the LiDAR units). The next section describes the Mapping Tool more comprehensively.
- **Decision Agent Module:** Analyses the latest available information about the surroundings and decides whether the current low-level tramming or turning command is safe to be executed or alternative corrective actions need to be taken.
- **Device Control Module:** Converts the decisions of the Agent into appropriate PWM signals and controls the transfer to the RC transmitter. Subsequently, the transmitter sends the signal to the onboard radio receiver.

AUTONOMOUS NAVIGATION FRAMEWORK

Mission planning

In order for the shuttle car to execute one mission (eg tram to the continuous miner's position and tram back to the feeder breaker), the mission must first be assigned to the shuttle car through the ALC application. To do so, the human operator needs to specify a few basic parameters (ie panel geometry, entry and pillar dimensions, maximum allowed speed of vehicle, coordinates of starting and ending point of mission etc). Based on these parameters, the ALC will determine the optimum path using Graph theory and visualise it (see Figures 7 and 8). However, the presence of ventilation devices, cables or other vehicles and infrastructure that are not mapped makes it necessary for the user to confirm the validity of that path and give permission to the ALC to assign the path as the executable mission. In the case that the provided path is not valid, the user can input the path using the manual path planner by providing a sequence of abstract instructions (low-level executable mission). More specifically, these instructions are in the form of *Traverse along one pillar and cross the next intersection* or *Traverse along one pillar and turn left/right at the intersection*.

Mission Planner

Stanley Gains	Driving Params	Main Traversing Sensor:	Path Cmds List:
Proportional: 0.25	Max Motor Speed: 35	<input checked="" type="button" value="LIDAR"/> <input type="button" value="USonic"/>	
1st term: 0.2	Min Rib Distance (cm): 10	Tuning Trigger Sensors:	
2nd term: 0.3	Obstacle Thresh. (cm): 30	<input checked="" type="button" value="USonic"/> <input type="button" value="IMU"/> <input type="button" value="RFID"/>	
Mine Geometry	Sh. Car Length (cm): 144.8	Traverse Mode:	
Panel Width (m): 11.4	Sh. Car Width (cm): 50.0	<input checked="" type="button" value="StayCentered"/> <input type="button" value="RibFollow"/> <input type="button" value="CC"/>	
Panel Length (m): 18.3	Driving Mission	Movement Direction: <input type="button" value="Inby"/> <input type="button" value="Outby"/>	
Pillar Width (m): 24.4	Initial X Coord (cm): 101.6	Target Spacing (cm): 15	
Entry Width (m): 10.2	Initial Y Coord (cm): 50.8	Wall Follow Direction: <input type="button" value="Of_side"/> <input type="button" value="To_side"/>	
Graph Edge Costs	Final X Coord (cm): 691.2	Tramming Speed: 25	
Straight Entrs: <input checked="" type="button" value="1.0"/>	Final Y Coord (cm): 396.4		
Straight Cuts: 2.0			
Turns: 50.0			
	<input type="button" value="Compute Optimum Path"/>	<input type="button" value="Add Optimum Path to Queue"/>	<input type="button" value="Clear"/>

Text Log

FIG 7 – Mission Planner form.

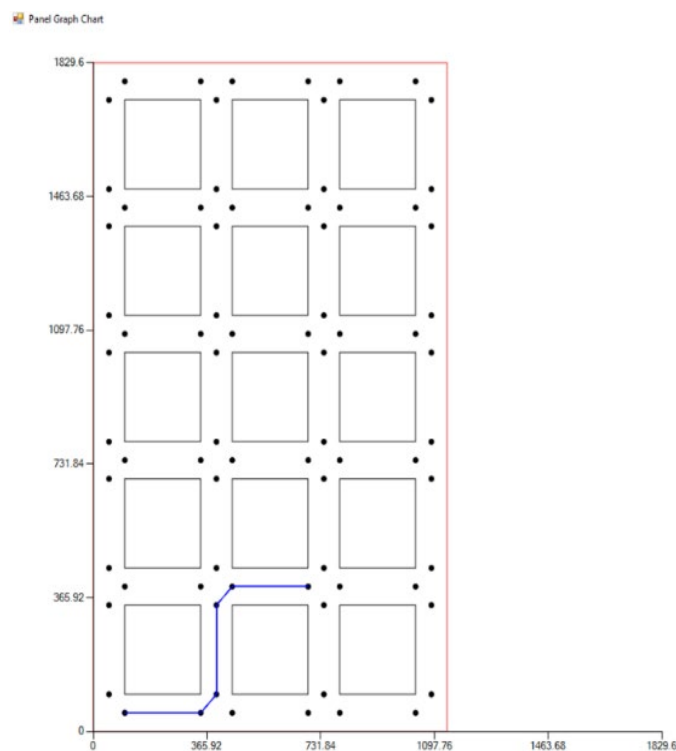


FIG 8 – Optimum path finder tool.

The low-level executable mission is defined in the form of a sequence of high-level commands. These commands instruct the vehicle to move inby/outby for a specific time interval (hundreds of milliseconds) at a specific speed or to change the steering angle of the vehicle. Each of these commands can be translated into a radio signal that is transmitted to the on-board radio receiver connected to the servomotors and traction motor controller. This initial sequence of commands is specified on the assumption that the movement of the shuttle car is not affected by external disturbances or by interruptions in the movement of the vehicle, and that the section does not deviate

significantly from the mine map (as in the map depicted in Figure 8). In order to take into account these disturbances and the dynamic nature of the mine section (eg obstacles, roof or rib falls etc) during the execution of the mission, this predefined queue is continuously cross correlated to the map of the vehicle's surroundings that is iteratively constructed based on the real-time sensor data. If the navigation algorithms determine that the top item of the queue is safe to be executed, the command will be sent to the radio transmitter and the algorithm will continue to examine the next item of the queue. Otherwise, modifications to the commands queue are applied and new corrective commands are added at the top of the queue.

Finite state machine

The autonomous navigation of the shuttle car in the proposed system is modelled through a deterministic finite state machine (FSM). FSMs are commonly used in cases where the assigned task can be modelled through a small number of states of the system. The simplicity and consistency that characterise the layout of the room and pillar mining method allows for the definition of such a small number of states for the shuttle car. Each item of the command queue that determines the executable mission is assigned one, and only one, of these states. Therefore, the shuttle car can encounter exactly one state at any given time. For the shuttle car to navigate around the pillars of the mining section, three main states are defined:

1. 'Centred' for following the centreline of the entry/cross-cut while traversing it.
2. 'CentredCC' for following the centreline of the entry/cross-cut ahead while passing an intersection.
3. 'TurnCCut' for turning in a cross-cut or entry.

A final state is specified for a neutral mode, called 'Agent', and is assigned to the corrective commands issued by the navigation algorithms based on the collected data.

Each state is associated with a different set of functions of the navigation algorithms, which means that different data interpretations, different commands queue – real-time data cross-correlation strategies, or different state transition rules, are followed for different states. Despite the relative rigidity introduced to the FSM by the predefined commands queue, state transitions can be initiated if this is dictated by sensor data. Such state transitions take place when the vehicle is in critical points of its route, eg close to the corners of intersections. At these critical points, the navigation algorithms need to select among the following four options:

1. Transition FSM from state 'Centred' to state 'CentredCC': The mission under execution dictates that the vehicle must cross the intersection ahead. The state transition is based on the distance of the vehicle from the pillar corners encountered as the vehicle enters the intersection.
2. Transition FSM from state 'CentredCC' to state 'Centred': After crossing an intersection the vehicle must navigate straight in the same entry between the pillars ahead. The state transition is again based on the distance of the vehicle from the pillar corners encountered as the vehicle leaves the intersection.
3. Transition FSM from state 'Centred' to state 'TurnCCut': The mission under execution dictates that the vehicle must turn at the intersection ahead. The state transition is based on the distance of the vehicle from the corners of the intersection.
4. Transition FSM from state 'TurnCCut' to state 'Centred': After turning at the intersection, the vehicle traverses the 'new' entry (or cross-cut) between the pillars ahead. The state transition is based on the orientation of the vehicle with regard to the 'new' entry/cross-cut.

Mapping

According to the discussion above, it becomes evident that the accuracy and reliability of the real-time maps of the vehicle's surroundings play the most critical role in the implementation of the FSM. In the proposed navigation system, the maps of the vehicle's surroundings are extracted from the LiDAR data. A Mapping Tool (MT) has been embedded into the front-end application for handling the creation of these maps.

The MT functionality is based on a two-step procedure that consists of:

1. A line-fitting process: a variation of the Random Sampling Consensus (RANSAC) algorithm, as developed by Fischler and Bolles (1981). This step processes the LiDAR data to determine a number of linear segments that model the ribs of the entries/cross-cuts.
2. A corner detection process: the linear segments defined in the first step are used to extract the corners of the intersections near the shuttle car.

Figures 9 and 10 show two examples of the constructed maps for two cases. The accuracy of the corner detection (between the entry and cross-cut around which the shuttle car needs to turn) is of critical importance to execute the turn reliably and safely. Delayed or erroneous detection of the corners will not enable collision avoidance with the ribs.

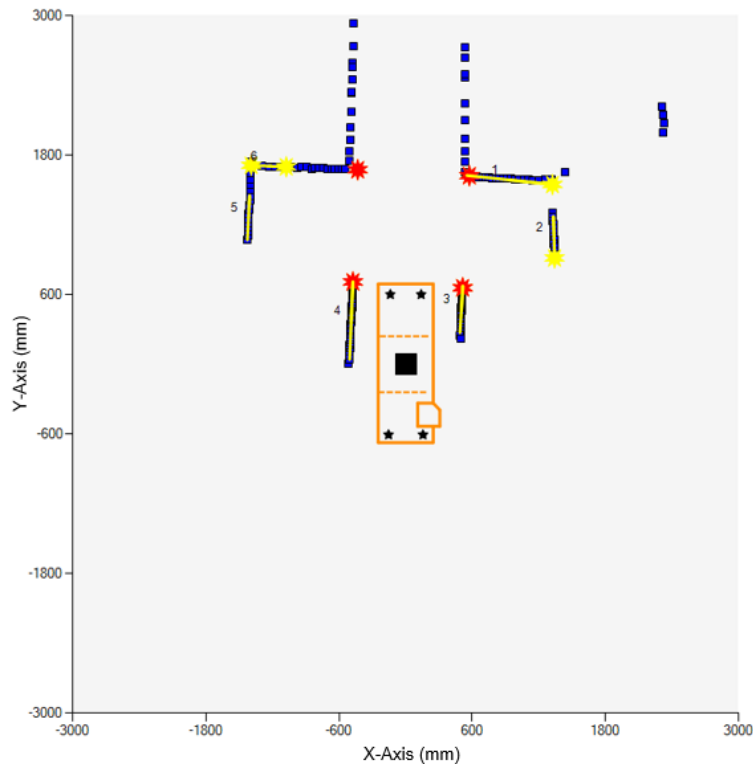


FIG 9 – Map derived by the two LiDAR units on the loading end of the shuttle car, while tramming towards the face (ie increasing values of y). Yellow lines are linear segments fitted by the custom multiRANSAC algorithm. The red stars denote the four closest (detected) corners, while the yellow stars denote the remaining detected corners. The black square denotes the centre of the shuttle car and is the origin of the axes. Movement is always in the direction of increasing values of y.

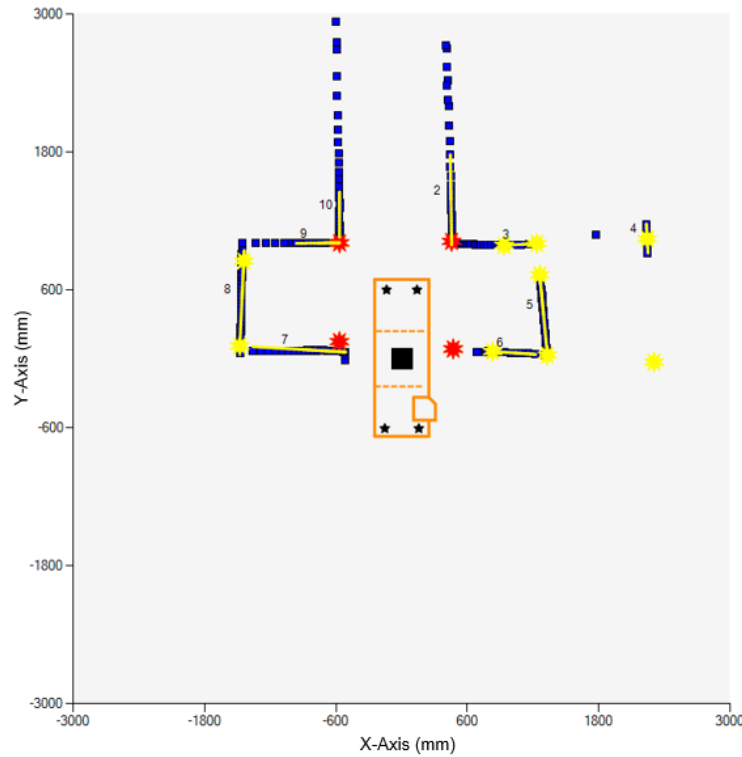


FIG 10 – Intersection map derived by the two LiDAR units on the loading end of the shuttle car, while moving inby (ie increasing values of y). Yellow lines are linear segments fitted by the custom multiRANSAC algorithm. The red stars denote the four closest (detected) corners, while the yellow stars denote the remaining detected corners. The black square denotes the centre of the shuttle car and is the origin of the axes. The direction of movement is always in the direction of increasing values of y.

The final output of the MT is not the maps per se, but rather the information of these maps is compressed into a few parameters. These parameters can be used by the navigation and decision-making functions of the proposed system. The MT outputs the following three parameters:

1. Orientation of the shuttle car, θ : angle of the longitudinal axis of the shuttle car and the operator-side rib of the currently traversed entry or cross-cut (measured in a counter clockwise direction starting from the rib).
2. Deviation of the shuttle car from the centreline: the distance of the middle of the front axle (reference point) from the centreline of the entry/cross-cut.
3. Distance to the nearest obstacle ahead (in the direction of movement).

Lateral control

The steering angle of the autonomous shuttle car while it is traversing along the entries is continuously corrected based on the deviations from the desired path as these are defined through the final outputs of the MT. The Stanley controller was chosen to act as the corrections model. The Stanley Controller is a non-linear lateral controller for autonomous vehicles for tracking a desired trajectory in real-time. It was implemented for the first time on ‘Stanley’, the Stanford Racing Team’s entry in the DARPA Grand Challenge 2005, which won the challenge after successfully traversing 132 miles over desert terrain in the Mojave Desert (Thrun *et al*, 2006).

The generic equation that describes the Stanley controller is:

$$\delta(t) = \psi(t) + \tan^{-1} \left(\frac{ke(t)}{k_s + v(t)} \right), \delta(t) \in [\delta_{min}, \delta_{max}]$$

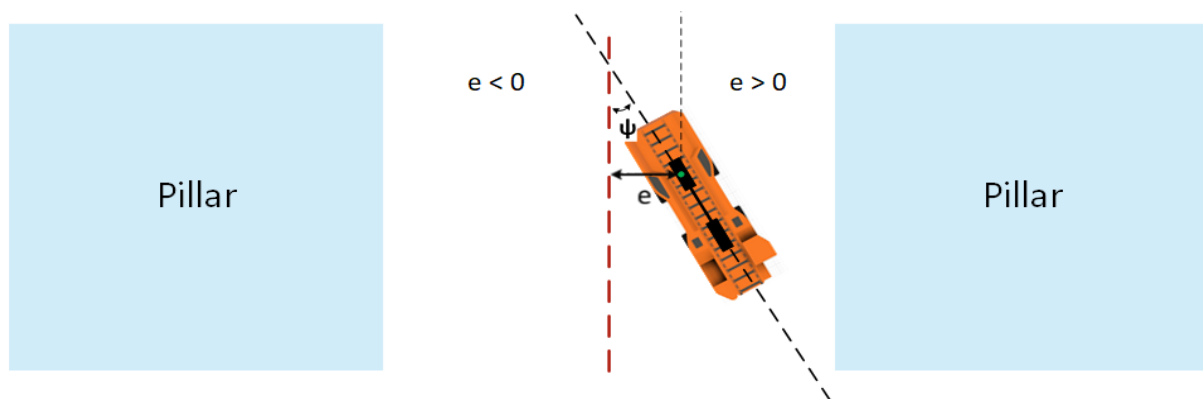
where:

δ : Steering angle

ψ :	Heading error
e :	Cross-track error
v :	Velocity of vehicle
k :	Proportional constant
k_s :	Softening constant

This equation can be intuitively explained by three principles (see Figure 11):

1. Eliminate the heading error (1st term of equation).
2. Eliminate the cross-track error, ie the distance between the closest point on the desired path with the front axle of the vehicle (2nd term of equation). The proportional constant, k , defines the contribution of that error in the corrective steering angle, while the softening constant, k_s , ensures a non-zero denominator.
3. Bound the steering angle with respect to the maximum and minimum allowable values.



DISCUSSION

Autonomous work without human presence is a highly sought-after solution in the underground mining environment. The proposed framework discusses the implementation of an automated shuttle car in underground room and pillar coalmines in a laboratory-scaled set-up. Because the environment is underground, it was necessary to design a GPS-denied navigation system without the aid of GPS information. The sensors selected were four 2D LiDAR scanners and four ultrasonic sensors. A data management system has been developed using a MySQL database to collect, store, and distribute the sensor data. The data from the scanning units are immediately and continuously processed using a custom variation of the RANSAC algorithm. Subsequently, the information derived from the maps is input into a Stanley controller to determine the next movement of the shuttle car.

The selection of the sensors to be integrated into the proposed system was influenced by three main considerations:

1. The lighting and air conditions in the typical underground room and pillar mine: the poor lighting conditions and the presence of suspended dust in the mine adversely affect cameras (sensors with the highest informative potential).
2. The dynamic change of pillar dimensions: the continuous resizing of the pillars and entries, either by human activity (eg retreat phase or mine expansion) or by roof or rib failure, renders the utilisation of landmark-based localisation techniques which require the instalment of additional infrastructure dispersed in the mine section.
3. The simplicity and the consistent geometry of the typical room and pillar mine: the inherent simplicity of the room and pillar mine geometry can be leveraged by the navigation algorithm to reduce the amount of data needed.

The first two considerations limit the applicability of two widely used localisation techniques, vision cameras and landmark-based techniques, and restrict the options between interoceptive sensors

(eg inertial measurement systems, rotary encoders etc) and distance ranging sensors that are not affected by the prevalent light conditions (eg LiDAR, ultrasonic, RADAR sensors etc).

On the other hand, the final consideration allows for reducing the complexity of the navigation system. The geometry of the room and pillar mine makes use of a complex sensor suite that collects a vast amount of data about the surrounding environment unnecessary. For example, under typical mining conditions (in the USA), the geometry of the mine along the vertical dimension does not change significantly and thus the system can be implemented with just a 2D mapping and navigation system. Additionally, the data collected from four LiDAR scanners provide adequate information to map the immediate surroundings of the shuttle car. The ultrasonic sensors are used only as an additional layer for proximity safety.

The room and pillar mine layout allows for further reduction of the problem's complexity in other aspects of the navigation system, as well. The path planning approach followed by the proposed system differs from the typical approach used for autonomous navigation. Typically, the path planner defines a sequence of desired poses for the vehicle to follow (ie a trajectory) to execute a given mission. Instead, the path planner of the proposed system defines a sequence of throttle and steering angle instructions. This simpler approach was selected because, in the case of a shuttle car, the motion planning functions do not need to determine the validity of any desired pose. Instead, the *a priori* known layout of the mine section allows the movement of the shuttle car to be dictated only by the clearance ahead of the vehicle. In addition, the mapping tool and the lateral control function are simplified by the geometry of the environment, since the information that the mapping tool needs to determine can be compressed into the small number of parameters described above. Subsequently, the Stanley controller can efficiently navigate the shuttle car using only these parameters.

Another aspect of the proposed autonomous system that plays a crucial role is the data management system. A reliable data management system is the backbone of the entire implementation, and its efficiency in seamlessly storing and distributing the data in near real-time (ie minimum latencies) determines the performance of the system. The DMS implemented in the current research attempts to: i) efficiently store the data collected from the onboard sensors; and ii) make the data accessible to any client request.

The DMS is separated into three subsystems: data collection, data storage, and autonomous logic controller, to ensure uninterrupted data flow. SQL databases are a commonly used solution that allows for asynchronous, real-time, and reliable data management. Asynchronous access from multiple sources ensures that the data will not be lost because of conflicts between the different writing processes, as well as ensuring that the data will be recorded in real-time or near real-time speed. A similar concept applies to data requests from multiple clients.

CONCLUSIONS AND FUTURE WORK

A laboratory-scale simulation system was developed as a test bed for autonomous shuttle car operation in underground coalmines. Despite the simplifying assumptions used during the development of this simulation system, it was shown that a shuttle car could successfully navigate the tight roadways present in coalmine entries and cross-cuts.

The sensor-data acquisition system, as well as the data management system, provide the required data for mapping and navigation. Improving sensor capabilities will help with improved accuracy in both mapping and localisation.

The RANSAC-like algorithm that is used to extract the models of the surrounding ribs performs sufficiently well for the data near the shuttle car. However, the probabilistic nature of the algorithm, as well as the need for manual fine-tuning of the basic parameters that the algorithm requires as inputs affect the accuracy of the line fitting. The increasing scarcity of the 2D point clouds, as the distance from the shuttle car increases, deteriorates this accuracy. The authors plan to further investigate these two issues and improve the preliminary observed overall performance of the mapping algorithm.

The lab-scale shuttle car is currently being tested in a mock mine set-up. The laboratory situations are idealised; however, they are sufficient for this pilot project. The authors plan to systematically

investigate the performance of the proposed system to determine possible inefficiencies and achieve sufficient navigation around the pillars.

Plans to equip a full-size shuttle car with the proposed system and test it in a real environment have been laid out in collaboration with industrial partners. This requires a multidisciplinary effort to properly integrate the current laboratory-scaled system with the actual-size vehicle. Several aspects of the current system must be converted for successful implementation at full scale: design for increased dataflow in the existing database schema, design the supervisor HMI that will provide connection and control over the ALC of the lab-scale system, etc. Additionally, unexplored issues regarding the full-size vehicle control through an innovative PLC design, connecting the throttle, steering, and brakes with appropriate actuators, and regulating the human-machine interactions are under investigation.

ACKNOWLEDGEMENTS

This study was sponsored by the Alpha Foundation for the Improvement of Mine Safety and Health, Inc. (Alpha Foundation). The views, opinions and recommendations expressed herein are solely those of the authors and do not imply any endorsement by the Alpha Foundation, its directors, or staff.

REFERENCES

- Androulakis, V, Sottile, J, Schafrik, S and Agioutantis, Z, 2020. Concepts for Development of Autonomous Coal Mine Shuttle Cars. *IEEE Transactions on Industry Applications* 56 (3):3272–3280. doi: <https://dx.doi.org/10.1109/TIA.2020.2972786>.
- Bodin, U, Andersson, U, Dadhich, S, Uhlin, E, Marklund, U and Häggströmff, D, 2015. Remote controlled short-cycle loading of bulk material in mining applications. *IFAC-PapersOnLine* 48 (17):54–59.
- Caterpillar, 2020. Cat® MineStar™ Command. Accessed January 8, 2021. https://www.cat.com/en_US/by-industry/mining/surface-mining/surface-technology/command.html.
- Fischler, M A and Bolles, R C, 1981. Random sample consensus: a paradigm for model fitting with applications to image analysis and automated cartography. *Communications of the ACM* 24 (6):381–395.
- Gleason, W, 2018. Autonomous Haulage Growing Fast; Komatsu Continues to Innovate in Driverless Fleet Sector. *Mining Engineering*.
- Hamada, T and Saito, S, 2018. Autonomous haulage system for mining rationalization. *Hitachi Rev* 67 (1):87–92.
- Hyder, Z, Siau, K and Nah, F, 2019. Artificial intelligence, machine learning, and autonomous technologies in mining industry. *Journal of Database Management (JDM)* 30 (2):67–79.
- Kempenaars, C, 2019. Implementation of mechanized roof-bolters for low-seam hard-rock mining. Masters, Faculty of Engineering and the Built Environment, University of the Witwatersrand.
- King, R L, Hicks, M A and Signer, S P, 1993. Using unsupervised learning for feature detection in a coal mine roof. *Engineering Applications of Artificial Intelligence* 6 (6):565–573.
- Magnusson, M, Lilienthal, A and Duckett, T, 2007. Scan registration for autonomous mining vehicles using 3D-NDT. *Journal of Field Robotics* 24 (10):803–827.
- Mäkelä, H, 2001. Overview of LHD navigation without artificial beacons. *Robotics and Autonomous Systems* 36 (1):21–35.
- Mansouri, M, Andreasson, H and Pecora, F, 2016. Hybrid Reasoning for Multirobot Drill Planning in Open Pit Mines. *Acta Polytechnica* 56 (1):47–56. doi: 10.14311/APP.2016.56.0047.
- Mine Safety and Health Administration, 2010. Safety practices around shuttle cars and scoops in underground coal mines. In *U.S. Department of Labor – Mine Safety and Health Administration*.
- Mine Safety and Health Administration, 2014. Mine Injury and Worktime, Quarterly. In *U.S. Department of Labor – Mine Safety and Health Administration*.
- Mine Safety and Health Administration, 2015. Mine Injury and Worktime, Quarterly. In *U.S. Department of Labor – Mine Safety and Health Administration*.
- Mine Safety and Health Administration, 2016. Mine Injury and Worktime, Quarterly. In *U.S. Department of Labor – Mine Safety and Health Administration*.
- Paraszczak, J, 2014. Maximization of productivity of autonomous trackless loading and haulage equipment in underground metal mines—a challenging task. *Mining Engineering* 66:24–41.

- Paraszcak, J, Gustafson, A and Schunnesson, H, 2015. Technical and operational aspects of autonomous LHD application in metal mines. *International Journal of Mining, Reclamation and Environment* 29 (5):391–403. doi: 10.1080/17480930.2015.1086553.
- Ralston, J C, Dunn, M T, Hargrave, C O and Reid, D C, 2010. Advances in continuous miner automation. Proceedings of the Mine Planning & Equipment Selection Conference (MPES 2010), Fremantle, Western Australia.
- Sahu, R, 2018. How harnessing computer vision and machine learning will revolutionize global mining. *Min Eng* 70 (6):33–35.
- Sammarco, J, Wesh, J, Reyes, M, Ruff, T and Sunderman, C, 2018. Mine of the Future: Disruptive Technologies that Impact our Future Mine Worker Health & Safety Research Focus. Internal NIOSH report (February 5, 2018): unpublished.
- Schunnesson, H, Gustafson, A and Kumar, U, 2009. Performance of automated LHD machines: A review. International Symposium on Mine Planning and Equipment Selection: 16/11/2009–19/11/2009.
- Thrun, S, Montemerlo, M, Dahlkamp, H, Stavens, D, Aron, A, Diebel, J, Fong, P, Gale, J, Halpenny, M and Hoffmann, G, 2006. Stanley: The robot that won the DARPA Grand Challenge. *Journal of field Robotics* 23 (9):661–692.

Assessment of excavation technologies for a small-scale mining robot and development of future concepts

M Berner¹ and N A Sifferlinger²

1. Senior Researcher Conveying Technology and Design of Mining Machinery, Department of Mineral Resources Engineering, Montanuniversitaet Leoben, Austria, A-8700.
Email: michael.berner@unileoben.ac.at
2. Professor Excavation and Conveying Technology and Design of Mining Machinery, Department of Mineral Resources Engineering, Montanuniversitaet Leoben, Austria, A-8700.
Email: nikolaus-august.sifferlinger@unileoben.ac.at

INTRODUCTION

Future challenges in mining due to sustainability and ecological aspects require additional efforts in research and development. With the help of fully automated machines and/or autonomous robots, new deposits can be accessed, or abandoned mines can be re-opened and operated economically. Possible tasks for robots in mining are the maintenance of machinery, exploration (eg of abandoned mines) and excavation (especially in difficult to access areas). Depending on mine layout, mining method and numerous other parameters, the design of autonomous robots can be drastically different compared to the current machinery. Outdated paths may have to be left to create room for thinking outside the box and to develop innovative solutions, which assist making future mining more sustainable and economical. The future scenarios require novel approaches and adaption of existing technologies. In particular, current excavation technologies must be assessed with new standards in order to fulfill the upcoming criteria (Hiltz, 2020; Khatib and Siciliano, 2016).

Several research and development projects are dealing with the development of robots for mining and exploration purposes. The comparatively small weight and low available power are the most limiting factors and therefore require – in addition to adaptations to commercial off-the-shelf (COTS) products – new approaches. The interaction between an excavation tool and rock creates reaction forces, which the machine needs to be capable of handling. Excavation methods can be separated into drill and blast, mechanical, alternative and combined excavation technologies, whereas the first two listed are the most commonly applied in standard excavation engineering. In order to ensure an efficient and economic application, the excavation tool needs to fulfill a number of requirements such as reasonable advance and excavation rates as well as flexible and mobile handling to adapt to the *in situ* conditions. A developed methodology is used to compare the most promising excavation methods by defining certain parameters (specific energy, reaction forces etc) and to assess their application for different rock strengths. Based on those studies, the feasibility and applicability of certain excavation tools for different scenarios and rock strengths are analysed.

ASSESSMENT

To assess the applicability of the eligible excavation methods, a classification and rough analysis of them are done. Generally, excavation systems can be divided into: drill and blast, mechanical excavation systems, alternative excavation systems and combined excavation systems (see Figure 1) (Bilgin, Copur and Balci, 2013; Vogt, 2016).

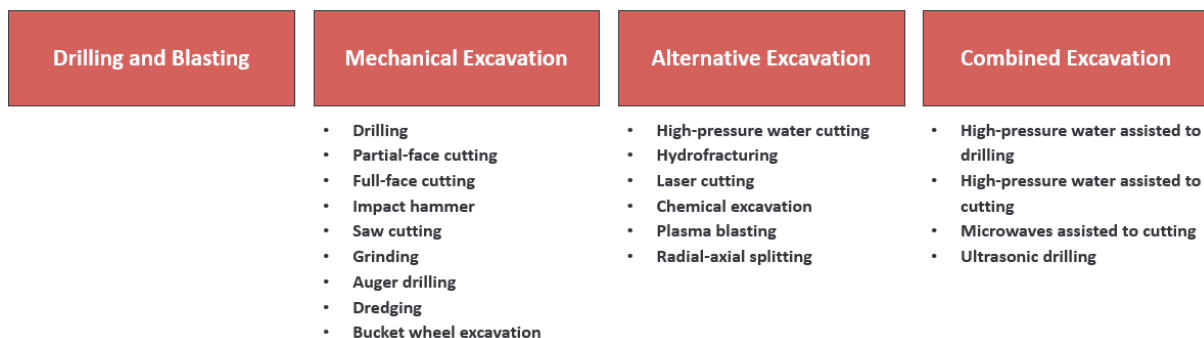


FIG 1 – Classification of excavation systems.

In the first step, these technologies are examined, analysed and evaluated according to selected criteria. Many of these methods are used for the extraction of raw materials or for tunnelling, but not all are economically viable on such a small scale. Firstly, the following features are assessed, which are mandatory for future production tools of small-scale, mobile mining robots:

- Ability to continuously excavate material.
- The capability to excavate tunnels for the robot's own locomotion.
- Limitations (maximum compressive strength and abrasivity of rock to be excavated etc).

Drill and blast is one of the most used excavation technologies due to the generic applicability in mining and tunnelling and its high production rate. Mechanical excavation systems are at least equally popular compared to drill and blast and exhibit some benefits, such as a safer operation, a better ability for selective mining and the continuous material excavation. Alternative excavation systems cover non-conventional excavation methods apart from mechanical excavation and drill and blast. The main application areas are precision tasks, pre-weakening of the rock to be excavated (used in combined excavation systems) and tasks for which the ambient conditions do not allow conventional methods. Combined excavation systems unite the advantages of mechanical excavation systems with alternative, auxiliary methods. Auxiliary tools provide an additional energy input to pre-fracture the rock or to amplify the effect of the mechanical excavation system (Bilgin, Copur and Balci, 2013; National Research Council, 1994; Sifferlinger, Hartlieb and Moser, 2017).

The tools most commonly applied in practice, include in some way a mechanical excavation tool. Because of this, it is inevitable to examine those systems in great detail. The high masses of the mechanical tools in relation to the mass of the robot pose an additional challenge. Therefore, even if they are irrefutably marked by high specific energies, alternative excavation technologies are also taken into account, because the required forces provided by the robot to penetrate the rock are comparatively low.

In the detailed investigations, the applicability of the technologies is assessed in terms of the following parameters:

- specific energy
- production rate
- excavation force/reaction force.

Power, mass and capability of handling the reaction forces are determined as the most crucial parameters influencing the ability of designing a small-scale excavation tool. In this case, the power and mass of the robot are assumed to be 40 kW and 1500 kg. The nature and strength of the rock to be excavated define the efficiency of the excavation process greatly and most importantly set strict boundary conditions for each mining system. In theory, for many excavation methods, the obtained results for specific energies and production rates sound reasonable and suggest a potential feasibility of a certain technology. However, these results do not provide any information about the practical feasibility. In reality, the machine/robot has to generate the required forces for penetrating the rock – or other way around – needs to handle the reaction forces exerted on it. Usually, the reaction forces are countered by the high mass of the machine and, depending on application and design, additional anchoring mechanisms. This issue constitutes the most fundamental consideration regarding the development of a small-scale production tool.

The minimum thrust forces of full-face cutting for excavating very soft rock already exceed the robot's capabilities. Partial-face cutting appears to be viable for soft rock material. Hydrofracturing can tackle stronger rocks, whereby alternative methods demand higher specific energies. High-pressure water jets assisted to cutting do lower the cutting forces of partial-face methods, but on the other hand also require a greater energy input. In this scale, drill and blast is the only remaining option for excavation of hard rock material, due to the low drilling forces and high efficiency of blasting rock. In this step, the technical feasibility is of lesser importance and will be covered in prospective activities.

Based on this premises, minimum requirements for each excavation method are defined, including the minimum mass of the robot and the minimum supplied power, to excavate rock with a defined strength.

Eventually, the results of the previous studies will be used for developing excavation tool concepts to be integrated in small-scale mining robots.

REFERENCES

- Bilgin, N, Copur, H and Balci, C, 2013. *Mechanical Excavation in Mining and Civil Industries*. CRC Press.
- Hiltz, R, 2020. Taking a step into the robotic future. Available from: <https://www.miningmagazine.com/innovation/news/1387411/taking-step-into-the-robotic-future> [17 June 2021.242Z].
- Khatib, O and Siciliano, B, 2016. *Handbook of robotics*, Springer.
- National Research Council, 1994. *Drilling and Excavation Technologies for the Future*. The National Academies Press. <https://doi.org/10.17226/2349>.
- Sifferlinger, N A, Hartlieb, P and Moser, P, 2017. The Importance of Research on Alternative and Hybrid Rock Extraction Methods, *BHM Berg – und Hüttenmännische Monatshefte*, vol. 162, no. 2, pp. 58–66.
- Vogt, D, 2016. A review of rock cutting for underground mining: past, present, and future, *Journal of the Southern African Institute of Mining and Metallurgy*, vol. 116, no. 11, pp. 1011–1026.

Intelligent characteristics and technical path of fully mechanised mining

H M Li¹, Z G Wang², S R Wang³ and W Wang⁴

1. Professor, School of Energy Science and Engineering, Henan Polytechnic University, Jiaozuo 454003, China. Email: lihm@hpu.edu.cn
2. PhD Candidate, School of Energy Science and Engineering, Henan Polytechnic University, Jiaozuo 454003, China. Email: 111702010004@home.hpu.edu.cn
3. Professor, School of Civil Engineering, Henan Polytechnic University, Jiaozuo 454003, China. Email: shurenwang@hpu.edu.cn
4. Associate Professor, School of Energy Science and Engineering, Henan Polytechnic University, Jiaozuo 454003, China. Email: wangwen2006@hpu.edu.cn

ABSTRACT

The intelligent mining in China is still in the initial stage and the technical system is still being improved. Through analysing the technical characteristics of production information acquisition, processing and control technology in different coal mining stages in China, it is believed that information perception, analysis and control technology are the essential features of the progress of coal mining methods. The connotation of intelligent mining in the fully mechanised mining was clarified to use the 'interconnected' intelligent set of fully mechanised mining equipment as the carrier. Based on the deep integration of modern technologies such as internet of things technology, artificial intelligence technology, big data technology, cloud computing technology, and communication technology with coalmine production, the automatic coal mining technology with artificial intelligence features was realised to apply the intelligent information perception, intelligent information analysis and decision-making, intelligent control and feedback. The key of intelligent mining lied in accurate information perception, rapid decision analysis, precise coordinated control, and real-time feedback learning. The technical path to realise the intelligent mining included three aspects: intelligent perception of production physical scenes and big mine data storage, association analysis and intelligent decision-making of big mine data, and precise coordinated control of intelligent production equipment. These key technologies constituted the intelligent mining, such as accurate geological detection technology throughout the mining life cycle, precise perception technology for production scenarios, multi-source information fusion technology, intelligent decision-making technology under complex production environments, and reliability enhancement technology for fully mechanised mining equipment systems. Combining with the actual engineering, the preliminary application of the intelligent fully mechanised caving mining mode for extra-thick coal seams was introduced based on 'man-machine-environment' multi-source information data.

INTRODUCTION

As the main component of basic energy, the coal resource has long occupied an important position in China's energy structure, which will continue to be the main energy source in China for a long time in the future (Xie *et al*, 2012; Xie, Wu and Zheng, 2019; Song, 2014; Yuan, 2017; Wang *et al*, 2018). With the new technological revolution, especially the breakthrough of information technology, artificial intelligence technology and intelligent manufacturing technology, the concept of intelligent mining has been proposed and a wave of exploration has emerged in the coal industry (Sun, 2015; Li, 2019; Yu *et al*, 2019; Wang, Pang and Ren, 2020). In the field of coal production, many experts and scholars plan the development direction of coal in the intelligent era from a strategic height. At the same time, they have conducted in-depth research on issues such as intelligent coal mining or intelligent mine construction, and put forward important theoretical frameworks and technical roadmaps (Wang *et al*, 2016; Lu, 2018; Li, Ji and Zhang, 2019; Luo and Fu, 2019; Li *et al*, 2019; Niu, 2019).

The traditional mining mode of coalmines is mainly based on the understanding of the physical phenomena in the mining process, using on-site observation, physical and mechanical analysis, and numerical analysis to explain the coal mining law from the perspective of mechanism, and establish a control model reflecting the coal mining. By continuously adjusting the mining parameters and control parameters to modify the model until it meets the needs of on-site

production, or through clustering standardisation to broadly classify the mines with different production and geological conditions, so as to achieve the effect of divide and conquer. Traditional coal mining is still in the stage of 'static' and 'trial and error'. It is unable to adapt to the complexity of the mining environment. It is difficult to achieve dynamic and accurate disaster management, which is difficult to quantify some mining problems and clarify some disaster mechanisms.

Intelligent mining is the deep integration of coal mining technology with intelligent manufacturing technology, information technology, communication technology, computer technology, internet technology, and automatic control technology. Through the perception systems at all levels, the structured and unstructured process of coalmine multi-source heterogeneous data is collected, and dynamically stored and released through database technology. Then, big data analysis and artificial intelligence algorithms are used to perform correlation analysis on the production data. The correlation among the production data is deeply explored to find out the decision variables and the related variables. The best cooperative operation logic of the production system is quickly decided according to the changes of the production environment, and the controlled equipment group of the production system is coordinated and controlled through the high-speed communication network. The feedback information of the equipment group is obtained in real time. To store and learn, and dynamically modify the decision-making algorithm. Intelligent mining enables the dynamic production scene to form a closed-loop control system of 'real-time perception-intelligent analysis and decision-making-collaborative control-real-time feedback', which realises the dynamic and precise control of the production system of coalmine under complex environmental conditions.

China is still in the initial stage of the development of intelligent coalmines (Wang *et al*, 2019), and the theoretical system of intelligent mining still needs continuous improvement. This paper analyses the difference between the intelligent mining and traditional mining methods in terms of information perception, information recognition and mining control, reveals the connotation and technical path of intelligent mining in fully mechanised mining face, and condenses the key to realise intelligent mining in fully mechanised mining face

CHARACTERISTICS OF INFORMATION PERCEPTION, ANALYSIS AND CONTROL TECHNOLOGY IN DIFFERENT COAL MINING STAGES

China's coal mining has gone through the processes of manual mining, general mechanisation, comprehensive mechanisation, automated mining and intelligent mining. Coal mining technology has developed in a progressive form. The internal driving force and driving mechanism for its development and evolution is fundamentally the acquisition of production information. The changes in methods, mine production information analysis methods, and working production environment and equipment control methods are also an intuitive manifestation of the level of scientific and technological development.

1. At the stage of manual coal mining, people use manpower or simple machinery (hoes, bamboo baskets, blasting) to mine coal. The production information in the coal mining process is completely obtained by human senses. Therefore, the understanding of coal mining is only based on workers' experience, which cannot form a systematic knowledge system. The most direct and primitive manual control methods are adopted for the control of the mining environment, such as knocking on the top and wood support. In this mining stage, human beings use their own power to fight against nature (mineral pressure, coalmine gas etc).
2. In the stage of ordinary mechanised mining, the initial mechanisation of coal loading and falling coal has been realised. People's perception of information in the mining process comes from personal senses and simple mechanical contact perception. People begin to obtain mining information through mechanical senses, but only it is simple and crude. People used these simple perceptual information to summarise the laws and formed the early mining pressure theory, rock mechanics and other theories. They used these theories to control and improve the coal mining environment. However, due to the limitation of the level of machinery manufacturing, the control over the mining environment is very limited.
3. In the stage of comprehensive mechanised mining, the main links of coal mining have been

realised, including the mechanisation of tunnelling, coal breaking, coal loading, coal transportation, support, goaf treatment, and mining roadway transportation. People are concerned about the coal mining process. With the development of advanced technologies such as sensor technology and communication technology, the ability of information perception has also achieved a great leap. People have begun to obtain more microscopic, detailed and comprehensive mining information through mechanical and electronic monitoring, detection, and sampling statistical analysis. These promote people's cognition of coal mining, and a relatively complete mining and mine pressure theory system is formed, such as masonry beam theory, key layer theory, and transfer rock beam theory. At the same time, the application of mechanised equipment such as coal mining machines, hydraulic supports, and scraper conveyors has greatly enhanced people's ability to control and change the mining environment. People have begun to widely use machinery instead of manpower for mining operations, expanding human physical capabilities. However, due to the limitations of technical conditions, the information obtained at this stage is still incomplete and static. People have obvious characteristics of hysteresis, static and qualitative analysis in the use of production information, and cannot perform real-time dynamic and qualitative analysis of the mining environment, while the influence of human factors still occupies a large part.

4. The automated mining stage is to further realise equipment interconnection, information exchange, process flow, and control system automation on the basis of comprehensive mechanised mining. At this stage, human perception capabilities have been greatly expanded, mine production information has been widely acquired, and information such as equipment status, environmental conditions, and personnel location can be monitored more completely. At the same time, due to the further advancement of machinery manufacturing, industrial internet, and perception technology improvement, the interconnection of production equipment, the interconnection of production information, the automation of control systems have been realised, thus an automated operation process for coal mining operations has been formed. However, the understanding of coal mining is still based on traditional mining theories. The operation and actions of equipment are executed in accordance with established patterns or commands. Sudden changes in the mining environment, changes in the operating status of mining equipment, and interference among the machines are inability to make timely decisions and responses, it still needs to be controlled by modifying parameters or manual operations. The automatic mining stage realises the basic function of intelligent perception of production information, but due to the lack of intelligent decision-making technology, it is impossible to realise the dynamic and accurate analysis and decision-making of production information, so that the independent control of production operations cannot be realised.
5. The intelligent mining is a stage in which coal mining undergoes fundamental changes. People will be greatly or completely separated from the underground operating environment. Intelligent complete sets of fully mechanised mining equipment and various coal mining operations will realise autonomous operation, control the production behaviour by remote controlling. At this stage, the perception network can obtain production big data in an all-round, multi-dimensional, complete, and real-time manner. Through database, cloud computing, artificial intelligence and other technologies, it can perform correlation analysis among production big data, and obtain the internal data that cannot be detected by humans. To learn and predict the development law of data, the powerful information analysis and decision-making ability in the stage of intelligent mining expands human wisdom. At this stage, people's understanding of coal mining will break through the traditional mining theory and extend to the internal connection among the big data, and even bypass the 'mechanism' to control coal mining. The theoretical dimension of intelligent mining is higher than the current one. The coal mining theory still needs further exploration and improvement. In the stage of intelligent mining, real-time and accurate analysis of big data in mines, low-latency transmission of feedback information, and high-precision control of mining equipment ensure the interconnection and intercommunication of equipment groups within the mining system, forming a single point, group, and system of different forms of autonomous control, which can ensure the independent, coordinated and continuous advancement of coal mining operations.

Information perception, analysis and control technology are the essential reasons for the advancement of coal mining methods. The development of each mining stage is restricted by the current level of science and technology, coal mining cognition level, equipment technology level and other conditions, as shown in Figure 1. The intelligent mining stage is the organic integration of the experience, theory and advanced intelligent technology of the past mining stage. It represents the current development direction of coal mining. At the same time, the development of intelligent mining is phased. At present, China is in the initial stage of the development of intelligent mining. The essential connotation, characteristics and key technologies of intelligent mining still need to be continuously explored and improved.

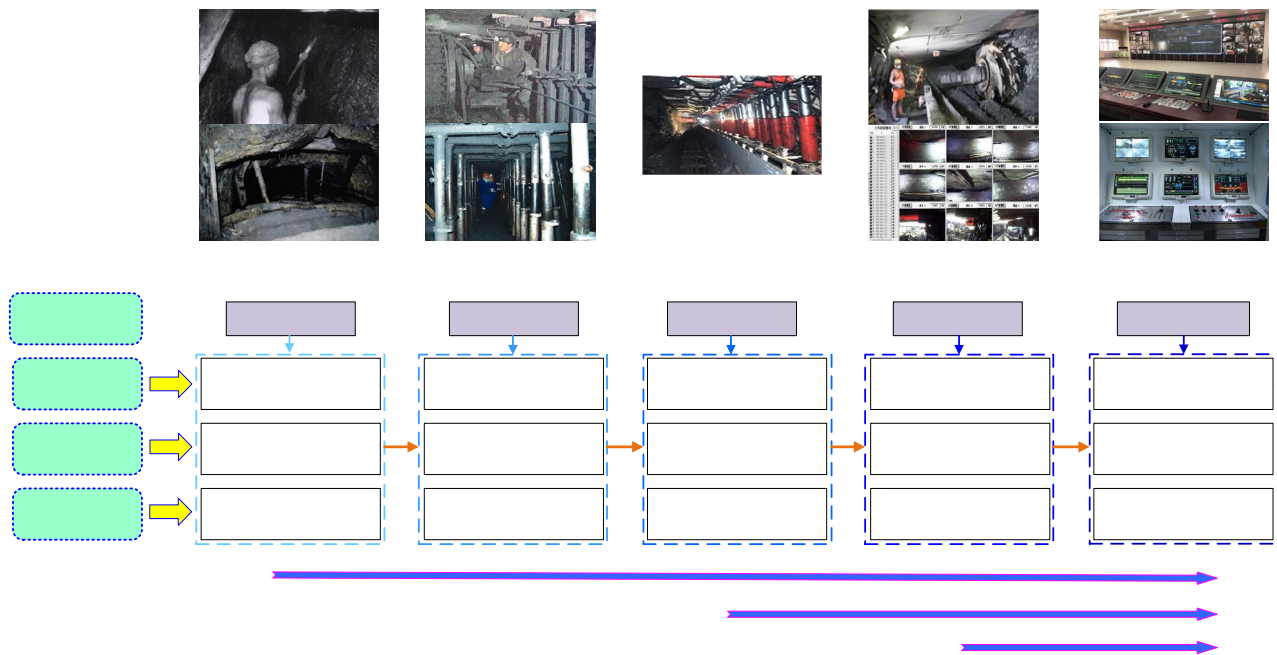


FIG 1 – Diagram of coal mining information collection, analysis and control in different mining stages.

CONNOTATION AND TECHNICAL PATH OF INTELLIGENT MINING IN FULLY MECHANISED MINING FACE

The intelligent mining of the fully mechanised mining face is based on the ‘interconnected’ intelligent complete set of fully mechanised mining equipment as the carrier. It uses the internet of things technology, artificial intelligence technology, big data technology, cloud computing technology, communication technology and coal production technology. Based on in-depth integration, through intelligent information perception, intelligent information analysis and decision-making, intelligent control and feedback, automatic coal mining technology with artificial intelligence features is realised. Its essential core includes two aspects: (1) Realise the closed-loop management of ‘ubiquitous perception-dynamic analysis-intelligent decision-real-time feedback’ of the production process of coalmine. (2) Build an ‘interconnected’ intelligent complete set of fully mechanised mining equipment system through the internet of things technology. That is, through sensing technology, communication technology, internet of things technology, digital image technology, and database technology. These various dynamic and static data such as geological exploration data, equipment operating status data, production environment data, and personnel positioning data during the production process. To carry out ubiquitous perception, stable high-speed transmission and centralised storage, use cloud computing, artificial intelligence and big data analysis technologies to conduct in-depth mining and learning of coal production big data, discover the associations between multi-source heterogeneous data, and establish equipment operation strategies and the coupling relationship model of environmental parameters. The corresponding control logic can realise the global optimal control path planning and adaptive control parameter decision-making under the mining environment and space constraints. The decision-making information is transmitted to the control and executive mechanism of the intelligent fully-mechanised mining equipment system in real time through the comprehensive

management and control platform of the working face. The single-unit, group and other modes of precise coordinated control of the equipment of the working face are carried out, and the fully-mechanised mining equipment is executed. The situation is fed back to the decision-making model in real time for dynamic correction.

As shown in Figure 2, according to the connotation of intelligent mining in fully mechanised mining face, its technical path is divided into three parts: intelligent perception of production physical scene and production big data storage, production big data association analysis and intelligent decision-making, and intelligent fully mechanised mining equipment precise coordinated control.

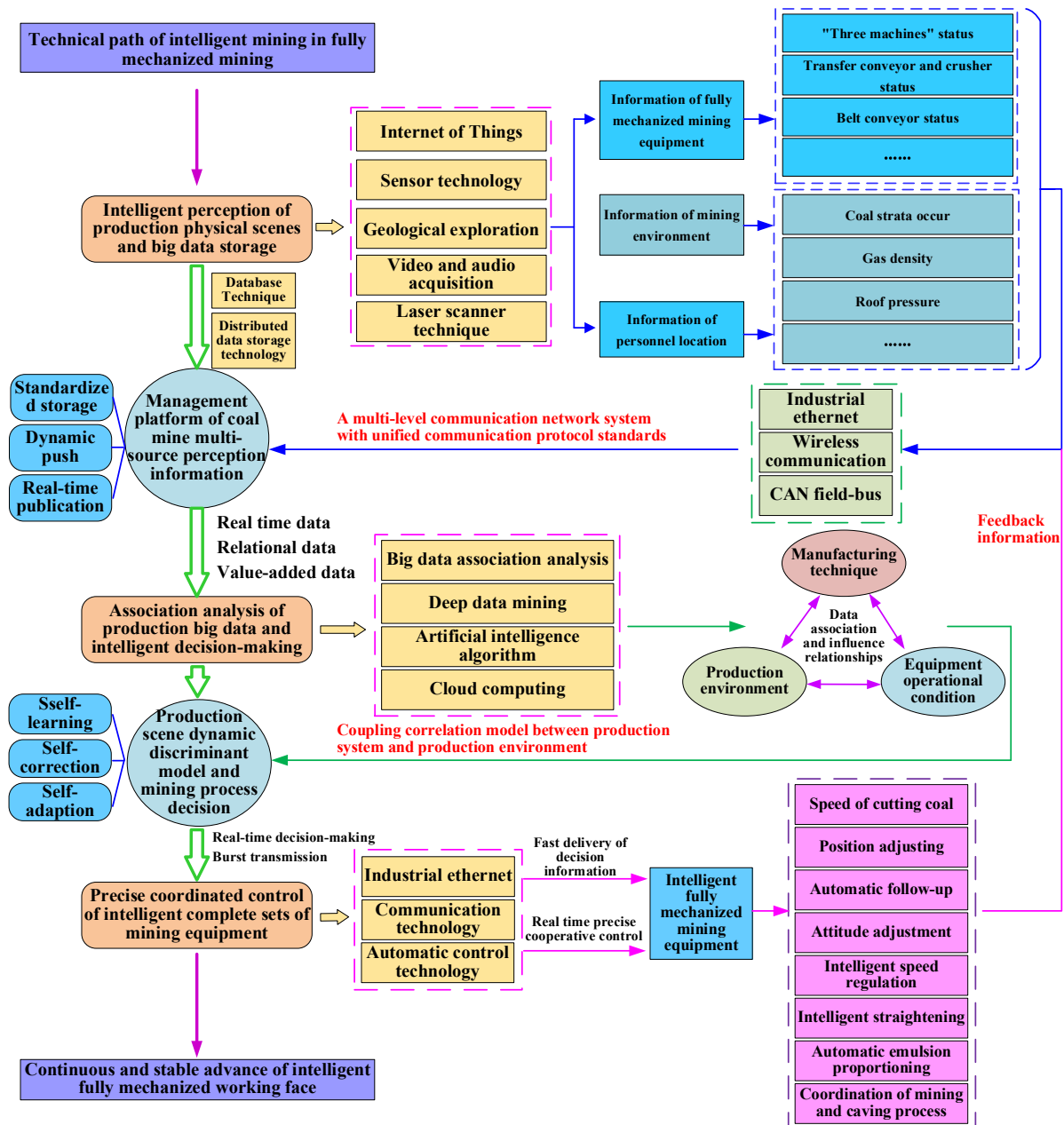


FIG 2 – Technical path of IM in fully-mechanised coal mining face.

Intelligent perception of production physical scenes and production big data storage

The intelligent perception and safe storage of the physical scene information of coalmine production are the basis for intelligent mining of fully mechanised coal mining faces. The coalmine production system is a complex and open system, including multiple types and multi-level subsystems, and there is a strong nonlinear coupling relationship between the subsystems. At the same time, the system and the external environment are undergoing material, exchange of energy

and information. Therefore, the production process of the working face will generate huge amounts of data and information, including structured data such as geomechanics data, electro-hydraulic control data, various monitoring data, mine design data, manual recording data, development mining layout and replacement information, etc. Structured data, as well as unstructured data such as video monitoring data and audio monitoring data (Li *et al*, 2019), these data are dynamic, fast, massive, multi-source, heterogeneous big data characteristics. Production big data is the key to intelligent mining. It not only provides the basis for the adaptive, self-control, and self-decision-making of the intelligent fully-mechanised mining equipment system, but also provides historical data learning samples for the artificial intelligence model to achieve dynamic prediction and control of the operating environment. The early warning control of the fully mechanised mining equipment system also provides a source for the visualisation of production data and the virtual reproduction of the mining environment (Li *et al*, 2019).

Intelligent perception of production physical scenes and mining big data storage mainly include two aspects of research content: (1) Establishing an intelligent perception network of coal production systems with internet of things technology, big data technology and other information technologies as the core, forming a comprehensive production system for mine ubiquitous information perception Information field. (2) Building a coalmine multi-source perception information management platform based on cloud database technology, distributed file storage technology and other big data storage technologies as the core to realise the unified standardised storage, dynamic push and real-time release of multi-source heterogeneous data in coalmine production.

Production big data association analysis and intelligent decision

Big data association analysis and intelligent decision-making of coal production are the core of intelligent mining in fully mechanised caving face. Artificial intelligence methods represented by deep data mining, big data association analysis, and reinforcement learning provide conditions for the full and effective use of coal production big data, which can realise the association analysis and intelligent decision-making of coal production big data, and make the data 'smart' stand up. Constrain the training of intelligent algorithms based on traditional physical models and expert experience, realise the self-discovery of the correlation law between production data, establish a coupling relationship model that can describe the production system and the mining environment (Ren *et al*, 2019), and realise the data of 'data-driven + physical guidance' cognition. Combining data cognition with dynamic mining environment changes and technological process requirements to realise the behaviour prediction and optimal operation path decision of the intelligent equipment group under multi-parameter conditions, thereby forming a global optimal control strategy for the production system.

Mine big data association analysis and intelligent decision-making mainly include two aspects of research content: (1) Adopting big data association analysis, deep data mining, web crawler and other artificial intelligence technologies to conduct production big data association analysis, discover the association mechanism between production data, and establish production Coupling correlation model between the system and the production environment. (2) Using artificial intelligence, cloud computing and other technologies to establish a production scene dynamic discrimination model and a mining process decision model, and carry out dynamic adjustment and self-learning of the model according to the control effect to realise the self-correction and self-learning of the decision model.

Precise coordinated control of intelligent complete set of fully mechanised mining equipment

The precise coordinated control of intelligent complete sets of fully mechanised mining equipment is the purpose of intelligent mining in fully mechanised caving face. The coal production system has the characteristics of complex operating environment, huge equipment system, and closely related subsystems. The intelligent mining face is a multi-agent system composed of multiple intelligent equipment. The self-decision-making of intelligent fully mechanised mining equipment should be related to production. The system's global control strategy is unified, while it is necessary to realise the rapid and accurate delivery of decision-making information to the equipment control system, the equipment executive components to accurately perform the required

actions, and the action feedback information to be submitted to the information management platform in real time to ensure the stable and reliable operation of the intelligent mining system.

The realisation of precise coordinated control of intelligent complete sets of fully mechanised mining equipment requires a unified standard protocol data information transmission network and high-reliability intelligent complete sets of fully mechanised mining equipment and other two basic guarantees, so it mainly includes two parts of research content: (1) Based on 10 Gigabit Industrial ethernet technology, internet of things technology, and 5G communication technology, establishing a unified communication protocol standard multi-level communication network system to realise the low-latency transmission of decision information, feedback information, the interconnection and intercommunication of information among various subsystems. (2) Based on Intelligent manufacturing technology, strengthening the processing accuracy of key control and executive components of intelligent fully mechanised mining equipment, and planning a complete set of manufacturing program of intelligent fully mechanised mining equipment based on top-level design to form a unified intelligent fully mechanised mining equipment system supporting specifications.

KEY TECHNOLOGIES OF INTELLIGENT MINING IN FULLY MECHANISED MINING FACE

The distinguishing feature of intelligent mining is 'intelligent perception, intelligent decision-making and automatic control', that is, the automatic collection of mine production process information, the intelligent analysis and processing of mining production big data, and the independent control of mine production equipment. Coal mining technology is developing in a progressive form. With the advancement of mining concepts, mining technology is constantly innovating and developing. At present, China is still in the initial stage of intelligent mining. According to the characteristics of intelligent mining, the following key technologies need to be studied.

Accurate geological detection and modelling technology for the whole life cycle of mining

The whole life cycle of mining includes the stages of working face planning, circle out and mining. By detecting and reconstructing the geological environment of the mining face throughout its life cycle, it provides prerequisites for the adaptive control of the fully mechanised mining equipment system at the mining face. The purpose of accurate geological detection in the whole life cycle of mining is to achieve transparency in the geological environment of the working face, that is, to use geological exploration technology, GIS (geographic information system), environmental sensors, three-dimensional laser scanning, video image monitoring and other technologies (Wang and Rong, 2019).

Multi-source, multi-dimensional, full-process, and all-round collection of geological information and geological information along with mining. Use machine vision, three-dimensional modelling, point cloud recognition, image recognition and other methods to analyse and merge the initial and mining information of the mining face to construct a dynamic three-dimensional model of the mining face's geological environment. Through GIS, virtual reality and other means, the preliminary geological information, mining geological information and coordinate information of the working face are merged to form a transparent and fine three-dimensional model of the working face, and finally realise the digital, model and visual reproduction of the invisible geological environment. Figure 3 shows the precise geological detection and modelling path for the entire production cycle.

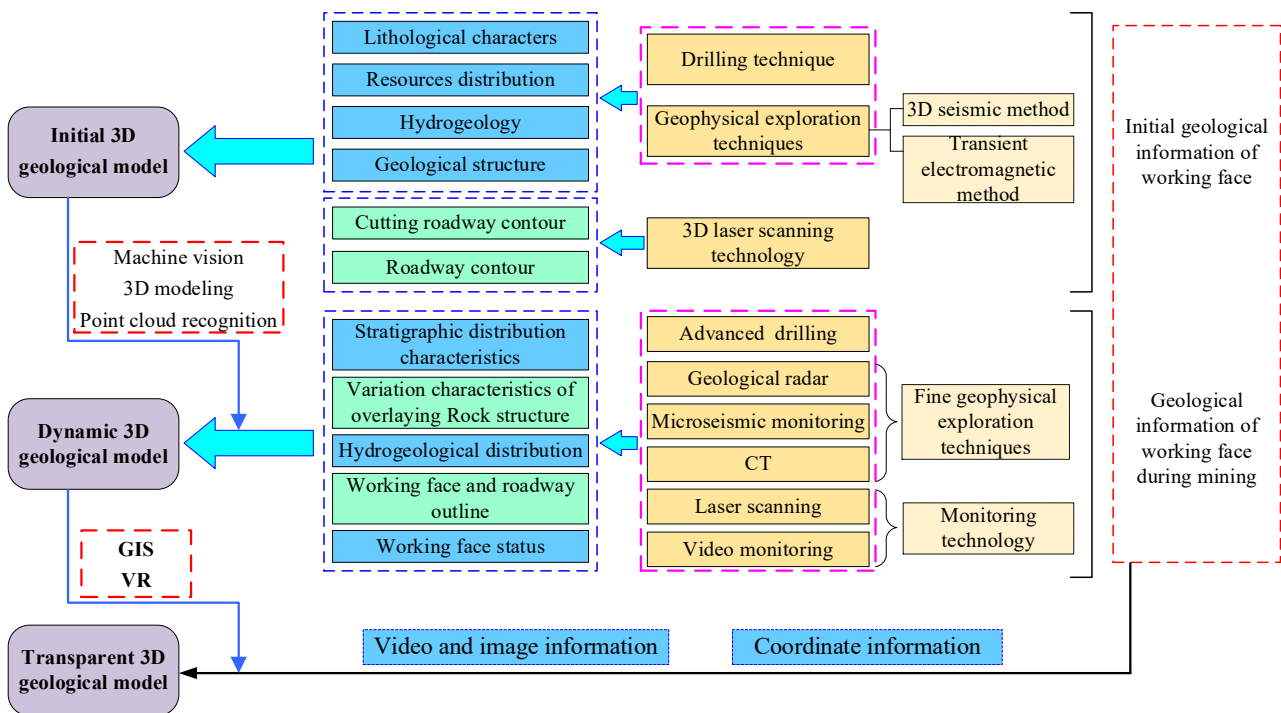


FIG 3 – Geological accurate detection and modelling approach of production full cycle.

Accurate perception technology for working face production scene

The working face production scene is a complex scene composed of mining environment, fully mechanised mining equipment and people. It includes the extensive connection of people-equipment-environment in time and space. The production of big databased on structural characteristics. Accurate production scene information perception is the basis for intelligent decision-making and adaptive control. However, it is limited by the complex underground working environment and the lack of high-reliability mining sensors, the production scene perception accuracy of the working face is low and continuous and stable perception cannot be realised.

At the same time, the lack of a distributed perception network covering the entire production link makes it difficult to form a ubiquitous perception of the production system, and there are perception blind spots. Therefore, it is necessary to develop high-performance, high-reliability, and long-life mining sensors that adapt to the complex environment of coalmines, and establish an intelligent perception network for production systems based on the internet of things technology to build a precise ubiquitous perception information field for production scenarios.

Establish information transmission system with standardised communication protocols

The intelligent fully mechanised mining face is a multi-agent system, and there are multiple technical links such as exploration, mining, transportation, monitoring and control. The interconnection of various subsystems and production links requires a smooth information transmission system, but the current intelligent fully mechanised mining work The equipment system on the front is only a shallow level of integration. There are many kinds of comprehensive mining equipment data interfaces and communication protocols, the working face communication protocol standards are not unified, wireless networks and industrial ethernet networks coexist etc, resulting in the interconnection and interoperability of production big data, obstacles, poor network carrying capacity, poor timeliness of data transmission, and difficulty in multi-source heterogeneous data fusion, which cannot achieve timely reception of intelligent decision-making and rapid response of intelligent control.

The production big data communication protocol standard system should be established on the basis of industrial ethernet communication technology and internet of things technology, and a 'one net to the end' mine production system network architecture should be established to realise the real-time and rapid transmission of production equipment data and the height of heterogeneous

data, increase the reliability of data communication and anti-interference. At the same time, 5G communication technology has the characteristics of enhanced mobile broadband, ultra-reliable and ultra-low latency, and large-scale machine connections. It has good development prospects in production scenarios such as precise positioning of production equipment, real-time control, and remote coordinated operation and maintenance (Wang, Zhao and Hu, 2020). The research of 5G communication technology in the field of coal production information transmission should be strengthened.

Intelligent decision-making technology in complex production environment

At present, the key to the difficulty of intelligent mining in China for normalised and intelligent mining lies in the lack of autonomous decision-making and adaptive control capabilities for the dynamic environment of the fully mechanised mining equipment system, the lack of algorithms for in-depth mining of multi-source heterogeneous production big data. The theory and model of the impact mechanism of mining environment on fully mechanised mining equipment are not yet complete. It is impossible to effectively detect the correlation relationships among the multi-source, multi-dimensional, and multi-modal data in the mining process, and difficult to make optimal path decisions for equipment behaviour according to environmental changes.

The intelligent decision-making technology in the complex environment is the deep integration of the internet, artificial intelligence, data standardised transmission, cloud computing and other technologies to conduct correlation analysis, in-depth mining, and in-depth learning of big data in mine production, and analyse the operation status of equipment in the process of mining, the stress field of surrounding rock, gas distribution field and other multi-level, multi-characteristic information coupling and influence relationship, establish intelligent decision-making model in complex mining environment, and assist intelligent decision-making through human-computer interaction, and continuously optimise the model until it can achieve real-time, fast and accurate analysis and decision-making of big data in production.

Reliability enhancement technology of intelligent fully mechanised mining equipment system

Intelligent fully mechanised mining equipment is the carrier to realise the intelligent mining of fully mechanised mining face. It is an intelligent body that organically integrates sensing components, control systems, communication systems and mechanical structures. The high-reliability and intelligent complete set of fully mechanised mining equipment realises intelligent perception, intelligent decision-making and automatic control and other intelligent mining functions. The traditional decentralised manufacturing model of fully mechanised mining equipment and the mining control concept of 'mainly single-machine equipment and overall coordination' make the production systems separate and independent of each other, resulting in insufficient reliability of the single-machine and system of intelligent fully-mechanised mining equipment, restricting the cooperative operation capability of fully mechanised mining equipment.

It should be based on the concept of top-level design to develop intelligent comprehensive mining equipment and its auxiliary systems to improve the level of intelligent manufacturing and supporting equipment. At the same time, based on the standardised information transmission system, the 'intelligent equipment master control system integrated decision-making, stand-alone equipment distributed execution' should be constructed. The control system architecture of the company forms an intelligent comprehensive mining equipment system that is coordinated, adapted and linked to each other, and realises the precise coordinated management and centralised coordinated control of the production equipment group of the working face.

CONCLUSIONS

Based on the above mentioned analysis, the main conclusions can be obtained as following:

1. The characteristics of information perception, analysis and control technology in different mining technology stages is analysed, and the core of that the intelligent mining is to transform the mining problem into an information processing problem is clarified. Based on the 'interconnected' intelligent comprehensive mining equipment system, the closed-loop

management of 'ubiquitous perception-dynamic analysis-intelligent decision-real-time feedback' of big data in mine production is realised.

2. It is clear that the connotation of intelligent mining is to use the 'interconnected' intelligent comprehensive mining equipment as the carrier, and use the internet of things technology, artificial intelligence technology, big data technology, cloud computing technology, communication technology and other modern technologies and coalmine production technology. Based on in-depth integration, through intelligent information perception, intelligent information analysis and decision-making, intelligent control and feedback, the automatic coal mining technology with artificial intelligence features is realised.
3. The path to realise intelligent mining technology is given as the intelligent perception of production physical scenes and the storage of big data in mines, the associated analysis and intelligent decision-making of big data in mines, and the precise coordinated control of intelligent production equipment. The key technical issues that need to be solved urgently in intelligent mining, such as the precise geological detection and modelling technology for the whole life cycle of mining, the precise perception technology of working face production scene, the establishment of an information transmission system with standardised communication protocol, intelligent decision-making technology under complex production environment, and reliability enhancement technology of intelligent fully mechanised mining equipment system.

ACKNOWLEDGEMENTS

This study was supported by the National Key R and D Program Funding Project (2018YFC0604500), and provided the industrial test site by Jinneng Holding Group Tongxin Coalmine, China.

REFERENCES

- Li, H, Ji, Y and Zhang, X, 2019. Study on autonomic tilting and offsetting technology of hydraulic support in fully-mechanised working face, *Coal Science and Technology*, 47(10): 167–174.
- Li, H M, Wang, S, Li, D Y, Wang, W, Yuan, R F, Wang, Z G and Zhu, S T, 2019. Intelligent ground control at longwall working face, *Journal of China Coal Society*, 44(1): 127–140.
- Li, S B, 2019. Progress and development trend of intelligent mining technology, *Coal Science and Technology*, 47(10): 102–110.
- Lu, C C, 2018. General structure design of intelligent control system for shearer, *Mineral Engineering Research*, 33(1): 54–57.
- Luo, Y G and Fu, R L, 2019. Control system of intelligent scraper conveyor in coalmine based on frequency conversion technology, *Colliery Mechanical and Electrical Technology*, 40(5): 18–22.
- Niu, J F, 2019. Research on unmanned key technology of fully-mechanised mining face based on video inspection, *Coal Science and Technology*, 47(10): 141–146.
- Ren, H W, Wang, G F, Zhao, G Y, Du, Y B and Li, S S, 2019. Smart coalmine logic model and decision control method of mining system, *Journal of China Coal Society*, 44(9): 2923–2935.
- Song, Z Q, 2014. Intelligent safe and efficient mining technology present situation and prospect, *Coal and Chemical Industry*, 37(1): 1–4.
- Sun, J P, 2015. 'Internet+coal' and coalmine informationalization, *Coal Economic Research*, 35(10):16–19.
- Wang, C F and Rong, Y, 2019. Concept, architecture and key technologies for transparent longwall face, *Coal Science and Technology*, 47(7): 156–163.
- Wang, G F, Liu, F, Meng X J, Fan, J D, Wu, Q Y, Ren, H W, Pang, Y H, Xu, Y J, Zhao, G R, Zhang, D S, Cao, X G, Du, Y B, Zhang, J H, Chen, H Y, Ma, Y and Zhang, K, 2019. Research and practice on intelligent coalmine construction (primary stage), *Coal Science and Technology*, 47(8):1–36.
- Wang, G F, Pang, Y H and Ren, H W, 2020. Intelligent coal mining pattern and technological path, *Journal of Mining and Strata Control Engineering*, 2(1): ID 13501.
- Wang, G F, Wang, H, Ren, H W, Zhao, G R, Pang, Y H, Du, Y B, Zhang, J H and Hou, G, 2018. 2025 scenarios and development path of intelligent coalmine, *Journal of China Coal Society*, 43(2): 295–305.
- Wang, G F, Zhao, G R and Hu, Y H, 2020. Application prospect of 5G technology in coalmine intelligence, *Journal of China Coal Society*, 45(1): 16–23.

- Wang, J B, Wang, Z B, Zhang, L, Xu, J and Li, F S, 2016. Research on electro-hydraulic control system of hydraulic support based on Ethernet and CAN-Bus, *Journal of China Coal Society*, 41(6): 1575–1581.
- Xie, H P, Wang, J H, Shen, B H, Liu, J Z, Jiang, P F, Zhou, H W, Liu, H and Wu, G, 2012. New idea of coal mining: scientific mining and sustainable mining capacity, *Journal of China Coal Society*, 37(7): 1069–1079.
- Xie, H P, Wu, L X and Zheng, D Z, 2019. Prediction on the energy consumption and coal demand of China in 2025, *Journal of China Coal Society*, 44(7): 1949–1960.
- Yu, B, Xu, G, Huang, Z Z, Guo, J G, Li, Z, Li, D Y, Wang, S B, Meng, E C, Pan, W D, Niu, J F, Xue, J S and Zhao, T L, 2019. Theory and its key technology framework of intelligentized fully-mechanised caving mining in extremely thick coal seam, *Journal of China Coal Society*, 44(1): 42–53.
- Yuan, L, 2017. Scientific conception of precision coal mining, *Journal of China Coal Society*, 42(1): 1–7.

Development of spilling judgment system for dump truck loading using digital twin technology

T Sato¹, K Yoshino², H Toriya³, M Saadat⁴, H Kuroki⁵, Y Goto⁶, I Kitahara⁷ and Y Kawamura⁸

1. Masters student, Graduate School of International Resource Sciences, Akita University, 1-1 Tegatagakuen-machi, Akita City 010-8502, Japan. Email: t.sato.mtl@gmail.com
2. Masters student, Degree Programs in Systems and Information Engineering, University of Tsukuba, 1-1-1 Tennoudai, Tsukuba City 305-0006, Japan. Email: yoshino.kohei@image.iit.tsukuba.ac.jp
3. Assistant Professor, Graduate School of International Resource Sciences, Akita University. 1-1 Tegatagakuen-machi, Akita City 010-8502, Japan. Email: toriya@gipc.akita-u.ac.jp
4. Associate Professor, Graduate School of International Resource Sciences, Akita University. 1-1 Tegatagakuen-machi, Akita City 010-8502, Japan. Email: mahdi.saadat1@gipc.akita-u.ac.jp
5. Group leader, ICT Engineering Group, Mechatronics Engineering Department, Technology Institute, Asunaro Aoki Construction, 36-1 Kaname, Tsukuba City 300-2622, Japan. Email: hirotadakuroki@aaconst.co.jp
6. Researcher, ICT Engineering Group, Mechatronics Engineering Department, Technology Institute, Asunaro Aoki Construction, 36-1 Kaname, Tsukuba City 300-2622, Japan. Email: yoshiko.goto@aaconst.co.jp
7. Professor, Center for Computational Sciences, University of Tsukuba, 1-1-1 Tennoudai, Tsukuba City 305-0006, Japan. Email: kitahara@ccs.tsukuba.ac.jp
8. Professor, Faculty of Engineering, Division of Sustainable Resources Engineering, Hokkaido University, Kita 13, Nishi 8, Kita-ku, Sapporo City 060-8628, Japan. Email: kawamura@eng.hokudai.ac.jp

ABSTRACT

The incorporation of digital technology in the mining industry has received many positive feedback in recent years. A good example is the utilisation of autonomous dump trucks in haulage operations. This application, however, does not come without shortfalls such as spilling due to overloading. When spilling occurs, dump trucks are more susceptible to a number of accidents including the reduction of brake performance, excessive exhaust gas emission, and the overall wearing of the body and engine. As a countermeasure, recently, several studies have been conducted regarding the development of loading volume measurement systems. One of such consists of measuring instruments directly mounted on dump trucks, as well as one based on volume measurement using laser scanning mounted orthogonally above the dump truck. These systems can however be complex and difficult to install on all heavy machinery and sites. Moreover, the systems can be expensive, time-consuming and are generally made for a single specialised purpose. This study therefore proposes an improvement to these systems via use of drones and digital twin technology for detecting dump truck overloading and spilling. The utilisation of drones is already prevalent in the mining industry looking to digitise the operations, and as such, the possible application of this technology would be smooth and cost-efficient loading and haulage operation. This system works by capturing several photographs using a drone from multiple points around the truck during loading. From these images, photogrammetry is used for constructing a 3D point cloud model of the dump truck plus load. By analysing this model, the shape and volume of the load are derived to extrapolate the loading status of the dump truck. Based on this technology, the proposed method has the potential to allow better load control for dump trucks, thereby increasing the overall productivity of a mine through system optimisation.

INTRODUCTION

The mining industry is currently facing a dire situation where the cost of development and investment is on the rise due to declining ore grades and deepening mine depths. A drop of a few dollars per ton in the price of ore can, in some cases, be enough to render a mine completely unprofitable. The implementation of smart mining technologies for the purpose of reducing operating costs, improving efficiency, safety and productivity is increasingly becoming popular. Thus, the need to reduce costs by optimising operations and implementing predictive maintenance.

When dump trucks are used in mining operations to transport mined material, there is a risk of material spillage due to overloading or off-centre loading. This may especially be the case in mines where vehicles are becoming increasingly automated as a single piece of spilt material on the haulage road can lead to an accident that interferes with operations. When overloading occurs, dump trucks are more susceptible to incidents from reduced brake performance, poor steering control, noise pollution, excessive exhaust gas emission, and the overall wearing of the body and engine (Shah *et al*, 2016; Scott *et al*, 2010). A few studies have been conducted with the aim of optimising the loading and hauling process, one of which is the development of loading volume measurement systems. One of the systems was created by Caterpillar (Caterpillar, 2021) which consists of measuring instruments directly mounted on dump trucks. The other system is based on volume measurement using laser scanning (Duff, 2000) mounted orthogonally above the dump truck. However, since these systems have to be specially installed in dump trucks, an improvement may be made in the form of assigning this particular task to a drone, something that is already prevalent nowadays in most of the mine sites.

In recent years, drones (Clarke, 2014) have been used to survey mines in order to improve efficiency and reduce operating costs, as they are relatively inexpensive compared to laser scanning and can be easily installed at any site.

Drone mining surveys (Shahmoradi *et al*, 2020) mainly use a drone equipped with a downward-facing RGB camera to capture images of the site from various viewpoints. Photogrammetry is then used to create digital surface models from the captured images. This creation of a 3D replica of physical features constitutes a part of Digital Twin Technology. As Digital Twin Technology becomes popular in the mining industry, drone surveying will most likely proliferate in mines, even more than before.

The purpose of this study is to develop a spilling judgment system for dump truck loading using Digital Twin Technology by analysing the shape and volume of the dump truck loading from a 3D point cloud model created using photogrammetry from an image data set captured by a drone. The system overview for the described process is shown in Figure 1.

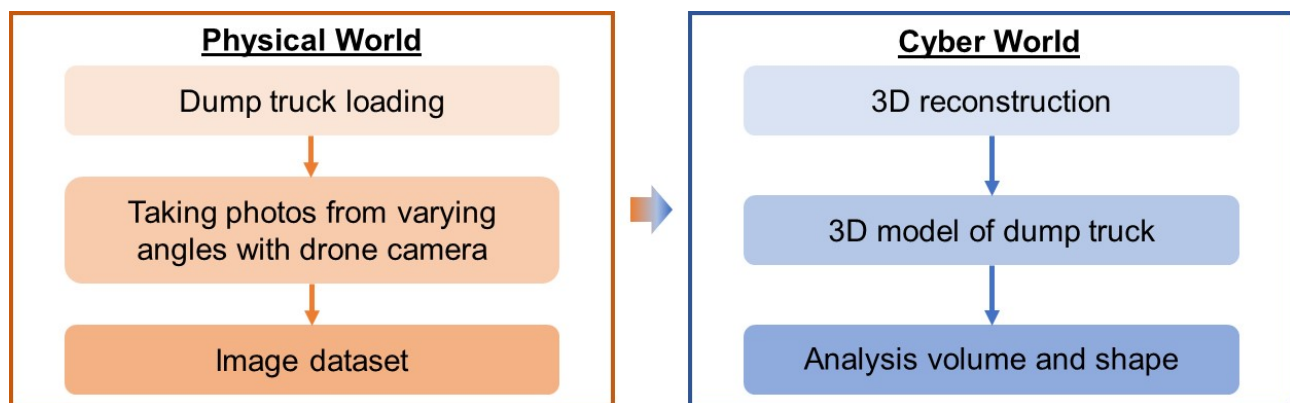


FIG 1 – System overview.

LITERATURE REVIEW

The development of spilling judgment system for dump truck loading will lead to the optimisation of the entire hauling process by preventing accidents, reducing hauling costs, and improving the technical skills of operators. In addition, by preventing unexpected spillage of rocks in mines, it is possible to prevent accidents involving vehicles that operate autonomously. The points considered in the present research are volume, off-centre loading, and payload.

Volume

Calculating the volume of a dump truck load can lead to increased profits as incorrectly loaded trucks can easily be identified and repaired. In addition, calculating the volume of a dump truck load allows for accurate measurement that takes into account the water content and density of the load, which can change the weight of the load. In the past, due to the variation in the density of the rock, there was a discrepancy between the amount of rock actually transported by the dump truck and the

amount delivered at the mill for processing, hence, this discrepancy should be eliminated. In addition, visual confirmation of the volume using laser scanning can lead to improved operator performance and optimisation of the trucking factor. A volume scanning system has been developed (Duff, 2000) to analyse the volume of the load as well as the detection of off-centre-loading. However, this system is specifically used for this one task – ‘measuring the volume of a dump truck’. The proposed system, on the other hand, utilises multi-purpose UAV technology, which is also already prevalent in most modern mining operations (Said *et al*, 2021).

Off-centre loading

Off-centre loading is a condition in which the load distribution is off centre and uneven when loading crushed rock into a dump truck. Therefore, off-centre loading is a cause of load collapse and should be taken into consideration when loading. In recent years, in order to measure off-centre loading, Loadscan have installed a Load Volume Scanner (LVS) system (Loadscan, 2021) in advance at the point where the dump truck passes. This allowed implementation of 3D scanning from overhead so as to recognise the shape of the load. Moreover, this allows for easy identification of the load and visual confirmation of the loading process, which in turn helps train operators.

Payload

Payload fluctuations affect mine productivity, load shedding, and overall costs. However, it is very difficult for even the most experienced operators to load the correct amount of crushed rock into a dump truck. Payload variance can be reduced by utilising the latest developed technologies such as the online fleet monitoring system, the truck on-board payload measurement system, and its connection with the shovel control system. Payload variance affects the truck availability, maintenance costs, the production rate, and the fuel consumption. In recent years, CAT (Caterpillar, 2021) have developed a system to install a measuring device directly on heavy machinery, which allows for the determination of the weight of rock in the payload, as well as in the bucket. However, weight alone is not an accurate standard for defining payloads and load shifting as it does not take into account the water content and density of the rock.

METHODOLOGY

The first step in this system is to capture images of the dump truck from multiple viewpoints using a drone. The image data set obtained by the drone is then used to create a 3D point cloud model of the dump truck. Structure from Motion (SfM) (Snavely, Seitz and Szeliski, 2006) is then used as a technique to create this 3D point cloud model. The shape and volume of the created 3D point cloud is consequently used to analyse the loading status of the dump truck, such as whether it is off-centre or overloaded.

Advantages of drone photography

A drone is a computer-controlled flying robot capable of autonomous flight, also known as a small unmanned aircraft, Unmanned Aerial Vehicle (UAV), or Unmanned Aerial System (UAS) (Clarke, 2014). There are at least three advantages of using a drone for imagery surveys. The first is that it is easier and cheaper to obtain high-resolution photos than conventional manned aircraft. Second, the ability to hover at low altitudes and move freely up, down, left, and right makes it possible to take photographs from various angles, even of complex target sites. Third, it is possible to take detailed photographs of mines, volcanoes, swollen rivers, and landslides that are dangerous or difficult for humans to survey directly.

3D reconstruction in cyber world using Structure from Motion (SfM)

SfM is a 3D photogrammetric technique that simultaneously recovers the position and orientation of the camera and the 3D shape of an object from multi-view images of the object taken from various angles. SfM is a linear formulation of the factorisation method and uses a numerically stable matrix singular value decomposition to recover the camera motion and shape and output the object as a point cloud. The process of 3D photogrammetry is shown in Figure 2, where the 3D shape is constructed by simply transforming the 2D image coordinates (x, y) of multiple photos into 3D coordinates (X, Y, Z). This is performed with assumption that the two photographic directions for the

projection centre point (C_1, C_2) and the entity point (m_1, m_2) are known. Thereafter, the object point (M_1) in 3D imaginary coordinates is represented by finding the intersection of two matching entity points in photo 1 and 2, which is called image matching. The result of SfM reconstruction is often spatially sparse, hence the Patch-based Multi-View Stereo (PMVS) (Furukawa and Ponce, 2009) is applied. A typical sequence of 3D model reconstruction is shown in Figure 3, where image data acquisition and processing are first performed, followed by 3D shape reconstruction and texture reconstruction.

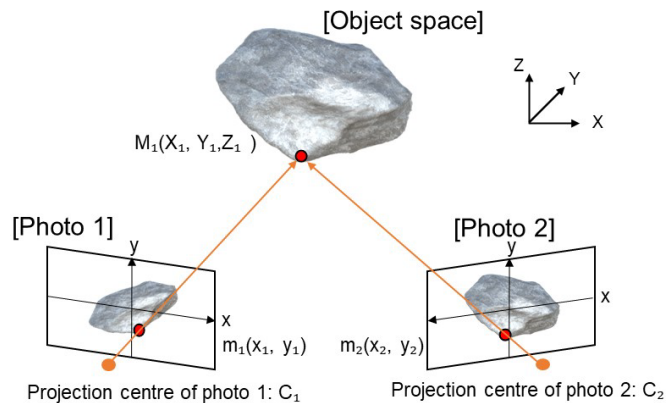


FIG 2 – The process of 3D photogrammetry.

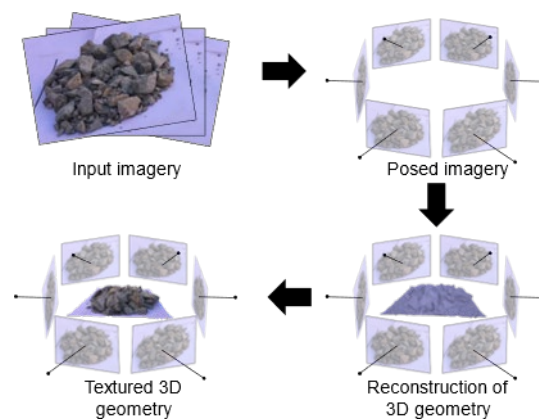


FIG 3 – 3D reconstruction process.

Distance measurement methods

Distance measurement methods were used to analyse the geometry of the point cloud. There are various ways in which this method may be applied. The first is the differential Digital Elevation Models (DEM) (Wheaton *et al*, 2010). DEM of difference is the most common method of point cloud comparison in earth sciences when the large-scale geometry of the scene is planar. The two point clouds are gridded to generate DEMs either directly if the large scale surface is near horizontal (Lane, Westaway and Hicks, 2003; Milan, Heritage and Hetherington, 2007; Wheaton *et al*, 2010; Schürch *et al*, 2011) or after rotation (Rosser *et al*, 2005; Abellán *et al*, 2010; O'Neal and Pizzuto, 2010). The two DEMs are then differentiated on a pixel-by-pixel basis which is similar to measuring a vertical distance (Lague, Brodu and Leroux, 2013). The second is direct cloud-to-cloud comparison with closest point technique (C2C). This method is the simplest and fastest direct 3D comparison method of point clouds as it does not require gridding or meshing of the data, nor calculation of surface normal (Girardeau-Montaut *et al*, 2005). For each point of the second point cloud, a closest point can be defined in the first point cloud. In its simplest version, the surface change is estimated as the distance between the two points. Improvements can be obtained by a local model of the reference surface either by an height function or by a least square fit of the closest point neighbours (Girardeau-Montaut *et al*, 2005). This technique is also used in cloud matching techniques such as the ICP (Chen and Medioni, 1992; Besl and McKay, 1992). The third method is Multiscale Model to Model Cloud Comparison (M3C2). This difference analysis is a method for calculating and analysing the differences between 3D models by approximating and calculating the plane shape from a set of

points extracted at an arbitrary density from the point cloud data, and then calculating the distance from the calculated plane to the individual point cloud data. The calculation result is a set of data with point coordinates and differences, which can be handled quantitatively. In this study, the third method was used.

Volume analysis

To compute the volume of the 3D point cloud, the method used CloudCompare's calculate 2.5D Volume tool (CloudCompare, 2021), which generalises the point cloud to a surface elevation model, then calculates volume on the basis of the difference between the surface model and a fixed ground elevation. In this calculation, each cell's contribution is summed. This contribution is simply the volume of the elementary parallelepiped corresponding to the cell footprint multiplied by the difference in heights. Only the cells which have a valid height value for both the 'ground' and the 'cell' are used for the global volume estimation.

Slope of the load analysis

In order to analyse the angle of repose, the shape and slope of a truck load is analysed. The angle of repose is an important concept in understanding the slope made of non-adhesive debris such as rocks and sand as shown in Figure 4, and is generally the maximum angle of inclination at which these objects can remain stationary without external disturbance. The angle of repose can then be applied to the loading of a dump truck and analysed to understand the slope. In the case of a dump truck, it is not in a state of no disturbance but in a state of constant movement, hence, if the slope is equal to or greater than the angle of repose, it is referred to as overloading. There are standards for angle of repose as shown in Table 1, and the angle of repose for limestone is 30–40° (Omega, 2013). In the analysis, the point cloud model of the dump truck is rasterised and contour lines are created every 0.05 m, and the inclination angle is calculated from the height and width of the contour lines.

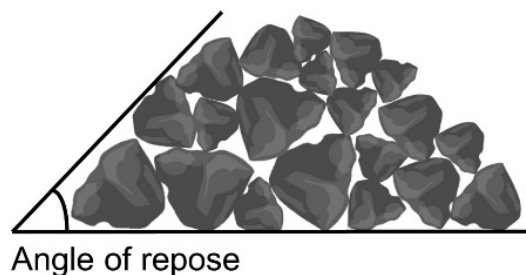


FIG 4 – Overview of angle of repose.

TABLE 1

Angle of repose for limestone.

Material	Density (lbs/ft ³)	Angle of repose
Lime, pebble	55-65	30-40°
Limestone, crushed	85-95	30-40°
Limestone, dust	68	45°

EXPERIMENTAL AND ANALYTICAL RESULTS

Experimental conditions

The dump truck used for the study was 2.8 m high and 8 m long. Photography experiments were conducted using DJI's drone under normal loading and overloading conditions. In the experiment, the route was set such that the truck could be photographed from the centre, allowing for a 360° view. The flight, photography, and return were pre-set to take place automatically. Figure 5 shows the photos of the dump truck taken by the drone. These photos were used as a data set for 3D reconstruction.

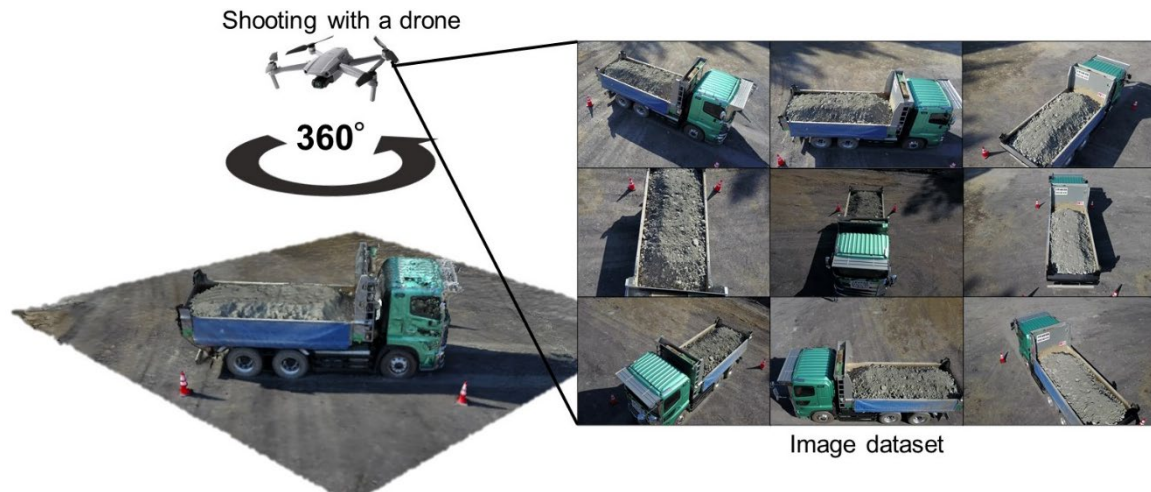


FIG 5 – Photos of the dump truck taken by the drone.

3D reconstruction using SfM

The output of the dump truck model from the data set was performed according to the workflow shown in Figure 6. Agisoft Metashape (Agisoft, 2021) was used to deduce the camera position as well as point cloud data coordinates. A PC with an Intel Corei7–9750H 2.60 GHz CPU and an NVIDIA GeForce RTX 2060 16 GB GPU was used for data processing. The number of photographs used in the model was 132 for both normal loading and overloading, and a point cloud with about 1.61 million points was generated. Figure 6 also shows the 3D reconstructed dump truck with left side showing the sparse point cloud. The estimated shooting position is shown above the dump truck.

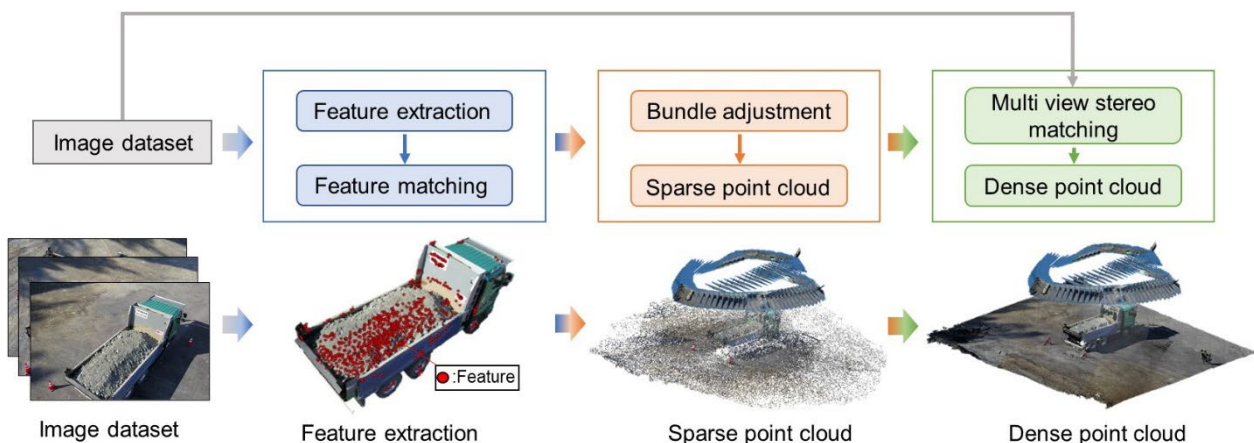
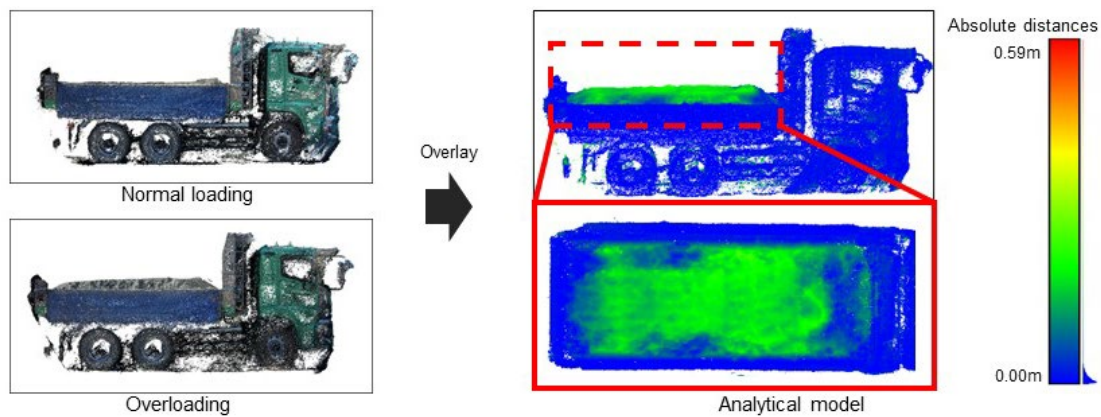


FIG 6 – Typical 3D reconstruction pipeline.

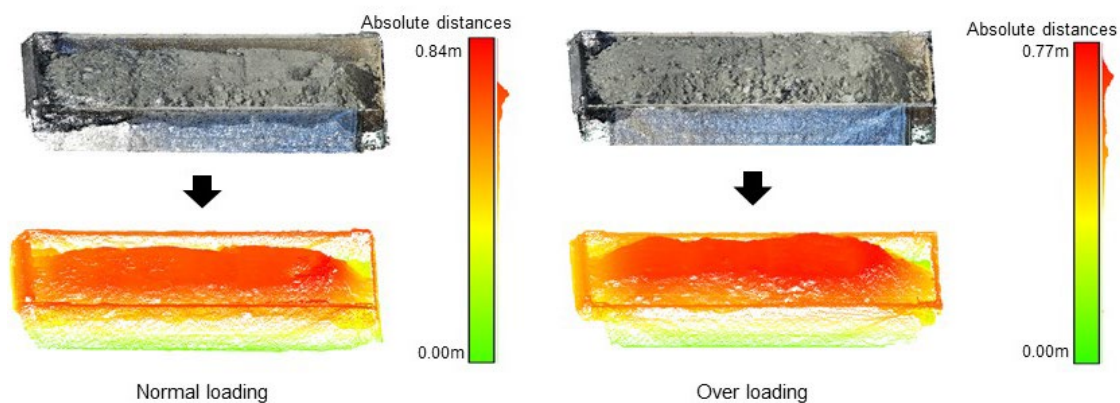
SfM Analysis of 3D model

The output data was analysed using CloudCompare, a point cloud analysis software for 3D models. In the analysis using distance measurement methods, the analysis was conducted between the 3D models of a normal loaded dump truck and an overloaded dump truck. The results are shown in Figure 7(a). CloudCompare's M3C2 plug-in was used to analyse the point cloud data (Lague, Brodu and Leroux, 2013). A blue dot indicates that the distance is zero, and the closer the dot is to red, the greater the distance is in metres from a normal load (blue colour). According to this analytical model, it is relatively easy to see where the load is clearly overloaded. In addition, the front area (green colour) of the loading area is particularly overloaded, hence the centre of gravity is shifted, indicating that load spillage may occur.

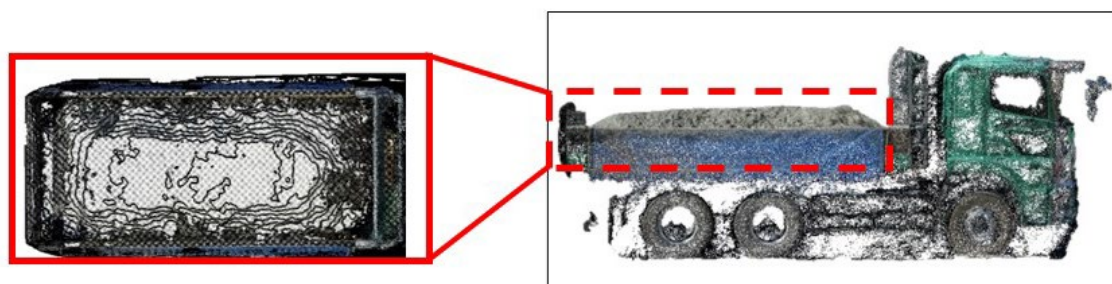
For the volume analysis, the 2.5D Volume tool with CloudCompare to calculate the 2.5D grid of the 3D reconstructed dump truck and estimate the volume using each cell in the grid was used. Figure 7(b) shows the output results of the experiment. The volume of a normal load was 6.476 m^3 , whilst the overloaded load volume was 7.215 m^3 . From the difference of the volumes, the overloaded volume turns out to be 0.739 m^3 .



(a) The flow of distance measurement and result



(b) Result of volume calculation



(c) Result of slope of load analysis

FIG 7 – Three-way analysis of the SfM-generated 3D model.

For the angle of repose analysis, the data in point cloud format was converted to raster format in order to simplify the process of drawing contour lines every 0.05 m, aiding in easier extrapolation of the slope angle based on the distance between contour lines. As a result of the calculation, the angle of repose in the case of overloading was 45°. Figure 7(c) shows contour lines (right) from an aerial view, as well as the cross-sectional view of the truck (left). From this figure, the concentration of contours at the front side of the dump truck is made obvious.

CONCLUSIONS

In this study, spilling assessment of dump truck loading using digital twin technology was performed. An automatic route was set-up from take-off to shooting and return, which allowed efficient acquisition of photos from multiple views, thereby creating an image data set of the dump truck. Using the data set comprised of 132 photos, an elaborate dump truck model with a point cloud of about 1.61 million points was created. The shape of the point cloud was analysed, and the distance measurement between the overloaded and normal loaded dump truck revealed where the truck was overloaded, as well as confirming the inconsistencies in truck material loading. In the inclination analysis, overloading of the truck by comparing it with the angle of repose was detected. The

volumetric analysis was able to compute how much the load was overloaded compared to the normal loading. As a result of the above observations using the digital twin technology, it was determined that this method is effective in determining the loading status of dump trucks. In general, in Japan, weight restrictions are installed on dump trucks to prevent load shifting, but weight restrictions alone are insufficient. However, based on the results of this experiment, it is possible to reduce the risk of spillage by using the proposed methods as they take advantage of drone technology, which make it easy to employ in almost any site. Future research can be continued to reduce the computational cost of 3D reconstruction and analysis.

REFERENCES

- Abellán, A, Calvet, J, Vilaplana, J, M and Blanchard, J, 2010. Detection and spatial prediction of rockfalls by means of terrestrial laser scanner monitoring. *Geomorphology*, 119 3–4, pp 162–171.
- Agisoft, 2021. *Agisoft*, viewed 3 June 2021, <<https://www.agisoft.com/>>.
- Besl, P, J and McKay, N, D, 1992. Method for registration of 3-D shapes, in *Sensor fusion IV: control paradigms and data structures*, Vol 1611, pp 586–606 (International Society for Optics and Photonics).
- Caterpillar, 2021. *Cat Payload Technology*, viewed 3 June 2021, <https://www.cat.com/en_US/by-industry/construction-industry-resources/technology/payload.html>.
- Chen, Y and Medioni, G, 1992. Object modelling by registration of multiple range images, *Image and vision computing*, 10.3, pp 145–155.
- Clarke, R, 2014. Understanding the drone epidemic, *Computer Law and Security Review*, 30.3, pp 230–246.
- CloudCompare, 2021. *CloudCompare*, viewed 3 June 2021, <<https://www.danielgm.net/cc/>>.
- Duff, E, 2000. Automated volume estimation of haul-truck loads, In *Proceedings of the Australian Conference on Robotics and Automation*, pp 179–184 (CSIRO).
- Furukawa, Y and Ponce, J, 2009. Accurate, dense, and robust multiview stereopsis, *IEEE Transactions on Pattern Analysis and Machine Intelligence*, 32.8, pp 1362–1376.
- Girardeau-Montaut, D, Roux, M, Marc, R and Thibault, G, 2005. Change detection on points cloud data acquired with a ground laser scanner, *International Archives of Photogrammetry, Remote Sensing and Spatial Information Sciences*, 36 3, W19.
- Lague, D, Brodu, N and Leroux, J, 2013. Accurate 3D comparison of complex topography with terrestrial laser scanner: Application to the Rangitikei canyon (N-Z), *ISPRS Journal of Photogrammetry and Remote Sensing*, 82, pp 10–26.
- Lane, S, N, Westaway, R M and Hicks, D M, 2003. Estimation of erosion and deposition volumes in a large, gravel-bed, braided river using synoptic remote sensing, *Earth Surface Processes and Landforms*, 28.3, pp 249–271.
- Loadscan, 2021. *Technical Specifications*, viewed 3 June 2021, <<https://www.loadscan.com/load-volume-scanner-2/specifications/>>.
- Milan, D, J, Heritage, G, L and Hetherington, D, 2007. Application of a 3D laser scanner in the assessment of erosion and deposition volumes and channel change in a proglacial river, in *Earth Surface Processes and Landforms: The Journal of the British Geomorphological Research Group*, 32.11, pp 1657–1674.
- OMEGA, 2013. *MATERIAL CHARACTERISTIC GUIDE*, viewed 1 June 2021, <https://www.omega.co.uk/green/pdf/MaterialChar_Guide.pdf>.
- O'neal, M, A and Pizzuto, J, E, 2010. The rates and spatial patterns of annual riverbank erosion revealed through terrestrial laser-scanner surveys of the South River, Virginia, *Earth Surface Processes and Landforms*, 36.5, pp 695–701.
- Rosser, N, J, Petley, D, N, Lim, M, Dunning, S, A and Allison, R, J, 2005. Terrestrial laser scanning for monitoring the process of hard rock coastal cliff erosion, *Quarterly Journal of Engineering Geology and Hydrogeology*, 38.4, pp 363–375.
- Said, K, O, Onifade, M, Githiria, J, M, Abdulsalam, J, Bodunrin, M, O, Genc, B, Johnson, O and Akande, J, M, 2021. On the application of drones: a progress report in mining operations, *International Journal of Mining, Reclamation and Environment*, 35.4, pp 235–267.
- Schürch, P, Densmore, A L, Rosser, N J, Lim, M and McArdell, B, W, 2011. Detection of surface change in complex topography using terrestrial laser scanning: application to the Illgraben debris-flow channel, *Earth Surface Processes and Landforms*, 36.14, pp 1847–1859.
- Scott, B, Ranjith, P, G, Choi, S, K and Khandelwal, M, 2010. A review on existing opencast coal mining methods within Australia, *Journal of Mining Science*, 46.3, pp.280–297.
- Shah, R, Sharma, Y, Mathew, B, Kateshiya, V and Parmar, J, 2016. Review paper on overloading effect, *International Journal of Advanced Scientific Research and Management*, 1.4, pp 131–134.

- Shahmoradi, J, Talebi, E, Roghanchi, P, and Hassanalian, M, 2020. A comprehensive review of applications of drone technology in the mining industry, *Drones*, 4.3, pp 34.
- Snavely, N, Seitz, S, M and Szeliski, R, 2006. Photo tourism: Exploring photo collections in 3D, In *ACM siggraph 2006 papers*, pp 835–846.
- Wheaton, J, M, Brasington, J, Darby, S, E and Sear, D, A, 2010. Accounting for uncertainty in DEMs from repeat topographic surveys: Improved sediment budgets, *Earth surface processes and landforms: the journal of the British Geomorphological Research Group*, 35.2, pp 136–156.

Application of use case modelling to achieve safe, efficient mining equipment automation

W X Tong¹, P Knights², T Phillips³, M S Kizil⁴ and M Nehring⁵

1. Mining Engineer, TAKRAF Australia Pty Ltd, Brisbane Qld 4000. Email: wenxiao.tong@uqconnect.edu.au
2. Professor, School of Mechanical and Mining Engineering, Faculty of Engineering, Architecture and Information Technology, Brisbane Qld 4000. Email: p.knights@uq.edu.au
3. Lecturer, School of Mechanical and Mining Engineering, Faculty of Engineering, Architecture and Information Technology, Brisbane Qld 4000. Email: t.phillips1@uq.edu.au
4. MAuslMM, A/Professor, The University of Queensland, School of Mechanical and Mining, St Lucia Qld 4067. Email: m.kizil@uq.edu.au
5. Lecturer, School of Mechanical and Mining Engineering, Faculty of Engineering, Architecture and Information Technology, Brisbane Qld 4000. Email: m.nehring@uq.edu.au

ABSTRACT

An In-Pit Crushing and Conveying (IPCC) system is a series-connected and continuously operating system. Therefore, every single equipment failure or delay will affect the utilisation of the throughput of the entire system (Foley, 2011). Moreover, the system downtime, including scheduled and unscheduled downtime, has negative impact on the system availability (Spriggs, Engineer, C M and Director, 2005). Effective system utilisation represents the productive hours used by the IPCC system during a period of time. The effective utilisation rate of a typical IPCC system is around 63 per cent, equivalent to 5500 effective working hours per annum. One of the significant system utilisation losses is the positioning and relocation of equipment, accounting for around 10 per cent of calendar hours. According to Harcus IPCC Time Utilisation Modelling (TUM) diagram, automated shovel/hopper locating has the potential to reduce this loss to 4 per cent due to equipment repositioning (Harcus, 2011). Teichman and Hegde (1986) indicate that the IPCC system's productivity and efficiency are limited by the achievable effective operating time of the single machine as well as their required moving or relocation time. McAree (2013) states that:

automation is not only a technology that can reduce the cost of production, but can enhance mining precision in terms of the optimised excavation sequence, guiding the machine's motions with precision at maximum mining capacity, creating a fully coordinated mining system with integrating of individual smart machines.

At the user requirements stage of designing a complex automated relocation system for the IPCC system, Use Case Modelling (UCM) is a fundamental analysis tool. The UCM approach is commonly applied to develop complex software that can be effectively applied to help define function and performance requirements (FPR) for automation projects involving complex system interactions. This paper demonstrates examples of applying UCM to analyse bench excavation strategies for hopper/shovel interactions in a fully autonomous mobile in-pit crushing and conveying system. The paper also introduces the use of the Enterprise Architect (EA) program to document all Use cases systematically and generate sequence diagrams, test cases, and activity with action diagrams.

INTRODUCTION

An understanding of performance and systems requirements of a complex automated relocation system for the Fully Mobile In-pit Crushing Conveyor (FMIPCC) system is critical. Systems engineering is defined as an 'integrated composite of processes, products, and people that is capable to meet specific customer requirements or objectives' (Department of Defence, 2001). Figure 1 is a flow chart of design process of a complex system that includes process inputs, requirement analysis, functional analysis or allocation, synthesis, system analysis, and control and process output.

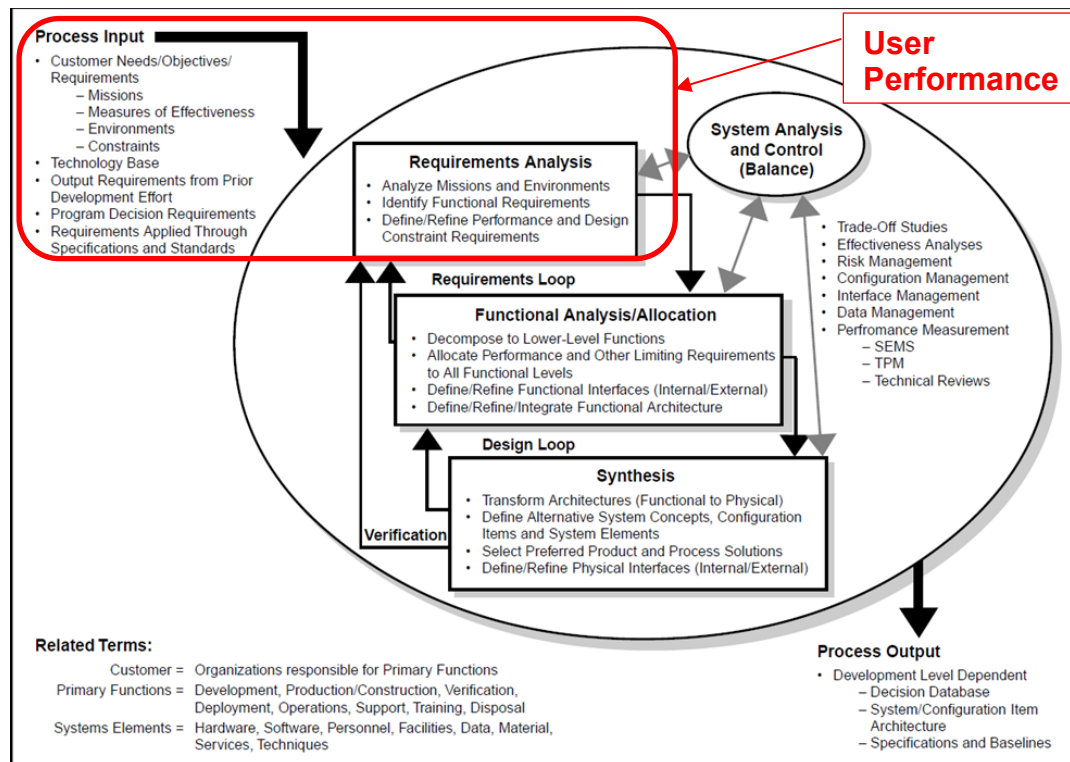


FIG 1 – Design process of a complex system (Department of Defence, 2001).

For the auto-relocation system design, this paper will focus on user performance that including the process input and requirements analysis which aims to identify and document the shovel and hopper interactions under the defined mining parameters and conditions, mining methods, and operation sequences. According to the Unified Software Development Process (USDP) (Somé, 2006), UCM can be applied to fill the gap between users and the system development caused by the manual nature of the requirement engineering process. Use case interaction diagrams can be generated along with enterprise diagrams.

FMIPCC OPERATION MODEL

The aim of using an FMIPCC system is to minimise or remove the requirement of truck haulage. Run-of-mine (ROM) material is mined by the excavator and fed into a fully mobile crusher directly. The material will be crushed into a conveyable size and discharged onto a short mobile transfer conveyor, then finally discharged into the continuous material haulage conveying system.

In order to simplify the operation sequence and minimise the required machine numbers, this analysis is limited to a typical FMIPCC operation scheme employing a single bench double block mining method. Under the selected operation scheme, the system requires one single mobile crushing unit (TMCS 9000) with the capability of loading, crushing, conveying and discharging material without a Belt Wagon and one typical electric rope shovel (P&H 4100 XPC). The mobile crusher operating capacity has to be designed to match the production rate of the shovel. Figure 2 shows the detailed operation scheme of the TAKRAF FMIPCC single bench double block operation.

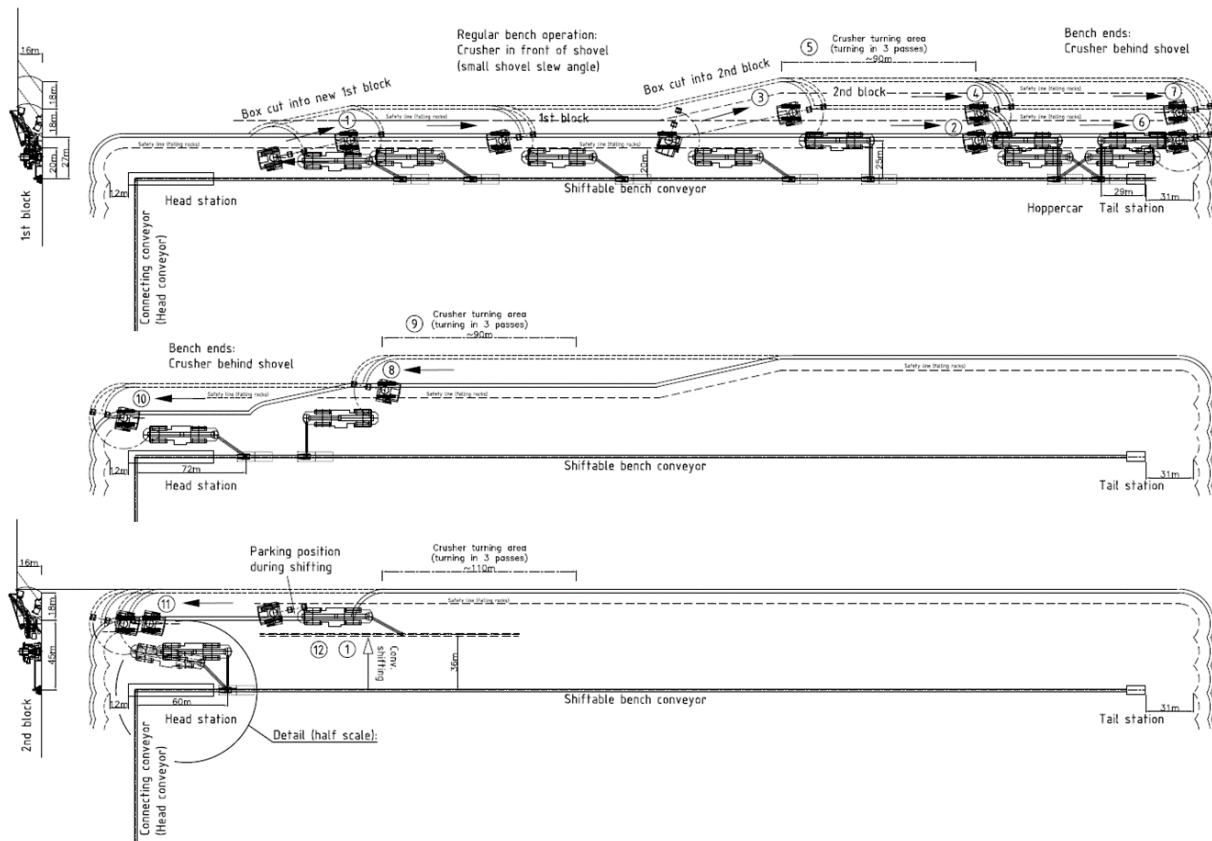


FIG 2 – TAKRAF FMIPCC single bench double block operation scheme.

The selected FMIPCC single bench double block operation scheme operation includes the following operation sequences:

1. Box cut into 1st block
2. Parallel mining 1st block
3. Box cut into 2nd block
4. Parallel mining 2nd block
5. Mobile Crusher self-turning 1 (6 stages/180 degrees)
6. Parallel mining 1st block (Block end)
7. Parallel mining 2nd block (Block end)
8. Reverse parallel mining 2nd block
9. Mobile Crusher self-turning 2 (6 stage/180 degrees)
10. Reverse parallel mining 1st block (Block end)
11. Reverse Parallel mining 2nd block (Block end)
12. Bench conveyor shifting.

All 12 operation sequences will be repeated in a loop after one bench has been excavated completely. The loop starts with the box cut into 1st block and ends with the bench conveyor shifting. Those operation sequences will be translated and documented in detail using the use case modelling (UCM) method.

USE CASE MODELLING

A use case is defined as ‘the specification of a sequence of actions, including variants that a system (or a subsystem) can perform, interacting with actors of the system’ In short, it is a description of

how a system will be used (or behave) in a particular circumstance. Use cases are normally presented as a text form, but they can be written in forms of flow charts, programming languages, sequences charts or petri nets. Under normal conditions, use cases can be used as a communication tool from one person to others who often have no special training (Cookburn, 2000). According to Unified Modelling Language (UML), a use case is defined as 'the specification of a sequence of actions, including variants that a system (or a subsystem) can perform, interacting with actors of the system'. A use case modelling describes a single piece of system behaviour which is ideal for requirement validation through prototyping (Somé, 2006). Use case modelling is an approach applied in the complex system, which is designed to identify, clarify, and organise system requirements and describe the system's requirements under various conditions, as the system responds to a request from one of the stakeholders. The use case can gather various information together, such as different sequence behaviour, scenarios, depending on the request and the environment conditions of the request. The single scenario has a set of sequences of steps showing how the action and interactions unfold. Some of the scenarios show achieved the goal and some of them result in a goal failure. The use cases provide a convenient means of describing system requirements in error situations and highlights appropriate error handling (Cookburn, 2000).

In this research, use case modelling provides a semi-formal framework for structuring the scenarios of the shovel and hopper interactions. In addition, UCM provide a means for documenting all the sequences between the shovel and hopper during the operations scenarios and parameters, and providing descriptions of system behaviour in failure or error situations. This in turn leads to early identification of error situations and appropriate error-handling solutions.

ENTERPRISE ARCHITECT

Enterprise Architect (EA) is a software product developed by SPARX that can be utilised to create use cases by the Use Case Modelling diagram function. EA helps a systems developer systematically organise and documents Use Cases and develop the system's Functional Performance Requirements. EA has been widely used in the automation development area.

This diagram is one of the Unified Modelling Language (UML) Behavioural diagrams that can be applied to describe the actors and record interactions between actors and the system. It also shows how the use case connects to other system elements, including upstream elements such as requirements and downstream elements such as components. A use case diagram describes goals that users want to achieve, which can represent a whole system or different parts of a system that always describes the goal from the perspective of actors.

The primary purpose of using The SPARX Enterprise Architect system in this thesis is to document the use cases.

RESEARCH OUTCOMES

This research is the first fundamental step toward automating the shovel and hopper interaction. At the current research stage, the outcome can't evaluate the improvement level of the time utilisation of the IPCC system, as no functional performance requirements have been implemented and simulated. However, the production improvement through implementing an automated IPCC system is a fact. The research analysed the use cases for all the operation sequences of FMIPCC single bench double block mining operation. Figure 3 outlines a use case writing example for a Box cut into the 1st block, including triggers, pre-conditions, functional requirements, operation schemes, use case writing and extensions. All the use case writing of the operation sequences has been documented into the enterprise architect. The interaction diagram of use cases shown in Figure 4 has been generated by the Enterprise diagram describing the interactions between the actors. The Enterprise Architect program generates the use case flow diagrams, and one example shows in the attached appendix – 'Appendix-IPCC system activity diagram example.'

- **Constraints**

Trigger: Box cut required for the first stage of mining operation

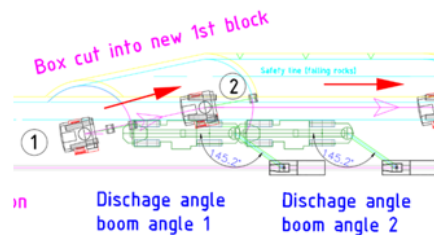
Preconditions:

- Pre-condition 0001 Assigned equipment are prepared for operation
- Pre-condition 0002 Target mining area is prepared for mining
- Pre-condition 0003 Machines are within the safe working area

Functional Requirements:

- REQ 0001- Required discharge boom angle 1
- REQ 0002- Required discharge boom angle 2
- REQ 0005- Pre-determined position 1
- REQ 0006- Pre-determined position 2
- REQ 0014- Operation Safety line

- **Operation Schemes**



- **Use cases writing**

1. Control center sends the required box cut operation information to the shovel and mobile crusher.
2. Shovel and mobile crusher move to the pre-determined position.
3. Control center validates the operation position of shovel and mobile crusher and sends out the permission of operation.
4. Shovel cuts into the block with the requested angle and path from pre-determined position 1.
5. Shovel loads each bucket material onto the mobile crusher.
6. Mobile crusher crushes the material and discharging onto the shiftable bench conveyor.
7. Shovel will relocate after finish the excavation of each working block until shovel reaches the pre-determined position 2.

- **Extensions**

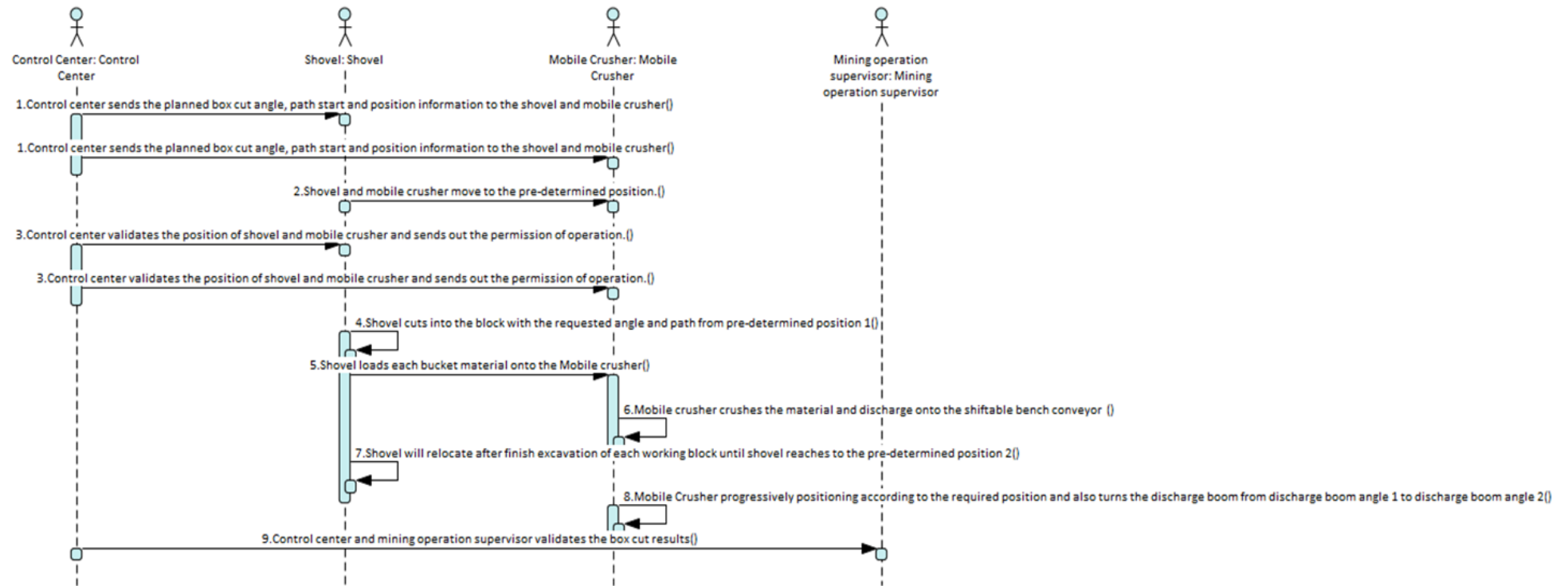
Extensions use cases has included in the report section 5.2.3.

- a) Shovel failed during mining operation
- b) Mining face slope failure
- c) Mobile Crusher failure during the operation
- d) Incorrect positioning of mobile crusher
- e) Incorrect discharge boom angle of mobile crusher
- f) Shovel excavating material failure
- g) Mobile crusher material crushing failure
- h) Incorrect positioning of the shovel

The extension of “Box cut 1st block” use cases includes the following steps:

- Step 2: 2a, 2c,
- Step 3: 3d,3h,
- Step 4: 4a-4h,
- Step 5: 5a-5h,
- Step 6: 6b, 6c, 6g, 6e
- Step 7: 7a,7b,7f,7h,
- Step 8: 8b,8c,8g,8e
- Step 9: 9J

FIG 3 – Use case writing example.



1_Basic_Path : Interaction diagram

Created: 13/03/2020 2:52:52 PM
 Modified: 13/03/2020 2:52:52 PM
 Project:
 Advanced:

CONCLUSIONS

This paper demonstrates that Use Case Modelling (UCM) approaches commonly used to develop complex software can be effectively applied to define function and performance requirements (FPR) for mine automation projects involving complex system interactions. In particular, this work applies UCM to analysis bench excavation strategies for hopper/shovel interaction in an autonomous fully mobile in-pit crushing and conveying system. The FMIPCC relocation automation system will potentially increase system utilisation by reducing the relocation time. UCM documents the use cases for the shovel and hopper interactions as a fundamental step of the FMIPCC relocation automation. The same method can be applied to other mining systems, such as complex dozer and shovel interactions.

ACKNOWLEDGEMENTS

The authors would like to acknowledge the support of TAKRAF GmbH in developing this work.

REFERENCES

- Cookburn, A. (2000). *Writing Effective Use Cases*. 1st ed. Boston: Addison-Wesley.
- Department of Defense (2001). System Engineering Process Overview, *System Engineering Fundamentals*, pp. 31–33.
- Harcus, M. (2011). Back to the Future. *Mining Magazine*, pp. 45–59.
- McAree, P R. (2013). Report on ACARP project C16031 Phase 2, Brisbane: The University of Queensland.
- Spriggs, G, Engineer, C M and Director, L. (2005). In-Pit Crushing Considerations for Conveying and Materials Handling Systems, *Bulk Solids Handling* 25 pp. 14.
- Somé, S S. (2006). Supporting use case based requirements engineering, School of Information Technology and Engineering (SITE), University of Ottawa, *Information and Software Technology* 48 (2006) 43–58, <www.sciencedirect.com>.
- Tejchman, L and Hegde, A S. (1986). Feasibility of in-pit crushing and conveying of waste rock at Mt Whaleback mine, in *Large Open Pit Mining Conference*, J R Davidson (ed.) (The Australasian Institute of Mining and Metallurgy: Melbourne), pp. 366–371.

Roof bolting module automation for enhancing miner safety

A Xenaki¹, H Zhang², S Schafrik³, Z Agioutantis⁴ and S Nikolaidis⁵

1. Graduate Research Assistant, University of Kentucky, Mining and Minerals Resources Building, Lexington KY 40506, USA. Email: anastasia.xenaki@uky.edu
2. PhD Candidate, University of Southern California, Ronald Tutor Hall, Los Angeles CA 90007, USA. Email: hejiazha@usc.edu
3. Associate Professor, University of Kentucky, Mining and Minerals Resources Building, Lexington KY 40506, USA. Email: steven.schafrik@uky.edu
4. Professor, University of Kentucky, Mining and Minerals Resources Building, Lexington KY 40506, USA. Email: zach.agioutantis@uky.edu
5. Assistant Professor, University of Southern California, Ronald Tutor Hall, Los Angeles CA 90007, USA. Email: nikolaid@usc.edu

ABSTRACT

The mining sector is currently in the stage of adopting more automation and with it, robotics. Autonomous bolting in underground environments remains a hot topic for the mining industry.

Roof bolter operators are exposed to hazardous conditions due to their proximity to the unsupported roof, loose bolts and heavy spinning mass. Prolonged exposure to the risk inevitably leads to accidents and injuries.

This study focuses on developing a robotic assembly capable of carrying out the entire sequence of roof bolting operations in full or partial autonomous sensor-driven rock bolting operations to achieve a high-impact health and safety intervention for equipment operators. The automation of a complete cycle of drill steel positioning, drilling, bolt orientation and placement, resin placement and bolt securing is discussed using an anthropogenic robotic arm. A human-computer interface is developed to enable the interaction of the operators with the machines. Collision detection techniques will have to be implemented to minimise the impact after an unexpected collision has occurred. A robust failure-detection protocol is developed to check the vital parameters of robot operations continuously. This unique approach to automation of small materials handling is described with lessons learned.

INTRODUCTION

Roof bolting is an essential operation within the underground mining cycle, as it aims to provide support to the exposed roof and ribs of the new excavation. Roof bolting operations can also be utilised to provide a preliminary characterisation of the competence of the roof. However, roof bolter operators are often exposed to dangerous conditions – the risk increases due to their proximity to the unsupported roof. Dust and noise exposure due to rock drilling and bolting should not be discounted. Roof bolting has been the principal means for enhancing miner safety regarding preventing different roof falls in underground mines in recent decades (Christopher, 2002). Based on previous research, underground roof bolting operators show an extended risk concerning overexposure to airborne levels of respirable coal and crystalline silica dust (size <10 µm) from the roof drilling operation (Goodman and Organiscak, 2018). Inhaling these clouds of dust can cause coal workers' pneumoconiosis (CWP) and another job-related lung disease, silicosis. Both illnesses are disabling even fatal and irreversible conditions.

In recent decades, the development and utilisation of autonomous equipment have been integrated into many engineering and scientific applications. Some applications include intelligent transportation (Zhang *et al*, 2011), agriculture (Li *et al*, 2009), marine and planetary environment exploration (Leitner, 2009; Wynn *et al*, 2014), mining (Larsson *et al*, 2008; Lösch *et al*, 2018) and disaster reconnaissance and rescue (Zhang *et al*, 2020). The main reason for developing a robotic assembly capable of carrying out the entire sequence of roof bolting operations; in a full or partial autonomous manner is to achieve a high-impact health and safety intervention for roof bolter operators.

BACKGROUND

Current circumstances of underground mining automation

Robots equipped with robotic arms can improve the performance of human workers in harsh working environments like underground mines. Xie *et al* (2017) showcased an automated system that has a UR5 robotic arm and a 3-Finger Adaptive Robot Gripper from Robotiq, with which the system can then install, rearrange and remove Smart Sensor Boxes (SSBs) of an internet of things (IoT) infrastructure. Robotics researchers also work together with mining experts to autotomise existing machines in the mining industry. Bonchis *et al* (2013) adapted a mechanical manipulator from a Palfinger truck crane for the explosive charging tasks. They designed an end-effector that carries the laser range-finder to detect the blastholes' location and several video cameras and LED lights used to support the automatic and manual host insertion process.

To insert the tool into the blasthole, the manipulator is first controlled by a planning algorithm and then teleoperated by a human operator to refine the position and direction of the end-effector. To perform different tasks underground, the robotic manipulator can be very different from conventional robotic arms. Huh *et al* (2011) designed a teleoperated mining robot with a boom, an arm and a bucket to replace human coalminers.

Moreover, most robotic manipulators are equipped with hydraulic actuators for heavy-duty tasks, which propose unique challenges in controlling (Huh *et al*, 2011; Bonchis *et al*, 2013; Lösch *et al*, 2018). Hydraulic actuators can be a direct drive for linear or rotary motions. Lu (2009) shows how a bucket wheel reclaimer can be converted into a robotic arm and how it can be controlled automatically. He first modelled three joints of a typical BWR based on which the kinematics and dynamics are modelled in his work. In the study of Colgate *et al* (2008), the authors conclude that Lagrangian dynamics models and Newton-Euler dynamics-based models for hydraulic robotic manipulators provide superior control performance and give solutions to the highly nonlinear behaviour of energy inefficient hydraulic systems.

Human-machine interface

The human-robot communication interface is crucial for the safe deployment of robots in underground mining because of its complex and various environments. Ideally, humans should monitor and interrupt the working progress of robots remotely in a safe place. In Yamada *et al* (1997) study, a teleoperation system is implemented as a remote-control station where humans can control the robot with joysticks. It is also important to inform humans of the robot's status and the working progress in a human-friendly way. The remote-control station has two monitors that show the robot and obstacles in the work area. Wilkinson (2004) suggests a new, cooperative approach to teleoperation in mining environments to enable an equipment sharing scenario. He also proposes an interactive telemining simulator to help quantify the interaction between operators in a dual operator configuration.

Collision detection techniques

In real case scenarios, it is almost impossible for humans to collaborate with robots without a certain level of physical contact. Post-collision techniques detect a collision as it occurs. The purpose of this method is to minimise the impact after an unexpected collision has occurred.

Based on real-time detection techniques (pre-collision techniques) and reactive planning algorithms, researchers have allowed a higher degree of coexistence and interactions between humans and robots (Ebert *et al*, 2005; Schiavi, Bicchi and Flacco, 2009; Flacco and De Luca, 2010; Fenucci, Indri and Romanelli, 2014). Green *et al* (2012) examined sensing technologies that could enable the development of underground autonomous vehicles. Combining three-dimensional cameras and a thermal imaging sensor created 3D thermal models of narrow mining stops, which can be used to determine the risk of rockfall in an underground mine. Kulić and Croft (2005) also presented a strategy for improving the safety of human-robot interaction by minimising a danger criterion during the planning stage.

AUTONOMOUS ROOF BOLTING DEVELOPMENT FOR MINING APPLICATIONS

A detailed study of human motion is carried out using sensors and computer software. Results are used to guide the development of a robust remote calibration diagnostics and self-monitoring system, the integration of a human-machine interface to enable a manual approval of the tasks and as well as to override the system in the event of unpredicted or unsafe actions. Although this project aims to provide a better working environment for the operators, productivity and the value of immediate roof observations should not be discounted.

Autonomous process description

The construction of a robust autonomous roof bolter able to carry out required tasks is based on an appropriate architecture that will enable it to make decisions similar to those made by humans. The autonomous roof bolter must be capable of sufficient robotic spatial perception, robust remote calibration diagnostics and self-monitoring capabilities. Overall, the autonomous roof bolter must successfully perform the following functions: drill steel positioning, drilling, bolt orientation and placement, resin placement and bolt securing. Figure 1(b) shows a flow chart of the robotic arm controller.

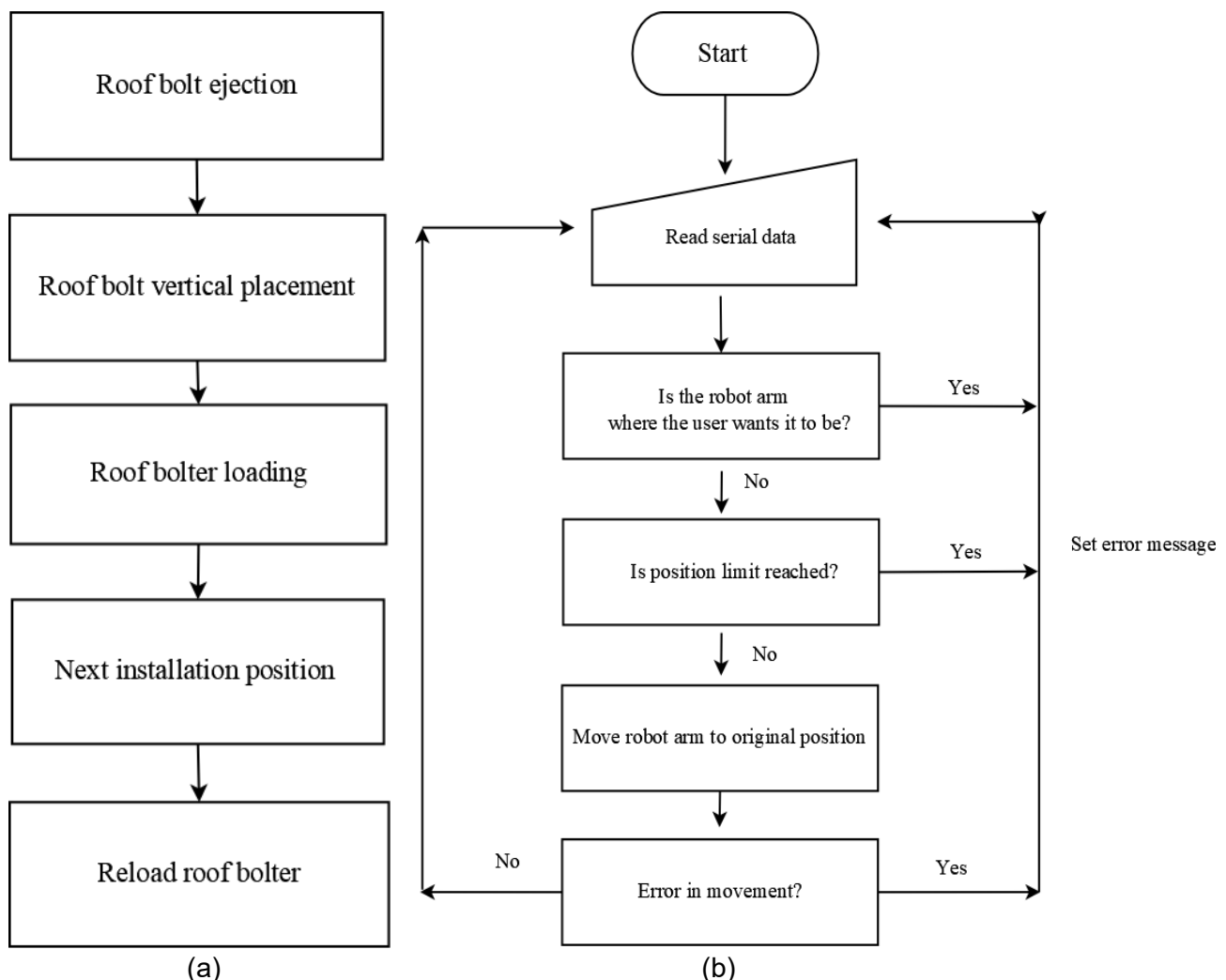


FIG 1 – Flow chart of: (a) the human motion states; (b) the robotic arm controller.

The foundation of an autonomous roof bolter is the control module. A Programmable Logic Controller (PLC) is developed to monitor drilling operations. A Drill Control Unit (DCU) is also set-up to automate the drilling and bolting cycle for improved safety and productivity. The systems are tested in the Rock Mechanics laboratory at the Mining Engineering Department, University of Kentucky. The display and control can be activated through a rugged touch screen panel. A CAN Bus system

interface is integrated directly in the valve section to connect to the master control unit and control the roof bolter's hydraulic system. The CAN Bus system has the bandwidth to cope with real-time control and data collection while significantly improving flexibility. A joystick controls the drilling operations of the roof bolter. Sensors monitored by this centralised system used for controlling or monitoring roof bolting parameters (temperature, pressure, height of roof) by using CAN interface are connected to the Expansion block. This module continuously operates and is responsible for monitoring that the control module is working correctly and that the robotic arm does not deviate from the desired planned path.

The determination of contact incidents for each component resulted in the following possible occurrences:

In the case of a collision between the machine and the operator, the user can immediately stop the operation and release the operator.

A complete analysis of the interaction allowed us to analyse situations where no contacts or avoid incidents occurred.

This analysis provides information that helps make recommendations to reduce the likelihood that roof bolter operators get injured from contact with the robotic arm and roof bolter boom arm.

Bolt module set-up and testing

Studying the human motion

The robotic arm functions similarly to the roof bolter operator that will be described below. Table 1 shows all the possible states for the robotic arm to be in, with when they are processed, in regard to the roof bolter and a flow chart that shows the state process (Figure 1(a)).

TABLE 1
Descriptive study of the human motion states.

State	Description
Roof bolt ejection	The first state of the installation process involves the ejection of a roof bolt from the storage magazine.
Roof bolt vertical placement	This state occurs when the bolt is placed at the bolt base. The robotic arm moves away. Once at the bolt base a small hydraulic jack and clamp arrangement rotates the roof bolt vertically.
Roof bolter loading	This occurs when the roof bolter extends the drill motor up so the roof bolt sits in the chuck. The robotic arm remains in the previous state. Once the roof bolt is seated, the bolt base releases the clamps on the roof bolt so the roof bolter can assume the next roof bolting installation process.
Next installation position	The loaded roof bolter assumes the following installation process. The robotic arm moves towards the storage magazine and grabs the specified chemical resin. The chemical resin is injected. The chemical resin can go off before the drill head rotates.
Reload roof bolter	The robotic arm returns to its original position. Then moves towards the storage magazine and grabs a new bolt. Once in the bolt base the bolter docks in position to load the bolt.

Simulated Robot Roof Bolting

A roof bolting scenario is set (see Figure 2) in the ABB RobotStudio (robot simulator developed by ABB). The simulated roof bolting scenario is constructed based on the actual roof bolter at the University of Kentucky (UK) shown in Figure 3.

The simulation phase of the automated roof bolting project provides a representation of the planned autonomous roof bolter lab structure. The simulation environment, incorporated by the IRB 1600

robotic arm and drill steel, is based on actual evaluations to develop the roof bolter structure and other functional components. Combined with the specifications (robot arm reach and actual payload), defines the limits for the system capabilities.

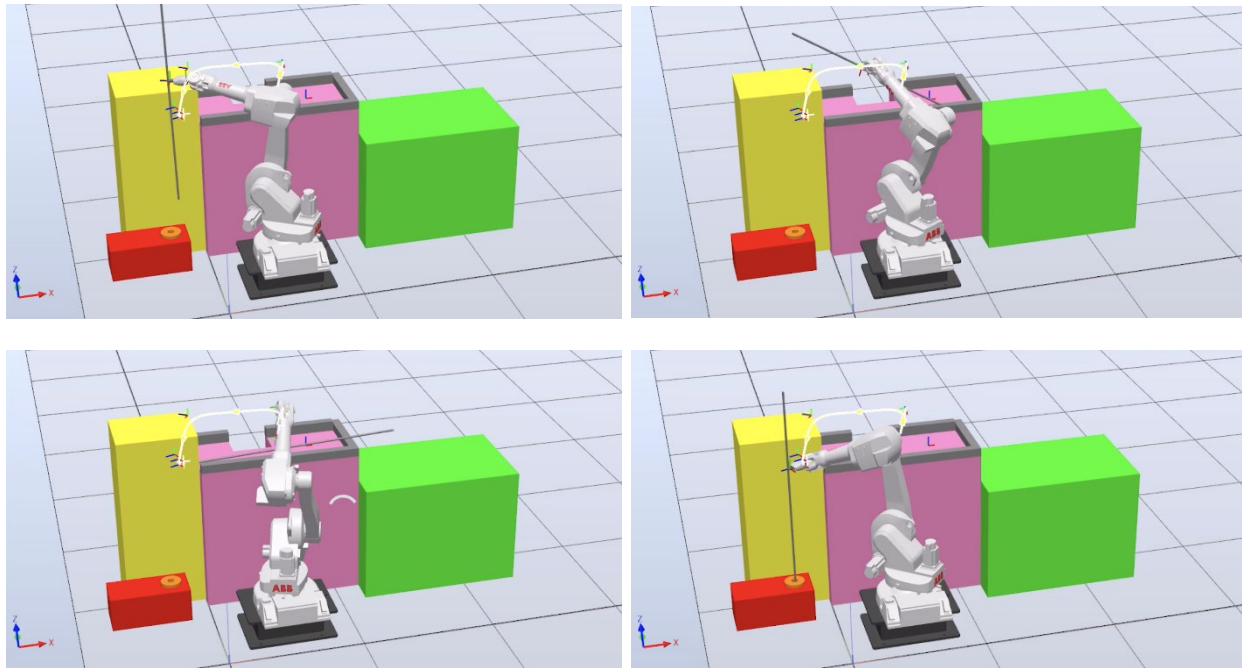


FIG 2 – Simulated robot roof bolting.

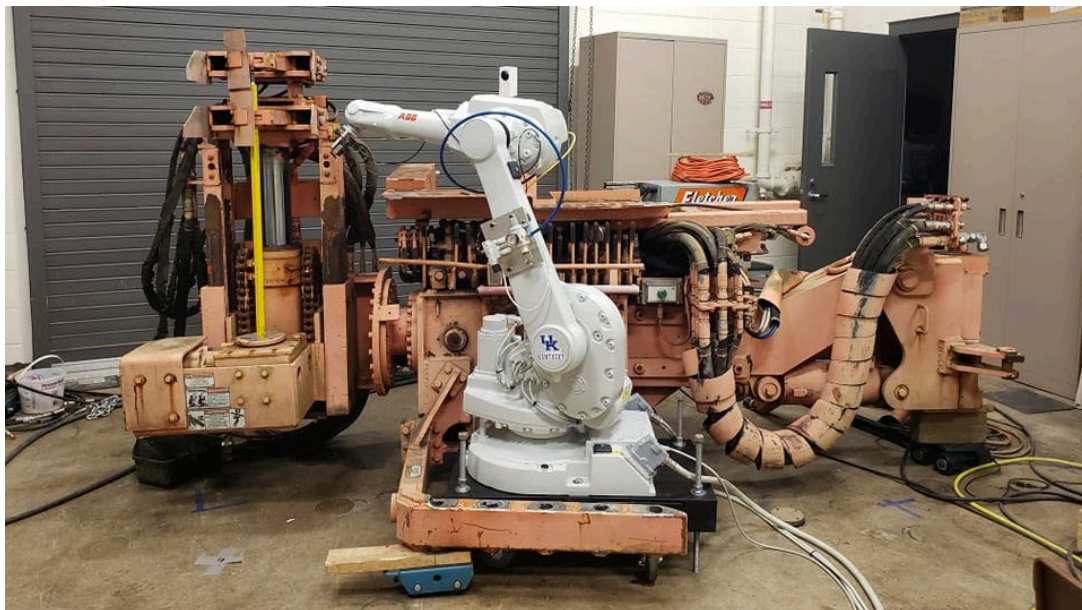


FIG 3 – Roof bolter in the lab.

Developing and testing motion patterns

Different motion patterns are developed and tested for the roof bolting required tasks. This is done by setting important waypoints as targets for the robot. Consequently, the robot follows the waypoints automatically. Once the motion patterns are set, the robot accurately and repeatedly executes the tasks. These motion patterns are implemented in RAPID (Table 2).

It is crucial to analyse how different levels of the location of the robotic arm affect the performance of the roof bolting cycle. The algorithm used in this project (Table 2) uses the whole roof bolting motions to generate a process (line 1). First, two positions are specified for the robot to reach. Then, the robot moves to the initial position (line 2) and grabs the drill steel (line 3) and finally retracts the drill steel towards the drill head (line 4). Notably, the retract motion must be carefully designed to

avoid the potential collision between the robot and the roof bolter. Subsequently, the robot places the drill steel into the drill head (line 5). The robot reaches the positions only when the relative transforms between the robot and the roof bolter is correct.

TABLE 2

The pseudocode for generating roof bolting motions.

<p>Generate_Roof_Bolting_Motions</p> <p><i>Input:</i> A calibration pose cp, initial pose ip, grab pose gp, place pose pp, gripper close position gcp.</p> <p><i>Result:</i> The drill steel successfully placed in the roof bolter.</p> <ol style="list-style-type: none"> 1. Calibrate(cp) 2. Move the robot to ip 3. GoPick(gp, gcp) 4. Retract(ip) 5. GoPlace(pp) <p>Calibration(p)</p> <ol style="list-style-type: none"> 6. Move the robot to p. 7. Verify if the whole system is in the right position. <p>GoPick(p, gcp)</p> <ol style="list-style-type: none"> 8. Move the robot to p. 9. Move the gripper to gcp. <p>Retract(p)</p> <ol style="list-style-type: none"> 10. Move the robot to p. <p>GoPlace(p)</p> <ol style="list-style-type: none"> 11. Move the robot to p. 12. Verify the drill steel is successfully placed inside the roof bolter.

Design and implementation of the human-robot interface

The adoption of flexible, more intuitive and user-friendly human-robot interaction is a key goal of this project—the developed HMI system is composed of a touch screen and joystick and a FlexPendant device. The user can send commands to the robot and monitor the robot status in real-time for both computer and FlexPendant devices.

The human-robot interface for computer environments is targeted at providing an easy-to-use interface for users to command the robot on desktop computers, smartphones, or tablets (see Figure 4). It has three components: GUI client, server and video streaming server.

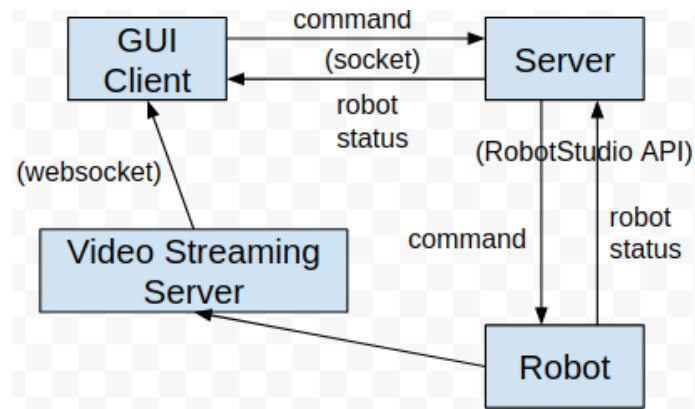


FIG 4 – Human-robot interface for computer environments.

The Qt cross-platform library is used to develop the graphical interface (see Figure 5). There are three components of the graphical interface: logging area, command sender and real-time robot video streaming player. The logging area is where the messages sent from the robot, eg., the last command is finished, are printed. The command sender has different buttons corresponding to different robot motion modules. The real-time robot video streaming player is where the user can monitor the robot's movement in real-time.

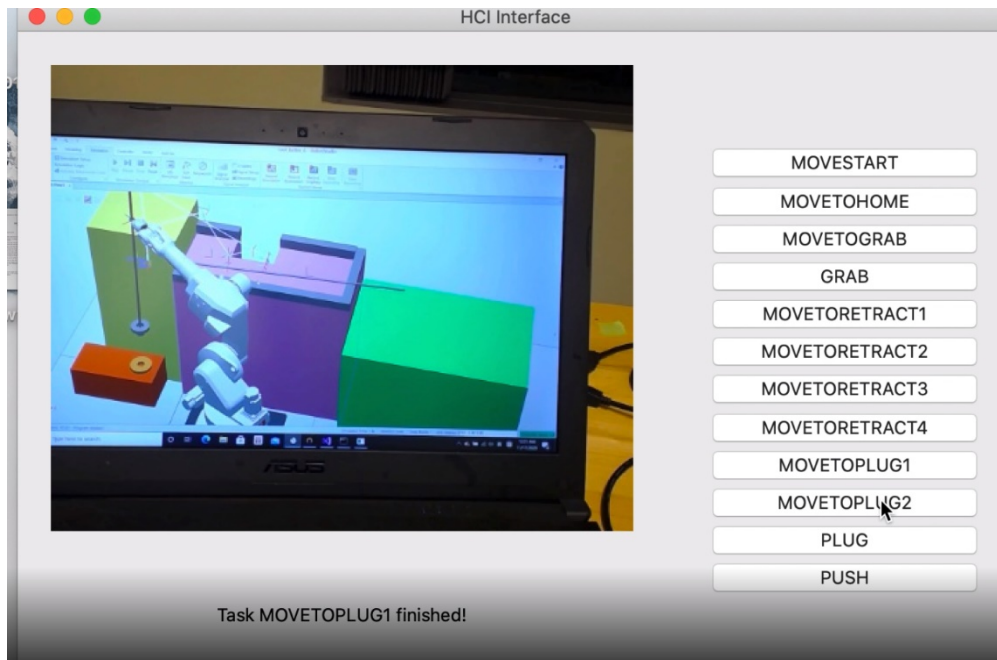


FIG 5 – Graphical interface.

The video streaming server is a program that can efficiently decode and transmit images. It communicates with the client through the WebSocket protocol. The server connects with the RobotStudio API module which is connected directly with the robot and it listens continuously for connections with a client through a static IP address. The server also interfaces all the functions implemented in the RobotStudio API module. This allows an external client to connect to the server and send commands to the robot.

The FlexPendant is a handheld operator unit used to perform many of the tasks involved when operating a robot system. In this work, the FlexPendant is used when the human operator is required to work closely with the robotic arm in various roof bolting activities, or for maintenance. The human-robot interface for the FlexPendant is developed using the ABB ScreenMaker software. The interface consists of different buttons corresponding to different motion modules.

Implementing and verifying robot motions on the real robot

For validation, the simulation results are run on the actual roof bolting system (see Figure 6). The currently implemented robot motions include self-positioning, drill grabbing and drill plugging. The successful execution of commands by the robot generates feedback signals delivered to the HMI system. Upon completion of a task, a green light indicator is activated on the user interface. After the robot executes assigned commands, feedback information can be transmitted to the human operator to inform him of the task's status. It is possible to verify that the robot is at the correct position with self-positioning before performing the task. The program implements a general picking and placing drill steel process corresponding to Figure 6, and it is straightforward to extend the program to other processes in the whole task. The roof bolting cycle executions are based on a logic that follows the flow diagram in Figure 7 that shows the preliminary flowchart of the semi-autonomous roof bolting cycle.

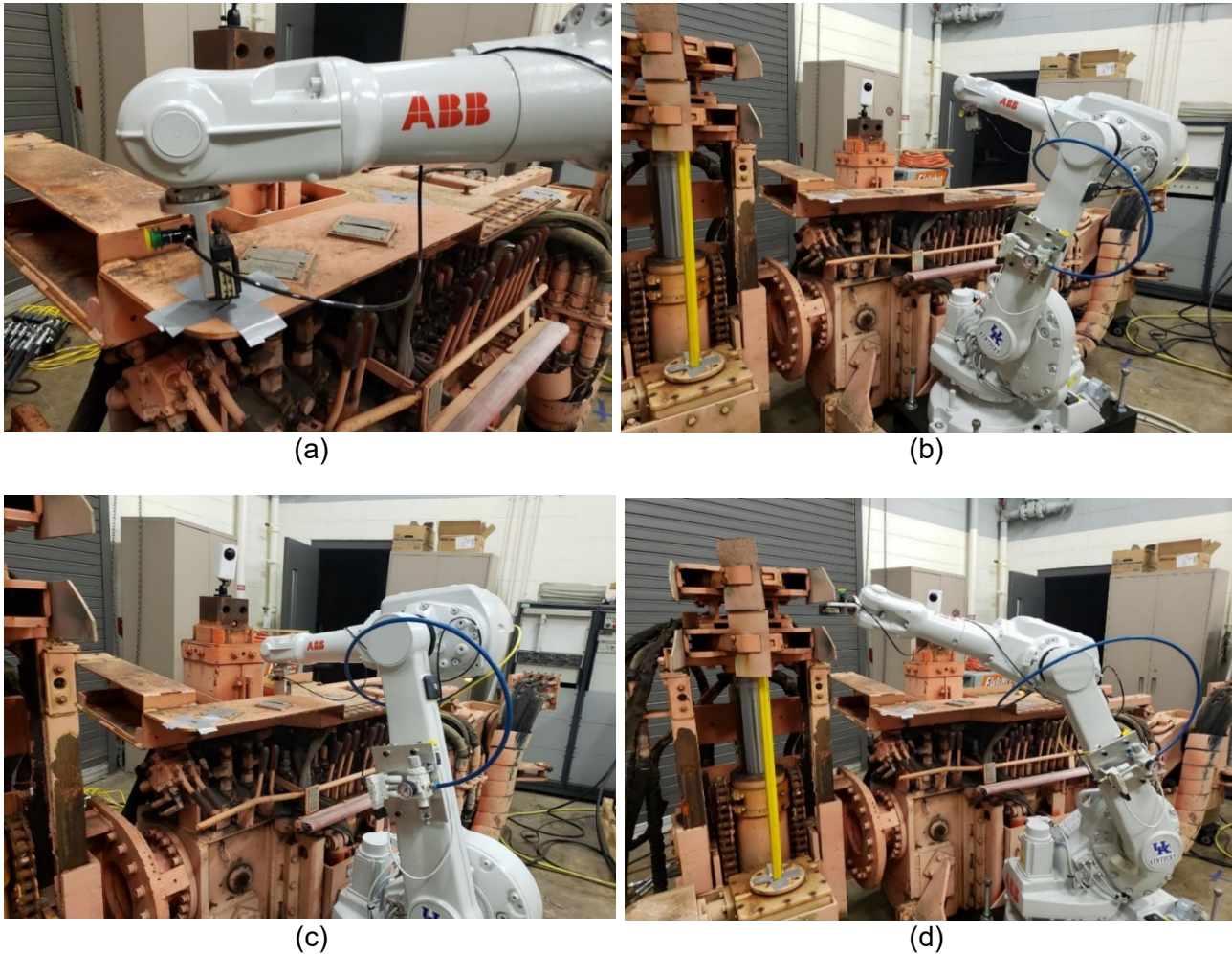


FIG 6 – Overview of the robotic arm in (a) Self-positioning; (b) home position; (c) grabbing position; (d) plugging position.

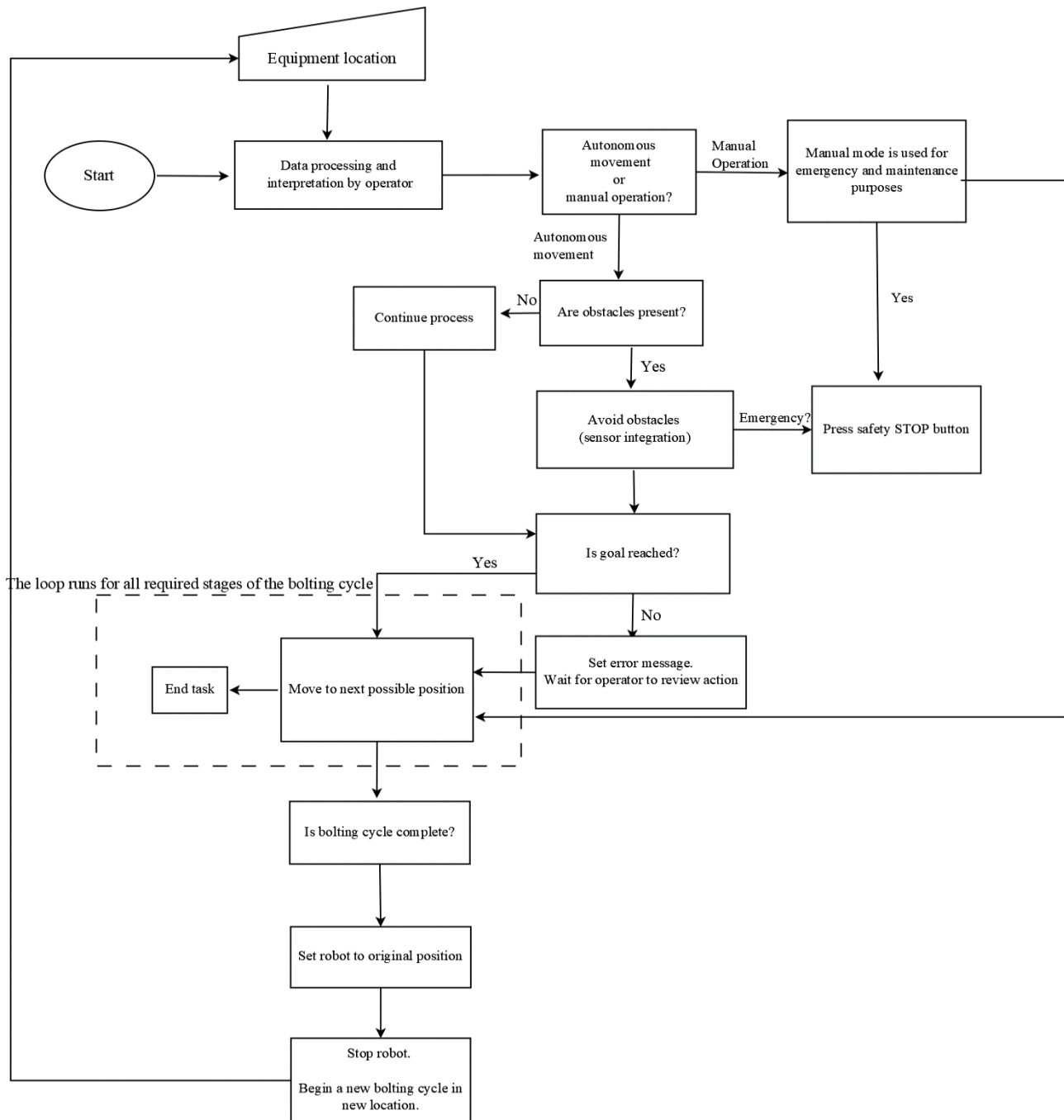


FIG 7 – Preliminary flow chart of the semi-autonomous roof bolting cycle.

DISCUSSION

One of the most challenging tasks of automating the operation of the roof bolter is that the manipulator should perform the specified operations while in limited space. So, the placement of the robotic manipulator in the vehicle is crucial. The robotic arm should also be able to pick up and install longer than seam height bolts, both resin and mechanical, with the various ancillary parts required of roof bolting. Its storage needs not to be kept in the module, but arrangements are made to provision the module from onboard storage and minimise onboard storage re-provisioning.

CRITICAL MILESTONES

The robotic arm installation project requires re-imagining the bolt installation procedure on the dexterity of the human operator. Historically, locating the installation assembly relied on the operator. The basis of the project is to use an automated machine-positioning system, which is a 6-axis anthropomorphic robot in place of a human to handle the drill steels, bolts and other consumables. This robotic assembly will carry out the entire sequencing of the roof bolting. The hydraulic system

will be synchronised with the robot's operations. A human operator will be required to approve major operations while also maintaining the ability to operate the robot and the hydraulic system. The only human interaction with the autonomous roof bolter should be re-provisioning the onboard storage, maintenance and supervisory control of the machine (Jobes, 1990).

CONCLUSIONS

Mining is a rapidly growing industry and recent advances in engineering automation can substantially improve the safety of operations, while increasing operational efficiency and production capability. This requires combining expertise from mining operations with control methods in robotics. Future work will focus on enabling automated equipment to adapt dynamically to changes in the environment, rather than executing pre-planned motions. It will also expand the proposed capabilities to more tasks beyond roof bolting, such as autonomous navigation and tool delivery.

ACKNOWLEDGEMENTS

This study was sponsored by the Alpha Foundation for the Improvement of Mine Safety and Health, Inc (ALPHA FOUNDATION). The views, opinions and recommendations expressed herein are solely those of the authors and do not imply any endorsement by the ALPHA FOUNDATION, its Directors and staff.

REFERENCES

- Bonchis, A, Duff, E, Roberts, J and Bosse, M, 2013. Robotic explosive charging in mining and construction applications. *IEEE Transactions on Automation Science and Engineering*, 11(1), 245–250.
- Christopher, M, 2002. August 6–8. The introduction of roof bolting to US underground coal mines (1948–1960): a cautionary tale. In *Proceedings of the 21st International Conference on Ground Control in Mining*, pp 150–160.
- Colgate, E, Bicchi, A, Peshkin, M A and Colgate, J E, 2008. Safety for physical human-robot interaction. In *Springer handbook of robotics*, pp 1335–1348.
- Ebert, D, Komuro, T, Namiki, A and Ishikawa, M, 2005. August. Safe human-robot-coexistence: emergency-stop using a high-speed vision-chip. In *Proceedings of the 2005 IEEE/RSJ International Conference on Intelligent Robots and Systems*, pp 2923–2928.
- Fenucci, A, Indri, M and Romanelli, F, 2014. A real time distributed approach to collision avoidance for industrial manipulators. In *Proceedings of the 2014 IEEE Emerging Technology and Factory Automation (ETFA IEEE)*, pp 1–8.
- Flacco, F and De Luca, A, 2010. May. Multiple depth/presence sensors: Integration and optimal placement for human/robot coexistence. In *2010 IEEE International Conference on Robotics and Automation*, pp 3916–3923. IEEE.
- Goodman, G and Organiscak, J, 2018, February 7. An evaluation of methods for controlling silica dust exposures on roof bolters. *Health National Institute for Occupational Safety and Health*.
- Green, J J, Hlophe, K, Dickens, J, Teleka, R and Price, M, 2012. Mining robotics sensors.
- Huh, S, Lee, U, Shim, H, Park, J B and Noh, J H, 2011. October. Development of an unmanned coal mining robot and a tele-operation system. In *2011 11th International Conference on Control, Automation and Systems*, pp 31–35. IEEE.
- Jobes, C C, 1990. Applied automation for the proposed automated roof reinforcement installation system. *U S Bureau of Mines – Electrical Electronic Systems*.
- Kulić, D and Croft, E A, 2005. Safe planning for human-robot interaction. *Journal of Robotic Systems*, 22(7), 383–396.
- Larsson, J, Appelgren, J, Marshall, J and Barfoot, T, 2008. Atlas Copco infrastructureless guidance system for high-speed autonomous underground tramming. In *Proceedings of 5th International Conference and Exhibition on Mass Mining*, pp 585–594.
- Leitner, J, 2009. July. Multi-robot cooperation in space: A survey. In *2009 Advanced Technologies for Enhanced Quality of Life*, IEEE, pp 144–151.
- Li, M, Imou, K, Wakabayashi, K and Yokoyama, S, 2009. Review of research on agricultural vehicle autonomous guidance. *International Journal of Agricultural and Biological Engineering*, 2(3), 1–16.
- Lösch, R, Grehl, S, Donner, M, Buhl, C and Jung, B, 2018. October. Design of an autonomous robot for mapping, navigation and manipulation in underground mines. In *2018 IEEE/RSJ International Conference on Intelligent Robots and Systems (IROS)*, pp 1407–1412. IEEE.
- Lu, T-F, 2009. Bucket wheel reclaimer modeling as a robotic arm. In *Proceedings, 2009 IEEE International Conference on Robotics and Biomimetics (ROBIO)*.

- Schiavi, R, Bicchi, A and Flacco, F, 2009. May. Integration of active and passive compliance control for safe human-robot coexistence. In *2009 IEEE International Conference on Robotics and Automation*, pp 259–264.
- Wilkinson, N, 2004. Cooperative control in tele-operated mining environments. In *Proceedings of the UBC Human Interface Technology Conference*.
- Wynn, R B, Huvenne, V A, Le Bas, T P, Murton, B J, Connelly, D P, Bett, B J, Ruhl, H A, Morris, K J, Peakall, J, Parsons, D R and Sumner, E J, 2014. Autonomous Underwater Vehicles (AUVs): Their past, present and future contributions to the advancement of marine geoscience. *Marine Geology*, 352, 451–468.
- Xie, J, Yang, Z, Wang, X, Wang, S and Zhang, Q, 2017. A joint positioning and attitude solving method for shearer and scraper conveyor under complex conditions. *Mathematical Problems in Engineering*, Article ID 3793412, 14 p.
- Yamada, Y, Hirasawa, Y, Huang, S, Umetani, Y and Suita, K, 1997. Human-robot contact in the safeguarding space. *IEEE/ASME transactions on mechatronics*, 2(4), 230–236.
- Zhang, J, Wang, F Y, Wang, K, Lin, W H, Xu, X and Chen, C, 2011. Data-driven intelligent transportation systems: A survey. *IEEE Transactions on Intelligent Transportation Systems*, 12(4), 1624–1639.
- Zhang, P, Ou, Y, Sun, B and Liu, C, 2020. A case study of floor failure characteristics under fully mechanised caving mining conditions in extra-thick coal seams. *Journal of Geophysics and Engineering*, 17(5), 813–826.

Digital transformation

Integrated operations for complex resources

P A Dowd¹

1. Director of the Australian Research Council Industrial Transformation Training Centre for Integrated Operations for Complex Resources (ARC ITTC IOCR), The University of Adelaide, Adelaide SA 5005. Email: peter.dowd@adelaide.edu.au

INTRODUCTION

This presentation covers the research program for the Australian Research Council Industrial Transformation Training Centre for Integrated Operations for Complex Resources (ARC ITTC IOCR), an \$11.5M, four-year program comprising three university partners (University of Adelaide, University of South Australia, Curtin University), two end-user mining companies (BHP and OZ Minerals) and 19 METS companies and other organisations.

The Training Centre will deliver the enabling tools – advanced sensors, data analytics and artificial intelligence – for automated, integrated and optimised mining. It will train the next generation of engineers and scientists in developing and applying these enabling tools, which are knowledge priorities for the mining industry.

Automating a mine requires integrating all stages of the mining and processing system so that intelligence across the value chain can automatically be generated, delivered and exploited. This is a complex, inter-disciplinary systems problem that requires an inter-disciplinary, as opposed to a multi-disciplinary, approach and includes researchers from mining engineering, mineral processing, geology, physics, chemical engineering, mathematics, computer science, mechanical engineering, electrical engineering and chemistry.

Mining as a complex system

The mining system is a sequence of interdependent inputs and outputs that deliver a final product as depicted in Figure 1.

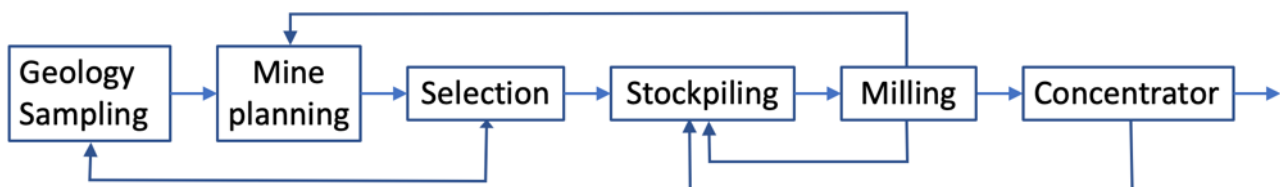


FIG 1 – Interdependent inputs and outputs of the mining system.

Independently optimising the components of this system does not optimise the system. The systems approach is a comprehensive analysis focused on the inter-relationships of the constituent parts of the system and how the system functions over time. Complex systems problems necessarily require inter-disciplinary approaches. Inter-disciplinarity is not simply multi-disciplinarity – it requires:

- the use and understanding of super-concepts.
- Integration of knowledge and methods.
- large systems-oriented teams to solve complex systems problems.

The general approach is summarised in Figure 2.

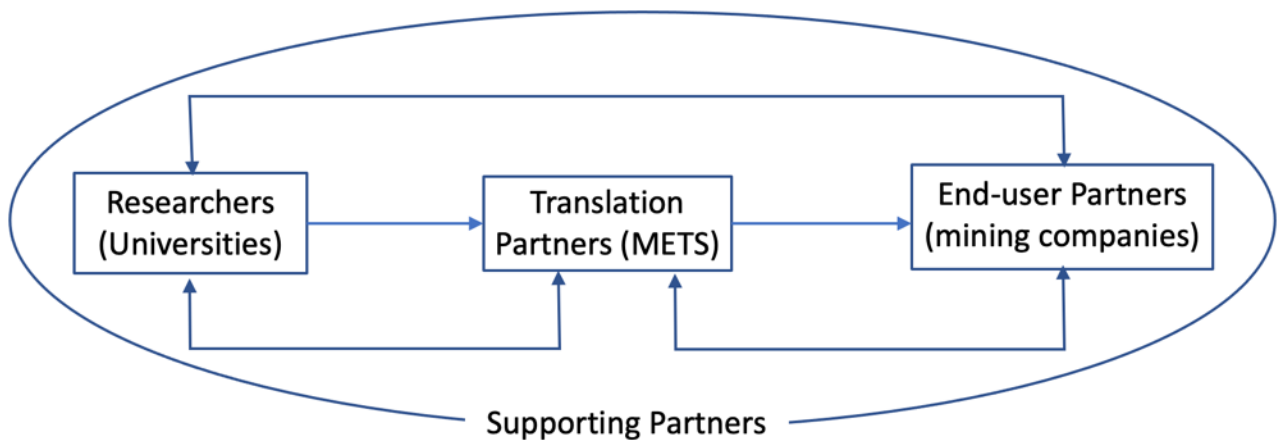


FIG 2 – The general approach.

Focus: sensors, data integration, data analytics, machine learning, real-time updating of models, mine system optimisation in near real-time.

Application: Complex resources.

The inter-disciplinary technologies are summarised in Figure 3.

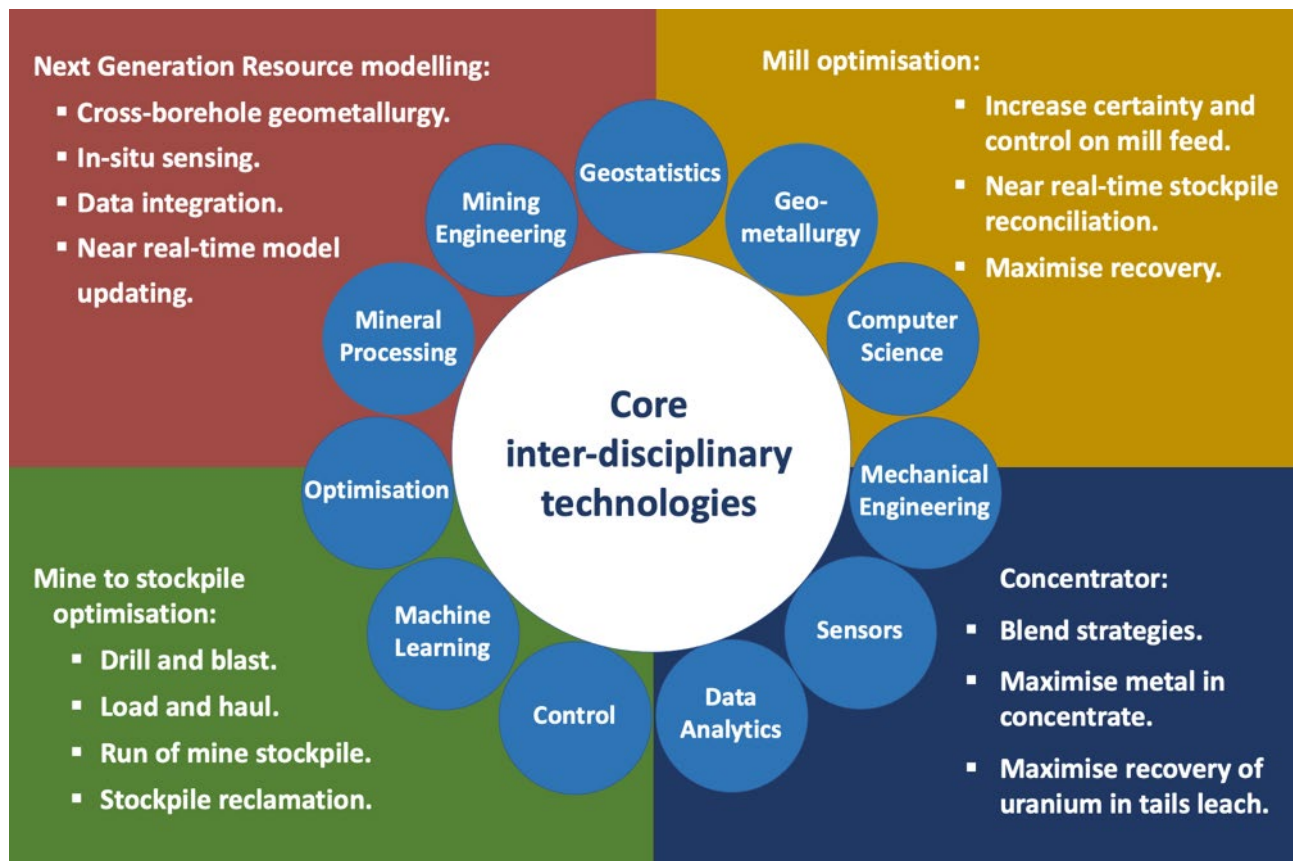


FIG 3 – The core inter-disciplinary technologies and the research challenges.

The Training Centre comprises three research nodes:

- Node 1: Smart Sensing.
Focus: new, field-deployable sensor tools and the interaction of the sensor tools with the resource at different stages.
- Node 2: Data Analytics and Integration.

Focus: data analytics to derive data-driven, real-time online and process models from existing and new sensor suites and plant operating data feeds.

- Node 3: Optimisation through Integration.

Focus: integration to optimise overall value by linking upstream and downstream stages.

The vertical and horizontal integration of the nodes and research themes is summarised in Figure 4.

Vertical and horizontal integration – links reflect integrated systems approach

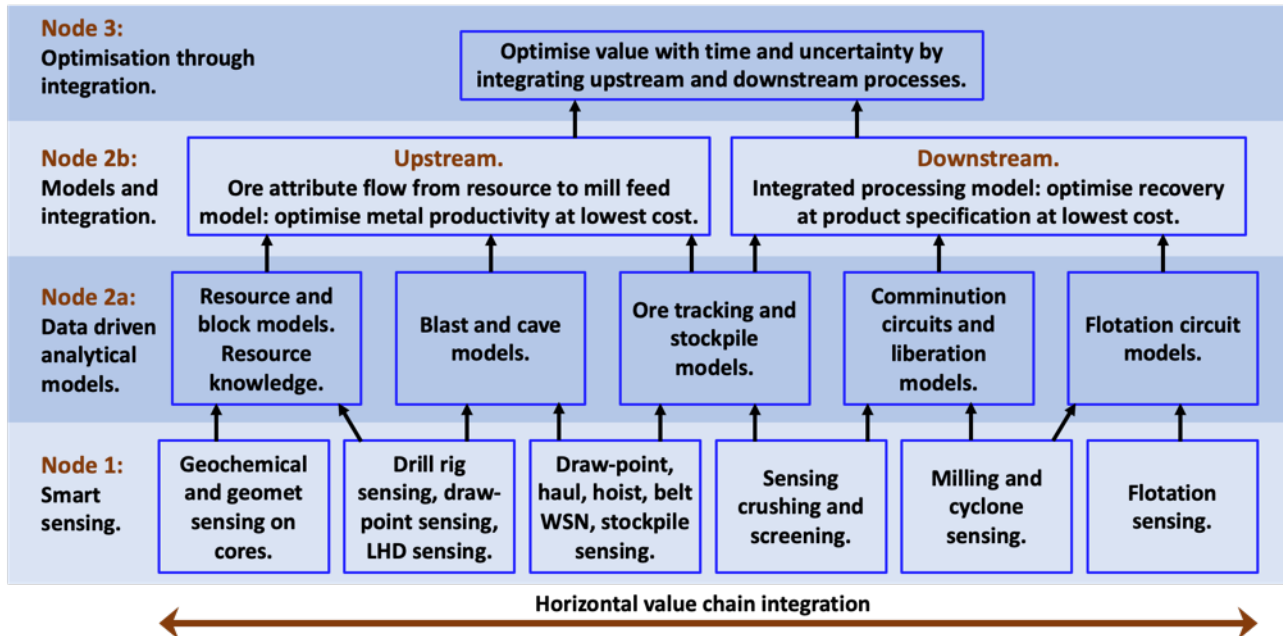


FIG 4 – Vertical and horizontal integration of the research nodes and research themes.

The PhD and Post-Doctoral Research projects

The research is being conducted by 16 PhD scholars and three Post-Doctoral Researchers (PDR). The 16 PhD projects and the three PDR positions together with academic and industry supervisors and translation partners will deliver the Training Centre outcomes and translate them into industry-ready implementations. The 16 PhD projects are:

1. Cross-borehole seismic interferometry to interpolate rock mass and geometallurgical variables.
2. Drawpoint and cave operations and fragmentation sensing.
3. Wireless sensor network RFID for continuously deployable tagging.
4. Gold sensing: low chemical-low energy biological extraction.
5. Vibration and accelerometer sensing for early stage roping detection in hydrocyclones.
6. Pulp chemistry monitoring for leach applications.
7. Integration and analytics of drill sensor information to derive geometallurgical attributes.
8. Fingerprinting ore types and blends by fusing hyper-spectral and other sensors using machine learning.
9. Ore tracking model from uncertain resource model to belt sensors and run-of-mine stockpiles.
10. Integrating sensors to maximise crushing plant throughput.
11. Integrating grinding circuit sensors including ultrasonics for particle size distributions to maximise mill throughput.

12. Integration and analytics of pulp chemistry sensor information with in-stream analysis for flotation plant optimisation.
13. Integrating in-stream and particle size measurements.
14. Rapid updating of resource knowledge with sensor information for rapid decision-making.
15. Measuring and monitoring particle size distributions and grade to divert low-value waste.
16. Linking the resource to downstream products.

Under the training component of the Centre, each PhD scholar will spend a total of 12 months conducting their research within the partner industry companies to ensure that their research is industry relevant, and outcomes are at meaningful technology readiness levels.

The Postdoctoral Researchers contribute to the following research projects:

- PDR1:
 - Wireless sensor network radio frequency identification for continuously deployable tagging (linked to PhD project 3).
 - Decreasing acquisition time on high tonnage run-of-mine belts using Prompt Gamma Neutron Activation Analysis, possibly in combination with other sensors such as X-ray Transmission and hyper-spectral imaging.
 - Vibration and accelerometer sensing for early stage roping detection in hydrocyclones (linked to PhD project 5).
 - An ore tracking model from uncertain resource model to belt sensors and run-of-mine stockpiles (linked to PhD project 9).
 - Sensing variable mineralogy on high tonnage run-of-mine belts by fusing multi-sensor data.
 - Integration of sensors to maximise crushing plant throughput (linked to PhD project 10).
- PDR2: contributes to the following research projects:
 - Integration and analytics of pulp chemistry sensor information with in-stream analysis for flotation plant optimisation (linked to PhD project 12).
 - Integration of leaching sensor information for hydrometallurgical processing.
- PDR3: contributes to the following research projects:
 - Rapid updating of resource knowledge with sensor information including structures (linked to PhD project 14).
 - Drawpoint and LHD productivity based on optimised fragmentation through blast control (linked to PhD project 2).
 - Optimising resource value through ore selection to downstream processing.

All three PDR positions contribute to an integrated simulator to link resource knowledge to models across the value chain for optimisation.

Industry partners

Current industry partners are as follows.

- End-users: BHP Olympic Dam, OZ Minerals
- Translation partners: Boart Longyear, Bureau Veritas, CRC ORE, Datanet Asia Pacific, Dassault Systèmes, EKA Software Solutions, Magotteaux, Manta Controls, Maptek, MZ Minerals, Orica, Petra Data Science, Rockwell Automation, RoqSense and Scantech,
- Supporting Partners: AMIRA Global, METS Ignited, Resources and Engineering Skills Alliance, South Australia Government Department for Energy and Mining.

Governance

The governance structure of the Training Centre includes an Advisory Committee and a Science Advisory Committee with membership that comprises leading researchers and industry leaders from Australia and around the World. This ensures that the Training Centre performs at international levels and engages with the highest levels of research and industry practice worldwide.

Key metrics for success

Key breakthrough: significant reduction in the time taken to sense variations in ore attributes across the value chain to enable decision-making in both mining and processing in the shorter term, preferably in real time.

The key outcomes are:

- Diagnostic tools (eg sensor fusion, tracking) to determine the causes of short-term variability in performance and to enable rectification.
- Increased productivity and value.

Summary

The presentation will expand on the research component and the general approach to interdisciplinary research. It will also provide examples of research outputs to date.

ACKNOWLEDGEMENTS

Members of the Training Centre, all of whom have contributed to establishing this enterprise.

Creating the modern mine – beyond 2025 at Prominent Hill Operations

G Iwanow¹, K Mant² and K Hobbs³

1. General Manager, Prominent Hill, OZ Minerals, Adelaide SA 5950.
Email: gabrielle.iwanow@ozminerals.com
2. Manager, People and Transformation, OZ Minerals, Adelaide SA 5950.
Email: kevin.mant@ozminerals.com
3. Manager, Studies, Prominent Hill, OZ Minerals, Adelaide SA 5950.
Email: kate.hobbs@ozminerals.com

INTRODUCTION

Prominent Hill is a copper-gold-silver mine in South Australia, which has delivered on its annual production guidance for the past six years and operates in the lowest cost quartile globally. Prominent Hill first came on stream in 2009 and in 2018, transitioned to an underground-only operation. It ramped up to a 4 million tonnes per annum (Mtpa) run rate in 2020. Further plans are in place to increase production to between 4–5 Mtpa from 2022. Upon completion of the Wira shaft installation in 2024, the underground production rate will increase to 6 Mtpa from 2025.

In 2019, the Site Leadership Team commenced a broader transformation program (Figure 1) so Prominent Hill is well positioned for the future as a Modern Mine; delivering value for OZ Minerals' five stakeholder groups and ensuring the safety, cost, and production fundamentals as a long-life asset.

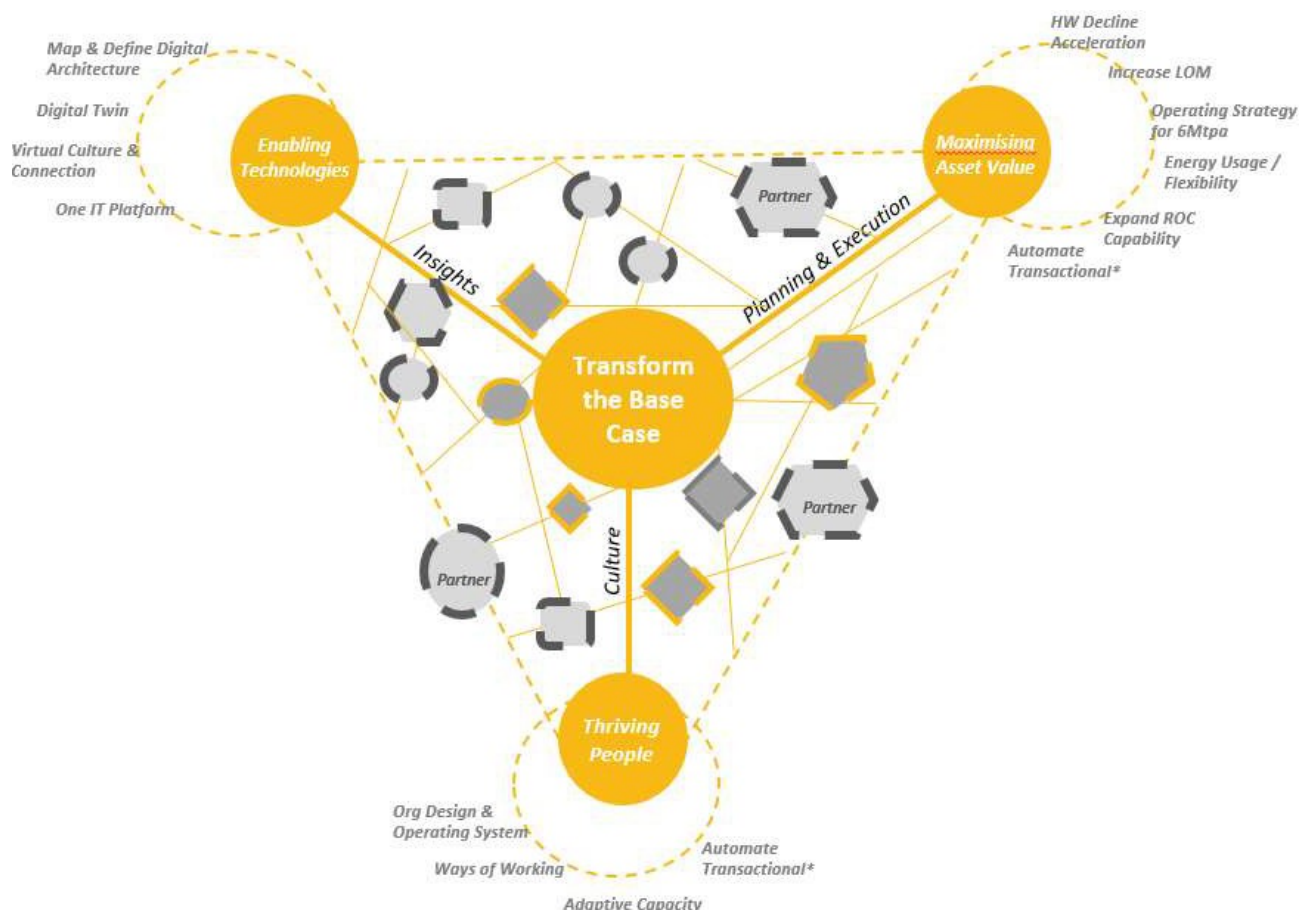


FIG 1 – Prominent Hill transformation program.

Enabling technologies

Prominent Hill has a digital strategy to deliver positive, measurable business impact by focusing on four key areas:

1. Product optimisation: providing an ability to turn data into insights for downtime analysis, delay accounting and process optimisation.
2. Value chain optimisation: providing visibility across the entire value chain in a unified environment.
3. Asset performance management: providing predictive equipment failure warnings and digitalisation of maintenance procedures.
4. Workforce transformation: creating a mobile workforce, enhanced collaboration and state-of-the-art training options through mobile applications, digital collaborations, augmented reality, and operator training simulation.

Maximising asset and orebody value

The Prominent Hill mineralisation consists of lenses found across five main zones. These include:

1. Malu, the main mineralised corridor that plunges down from the base of the open pit.
2. Ankata, an independent area to the west of Malu and relatively close to surface.
3. Kalaya, an area directly to the west of, and along strike from Malu.
4. Papa, a small area of mineralisation to the east of the open pit.
5. Walawuru, a thin, tabular zone of mineralisation on the western side of the open pit.

Mining activities are currently undertaken in Ankata and the upper region of Malu. Prominent Hill has significant Inferred Mineral Resources with the Malu and Kalaya mineralisation zones both open at depth (Figure 2).

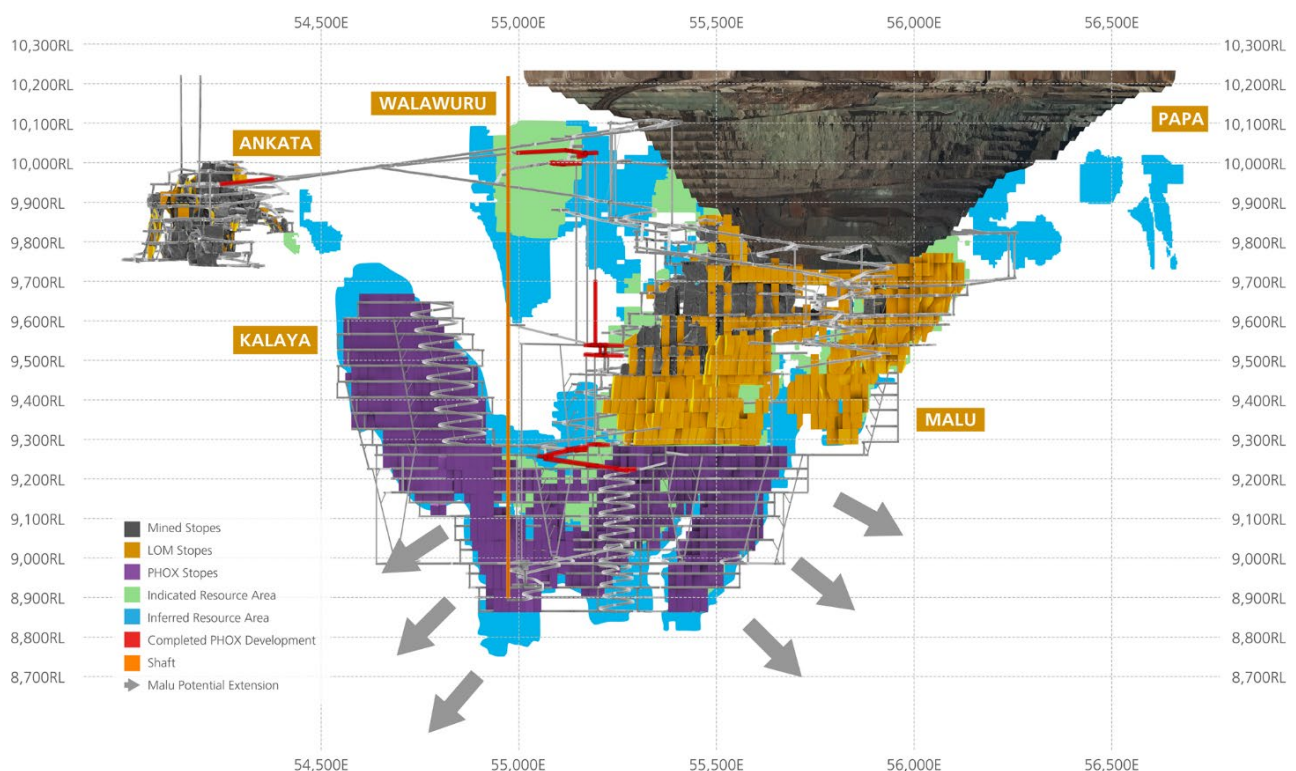


FIG 2 – Conceptual Prominent Hill expansion study update mine layout in the context of Prominent Hill mineral resources, ore reserves and exploration potential, Prominent Hill expansion study update, August 2021.

In 2020, the operation started to take a more assertive approach to understand its orebody. The Prominent Hill (PHOX) Expansion Study was established to examine the safety, economic and technical feasibility of installing a shaft which would further increase the annual underground mining rate, extend the mine life, and reduce the overall operational risk.

In August 2021, the OZ Minerals Board approved construction of a hoisting shaft at the mine which will extend the mine life to at least 2036 at 6 Mtpa. The \$600 m Prominent Hill Wira shaft investment provides access to further value upside with approximately 45 per cent of the mineral resource remaining outside the shaft mine plan.

Thriving people

Prominent Hill is working to evolve traditional work arrangements into arrangements that support different lifestyles and requirements. The goal is to align the needs of the operation (performance, cost, innovation) with the needs of the workforce (meaningful work, personal growth, fair rewards, connection, and impact) through flexibility. Operations are supported by Prominent Hill employees and partner organisations (in mining production and shutdown activities), with some alliance partnerships in place. Previously:

- Work was expected to be done on-site.
- Working patterns were expected to be mostly on 12-hour or 12.5-hour shifts, over typical shift arrangements such as 8:6, 2:2 and 2:1 swings.
- The assumption was that all operational work must have 24/7 coverage.

Mapping the work across the operation has created a baseline for re-imagining how and where work occurs in the future Prominent Hill. Having a strong understanding of the work activities also ensures that future process automation impacts are effective and impacts to specific roles are thoughtfully managed.

Adopting an agile approach to driving change has already delivered results:

- On any given day, approximately 30 per cent of the Prominent Hill workforce is working remotely, on work patterns tailored to suit their lifestyles (this peaked at 40 per cent during the initial period of Covid-19 lockdowns).
- OZ Minerals has embedded a work standard to continually encourage people to review their personal needs with the needs of the operation and seek tailored work arrangements through an agreed Work-Life Plan. As well as creating opportunities on an individual level, the benefits to Prominent Hill includes lower cost operations and the ability to attract a different cohort of people who would not have been able to manage traditional FIFO arrangements.
- The current state mapping of the work of the operation has enabled leaders to understand how the current organisation design performs in practice, and where there may be optimisation opportunities in the short and longer term (for example, removing duplication, reducing bureaucracy).
- Understanding the current state and future options for designing teams around the work has led to the 2025 Prominent Hill Operating Model. The operating model will contribute to a modern mine by grouping work where, when and by whom it can be completed in the most effective, efficient and inclusive manner. It unlocks significant value through adoption of process automation, robotics, and digitalisation to free people up for creative problem solving and opportunity responsiveness.

ACKNOWLEDGEMENTS

This abstract has been approved for release by OZ Minerals. We would like to thank the entire Prominent Hill workforce, and Sam Rees, Keaveney Consulting.

Forward looking and cautionary statements

This document has been prepared by OZ Minerals Limited.

Some statements in this document are forward-looking statements. By their nature, forward-looking statements involve risk and uncertainty because they relate to events and depend on circumstances that will occur in the future and may be outside OZ Minerals' control. Actual results and developments may differ materially from those expressed or implied in such statements because of a number of factors, including levels of demand and market prices, the ability to produce and transport products

profitably, the impact of foreign currency exchange rates on market prices and operating costs, operational problems, political uncertainty and economic conditions in relevant areas of the world, the actions of competitors, activities by governmental authorities such as changes in taxation or regulation.

Given these risks and uncertainties, undue reliance should not be placed on forward-looking statements which speak only as at the date of the document. Subject to any continuing obligations under applicable law or any relevant stock exchange listing rules, OZ Minerals does not undertake any obligation to publicly release any updates or revisions to any forward looking statements contained in this document, whether as a result of any change in OZ Minerals' expectations in relation to them, or any change in events, conditions or circumstances on which any such statement is based.

This document should be read in conjunction with the Prominent Hill Exploration Results and the Prominent Hill 2020 Mineral Resource and Ore Reserve Statement and Explanatory Notes which can be found on www.ozminerals.com.

Developing a foundation of a framework for evaluating the impact of mining technological innovation on a company's market value

P Mugebe¹, M S Kizil², M Yahyaei³ and R Low⁴

1. MAusIMM, PhD student, The University of Queensland, School of Mechanical and Mining, St Lucia Qld 4067. Email: p.mugebe@uq.edu.au
2. MAusIMM, A/Professor, The University of Queensland, School of Mechanical and Mining, St Lucia Qld 4067. Email: m.kizil@uq.edu.au
3. A/Professor, The University of Queensland, Julius Kruttschnitt Mineral Research Centre, Indooroopilly Qld 4067. Email: m.yahyaei@uq.edu.au
4. A/Professor, The University of Queensland, School of Business, St Lucia Qld 4067. Email: r.low@business.uq.edu.au

INTRODUCTION

Technological innovation development plays a pivotal role in the economics of minerals mining. History shows that the difference between a mineral deposit's economic status and its uneconomic status lies in the mining technological innovation most prevalent. The significance of mining technology is that it curbs the negative impact of mineral deposit depletion by improving productivity, thereby keeping mineral exploitation profitable. This relationship makes it imperative to develop a framework that utilises this concept to sustain mining in the future. The framework will incorporate the benefits of technological innovation implementation to demonstrate its impact on a company's share price.

This paper demonstrates how applying technological development and innovation affects mining processes and its economics. This relationship is evident throughout the four historical mining technological stages, which started in the 18th century with mechanisation, then remote control, automation, and currently, autonomous technology systems. At each stage, the need for a more productive technology arose as the effects of mineral resources depletion threatened mining's profitability. Thus, it is evident that the future of mining profitability lies in the current advanced technologies that leverage artificial intelligence and machine learning systems. Nonetheless, while mineral commodity miners profit and firm market values grow, the growth is not empirically linked to the technological innovation development that drives it. Conversely, in other industries, the firm's technological development innovation resultant economic metrics, along with macroeconomic factors, are captured and empirically linked to stock market value. This exposes a gap in the financial impact evaluation of mining technology innovation implementation. Therefore, it is necessary to lay the basis for developing that framework for the mining industry. The work involves identifying improved productivity and cost metrics, profit margin growth, and the resultant share price performance.

The mining industry is faced with many challenges which threaten its continued viability. The first problem is the depletion of high-grade mineral deposits, at the backdrop of global mineral demand for industrial growth and socio-economic welfare (Mitra, 2019; Ren *et al*, 2019; Brundrett, 2014). For industry sustainability, methods to increase productivity must be found to combat the effects of resource depletion (Coulson, 2012; Hartwick, Olewiler and Preuss, 1986; Humphreys, 2019b; Nebot, 2007; Tilton, 2018). The rising costs of labour, equipment maintenance, safety, and environmental stewardship (Humphreys, 2019a; Brundrett, 2014) are another challenge. For all these challenges, the rescue can be found in a cost-saving mining technological innovation which comes as a capital cost but with operating cost trade-offs in incremental "benefits in safety, productivity, tyre life, maintenance, personnel management and environmental stewardship" (Price, 2017). Such trade-off benefits ensure that the mining industry remains profitable and hence sustainable.

This study aims to address a research question from the standpoint that the difference between the economic status of a mineral deposit and its uneconomic status lies in the level of mining technological innovation most prevalent in each time (Wright and Czelusta, 2003; Wellmer and Scholz, 2017; Hartwick, Olewiler and Preuss, 1986). Several studies show that mining technological innovation improves the profitability of mineral deposit exploitation by improving mining productivity

(Tilton, 1989, 2014; Mitra, 2019; Humphreys, 2019a, 2019b; Topp, 2008; Bartos, 2007; Accenture, 2010; Sánchez and Hartlieb, 2020). Thus, based on a direct relationship between technological innovation and firm market value in other industries (Sood and Tellis, 2009; Nicolau and Santa-Maria, 2013; Schroeder, Scudder and Elm, 1989; Koellinger, 2008), it is expected that share price performance of mineral commodities conforms to the same relationship. Therefore, the research question is whether mining technological innovation has ultimately been linked to sharing price performance for mineral commodities. If so, could that relationship be used by both mineral commodity operators and the public investors for investment decision-making?

Interestingly, the literature shows no evidence of an empirically defined impact of mining technological innovation on a mineral commodity's share price performance. Most literature concentrates on cost benefits, improved productivity, and safety (Tilton, 2014; Mitra, 2019; Brown, 2012; Fan, Yan and Sha, 2017). Even more benefits are realised with the introduction of autonomous haulage system (AHS) technology implementation in open pit mining. However, mining technological innovation impact on share price performance has not been described. This void presents a loss of opportunity to have an empirical relationship between mining technological innovation and share price performance. This study sets the foundation for building that scientific framework.

The framework results in a tool that mineral commodity operators and other investors can use to make investment decisions. It will be an additional tool for mining technology projects investment approval process for the mineral commodity operators. The public investors will use it to decide whether to invest in a mineral commodity company that is implementing a radical mining technological innovation. As indicated by (Sorescu *et al*, 2018), many investors follow developments and news about certain organisations. Their investment into or divestment from the organisations is informed by what they find. This two-pronged usefulness of the framework makes this study a worthy exercise.

To test the validity of a relationship between mining technological innovation implementation and share price performance, an investigation into the potential impact of AHS implementation on iron ore stock price of Fortescue Metals Group (FMG) was conducted. It is demonstrated that FMG commenced the implementation of autonomous haulage system in 2012 and realised significant mining productivity and cost improvement (FMG, 2020; Gölbaşı and Dagdelen, 2017; Leonida, 2019), profit margin growth, and a subsequent skyrocketing of share price performance (ASX, 2021). This is shown in Figures 1 and 2.

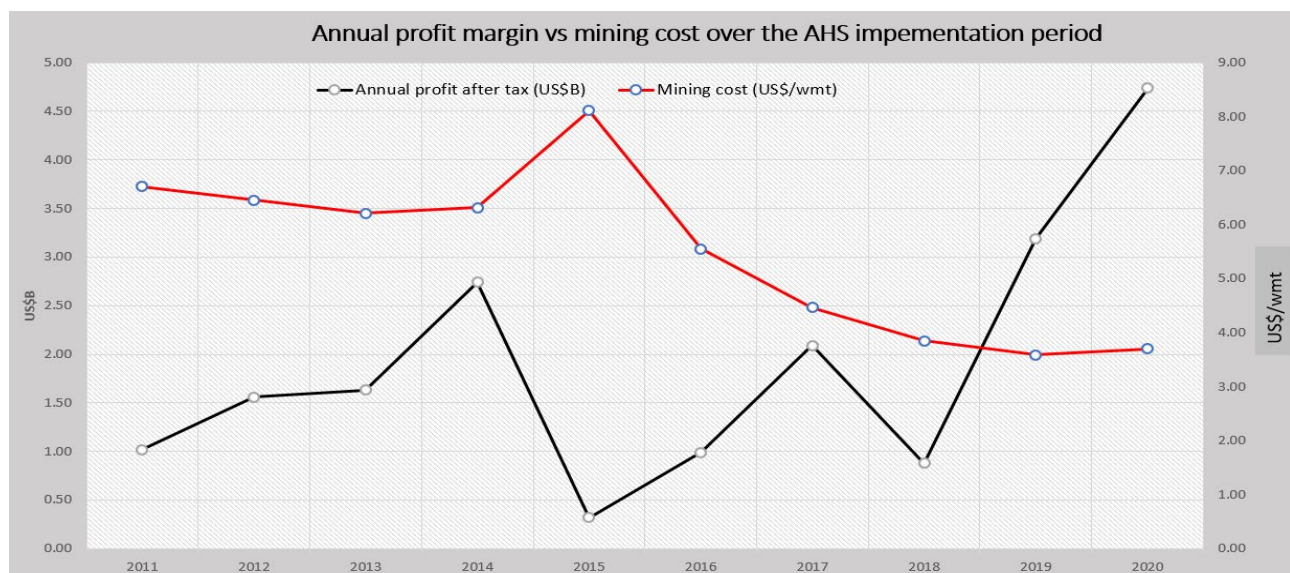


FIG 1 – Annual profit versus mining cost over AHS implementation period.

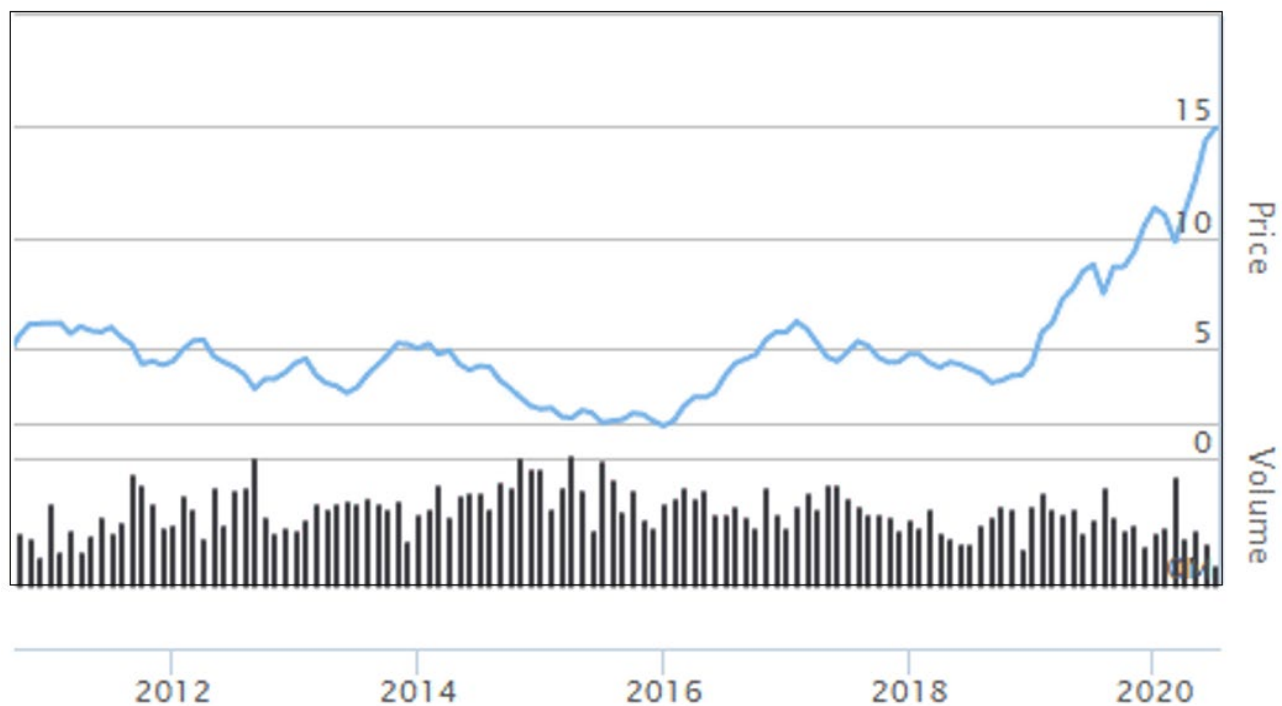


FIG 2 – FMG stock price over AHS implementation period (ASX, 2021).

The case study showed evidence of a relationship between mining technological innovation implementation and share price performance. Consequently, this study lays the foundation for the development of a framework for evaluating mining technological innovation impact on a company's market value.

ACKNOWLEDGEMENTS

Sincere gratitude goes to the research advisors, Associate Professors Mehmet Kizil, Mohsen Yahyaei, and Rand Low, for their support and encouragement. The University of Queensland is equally acknowledged for providing the necessary resources for the research.

REFERENCES

- Accenture, 2010. Using autonomous equipment to achieve high performance in the mining industry. *Accenture*.
- ASX, 2021. *Fortescue Metals Group* [Online]. 2021: ASX. Available: <https://www2.asx.com.au/markets/company/FMG> [Accessed 18/06/2021].
- Bartos, P J, 2007. Is mining a high-tech industry?: Investigations into innovation and productivity advance. *Resources Policy*, 32, 149–158.
- Brown, C, 2012. Autonomous vehicle technology in mining: how it works and how it's applied from user assist to full autonomy (Autonomous Mining). *E&MJ – Engineering & Mining Journal*, 213, 30.
- Brundrett, S, 2014. *Industry Analysis of Autonomous Mine Haul Truck Commercialization*. Simon Fraser University.
- Coulson, M, 2012. *The history of mining: The events, technology and people involved in the industry that forged the modern world*, Great Britain, Harriman House Ltd.
- Fan, S, Yan, J and Sha, J, 2017. Innovation and economic growth in the mining industry: Evidence from China's listed companies. *Resources Policy*, 54, 25–42.
- FMG, 2020. Fortescue automation deployment reaches significant milestone. *FMG News*.
- Gölbaşı, O and Dagdelen, K, 2017. Equipment replacement analysis of manual trucks with autonomous truck technology in open pit mines. *Proceedings of the 38th International Symposium on the Application of Computers and Operations Research (APCOM 2017) in the Mineral Industry*.
- Hartwick, J M, Olewiler, N D and Preuss, R, 1986. The economics of natural resource use.
- Humphreys, D, 2019a. The mining industry after the boom. *Mineral Economics*, 32, 145–151.
- Humphreys, D, 2019b. Mining productivity and the fourth industrial revolution. *Mineral Economics*, 33, 115–125.

- Koellinger, P, 2008. The relationship between technology, innovation, and firm performance—Empirical evidence from e-business in Europe. *Research policy*, 37, 1317–1328.
- Leonida, C, 2019. Optimising Autonomous Haulage. *Engineering and Mining Journal*, 220, 36–43.
- Mitra, S, 2019. Depletion, technology, and productivity growth in the metallic minerals industry. *Mineral Economics* 32, 19–37
- Nebot, E M, 2007. Surface mining: main research issues for autonomous operations. *Robotics Research*. Springer.
- Nicolau, J L and Santa-María, M J, 2013. The effect of innovation on hotel market value. *International Journal of Hospitality Management*, 32, 71–79.
- Price, R, 2017. Autonomous haulage systems-the business case. *AusIMM Bulletin*, 80.
- Ren, H, Zhao, Y, Xiao, W and Hu, Z, 2019. A review of UAV monitoring in mining areas: current status and future perspectives. *International journal of coal science & technology*, 6, 320–333.
- Sánchez, F and Hartlieb, P, 2020. Innovation in the Mining Industry: Technological Trends and a Case Study of the Challenges of Disruptive Innovation. *Mining, Metallurgy & Exploration*, 37, 1385–1399.
- Schroeder, R G, Scudder, G D and Elm, D R, 1989. Innovation in manufacturing. *Journal of Operations Management*, 8, 1–15.
- Sood, A and Tellis, G J, 2009. Do innovations really pay off? Total stock market returns to innovation. *Marketing Science*, 28, 442–456.
- Sorescu, A, Sorescu, M S, Armstrong, J W and Devoldere, B, 2018. Two Centuries of Innovations and stock market bubbles. *Marketing Science*, 37, 507–529.
- Tilton, J E, 1989. Changing trends in metal demand and the decline of mining and mineral processing in North America. *Resources Policy*, 15, 12–23.
- Tilton, J E, 2014. Cyclical and secular determinants of productivity in the copper, aluminum, iron ore, and coal industries. *Mineral Economics* 27, 1–19.
- Tilton, J E, 2018. The Hubbert peak model and assessing the threat of mineral depletion. *Resources, conservation and recycling*, 139, 280–286.
- Topp, V, 2008. Productivity in the mining industry: measurement and interpretation.
- Wellmer, F-W and Scholz, R W, 2017. Peak minerals: What can we learn from the history of mineral economics and the cases of gold and phosphorus? *Mineral Economics*, 30, 73–93.
- Wright, G and Czelusta, J, 2003. Mineral resources and economic development. Conference on Sector Reform in Latin America, Stanford Center for International Development. 13–15.

Digital twins meet virtual reality in the Australian mining industry

J Qu¹, M S Kizil², M Yahyaei³ and P Knights⁴

1. PhD student, The University of Queensland, School of Mechanical and Mining, St Lucia Qld. Email: juncong.qu@uq.net.au
2. MAusIMM, A/Professor, The University of Queensland, School of Mechanical and Mining, St Lucia Qld 4067. Email: m.kizil@uq.edu.au
3. A/Professor, The University of Queensland, Julius Kruttschnitt Mineral Research Centre, Indooroopilly Qld. Email: m.yahyaei@uq.edu.au
4. MAusIMM, Professor, The University of Queensland, School of Mechanical and Mining, St Lucia Qld. Email: p.knights@uq.edu.au

INTRODUCTION

Mining in the 21st century presents a complex set of challenges to the Australian mining industry. With shifting global demands due to the COVID-19 pandemic and shifted focus from a booming phase into an operational phase, mining companies are looking for ways to maximise long-term sustainability. Meanwhile, in the booming age of Industry 4.0 and IoTs, Virtual Reality (VR) simulation had demonstrated its values in training and incident reconstruction by providing an immersive, realistic, and team-orientated experience for the human operators in a safely controlled learning environment (Schroeder, 1993; Dorey and Knights, 2015; Bellanca *et al*, 2019).



FIG 1 – Virtual reality training in mining (University of Wollongong)

However, the adaptation of VR technologies remains limited around more advanced mining applications such as real-time data analysis, scenario simulation, and process optimisation with greater potentials to improve long-term operational decision-making and efficiency. While the manufacturing industry had been using Digital Twins (DT) – an accurate virtual replication of a physical entity providing human-readable, semantic, data-model of reality enabled by sophisticated AI algorithms to handle these tasks (Tao *et al*, 2018), the mining industry is presented with a unique set of challenges characterised by a lower level of automation, higher risk factor and greater emphasis on sustainability. These challenges call for a human-centred approach to the development of new technologies in the pursuit of a future of autonomous mining in Australia (Stothard *et al*, 2019). The concept of integrating Digital Twins (DT) with VR visualisation presents an opportunity for the Australian mining industry to balance resource extraction efficiency, environmental sustainability, and economy of throughput in remote operations while providing a more intuitive interface for human interaction, data presentation, knowledge sharing, team collaboration, and safer on-the-job training. This study aims to answer whether VR Digital Twins (VRDT) would be of value in the long run. To achieve this, the purpose and context for employing such a concept will be examined against current needs. Doing so would help set priorities by filtering out the hypes from the facts around the emerging technologies. Furthermore, the human factors around VR visualisation will be studied against the traditional dashboard-based DT interfaces to better understand its true potentials from a user perspective in terms of job effectiveness, possible VR-induced sickness, development cost, and user-friendliness.

As a baseline, businesses are interested in developing DTs capable of supporting plant productions throughout their entire life cycle, starting from surveying, plant design, engineering, and leading to plant construction, commissioning. The latest DT-related research trend in the mining sector focuses on supporting operational tasks such as real-time monitoring and control, system prognostic and process optimisation enabled by Artificial Intelligence and machine learning algorithms (Qi *et al*, 2021).



FIG 2 – The future of DT-related research in mining focuses on supporting operation and process optimisation.

A common issue of the traditional dashboard-based user interfaces developed for DT data visualisation is the lack of representation of the real-world space, geometries, scale, and sounds, making it difficult for an untrained set of eyes to gain an equivalent level of situational awareness from 2D charts and figures compared to conducting on-site inspections. Virtual Reality (VR), on the other hand, provides the tools to bridge the gap in human cognition between the physical world and a highly detailed 3D virtual environment that houses DT models of real-world mining assets (Stone, 2012; Stothard *et al*, 2015).

Using VR technologies also greatly enhances team collaboration across multiple users. A study conducted in 2018 outlined the distinct benefits of VR in attention management, developing shared mental models, and creating the perception of interdisciplinary knowledge (Litvinova *et al*, 2018).



FIG 3 – How VR facilitates team collaboration (modified from Litvinova *et al*, 2018).

VR can also influence how DT controls the physical entity by allowing operators to take manual control of the Digital Twin in an intuitive way, thanks to its human-centred interactive functionalities. In case of a manual override, DT can act as an agent that passes human decisions to the physical entity in the real world. Since a functional DT is modelled with a set of rules and constraints based on physical limitations and safety guidelines, human errors can be effectively filtered out by the evaluation from the Digital Twin. In a conceptual sense, this works similarly to the fly-by-wire systems installed in modern aircraft.

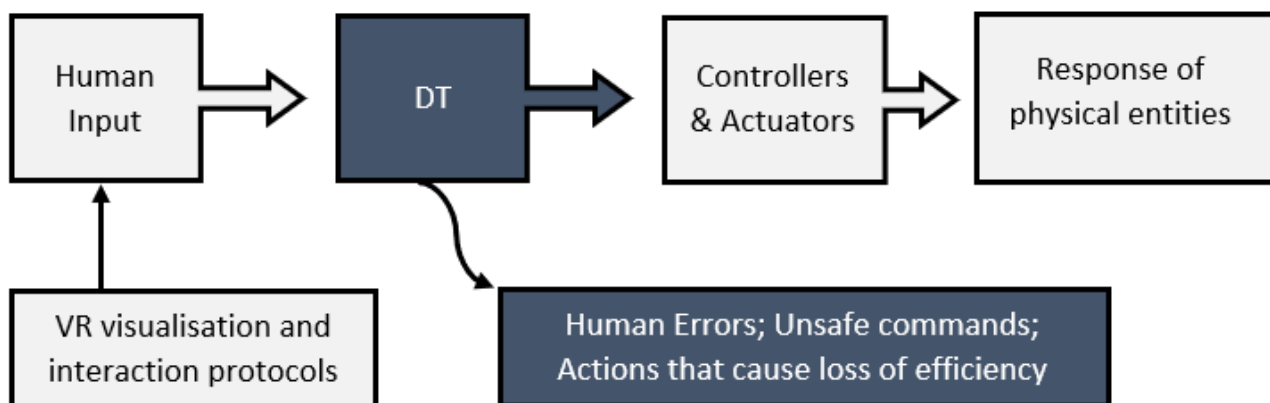


FIG 4 – Concept of VR digital twin acts as safeguard in manual override.

For a long time, the adoption of Virtual Reality simulation technologies had faced bottlenecks in the mining industry due to the time-consuming nature of creating a detailed 3D environment (Stothard *et al*, 2019). In recent years, advancements in autonomous robotic and lidar scanning technologies opened the door to fast geometric mapping of mine sites, therefore significantly shortening the human overhead previously needed to create a virtual environment. The study suggests that combining the full benefits of Digital Twins and Virtual Reality would require a strategic approach by the mining industry and would complement future advancements towards autonomous mining in Australia. In the short-term, VR Digital Twins shows excellent potential in lowering sustainment costs of mining operations by bridging the gap between on-site workers with off-site supports.

REFERENCES

- Bellanca, J L O, Timothy, J, Helfrich, W J, MacDonald, B, Navoyski, J and Demich, B. (2019). Developing a Virtual Reality Environment for Mining Research. *Mining, metallurgy and exploration*, 36(4), 597–606. doi:10.1007/s42461-018-0046-2
- Dorey, F and Knights, P F. (2015). Quantifying the benefits of simulator training for dragline operators. *Transactions of the Institution of Mining and Metallurgy. Section A, Mining technology*, 124(2), 97–106. doi:10.1179/1743286315Y.0000000007
- Litvinova, Y, Rehm, S-V, Goel, L C and Junglas, I. (2018, 1 January). *Collaborating in Virtual Reality by using Digital Twins*. Paper presented at the ISPIM Conference Proceedings, Manchester.
- Qi, Q, Tao, F, Hu, T, Anwer, N, Liu, A, Wei, Y, Wang, L and Nee, A Y C. (2021). Enabling technologies and tools for digital twin. *Journal of manufacturing systems*, 58, 3–21. doi: 10.1016/j.jmsy.2019.10.001
- Schroeder, R. (1993). Virtual reality in the real world: History, applications and projections. *Futures: the journal of policy, planning and futures studies*, 25(9), 963–973. doi:10.1016/0016-3287(93)90062-X
- Stone, R J. (2012). *Human Factors Guidance for Designers of Interactive 3D and Games-Based Training Systems* (2 ed.). Birmingham (UK): University of Birmingham (UK).
- Stothard, P, Squelch, A, Stone, R and van Wyk, E. (2019). Towards sustainable mixed reality simulation for the mining industry. *Mining technology* (2018), 128(4), 246–254. doi:10.1080/25726668.2019.1645519
- Stothard, P, Squelch, A, Stone, R, van Wyk, E, Kizil, M, Schofield, D and Fowle, K. (2015). Taxonomy of interactive computer-based visualisation systems and content for the mining industry. *Transactions of the Institution of Mining and Metallurgy. Section A, Mining technology*, 124(2), 83–96. doi:10.1179/1743286315Y.0000000006
- Tao, F, Cheng, J, Qi, Q, Zhang, M, Zhang, H and Sui, F. (2018). Digital twin-driven product design, manufacturing and service with big data. *International journal of advanced manufacturing technology* 94(9): 3563-3576.

Global digitalisation trends in mining and their impact on aspects of sustainability

A Sörensen¹, F Uth², R Mitra³, F Lehnen⁴, B Schwarze⁵ and E Clausen⁶

1. Scientific Research Assistant, Institute for Advanced Mining Technologies (AMT), RWTH Aachen University, Aachen, Germany. Email: asoerensen@amt.rwth-aachen.de
2. Mining Engineer, Regierung von Oberbayern, Munich, Germany. Email: fabian.uth@reg-ob.bayern.de
3. Head of Research, Institute for AMT, RWTH Aachen University, Aachen, Germany. Email: rmitra@amt.rwth-aachen.de
4. Head of Business Area 'Radwaste Disposal, Mining and Environmental Management', Brenk Systemplanung GmbH (BRENK), Aachen, Germany. Email: f.lehnen@brenk.com
5. Geoscientist, BRENK, Aachen, Germany. Email: b.schwarze@brenk.com
6. Director, Institute for AMT, RWTH Aachen University, Aachen, Germany. Email: eclausen@amt.rwth-aachen.de

INTRODUCTION

There is an increasing demand and rising expectation in the mining industry towards governance issues such as transparency, sustainability and responsibility. This demand arises from across the value chain and stakeholder groups. Shareholders want to make sure they get a return on investment while increasingly caring about the 'triple bottom line' of social, environmental and economic performance – also reflecting the three pillars of sustainability. This new species of 'Social Investors' is looking for good Environmental, Social and Governance ratings of the companies in which they invest. The demand for transparency in the supply chain of the minerals from the customers of the end product are also increasing. At the same time, local communities have increasing demands for communal engagement and their long-term benefits. Regulatory pressure results from requirements for environmentally sustainable production (eg carbon taxes). Governments, including Germany's, are committed to supporting responsible extraction and efficient use of materials as well as improving transparency in raw materials supply chains and decreasing the environmental footprint of mining operations – both domestic and abroad (BMW, 2020). At the same time, news travels the globe in an instant through social and online media and can have a huge impact on stock performance of mining companies or the social license to operate of individual mining projects.

Excess capital spending during commodity boom cycles has confronted the industry with enormous pressure for cost cutting and productivity improvements. Moreover, while technological advances have improved methods for locating and extracting raw materials, high-grade deposit zones in easy to access locations have been largely depleted. The technical possibility of mining ores at lower grades increases both the cost as well as the amount of waste rock generated. In addition, remote and deeper deposits drive up development and operational costs and may pose additional challenges. These challenges may also have implications for energy consumption and greenhouse gas emissions, for example through long distance transports of material and people or the increased amount of energy needed for ventilation in greater depths.

It follows, that mining operations today are under two kinds of pressure: On the one hand, they have to address challenges that can be considered inherent to the industry, such as changing geology, rising operational costs along with commodity price cycles. To meet these challenges mining operations need to become more efficient. On the other hand, mining operations are facing pressure from external stakeholders, which are forcing the industry to take governance issues such as transparency, sustainability and responsibility seriously. Sustainable business practices are no longer a 'nice to have', but are increasingly becoming indispensable for long-term productivity, and consequently, economic survival (Ellis, 2020).

To date, digitalisation and automation can be seen as two of the key answers to these challenges leading to measurable improvements in productivity and cost management as well as transparency. Figure 1 provides a schematic of the mining processes affected by digitalisation technologies. Although mining is still in the early stages of digital transformation compared to other industries, the global mining industry has begun the digitalisation journey and has been undergoing significant

changes over the past decade. However, success is not guaranteed by simply introducing new technologies. The landscape of digitalisation in mining is heterogeneous and success factors are still being evaluated.

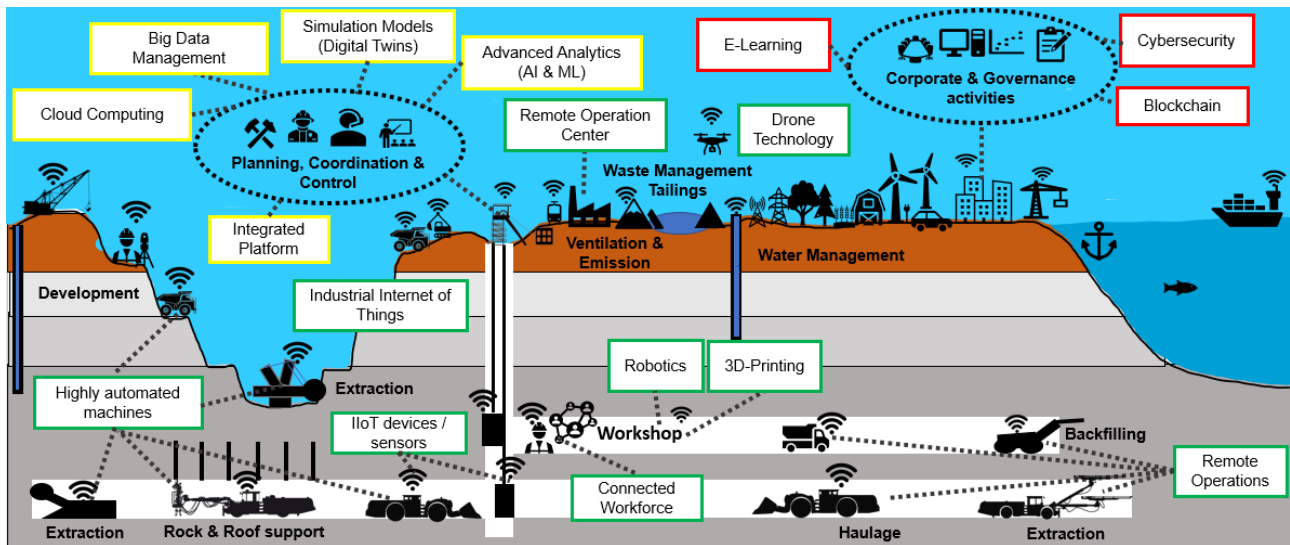


FIG 1 – Schematic illustration of mining processes affected by digitalisation technologies (Clausen *et al*, 2020a).

The complex relationship between digitalisation and sustainable business practices has not been investigated systematically yet. Therefore, the German Federal Institute for Geosciences and Natural Resources (BGR) recently commissioned a study on the ‘Assessment of the effects of global digitalisation trends on sustainability in mining’ (Clausen *et al*, 2020a, 2020b). The purpose of the study was to provide a systematic investigation into the correlation between digitalisation and sustainability. It contributes to understanding the current process of change in the global mining sector, especially with regard to the assumed interconnection between processes of digitalisation and sustainability on a global scale. While the study focused on metal mining, all forms of mining, from artisanal and small and medium-sized enterprise to industrial large-scale mining (LSM), were included. However, since the current process of digital transformation, albeit still in its early stages, is taking place predominantly at large-scale, highly mechanised and automated mining operations, this publication focuses on the results concerning LSM operations only.

The study presumed, as a hypothesis, that processes of digitalisation are closely linked to various aspects of sustainability. Thus, the study examined digitalisation trends in mining and their impact on sustainability at a mining process level as well as with regard to the global development of the sector and related markets. Secondly, the study investigated whether the level of implementation as well as the impact and benefit of digitalisation trends vary in relation to certain influencing factors, ie the geographical region, type of commodity, mining method, size of operation or company size.

CONCLUSIONS

Within the framework of the study, the following conclusions were drawn, among others.

The leading technological trends included integrated platform, automation, advanced analytics, simulation/visualisation, industrial internet of things (IIoT), remote operation centre and connected worker, among others.

At the current level of implementation of digital initiatives, mining companies seem to prioritise and focus on optimising certain areas of the operation. Consequently, not all available technologies are found to be implemented in a single operation.

Mining companies have to cope with implementation challenges such as interoperability and standardisation as well as legal issues, which are not just technological in nature. Another pressing challenge is talent management, followed by challenges related to data management and change management, as well as innovation and collaboration.

While OEMs originally pushed the market, now the mining companies are pulling the market and driving transformation. Today, mining companies are more aware of the available technologies and their specific requirements, technical needs, and expected outcomes. Both mining companies and technology suppliers foster a corresponding ecosystem of innovation and change. Accordingly, partnerships, especially with respect to interoperability, appear and lighthouse projects are being built – capable to address the challenges and opportunities of the upcoming years.

The size of the operation in conjunction with the size of the company has the highest influence on the level of implementation of digital initiatives and related technologies. In contrast, geographical region and commodity type were found to have the lowest influence.

Although mainly globally operating corporations were found to drive the digital transformation, it should be noted that there are a number of smaller, but highly mechanised and technologically advanced mining companies that drive digital transformation, especially in Europe and in Canada.

Regional clusters form where certain digital technologies have already been implemented to a higher degree exist, for example in the Pilbara region in Australia.

The advancement of sustainability, just as the implementation of digital initiatives, is closely inter-related with the respective company's priorities in conjunction with the company's specific decisions on how to address specific aspects of digitalisation and sustainability.

- Digitalisation and sustainability are already intrinsically linked. Digitalisation was found to be an important enabler for sustainable operations. The analysis of the drivers and incentives for digital transformation clearly shows that economic profits, OHS and sustainability are linked to one another and the digitalisation technologies as such.

In conclusion, mining companies are being challenged to change, adapt, and innovate in order to remain competitive and economically viable in the future. Both, digital transformation and sustainability have thus become hallmarks of the discussion on how mining companies can master the challenges of the future.

ACKNOWLEDGEMENTS

The authors would like to thank German Federal Institute for Geosciences and Natural Resources (BGR) for their financial support for the study. They would also like to thank all the experts who agreed to be interviewed and shared their opinion in regard to this topic.

REFERENCES

- BMWi, 2020. Rohstoffstrategie der Bundesregierung. [Accessed 10 May 2020], Available from: <https://www.bmwi.de/Redaktion/DE/Publikationen/Industrie/rohstoffstrategie-der-bundesregierung.pdf?__blob=publicationFile&v=4>
- Clausen, E, Sörensen, A, Uth, F, Mitra, R, Lehnen, F and Schwarze, B, 2020a. Assessment of the Effects of Global Digitalization Trends on Sustainability in Mining – Part I: Digitalization Processes in the Mining Industry in the Context of Sustainability. Commissioned by: Bundesanstalt für Geowissenschaften und Rohstoffe (Federal Institute for Geosciences and Natural Resources), Sep 2020, ISBN: 978–3-948532–14–7. Available from: <https://www.bgr.bund.de/EN/Themen/Min_rohstoffe/Downloads/digitalization_mining_sustainability_part_I_en.html> [Accessed 1 May 2021].
- Clausen, E, Sörensen, A, Uth, F, Mitra, R, Lehnen, F and Schwarze, B, 2020b. Assessment of the Effects of Global Digitalization Trends on Sustainability in Mining – Part II: Evaluation of Digitalization Trends and their Effects on Sustainability in the Global Mining Sector. Commissioned by: Bundesanstalt für Geowissenschaften und Rohstoffe (Federal Institute for Geosciences and Natural Resources), Dec 2020, ISBN: 978–3-948532–31–4. Available from <https://www.bgr.bund.de/EN/Themen/Min_rohstoffe/Downloads/digitalization_trends_mining_sustainability_part_II_en.html> [Accessed 1 May 2021].
- Ellis, I, 2020. Why Sustainability will be a Key Issue to the Mining Industry's Future. Available from: <<https://www.nsenergybusiness.com/features/sustainability-mining/>> [Accessed 15 May 2020].

The breakthrough technology for digital transformation of mining business

B Vorobyov¹, S Reznichenko² and V Monastyrov³

1. Chairman of the Board, SightPower Inc., Ottawa Canada K1T 0C6.
Email: borys.vorobyov@sight-power.com
2. President and CEO, SightPower Inc., Johannesburg SAR 2192.
Email: sergey.reznichenko@sight-power.com
3. CTO, SightPower Inc., Ottawa Canada K1T 0C6. Email: vitalii.monsatyrrov@sight-power.com

INTRODUCTION

Within last few years, the concept of digital transformation of mining business made its way from futuristic dreams to the practical implementation. Although not too many mining companies already reorganised their style of operations towards digitalisation, they mostly realise that the process of digitalisation is unavoidable.

SightPower globally provides digital transformation of a mine site and integration of all mining operations under the trademark Digital Mine™. The concept of digital transformation assumes implementation of Digital Twin: dynamic data model of a mine. Digital Twin reflects in a real time any developments and changes which are being happened to a mine. The concept of Digital Mine assumes integration into unified informational space data provided by monitoring, IoT and fleet management systems as well as simulation and modelling systems which are being used. Digital Mine™ allows the client to make effective business decisions by obtaining uninterrupted access to the distributed newly collected and historical mine spatial data regardless of its volume and actual location of data servers. Digital Mine™ concept facilitates to optimise Mine to Mill operations providing operational transparency and effective microplanning.

Real-time information support of mine operations in continuously changing environment causes the necessity to process on the fly or at least very operatively enormous volumes of spatial data. The problem exacerbates by the additional data, which permanently comes from various monitoring sensors. SightPower technology suggests the universal and effective solution for Big Spatial Mining Data management. The customers may get full access to the 3D models of mine or 2D thematic maps or any other information which is always up to date momentarily. In certain situations, access can be provided even through the web interface any time from any point of the world.

Effective planning of mining operations is a critical factor that determines the successful development of any underground or open pit mine. Setting the right sequence of mining development, ore extraction, and ground handling operations, optimal resource allocation, and risk management, are all an integral part of the planning process.

At any modern mine, the automation of mine planning is an essential component of information management in a mine development. Long-term and mid-term planning usually suggest longer planning horizons from years to months accumulating information from various and different sources in semi-automated way or even manually. The existing solutions are not capable to secure micro-planning which may at one hand rely on actual up-to-date information provided by Digital Twin, and on other hand introduces instant changes to Digital Twin of a mine reflecting all instant operational developments. Integration of shift-to-shift planning methods into a Digital Twin is a sound approach since the effective optimisation of mine planning is possible only inside a unified and actual informational space. The latter includes in particular regularly refined geological model, mine survey information, the configuration and the status of mining fleet and transportation equipment, economic indicators, etc.

Implementation of Digital Mine™ concept is based on Mine Advisor™ platform which includes not only integration capabilities but also suggests suite of instruments for geological modelling, mine design and planning, automated surveying with laser-based technologies, and informational support of mineshaft life cycle, including ice-wall simulation models for mineshafts which are being built, and automated mineshaft inspection systems. SightPower suggests best-in-class visualisation engine with practically unlimited capabilities to combine spatial data of any type and any size (geological,

CAD, GIS, seismic etc) which are enhanced by unique innovative mixed and augmented reality features developed by our partner company Arvizio Inc.

Practical steps on the way to digital transformation is, first, a special reorganisation of work processes that allow participants in each work process to receive prompt and reliable information from the Digital Twin at any time, and then transfer information to the right place and in the right form. Digital Mine™ principal scheme is displayed in Figure 1.

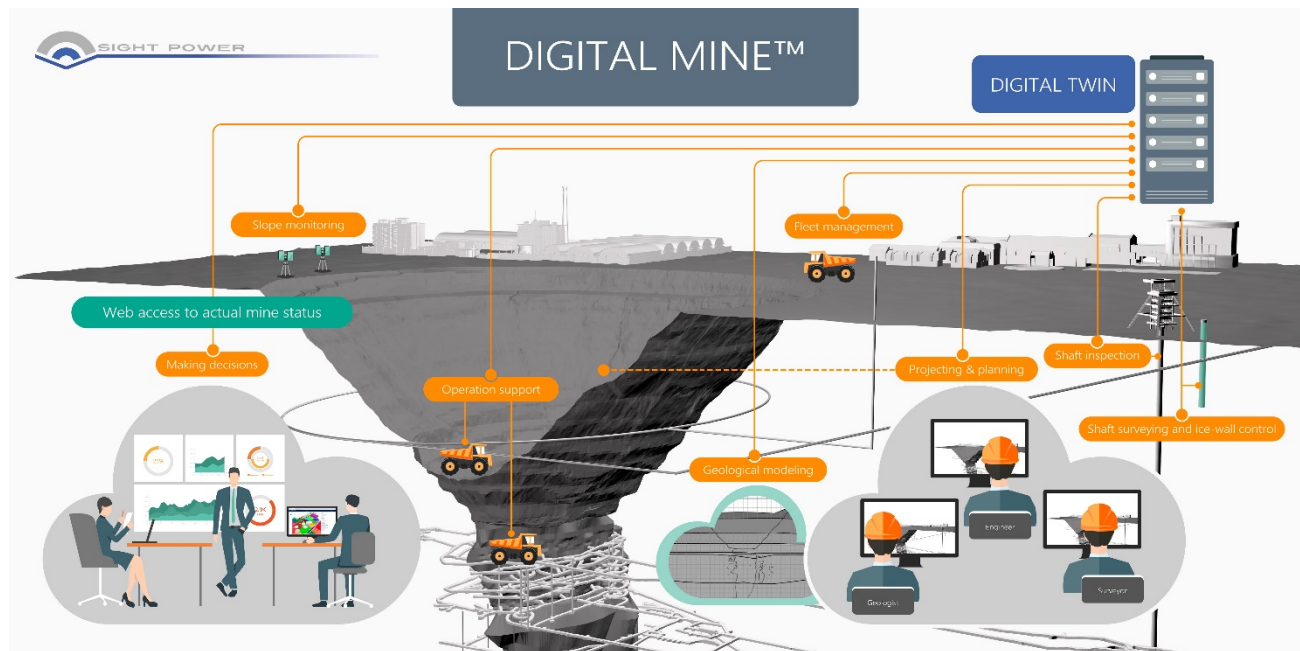


FIG 1 – Schematic representation of a Digital Mine.

Therefore, the Digital Twin becomes an information control centre, which reflects the current state of an enterprise, allows the client to investigate the past by storing the history of development, and foresee the future due to effective planning mechanisms and variant simulation of possible development of events.

Summarising the advantages suggested by the Digital Mine™ concept it is worth to notice the following most important benefits:

- Ability to remotely control everyday operations
- Efficient automation and robotisation of production processes
- An option to provide virtual presence at a mine without leaving office
- Access to information about the actual state of work in a mine or quarry, the state of equipment, availability of resources etc at any time
- Ability to conduct a quick variant analysis to make the best operational decision
- Permanently operating warning system about a possible unfavourable combination of technogenic factors which helps to reduce risks of emergencies, industrial accidents and/or man-made disasters
- Customisable system of automatic distribution of informational reports, easily adaptable to the needs of a particular specialist or manager
- Full integration with strategic planning systems to build models for the long-term development of an enterprise
- Smooth integration with Mine to Mill operational workflows.

Energy systems and sustainability

Hydrogen power for the mining industry

F Aguey-Zinsou¹

1. School of Chemical Engineering, UNSW, Kensington NSW 2052. Email: f.aguey@unsw.edu.au

INTRODUCTION

As solar panels and wind turbines becomes common place on mining sites, the effective deployment of renewable energy storage solutions could enable game changing opportunities for the mining industry. The renewable energy produced on-site can be stored with batteries. However, their energy density is limited, cost is high, and life cycle relatively short (<5000 cycles). Furthermore, batteries have intrinsic issues of safety in particular in confined mining environments where any spark can be catastrophic.

In contrast the potential of converting renewable energy with an electrolyser into hydrogen offers new opportunities, in particular when considering the challenges associated with a mine's 24/7 production cycle and off-grid mines. Hydrogen, as a clean energy vector, has the flexibility to address some of the processing and operational challenges being experienced by the mining sector while enabling the full utilisation of the renewable energy produced on-site with significant round trip efficiency. Unlike batteries, delivering only electricity, hydrogen has the unique attribute of being usable in a variety of different processes around a mine, including as fuel for trucks and loaders, as energy for heating and cooling systems, and as a secondary or backup fuel stock for electricity generation, providing enhanced energy security.

This last application could potentially become a mechanism that allows mines to move away from the traditional reliance on diesel backup generators and toward a cleaner source of generation that can be efficiently incorporated into the heavy industrial sector.

Renewables for green hydrogen production include solar and wind coupled with water electrolysis, solar-thermal and in a distant future direct photochemical hydrogen generation. Renewable methods to produce H₂ from water and biomass, along with their associated costs – in USD are summarised in (Figure 1) and compared to the production cost of hydrogen from steam methane reforming (\$1.9–\$2.6/kg H₂) and the 2020 US Department of Energy (DOE) target (\$2/kg H₂). In the mass manufacture of electrolysers the cost of hydrogen is expected to decrease. One of the major bottleneck remains the effective storage of hydrogen for on-site use and distribution. The main problem with storing hydrogen is its low volumetric density. Hydrogen is the lightest element, and at ambient condition it is a gas with a low density of 0.0899 kg/m³. Even when liquefied at -253°C, the density of H₂ is only 70.8 kg/m³, which is one fifteenth of water's density. Hydrogen is also a very small highly diffusive molecule and thus hydrogen leaks can easily occur. Besides, the use of hydrogen is associated with difficulties in terms of materials' compatibility. In particular, the dissociation of hydrogen molecules at the surface of metals and further hydrogen diffusion at metallic interstitial sites can lead to piping embrittlement and accidental fracture as a result of the reduced ductility and weakening of metals subjected to high purity/pressure hydrogen. The storage of hydrogen is also more delicate than other fuels, because hydrogen has higher laminar burning, buoyant and propagation velocities that results in higher flammability than other fuels. In addition, hydrogen is also very sensitive to detonation due to its wide volume fraction range of ignition (4–74 per cent) and detonation (18–59 per cent).

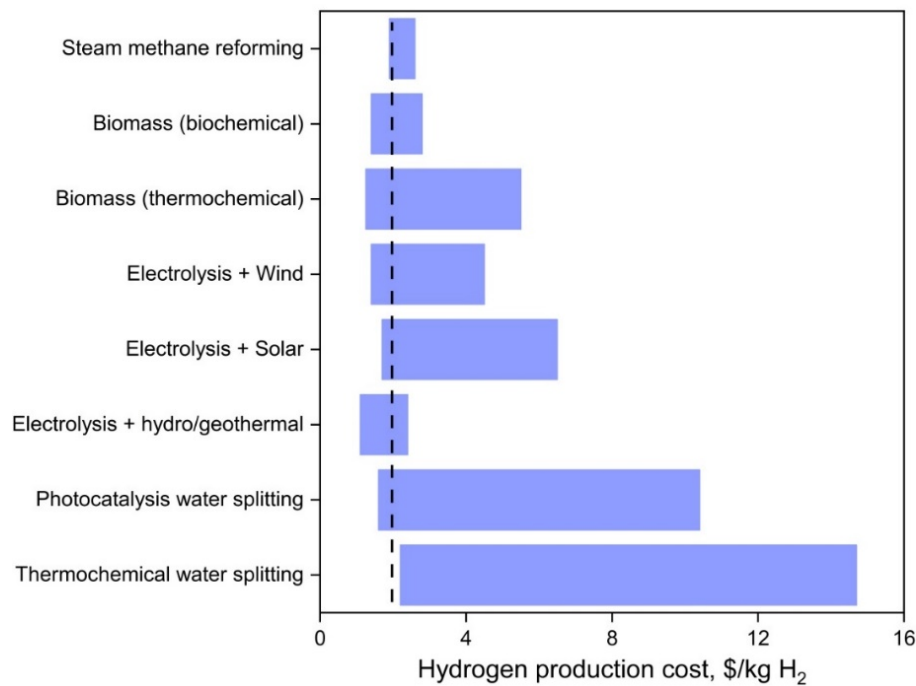


FIG 1 – Average hydrogen production cost from various methods. The black dotted line represents the 2020 DOE target of \$2/kg H₂.

Existing methods to store hydrogen are summarised Figure 2. Storing hydrogen in high pressure vessels (up to 700 bar in lightweight composite cylinder) is the most common method so far, but the resulting low volumetric storage density, high cost of the composite vessels (~\$13/KWh for 100 000 vessels per annum) and their maintenance/safety are still a concern. Cryogenic tanks are designed to store liquid hydrogen at -253°C under ambient pressure (the pressure can increase to 10⁴ bar in a closed storage system due to the low critical temperature (-239.95°C) of hydrogen. As a general observation and depending on the vessel design, conventional cryogenic tanks can store twice more hydrogen per volume as compared to 700 bar hydrogen gas tanks. However, with such a storage technology, it is inevitable to avoid the loss of hydrogen even with a perfect insulation because of heat leakage. The boiling losses of 0.4 per cent per day for a 50 m³ double-walled vacuum-insulated spherical Dewar vessel have been reported. In addition, hydrogen liquefaction is a very energy intensive process with at least 30 per cent of the energy stored lost through the liquefaction of hydrogen.

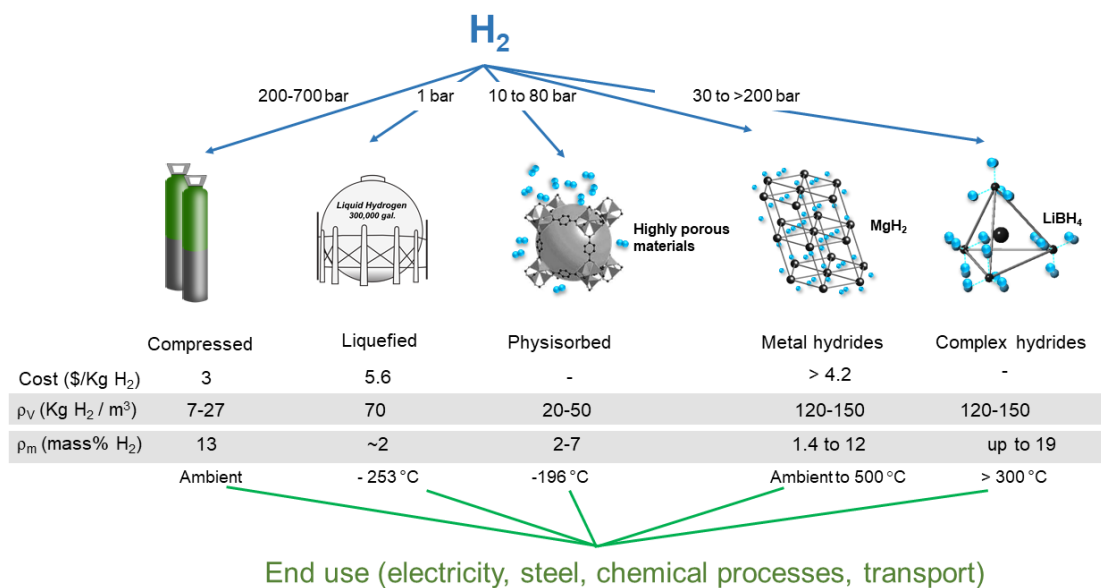
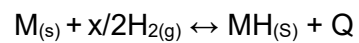


FIG 2 – Hydrogen storage methods with their respective volumetric densities.

The presentation will discuss advanced hydrogen storage methods and their integration to innovative technologies to benefit the mining industry. An alternative method to store hydrogen is in the use of materials storing hydrogen within their structure to form a hydride. Metal hydrides are usually formed by the reaction between metals or intermetallic compounds with hydrogen by the reversible reaction below:



where M is either a metal, an alloy or an intermetallic compound, MH is the metal hydride formed and Q is the heat generated during the reaction.

Safety culture survey in coal-fired powerplant (PT X) at South Kalimantan, Indonesia

M Ashifa¹

1. Industrial Hygiene and Occupational Health Department Head, PT Adaro Energy Tbk, Jakarta Indonesia 12950. Email: muthia.ashifa@adaro.com

ABSTRACT

Safety culture has been defined as a product of the interaction between people, work and organisation. The aim of safety culture is to create an atmosphere where employees are aware of the risks they face in the workplace and how to prevent them. Despite many different factors underlying safety culture, the factors most commonly measured as culture include: safety policies, procedures, sanctions, rewards, training, communication, employee engagement, and management commitment and employee safety behaviour.

One approach to understanding safety culture is to use a safety culture maturity model that focuses on organisational characteristics. The cultural maturity model used in this study is based on the concept developed by Hudson (2001). From the result of the investigation of the accidents at one of the coal-fired powerplant, it can be concluded that the human factor is one of the dominant causes of work accidents. Thus, a comprehensive evaluation of human factor is needed by measuring the maturity level of safety culture in the plant. A safety culture survey was conducted in all work areas that were randomly selected. Workers who took part in the safety culture survey were taken from employees and contractors and sub-contractors consisting of operator and supervisor levels. The output of this survey are to provide an overview of employees' perceptions in understanding the implementation of safety aspects as well as employee compliance with the safety regulations, define appropriate remedial actions as effective recommendations for enhancing safety culture to support zero accident mindset.

INTRODUCTION

Energy demand in Indonesia has increased significantly over the last 10 years. PT X is a Coal-Fired Powerplant (PLTU) company that contributes to the supply of electricity in Indonesia. The company is also classified as a high-risk industry, where a work accident can cause disruption of operation and major impacts, such as interruption of electricity supply. On the other hand, work accidents can cause death, injuries that cause the loss of working days (Loss Time Injury – LTI), a decline in company reputation, environmental pollution and financial losses for the company and society.

The term 'safety culture' was introduced by the International Atomic Energy Agency in their report on the Chernobyl nuclear powerplant disaster in 1986. The identification of poor safety culture as a contributing factor to accidents has led to a large amount of research being undertaken to investigate and attempt to quantify safety culture in various industries with high safety risks. Although the importance of safety culture is widely accepted, there are slight differences in the definition of culture. In Indonesia, a safety culture is still new and many companies fail to create an effective safety culture.

Safety culture is a polemic and complex concept that requires theoretical and empirical clarification (Wilpert and Itoigawa, 2001). Safety culture has been defined as a product of the interaction between people (psychological factor), work (behavioural factor) and organisation (situational factor) (Cooper, 2001).

Fernandez-Muniz, Montes-Peon and Vasquez-Ordas (2007) consider safety culture as a component of organisational culture which refers to individual, occupation, and organisational characteristics that can affect their health and safety. The aim of safety culture is to create an atmosphere where employees are aware of the risks they face in the workplace and how to prevent them.

In summary, despite the many different factors underlying safety culture, the factors most commonly measured as culture include: safety policies, rules and procedures, sanctions and rewards, training, communication, employee engagement, management commitment and employee safety behaviour.

One approach to understanding safety culture is to use a safety culture maturity model that focuses on organisational characteristics. The cultural maturity model used in this study is based on the concept developed by Hudson (2001). This model is suitable for use because it has a focus including an adequate occupational safety and health management system, emphasising human factor as the main cause of accidents, and compliance with occupational safety and health laws and regulations.

The most important problem in running production operations is to build a culture of occupational safety and health that can provide assurance to support and promote accident prevention behaviour at all times. Multiples of the occurrence of unsafe conditions and behaviour which if not managed will have a greater further impact.

Based on Figure 1, it can be seen that from year to year there were work accidents that happened to workers at PT X and the trend shows unfavourable symptoms. From the result of the investigation of the work accidents, it can be concluded that the human factor is one of the dominant causes of work accidents. Thus, a comprehensive evaluation of human factor is needed by measuring the maturity level of Occupational Health and Safety (OHS) culture in PT X.

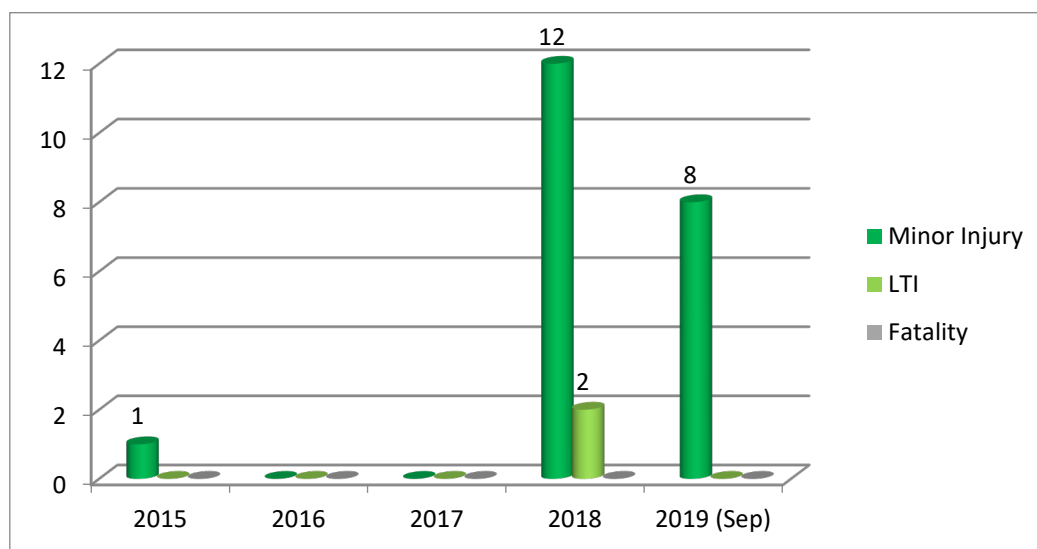


FIG 1 – Number of minor injury, loss time injury (LTI) and fatality in PT X.

A safety culture survey was conducted in all PT X work areas that were randomly selected. Workers who took part in the safety culture survey were taken from PT X employees and contractors and sub-contractors consisting of operator and supervisor levels.

The objectives of the research are:

- To provide an overview of employees' perceptions in understanding the implementation of occupational safety and health aspects, as well as employee compliance with the OHS regulations applicable at PT X.
- To define appropriate remedial actions as effective recommendations for enhancing safety culture.
- To improve safety culture to support 'PT X Zero Accident Mindset'.

LITERATURE REVIEW

OHS culture

Definition

OHS culture has various definitions such as from INSAG (1991) defines OHS culture as the formation of the characteristics and attitudes of an organisation and the individuals in it as a top priority. According to the UK Health and Safety Executive (1993), OHS culture is the result of individual and group values, attitudes, perceptions, competencies, and behaviour patterns that

determine the commitment, style and skill of the organisation's management in managing OHS. According to Guldenmund (2000), OHS culture is the aspects of organisational culture that have an influence on attitudes and behaviours related to increased or reduced risk. Barnes (2009) explains that OHS culture is the values, attitudes, motivation and knowledge that give influence on OHS so that it can be developed so that it can influence policy and behaviour.

Characteristics of OHS culture

In forming an OHS culture, a foundation is needed starting from the organisational culture. According to Reason (1997), an OHS culture can be formed if an organisation has the following characteristics:

- Informed-culture: workers who are in the system have knowledge of OHS and the factors that affect OHS in the system as a whole.
- Reporting culture: the culture of workers who have the willingness to report incidents, errors or near misses in the workplace.
- Just culture: a culture of not blaming each other and the presence of a sense of trust and enthusiasm for workers or even giving awards or gifts to workers who provide information related to occupational safety and health in the workplace.
- Flexible culture: a culture that can accept various forms or adapt well from conventional hierarchical changes to a more professional structure.
- Learning culture: the willingness and competence to be able to learn from the OHS information system and the willingness to implement major changes when it is needed.

The characteristics of the organisational culture above have values that are interrelated with the OHS culture. From these five characteristics, a sense of trust will be formed in each worker. This sense of trust is needed when there are reports of accidents or near misses involving other people, so that there is no blame for the perpetrator and the reporter. Reporting is a form of belief or trust that people have tried their best in providing lessons from a failure on the problem that they face.

The development of the OHS culture maturity model

According to Schein (2004), there are three stages of organisational culture evolution, namely founding, early growth, midlife and maturity. In organisations in the founding and early growth stages, the main culture emerges from the company founders and their assumptions. In the midlife stage, the leader makes no other better assumptions, so he has the same choices as the owner. At the maturity stage, continued success will create the sharing of positive assumptions at all levels in the company so as to create a strong OHS culture. Westrum (1993, 2004) created a model to identify the types of culture of an organisation based on its information processes, namely pathological, bureaucratic and generative.

Fleming (2001) developed a maturity model for OHS culture with the aim of helping organisations identify the maturity level of their OHS culture. The model is based on the capability of the maturity model used in software engineering organisations and has five maturity levels: emerging, managing, involving, cooperating and continually. For each of the five maturity levels of the OHS culture, the levels will be seen in the ten elements. The ten elements are management commitment and visibility; communication, productivity versus safety, learning organisation, safety resources, participation, shared perceptions about safety, trust, industrial relations job satisfaction and training. The level of maturity of an organisation's safety culture is determined based on the ranking of these elements.

Hudson (2001) also proposed a model of OHS culture maturity, based on a model originally developed by Westrum (1993) to be pathological, reactive, calculative, proactive, and generative. Figure 2 is of the OHS culture maturity model based on Hudson (2001):

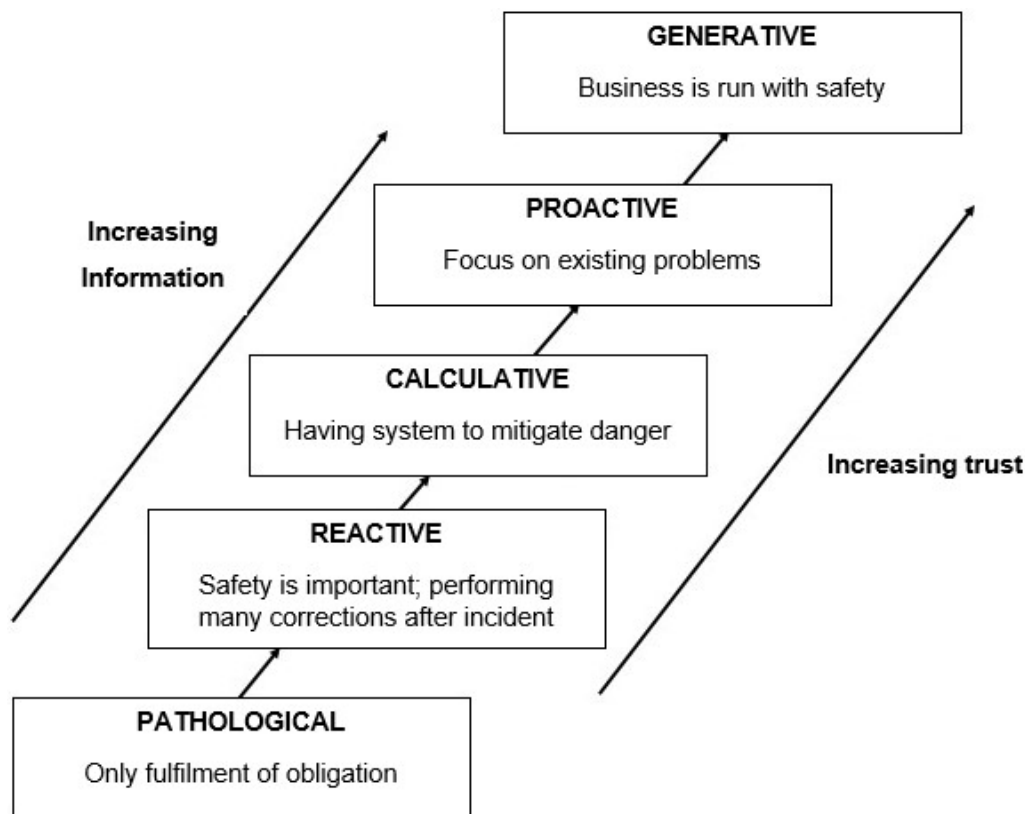


FIG 2 – OHS culture maturity model by Hudson (2001).

The explanation of each level of the OHS culture maturity model according to Hudson (2001) is as follows:

- **Pathological**
OHS is considered a problem caused by workers. The main driver of the company is the business itself and emphasises not being blamed by regulators.
- **Reactive**
Company start to take OHS seriously but real action is taken solely after an incident occurs.
- **Calculative**
OHS is driven by the OHS management system, by collecting a lot of OHS data. OHS is still mainly driven by the management and there is an impression of coercion on workers.
- **Proactive**
The company already has a system for managing hazards and OHS has begun to form, as seen from the involvement of workers and the implementation of OHS programs at all levels of management.
- **Generative**
There is active participation at all levels of the company. OHS is considered as an inherent part of business. The company is characterised by chronic restlessness as opposed to complacency.

Determination of PT X's OHS culture maturity model criteria based on the Hudson model

By adopting the OHS culture model from Hudson (2001), PT X created criteria in determining the extent of the maturity of the OHS culture. The complete criteria for the OHS culture model of PT X can be seen in Table 1.

TABLE 1

Criteria of OHS culture maturity model of PT X based on Hudson Model.

	1. Information	2. Incident Analysis & Correction	3. Participation	4. Communication	5. Commitment
Generative ★★★★★					
Proactive ★★★★★					
Calculative ★★★					
Reactive ★★					
Pathological ★					

Modified from Hudson, 2001

METHODOLOGY

Population and sample

The population of the assessment is all workers at PT X. The population of workers at PT X is 210 workers. The number of samples in this study were obtained using the Slovin formula as follows:

$$\frac{N}{1+N(e^2)}$$

$$\frac{210}{1+210(5\%^2)}$$

$$n = 137.70 \sim 138 \text{ Respondent}$$

n = Number of minimum samples

N = Number of populations

e = Tolerable error rate (5 per cent)

From the results of distributing questionnaires to 210 people, 148 questionnaires were successfully returned. The number of questionnaires has met the required minimum number of samples.

Method of data collection

Questionnaire

By using a safety culture development model which was arranged based on the Hudson model, the questionnaire instrument consisted of two types of questionnaires and two content sections. The type of questionnaire was made based on the target respondents, namely operators and supervisors. Each consists of two parts; first part is expected to describe the dissemination of accident information

to employees in the PT X area. The second part of the questionnaire is expected to describe the implementation of OHS which consists of 20–25 questions according to the five safety culture survey criteria which have been defined, namely, information, incident analysis and correction, employee participation, communication and commitment.

The feasibility test was carried for the operator and supervisor questionnaire instruments. The feasibility test was carried out by testing the validity and reliability of 40 respondents who were randomly selected. The validity test was used to measure the accuracy of a measuring instrument in measuring data. While the reliability test was used to determine the extent of the consistency of the measurement results when two or more measurements are made against the same conditions and with the same measuring instrument.

The validity and reliability of the questionnaire were tested randomly to 40 respondents. Both of these tests were carried out using Statistical Package for the Social Sciences (SPSS) by performing the Cronbach alpha test by looking at the r coefficient on the test. It is known that $r_{table} = 0.312$, if $r_{count} > r_{table}$, it means that the variable is valid. If $r_{Alpha} > 0.6$, it means that the question is reliable. After the validity and reliability tests were carried out, the validity test results showed that all questions from the operator and supervisor questionnaires had a value of r results (Corrected Item-Total Correlation) above the r_{table} , so it can be concluded that the five safety culture survey criteria are valid. After everything is valid, from the results of the reliability test above, it turns out that, of the five safety culture survey criteria, the value of r_{Alpha} is greater than the value of 0.6, then the five criteria above are declared reliable.

Focus group discussion (FGD)

Focus Group Discussion (FGD) was held for two days on Tuesday, 15 October 2019 and Wednesday, 16 October 2019. The FGD was conducted in two sessions throughout the day, session one took place at 09.00–11.00 Central Indonesian Time (WITA), and session two took place at 14.00–16.00 WITA. The FGD participants are representatives of each PT X department and work partners. The participants consisted of eight different operators and six supervisors in each session. The FGD was conducted for the purpose of data triangulation, to convince researcher of the data obtained from the questionnaire.

Meanwhile, the FGD participants were determined by meeting one of the following criteria:

- Position Operator, Mechanic, Supervisor
- Working Period ≤ 2 years, 2–5 years and > 5 years
- Age ≤ 25 years, 25–30 years and > 30 years
- Incident Experience There have been those who have and have never experienced an incident.

The questions of FGD session for Operator consisted of four criteria: information, participation, communication and commitment. The criteria for incident analysis and correction were not included in the list of questions because they were not included in the job description of the operator but was a supervisor.

Meanwhile, the questions of FGD session for Supervisor consisted of five criteria: information, incident analysis and correction, participation, communication and commitment. Specifically, for the communication criteria, the researcher did not make a list of questions, but did it with field observations. The researcher wanted to know directly how the communication process of a supervisor to his subordinates.

Interview of top management

The Interview of top management was conducted as an effort to see the commitment and management's point of view in managing OHS and used as a variable to confirm the results of the questionnaire and FGD.

Observation

Observation was made for data triangulation purposes. Observation was made when the researcher was at the site to conduct FGDs with the respondents. During the observation, the researcher observed the actions of both operators and supervisors, especially regarding their awareness of OHS and the communication process between supervisors and their subordinates.

Method of data processing

Questionnaire

The results of the questionnaire were processed in such a way using SPSS to see the frequency distribution of the observed variables, such as: the proportion of supervisors and operators, age, years of service and the five criteria of safety culture, namely information, incident analysis and correction, participation, communication and commitment.

Focus group discussion (FGD)

The FGD was processed using a list of questions that had been compiled from the start, where there were five options of answers that were close to each of the FGD questions according to the criteria for each stage of the safety culture.

Data analysis

The final analysis to determine the level of safety culture survey at PT X used the combined results of a questionnaire with a weight of 60 per cent and FGD with a weight of 40 per cent.

RESULTS AND DISCUSSION

Results

Safety culture survey questionnaire

The questionnaires were distributed to 210 employees of PT X with positions as operators and supervisors, with a sample of the questionnaire obtained as many as 148 workers. Table 2 shows the results obtained from the safety culture survey questionnaire.

TABLE 2
Respondents characteristics.

Characteristics	Operator	Supervisor
Proportion	61%	39.8%
Age		
Mean	34	37
Min-max	21-62	23-52
Years of service		
Mean	7 years	5 years

Safety culture maturity level

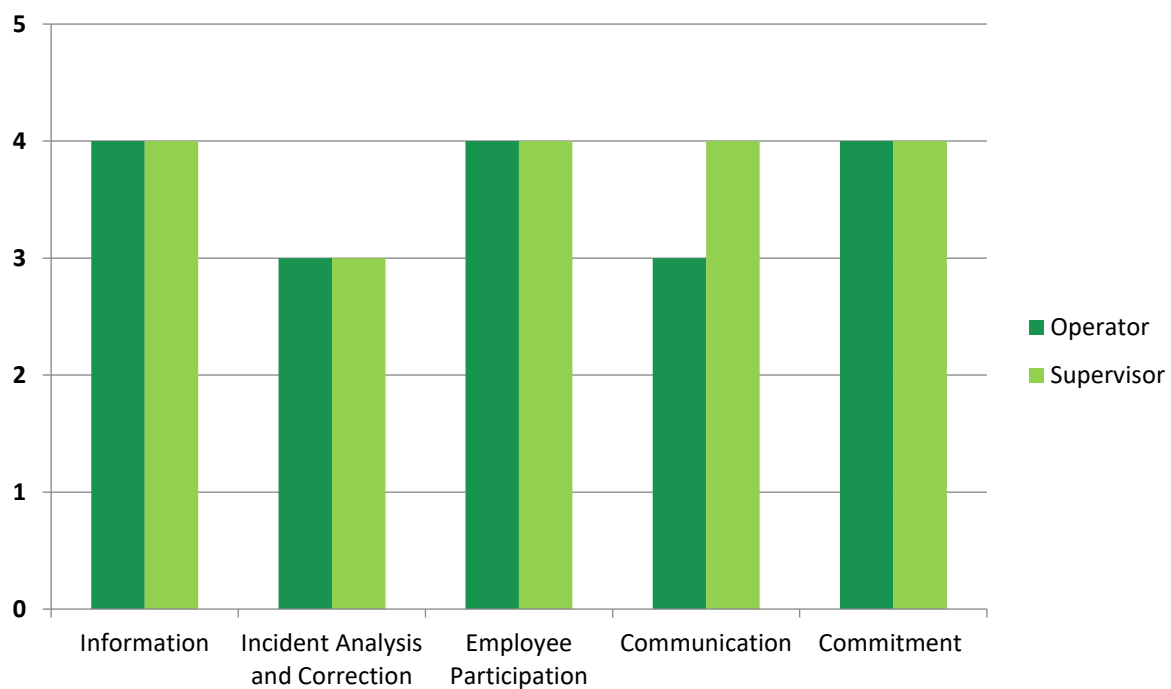
A questionnaire was distributed to 210 PT X employees with positions of operator and supervisor; and a sample of 148 employees results were obtained from the questionnaire. Table 3 shows the mean distribution and calculation of safety culture maturity level in PT X based on the safety culture criteria of operators and supervisors.

TABLE 3

Calculation of safety culture maturity level questionnaire on scale 1–5 at PT X.

Position	Information	Incident analysis and correction	Employee participation	Communication	Commitment	Mean
Operator	4.0	3.0	4.0	3.0	4.0	3.6
Supervisor	4.0	4.0	4.0	4.0	4.0	4.0
Mean	4.0	3.5	4.0	3.5	4.0	3.8

Figure 3 shows the overall results of safety culture maturity level in PT X for all criteria of operators and supervisors.

**FIG 3** – Results of safety culture level from questionnaire at PT X.

Focus group discussion (FGD)

Table 4 and Figure 4 are the results obtained from the FGD of the safety culture survey at PT X.

TABLE 4

Calculation of the safety culture survey FGD in percentage at PT X.

Position	Information	Incident analysis and correction	Employee participation	Communication	Commitment	Mean
Operator	66%	N/A	76%	60%	52%	64%
Supervisor	67%	63%	76%	-	64%	67%
Mean	67%	63%	76%	60%	58%	65%

Note: (-) Data of communication as FGD result was not recorded.

Score reference	
Level	Percentage
1	0–39%
2	40–59%
3	60–69%
4	70–89%
5	90–100%

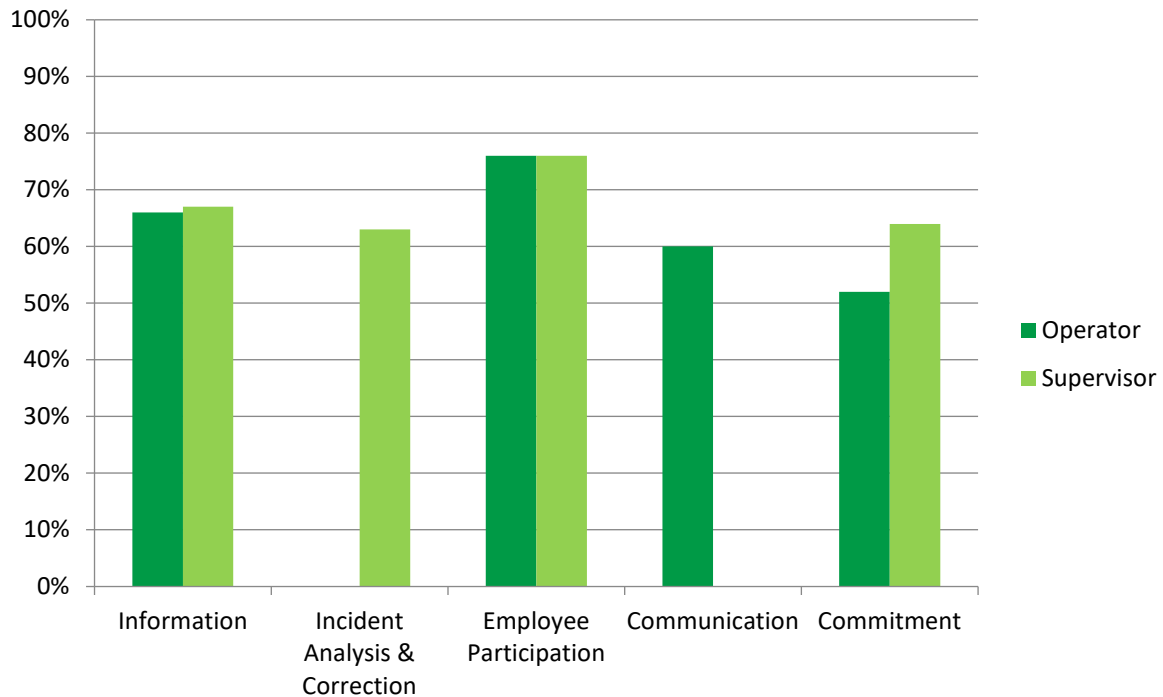


FIG 4 – Results of safety culture level FGD at PT X.

Meanwhile, the explanation of the FGD in the field can be seen in Table 5 as follows.

TABLE 5
Description of safety culture based on FGD at PT X.

Criteria	Supervisor	Operator
Information	<ul style="list-style-type: none"> Near miss, minor injury, lost time injury, and fatality were reported by supervisors, but dangerous actions have not been fully reported. Supervisors are aware of procedures that allow employees to inform all minor accidents, serious, dead and dangerous incidents. Supervisors considered the implementation of OHS to be a priority but not yet fully implemented in daily operational activities. Some employees are comfortable enough to be able to inform about accidents in the organisation. 	<ul style="list-style-type: none"> Near miss and minor injuries were reported by operators. Reporting is only for meeting targets, not yet assessing the quality of the reporting. Operators know the safety reporting rules but they are limited to serious accidents and death. Operators considered the implementation of OHS to be a priority but not yet fully implemented in daily operational activities. Some employees are comfortable enough to be able to inform about accidents in the organisation.

Incident analysis and correction	<ul style="list-style-type: none"> Supervisors assumed investigation has been carried out to determine the underlying causes of an accident and to take corrective actions. Supervisors know corrective action as a follow-up to the incident that occurred. 	-
Employee participation	<ul style="list-style-type: none"> Both supervisors and operators felt that they and their subordinates are motivated to participate actively in safety issues and in complying with applicable safety regulations. Supervisors and operators have participated in safety issues not only through mining safety committee forum but also through safety talks and toolbox meeting. 	
Communication	-	<ul style="list-style-type: none"> Operators felt that the company only informed about safety in the event of a fatal accident. There were employee communication programs with organisations that address safety information but are structural in nature and are based on (rigid) norms and procedures. The organisation only checked the effectiveness of the safety communication program in areas where safety risks can occur.
Commitment	<ul style="list-style-type: none"> Both supervisors and operators felt that safety planning is based on the results of risk identification and analysis, field requests and compliance with regulations. The organisation conducted a safety audit program in all work areas based on national standards. Supervisors and operators felt that the organisation already has a standard occupational safety training for all employees in accordance with the rules, duties and responsibilities but has not been well disseminated. The organisation in selecting subcontractors already has pre-qualified, detailed safety requirements in the contract and carries out supervision for all work. Workers felt there is a safety reward system for employees only under special conditions. 	

Final results of safety culture maturity level

The final results of the safety culture maturity level at PT X can be seen in Table 6 and Figure 5, where these results were obtained from a combination of methods between a questionnaire with a weight of 60 per cent and an FGD with a weight of 40 per cent.

TABLE 6

Final results of safety culture maturity level at PT X.

Questionnaire	FGD	Total
2.28	1.04	3.32

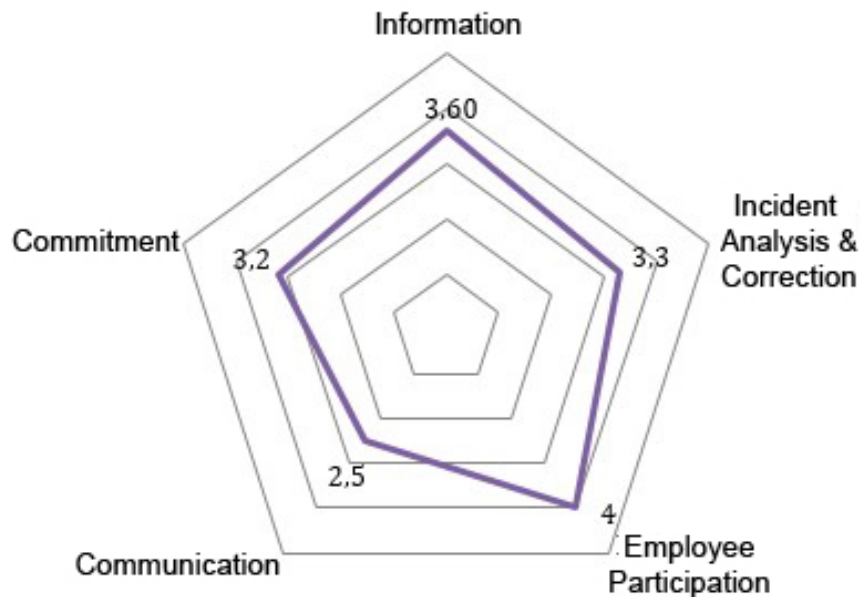


FIG 5 – Final results of safety culture maturity level at PT X.

Discussion

The overall maturity of PT X's safety culture is at level three. There are several driving factors. First, so far PT X has been trying to improve safety and achieve a high level of safety performance. Throughout 2019, there were 0 LTIFR per one million working hours, compared to 0.19 LTIFR for the Energy and Mineral Resources Ministry in Indonesia. PT X is also designated as a role model in the PT X Power Group in the field of electrical energy generation, so that everything needs to be developed and implemented so that its function as a role model can be carried out, including in the field of OHS. A real reflection of this is the Permit-To-Work (PTW) system at PT X which PT Z' lenders consider a good model and needs to be implemented in PT Z. The determination of the OHS work program is based on the achievement of jobs in the previous year. The budget in the OHS sector is of course an unlimited budget.

Second, apart from being in the holding group, PT X also works under the direction of the HSE Steering Committee at the corporate level. This committee has a role to encourage PT X Group's MOHS Policies that are guided by laws and regulations, standards and best practices to be implemented by all parties. One of the policies is Zero Accident Mindset (ZAM). At PT X, OHS is an objective that needs to be set and passed down to all personnel. The OHS objective is emphasised on the implementation of leading indicators to ensure lagging indicators do not occur (fatality, LTI, near miss, incident). In addition, there are awards to increase safety motivation because the company rewards each company with the best safety performance.

Third, what is no less important is PT X as the contractor of PT Y. PT X realises that the risks they face are representative of PT Y so that the required OHS regulations must always be obeyed. Further explanation of each criterion is as follows:

- Information

Information is at level three. This factor is because PT X has implemented an OHS Management System, where there is a reporting system for all types of accidents, dangerous incidents and near miss. Most employees also think that occupational safety is a top priority at work so that it influences the decisions taken at each step in their work.

- Incident analysis and correction

This criterion is still at level three, several factors include:

- The system of sanctions for those who violate safety rules and those who are involved in incidents has not been in operation.

- Some Supervisors feel that accident investigations are still being carried out only to find the direct cause without involving the search for basic causes such as personal and occupational factors.
- Corrective action from an existing incident has not been implemented effectively and learning information has not been communicated effectively.

- Employee Participation

The OHS steering committee has been formed to give a positive value, but it needs to be realised that the role and function of this committee is not yet running effectively. The perception of supervisors and operators has not felt the added value of this committee. The roles and functions of the committee must be reviewed so that employee participation in safety can increase.

Based on the top management interview, in general the implementation of the procedure was considered to have gone well. However, it is realised that in several situations, incidents or violations of a procedure still occur. OHS is expected to be born from each part, not only from the HSE division. In this case the HSE department is expected to play a role as the main trigger. Until now, it is felt that the quality of the implementation of occupational safety aspects has not reached 100 per cent. There are still workers who do not comply with the rules. The range of non-compliant workers is 5 per cent or approximately 10 people. Another issue that needs to be implemented is a review of the JSA documents so that their quality is better. Another factor is the role of the sub-leader who is not strong enough, or still relies on the role of the OHS department. Procedures were carried out, but the responsibility was still felt to be with OHS. The basic philosophy of why safety is needed at work has not been understood and has become a self-value.

- Communication

The criterion of communication was not responded positively. Safety information was conveyed to employees in the form of induction, toolbox talk, safety meeting, OHS advisory committees and other methods. However, the effectiveness of the communication method or program must be evaluated. Some supervisors and operators felt that not all employees have received information about accidents, for example how the methods are to provide information to off-duty personnel. Operators also felt that the company only informed safety in the event of a fatal accident.

Another important thing is that workers still prioritised work completion, as a result there are still jump-in work processes for reasons of wanting to finish work quickly. The number of workers who have worked for more than five years raises the stigma that 'I already understand my job' and will make workers overconfident. Sometimes, this is influenced by the work culture of workers in the old place, where if a jump-in is a procedure, the boss does not reprimand and is left alone. This issue cannot be separated from the typical work in the maintenance department which tends to be urgent/sudden that needs to be done immediately.

- Commitment

PT X employees have no doubts about the commitment of company management in improving safety, because of the existence of an OHS Policy, safety objectives, goals and programs and investment for safety. Based on interviews with Top Management, there is also a visible commitment to safety. In general, management deemed that the implementation of safety procedures has not been going well, as seen in several incidents caused by violations of a procedure.

In the end, competence is closely related to culture. In general, the competence of workers at PT X is sufficient because this is required by the Ministry of Energy and Mineral Resources in the electricity sector. Competency elements are: skill, knowledge and attitude. Attitude mapping still needs to be improved and is more challenging to form a culture in the workplace. Attitude also reflects the skills and knowledge of these workers.

CONCLUSIONS

- The maturity level of occupational safety culture at PT X in 2019 was at level 3, where the participation criterion had the highest score with a score of 4, while the communication criterion had the lowest score with a score of 2.5.
- The criterion of employee participation was at level 4. The OHS steering committee has been established and is running, but it needs to be realised that the role and function of this committee is not yet effective. Supervisors and operators still do not feel the added value of this committee.
- The information criterion was at level 3. This factor was because PT X has implemented an OHS Management System, where there is a reporting system for all types of accidents, dangerous incidents and near miss.
- The criterion of incident analysis and correction was still at level 3, several factors include the not yet functioning system of sanctions for those who violate safety rules and those involved in incident and some supervisors felt that accident investigations are still being carried out only to find the direct cause without involving the search for the basic cause such as personal and occupational factors.
- The criterion of management commitment was at level 3. PT X employees have no doubts about the commitment of company management in improving safety. This is reflected in the existence of OHS Policies, OHS objectives, targets and programs and OHS investment.
- Communication criterion was at level 2. Safety information was conveyed to employees in the form of induction, toolbox talk, safety meetings, OHS steering committee and other methods. Some operators felt that not all employees have received information about accidents, for example how to provide information to off-duty personnel. Operators also felt that the company only informed about safety in the event of a fatal accident.

The results of the safety culture survey at PT X provide an opportunity for improvement through these recommendations:

- The results of the OHS steering committee meeting contain important decisions, and all employees at PT X must be informed and understand. Systems and procedures need to be reviewed to accommodate this matter.
- From the communication criterion, the effectiveness of the communication method or program must be evaluated. Information on all types of accidents must be communicated to workers. Another thing is the matter of jumping in a procedure, it is better if the direct supervisor can give sanctions. PT X should compile a list of violations and sanctions and accommodate them in a cooperation agreement as stipulated in the business pillars of PT X's OHS Management System.
- From the criterion of incident analysis and correction to always consider determining long-term corrective actions so that similar accidents do not occur and the imposition of sanctions and a monitoring system for corrective actions to monitor their effectiveness.

ACKNOWLEDGEMENTS

Mr Rusdi Husin – Division Head of HSE and Risk Management PT Adaro Energy

Mr Harry Tri Pamungkas – Marine Safety Superintendent at PT Adaro Energy

Mr Nurhidayad Dawoed – HSE Manager PT MSW (PT X)

Mr Joko Sudiyanto – Safety System Officer at PT Adaro Energy

Mr Jayadi Pide – Industrial Hygiene Supervisor PT Adaro Energy

Ms Vina Dwi – Internship at HSE and Risk Management Division PT Adaro Energy

REFERENCES

- UK Health and Safety Executive, 1993. ACSNI Human Factors Study Group, third report – Organising for safety, HSE Books. Available from: <<https://www.hse.gov.uk/humanfactors/topics/common4.pdf>> [Accessed: October 5th 2021].
- Barnes, V, 2009. *What is safety culture? Theory, research and challenges* (United States Nuclear Regulatory Commission: Maryland).
- Cooper, D, 2001. *Improving safety culture. A practical guide* (John Wiley & Sons Ltd:UK).
- Fernandez-Muniz, B, Montes-Peon, J and Vasquez-Ordas, C, 2007. *Safety culture: analysis of the causal relationships between its key dimensions* (National Library of Medicine).
- Fleming, M, 2001. *Safety culture maturity model* (Health and Safety Executive: Coalgate, Norwich).
- Guldenmund, F, 2000. The nature of safety culture: a review of theory and research, pp 215–257 (*Safety Science* 34).
- Hudson, P, 2001. Aviation Safety Culture, pp 23 (*Safe Skies* 1).
- International Nuclear Safety Advisory Group (INSAG), 1991. Safety Culture: Safety Series No.75-INSAG-4. (International Atomic Energy Agency: Vienna).
- Reason, J, 1997. Indicators of safety culture, in *Safety Culture Definition and Enhancement*, p 12, Civil Air Navigation Services Organization (CANSO) 2008.
- Schein, E H, 2004. *Organisational culture and leadership* (Jossey-Bass: San Francisco).
- Westrum, R, 1993. Cultures with requisite imagination. In: Wise, J A, Hopkin, V D, Stager, P (Eds.), *Verification and validation of complex systems: Human factors issues* (Springer-Verlag: New York).
- Westrum, R, 2004. A typology of organisational cultures, pp 22–27 (*Quality and Safety in Healthcare* 13).
- Wilpert, B and Itoigawa, N, 2001. *Safety culture in nuclear powerplant*, pp. 5–18 (Taylor & Francis: London).

A simulation based feasibility evaluation of renewable power generation on an off-grid mine (Jundee Gold Mine)

*S Bacich*¹

1. MAusIMM, Senior Mining Engineer, Northern Star Resources, Perth WA 6000.
Email: sbacich@nsrltd.com

ABSTRACT

This paper covers key aspects from the literature review and the methodology used to simulate the techno-economic feasibility of integrating renewable power generation with existing reciprocating gas generation at Northern Star's Jundee Gold Mine. This paper presents an approach to guide mining professionals when evaluating the feasibility of integrating renewables at their operation.

Topics covered include:

- The business case for renewables.
- The role of power in mining.
- Site suitability for renewables and natural resource evaluation.
- Renewable power generation and storage technology overview, including hybrid generation systems.
- Current renewable power generation and storage technology costs, and forward looking cost estimates.
- How to develop site-specific natural resource data sets using publicly available information.
- Key parameters configured within the HOMER simulation software including justifications.
- Model results and sensitivity to natural resource variability and gas price.
- Conclusions and study limitations.

INTRODUCTION

The world is increasingly focused on developing low-carbon energy to combat climate change, and a clear business case has emerged for companies to pursue renewable power generation; providing an opportunity to reduce exposure to fuel price volatility with a diversified energy portfolio, and allowing companies to consolidate their sustainability credentials and strengthen their social license to operate (ARENA, 2017). These elements allow companies to differentiate themselves and gain competitive advantage as an investment that is socially and environmentally sustainable.

In response to the identified business case for renewables, this paper outlines the case study conducted to evaluate the feasibility of renewable generation at Northern Star's Jundee Gold Mine, incorporating current cost estimates and locally representative natural resource data. Several hybrid generation configurations were considered, which included solar photovoltaic (PV), wind turbines and lithium-ion (li-ion) battery storage.

Research methodology

Central to the evaluation was HOMER, a techno-economic optimisation software solution that nests simulation, optimisation and sensitivity analysis to assess the least cost solutions for hybrid renewable generation systems (HOMER Energy, 2020). HOMER simulates the operation of an electric power system in time-steps determined by the input data resolution and finds the most cost-effective way to meet the electric load based on natural resources, costs, and technical specifications.

THE ROLE OF POWER IN MINING

A continuous and reliable power supply is crucial to the revenue stream of a mining project. Although power generation costs are significant, they are low in comparison to commodity revenue; therefore, power reliability is more important than any marginal cost savings in its supply (Ekstica, 2018). If grid-connected power is not feasible, mining projects produce power off-grid, which is generally gas or diesel derived, or a combination of both.

Off-grid electricity generation arrangements are typically procured from Independent Power Providers (IPPs) on 5 to 10 year contracts that are constructed with a fixed monthly capacity charge and a variable consumption charge (excluding fuel). Benefits of IPP procurement include flexibility and minimal capital outlay. The IPP is generally responsible for all operating and maintenance costs, but the mine owner remains exposed to fuel price, which accounts for most of the electricity operating cost (SunSHIFT, 2017).

Fuel prices

Complete reliance on fossil fuels results in maximum exposure to fuel price volatility. Figure 1 shows the unpredictable nature of fuel prices, with diesel and gas both fluctuating significantly in the decade to 2017. Japanese pricing is used as a proxy in the absence of an Australian wholesale benchmark.

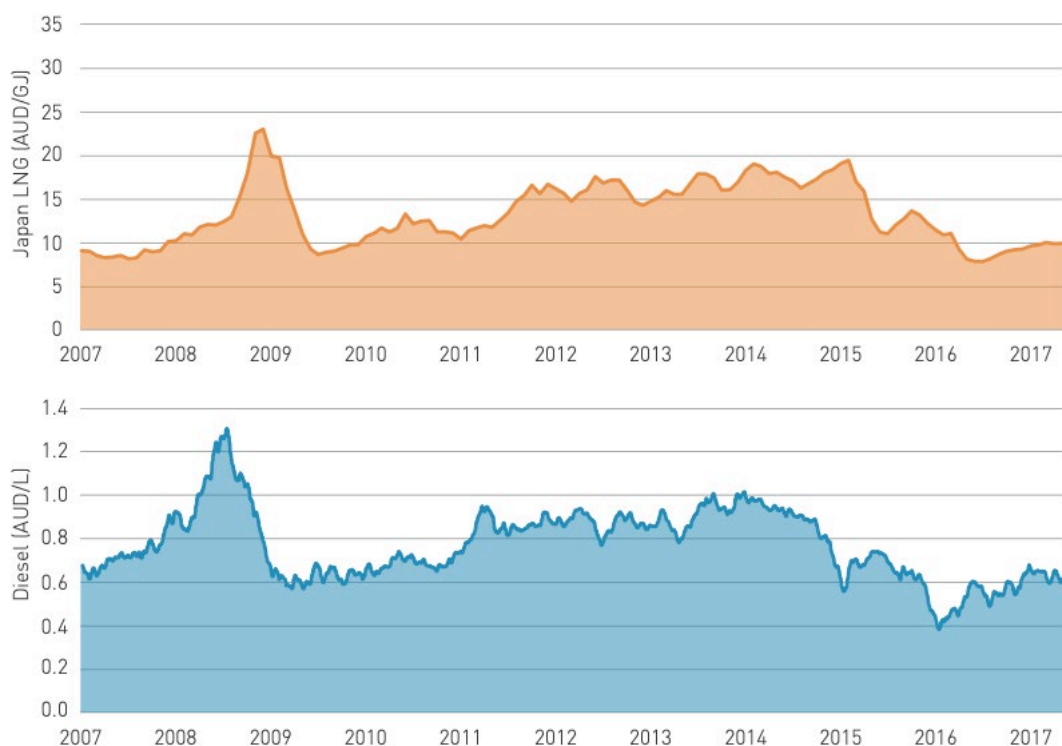


FIG 1 – Historical Japanese LNG pricing (monthly) and Australian diesel terminal gate price (daily) excluding GST and excise (SunSHIFT, 2017).

Note: Diesel transportation typically adds \$0.15/L to \$0.45/L to diesel terminal gate prices.

Load profile and power demand

Most mines operate 24/7 with limited fluctuations in the daily load profile, which is typical of industrial demand profiles (HOMER Energy, 2020). Processing alone can consume up to 75 per cent of electrical demand (Ekstica, 2018), but the mine itself can also be a major source of demand.

Underground mines draw significant power which can be categorised into main sources of demand:

- Primary ventilation
- Secondary ventilation
- Underground drills (development/production/exploration/grade-control)

- Dewatering (primary and secondary pumps)

When estimating power requirements, a spinning reserve needs to be considered to manage short-term fluctuations in demand. Spinning reserve is the extra online generation capacity created to cover contingency events such as the failure of a generator, or a sudden unscheduled increase in demand. In the mining context, spinning reserve addresses intermittent loads and supports the start-up of large equipment. Processing loads can be more sensitive, and large processing plants can generally only be started with powerhouse co-operation due to the significant load created by each module (Ekstica, 2018).

SITE SUITABILITY FOR RENEWABLES

The economic feasibility of a hybrid generation system incorporating renewables relies on-site suitability characteristics that are assessed to determine the potential design, technology selection and scope (see Table 1).

TABLE 1

Key considerations for site suitability of renewables (Ekstica, 2018).

Land
Life of mine
Existing power infrastructure (capability and service life)
Existing IPP/PPA terms and conditions
Load profile
Natural resources (wind/solar)

Factors to consider are the natural resources typical of the location, available land area, remaining life-of-mine, and constraints around existing infrastructure and contracts (Ekstica, 2018). Sterilisation drilling may be required as wind and solar farms can cover significant land areas, and additional geotechnical and hydrological evaluations are required to confirm structure stability and ensure compliance with all legislation.

A comprehensive understanding of the load profile and power demand components is required, as load characteristics form the basis of any hybrid power configuration. The variable nature of solar and wind resources makes it crucial that hybrid configurations are designed for load characteristics, and inadequate design may result increased operating costs due to mismatched components and inefficient operation (Ekstica, 2018).

The key metric used to measure and compare the effectiveness of renewable generation technologies is the capacity factor, which is the ratio of actual electrical energy output compared to the nameplate capacity of that asset (Comino, 2018).

Natural resource evaluation

Evaluating the site-specific natural resources is fundamental to hybrid powerplant design. Solar radiation and wind speed data form the natural resource data set. The minimum acceptable data resolution is hourly, but better results are achieved with minutely resolution. Minute resolution best captures natural resource variability and is particularly important for solar PV (Ekstica, 2018). Historical data can provide guidance on daily and seasonal trends, and complementarity of solar and wind resources is not guaranteed (Jurasz *et al*, 2020).

The cost of collecting site-specific data can vary considerably, depending on the equipment used (see Table 2), but it is possible to lease equipment, which is practical and cost-effective if only one site is to be considered.

TABLE 2

Natural resource measurement equipment and cost (Ekstica, 2018).

Equipment	Measurement	Approximate cost/yr
Pyranometer	Solar irradiance (PV)	\$2,000 - \$7,000
High Quality Satellite Data	Solar irradiance (PV)	\$3,000 - \$15,000
Metmast	Wind	\$100,000 - \$150,000
SODAR	Wind at various heights	\$36,000

Solar resource evaluation

Australia has the highest solar radiation per square metre of any continent in the world (ARENA, 2013). Radiation intensity shifts predictably throughout the seasons, but cloud cover causes rapid short-term losses of PV output by up to 70 per cent, requiring significant levels of operating reserve in the form of spinning reserve or battery storage (Ekstica, 2018). The data collection required to justify a solar farm is less involved than for wind turbines due to Australia's solar resource consistency, which is illustrated in Figure 2. Regional solar radiation data can be sufficient for solar farm justification, but some site-specific data may be required depending on the method of financing (EDL, 2019).

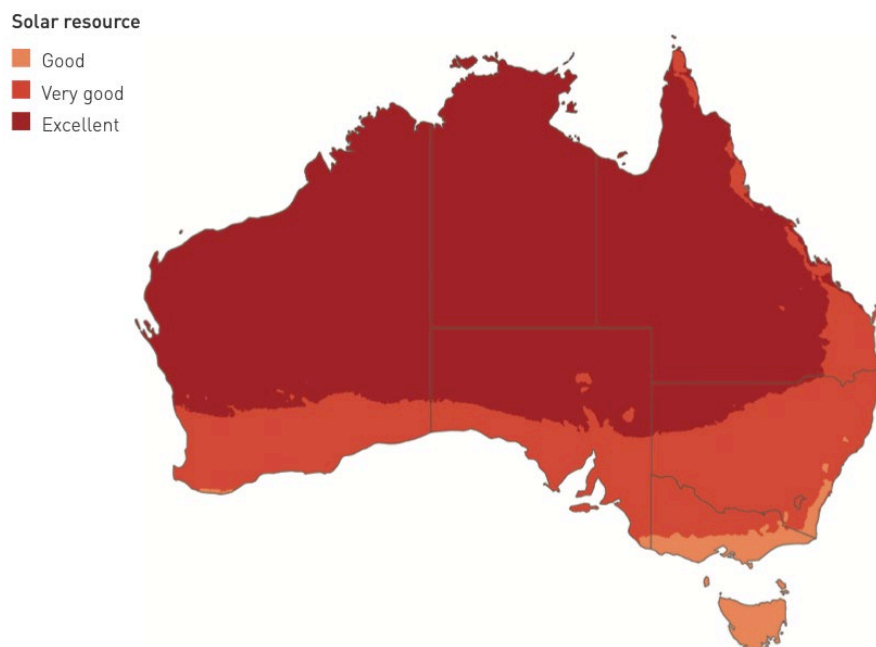


FIG 2 – Australia's solar resource availability (SunSHIFT, 2017).

Note: Good = 3.3–4.4 kWh/m²/day, very good = 4.4–5.5 kWh/m²/day, and excellent = 5.5–6.6 kWh/m²/day

Free satellite data from providers such as NASA, BOM and Global Solar Atlas is readily available, but should only be used for calibration purposes, as satellite data is very high-level and doesn't consider short-term variability. An on-site measurement campaign using a pyranometer produces the best results and can accurately capture short-term variability, which can then be correlated with a high-level data set. Figure 3 demonstrates the solar irradiance variability during a clear day versus a cloudy day. An additional predicament for solar PV is that solar irradiance falls to zero every night, further impairing solar PV's capacity factor against wind turbines.

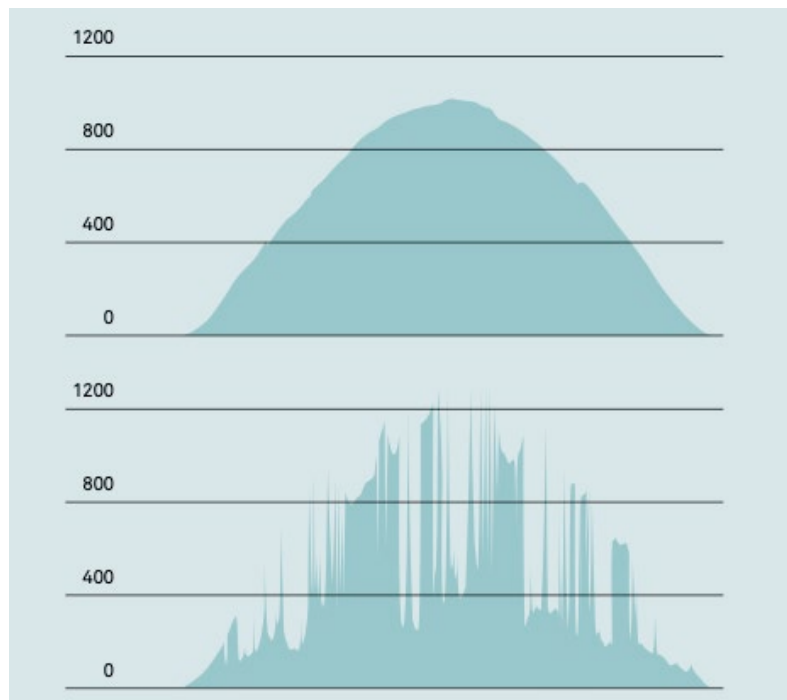


FIG 3 – Demonstration of solar irradiance variability recorded with a pyranometer during a clear sky day (top) and cloudy day (bottom) (W/m^2) (Ekstica, 2018)

Wind resource evaluation

Figure 4 shows that wind resource availability across Australia is typically very good, and Figure 5 demonstrates the variability of wind speeds over a 10 day period, with the added identification of a typical wind turbine cut-in and cut-out speed.

Wind is highly influenced by the terrain and local weather patterns, so it is important to obtain site-specific data. The current risk climate for wind farms requires around 12 months of site-specific data to justify the significant capital investment.

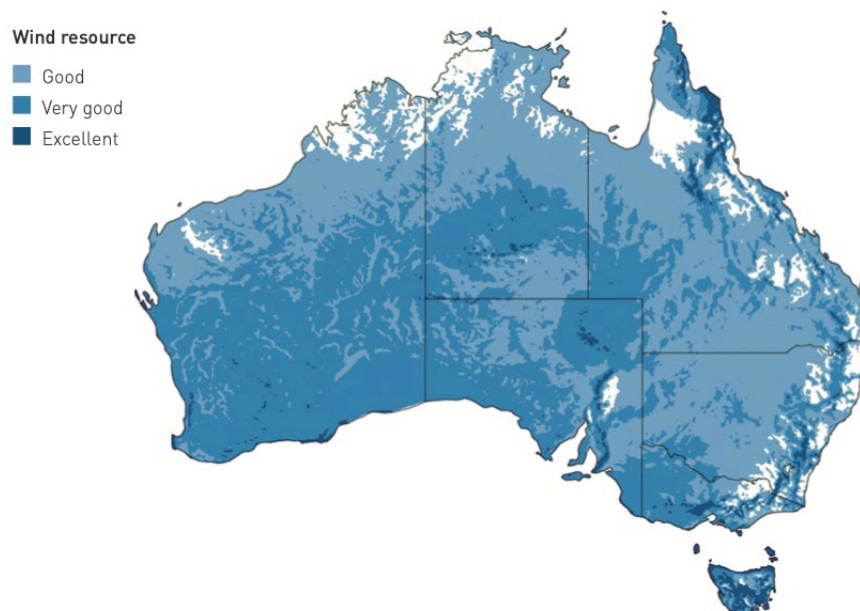


FIG 4 – Australia's wind resource availability (SunSHIFT, 2017).

Note: Good 6–7 m/s, very good 7–8 m/s, and excellent 8–9 m/s. (Wind speed measured at 100 m).

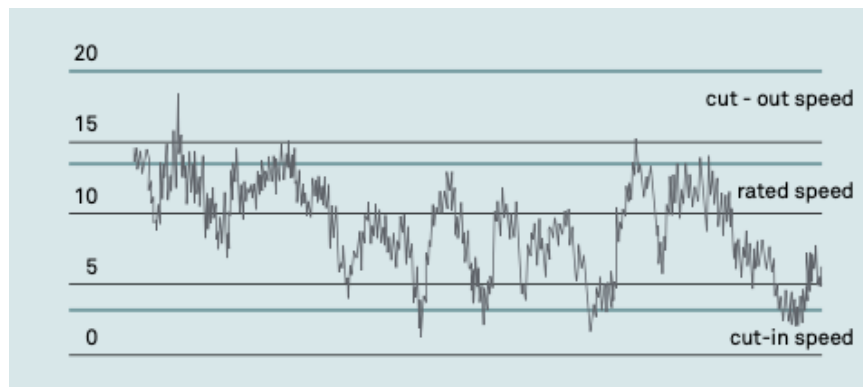


FIG 5 – Demonstration of wind speed variability during 10 days (m/s) (Ekstica, 2018).

Wind speed data can be acquired from a local BOM weather station and is a good approximation for initial evaluations. The quality of weather station data may be assessed as ‘high quality’ for stations less than 20 km away with simple terrain, and ‘medium quality’ for stations up to 50 km away with more complex terrain (Ekstica, 2018). Weather stations typically measure wind speed at 10 m above ground. This data requires ‘scaling up’ to the approximate height of the desired wind turbine.

Wind data can be upscaled with various logarithmic and power-law equations, which can produce varying results due to factor assumptions. An easy way to upscale wind speed data is with a publicly available satellite data source such as Global Wind Atlas (GWA), which is used by policymakers, planners and investors to identify high-wind areas for wind power generation (Global Wind Atlas, 2020).

There are multiple ways to collect high-resolution site-specific data, which can then be correlated with long-term satellite-derived averages to enhance data quality. Wind monitoring masts (Metmasts) have been traditionally used, but new ground-based SODAR wind monitoring devices are a cost-effective alternative that can measure wind speeds at various heights.

A SODAR is a doppler lidar measurement device that measures wind speeds using sound pulses (Fulcrum3D, 2020). An added benefit of the SODAR is that it can record wind speed and direction measurements in 10 m intervals, which can assist with wind turbine selection to achieve the most cost-effective and efficient solution based on local wind resource characteristics.

RENEWABLE ENERGY TECHNOLOGIES

The critical challenge associated with solar PV and wind energy technologies is managing natural resource variability and uncertainty. For hybrid generation systems with a low renewable energy fraction, thermal generation manages this variability with spinning reserve.

When the renewable energy fraction is high, additional mitigation and control measures are required to provide system flexibility (Ekstica, 2018). Energy storage is the most effective solution for creating system flexibility, but other opportunities exist, such as load-shifting (IRENA, 2020). Electric vehicles (EV) will become a load-shifting opportunity as their use increases, and sector coupling such as hydrogen production with renewable energy may become the norm if large-scale commercialisation of this technology is successful (IRENA, 2020).

Installing wind and solar PV together has the potential to reduce overall renewable output variability, but outcomes are highly site-specific and depend on local weather patterns. High-quality natural resource measurement data needs to be obtained to estimate natural resource correlation before any assumptions are made (IRENA, 2017).

Solar PV

There are three main types of solar PV installations:

1. Fixed flat-plate systems, which can be mounted on roofs or in a field array, in a fixed position.
2. Single-axis tracking systems, which typically track the sun daily from east to west.
3. Dual-axis tracking systems, which track the sun both seasonally and daily.

Fixed flat plate systems are used for residential and other urban installations, as they are easily mounted on roof-tops, but can also be used for large-scale solar PV. Single-axis tracking systems are most commonly used for large-scale solar PV and can achieve up to 30 per cent more solar production by following the sun throughout the day (Campbell *et al*, 2018). Single-axis tracking systems take up more area per kW installed, but output is similar to fixed plate installations of the same footprint. Dual-axis tracking systems can deliver a further 10 per cent of additional electricity output but can be more susceptible to mechanical malfunctions (Campbell *et al*, 2018).

A significant drawback with PV technology is that it only produces reliable output when there is clear sunlight, and typically achieve capacity factors around 22–32 per cent (Graham *et al*, 2018). Output variance from passing clouds can rapidly reduce power produced by up to 70 per cent. This variance is known as the ramp rate (Ekstica, 2018; Campbell *et al*, 2018). When solar PV output is intermittent during a cloudy day, the intermittent source is most often curtailed as wasted energy to preserve grid stability (Dickeson *et al*, 2019; Ekstica, 2018; Blanksby, 2018). An example of solar PV ramp rate control and energy curtailment can be seen in Figure 6.

Additional mitigation techniques include geographically dispersing the PV arrays to reduce output variability, and weather monitoring devices to forecast PV generation so that thermal generation can be efficiently scheduled to minimise spinning reserve (Ekstica, 2018).

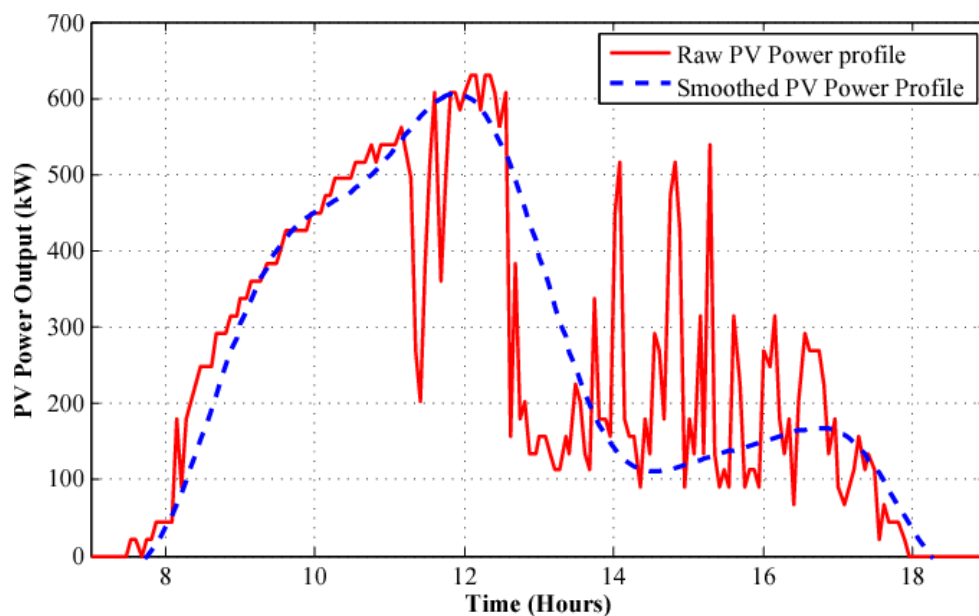


FIG 6 – Ramp rate control and energy curtailment of solar PV with battery (Bhattacharjee *et al*, 2017).

Battery storage can be used to store daytime output for night-time demand but is currently economical for small domestic installations only. For large scale installations with a high renewable energy fraction, batteries provide ramp rate control and grid stability (voltage and frequency). Battery support provides enough time for thermal generators such as gas or diesel to come online and replace supply as required. For systems with a low to moderate renewable energy fraction, excess power generated by thermal generators (otherwise known as spinning reserve) can load follow to smooth the raw PV power profile (ramp rate).

The ground area required for a fixed, ground-mounted PV array installation is about one hectare (2.5 acres) per MWDC. The footprint required is linearly scalable to capacity, and additional area is required if the terrain is sloped or where other structures or geographical features induce shadow (Ekstica, 2018). Installation and maintenance vehicle access also needs to be considered for single and dual-axis systems, and tracking systems require special considerations to prevent shading between adjacent rows or arrays. The ground area occupied by PV modules compared to the total area of the PV site is often described as the ground coverage ratio (GCR), and typically ranges between 30–60 per cent (Ekstica, 2018).

Wind turbines

Onshore wind turbines are typically 1.5–3.0 MW in output and 80–100 metres high, and offshore wind turbines are typically 3.5–5.0 MW and 100–120 metres high. Offshore wind turbines are larger than their onshore counterparts as a way to increase output to offset higher costs (Campbell *et al*, 2018). The increased height also increases efficiencies due to lower wind friction losses at increasing heights.

Wind generation technology is a mature technology and is the fastest growing in terms of global annual and cumulative installed capacity (Lawan and Abidin, 2020). The installation rate is likely due to the superior capacity factors achieved versus solar PV, making it the most economical renewable energy source at current prices. It is not uncommon for large inland wind turbines to achieve a capacity factor between 40–50 per cent, and with day and night time production, wind technology makes higher renewable penetrations more achievable (Steggel, 2019; Graham *et al*, 2021).

Wind turbines should be installed in places with a fully developed wind velocity profile and low surface roughness. Wind farms are generally dispersed across a large area. However, individual turbines have a comparatively small footprint, with foundations typically 8–20 m in diameter for turbines 40–120 m high, accompanied by a crane pad occupying approximately 0.2–0.3 ha. A general rule of thumb for spacing larger turbines (1.5–4.5 MW) to avoid wake effects, is an inter-turbine spacing of 2.5 times the rotor diameter (Ekstica, 2018).

Wind turbine performance can be affected by high temperatures, and wind turbines are typically designed to de-rate from 40°C, and shutdown at 50°C (measured at the nacelle) (EDL, 2019; Goldwind, 2018). Wind turbines cannot be scaled as easily as solar PV installations, and planning and approvals may take longer, with at least one year of site-specific data required. High-quality site-specific data confirms wind turbine feasibility and ensures the most cost-effective design via the turbine selection process.

Electricity storage technologies

There are many types of energy storage technologies; some are on the cusp of commercial development, but others have been in use for years. One of the oldest forms of energy storage is pumped hydro energy storage (PHES), which requires favourable topography conditions to control construction costs. Electrochemical batteries are developing at a fast pace, with li-ion variations showing the highest potential. Other battery technologies still exhibit relatively high costs despite being in research and development for many years (IRENA, 2020).

Electricity storage can mitigate the risk of natural resource variability and uncertainty in renewable energy systems by providing ancillary services such as system inertia, frequency regulation, and operating reserves, while maintaining grid stability (IRENA, 2017). The importance of ancillary services increases with the renewable energy fraction, enabled by the rapidly improving capabilities of power electronics and control systems (Blanksby, 2018).

Electricity storage provides operational reserves for renewable systems via ramp rate support, as well as black start services and capacity firming (IRENA, 2020), and can also be used for load following or shifting. An example of load shifting is when excess solar power stored during the day is used to provide power overnight. This requires large amounts of storage, and the only technologies that currently fulfil this role cost-effectively are PHES, compressed air energy storage (CAES) and flow batteries (Blanksby, 2018; IRENA, 2020).

Figure 7 illustrates the various applications of storage technologies across different timescales. As performance improves and costs fall, the uses of technologies may change, with batteries expected to provide load-following and time-shifting services with successful research and development.

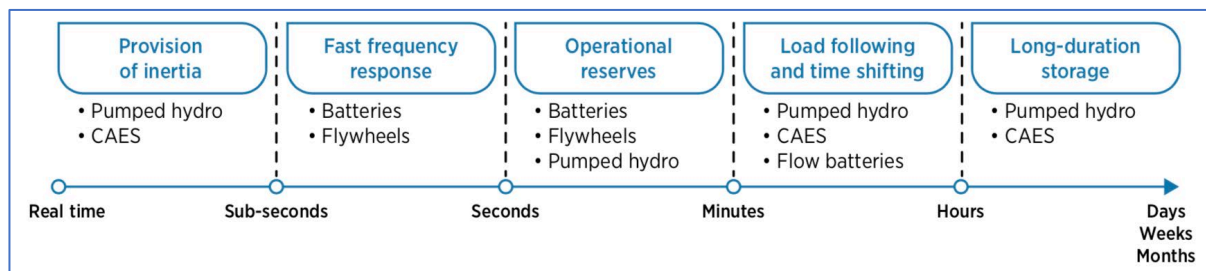


FIG 7 – System services that electricity storage can provide at varying timescales (IRENA, 2020).

Hybrid control systems

Control systems are required in hybrid generation systems to manage each component and the overall output against demand. If the total renewable power fraction is low, then wind or solar PV can be retrofitted without a central control system, as the issue of controlling variability is relatively minor. A hybrid system with a high percentage of renewable power inherits its own set of challenges, and an overarching control system is critical to its success (Ekstica, 2018).

Integrated control systems require each form of generation to have a standalone control system, with an overarching hybrid programmable logic control system (PLC) that schedules the required generation to meet the load while respecting a hierarchy of principles. The priorities depend on individual site requirements (Ekstica, 2018), but a typical hierarchy of principles follows the order of:

1. Security of supply
2. Maximise renewables
3. Efficiency of thermal plant.

Innovative operational practices can also be integrated to maximise renewable energy use and maintain system security, including resource forecasting, dynamic load shedding, and IPP-controlled load management (ARENA, 2019). EV's provide a load management opportunity, as charging can be scheduled for when demand is low.

ELECTRICITY GENERATION TECHNOLOGY COSTS

The cost of renewable energy technologies has fallen dramatically in recent years which is directly linked to the rate of deployment, as supply chains develop, competition increases, and economies of scale are achieved by manufacturers (Graham *et al*, 2020).

There are several publicly available cost resources for renewable energy and associated technologies, but the only comprehensive Australian release is CSIRO's annual GenCost report. Current capital cost estimates from the latest GenCost report for generation technologies are shown in Figure 8.

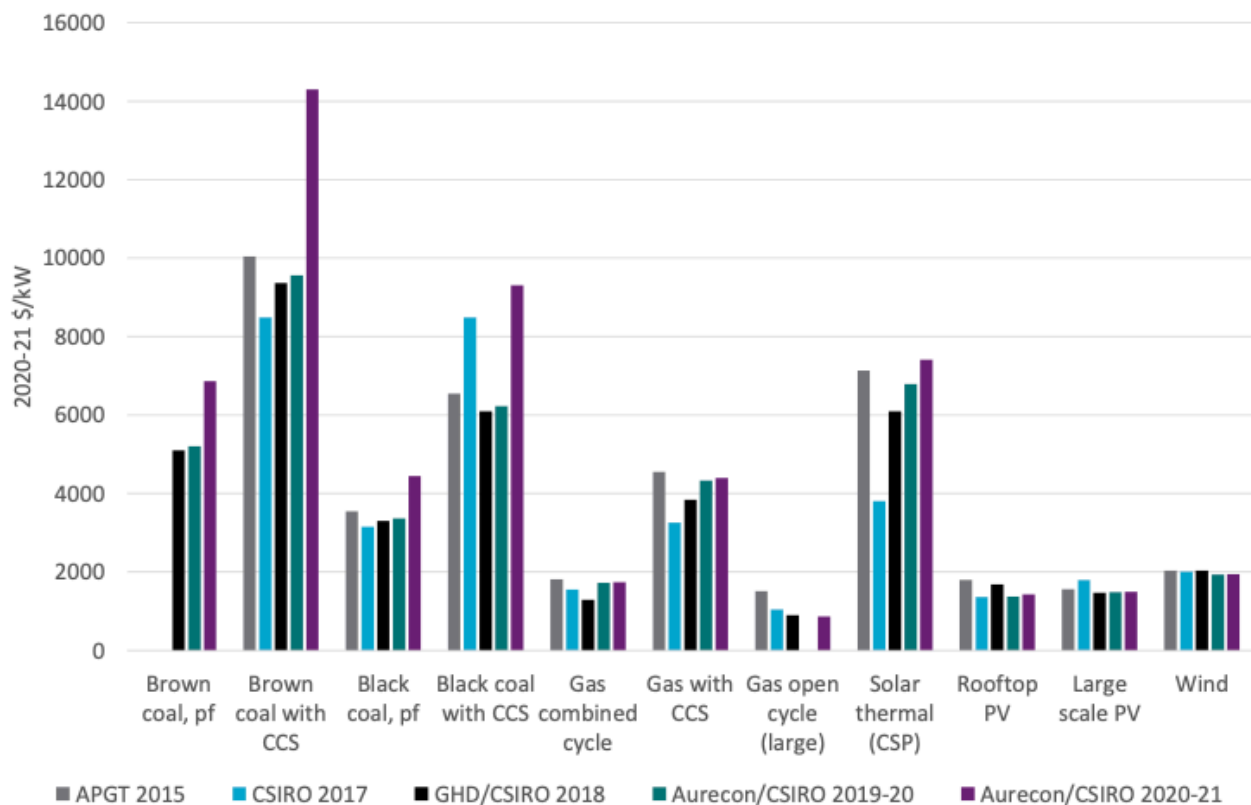


FIG 8 – Comparison of generation technology capital-cost estimates for 2020–21 (Graham *et al*, 2021).

GenCost models cost projections for three climate policy response scenarios, outlined in Table 3. The central scenario was used for capital cost projections as a conservative case scenario. The Central scenario has the least climate policy ambition and as a result it has the highest amount of coal, gas and oil-based generation in 2030 and 2050.

TABLE 3
GenCost capital cost projection scenarios.

Scenario	CO ₂ pricing / climate policy
High renewable energy	High
Diverse technology	High (to support non-RE technology)
Central	Moderate

Figure 9 shows the 2019–2020 and 2020–2021 GenCost projection for renewable energy capital costs, against reciprocating gas engines for the central case. The graph shows that the capital costs of solar PV and battery technologies can expect significant capital cost reductions to 2030, while the capital costs of wind and gas remain stable, as they are mature technologies. In the 2021 update, large scale solar PV cost reductions have slowed, reflecting local challenges in the Australian industry where several solar developers went out of business. These developments have reduced competition and led to more conservative outcomes. The modelling has not built any further industry disruptions into the projection and so cost reductions resume in forward years (Graham *et al*, 2021).

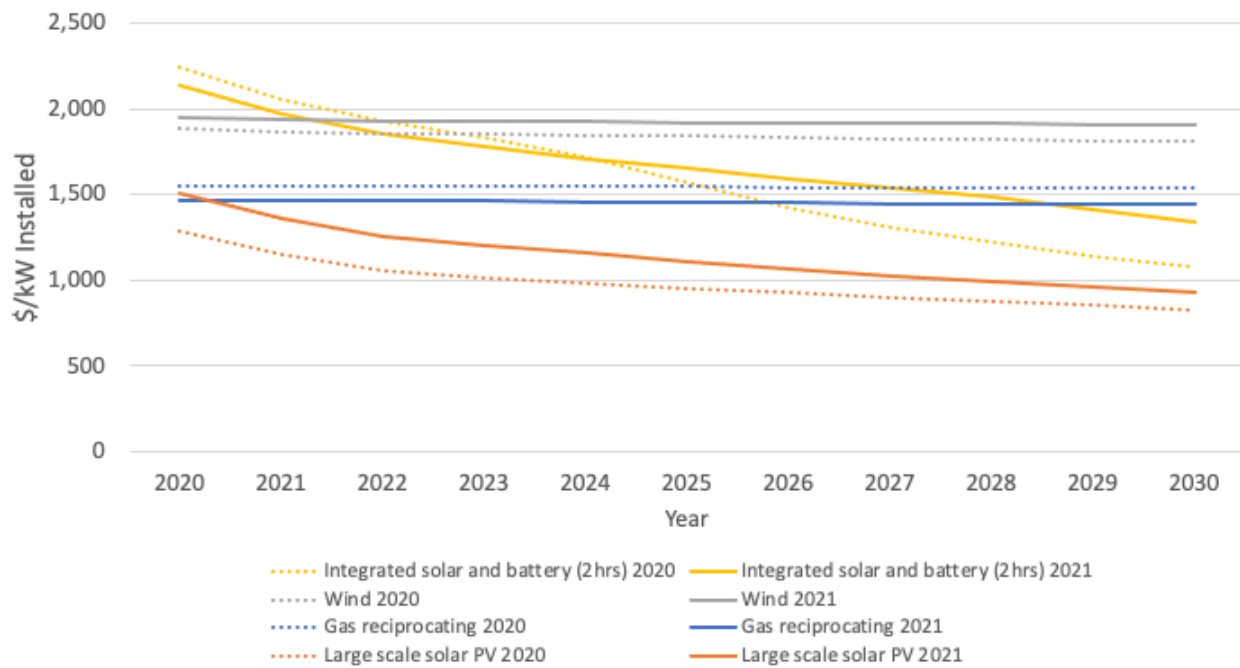


FIG 9 – Projected generation technology capital costs (central case) (Graham *et al*, 2020, 2021).

Levelised cost

Capital costs on their own cannot be used as an indicator of competitiveness between technologies. The economics of power generation methods are driven by several key factors:

- CAPEX (\$/MW)
- Capacity factor (actual generation versus potential)
- OPEX (\$/MWh)
- Asset Life.

These aspects contribute to the levelised cost of electricity (LCOE), which can be used to compare the relative competitiveness of electricity generation technologies (Graham *et al*, 2020). The LCOE represents the average cost of electricity generated, incorporating the cost of building and operating a generating plant during an assumed financial life (EIA, 2020), and is expressed in terms of cost per energy unit (\$/kWh). See Equation 1 for the LCOE calculation (Ekstica, 2018), and Figure 10 for the current LCOE by technology and category from the GenCost 2020–2021 report.

$$LCOE = \frac{\sum_{t=1}^n \frac{I_t + M_t + F_t}{(1+r)^t}}{\sum_{t=1}^n \frac{E_t}{(1+r)^t}} \quad (1)$$

Where:

LCOE	= Average lifetime levelised electricity generation cost
I_t	= Investment in year t
M_t	= Operations and maintenance
F_t	= Fuel expenditure
E_t	= Electricity generation (capacity factor)
r	= Discount rate
n	= Life of system (amortisation period)

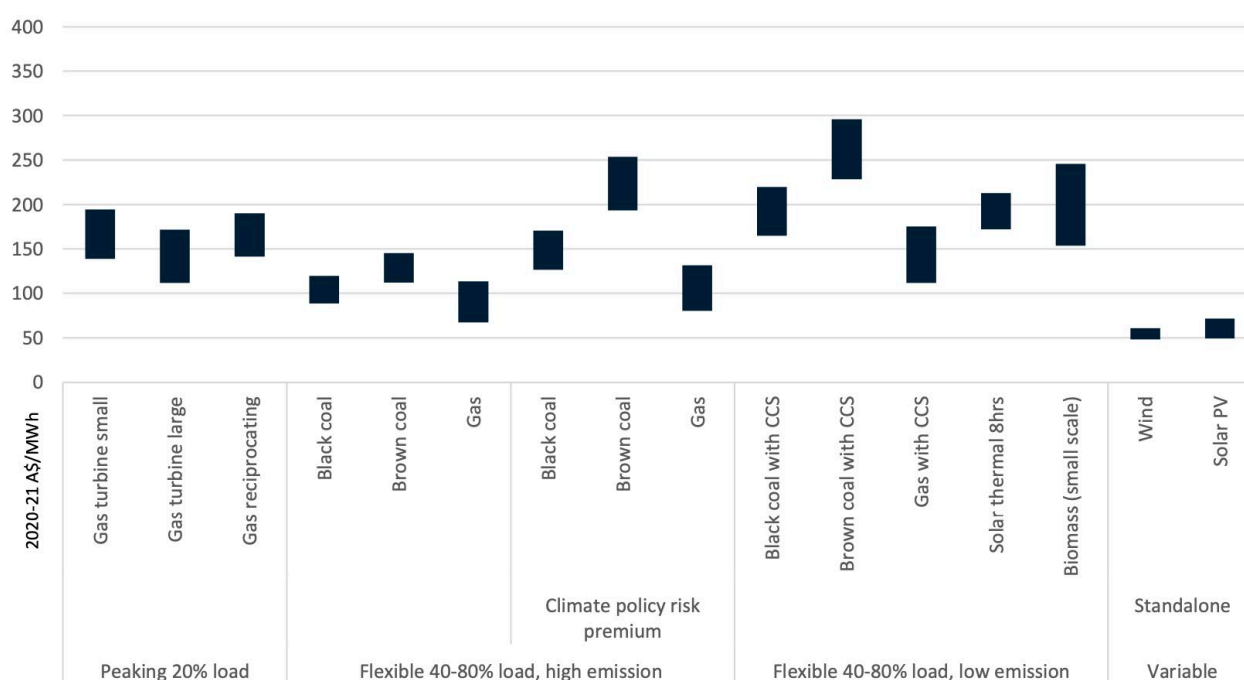


FIG 10 – Calculated LCOE by technology and category for 2020 (Graham *et al*, 2020).

The operating costs of wind and solar PV technologies are very low, and LCOE is primarily affected by capital cost and capacity factor. For fossil fuel technologies, the major LCOE influences are fuel and capital costs (EIA, 2020). Fuel costs are not only significant but are uncertain due to fuel price volatility (ARENA, 2017). The primary source of LCOE uncertainty for renewables is the capacity factor, which relies on natural resources.

Simply citing LCOE from a source can be misleading and a poor indicator of the real unit price of generation if the lifetime and energy yield assumptions are not studied carefully. A low amortisation period and a low solar or wind natural resource will increase the LCOE, and vice versa (Ekstica, 2018). Additionally, LCOE does not take into account the additional balancing costs associated with renewable energy technologies, applies the same discount rate across all technologies, and does not recognise that different technologies have different roles in the system (Graham *et al*, 2020).

The following tables outline the LCOE factors taken from the GenCost 2019–2020 report for various electricity generation technologies. Tables 4 to 6 show the 2020 LCOE factors for gas reciprocating, large scale solar PV and wind turbines, respectively.

TABLE 4
Gas reciprocating LCOE factors (Graham *et al*, 2020).

Economic life	25 years
Construction time	0.8 years
Efficiency	41%
Capital cost	\$1,551/kW
O&M fixed/year	\$24.1/kW
O&M variable	\$7.6/MWh
Capacity factor	20%

TABLE 5

Large scale solar PV (single-axis tracking) LCOE factors (Graham *et al*, 2020).

Economic life	25 years
Construction time	6 months
Capital cost	\$1,285/kW
Replacement cost	\$601/kW
O&M fixed/year	\$17/kW
O&M variable	\$0/MWh
Capacity factor	22-32%

TABLE 6

Wind turbine LCOE factors (Graham *et al*, 2020).

Economic life	25 years
Construction time	1 year
Capital cost	\$1,884/kW
Replacement cost	\$1,734/kW
O&M fixed/year	\$21.9/kW
O&M variable	\$2.7/MWh
Capacity factor	35-44%

The costs extracted from the GenCost 2019–2020 report were used for all HOMER simulation cost inputs. Alternative cost and capacity factor figures were sourced to confirm the validity of the GenCost figures, but are not outlined in this paper.

ELECTRICITY STORAGE TECHNOLOGY COSTS

Figure 11 shows the current capital costs of electricity storage types from various sources. The cost of batteries increases with duration (\$/kW), and the cost of longer duration batteries (4–8 hours) used for load following or shifting purposes is higher than the cost of PHES with a similar storage capacity. This highlights the competitive advantage that PHES currently holds for long-duration storage applications (Graham *et al*, 2020).

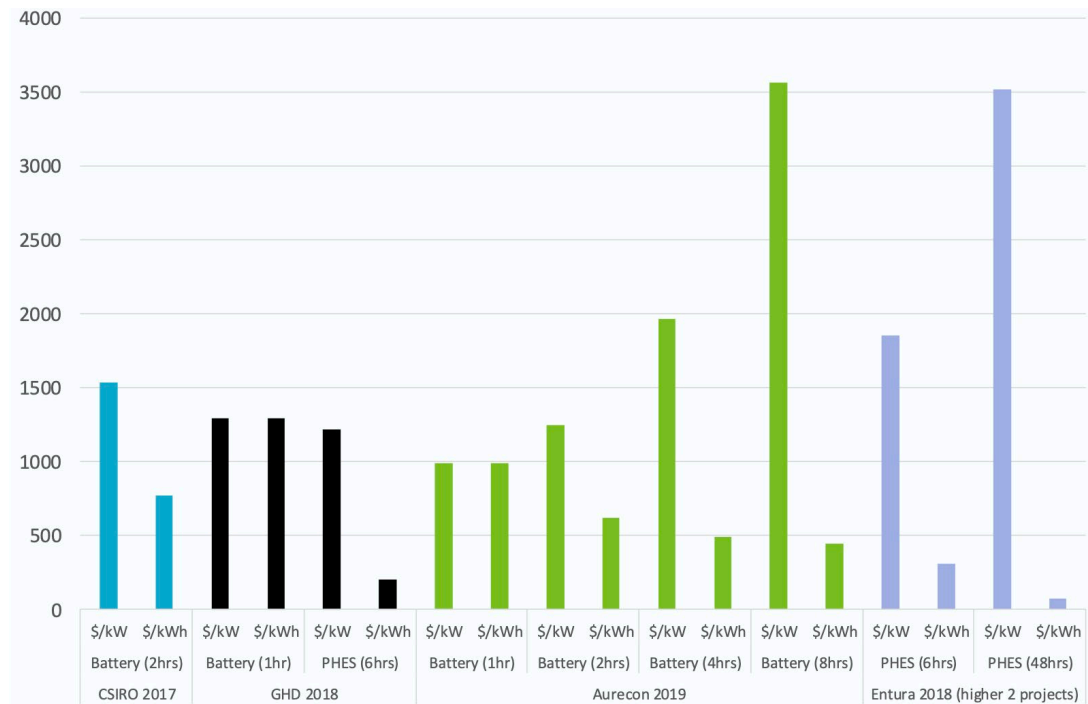


FIG 11 – Capital costs of storage technologies (total cost basis) (Graham *et al*, 2020).

PHES is a mature technology, so capital costs are expected to remain stable. However, costs are rapidly moving for battery technologies, as ongoing research and development improves degradation rates and energy density (IRENA, 2019).

Figure 12 illustrates the expected trajectory of battery storage costs compared to PHES costs (\$/kWh). As the storage duration of a project increases then more batteries or larger reservoirs need to be included in the project, but the power components of the storage technology remain constant. As a result, \$/kWh costs tend to fall with increasing storage duration. In the 2020 estimate, low and high duration battery costs were forecast to fall by more than 50 per cent to 2030. The 2021 update saw a reduction in battery costs across duration based on projects deployed, and an upwards revision in PHES costs. Despite the downwards revision in battery costs, further cost reductions in the order of 30–35 per cent are expected to 2030 (Graham *et al*, 2020, 2021).

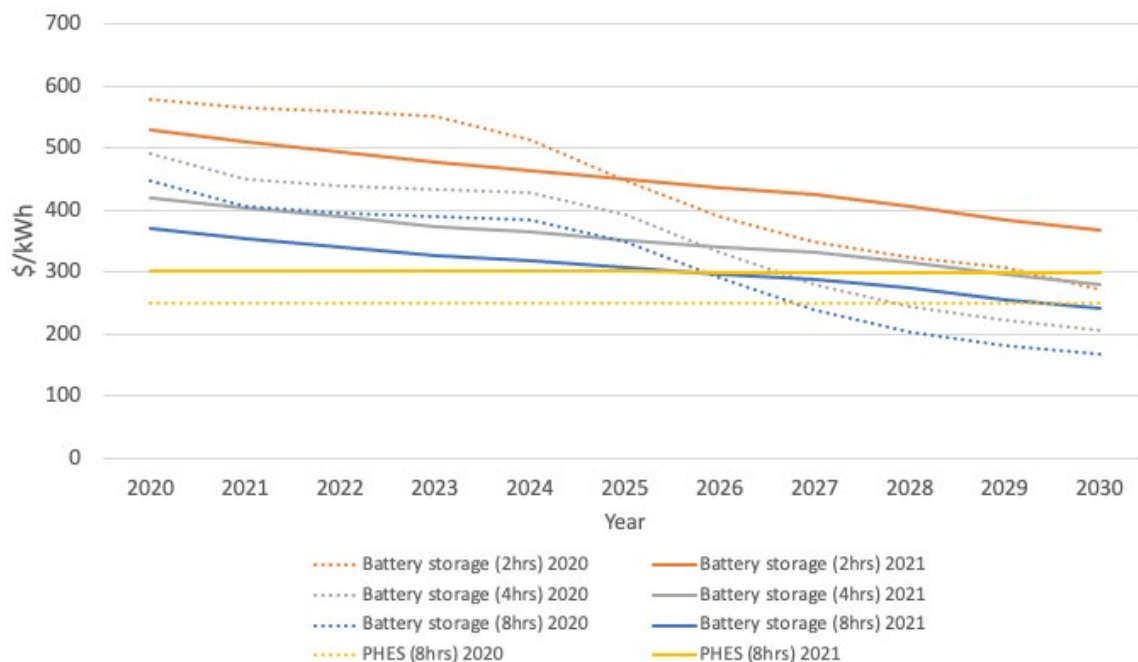


FIG 12 – Projected storage capital costs (central case) (Graham *et al*, 2020, 2021).

JUNDEE GOLD MINE

Northern Star's Jundee operation is located 790 km north-east of Perth in the Mid-West region of Western Australia and is 50 km north-east of Wiluna, the nearest township. The local climate is classed as arid with annual rainfall of approximately 250 mm per annum, an average maximum temperature of 38°C in January and 19°C in July, and an average minimum temperature of 23°C in January and 6.5°C in July (Northern Star, 2018). Jundee's surrounding topography is characterised as flat and non-complex.

Jundee commenced production as an open pit operation in 1995, and underground production commenced in 1997. Jundee has an estimated remaining mine life of eight years, with active infill and exploration projects looking to continue the track record of resource conversion.

Ore is predominantly sourced from three underground mines (Barton, Gateway and Invicta). Figure 13 shows the extensive nature of underground workings across the three underground mines at Jundee.



FIG 13 – Jundee underground workings (plan view).

Natural gas supply

Northern Star Jundee owns a 42 km lateral pipeline connecting to the Goldfields Gas Pipeline (GGP) East of Wiluna. Gas is purchased through a supply contract, which is supplemented by energy trading platform (ETP) swaps at spot price. The supply contract dictates a minimum and maximum annual quantity at an agreed price, which is supplemented by the ETP to top-up throughput as required, and to reduce consumption costs when the spot price is lower than the supply contract rate.

Natural gas costs

Jundee's natural gas resource is maintained with an assortment of contracts and purchasing methods, which required simplification to prepare as inputs for HOMER simulations. The gas

transport cost was configured as a fixed cost in the initial gas models. This was later configured as a variable cost in the hybrid models so that the cost benefits of reducing gas consumption could be captured.

Electricity generation

Electricity is supplied to Jundee via a Power Purchasing Agreement (PPA) with an Independent Power Provider (IPP). The IPP own, operate and maintain the power station site, bearing all related costs, and Northern Star supply gas and diesel fuels at their own cost.

The PPA consists of fixed and variable cost components. The fixed cost is a capacity cost and represents the capital cost incurred by the IPP and the standing fixed costs for the duration of the PPA. The variable cost is a consumption cost and represents the operating and maintenance costs incurred by the IPP.

Jundee benefits greatly from being connected to the GGP, which results in a low power cost compared to other sites that don't have gas pipeline access or that use diesel generators as their primary source.

Electricity demand

Table 7 outlines the electricity demand breakdown for Jundee, showing that the underground mines consumed nearly 60 per cent of electricity generated in 2019. The projected breakdown represents the processing-plant ball mill upgrade which was at early stages of commissioning in April 2020.

TABLE 7
Jundee electricity demand breakdown.

	2019	Projected
Processing plant	39%	48%
Underground mines	58%	49%
Village	2%	2%
Administration buildings	1%	1%

Hourly resolution power demand data was acquired from the powerhouse to produce a daily demand profile. Figure 14 illustrates the daily profiles constructed from the data obtained. An average of seven days was first collated, and three days were selected out of the seven for exhibiting the most consistent daily demand, forming the smoothed average. The smoothed average was then augmented with 3 MW of constant load, representing the ball mill upgrade. This demand profile is the projected profile, and was used for the HOMER simulations.

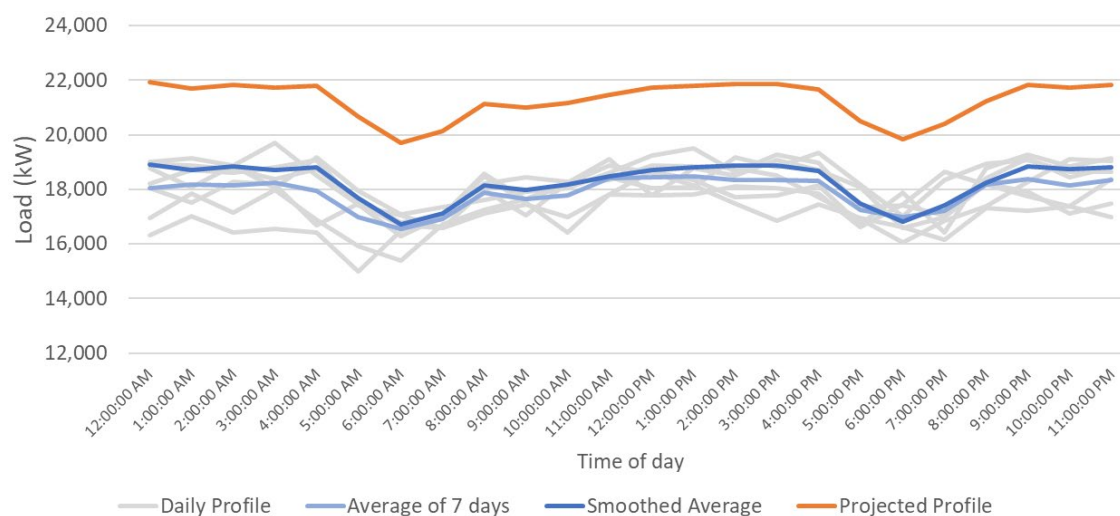


FIG 14 – Jundee hourly electricity demand profiles.

Natural resources

Solar

Three Global Horizontal Irradiation (GHI) data sets were considered for the HOMER simulations, with monthly averages shown in Figure 15.

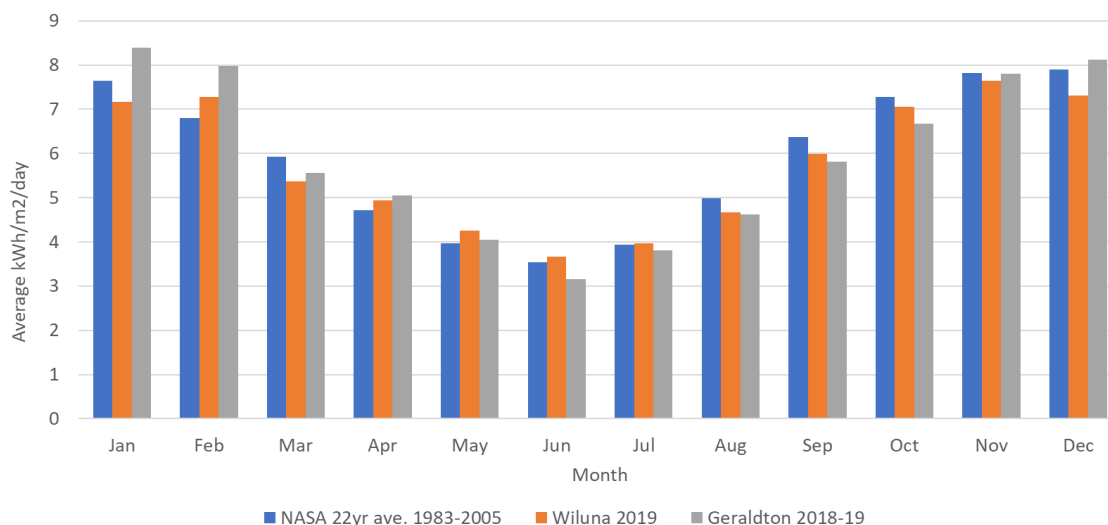


FIG 15 – Monthly GHI average by source.

The rapid variability of solar radiation from passing clouds means that the highest data resolution practically obtainable is required, to properly evaluate spinning reserve and battery requirements to balance the plant.

Minutely resolution solar data is available free-of-charge from the BOM for key locations across the country. Unfortunately, no available minutely data sources were located within 500 km of Jundee, but Geraldton was considered as the best available proxy for Jundee and Wiluna. Additionally, the 2019 Geraldton minutely solar data was incomplete, with data existing from January to August only, so September to December 2018 values were appended to the 2019 data. Figure 16 shows the daily mean GHI of the combined Geraldton 2018–2019 data set used for the HOMER simulations, illustrating seasonal variation and output variability.

Figures 17 and 18 illustrate the importance of using minute resolution data to capture output variability from passing clouds, showing the same day with different resolutions.

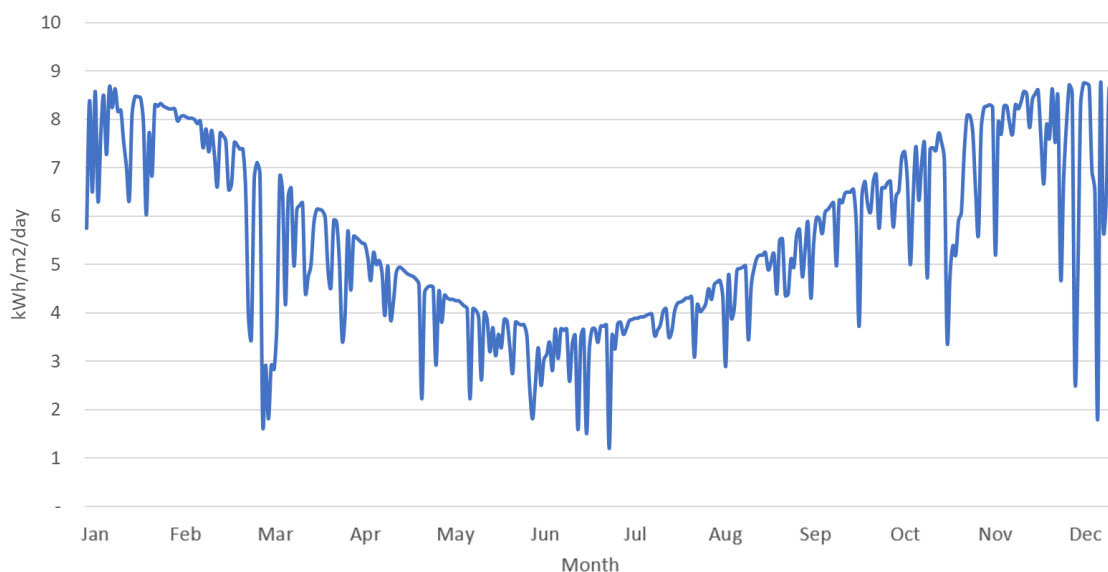


FIG 16 – Daily mean GHI (kWh/m²/day) for combined Geraldton 2018–2019 solar resource (used in HOMER simulations).

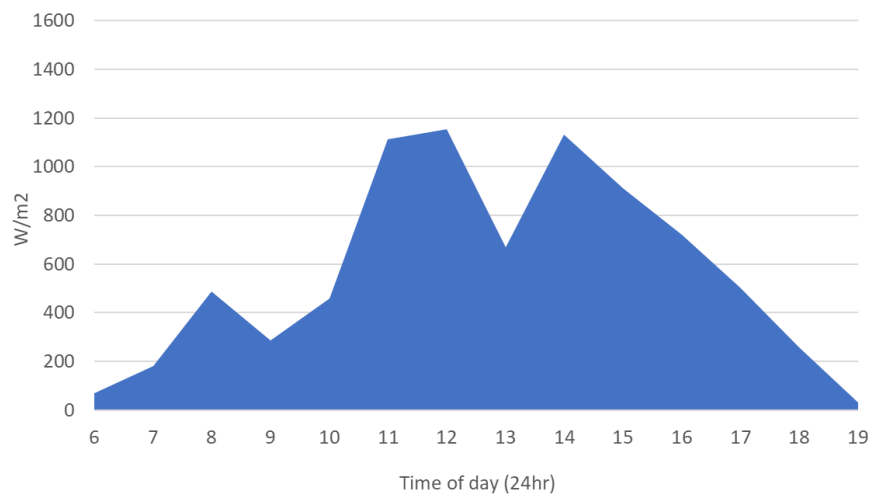


FIG 17 – Hourly GHI (W/m^2) for 1st of January 2019.

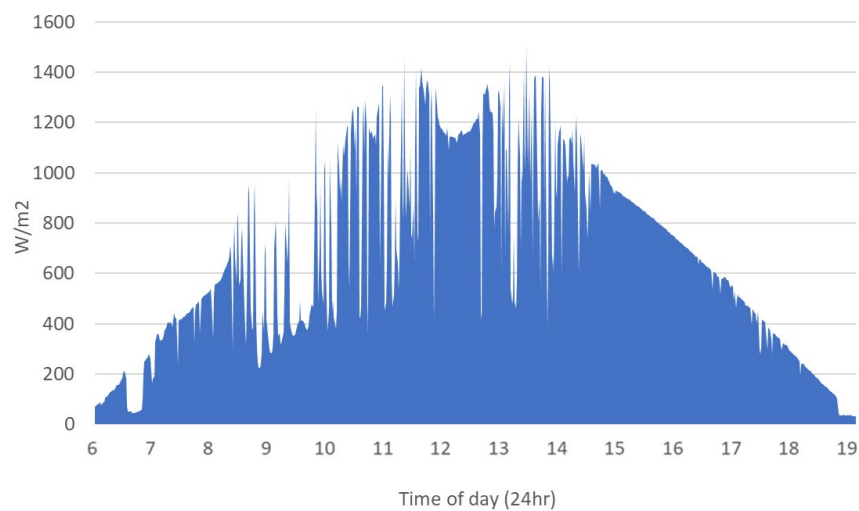


FIG 18 – Minutely GHI (W/m^2) for 1st of January 2019.

Wind

Two wind speed data sets were considered for the HOMER simulations. Hourly 2019 wind speed data was purchased from the BOM for the Wiluna weather station measured at the typical weather station anemometer height of 10 m above ground. This data was scaled to a 50 m height above ground with Global Wind Atlas (GWA) for comparison purposes, showing a reasonable correlation to HOMER's default data set (see Figure 19). The Wiluna data set was scaled to 100 m above ground for the HOMER simulations using GWA, which is the approximate height of the wind turbine modelled.

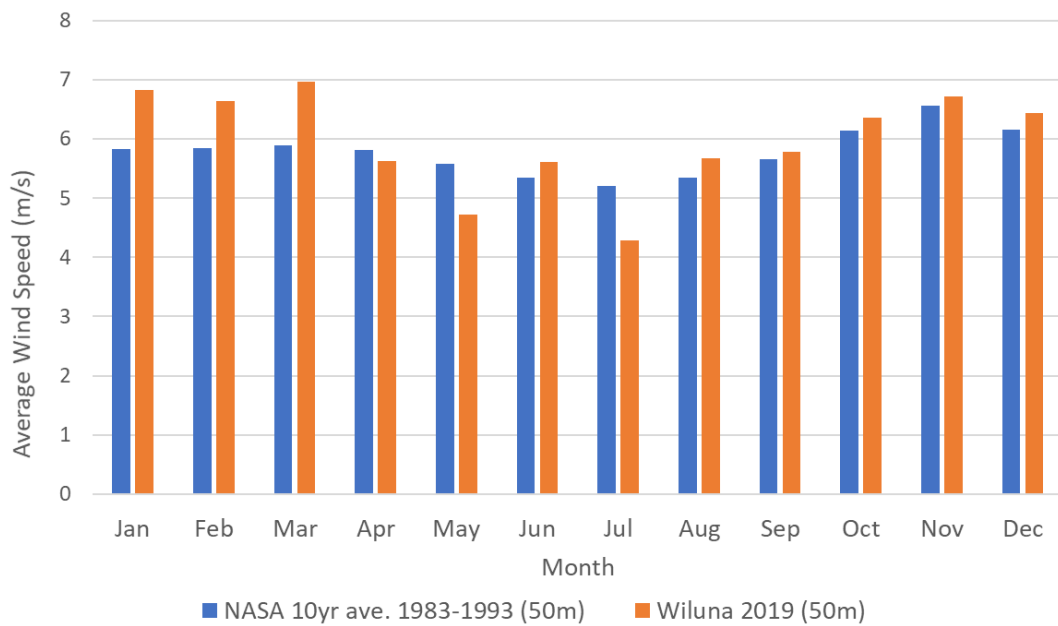


FIG 19 – Monthly wind speed average by source.

Figure 20 shows the daily average wind speed for 2019 scaled to 100 m above ground, incorporating the cut-in speed and rated speed of the wind turbine modelled in HOMER. Figure 21 similarly shows the hourly wind speed for the first week of 2019.

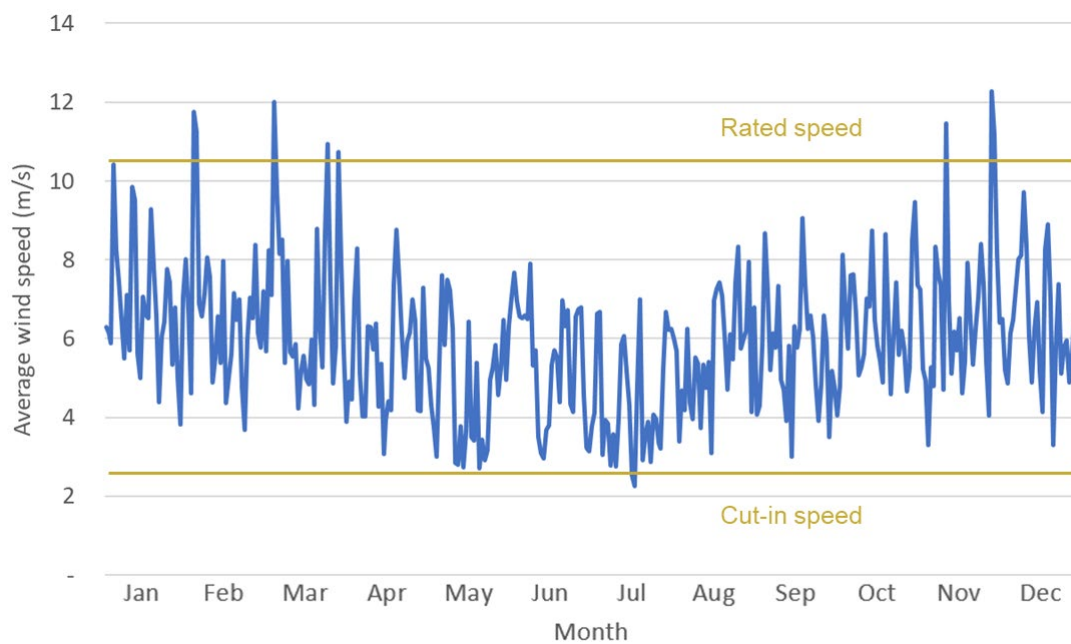


FIG 20 – Wiluna Daily average wind speed for 2019 – scaled to 100 m above ground.

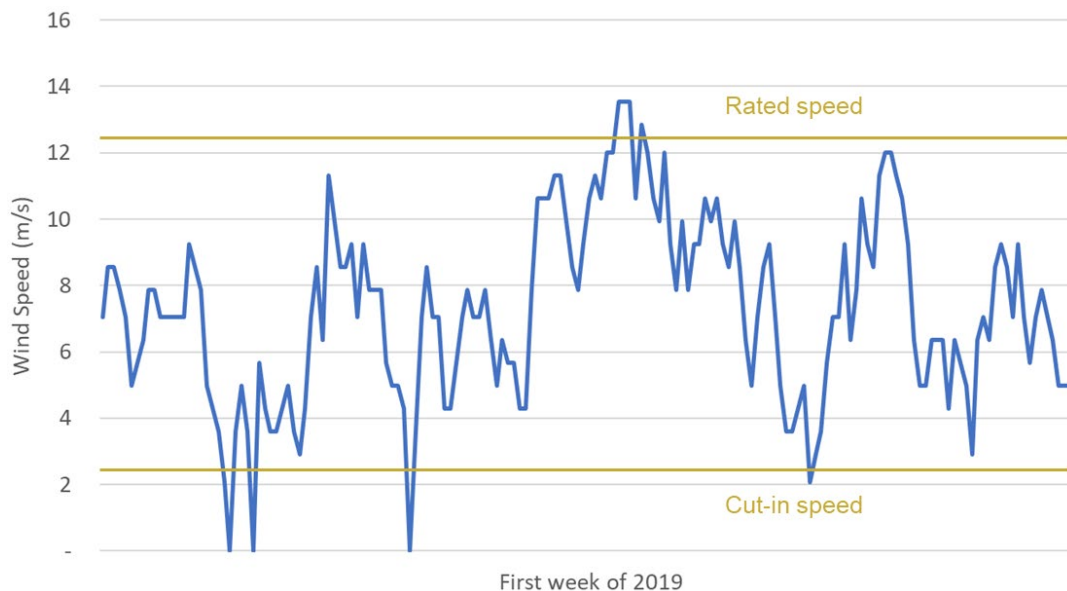


FIG 21 – Hourly wind speed for the first week of 2019 – scaled to 100 m above ground.

Figure 22 shows the average wind speed by the hour of the day. This graph suggests that wind and solar resources are not complementary at Jundee, which needs to be confirmed with on-site measurement.

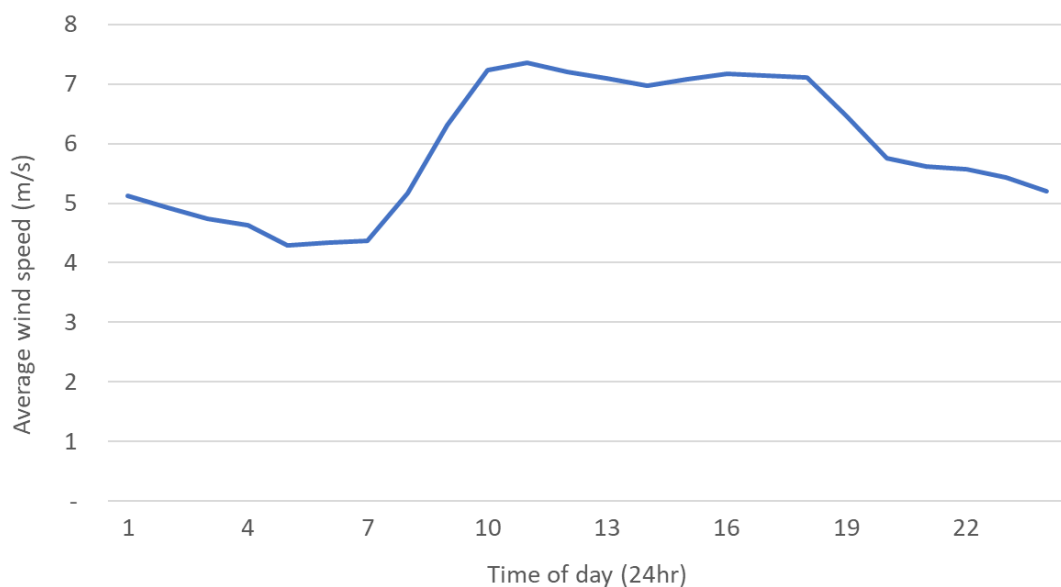


FIG 22 – Wiluna Average wind speed by hour of the day – scaled to 100 m above ground.

HOMER SIMULATIONS

Introduction

Several scenarios were evaluated to consider the feasibility of renewables at Jundee. HOMER was initially configured to replicate Jundee's gas powerplant, and costs were adjusted to replicate the long-term average unit cost of gas power (\$/kWh). The projected load profile was then imported to represent the ball mill upgrade, which was followed by the configuration of solar PV, wind turbine and li-ion battery components. Project lifetimes of 7 and 10 years were tested for all hybrid simulations representing typical PPA durations.

Gas model

The real-world Jundee power cost structure differs from the available configuration in HOMER. Gas generator variable costs are configured in HOMER on an operating hour basis, whereas the Jundee

historical costs are determined on a kWh basis. The gas generator O&M cost per operating hour was adjusted to replicate the overall power cost (\$/kWh) and captures the PPA consumption charge as well as other O&M costs for the gas plant. The cost specifics are not covered in this paper.

Hybrid model

The HOMER model was configured with the solar and wind natural resources developed – in addition to a temperature resource, which allows HOMER to model the detrimental effects of high temperatures on PV and wind turbine output. All cost and technical parameters for solar PV, wind turbine and li-ion components were configured at this stage.

A key constraint in the hybrid model was the differing operating reserve requirements for each generation component, highlighting the ‘balance of plant’ costs of natural resource variation (see Table 8).

TABLE 8

Hybrid model operating reserve by component.

Hybrid model operating reserve	
% of gas power output	10%
% of solar power output	80%
% of wind power output	50%

The hybrid power generation components modelled in HOMER are summarised in Table 9. The Goldwind 3.5 MW turbine was chosen for modelling as it is the turbine used at the nearby Goldfields Agnew mine. All cost factors were taken from the 2019–2020 GenCost report (Graham *et al*, 2020).

TABLE 9

Hybrid model modelled in HOMER.

Hybrid components modelled
Generic single-axis tracking solar PV
DC-AC inverter
Goldwind 3.5MW wind turbine
Generic 1MWh li-ion battery

Initial hybrid results

An initial hybrid simulation was conducted using the solar PV and wind turbine LCOE factors derived from the 2019–2020 Gencost report (Graham *et al*, 2020). All new assets were salvaged at the end of the project time frame, at a value determined by the asset’s economic life, capital cost, and replacement cost differential. The results generated in this scenario over-stated the cost benefits of renewables are not representative of a PPA cost environment.

Zero salvage hybrid results (PPA environment)

The initial hybrid simulations found that the COE and operating cost was heavily influenced by salvage costs at the end of the project lifetime. A typical PPA includes a fixed capacity cost that represents payback of the capital costs incurred by the IPP. A PPA cost environment was simulated by matching the useful lifetime of the renewable assets to the project lifetime. The capital costs were then amortised over the project lifetime to form the total cost (\$/a), which was the key metric used to compare results.

Table 10 lists the lowest COE configurations for the 7 and 10 year project periods, indicating that for a 7 year PPA period, gas-only generation is preferred. When a 10 year PPA is considered, a hybrid configuration with five 3.5 MW wind turbines results in a total annual cost reduction of \$700 000/annum and a COE of \$0.110/kWh.

The five wind turbine configuration was further simulated as a 7 year PPA, resulting in an annual cost increase of \$1.4M and a COE increase to \$0.118/kWh (see Table 11).

TABLE 10

Zero salvage Hybrid simulation – lowest COE.

Project lifetime (years)	GW 3.5 turbine	Initial Capital	Ren. Frac.	Ave. Gas Load	COE (\$/kWh)	Operating Cost (\$/yr)	Total Cost (\$/yr)
7	0	\$0	0%	21.3MW	0.112	\$20.8M	\$20.8M
10	5	\$33M	34%	14.1MW	0.110	\$16.8M	\$20.1M

TABLE 11

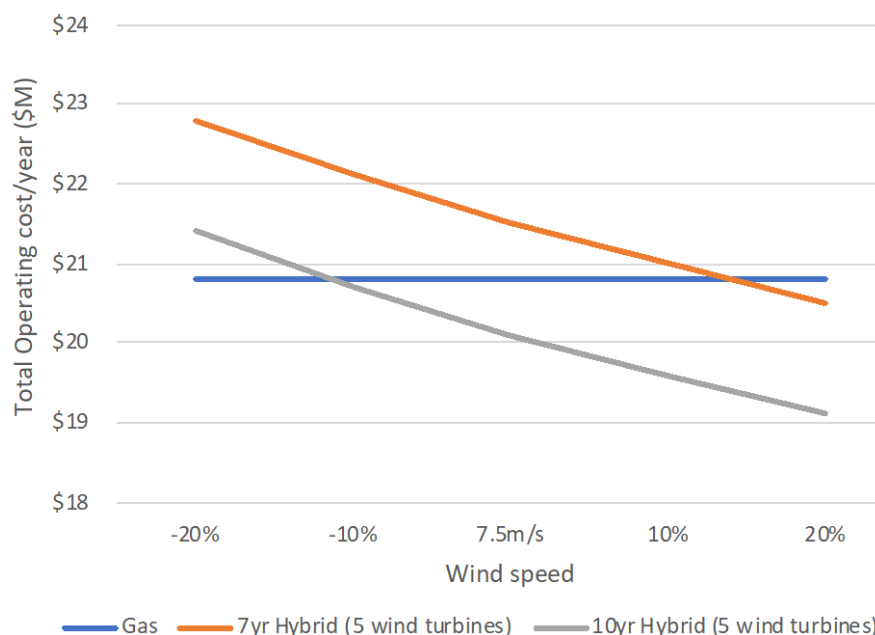
Zero salvage Hybrid simulation – gas and wind turbine PPA comparison.

Project lifetime (years)	GW 3.5 turbine	Initial Capital	COE (\$/kWh)	Operating cost (\$/yr)	PPA Estimate (\$/yr)	Total Cost (\$/yr)
7	5	\$33M	0.118	\$16.8M	\$4.7M	\$21.5M
10	5	\$33M	0.110	\$16.8M	\$3.3M	\$20.1M

Sensitivity analysis

Natural resource sensitivity

A sensitivity analysis was completed to evaluate the impact of a diminished average wind speed on the COE. The cost-benefits of wind turbines are sensitive to average wind speed, and the default wind speed with a 10 year PPA is the only scenario where wind turbines provide the lowest COE. The cost relationship between the hybrid and gas configurations for 7 and 10 year project lifetimes is also illustrated in Figure 23.

**FIG 23** – Zero salvage gas and wind hybrid – natural resource sensitivity on operating cost.

Additional data was purchased from the BOM to evaluate annual wind speed variability. Long-term annualised data was not available for Wiluna but was available for Leinster and Meekatharra. Figure 24 shows the mean wind speed by year from 2000 to 2019 with minimal variation year-on-year. This suggests that wind turbines can be installed with a comparatively high level of confidence due to the regularity of natural resources, a contrast to fossil fuel price volatility, which fluctuates with varying supply and demand.

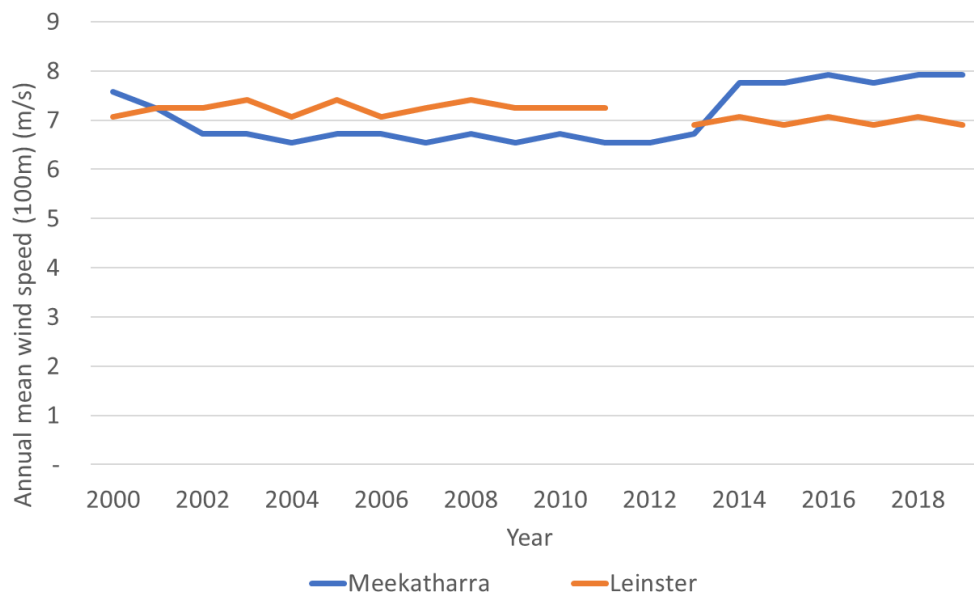


FIG 24 – Mean wind speed by year for Meekatharra and Leinster (purchased from BOM).

Gas price sensitivity

An additional sensitivity analysis was conducted for gas prices ± 40 per cent the current gas price (Figure 25), showing that the 10 year hybrid wind turbine configuration withstands a 20 per cent fall in gas price before the gas-only configuration provides the lowest COE.

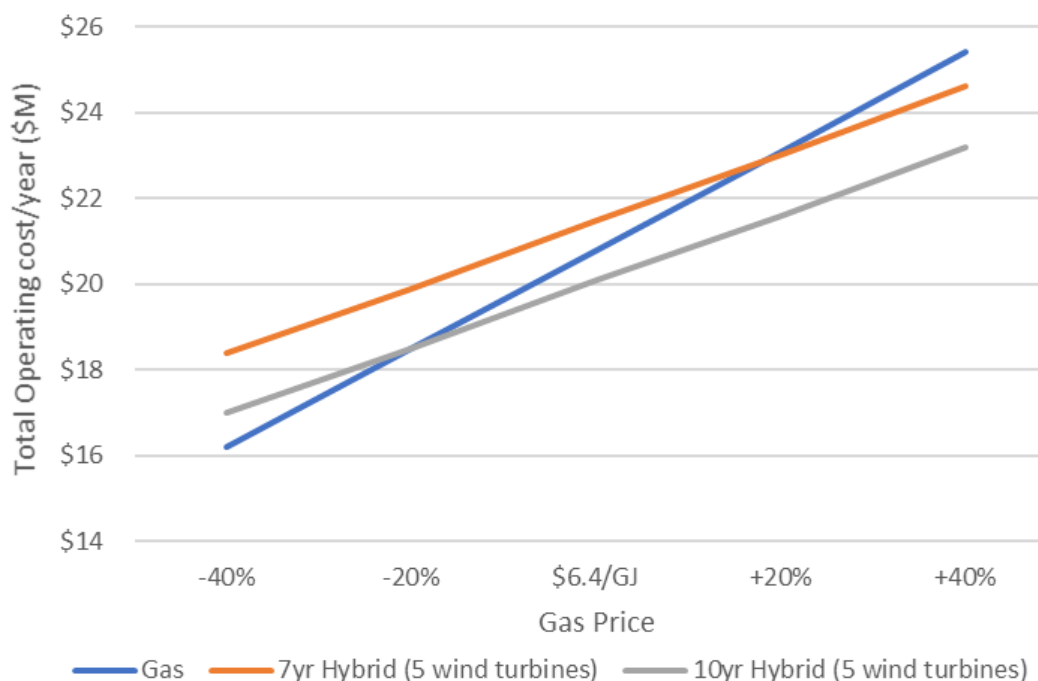


FIG 25 – Zero salvage hybrid simulation – gas price sensitivity versus five wind turbine configuration total cost/annum.

Renewable generation performance

Table 12 compares the LCOE for solar PV and wind for the 7 and 10 year scenarios. The results illustrate the value proposition of wind, with a resulting higher capacity factor and lower LCOE than solar PV. Solar PV capital costs are currently 30 per cent less than wind per kW installed, implying that costs need to fall further and additional technology improvements are required before solar PV becomes more cost-effective than wind. Additional solar PV costs not captured in the LCOE are the additional operating reserves required to 'balance the plant' through natural resource variation – and the integrated battery support required for ramp rate control.

TABLE 12
Zero salvage LCOE comparison table.

	Capacity factor	LCOE (\$/kWh) (7 years)	LCOE (\$/kWh) (10 years)
Solar	25%	0.1020	0.0762
Wind	40.8%	0.0904	0.0676

Figure 26 shows that the LCOE of solar PV and integrated solar and battery is expected to fall over the coming years. In contrast, the LCOE of the mature wind turbine technology is stable, suggesting that solar PV will become increasingly cost-competitive in due course.

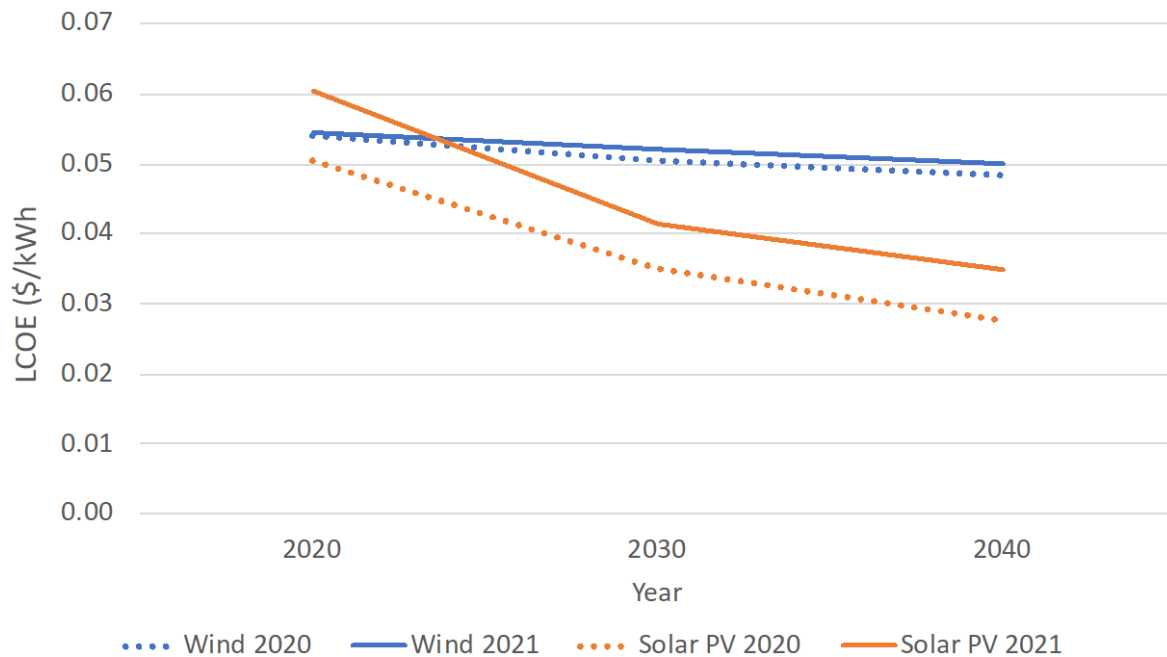


FIG 26 – Solar PV and Wind projected LCOE (Graham *et al*, 2020, 2021).

CONCLUSIONS

The purpose of this study was to evaluate the techno-economic feasibility of renewable power generation at Jundee. HOMER techno-economic simulation software was used for the evaluation and relied on natural resource data, load data and cost and technical parameter inputs. Jundee's gas-only generation method was satisfactorily modelled in HOMER, and the model was further developed to consider wind turbines, solar PV and li-ion battery storage components. Multiple scenarios were simulated, and HOMER provided the lowest COE configuration for each possible combination of components, for each scenario.

HOMER simulations were conducted for 7 and 10 year periods, to create two PPA considerations. All renewable generation assets were configured with a useful life matching the PPA length, and the initial capital cost was amortised over the project life to represent the fixed cost component of a PPA. Additional results were evaluated for sensitivity against varying average wind speeds and gas prices.

Based on the modelling, HOMER found that a gas and hybrid configuration with five 3.5 MW wind turbines providing 34 per cent of Jundee's electricity over a 10 year PPA can provide a slightly lower cost of electricity than the status quo.

The operating cost benefit of reducing reliance on fossil fuels was illustrated with a gas price sensitivity analysis, showing that the hybrid system costs are less sensitive to gas price volatility because of reduced exposure to gas prices. Additionally, the 10 year gas and wind configuration remains the cheapest configuration until the gas price falls more than 20 per cent below the contract price.

Jundee has had a long and prosperous mine life which is expected to prolong. Still, the ongoing feasibility of renewables at Jundee relies on additional resource conversion extending mine life beyond the current 8 year estimate. A wind turbine definitive feasibility and construction process could take between 2–3 years, and the cost-effectiveness of the hybrid gas and wind solution relies on a 10 year mine life at the commissioning date.

STUDY LIMITATIONS

The key limitations of this study were compromises made developing natural resource data sets for the simulations. The nearest available BOM source of minutely resolution solar GHI data was Geraldton, and the data available for 2018 and 2019 was incomplete, so the available months were merged to create a complete calendar year. The annual average radiation was consistent with long-term averages for Wiluna, so the data was considered as an acceptable alternative. The direction taken here was still superior to using hourly resolution data from a site closer to Jundee, which would have produced conservative results and inadequately estimated the 'balance of plant' costs of managing output variability, resulting in increased operating costs due to mismatched components.

A compromise was also made for the wind speed data. Hourly wind speed data was purchased from the BOM for Wiluna, which is approximately 50 km from Jundee. Additionally, this data was measured at 10 m above ground, which is typical for weather stations, but required scaling to 100 m above ground speeds with satellite data. Scaling wind speed data with satellite-derived long-term averages is acceptable for an initial evaluation. Still, site-specific measurement is required to confirm the effects of local terrain and to evaluate wind shear loss caused by high temperatures.

A final but minor limitation was that the cost estimates used were extracted from the CSIRO 2019–2020 GenCost report – and were not based on direct quotes from IPP's. The lack of direct quotes may add some risk to the cost estimates, but several additional sources were evaluated in the literature review, validating the GenCost report estimates. Despite an increase in renewable energy capital costs in the 2020–2021 GenCost report update, continued cost reductions for renewable generation and storage technologies are expected.

ACKNOWLEDGEMENTS

The author would like to acknowledge Northern Star Resources for allowing this paper to be published.

REFERENCES

- ARENA. 2013. Australian Energy Resource Assessment. <https://arena.gov.au/assets/2013/08/Chapter-10-Solar-Energy.pdf>.
- ARENA, 2017. The Business of Renewables. Australia. <https://arena.gov.au/assets/2017/07/AU21476-ARENA-Corporate-Report-REVISED-v1-1.pdf>.
- ARENA, 2019. Fringe of Grid Mines Embrace Renewables. Accessed 7th May 2020, <https://arena.gov.au/blog/hybrid-renewables-mines/>.
- Bhattacharjee, A K, Batarseh, I, Hu, H and Kutkut, N, 2017. An Efficient Ramp Rate and State of Charge Control for Pv-Battery System Capacity Firming, *2017 IEEE Energy Conversion Congress and Exposition (ECCE)*.
- Blanksby, C, 2018. Are Batteries the Best Way to Go? Entura. Accessed April 6 2020, <https://www.entura.com.au/are-batteries-the-best-way-to-go/>.
- Campbell, A, Draper, G, McKenzie, P, Ramli, H and O'Brien, L, 2018. Nem Outlook and Snowy 2.0. Australia: Jacob Marsden.
- Comino, T, 2018. Calculating Capacity Factor. AGL. Accessed June 5 2020, <https://thehub.agl.com.au/articles/2018/09/calculating-capacity-factor>.
- Dickeson, G, McLeod, L, Dobb, A, Frearson, L, Herteleer, B and Scheltus, D, 2019. Ramp Rate Control for Pv Plant Integration: Experience from Karratha Airport's Hybrid Power Station.
- EDL, 2019. Coober Pedy Hybrid Renewable Project – Second Year Performance Review. Australia: ARENA. <https://arena.gov.au/assets/2017/02/coober-pedy-hybrid-renewable-project-second-year-performance-report.pdf>
- EIA, 2020. Levelised Cost and Levelised Avoided Cost of New Generation Resources in the Annual Energy Outlook 2020.
- Ekstica, 2018. Hybrid Power Generation for Australian Off-Grid Mines. ARENA. <https://arena.gov.au/assets/2018/06/hybrid-power-generation-australian-off-grid-mines.pdf>.

- Fulcrum3D, 2020. Fulcrum3D Sodar. Accessed 11th May 2020, <http://www.fulcrum3d.com/sodarf3d/>.
- Global Wind Atlas, 2020. Global Wind Atlas. Accessed 8th May, <https://globalwindatlas.info/>.
- Goldwind, 2018. 'Goldwind 3.0 mw(S) Pmdd Wind Turbine Brochure.'
- Graham, P, Hayward, J, Foster, J and Havas, L, 2020. Gencost 2019–2020. Australia. <https://doi.org/10.25919/5eb5ac371d372>.
- Graham, P, Hayward, J, Foster, J and Havas, L, 2021. Gencost 2020–2021. Australia.
- Graham, P, Hayward, J, Foster, J, Story, O and Havas, L, 2018. Gencost 2018.
- HOMER Energy, 2020. Homer Pro 3.13 User Manual. Accessed 3rd May 2020, <https://www.homerenergy.com/products/pro/docs/latest/index.html>.
- IRENA, 2017. Electricity Storage and Renewables: Costs and Markets to 2030.
- IRENA, 2019. Global Energy Transformation – a Roadmap to 2050.
- IRENA, 2020. Electricity Storage Valuation Framework.
- Jurasz, J, Canales, F A, Kies, A, Guezgouz, M and Beluco, A, 2020. A Review on the Complementarity of Renewable Energy Sources: Concept, Metrics, Application and Future Research Directions. *Solar Energy* 195: 703–724. doi: 10.1016/j.solener.2019.11.087.
- Lawan, S M and Abidin, W A W Z, 2020. A Review of Hybrid Renewable Energy Systems Based on Wind and Solar Energy: Modeling, Design and Optimization. In *Wind Solar Hybrid Renewable Energy System*. IntechOpen.
- Northern Star, 2018. Northern Star Jundee Operations Fact Sheet. Accessed 13th April 2020, <https://www.nsr ltd.com/wp-content/uploads/2018/08/NSR-Jundee-Operations-Fact-Sheet-July-18.pdf>.
- Steggel, N, 2019. Wind Futures: 'How Low Can It Go?'. Accessed 4th May 2020, <https://www.dropbox.com/s/1fnio0opz0urj3b/2b%20Steggel%20WindEnergy.pdf?dl=0>.
- SunSHIFT, 2017. Renewable Energy in the Australian Mining Sector – White Paper. Australia. <https://arena.gov.au/assets/2017/11/renewable-energy-in-the-australian-mining-sector.pdf>.

Hydro-electrical power potentials in the Peruvian mining industry

Y Feldmann¹, G Blauermel², M Roth³, B Alapfy⁴, T Hillig⁵ and B G Lottermoser⁶

1. Research Fellow, Institute of Mineral Resources Engineering, RWTH Aachen University, 52062 Aachen, Germany. Email: feldmann@mre.rwth-aachen.de
2. Research Fellow, Institute of Mineral Resources Engineering, RWTH Aachen University, 52062 Aachen, Germany. Email: blauermel@mre.rwth-aachen.de
3. Research Fellow, Chair of Hydraulic and Water Resources Engineering, Technical University of Munich, 80333 Munich, Germany. Email: moritz.roth@tum.de
4. Research Fellow, Chair of Hydraulic and Water Resources Engineering, Technical University of Munich, 80333 Munich, Germany. Email: bertalan.alapfy@tum.de
5. Managing Director, Thomas Hillig Energy Consulting – THEnergy, 80333 Munich, Germany. Email: thomas.hillig@th-energy.net
6. Professor, Institute of Mineral Resources Engineering, RWTH Aachen University, 52062 Aachen, Germany. Email: lottermoser@mre.rwth-aachen.de

INTRODUCTION

For many decades, the mining sector has predominantly relied on fossil fuels to meet its energy demand in the extraction and processing of mineral resources. Recently, mining companies have increasingly begun to incorporate renewable power sources into their operations, mostly solar and wind power. The implementation of renewable energy in the mining sector offers the potential to lower greenhouse gas emissions, increase profitability, create new employment opportunities, support sustainable resource development and to increase energy efficiency at mine sites.

In Peru, hydropower has traditionally been a reliable major source of energy. However, in recent decades its share in national power generation has fallen significantly due to increased natural gas extraction in the Amazon region. Simultaneously, the energy demand of the Peruvian mining sector is expected to increase further.

In this project, an international collaborative research team led by RWTH Aachen University and consisting of the Technical University of Munich, the consulting company THEnergy, Ergon Power S.A.C. (Peru) and a Peruvian mining company aims to develop comprehensive concepts and applications that help to unlock the untapped hydroelectric power potential in the Peruvian mining sector. The goal is to identify, develop and assess scenarios for the implementation of hydro-electric power generation from water or other fluid flows at mine sites. In particular, the scope of this project includes the development of scenarios for individual mine sites and their associated infrastructure as well as the identification of hydro-electric power potentials at mine site clusters.

In the initial project stage, mine water balances were analysed for large water or fluid volume flows resulting in points of interest. These points of interest were then characterised regarding their hydro-electrical potential, focusing on parameters relevant to hydro-electric power generation. Considering the fact that many mineral processing fluids contain solids, the list of relevant criteria also included the fluids' solids content, hydrochemistry, rheological and physical properties, as well as the potential hydro-electric drop head. This analysis resulted in the identification of seven domains for the possible production of hydro-electric power at individual mine sites or mine site clusters:

1. natural water bodies in the direct vicinity of a mine
2. water supply and discharge systems
3. fluid flows within the mineral processing plants
4. transportation of tailings to tailings storage facilities or slurry transport of concentrates by pipeline
5. water management systems for natural precipitation on heap leaching pads
6. water supply pipelines for underground mines
7. mine water flows.

Evaluation of the different domains was done using freely accessible satellite images and technical reports. Modelling of changing parameters at the points of interest was performed using the commercially available simulation software GoldSim and a purpose-designed adjustable mine water balance model. Time-dependent values of fluid quantities and characteristics for the different domains were simulated based on production figures from various mines in Peru.

To date, several operational domains of mine sites have been identified that show promising potentials for the generation of hydro-electric power:

1. natural water bodies in the direct vicinity of mines
2. fluid flows within the mineral processing plants
3. hydraulic transportation of tailings
4. precipitation on heap leaching pads.

The specific volumes required vary depending on the turbine technology utilised, for the identified domains volumes of 0.5–3 m³/s are expected.

Established and unconventional technologies for generating hydroelectric energy were evaluated and assessed using Computational Fluid Dynamics (CFD) simulations. Due to the high sediment content of the fluid, conventional turbines – such as Francis, Pelton or Kaplan turbines – cannot be used, as high speeds – for maintenance reasons – are to be avoided. Therefore, unconventional hydropower turbines such as the cross-flow or spherical turbine (also Gorlov turbine) are used. These turbines are characterised by the fact that they have a low rotational speed and can be integrated into an existing pipe system without major piping construction. The self-cleaning effect is particularly pronounced in the cross-flow turbine. It results from the fact that the fluid flows through the entire blade ring and flushes out the accumulated deposits.

The SmartH₂OEnergy-Project will ultimately establish a set of principles and parameters that determine the development potential of hydro-electric power at Peruvian mine sites. Moreover, the results of this project will be extended from Peru to establish guiding principles for hydro-electric power development at mine sites in general. It is expected that the installation of small hydropower schemes at mine sites will yield many benefits:

- the establishment of much needed and long-lasting power infrastructure for local communities
- less reliance on unreliable electricity networks
- less dependence on fossil fuels
- lower carbon dioxide emissions at industrial sites.

ACKNOWLEDGEMENTS

This work was supported by the German Federal Ministry of Education and Research and is part of the SmartH₂OEnergy project (grant number 033R206A).

Sustainable power generation for mining operations with natural ester technology

K Y Lam¹, A Sbravati², P Reilly³ and J Tan⁴

1. Technical Service Representative, Cargill Bioindustrial, Singapore 048946.
Email: kinyu_lam@cargill.com
2. Global Technical Application Manager, Cargill Bioindustrial, Wayzata, MN 55391 (USA).
Email: alan_sbravati@cargill.com
3. Business Development Manager, Cargill Bioindustrial, Melbourne Vic 3006.
Email: philip_reilly@cargill.com
4. Marketing Specialist, Cargill Bioindustrial, Singapore 048946. Email: janet_tan@crgl-thirdparty.com

INTRODUCTION

With many industries placing sustainability high up on their business agenda and with the rapid deployment of solar panels, wind mills and other renewable and low-emission energy infrastructure driving up the demand for iron, copper, aluminium and other rare earth elements, the spotlight is on the mining sector to improve its output and efficiency in a sustainable way.

To meet their huge energy demand more sustainably, many mining operators are beginning to use renewable energy resources to replace heavy fuel oil generators, many of which are deployed at remote mining sites, while ensuring that reliability and continuity of their power supply are not compromised in their operations (Mellmann *et al*, 2020).

Simultaneously, as fire and environmental risks continue to be of concern – following a few major bushfire outbreaks – the use of mineral oil-based insulating fluid in transformers is increasingly viewed as unacceptable. With the use of dry-type transformers also limited by their low efficiency and stringent operating requirements, liquid-filled transformers with less flammable insulating fluids (or ‘K class’ fluid according to IEC Standard, 2008) are fast becoming the industry norm.

Developed more than 25 years ago to combat the fire and environmental hazards of liquid-filled transformers, natural ester is becoming the fastest growing insulating fluid in the market, as it is capable of improving equipment lifespan, reliability and loading capacity. As will be discussed later, these capabilities can play a key part in enabling mining operators to achieve economic, environmental, and social sustainability.

ECONOMIC SUSTAINABILITY THROUGH RELIABLE, RESILIENT AND SAFE TRANSFORMERS

One of the most significant properties of natural ester fluid is that it can absorb moisture produced during the ageing of cellulose paper as well as chemically remove it through hydrolysis (Rapp, McShane and Luksich, 2005; Lemm, Rapp and Luksich, 2006; Yang *et al*, 2010). This dual mechanism retards the ageing of transformer insulating systems comprising cellulose paper and natural ester and prolongs its lifespan by five to eight times, compared to mineral oil systems (Figure 1) (McShane *et al*, 2001, 2002).

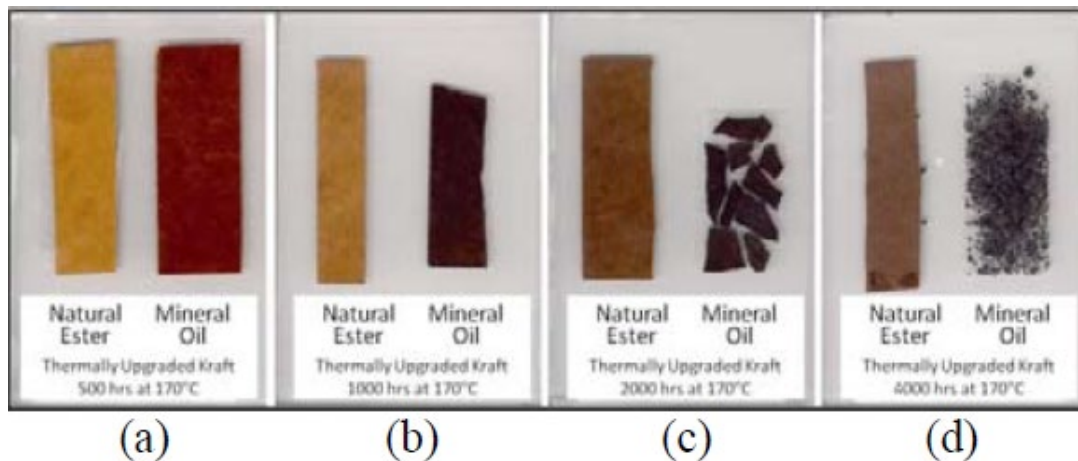


FIG 1 – Aging of thermally upgraded insulation paper in mineral oil and natural ester after: (a) 500 hrs, (b) 1000 hrs, (c) 2000 hrs, and (d) 4000 hrs at 170°C (McShane *et al*, 2001).

The extension of insulation and transformer lives reduces the life cycle costs through delaying asset replacement. Moreover, such benefits can also be reaped by retro-filling existing mineral oil transformers with natural ester fluid without extra capital outlay on new equipment (McShane *et al*, 2003).

The increased lifespan of the cellulose paper insulation system with natural ester also means that transformers can run at higher temperatures with additional loading, as recognised by IEC Standard (2013). Using this approach, transformers can be designed at a reduced size and improved cost-effectiveness without compromising on reliability and equipment life.

In one of the most significant projects (Vasconcellos, Franchini and Mak, 2010), a natural ester transformer, based on an original design of rated load at 45 kVA (rated at standard average winding temperature rise (AWR) of 65K) with a fluid tank size of 81 litres, was re-rated to 88 kVA at a higher temperature (AWR of 85K). Compared to a standard 75 kVA mineral oil transformer with a tank size of 102 litres, the natural ester transformer is not only more space economical and energy efficient (due to its lower no-load loss), its cost is also about one third lower on per kVA basis. More importantly, after about 2100 such transformers had been in use for over 5 million accumulated hours, the failure rate was found to be lower than standard transformers.

From the fire safety standpoint, there are clear benefits to using natural ester transformers in reducing the cost of infrastructure for mitigating fire hazards as required by the various fire codes (eg FM Global, 2019). But more importantly, in mining operations where the downtime cost can be very high, the benefit of minimising the consequence of a transformer failure can be much greater, even when all the precautions and safety measures are in place.

In one particular case study involving two similar transformer failure incidents at different mining sites (Sbravati *et al* (in prep)), one 100 kVA/15 kV mineral oil transformer caught fire, and normal work order could only be resumed after 20 days due to various procedures including cleaning up of the site, notification and inspection involving relevant external agencies, etc. In the other incident, since the transformer of similar size was filled with natural ester and there was no fire, the downtime was a mere four hours for replacing the faulty transformer.

ENVIRONMENTAL AND SOCIAL SUSTAINABILITY THROUGH A BIOBASED GREEN FLUID

From the environmental and social perspectives, the sustainability benefits of natural ester derive from its origin from renewable crops, as well as the feasibility of reducing raw materials required to build the transformer.

Being essentially a bio-based product means that the basic ingredient of natural ester fluid can be sourced from a large base of agricultural communities, making it more likely to benefit the local economy in a social context.

Environmentally, natural ester is intrinsically highly biodegradable and effectively carbon neutral. With carefully selected additives, natural ester insulating fluid can also be made non-toxic in all the key aquatic and oral toxicity tests. Based on its overall environmental impact as calculated according to Lippiatt (2007), natural ester is clearly the best green option among all the different types of insulating fluids, particularly when considering its higher fluid thermal class according to IEC Standard (2013) concurrently (Figure 2) (Bingenheimer, 2011).

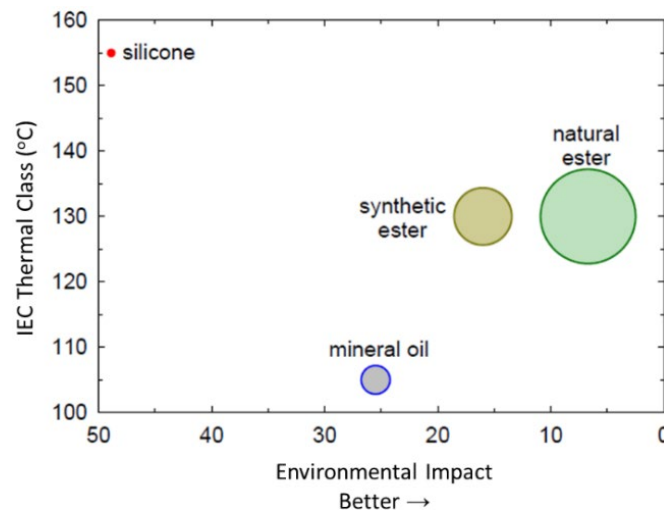


FIG 2 – Environmental impact (Lippiatt, 2007) and thermal class (maximum recommended operating temperature with an acceptable fluid life) (IEC Standard, 2013) of different types of insulating fluids. Symbol diameter represents OECD 301 biodegradability.

Apart from being a sustainable fluid, natural ester's contribution toward environmental and social sustainability is even more significant when its benefit of increasing the loading capacity of transformers is fully exploited. Other than the economic benefits mentioned earlier, the possibility of having a more compact transformer to meet the same loading requirement also means less metal is needed in the building of transformers, hence enabling conservation of precious non-renewable resources.

CONCLUSION

With its proven capacity in enhancing safety, reliability and resilience of power supply in a sustainable way, natural ester clearly has what it takes to meet the stringent requirements of the mining industry while enabling it to be a driving force towards true sustainability.

REFERENCES

- FM Global, 2019. *Property Loss Data Sheet 5.4*, FM Global, Norwood, MA. USA, July 2019.
- IEC Standard 2013. IEC 60076–14:2013 – Liquid-immersed power transformers using high-temperature insulation materials, Sep. 2013.
- IEC Standard, 2008. IEC 61039:2008 – Classification of insulating liquids, Jul. 2008.
- Lemm, A W, Rapp, K J and Luksich, J, 2006. Effect of natural ester (vegetable oil) dielectric fluid on the water content of aged paper insulation, in *Proceedings 10th Intl. Electrical Insulation Conference*, EIA, 65–70.
- Lippiatt, B C, 2007. *BEES 4.0 Building for Environmental and Economic Sustainability*, National Institute of Standards and Technology, Gaithersburg, MD, USA.
- McShane, C P, Corkran, J L, Rapp, K J and Luksich, J, 2003. Aging of paper insulation retrofilled with natural ester dielectric fluid, *Annual Report Conf. on Electrical Insulation and Dielectric Phenomena*, IEEE, 124–127.
- McShane, C P, Rapp, K J, Corkran, J L, Gauger, G A and Luksich, J, 2001. Aging of paper insulation in natural ester dielectric fluid, in *Proceedings Transmission and Distribution Conference*, IEEE, vol. 2, 675–679.
- McShane, C P, Rapp, K J, Corkran, J L, Gauger, G A and Luksich, J, 2002. Aging of plain Kraft paper in natural ester dielectric fluid, in *Proceedings 14th Intl. Conf. on Dielectric Liquids*, IEEE, 173–177.

- Mellmann, J, East, D, Knight, A and Baines, O, 2020. Mining & renewable energy – a greener way forward [online], Watson Farley and Williams. Available from: <https://www.wfw.com/articles/mining-renewable-energy-a-greener-way-forward/> [Assessed: 4 June 2021].
- Rapp, K J, McShane, C P and Luksich, J, 2005. Interaction mechanisms of natural ester dielectric fluid and Kraft paper, in *Proceedings 15th Intl. Conference on Dielectric Liquids*, IEEE, 393–396.
- Sbravati, A, Farren-Handford, J, Bloom, L and Scaquetti, D (in prep), Evaluation of the impacts of a catastrophic failure of electrical apparatus insulated with mineral oil and natural ester liquids.
- Vasconcellos, V, Franchini, L R and Mak, J, 2010. Transformador de distribuição de maior vida útil e menor agressividade ambiental', in *XIX Seminário Nacional de Distribuição de Energia Elétrica*, SENDI
- Yang, L, Liao, R, Sun, C, Yin, J and Zhu, M, 2010. Influence of vegetable oil on the thermal aging rate of Kraft paper and its mechanism, in *Proceedings International Conference on High Voltage Engineering and Application*, IEEE, 381–384.

Carbon footprint reduction with continuous mining equipment

M Schmid¹, A Heiertz² and S Blunck³

1. FAusIMM, Senior Mining Consultant, RWE Technology International GmbH, 45141 Essen, Germany. Email: martin.schmid@rwe.com
2. Head of Mining and Materials Handling, RWE Technology International GmbH, 45141 Essen, Germany. Email: arie.heiertz@rwe.com
3. MAusIMM, Department Head of Mining and Material Handling, RWE Technology International GmbH, 45141 Essen, Germany. Email: stefan.blunck@rwe.com

ABSTRACT

The mining industry has recently started to establish sustainable carbon emission reduction goals. The major source of carbon emissions in the mining process is the transport/haulage of ore and waste, especially over large horizontal and vertical distances. There are different approaches to reduce the carbon footprint in mining. While diesel fuel is still the main energy source used for conventional excavation and truck haulage, leveraging new technologies such as green hydrogen as a replacement for diesel may be one option. Another option is to partly or fully shift from fuel intensive haulage to conveyor-based technology driven by electricity generated from renewables.

RWE TI is an international mining engineering and consulting firm. Its parent company, the RWE Group, owns and operates three large-scale opencast mines in Germany with a total annual mining capacity of 90 million tonnes of ROM coal plus more than 500 million bank cubic metres of waste material. For more than 60 years now, the enormous amount of material has been moved by shiftable in-pit belt conveyors driven by electricity. The experience gained from operating the largest in-pit belt conveyors in the world (38 000 t/h, total length of 250 km, 7.5 m/s belt speed, 2.8 m belt width) has been successfully transferred to other commodities such as copper and iron ore in the last few decades. Coal-based electricity generation will be phased out in Germany by 2038, and RWE is committed to becoming a leading global provider of renewable energy and innovative engineering services.

The authors of this paper have developed a carbon emission estimation tool for the excavation and material handling process in a classic opencast strip mine. They have used the tool to compare the emissions as well as capital (CAPEX) and operating costs (OPEX) of a conventional Truck/Excavator (TEx) operation as a base case with various conveyor based continuous mining equipment (CME) applications, including bucket wheel excavator (BWE) and in-pit crushing and conveying (IPCC) systems. With respect to the latter technology, the required change in mine planning, the novel technology components and specific equipment productivities are derived from RWE's long-term operational experience. CAPEX, OPEX and the potential reduction in greenhouse gas (GHG) emissions are calculated for the mine's life. The results show a significant carbon reduction potential (30–85 per cent) depending on the energy mix used, accompanied by significant savings in OPEX.

INTRODUCTION

RWE owns and operates the largest continuous mining and material handling system in the world. The three mines Hambach, Garzweiler and Inden, all located in a densely populated area west of Cologne in Germany, are powered completely by electricity. Since the beginning, more than 60 years ago, RWE has invested in the development of continuous mining technology and knowhow. A waste excavation and material handling 'chain' consists of a bucket wheel excavator, a belt loading unit, shiftable belt conveyors, material transfer stations, relocatable and shiftable belt conveyors to and on the waste dump, a tripper car and a spreader. RWE and its technology development partners (OEMs) for continuous mining system components, such as the steel cord belts, the drive units, the idlers, the crawler mounted machines including excavators, tripper cars and spreaders, have developed this technology to an outstanding maturity level: Each belt conveyor chain is capable of transporting 38 000 t/h, featuring a 2.8 m wide steel cord belt (ST4500) running at a fixed speed of 7.5 m/s. The typical length of one chain is 8 to 12 km. It comprises three to four shiftable belt conveyors each on the mining side and on the dumping side, which lift the waste up to more than 300 m in height.

This conveyor-based technology is increasingly being adopted in copper and iron ore mines, ie hard rock mines, in combination with in-pit crushing technology. At such an application the bucket wheel excavator is replaced by a hydraulic excavator which is loading the coarse blasted rock into a fully mobile crushing rig to establish the same material handling 'chain' in waste material. This process is referred to internationally as In-Pit Crushing and Conveying (IPCC).

The industry-wide carbon emission reduction goals are forcing mine owners to reduce fossil fuel consumption in the next few decades. The major source of carbon emissions in the mining process is the transport/haulage of ore and waste, especially over large horizontal and vertical distances with diesel powered truck/excavator systems. One important option is to partly or fully shift from this fuel intensive haulage to a conveyor based technology driven by electricity generated from renewables.

Therefore, the authors of this paper have developed a carbon emission estimation tool for this excavation and material handling process in a classic opencast strip mine. They have used the tool to compare the emissions as well as capital (CAPEX) and operating costs (OPEX) of a conventional Truck/Excavator (TEx) operation as a base case with different In-Pit Crushing and Conveying (IPCC) applications, ie continuous mining and transportation variants.

With respect to the latter technology, the required change in mine planning, the novel technology components and specific equipment productivities are derived from RWE's long-term operational experience.

CONTINUOUS MINING EQUIPMENT

The main difference between conventional TEx and innovative IPCC systems is their mode of operation: 'discontinuous' versus 'continuous'. If the material transport is examined, the number of accelerations of the masses along the transport route is always accountable for the majority of total energy consumption. TEx systems are typically 'discontinuous': the freshly mined material is accelerated, loaded and rested on the truck. The truck is accelerated and stopped again multiple times along the transport route. Finally the truck stops again, reverses, stops again and unloads the material. In IPCC systems this chain can be regarded as 'continuous': The material is mined and loaded onto eg the fully mobile crusher. From here the material is only accelerated once. Along the total chain of conveyors no stops are necessary until the material is unloaded from the spreader. This technological advantage is the main reason for energy savings in the mining and transporting process (Schmid and Tappeiner, 2014).

The change towards IPCC systems needs careful planning as the conveyor lines require an adapted mine layout. If a decision is made in favour of fixed, semi-mobile or fully mobile crushing units, either shiftable in-pit conveyors or fixed rigid installed conveyors can be used. The main focus from an operational planning point of view are the downtimes of such systems. RWE has derived reliable time usage models (TUM) from its own operations. These are the basis for the investment decision in continuous mining technology: It is always a trade-off between reliably achievable operating hours and the necessary nominal capacity of the systems. The local situation and the target production must be thoroughly investigated in order to install a manageable IPCC system. Unlike TEx systems, IPCC systems are more vulnerable to overloading and working at 100 per cent capacity. A breakdown of only one component in the chain leads to an immediate production stop. Material-based production capacities therefore have to be considered.

Another important factor is largely unmanned, autonomous production. A typical manning of a continuous mining equipment chain at RWE is three operators at the excavator and two operators at the spreader. All other personnel needed for shifting of the conveyor lines and performing maintenance work is preparing the next planned stop of the system during production. These times also have to be utilised by providing the teams with continuous training in order to achieve the downtime targets for the year. Component expert teams must be set-up to collect operational experience and keep this experience alive. In comparison with RWE's operations, many operations in the world utilising IPCC systems underestimate this human factor. Instead of focusing on the efforts needed to reach the downtime plan, hasty decisions are made to bring the system back into operation as fast as possible, which often leads to longer downtimes a few weeks later.

A system inherent lack of flexibility and redundancy of IPCC systems is often assumed by TEx system owners and operators. Fully mobile IPCC systems (FMC) however offer greater flexibility

than typically estimated. In combination with belt bridges the accessible mining block can be extended in vertical and horizontal distance. It also can be mined from both sides of the belt. Where there are long horizontal mining faces, the mining block should be designed so that the conveyor does not need to be shifted more than three to six times a year. Along the face, each different quality can be reached within the day-to-day planning and by moving the FMC to the desired location. However, these quality-based downtimes have to be taken into account in the TUM as early as possible, eg during the Feasibility Studies.

The provision of redundancies in continuous mining systems is essential if the planned uptimes of a single conveyor line are not sufficient to fill the necessary stockpile, eg of a preparation plant. At RWE all three mines have redundant (two) conveyor lines allowing coal to be produced at the required quantity any time. Regarding the waste conveyor lines, redundancy can be achieved by installing a conveyor distribution point or belt splitter units. RWE uses both systems. At the large distribution station, multiple upstream conveyor lines from the excavation side overlap with all downstream conveyor lines of the dumping side. If for instance one spreader line has to be switched off, the excavator line can be reconnected to another spreader line by means of shuttle heads. Maintenance work on the spreader and the excavator side should be planned to take place during the same time frame, eg during major overhauls or conveyor shifting processes. As discussed earlier a certain degree of contingencies should also be considered when deciding on name plate capacities of the IPCC systems to allow for a larger production during short time periods.

The technology development partnership with various original equipment manufacturers (OEMs) is another important success factor that has been identified by RWE. The highest quality standards in combination with internal quality assurance testing, and a strategy to invest in high quality equipment result in fewer or no quality-related unplanned downtimes. Unplanned downtimes are the most expensive and most avoidable downtimes of an IPCC operation. RWE decided therefore to buy high-quality belt conveyor components only. Idler design and manufacture are expected to ensure that the idlers will last at least seven years in 24/7 operation. The belt itself has to pass the RWE standard tests, which are more detailed and adapted to RWE's mining conditions in order to reach a longer service life, especially of the splices. The pulley's lagging is important to reduce slippage. Recent advances in ceramic lagging allow for very long operating periods. Belt cleaning is essential for undisturbed production: The components must be able to withstand the most severe weather and wet material conditions. RWE's operation and maintenance experience, not only in these few areas of concern, should be considered during preliminary studies before an investment decision is made for a new IPCC system.

Taking these facts into account, the main further question discussed in this paper is: Is Continuous Mining Equipment (CME), incl. IPCC technology, a sustainable GHG emissions-reducing alternative to conventional Truck/Excavator (TEx) technology?

Key drivers

The key drivers in a comparison of continuous mining and materials handling equipment with discontinuous TEx technology, which are recognised across the industry, are listed in Figure 1. For many years, fixed- and semi-mobile conveyor systems have proven to be reliable and economically superior due to the main drivers 'large transport distance' and 'vertical lift' (Blunck and Schmitz, 2012; Heiertz, Schmitz and Durchholz, 2014; Heiertz, 2014; Schmitz, Franken and Blunck, 2010; Wolff, Boyan and Blunck, 2013).

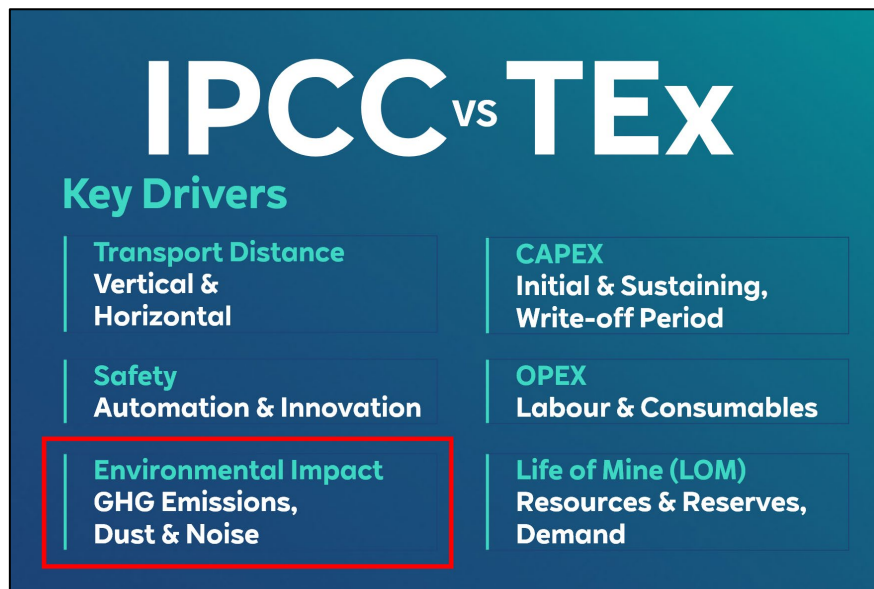


FIG 1 – Key drivers for continuous mining and material handling.

With the resolutions of the International Panel of Climate Change (IPCC(!)) another key driver in selection between TEx and CME is becoming more and more important for mine owners: the 'environmental impact' and, in particular the 'GHG emissions'.

Mining cost

An opencast mine can utilise various mining technologies. The decision which system is implemented depends primarily on the nature of the deposit, the hardness of the material mined, the estimated life-of-mine, the availability of skilled personnel and last but not least on the initial CAPEX. Earlier studies by RWE revealed that especially for waste material continuous mining and conveying technologies can have significantly lower unit costs compared to the discontinuous Truck/Excavator baseline. The comparison in Figure 2 shows an example of relative mining prime unit costs, which were estimated for a 4 km long strip mine with 20 years life-of-mine in a high-cost country (Australia). The various systems of this comparison are not all fully competitive, however the results are comparable. Especially the cross-pit (XPS) and around-the-pit (ATP) systems show significantly lower direct costs, whereas specifically the ATP systems can be also utilised for hard rock operations. The prime volume graph represents the annual mining capacity for only one unit of equipment or system (Blunck, 2021; Blunck and Langmaid, 2016; Blunck and Schmitz, 2012).

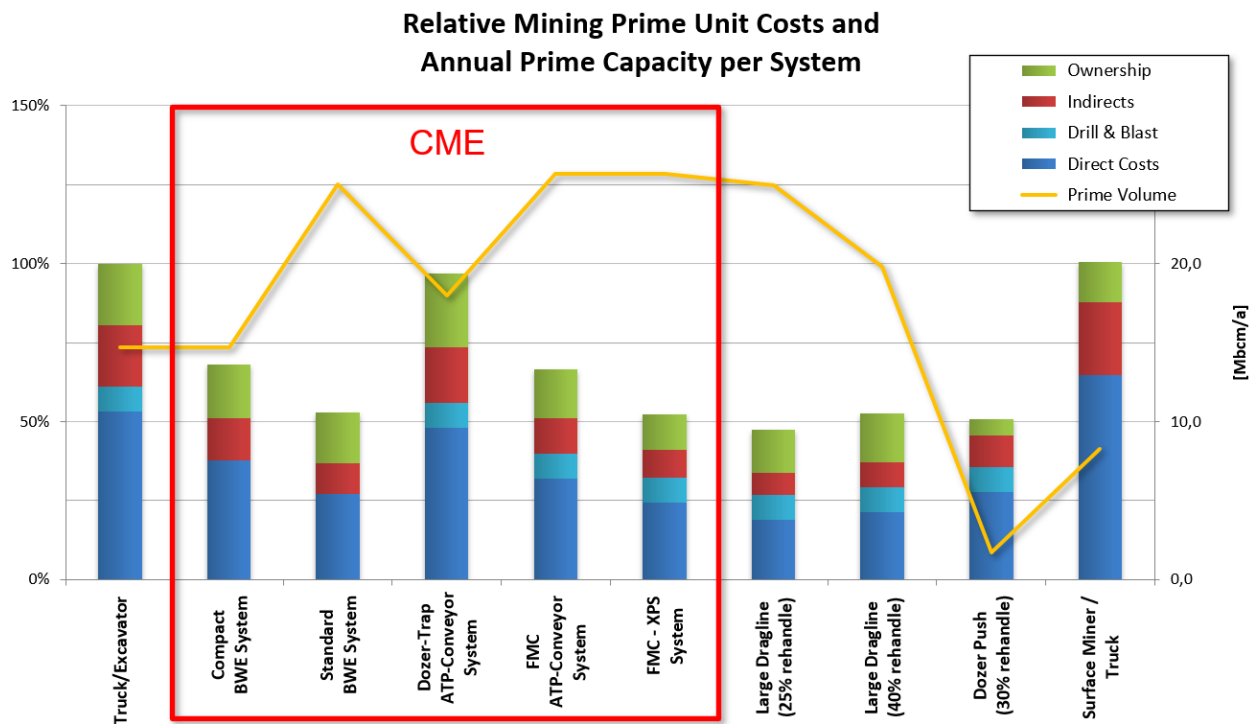


FIG 2 – Relative mining prime unit costs (bars) and annual prime volume (yellow line) for waste systems (Blunck and Langmaid, 2016).

The well-known bucket wheel excavator (BWE), belt conveyor and spreader application, a fully continuous mining-transportation-dumping process for unconsolidated material, is becoming increasingly attractive for other commodities than coal since crusher technology with larger capacity is available. The energy-efficiency is based on the above-mentioned fact that the mined material is accelerated only once. Thereafter, within the uninterrupted material flow, energy is only utilised to overcome system-inherent resistance and gravitation (vertical transport component) until the conveyed material is placed on the final dump or ROM stockpile location. Energy-consuming multiple material acceleration, the movement of large truck dead-weight (esp. empty return trips) as well as material rehandling, which are characteristic to TEx fleets, are avoided. This results in notable lower mining prime unit costs for nearly all of the CME systems in Figure 2 (red square).

Today successful implementation shows that IPCC technology enables the use of shiftable or relocatable in-pit conveyors also in hard rock mines. The extracted waste rock is crushed to a conveyable grain size via semi – or fully mobile crushing units (SMC/FMC).

Specific energy consumption of transport systems

Another recent study led by RWE compared the specific energy consumption of trucks and conveyors in kilowatt hours per tonne and kilometre (Figure 3) (Naghshi, 2020). Two main findings are:

- The actual fuel consumption of trucks is significantly higher than the theoretical fuel consumption.
- The actual power consumption of conveyors is negligibly higher than the theoretical calculated consumption.

Furthermore, as shown in Figure 3, this comparison reveals the increasing advantage of conveyors over trucks with steeper gradients. The specific energy consumption for continuous mining applications is significantly lower than TEx-based mining systems. The presented numbers are based on RWE's and other operating partners experiences.

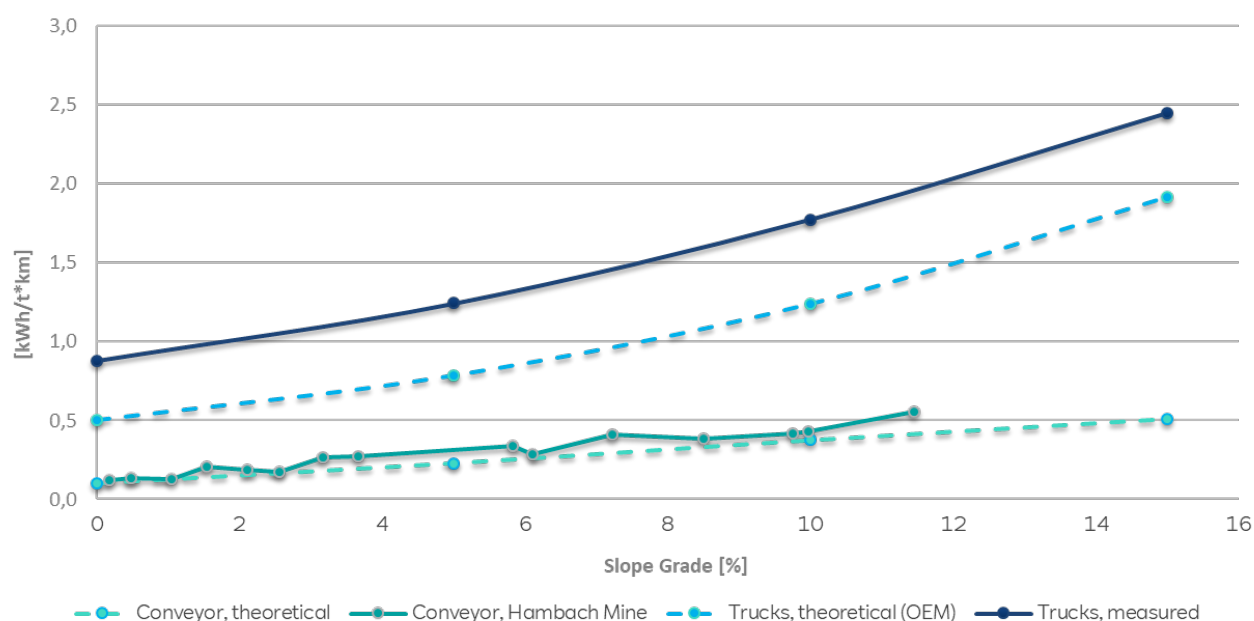


FIG 3 – Comparison of specific energy consumptions of trucks and conveyors (Naghshi, 2020).

REDUCTION OF GHG EMISSIONS

Electrically powered CME, incl. IPCC, can substantially and sustainably reduce the GHG emission footprint compared to an equivalent diesel-powered operation, provided that only renewable energy or at least an energy mix containing a substantial share of renewable energy is used (Heiertz, 2021).

Whereas the substitution of diesel fuel with lignite/coal-based energy may contradict the goal of GHG emission reduction, the availability of renewable electrical energy (biomass, hydro, solar, wind) on-site justifies the investment in CME/IPCC systems. Carbon taxes and subsidies may further accelerate this process.

RWE as a global Tier 1 company in continuous mining operations and renewable power generation can help investigate how to bring renewable energy generation to remote sites and, just as challenging, how to store and integrate climate friendly energy in the operation's local grid.

Life cycle of asset emissions

It needs to be acknowledged that renewable energy is not free of GHG emissions. The Life cycle-of-Asset (LCA) emissions are to be considered (eg including emissions released during production, transport, erection, dismantling and recycling of wind generators blades). Figure 4 provides an LCA emission comparison of different energy sources and associations on the right-hand side of the chart in kg CO₂ per kilowatt hour. Additionally, the average CO₂ emissions produced when burning fossil fuels are shown in kg CO₂ per litre on the left. As a result, these are negligibly small compared to the CO₂ emissions savings potential when changing from fossil to renewable fuels.

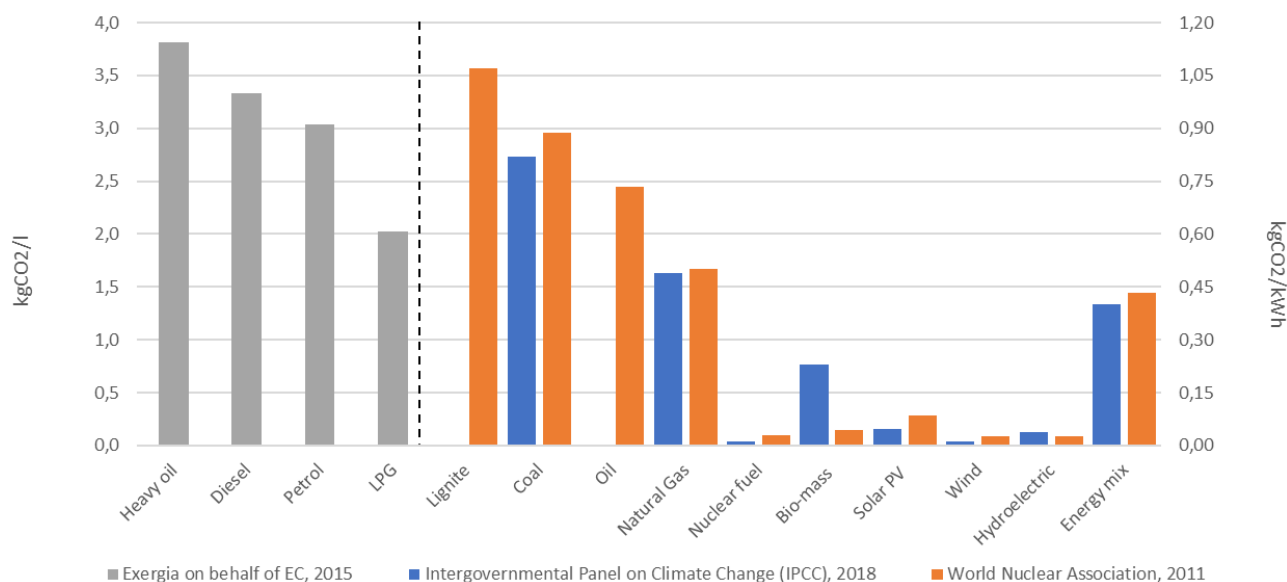


FIG 4 – Life cycle GHG emission comparison of different energy sources.

Renewable energy application potential

IPCC technology, especially in-pit and ex-pit conveyors, can typically replace a diesel-based truck fleet entirely in some operations. In general, however, despite the use of electric powered equipment, trucks are still required, but truck operation is limited to a radius that is justifiable in economic and environmental terms. In addition, by bringing electrical power closer to the face through the implementation of CME, the excavation process, which may still be diesel-based in the conventional baseline, can likely be electrified as well.

In summary, CME/IPCC technology, which has proven to be more economic not only in RWE mines, is also more environmentally friendly (Heiertz, 2016). The advantages are most obvious when:

- the movement of large masses is required
- a vertical transport component (lift) is significant
- the lifetime of the operation justifies the corresponding investment
- the source of electric power has a renewable component.

Since RWE is an energy utility using all sources of energy (lignite, hard coal, nuclear, gas, hydro, biomass, wind, solar, hydrogen) as well as a mine owner and the operator of the largest and most efficient CME system worldwide, RWE has developed a general GHG emissions calculator for order-of-magnitude comparisons, which is presented here.

Substituting diesel-powered truck fleets with CME equipment driven by renewable-based electricity will have further positive side effects such as

- a high degree of automation
- reduction in dust emissions
- lower water consumption
- a reduced exposure to (future) carbon taxes.

GHG EMISSION CALCULATIONS

General assumptions

Figure 5 depicts a typical opencast strip mine with different mining systems, a four-bench system and ex-pit as well as in-pit dumping of waste. On the first bench the typically unconsolidated or weathered overburden material is mined by a bucket wheel excavator. On the second bench the semi-hard material is blasted and loaded by a diesel or electric shovel onto an FMC system. The

third bench material is directly dumped (with a certain amount of rehandle) by a dragline. The coal is extracted conventionally from the fourth bench by TEx. The mine uses two belt conveyor systems: Waste from the first bench is transported to an ex-pit dump spreader. Waste from second bench is used to refill the mine with an in-pit spreader. This model set-up has been used in RWE's carbon emission estimation tool for this paper.

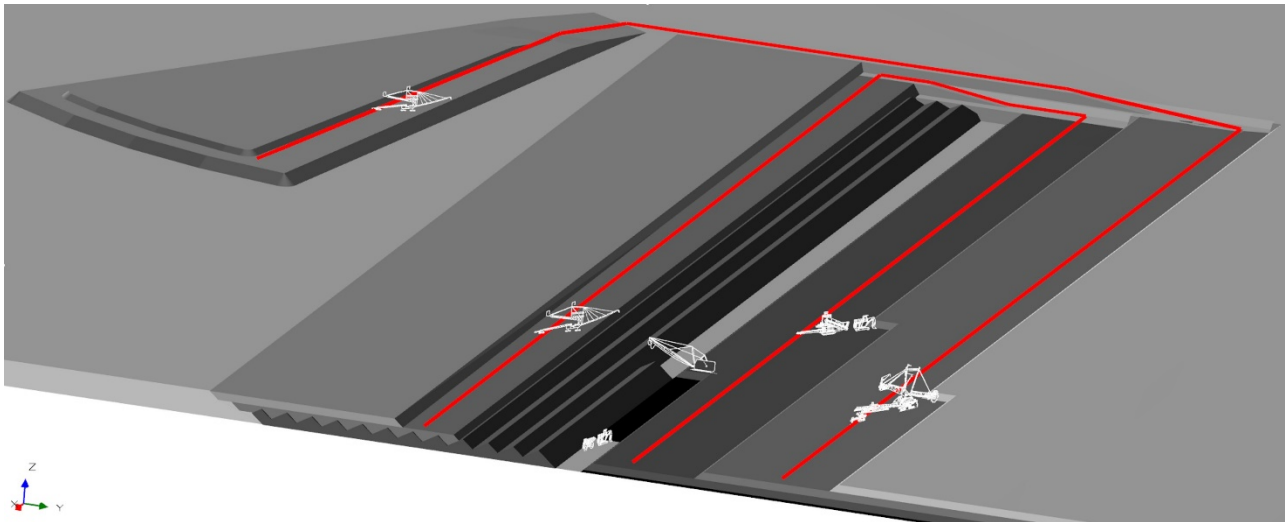


FIG 5 – A typical opencast strip mine with different mining systems.

Figure 6 shows the cross-section of this typical opencast strip mine. The first example discussed in this paper is a conventional TEx operation on the second bench (behind a drilling and blasting strip) compared to a fully-mobile crushing plant, which is also connected via an ATP conveying system to an in-pit spreader on the second bench on the dump side. The carbon emission estimation tool uses a typical material haulage profile – without truck bridges – and is not based on specific mine planning efforts. Auxiliary equipment is considered as percentage of digging/trucking hours. The GHG emissions as well as the corresponding capital and operational costs are estimated in order to compare different systems and set-ups.



FIG 6 – Cross-section of a typical opencast strip mine with different mining systems.

The following general assumptions for the GHG emission calculations were used for the comparison of TEx with an equivalent conveyor-based IPCC system for waste:

- Typical opencast strip mine.
- Truck/Excavator (TEx) base case:
 - 800 t hydraulic excavator (diesel powered)
 - 360 t ultra-class truck (diesel powered)
 - corresponding auxiliary equipment.
- Base case versus two IPCC alternate options:
 - Bench-wise comparison of CME applications
 - Waste: second bench face excavation – horizontal around pit conveying system – in-pit dump (diesel powered excavator)

- Waste: first bench excavation face – out of the pit conveying system – ex-pit dump (electric powered BWE)
- both: conveying routes similar to trucking routes.
- Energy mix of power supply: 1/3 coal + 1/3 gas + 1/3 renewables.

All inputs are variables and can be changed by manual input or drop down menus. Figure 7 shows a sample input parameter selection for the GHG emission calculation.

Project Lifetime	20	yr	Lifecycle GHG Emissions	
Densities			Fuel powered equipment	
Weathered	2.10	t/bcm	Diesel	3.331 kg _{CO2} /l
Waste	2.40	t/bcm	e-powered equipment	
Coal	1.45	t/bcm	Energy Mix	0.432 kg _{CO2} /kWh
			(33% coal, 33% gas, 33% renewables)	
Shift Regime			Haulage System (OB)	
Mine operating time	8,760	h/yr	Excavation bench (strip) length	4.0 km
Labour work hours	1,885	h _{work} /yr	Cross-pit haulage distance	1.5 km
Number of labour to fill job	4.65		Dump bench length	4.0 km
Labour Costs			> Truck haulage distance (base case)	5.5 km (one way)
Operator	110	USD/h	Truck haulage lift, avg.	22.5 m
Maintainer	120	USD/h	> Conveyor system length	5.5 - 9.5 km*
			Conveyor haulage lift	30 M
				* depending on option
Consumable Prices			Haulage System (ROM Coal)	
Diesel	0.85	USD/l	> Truck haulage distance (base case)	2.75 km (one way)
e-Power	0.085	USD/kWh	Truck haulage lift, avg.	150 m
GHG Impost			> Conveyor system length	1.85 km
CO ₂ tax/certificate	50.00	USD/t _{CO2}	Conveyor haulage lift, avg.	150 m

FIG 7 – General assumptions for GHG emission calculations.

Results for horizontal IPCC application

The bar charts in Figure 8 show the calculation results of the TEx baseline versus a conveyor-based IPCC system. A fully mobile crushing (FMC) unit is used, if BWE deployment is generally not feasible due to the limit unconfined compressive strength (UCS) of the digging material. The main findings are:

- The capital expenditure for implementing an IPCC system is higher than the initial CAPEX for a comparable TEx fleet. However, over a period of 20 years, total CAPEX is more or less the same (-2 per cent) due to higher relative re-investment costs for the conventional option.
- Initial and overall OPEX of the IPCC system is significantly (in this case: 41 per cent) lower than that of the compared TEx system.
- Taking into account the above-mentioned energy mix for the electricity used for the IPCC system, the GHG emissions are 34 per cent lower than the TEx baseline emissions.

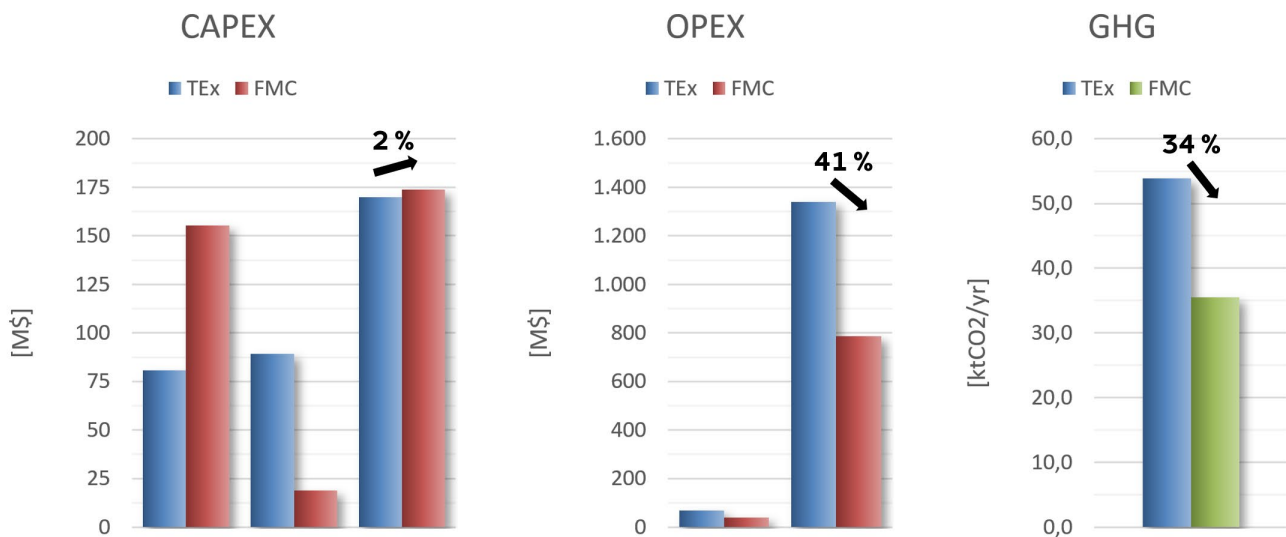


FIG 8 – Calculation results of TEx versus IPCC system with FMC.

Results for IPCC application with a substantial vertical lift component

The bar charts in Figure 9 show the calculation results of the TEx baseline versus a conveyor-based BWE system for the second example. The BWE mines and loads the waste onto the shiftable conveyor. The material is dumped on top of an ex-pit dump, which adds a substantial vertical lift component to this calculation. The main findings are:

- The capital expenditure for implementing an IPCC system is again higher than the initial CAPEX for a comparable TEx fleet. However, over a period of 20 years, total CAPEX is considerably lower (16 per cent) than that of a TEx system due to the much lower re-investment costs for the IPCC option.
- Initial and overall OPEX of the IPCC system is significantly (60 per cent) lower than that of the compared TEx system.
- Taking into account the above-mentioned energy mix for the electricity used for the IPCC system, the GHG emissions are 61 per cent lower than the TEx baseline emissions.



FIG 9 – Calculation results of TEx versus BWE system.

This clearly shows the advantages of a BWE or IPCC system for waste handling with a relatively high vertical transport component and a long transport distance. In general, applications can be modelled for any type of opencast mine and haulage profile. For example, steep angle conveying may be an attractive option for hard rock mines that could be worthwhile investigating with the RWE GHG calculator.

Limitations

The results of the GHG emissions calculation presented here have the following limitations:

- The energy mix used in the model is mainly based on conventional energy sources (2/3). As the contribution of renewables in the energy mix will increase substantially in the short to medium term, the GHG difference will increase to the benefit of the electrically powered equipment.
- The assumed diesel-powered hydraulic excavator used in the TEx baseline and IPCC alternative could be electrified (eg R 9800E) if power for the FMC system is supplied close to the face.
- The sample calculations in this paper only consider one bench of an opencast mine.
- Only direct costs are considered, no indirect or ownership costs.
- The estimations of CAPEX and OPEX are based on a pure cost model. No cost escalations over time nor interest rates as used in financial modelling are applied.
- Potential carbon taxation costs are not considered in this example.

CONCLUSION AND OUTLOOK

In conclusion, the answer to the initial question ‘Is CME, incl. IPCC, a sustainable GHG emissions-reducing alternative to conventional TEx technology?’ is definitely a ‘YES’ for a large number of mines worldwide. The inherent better energy efficiency of continuous mining systems has been described. In view of the operating and maintenance experience gathered by RWE thanks to the long-term successful use of CME systems in its own completely electrified mines, this technology should be transferred to other mines and commodities. The individual situation could be thoroughly investigated, eg with the presented tool.

The application examples show that GHG emission reductions can be accompanied by significant savings in OPEX that will eventually more than offset the initially higher CAPEX over 10+ years. The greater the rise in the haulage profile, the greater the potential for GHG emission reductions. The integration of any available renewable energy sources also plays a significant role in the site specific electrification of the mine.

Substituting diesel-powered fleets with CME equipment driven by renewable-based electricity will have further positive side effects such as a high degree of automation, reduction in dust emissions and water consumption, and a reduced exposure to (future) carbon taxes, which need to be quantified in further studies.

ACKNOWLEDGEMENTS

The authors thank the THIESS-RWE JV, Australia as well as RWE Power AG, Germany for their contribution of knowhow and actual mining data for TEx, CME and IPCC systems.

REFERENCES

- Blunck, S, 2021. Continuous Mining – Opportunities for more sustainable mining. In *Proceedings of Eco Mining Concepts Webinar*, Santiago de Chile, Chile 2021.
- Blunck, S, Langmaid, M, 2016. THIESS-RWE JV cooperation presentation. Brisbane, Australia 2016.
- Blunck, S and Schmitz, R, 2012. Determination of performance and utilization of IPCC systems – the key role of the belt conveyors. In *Proceedings of IPCC Conference*, Bali, Indonesia 2012.
- Heiertz, A-J, 2021. IPCC for greener mining: RWETI The carbon footprint reduction experts. *International Mining (IM)* 05/2021 p. 40f.
- Heiertz, A-J, 2016. Emission control optimization in the resource industry. In *Proceedings of ISCSM 13th International Symposium Continuous Surface Mining*, Belgrade, Serbia 2016.
- Heiertz, A-J, 2014. Investigations to apply continuous mining equipment in a shovel and truck coal operation in Australia. In *Proceedings ISCSM 12th International Symposium Continuous Surface Mining*, Aachen, Germany, 2014.
- Heiertz, A-J, Schmitz, R and Durchholz, R, 2014. Change Challenges for Large Open Pit Mines. In *Proceedings 8th AusIMM Open Pit Operators Conference* (The Australasian Institute of Mining and Metallurgy: Melbourne).

- Naghshi, S, (not published). *Comparison of mining systems with a special focus on energy efficiency*. Master thesis, Technical University Bergakademie Freiberg, not published.
- Schmid, M and Tappeiner, S, 2014. In-pit Crushing and Conveying (IPCC) – Projects in Chilean copper-mining operations as exemplified by the Los Pelambres opencast mine. *World of Mining. Surface & Underground* 66 (2014) No. 5, pp. 310–315.
- Schmitz, R M, Franken, H and Blunck, S, 2010. An empirical relationship to determine the performance of bucketwheel excavator, bench conveyor and spreader systems verified with data from the Rhenish lignite mining district. *Extracting the Science, a century of mining research* (Society for Mining, Metallurgy & Exploration Inc (SME): Littleton, Colorado).
- Wolff, J, Boyan, J and Blunck, S, 2013. RWE – Leading in Operation & Maintenance of Continuous Mass Mining Equipment. In *Proceedings of IPCC Conference*, Cologne, Germany 2013.

Do we have enough copper to decarbonise society? An overview of resources/production from porphyry ores/E-wastes

C B Tabelin¹, I Park², T Phengsaart³, S Jeon⁴, M Villacorte-Tabelin⁵, D Alonzo⁶, K Yoo⁷, M Ito⁸ and N Hiroyoshi⁹

1. Lecturer, UNSW Sydney, Sydney 2052 NSW. Email: c.tabelin@unsw.edu.au
2. Assistant Professor, Hokkaido University, Sapporo, Japan. Email: i-park@eng.hokudai.ac.jp
3. Lecturer, Chulalongkorn University, Bangkok, Thailand. Email: theerayut.p@chula.ac.th
4. Assistant Professor, Hokkaido University, Sapporo, Japan.
Email: shjun1121@eng.hokudai.ac.jp
5. Professor, MSU-IIT, Iligan City, Philippines. Email: mylah.tabelin@g.msuiit.edu.ph
6. Lecturer, UNSW Sydney, Sydney 2052 NSW. Email: d.alonzo@unsw.edu.au
7. Professor, Korea Maritime and Ocean University, Busan, South Korea.
Email: kyoo@kmou.ac.kr
8. Associate Professor, Hokkaido University, Sapporo, Japan. Email: itomayu@eng.hokudai.ac.jp
9. Professor, Hokkaido University, Sapporo, Japan. Email: hiroyosi@eng.hokudai.ac.jp

INTRODUCTION

Decarbonising society – envisioned in UN-SDG #13 ‘Climate Action’ – aims to rapidly reduce carbon dioxide (CO₂) emissions to combat climate change and achieve a carbon-neutral society by 2050. Decarbonisation of two of the largest CO₂ emitting sectors – electric power/heat generation and transportation – requires changing fossil fuels with clean storage and renewable energy technologies. Unfortunately, low-carbon technologies are more material, mineral and metal intensive than conventional fossil fuel technologies. A typical 3 MW wind turbine, for example, requires 4.7 t of copper, 2 t of rare earth elements (REEs) and 3 t of aluminium while electric vehicles (EVs) needs 1.7 to 11 times more copper than conventional cars aside from nickel, cobalt and lithium for their rechargeable batteries (Tabelin *et al*, 2021).

Because of this, the World Bank identified copper as one of the 17 critical metals/materials necessary for decarbonisation strategies to succeed. Copper is essential in at least eight clean storage and renewable energy technologies and by 2050, the demand for this metal is forecasted to increase to ~29 Mt from 2019 values of ~20 Mt assuming the 2-degree scenario (2DS). To put this increase in demand into perspective, ~550 Mt of copper has been produced for the last 5000 years and this amount is needed in the next 25 years.

GLOBAL COPPER AVAILABILITY

Two of the most important copper-bearing materials on the planet are copper ores and E-wastes. The global copper reserve from ores stands at 870 Mt (USGS, 2020), more than 75 per cent of which is found in only 11 countries – Chile (23 per cent), Australia (10.2 per cent), Peru (10 per cent), Russia (7 per cent), Mexico (6.1 per cent), USA (5.9 per cent), Indonesia (3.2 per cent), China (3 per cent), Kazakhstan (2.3 per cent), Zambia (2.2 per cent) and the Democratic Republic of Congo (2.2 per cent). Among the 10 types of copper-bearing deposits, porphyry copper ores are economically the most important because they are widely distributed and contain >1000 Mt of ore at >0.5 per cent copper. ~60 per cent of global copper production comes from these deposits and as of January 2020, 14 of the top 20 largest operating copper mines in the world are exploiting porphyry copper deposits (Tabelin *et al*, 2021).

Meanwhile, E-waste(s) is the fastest-growing copper-bearing waste but with the lowest recycling rates. Printed circuit boards (PCBs) in E-wastes, for example, contain ~20 per cent copper that is 40-fold higher than porphyry ores. In 2019, 53.6 Mt were generated globally, an increase of 9.2 Mt in just five years, and the global E-waste generation is projected to reached 74.7 Mt by 2030 and 243 Mt by 2050 (Forti *et al*, 2020).

Because copper ores are finite resources, they will be depleted rapidly without efficient recycling strategies. Several future copper supply scenarios were formulated using mass balance, reported global recycling rates and current resources estimates, and the results are shown in Figure 1. At the

current EoL recycling rate of 43 per cent and assuming a 29 Mt copper/annum consumption, the 2020 copper reserve of 870 Mt will be depleted in just 53 years. If a 90 per cent recycling rate scenario is assumed, the 2020 copper reserve will be available for the next 300 years.

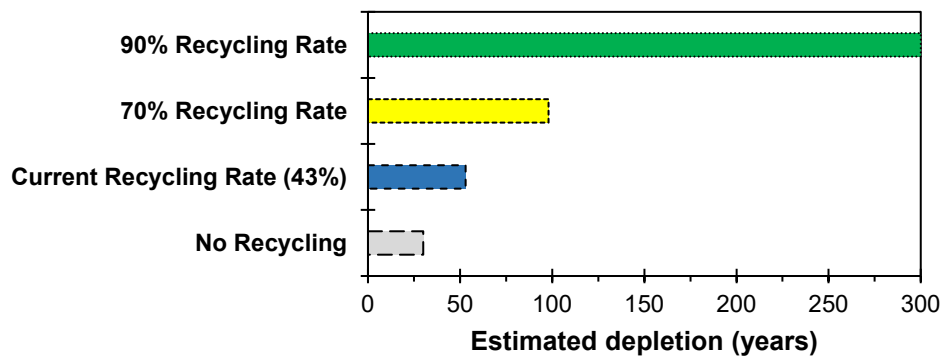


FIG 1 – Projected copper resource depletion time based on various recycling scenarios (Resource depletion (years) = current metal reserve (kt)/[metal consumption (kt/annum) – recycled metal (kt/annum)]).

CHALLENGES AND OUTLOOK

Stable copper supply for the clean energy transition is facing multiple challenges. Many major operating copper mines will close down in 10–20 years due to ore depletion while the majority of untapped porphyry deposits are located in low- to middle-income countries where access is challenging due to complex socio-political dynamics (Tabelin *et al*, 2021). For example, negotiations with the traditional landowners for the US\$5.9 B Tampakan Project in the Philippines took ~10 years to complete, but mine development has stalled due to an open pit mining ban imposed by the local government. As low-grade copper ores become the norm, processing/extraction challenges due to ore complexity, arsenic-rich/‘dirty’ concentrates and loss of fine (<10 µm) copper-bearing minerals to tailings will become commonplace. Improved/novel processing technologies have been proposed to address these issues including pre-treatment/direct leaching of ‘dirty’ concentrates and agglomeration-flotation.

Meanwhile, increasing E-waste collection efficiency is critical for recycling programs to succeed because only those properly tagged are collected and processed. Governments can improve E-wastes collection and recycling rates bypassing legislations that penalise their disposal together with municipal solid wastes as well as educating the public on proper waste segregation at home. Finally, E-waste recycling using existing smelter facilities is efficient, but this approach is difficult to implement in low – and middle-income countries because of economic and specialised know-how constraints, so alternative, less costly and more environmentally friendly strategies need to be developed.

REFERENCES

- Forti, V, Baldé, C P, Kuehr, R and Bel, G, 2020. The Global E-waste Monitor 2020: Quantities, flows and the circular economy potential. United Nations University (UNU)/United Nations Institute for Training and Research (UNITAR) – co-hosted SCYCLE Programme, International Telecommunication Union (ITU) and International Solid Waste Association (ISWA), Bonn/Geneva/Rotterdam.
- Tabelin, C B, Park, I, Phengsaart, T, Jeon, S, Villacorte-Tabelin, M, Alonzo, D, Yoo, K, Ito, M and Hiroyoshi, N, 2021. Copper and critical metals production from porphyry ores and E-wastes: A review of resource availability, processing/recycling challenges, socio-environmental aspects, and sustainability issues. *Resources, Conservation and Recycling* 170, 105610.
- USGS, 2020. Mineral commodity summaries 2020: US Geological Survey, 200 p, <https://doi.org/10.3133/mcs2020>

Future skills

Mine training for future skills

S Bowes¹

1. Managing Director, Edge Learning Services, West Perth WA 6005.

Email: sally.bowes@edgelearning.com.au

ABSTRACT

Future skills shortages are the most critical risk to the mining industry. Transfer of the knowledge and skills required for future positions will be a key factor in maintaining the success of the industry. Currently, mine training is largely failing to keep pace with the advances in technology and automation in the industry and has not addressed the changing learning styles of new generations entering the workforce.

Mine training has advanced significantly over the past two decades as safety and compliance requirements have increased and the cost of equipment, and therefore the cost of damage to equipment has risen substantially. In the past, the majority of mining companies did not have training departments and training activities and records were haphazard. While this has improved significantly, mainly due to compliance requirements, there are still many areas that require improvement in order to avoid future skills shortages.

This paper discussed the advances in mine training and the current state of mine training. Training activities and their effectiveness are discussed, particularly as they relate to new technologies. The paper covers advances in learning technologies and identifies some learning technologies in use and their advantages and disadvantages. It also outlines the requirements for the mining industry to take advantage and use these technologies effectively.

The paper discusses the changing demographics of the workforce and the changes in the nature of future skills that will be required to address new challenges in the mining industry. Training personnel and their required qualifications are discussed, including the structure of training departments, the qualification required by training personnel and how the arrival of future technologies will change the qualifications and knowledge required by training personnel.

The paper also briefly identifies some future training possibilities and how training will be integrated with continuous improvement and maintenance of standards to improve safety and production, not only for the trainee, but for workers with all levels of experience in the industry.

INTRODUCTION

In order to effectively deploy learning and development activities to support future skills, it is critical that mine training departments develop and effectively implement an overall strategy, apply necessary standards and allocate resources correctly. Training departments must be involved in planning for future adoption of technologies from the earliest stages and there must be processes in place requiring suppliers to work with training departments to develop or supply training for new equipment and technologies well before products are delivered. Training personnel must be upskilled in the identification and implementation of effective learning technologies that support the learning for the new technologies.

TRAINING ACTIVITIES

The most effective training activities are those that bring the trainee as close as possible to the real experience of work, without exposure to harm or risk of damage. Advances in technology have introduced new training methods that immerse the trainee into a simulated working environment. Where new technologies are introduced, simulation is particularly effective at preparing trainees for the real work environment. Examples of this are machine simulators, such as trucks and drills and system simulators. Research indicates that the use of machine simulators reduces the mean time for inexperienced operator training by 43 per cent and overall cost per tonne of mining by between 5 per cent and 7.5 per cent (Immersive Technologies, 2021). System simulators allow the trainee to operate a system in a 'sandbox' environment where they can experience the consequences of their actions without causing real damage. Examples are dummy mine control and mill control systems.

As new technologies emerge in the training space, organisations must ensure that training activities are an integrated part of a planned strategy to achieve outcomes, and not just the latest, most eye-catching trend. Where learning technologies are considered, the learning must always be considered before the technology. There are many examples of virtual and augmented reality training activities that require the trainee to spend most of their time and effort mastering the controls rather than actually carrying out the virtual task. The same task can often be practiced just as effectively using a dummy model. Examples of this include connecting distribution boards, applying CPR, and wiring in explosives.

There are more types of training activities available than ever before. Training activities must always be chosen by considering how close they bring the trainee to the actual experience of work. Sitting a trainee in a room to read a manual that is hundreds of pages long does not come anywhere near close to the experience of operating a piece of heavy machinery. But neither does giving a trainee a computer and asking them to master fifteen different keyboard shortcuts to operate a virtual crane on the screen. Cost constraints always have to be considered but a training activity that does not achieve the desired outcome is worthless, no matter how much it costs.

ATTRACTING FUTURE PERSONNEL

As retirements are delayed, and the younger workforce becomes more mobile, training must be adapted for a multi-generational, multi-cultural workforce. A one size fits all approach to training is no longer effective, if it ever was. Training must become more learner centred, more adaptable and more relevant.

A report for the Intergovernmental Forum on Mining, Mineral, Metals and Sustainable Development states that 'New technologies have uncovered a deeper challenge of skills gap and the skills mismatch, underlined by the fact that current workers' qualifications are not necessarily the ones needed for the new jobs' (Hoteit *et al*, 2020). There is a critical need to change the entrenched reputation of the mining industry as poor environmental stewards and unethical operators in order to attract younger workers who can manage these new technologies. It is almost ironic that the mining industry will be competing with big tech firms for the best people to drive industry progress. Investment in training and development opportunities is vital to attract these people.

TRAINING PERSONNEL

Trainers are often former operators who have taken training roles which only require a Certificate IV in Training and Assessment. This is manifestly inadequate and gives little to no instruction on adult learning principles, managing people or planning, all of which are required to be an effective trainer. Significantly more effort needs to be made in ensuring that the right trainers are recruited and equipped with the right skills, knowledge and resources to effectively build capability within the organisation.

Currently, training personnel often report to site management or site department management. While this makes geographical sense, it also results in inconsistencies, duplication of effort, major gaps and makes it impossible to apply a core strategy and direction to training planning, development, delivery and measurement. Training personnel also often take on split roles such as safety and training or training and operations. Operator mentors are a great asset to a training team (as long as they are correctly identified and trained in basic adult learning principles), but combining roles such as safety and training is bad practice for all but the smallest operation. While it is true that there is some overlap between safety and training, there is also some overlap between geology and engineering, yet it would be extremely difficult to find one role with those disciplines combined.

New learning technologies will assist training personnel, but only if they understand how to recognise which technologies will add value to their learning. In 2006 at an international Virtual Reality in Mining conference, it was recognised that 'Current mine safety and health instructors have varying levels of interest in, understanding of, and facility with the new technologies' (Mallet and Jenkins, 2006). Fifteen years later, there are still limited resources for training personnel to assist them to manage and utilise learning technologies effectively. Companies must make a significant commitment in their investment in all areas of their training, particularly in the skills of their training personnel to upskill them for the new challenges that are approaching.

PATHWAYS

Pathways for development are vital to ensure that learning activities effectively meet the needs of the organisation by developing and maintaining a workforce with the right skills for the right jobs at the right time. As new technologies are introduced into the mining industry, this becomes even more critical. Skill gaps, more than ever, will have the potential to stop production. A 2017 study (Institute for the Future and Dell Technologies, 2017) suggests that 85 per cent of the jobs of 2030 have not yet been invented.

Autonomous fleets are a good example of this. The World Economic Forum projects that automation and robotics could prevent 10 000 injuries in the mining and metals industries in the decade to 2025 (WEF, 2017) and productivity improvements of between 15 per cent and 30 per cent are currently being reported from autonomous haulage (Accenture, 2020). While autonomous machines reduce the need for machine operators, maintenance departments will need a completely new and different skill set to keep the fleet operational. Well planned and resourced pathways, developed in line with future mine plans, will allow training departments, and organisations, to pivot quickly and ensure the necessary skills are available when they are required.

MEASUREMENT

Measurement is critical to the success of all training. If the effectiveness of the training activity is being measured, productivity trends can be identified. Targeted, meaningful improvements are then possible. For example, if the productivity rates of truck operators in their first twelve months on-site are monitored in Tonne Kilometres per Hour (TKPH), the effectiveness, or ineffectiveness, of any changes to training activities are easily identified. Different sections of the workforce can also be monitored to identify areas where training may require adjustment. Indigenous trainees' productivity rates can be compared to non-indigenous trainee rates to check if adjustments to training activities are more or less beneficial. Training methods can then be adjusted to suit. It is also vital to assess the Return on Investment (ROI) of training activities to determine the most cost – effective solutions.

THE FUTURE

So what can the future of mine training look like? Imagine if training could be seamlessly incorporated into work and used for continuous improvement of work tasks and maintenance of standards as well as training. A mechanic with glasses that will show an augmented reality overview of the inner workings of a pump as she looks at it and guide her through the process of fault finding and repair. A grader operator who watches a heads up display of the feed from a camera on the blade and compares that to a best practice example. An underground operator who reviews a video taken from a camera on his helmet and played back through his cap lamp light showing him performing scaling a minute earlier.

Today, more than any time in history, we live in a world where anything is possible. The potential is almost limitless. But we have to be ready. And currently, we have a long way to go to get there.

CONCLUSION

Mining industry training has made significant advances in some areas over the last few decades but there are still some major gaps. It is critical that these are addressed thoughtfully and holistically to ensure that the future workforce is safe, productive and engaged and we are positioned to take advantage of the advances in training and operations that are coming.

REFERENCES

- Accenture, 2020. Mined Over Matter: The Not Too Distant Future of Autonomous Operations [online], Available from: https://www.accenture.com/_acnmedia/PDF-120/Accenture-Autonomous-Operations-Mining-Report.pdf#zoom=40
- Hoteit, L, Perapechka, S, El Hachem, M and Stepanenko, A, 2020. Alleviating the heavy toll of the global skills mismatch [online]. Available from: <https://www.bcg.com/publications/2020/alleviating-the-heavy-toll-of-the-global-skills-mismatch>
- Immersive Technologies, 2021. Cost per Ton [online]. Available from <https://www.immersivetechologies.com/solutions/cost-per-ton.htm>

- Institute for the Future and Dell Technologies, 2017. Emerging Technologies Impact on Society and Work in 2030 [online], Available from:
https://www.delltechnologies.com/content/dam/delltechnologies/assets/perspectives/2030/pdf/SR1940_IFFforDeIITechnologies_Human-Machine_070517_readerhigh-res.pdf
- Mallet, L G and Jenkins, T W, 2006. Virtual Reality in Mine Training, [online], Available from
<https://www.cdc.gov/niosh/mining/userfiles/works/pdfs/vrimt.pdf>
- World Economic Forum (WEF), 2017. Digital transformation initiative: Mining and Metals industry (White Paper). World Economic Forum, Geneva, p 36.

Aligning competency orientated work integrated learning models for mining engineers and mine surveyors

H C Grobler¹

1. Head of Department, University of Johannesburg, Gauteng, South Africa.
Email: hgrobler@uj.ac.za

ABSTRACT

Work Integrated Learning (WIL) is recognised in the revised Higher Education Qualification Sub Framework (HEQSF) published in 2013 as a credit bearing learning activity. A counter argument postulates that WIL is orientated to developing already learned theory in a practical environment and develops 'soft-skills' that should not bear credit. In response to the Higher Education Qualification framework of 2007, some institutions moved their focus away from including WIL in their academic programs. The 360 credit National Diploma programs was arguably impacted the most by the HEQF requirement that the institution would be responsible to find placement for WIL for all students registered in such a program. This paper defines three stages of WIL on the way to professional registration and argues that it is important that government, industry, academia and Professional bodies re-evaluate how the various stages of WIL can lead to a competency based evaluation of professionals prior to being allowed to complete Government Certificate of Competency examinations. The programs developed by mining companies to assist their bursars and Graduates in Training (GIT) through these three stages of experiential learning are discussed and used to propose a model that may improve the throughput in the final Government Certificate of Competency (GCC) examinations. It is unfortunately becoming increasingly rare that a student would be exposed to all three phases of experiential learning due to the current fluctuations in the South African mining industry. The author argues that WIL is an essential part of developing professional competency and should bear credit. The integration of these three forms of experiential learning would enable a sustainable model of development of future professionals.

INTRODUCTION

The various guidelines that exist in industry and professional organisations for Experiential learning was developed to introduce recent graduates to the workplace. Despite these programs there is sometimes a disconnect between the graduate expectations and that of the employer (SAIMM, 2015). In the rapidly changing technological environment, the desirable characteristics to be developed in graduates have changed fundamentally (Erol *et al*, 2016). In the formalised corporate environment of large multi-national corporates, graduates are more likely to be exposed to a more well-rounded introduction. On the opposite side of the spectrum however, a graduate employed in a small company may not be able to receive similar exposure and be expected to immediately take on the responsibilities expected from an experienced person.

This paper explores the development of graduates through three phases of experiential learning and argues for the need of graduate in training or 'second stage qualifications' within the current education environment that has in part been created through the reduction of work integrated learning in some university programs.

Through the analysis of common denominators used in various professional documents, Grobler defined competency as '*The ability by virtue of Education, Skills, Knowledge and Experience to identify potential hazards and deal with situations successfully*' (Grobler, 2016a). Dale's 'cone of experience' describes how people are able to define, list and explain based on reading and hearing information whereas people who participate in hands-on workshops, simulated experiences or performing the real action are able to analyse, design and evaluate while retaining up to 90 per cent of what they have done (Jason, 2016; Davis and Summers, 2016).

In order to develop a better understanding of how WIL facilitates the assimilation of theoretical knowledge into professional competence through experience, an analysis of the stages of WIL as they currently exist will be discussed. The changing needs of industry tempered by the constraints

of the socio-economic climate in which mining companies operate is considered in the development of a proposed model of experiential learning.

Commentators on Industry 4.0 predict that workers will increasingly focus on predictive, analytical and cross-disciplinary interaction requiring high levels of competency in communication skills (Erol *et al*, 2016) while leaving the dirty, boring and dangerous jobs to automated processes and equipment. Erol *et al* identified several personal-, social, action – and domain related competencies that will be required by professionals and workers alike in this environment. The main personal competency identified is the idea of flexibility regarding personal development, time management, workplace and work content. In the social competency environment, the ability to operate in a broader scope that requires the ‘building and maintaining of networks’ that can communicate complex challenges efficiently. The ability to integrate concept and more importantly, act based on the analysis of the information that has been obtained. Finally, the understanding of the workflow, domain specific language and tools are essential to evaluate the efficiency and interrelation between systems (Erol *et al*, 2016). It is therefore possible to see how these personal and interpersonal skills, when developed in the correct manner will lead to competencies that is required of the professionals of the future. The context of current WIL practices is evaluated within this framework.

Three phases of experiential learning

In the context of this paper three distinct stages of work integrated learning, could be identified. These stages are:

1. Work exposure prior to under-graduate training such as the no-longer used ‘learner official program’ or the ‘cadet program’ used by Lonmin. For the fortunate individual that was identified at school or directly thereafter and given an opportunity to join a mining company this stage of learning is of great benefit throughout the individual’s career.
2. Formal work integrated learning during undergraduate studies, managed by the educational institutions. WIL learning is formalised in the National Diploma programs within the mining related study fields. Due to the change in strategy in response to the HEQF of 2007 a significant number of these qualifications are now being phased out and replaced by three-year degree qualifications. The continuing argument for the recognition of the credit bearing aspect of WIL by the various professional bodies.
3. Graduate Development Programs for second stage qualifications. This stage is regulated mostly by the companies that employ recently graduated bursars. At the same time, professional bodies and government, require a minimum of three years of work experience before being allowed to register professionally. It is evident that there is a disconnect between the deliverables expected by the graduate, the employer and the professional bodies at this stage. Companies and disciplines that manages this critical stage well benefit from higher employee retention rates and improve the throughput rates in the Government Certificate of Competency examinations.

Work exposure prior to formal under-graduate education

Most persons entering the mining industry during the late 1970s and 1980s would be familiar with the Learner Official (LO) program. Individual mining companies developed this program to transition school leavers into the mining industry and included courses on basic surveying, first aid and other related topics. The introductory period which normally lasted around 12 months, enabled mining companies to identify persons that would be suitable for a Chamber of Mines (COM), Diploma or Degree routes of qualification. The LO model of industry exposure fell out of favour in the late 1990s.

Approximately a decade ago, Lonmin platinum mines developed a structured Mine Technical Services (MTS) program to develop a sustainable pipeline of potential bursary students to a structured development program to induct candidates to the specific requirements of a career in the mining industry (Visser, 2016). This program is designed to meet the mining company’s ‘Social Labour Plan deliverables’. During the first year of the program, identified ‘cadets’ are taken through basic competency and chamber of mines qualifications. During the second year of the program, cadets are exposed to and allowed to select one the various technical service departments (strata control, mine design, mine sampling, mine surveying, mine environmental or geology) as a field of

specialisation (Visser, 2016). The model bridges the knowledge of the potential pool of students in mathematics, computer – and basic reporting skills. In addition, the pre-university program introduces the potential bursary student to the corporate culture, time management and physical fitness requirements. In most of these aspects, the ‘cadet’ model mirrors that of the older Learner Official programs.

Anglo Platinum mining company provides an exposure year to students already identified for bursaries and are provided with additional mathematics and science tutoring through a third-party service provider in the year prior to registration (Roos, 2018). This approach is tailored to address to some extent the difficulty which some learners experience in the transition from the grade 12 public school education to adapting to the first year of university in modules. With the recent move in assets between Anglo Platinum and Sibanye Stillwater this model may require some revitalisation. Unfortunately, this model of additional tutoring does not address the critical industrial exposure that the Lonmin model provides for.

The major constraint of the pre-university phase of WIL is that only a limited number of students can participate in such a program. Privately funded (unencumbered) students without a bursary from a mining company will be unable to benefit from such a program. Because of these constraints, pre-university exposure is categorised as highly recommended but cannot form part of compulsory entry requirements.

Formalised WIL activities during undergraduate studies

The National Diploma qualifications all have a work integrated component of the qualification has moved from an initial ‘sandwich course’ that was in essence an after-hours academic program (Lurie, 1982) to a 50/50 model where each academic semester was followed by a full six months of practical training. That implies that a student that graduated with a National diploma from UNISA or the older National Diploma from a Technikon would have completed 18 months of academic study and 18 months of practical WIL training. It can postulated that a graduate with that much industry experience could be deemed as ‘immediately employable’ by a potential employer. In most cases such a graduate would have been a full-time employee of a mining company either as a Learner Official (LO) or as a mining – or surveying official. The original purpose of this blend of practical and academic training was to prepare mining officials for the GCC examinations. Meyer observed that a diploma course would assist persons that were unable of successfully completing the GCC examinations through self-study (Meyer, 1964).

In 2004 a new diploma model was introduced at the University of Johannesburg that replaced one semester of WIL with a semester of academic content, effectively reducing the total amount of WIL to one year. This model effectively represented a qualification composed of 240-credits of academic content (four semesters) and 120-credits of WIL (two semesters), SAQA reference number 62405 (SAQA, 2018). It is unclear if this development was in response to the argument from some quarters that WIL should not carry a credit value. It is important to note that at this point in the development of the WIL program, the diploma offered by UNISA, SAQA reference number 62405, retained the three semesters of academic content and three semesters of WIL (SAQA, 2018). Regardless of the model, both these Diplomas are categorised as 360-credit diplomas by the South African Qualification Authority (SAQA). Due to the uncertainty around credits, HEQF requirements and the overwhelming demand for a degree qualification from students, the model of a Diploma that includes WIL has been less favourable than a conventional three-year degree. The major risk identified with this strategy is that the new degree may not prepare graduates adequately for the rigours of the workplace and may be perceived as ‘not immediately employable’. The challenge of these new qualifications is to find alternative and supplementary activities which will adequately prepare the graduate to meet these expectations.

Supplementary WIL activities at the formal education level

It is accepted that theory can be learned readily enough but that mastery can only be acquired through experience (Willows-Munro, 1948), this argument is developed further by Greene who postulated that the time needed to master a particular skill depends on the ‘intensity of the focus’ of the individual (Greene, 2013). The WIL component has always been considered to be the defining factor or ‘niche’ aspect of the Mining Engineering and Mine Surveying module (Grobler, 2016b).

During the practical or experiential learning semesters, the student follows a guided exposure to the aspects of the mine value chain from safety, geology, sampling, assay, mining, surveying and metallurgical treatment. The student compiles a portfolio of evidence during these shifts spent in the various departments and the logbook is signed off by the supervisor and mentor. In the second semester, the student is expected to perform basic work in the production section of a mine and provide a signed portfolio of evidence in addition to the logbook includes a small project or investigation performed by the student. In the case of the mine surveyor, that project is in the form of a surveyed mine plan and in the case of the mining engineering student, takes the form of a small investigative project, normally on the ore flow process of the mining unit at which the semester was spent.

With the introduction of the new Bachelor of Technology degrees, most programs have adopted a strategy that includes more laboratory and workshop practical training within the formal curriculum of the program. These 'workshop practice' modules typically replicate tutorials and practical exercises that would normally have been completed by a student as part of the formal WIL modules in the old programs. Most situations can be replicated safely in a controlled environment under the supervision of a lecturer and laboratory assistants. In the case of mining and mine surveying, these workshop practice periods are divided between safety induction, theoretical refreshers on specific aspects of the work to be completed followed by practical sessions at the end of which a portfolio of evidence of completed work must be provided for a standard academic assessment. 'Soft skills' such as teamwork, team dynamics, safety awareness and project planning forms part of the competency areas that are developed during these practical sessions. These soft skills are the essential skills of interdisciplinary co-operation and communication that has been identified as essential skills in the fourth industrial revolution (Erol *et al*, 2016). Although the stress of a production mining environment cannot be replicated in every way, the students are exposed to real-life situations and are expected to manage these situations in a safe and responsible manner under the guidance of the facilitator.

Workshop practice as an integrated method of underpinning theory with practical exposure on campus. In this format the workshop practice is evaluated and assessed through continuous assessment and ensures that each individual complies with the minimum required competencies. In the new Bachelor of Engineering Technology qualification, mining engineering students are exposed to theoretical and practical aspects of each step in the mining value chain. The workshop practice module outcomes are based on the Experiential Learning 1 module of the diploma and is assessed through the portfolio work that the student presents.

For Mine Surveying students the workshop practice module includes a safety induction and practical survey work to be completed in a group under the supervision of a lecturer. The portfolio of evidence completed by each student during this module is assessed and a summative assessment mark is awarded. To develop the confidence and competency of students, each semester has a workshop practice module that builds on the previous module. Should a student not be successful in one of the workshop modules, the module must be repeated in the next academic cycle.

In the first term of the first year, all students in the mining study fields are taken on one or more mine site visits to familiarise them to a certain extent to the rigours of an actual mining operation. These visits are supplemented in the second and third year by further supervised and facilitated mine visits conducted during the university recess periods. Students are expected to complete daily reports and report on the experience at the conclusion of the tour.

Vacation work during academic recess periods is highly recommended and supported by Universities and employers alike, but this assumes that placement can be found for all students and the reality is that this is not always possible. The bursary student will be able to complete this through its sponsoring company but would place 'un-encumbered' students at a distinct disadvantage unless sponsored through the Mines Qualification Authority (MQA) or any similar incentive. Sadly, placement of 'un-encumbered' or 'non-bursary' students are becoming increasingly difficult to find as mining companies are averse to 'create expectations of permanent employment'.

The next step in WIL training experience that should be considered is the use of Virtual-, Mixed – or Augmented Reality experiences (Chmelina, 2010). Using these technologies, students and teachers can be immersed in varying levels of simulation into a realistic mining environment augmented with additional information supplied to the user during the experience that can 'produce compelling

results' (Jason, 2016). Mischo and Bruno describes the effective use of virtual reality training for student mine rescue teams to prepare the teams for the final phases of practical training (Mischo and Brune, 2017). In the South African context, a Virtual reality blast wall has been adopted by a number of mining companies in their training facilities and is claimed to merge practical and theoretical training that accelerates the learning experience (Bouwer, 2018).

Second level qualifications after under-graduate studies

The SAIMM and ECSA report on GDP recommends that the graduate be registered as a candidate with the professional body soon after graduation. The DMR requires a candidate to submit proof of three years of experience after graduation in profession specific activities. This view is supported by the Engineering Council of South Africa (SAGC) and the South African Geomatics Council (SAGC) that requires evidence of a minimum of three years of work experience (SAIMM, 2015) under the supervision of a registered person before being able to become eligible for professional registration. The differences in approach between the Mine Manager, Mine Engineer and Mine Surveyor portfolios of evidence are discussed and a comparison with a mining company's Graduate in Training program made.

The Mine Engineers (Mechanical or Electrical) Certificate of Competency (MEGCC) appears to be the most developed program between the three qualifications. An Engineer in Training (EIT) is required to complete a detailed portfolio of evidence as detailed in 'Annexure E' that includes amongst others, evidence of shifts on winding engines, lifting equipment, chairlifts, compressed air, material handling, environmental engineering, fluid handling and minerals processing plants. The documentation required by the board of examiners indicates that all shifts must be signed off by a mentor and certificated engineer (DMR, 2018a) and submitted with the application of the candidate.

The entry requirements to the Mine Managers Certificate of Competency (MMGCC) examinations requires a candidate to be 23 years old and provide evidence through a record of service of at least 500 shifts of mining specific experience of which '*6 months on the face*', which is assumed to imply six months of actual production mining (drilling and blasting) experience. The record of service requires a portfolio of evidence that provides evidence of specific aspects of experience such as the transport of explosives, support of a working place, blasting and transport of ore with rolling stock. In addition to these fundamental performance areas, the candidate is required to furnish proof of '*performing the duties of a Miner in a development face...*', taking environmental measurements and having been '*legally appointed*' as a miner and shift supervisor. For both the Mine Overseer (MO) and Mine Manager certificates, proof of time spent in the '*survey, sampling, geology, rock engineering and ventilation*' departments must be provided (DMR, 2018b).

The requirements of candidates to the Mine Surveyor Government Certificate of Competency (MSGCC) examinations stipulates '*...at least three years practical experience in mine surveying acceptable to the commission, provided that one year has been in the underground workings of a mine...*' (DMR, 2018c). The specific detail of the experience is not defined other than the evidence for one year of underground shifts. This requirement presents graduates employed at companies who solely operate in surface mining with an enormous challenge. From anecdotal evidence, candidates are sometimes forced to take leave or on extreme cases resign from their companies to gain the required experience. The greatest weakness in this qualification's pre-requisites is that most graduates are inadequately exposed to various aspects of mine surveying practice and no evidence of shifts or a portfolio of evidence is required. It is therefore very likely that a candidate to the mine surveying examination has no tangible additional training or exposure by the time they have completed the minimum requirement for shifts. Such a candidate would therefore not have had the benefit of exposure to practices and operations other than that that may have been available on the mine at that time.

The Mine Surveying graduate in training program of Anglo Platinum producers in South Africa provides insight into the area in which the graduates are to be developed in the period between graduation and becoming candidates to the GCC examinations. Areas of experience that is listed in the corporate document includes the completion of a trial survey as required by the GCC examiners before any of the theory components are attempted (a highly recommended practice) and shaft surveying, exposure to which is extremely difficult if the company is not undertaking vertical or inclined shaft development. Further to these practical exposure opportunities, the Graduate in

Training is expected to participate in the compilation of month-end figures, resource reconciliation, mine design and layout advice (Roos, 2018).

In a study conducted by Grobler, it was shown that a detailed portfolio of evidence is a requirement for the Australian, German Markscheider and British Mine Surveyor Boards of Examiners as well as the Royal Institution of Chartered Surveyors (RICS) (Grobler, 2016b). Based on this benchmarking study it was recommended that the DMR commission of examiners consider the reduction of examination subjects in preference to outcomes based portfolios of evidence (Grobler, 2016b).

The experience gained through PIT programs are arguably of great benefit to the development of the individual and the company but depends on the maturity of the company offering the program. Graduates in companies who may be less invested in PIT programs may not receive the full benefit of the intended exposure.

Current challenges and solutions

In a report on Graduate Development Programs (GDP) generated by the South African Institute of Mining and Metallurgy (SAIMM), difference in the expectations, responsibilities, lack of challenges and guidance in the work environment was identified as the major sources of discontent under recently graduated professionals (SAIMM, 2015). It is recognised that Professional bodies have the responsibility to set requirements and ensure that the qualifications meet the requirements for professional registration (DHET, 2012). The SAIMM GDP reports remarks that it is 'regrettable' that the current definition of a competent person according to the Mine Health and Safety Act (MHSA) does *'not reflect the outcomes based competency paradigm'* (SAIMM, 2015).

WIL is recognised as a part of professional qualifications that may include 'simulated work experience, work directed theoretical learning, problem-based learning, project based learning and workplace based learning' (DHET, 2012) to integrate workplace practice and 'formal learning' (Winberg *et al*, 2011). The problem originally identified in the 2007 version of the HEQSF was that the institutions offering a program was responsible to place students in an 'appropriate workplace' (DHET, 2012) which has become more challenging in the current economic climate. The sentiment that WIL Workplace Learning (WPL) is highly demanding on resources, support and follow-up visits (Winberg *et al*, 2011), ensuring 'cordial relationships with employers' (Martin and Hughes, 2009) and monitoring student progress that simply does not justify the amount of effort required for a low or zero credit bearing module.

The HEQSF states that the credit ratings in a qualification is *'independent of the mode of learning'* and recognises ten notional hours towards one credit. The framework defines that 'all learning activities' can bear credit and makes direct reference to Work Integrated Learning (WIL) in this regard (DHET, 2012). As a counterpoint it is argued in the WIL good practice guide that students undergoing workplace learning are exposed more to soft skills within their professional area rather than academic learning and as a result *'workplace learning is typically given either no credit points or it is given a low credit value...'* (Winberg *et al*, 2011). It is argued that professional societies and accreditation bodies alike should formally recognise the advantage of work exposure and place a premium on any credits to be allocated to these activities.

CONCLUSIONS AND RECOMMENDATIONS

The benefits of WIL include amongst others, the integration in industry specific culture and terminology, time management, financial acuity, increased sense of responsibility and the development of professionalism. An integrated policy that aligns pre-study Work exposure, Work Integrated Learning during undergraduate studies and post-qualification Graduate Development programs may serve to align the expectations of new professionals with the requirements of industry.

Trede concluded that there was a link between WIL and the development of the participant's professional identity (Trede, 2012). Grobler made a recommendation in 2015 that it industry should consider the registration of a 'second stage qualification' with a realistic NQF level that could be made a compulsory pre-requisite to the Government certificate of Competency examinations (Grobler, 2015). For the maximum benefit and credit to be awarded to Work Integrated Learning, it is recommended that the Professional Institutions enter a conversation with the DMR regarding a change in the manner in which a graduate professional becomes a candidate to the examinations

for the Government Certificate of Competency. In a draft proposal by an industry advisory board to the DMR in 2007, a second stage qualification qualified as a period of 'internship' of 18 and 24 months during which the 'intern' will be subjected to a program of intense, practical exposure based on a predefined curriculum of activities that will cover the theoretical and practical aspects of various types of mining production environments, under the guidance of a registered competent person acting as mentor and finally certifying the portfolio of work done by the applicant (Grobler, 2007).

The stages of WIL may be compared with Wallas' four stage model of creativity which describes the stages of 'Preparation, Incubation, Illumination and Verification' (Sadler-Smith, 2015). The process of preparing the student for the expectations of industry, followed by the academic underpinning of the experience and finally brought to an understanding of how theory and practice interact as verified by the experience gained in the graduate in training follows a similar process. In future the use of virtual reality technology will most likely provide tangible learning experiences that can be controlled in a safe environment.

The 'Lonmin MTS model' of pre-university exposure has demonstrated that the program creates motivated bursars that understands the requirements of the study field that they have chosen as well as the deliverables expected from the sponsoring company. The familiarisation of the student to the culture, the mining value chain and specific terminology used in the mining environment provides the first-year student with a tangible advantage over their class-mates. The preparation phases in mathematics and business literacy provides the student with an advantage but at the same time decreases the risk undertaken by the sponsor as the student stands a better chance to be successful academically. The challenge with pre-university exposure is how this option may be made available to all entrants to the mining study field in a fair and rational manner. It is proposed that mining companies consider making such an exposure year part of their community engagement and social responsibility obligations to the benefit of the local communities in which they operate.

McDougall and Storey observed that the original purpose for the GCC qualification for surveyors was to act as a preparatory phase for mine management and postulated that the skills required by surveyors in the next millennium will include excellent communication, information technology, core mathematical, analytical, measurement, processing, presentation and management skills (McDougall and Storey, 1999). These skills are the same as those listed by Errol *et al* required in the industry 4.0 paradigm (Erol *et al*, 2016).

The development of an integrated program of WIL through the three stages of development of a graduate in training should be considered by the Department of Mineral Resources (DMR) in order to align the Government Certificate of Competency (GCC) requirements, but more importantly should serve in the development of competent professionals that is well versed in the analytical and integration skills that is required in the latest industrial revolution.

REFERENCES

- Bouwer, J (2018). Virtual reality blast wall, cube providing 'memorable' training. (M Zhuwakinyu, Ed.) *Mining Weekly creamer Media*. Retrieved from http://www.miningweekly.com/article/worlds-first-virtual-blast-wall-virtual-cube-revolutionise-mining-training-2018-06-08/rep_id:3650
- Chmelina, K (2010). A virtual reality visualisation system for underground construction, Chapter 4. In G Beer, *Technology innovation in underground construction* (pp. 50–62). Graz, Austria: Graz university of technology, CRC Press Taylor and Francis.
- Davis, B, and Summers, M (2016). Applying Dale's Cone of Experience to increase learning and retention: A study of student learning in a foundational leadership course. In QScience (Ed.), *Engineering Leaders Conference 2014*, (pp. 2–7). West Lafayette, USA Retrieved from <http://www.qscience.com/doi/pdf/10.5339/qproc.2015.elc2014.6>
- DHET (2012, 12 14). The Higher Education Qualification Sub Framework as revised January 2013. (Notice 1040 of 2012), in terms of the National Qualifications Act, 2008 (Act 67 of 2008. *Government Gazette no 36003*. Department of Higher Education and Training.
- DMR (2018a, 09 18). *Examination%20rules%20and%20syllabi.pdf*. Retrieved from <http://www.dmr.gov.za/Portals/0/adam/Courses/Jkvs2v6NoUqvcVi-UGyC0w/Description/Examination%20rules%20and%20syllabi.pdf>
- DMR (2018b, 08 20). *gcc-examinations*. Retrieved from [www.dmr.gov.za: http://www.dmr.gov.za/mine-health-and-safety/gcc-examinations/certifications?id=2635](http://www.dmr.gov.za/mine-health-and-safety/gcc-examinations/certifications?id=2635)

- DMR (2018c, 09 18). *Mine Survey examinations*. Retrieved from www.dmr.gov.za: http://www.dmr.gov.za/mine-health-and-safety/gcc-examinations/certifications?id=2682
- Erol, S, Jäger, A, Hold, P, and Ott, K (2016). Tangible Industry 4.0: a scenario-based approach to learning for the future of production. *6th CLF – 6th CIRP Conference on Learning Factories* (pp. 13–18). Elsevier Science Direct.
- Greene, R (2013). *Mastery: Reprint edition (October 29, 2013)*. Penguin Books.
- Grobler, H C (2007). *Proposal for a future Professional Qualification structure for Mine Surveying (unpublished)*. Johannesburg: University of Johannesburg, Institute of Mine Surveyors of South Africa.
- Grobler, H C (2015). Work Integrated Learning for south African Mine surveyors, a seven year journey. Freiberg: Society of Mining Professors.
- Grobler, H C (2016a). 120 Years of Education for Mine Surveyors in South Africa A Framework for the Mine Survey Profession. *South African Journal of Geomatics Vol 5, No 2 (2016) ISSN 2225–8531*, pages 109 to 119.
- Grobler, H C (2016b). Can an examination guarantee competency? *16th International congress for Mine Surveying*, 49–56.
- Jason, J (2016). *The VR book, Human centred design for virtual reality*. Morgan Claypool books.
- Lurie, J (1982). The education of Mine surveyors. *The journal of the Institute of Mine Surveyors of South Africa*.
- Martin, A, and Hughes, H (2009). *How to Make the Most of Work Integrated Learning: A guide for Students, Lecturers and Supervisors*. Massey University Press.
- McDougall, K, and Storey, B (1999). Mine Surveying education – a model for the future. University of Southern Queensland.
- Meyer, F J (1964). Training and diplomas for Mine surveyors. *Journal of the Institute of Mine Surveyors of South Africa, Vol XIII No2*.
- Mischo, H, and Brune, J F (2017). Computer Simulation Programms in Mine Rescue Education and Training, on the Example of Student Mine Rescue Teams. *Society of Mining Professors. SOMP*.
- Roos, C (2018, August 15). Graduate program for Anglo Platinum. (H Grobler, Interviewer)
- Sadler-Smith, E (2015, 10 02). Wallas' Four-Stage Model of the Creative Process: More Than Meets the Eye? Routledge. Retrieved from <https://www.tandfonline.com/doi/abs/10.1080/10400419.2015.108727>
- SAIMM (2015). *Best practice guideline for the development of Graduate Development Programs for Mining and Metallurgy*. South African Institute of Mining and Metallurgy.
- SAQA (2018, 09 25). National Diploma Qualifications 62405 and 74099.
- Trede, F (2012). Role of work-integrated learning in developing professionalism and professional identity. *Asia-Pacific Journal of Cooperative Education*, page 159–167.
- Visser, J (2016). *Lonmin MTS Cadets – Training and Development*. Lonmin.
- Willows-Munro, S E (1948). *Quarterly annual General meeting of IMSSA 1948, page 19*. J. Institute of Mine Surveyors of South Africa.
- Winberg, C, Engels-Hills, P, Garraway, J, and Jacobs, C (2011). *Work-Integrated Learning: Good Practice Guide, HE Monitor No. 12*. Council on Higher Education.

Miners of the future – ensuring good working conditions in the future digital mine

J Johansson¹, L Abrahamsson² and J Löw³

1. Professor, Luleå University of Technology, 97197 Luleå Sweden. Email: jan.johansson@ltu.se:
2. Professor, Luleå University of Technology, 97197 Luleå Sweden.
Email: lena.abrahamsson@ltu.se
3. Associate Senior Lecturer, Luleå University of Technology, 97197 Luleå Sweden.
Email: joel.loow@ltu.se

INTRODUCTION

Future mining will be shaped in a context where it is necessary to produce resource-efficient at costs that are determined by international competition. The mining industry has overcome many challenges with the help of technology, but technology alone will not be enough in the future. So, while having a technical production process that is at the forefront is one the most important conditions for the future, having a competent workforce that can handle the technology is another but most important condition. Digitalisation is a recurring buzzword that is often claimed to be able to combine these two requirements. But how do we build such a production system?

MINING 4.0 – AN UPCOMING CONCEPT

Industry 4.0 is a strategy that was shaped by the German government in 2013 (Kagerman, Wahlster and Helbig, 2013) where the entire production process is included in internet-based networks that transform ordinary factories to *smart* factories. Industry 4.0 will also come to affect the mining industry. Gradually, mining gets closer to the visions of fully automated mines as well as more technologically sophisticated ore processing facilities, ie Mining 4.0. A Mining 4.0 operator is not confined to a control room. Instead, real-time process-data and the status of machines follow the miner as they move around the mine. The miner solves problems on the spot by remotely interacting with other operators, experts, suppliers and customers in multicompetent teams. Production control could even be done in a digital model (or 'digital twin') far away from the mine. In short, Mining 4.0 envisions an augmented miner with senses and memory extended through technology. This technology takes advantage of and supports human skills and increases situational awareness through sensors embedded in the clothes of operator, for example, while keeping an uninterrupted operational vigilance. Romero *et al* (2016) formed a typology of the future Industry 4.0 operator built on eight characteristics that can be seen as the core of the new technology (Figure 1).



FIG 1 – Operator 4.0 typology shaped by Romero *et al* (2016).

We have modified the typology by Romero *et al* (2016) to relate to the future miner:

- The *super-strength miner* uses biomechanical support for increased limb movement, increased strength and endurance.
- The *augmented miner* uses augmented reality (AR) for integrating information from the digital to the physical world. Examples include maintainers receiving direct assistance from equipment manufacturers. Through special glasses that send and receive live video, both parties would be able to see the problem – which can then be solved through instructions from the equipment manufacturer.
- The *virtual miner* using virtual reality (VR) for simulation and training of risky real-life situations is relatively common in mining. In principle, it is possible to place the entire control room and production control in a VR environment, and thus make it independent of location.
- The *healthy miner* uses wearable sensors for monitoring health-related metrics as well as GPS location. There are already advanced positioning systems in use and there have been projects on the application of sensors for monitoring miner's health.
- The *smarter miner* uses intelligent personal assistants for interfacing with machines, computers, databases, and other information systems. RFID tag systems are used together with a smartphone app to rapidly and easy report malfunctioning equipment.
- The *collaborative miner* uses collaborative robots for performing repetitive and non-ergonomic tasks. The repetitive and ergonomically strenuous task of driving to and from the muck pile is taken over by the machine.
- The *social miner* uses enterprise social networking services for interaction between operators and between operators and the Internet of Things.
- The *analytical miner* uses big data analytics to discover useful information and predicting relevant events.

This classification points to the numerous possibilities of integrating Industry 4.0 with human labour – some good and some bad. But this development is not about *creating new* kinds of jobs. Rather it is a development that means that most current jobs will be *influenced* by these characteristics and developments. Miners will not disappear, but they will be different in the future. We have chosen to call them Miners 4.0.

CONCLUSIONS

Mining 4.0 can definitely represent a positive development, but there are many questions that must be cleared. The development cannot and should not be stopped, but it requires reflection and consideration so that more problems are not created than are solved. Based on our experience in the EU funded project *Sustainable Intelligent Mining Systems* (SIMS), we want to bring forward a number of recommendations that can be considered as a beginning of a road map for the human side of Mining 4.0 (Löw, Abrahamsson and Johansson, 2019).

- First, there is the economic bottom line. A mine must be able to produce at costs that are determined by international competition. But more ways of measuring success may be required, ways that capture eg social factors.
- Mining 4.0 will cause a reduced need for traditional labor. Any reduction in the workforce must be managed with great transparency and in close cooperation with the trade unions.
- New competencies will be needed, and it is necessary to involve all employees in this competence development.
- A flat organisation based on sociotechnology that empowers employees and encourages their creativity is a key to success of Mining 4.0.
- Management of privacy and integrity issues must be done in close cooperation with the trade unions.
- All changes must be embedded in a context of great social responsibility.

ACKNOWLEDGEMENTS

The study is part of the project *Smart Intelligent Mining Systems* (SIMS) and received funding from the European Union (EU)'s Horizon 2020 program (Grant Agreement no. 730302)

REFERENCES

- Kagerman, H, Wahlster, W and Helbig, J, 2013. Recommendations for Implementing the Strategic Initiative Industry 4.0. München: Acatech.
- Löw, J, Abrahamsson, L and Johansson, J, 2019. Mining 4.0—the Impact of New Technology from a Work Place Perspective, J. Mining, Metallurgy & Exploration, 2019 36: 701–717.
- Romero, D, Stahre, J, Wuest, T, Noran, O, Bernus, P, Fast-Berglund, Å and Gorecky, D, 2016. Towards an operator 4.0 typology: a human-centric perspective on the fourth industrial revolution technologies. International Conference on Computers & Industrial Engineering (CIE46).

Human performance variability and responsiveness to training in traditional and autonomous haulage operations

G K Karadjian¹

1. Senior Vice President – Australia Pacific, Immersive Technologies, Perth WA 6017.
Email: gkaradjian@immersivetechologies.com

INTRODUCTION

Simulators of mining heavy equipment have been used as a tool in operator performance improvement for many years. As such, there is a substantial body of knowledge surrounding rates of human performance improvements in manned operations. With the growing population of autonomous haulage operations using simulator based training for manned roles, rates of human performance improvement in autonomous haulage operations are now becoming understood. This report summarises project methods, measures and results from simulator based operator improvement projects and compares these to methods, results and measures from traditional manned operations. It is anticipated that knowledge of human performance variability in autonomous operations may assist in improving autonomous project modelling accuracy.

Background

Simulation based human performance projects have been run successfully for surface (Dorey and Knights, 2015) and underground (Karadjian, de la Torre and Cerna, 2017) mining operations over a number of years. Whilst performance improvement must be confirmed via real world measurements to achieve validity, simulation based measurement offers a depth of behavioural information and repeatability of training environment which is superior for rapid comparison of operators. However, according to the author's knowledge, to date there has been nothing published surrounding its efficacy in operations utilising autonomous haulage systems, or how it compares to traditional operations.

Historical project methodologies

Whilst variation in project methodology exists between different mining organisations, most projects conform to the structures of the Plan, Do, Check, Act cycle (Johnson, 2020). In the 'Plan' stage, the performance goal is identified, as are the lowest performing operators. As noted by Nickel *et al* (2017), human performance is a relative measure, benefiting from assessment of local distribution, rather than external benchmarks. It is during this stage that a 3–6 month sample of historical fleet management data is captured, to establish a performance baseline. In the 'Do' stage, targeted curricula is prepared and training delivered. Simulator training delivery includes a baselining, whereby an operator is assessed with no coaching. Following the baseline, targeted training is delivered. And following this, a final assessment is performed to confirm skills adoption. In the 'Check' phase, following another sampling period a simulator based retention assessment is performed to measure skills decay (Childs, Spears and Prophet, 1983) and real world data is again measured to confirm the level of effective performance retention. Finally, in the 'Act' stage, the learnings from the 'Check' stage calculate the Return-On-Investment from the process and assess the findings.

Project sampling and variables

Two simulator based autonomous operator performance projects have been run. Both occurred in Australian Iron Ore operations, with hydraulic excavators, however both run autonomous haulage systems from different OEMs. Both projects reported improvements in instantaneous dig rate as t/h as reported by their dispatch systems following the final simulator assessment. In order to assess if there was a significant difference in the rate of human performance for autonomous operations, a sample of 14 comparable Australian hydraulic excavator simulator based training projects were selected for comparison.

To report environmental factors which may effect each project, additional variables reported were:

- whether the operation had autonomous haulage system ('AHS')
- the material being excavated ('Material') to report for differences in material hardness
- whether the material being excavated was waste or ROM, again to report differences in material hardness
- the number of equipment operators taking place in the project ('Ops').

A summary of the selected projects can be found presented in Figure 1 and summarised in Appendix 1.

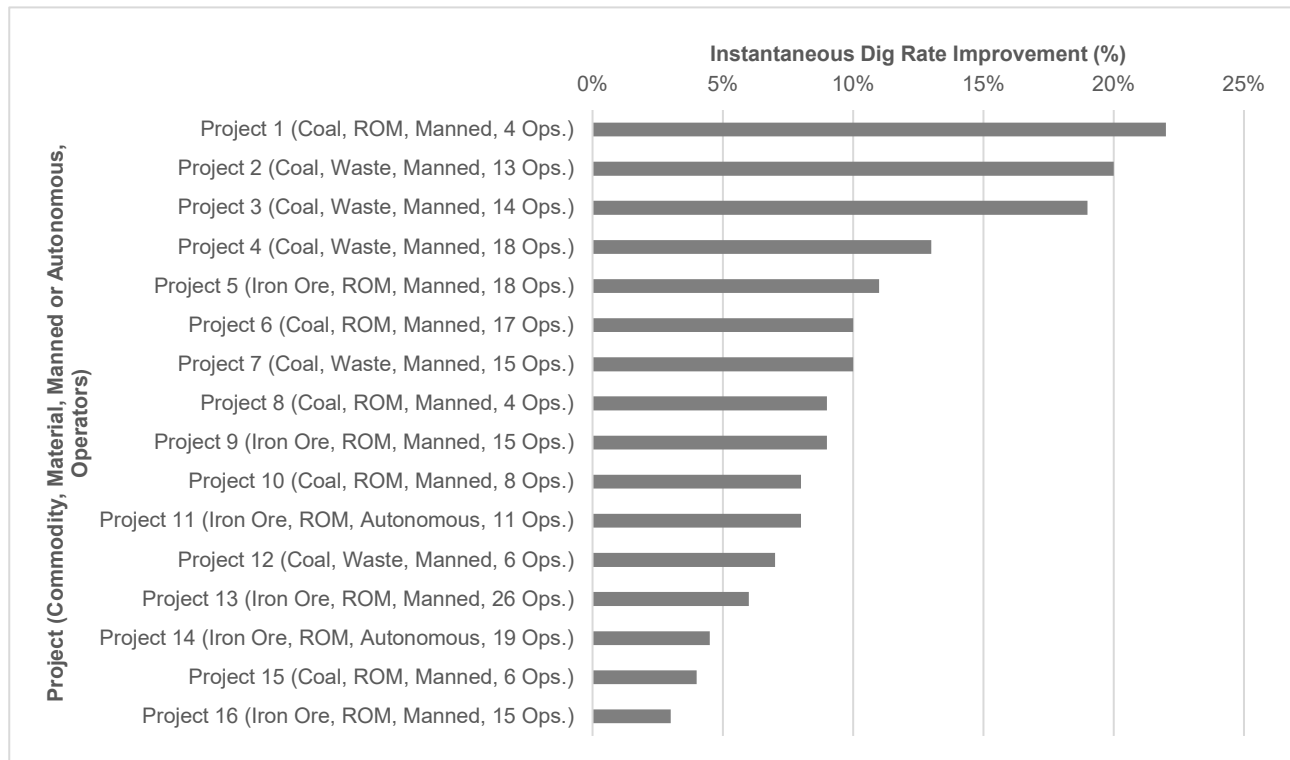


FIG 1 – Graphical summary of sampled excavator projects.

Findings

The mean rate of improvement observed across the sampled projects was 10.2 per cent, with a standard deviation of 3.5 per cent, a minimum of 3 per cent and a maximum of 22 per cent. This places both autonomous projects below the average yet within two standard deviations, with improvements of 4.5 per cent and 8 per cent.

CONCLUSIONS

Excavator dig rates within autonomous operations are still influenced by operator performance at similar rates to traditional operations. A review of the projects shows that the rate of performance improvement anticipated from simulation based continuous improvement varies little from traditional operations. However, the current sample size is insufficient to support a predictive model of anticipated rates of improvements from projects of this nature. It is therefore recommended that further simulation based performance improvement projects of this nature be performed to increase the number of samples for both manned and autonomous operations. Additionally, further studies should be performed into likely antecedents of excavator performance potential, to support building a predictive model of performance improvement.

REFERENCES

Childs, J M, Spears, W D and Prophet, W W, 1983. 'Private pilot flight skill retention 8, 16 and 24 months following certification', viewed 23 Jun, 2021, <<https://apps.dtic.mil/sti/citations/ADA133400> >.

- Dorey, F and Knights, P F, 2015. 'Quantifying the benefits of simulator training for dragline operators', *Mining Technology*, 124(2), 97–106, viewed 23 Jun, 2021, <<https://doi.org/10.1179/1743286315y.0000000007>>.
- Johnson, C N, 2002. 'The benefits fo PDCA'. *Quality Progress*, 35(5), p.120, viewed 23 Jun 2021, <<https://www.proquest.com/magazines/benefits-fo-pdca/docview/214762325/se-2?accountid=30812>>.
- Karadjian, G K, de la Torre, J A and Cerna, I R 2017, 'Innovations in underground hard rock operator efficiency – through simulation-based training technologies and processes', 13th AUSIMM Underground Operators' Conference 2017, Gold Coast, Queensland, 16–18 October 2017, viewed 23 Jun, 2021, <https://www.ausimm.com/globalassets/pdf-files/publications/8–17_underground-ops/8–17_karadjian.pdf>.
- Nickel, C, Knight, C, Langille, A and Godwin, A, 2019. 'How Much Practice Is Required to Reduce Performance Variability in a Virtual Reality Mining Simulator?', *Safety*, 5(2), 18. Viewed 23 Jun, 2021, <<https://doi.org/10.3390/safety5020018>>.

APPENDIX1 – SAMPLE EXCAVATOR PROJECT SUMMARY

TABLE 1

Summary of sampled excavator projects.

Project	Material	Waste	Haulage	No. of operators	Instantaneous dig rate improvement
Project 1	Coal		Manned	4	22%
Project 2	Coal	Yes	Manned	13	20%
Project 3	Coal	Yes	Manned	14	19%
Project 4	Coal	Yes	Manned	18	13%
Project 5	Iron Ore		Manned	18	11%
Project 6	Coal		Manned	17	10%
Project 7	Coal	Yes	Manned	15	10%
Project 8	Coal		Manned	4	9%
Project 9	Iron Ore		Manned	15	9%
Project 10	Coal		Manned	8	8%
Project 11	Iron Ore		Autonomous	11	8%
Project 12	Coal	Yes	Manned	6	7%
Project 13	Iron Ore		Manned	26	6%
Project 14	Iron Ore		Autonomous	19	4.5%
Project 15	Coal		Manned	6	4%
Project 16	Iron Ore		Manned	15	3%

Unlocking human creativity – people, technology and the changing role of organisations

B Kubat¹

1. MAusIMM, Founder, Resolve Coaching & Consulting, Brisbane Qld 4520.
Email: bev@resolvecc.com.au

ABSTRACT

Mining has followed the trajectory of each of the industrial revolutions. It began with the mechanical innovation of the first industrial revolution which saw the replacement of labour with machines. Then came a focus on scale and efficiency, with the introduction of mass production and electrification from the second industrial revolution. The third industrial revolution saw the utilisation of computers and the internet, reducing cognitive load for humans and increasing our connection. Each advance has affected the way organisations manage their resources.

Mining companies have at various times reached for the levers of cost reduction, productivity improvement and capital efficiency in order to find a competitive advantage. Often these levers have been deployed in a command and control style, where all-knowing leadership has focused efforts on cementing knowledge through the identification of best practice, an emphasis on efficiency and the assumption that replication is possible.

We are at the beginning of the fourth industrial revolution which is characterised by system-wide innovation, brought about by the interplay between digital, physical and biological fields. New tools are cheap, quickly scalable and accessible to all, meaning change and innovation is coming from more sources than ever. The pace and interconnected nature of change, and the resulting increase in complexity mean that one off organisational adjustments, targeting a well-defined solution, is no longer sufficient.

Instead, organisations will need to focus their effort on the process of continual response to an unfolding future if they want to realise the potential of technology adoption. This will require, paying attention to information that flows from actions, making sense of that information from the viewpoint of multiple perspectives, utilising collective sense making to drive decisions and ultimately delivering adjusted action. The term I'm using to describe this process is adaptive development, the ability to learn, change and become more advanced in response to changing conditions.

As illustrated in Figure 1, adaptive development requires two forces to drive it. The first is the process of learning, of acquiring new understanding that accumulates into knowledge. Learning first passes through the process of noticing information that emerges from our actions and then it proceeds to the process of sense making where we decide what that information means to us. The second force is the process of change, where we utilise the new knowledge developed to take action and in so doing, accumulate know-how. Change passes through the process of deciding based on the knowledge accumulated and then the process of doing, converting learning to action.

There are different levels of maturity in the adaptive development process that match the requirements of different levels of complexity that have emerged from the various stages of the industrial revolution. The four levels of maturity are shown in Figure 2.

Silo adaptive development focuses on the learning and change required within individual departments or elements of an organisation. The assumption is, that if each section performs well, then the whole will perform well. Learning tends to be limited to tracking internally gathered data against set targets and change emphasises compliance and the attainment of outcomes. Underlying assumptions are not examined because they are assumed to be known and unchanging. This focus of adaptive development can be useful to improving well known and understood processes that don't have complex interdependencies. Focus is on compliance to known and understood practices.

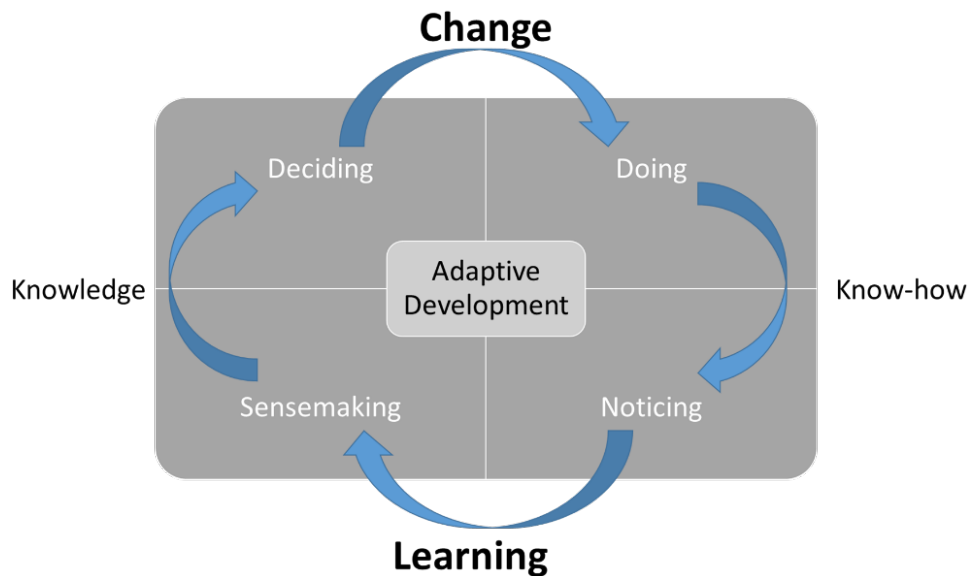


FIG 1 – Adaptive development (learning/change loop).

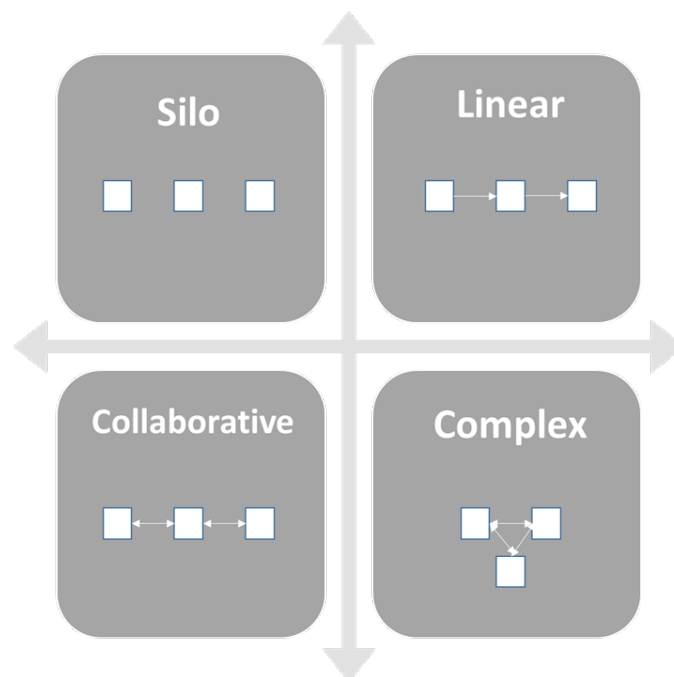


FIG 2 – Maturity levels of adaptive development.

Linear adaptive development understands that there is a dependence between elements but, it tends to be thought of in terms of clear cause and effect with connection flowing one way. Learning might start to include more analysis of the gaps between elements, with a focus on waste and inefficiency. Learning can also consider external benchmarking for equivalent activities, with the assumption that practices can be replicated at different locations. Change is focused on improving existing processes, often focusing on one element at a time. This level of adaptive development can be useful where there is little variation in context and conditions between operations eg factory settings. Focus is on improvement to existing practices.

Collaborative adaptive development begins to recognise a more interconnected nature of elements in an organisation, with cause and effect being less straightforward and operating in multiple directions simultaneously. Learning begins to look across discipline boundaries for information and scanning of the external environment occurs, looking for ideas outside of direct industry examples. Change comes from taking existing ideas but applying them in novel ways. Focus is on generating creativity and developing new applications from a wider scope of knowledge.

Complex adaptive development starts to build a more nuanced view of the complex ecosystem that we operate in, paying attention to the subtle influences from a wide variety of elements both within and external to the system. Learning moves to developing a shared understanding across discipline boundaries, encouraging the ability to look at a problem from multiple perspectives. Change involves being able to generate novel ideas, challenge underlying assumptions and adopt a language of experimentation where assumptions are held lightly. The focus is a move to the collective view, where wisdom and innovation is developed.

The ability for an organisation to shift to a more complex level of adaptive development relies on the interplay between three levers; technology adoption, individual mastery and collective capability. Each lever impacts the other as shown in Figure 3.

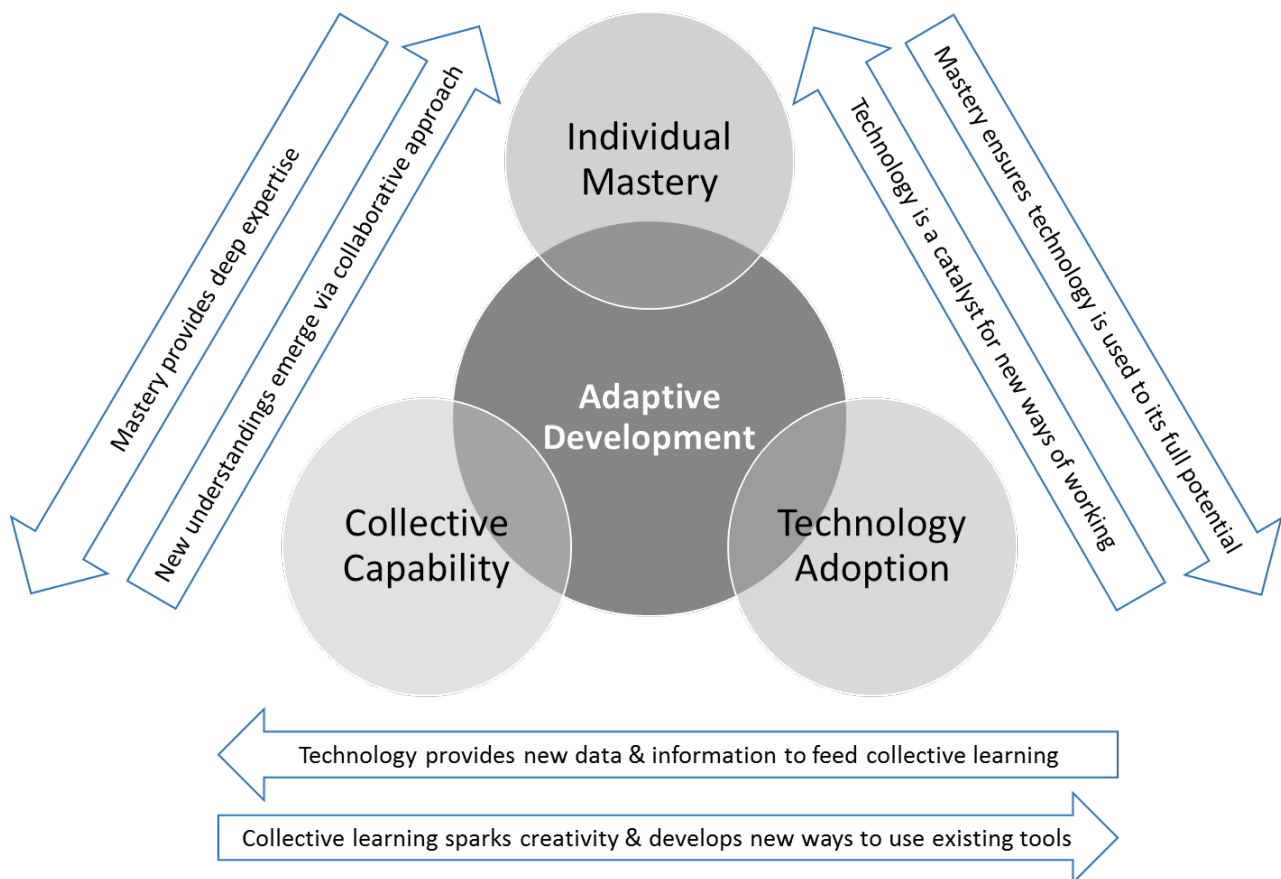


FIG 3 – Adaptive development levers.

There are three categories of skills required to support the development of each of these levers. The first, technical skills are the first category and are the most visible and tangible of the skill sets. They are the skills and knowledge you need to undertake organisational tasks. The fourth industrial revolution means that the lifespan of technical skills is shortening and changing, keeping pace with digital literacy is essential.

The second category of skills has been referred to by McGowan and Shipley (2020) as Uniquely Human Skills (UHS). UHS are those skills that are not yet replicated by technology. These are the skills that are often less visible and tangible but make us better at our job, both better as an individual and better functioning within a group. Examples of these skills are sense-making, social intelligence, novel and adaptive thinking, cross-cultural competency, computational thinking, new-media literacy, transdisciplinarity, design mindset, cognitive load management and virtual collaboration (Davies, Fidler and Gorbis, 2011).

The third category of skills can be thought of as our world view. This is our constantly evolving selves, how we view ourselves, how we view others, how we make sense of the world around us. It is generally accepted that we gain increasing complex ways of understanding the world as we move through childhood, adolescence and into adulthood. Adult development theory (Garvey Berger,

2012) can provide us with a framework that shows as we encounter increasingly complex situations, our way of making sense of the world also continues to evolve throughout our adult lives. Many believe that the fourth industrial revolution requires more of us to step through these later stages of adult development than we have previously required.

And so we come to the changing role of the organisation. In the rapidly changing context of the fourth industrial revolution, the organisations role is to provide the conditions in which individual development can thrive and be matched to organisational objectives. The delivery and implementation of each skill category is supported or inhibited by the organisational culture that individuals operate in. Mining brings many positive cultural attributes to play; optimism, resilience, action orientation, pragmatism and determination are some elements that spring to mind. However, mining is also known to display attributes that inhibit an organisations ability to respond to the changing world; risk adverse, conservative, hierarchical, conforming, hero-leader and bureaucratic. To shift the culture to one that supports an internal rate of change to match the rate of change demanded externally, there are a number of themes that companies need to pay attention to. These include, diversity and inclusion (building block to access a wide range of perspectives and experience), psychological safety (ensuring every person can contribute and a learning and experimental mind-set is supported), system thinking (understanding interdependency and complexity), transdisciplinary thinking (in order to build a shared understanding and develop novel solutions), participation of all (utilising the full human potential available to an organisation, not reliant on top down).

The shift in focus from individual achievement, control, efficiency and set outcomes to one that emphasises context, process and collective learning and change will not be easy but for those that succeed it will be rewarding.

REFERENCES

- Davies, A, Fidler, D and Gorbis, M, 2011. *Future Work Skills 2020*. Palo Alto, CA. Available at: https://www.iff.org/uploads/media/SR-1382A_UPRI_future_work_skills_sm.pdf [Accessed: 30 June 2021].
- Garvey Berger, J, 2012. *Changing on the Job*. Stanford University Press.
- McGowan, H and Shipley, C, 2020. *The Adaptation Advantage*. Wiley.

Highly sought-after mine managers – what qualifications, responsibilities and duties are of great importance to mining companies?

W E Oching¹ and G Bonci²

1. Faculty, British Columbia Institute of Technology, Burnaby BC, Canada V5G 3H2.
Email: woching@bcit.ca
2. Faculty, British Columbia Institute of Technology, Burnaby BC, Canada V5G 3H2.
Email: gheorghe_bonci@bcit.ca

ABSTRACT

Traditionally, operating mining companies offered mine manager positions to long-serving shift supervisors (bosses) with very good track record in decision-making. With numerous challenges posed by global economic cycles, mining companies' commonly sought after mine manager's qualifications, responsibilities and duties are showing a new trend and focus that include mining engineering education, proven experience, certification, health and safety, environment, meeting of production and financial goals, interpersonal relationships and other top leadership qualities. This paper focuses on the analysis and findings associated with the samples of job advertisements data collected in 2018, 2019 and 2021. The study demonstrates the shift in hiring practices that emphasizes on many different and challenging aspects of mine management. The prevailing hiring trend highlighted in this paper provides avenue for discussion and standardisation of mine manager's role globally, regionally or by countries like Canada, USA and Australia with similar mining regulations. This work offers mining professionals and academic institutions an opportunity to redesign or develop mine management education and training tailored for the current and future needs of the mining industry. It also highlights necessary areas for future research that could not be properly exhausted with the prevailing research resources and time constraints.

INTRODUCTION

Traditionally, most mines were managed by long-serving shift-bosses/supervisors appointed to make decisions and the rest of the workers implement their decisions (Musgrave, 1985). The mine managers' appointments have been mainly based on the number of years of experience in the mining industry and desirable leadership skills. With increasing volatile market for mining products posed by cyclical global economic challenges, human resources professionals in the mining industry are compelled to continue changing the qualifications, competencies and responsibilities of ideal mine managers to be hired. Globally, the mining industry is facing threats from regular changes in mining regulations, unstable commodity prices and higher cost of mining, as such mining companies are adapting to seek mine managers capable of providing not only the strategic leadership in many key aspects of mining operations but also managers with very important academic qualifications and professional certifications that this paper focuses on.

This work focuses on new revelations obtained from a study of many job postings associated with mine management. The job posting samples were collected from various world-class companies operating in North America, South America, Australia, Africa, Europe and Asia. Among the companies whose job postings are used for this work include Barrick Gold Corporation, Vale, Newmont, Teck Resources Ltd., Westmoreland Coal, Alamos Gold Inc, Suncor Energy, Lhoist, Lafarge, etc. This paper also provides mining executives and human resources professionals tasked with recruiting mine management professionals with the trend of top qualifications, duties and responsibilities associated with the highly sought-after general mine managers, mine managers, and mine superintendents. Examples incorporated in this paper are from a wide range of mining operations using different mining methods and extracting commodities such as gold, copper, nickel, coal, iron, limestone and oil sand, among others. This work may also assist operating mines reduce high turnover of mine managers by appointment of suitable leaders that possess the highly regarded requirements including academic credentials, mine manager certification, and experience, that subsequently lowers the cost associated with recruitment which directly also affects mine operating costs.

In accordance with the Mines regulations or codes of practice in several countries including Australia, Canada and the US, the mine manager or designate is responsible to enforce the regulations of the Mines Act and health and safety codes. In addition, mining companies also expect mine managers to have managerial responsibility and be accountable for the work of various mine departments including engineering, geology, environmental and safety. Mine manager candidates with additional qualification: mine manager's certificate of competence, valid driver's license, broad technical knowledge of operations, processes, excellent interpersonal skills and sound computer skills and project management experience etc, are required or sometimes are regarded as having added advantage (Manyuchi, Mbohwa and Muzenda, 2020). Therefore, this paper extracts the key technical, leadership and business competencies that enable contemporary mine managers to run the mining operations effectively.

METHODOLOGY

The data used for this paper was collected from various job banks commonly used by mining companies, suppliers, professionals, among other users. The criteria used include searching for job titles such as general mine manager, mine manager and mine superintendent as these terms can be used interchangeably based on the desire of an organisation. The main focus is to see that the duties and responsibilities are similar for the job posting to be considered as a sample. The mining operations considered for this work employ underground and surface mining methods including oil sand and quarries (Table 1). No preference was given to job postings by commodity mines or mining methods. The samples collected cover a wide range of minerals mined including gold, copper, nickel, iron, coal, oil sand, limestone, etc. A total of fifty job posting samples were collected in 2018, 2019 and 2021 during the months of January and February and tabulated in terms of years of experience, education and training, and type of mines (Table 1). The power of 'word cloud' was used to generate the summary of common words used in job postings to visualise data from these large documents (Figure 1).

TABLE 1
Mine types associated with the job postings.

Year	No. of postings	Type of mines		
		Open pit	Underground	Quarry
2018	16	6	9	1
2019	20	10	8	2
2021	14	6	8	-

Years of experience

From 2016 to 2017 the mining sector experienced a significant downturn, thus a continued contraction in mining employment. Many mining professionals decided to leave the industry to take an early retirement or to start their own businesses. The replacement of these workers, especially for those with extensive experience, was a significant burden for the mining companies. Hence the sector faced a huge skills gap including for the upper levels management. That generated costly downtime on some important mining projects due to lack of manpower.

The sector started a slowly recovering in 2018 as can be seen by the increased in the number of postings from 16 to 20 in the first two years of the recovery process. About 60 per cent of the mining companies require at least 10 years of mine operational and planning experience (with 5 years in management/supervisory role) for their mine managers. A few companies (three underground and two large scale surface operations) required more than 15 years of supervisory and production management experience. Ten per cent of job postings mainly by small mining operations (quarries) required a minimum 5 years' experience especially on operational role (Table 3).

TABLE 3
Manager's years of experience requirement.

Year	No. of postings	Years of experience			
		Under 5	5–10 years	10–15 years	Over 15 years
2018	16	-	5	11	0
2019	20	-	6	11	3
2021	14	-	4	8	2

Therefore, it is apparent that mining companies take significant years of experience at mine operations very seriously in their hiring decisions. No shortcuts for mining leadership positions without practical experience in the mining industry in addition to academic qualifications required for managerial positions.

Risks and responsibility

One question to be asked: how the mining sector is evolving to keep a balance between the economic development and the continuous sustainability pressure? The answer to this question is a key for the hiring process of the future managers. Despite the difficulties and challenges witnessed in the world economy, there is a continual growth of the global mining market. Over the years mining sector faced different types of risks/challenges. For the studied period beside the social license to operate, lowering the carbon footprint and energy usage, or water sources, finding the right workforce for the 'new mining' is one of the biggest challenges. The mining companies have a difficult time not only to hire and retain the best/right people for their operations, but to understand how actually their future employees might look like on the new conditions (mining in the digital era).

Roles/positions like 'digital specialist/expert', 'data expert analyst', 'data architect', 'optimisation engineer', 'interface engineer', 'chief digital officer', to name a few, didn't or still don't exist on the mining companies' classical structures. Then, another question arises: is the mining sector going to turn the mining companies into some high-tech companies? The answer is no, but it is something that must be changed into the traditional company models to accommodate for the intelligent mining organisations which represent the mining of the tomorrow. Indeed, there is a missed opportunity by mining human resources professionals and corporate executives to consider; that is the application of human-machines to select suitable candidates in management positions. Candidates with a good track record of innovative initiatives can help address the current and future challenges of recruitment and retention as there is high turnover in executive positions very common in the mining industry which can be proven by many mining professionals changing companies within short period of time.

The responsibilities of the mining managers evolved/shifted during the analysed period, but there are some common and very easy identifiable ones that can be extracted from all the postings: Ensuring, Mining, Production, Performance, and Improvement (Figure 1). The top and common

responsibilities and duties stipulated in the job postings used in this paper include: achieving production targets, through proper planning, implementation and overseeing the mining programs, effective management of mining operations, continuous improvement in all areas of mining operations, and attaining strong financial results on regular basis through enforcement of mining regulations, development of mining standards, procedures, and employees; and ensuring health and safety of mine workers is valued.

It is not a surprise to see the focus on production and successful mining operations performance especially during challenging mining cycles associated with low commodity prices or global financial recession where maximising production has proven to be effective to attaining acceptable financial performance as by maximising production volume or throughput, costs of production or unit costs are reduced (Cavender, 2001). Cost reduction solutions are less focused on traditional set of top-down managerial strategies such as reduction in production volume, cancellation of employee training, restrictions on travel, reductions in office supplies, and so forth (Cavender, 2001).

However, the summary of responsibilities and duties also clearly shows that health and safety is not the top priority as mining executives usually stress in company's values and press conferences yet operating unsafe mines tend to be costly and unprofitable mines shutdown or close (Fiscor, 2013) as also demonstrated by Westray Mine explosion in Nova Scotia, Canada in 1992 which claimed 26 miners resulting in financial collapse of Curragh Inc and criminal charges of two former mine managers (Ottawa Citizen, 1993).

CONCLUSION

Mining industry has evolved from mainly considering significant years of experience in mining operations as a top qualification for a position of a mine manager to a new set of qualifications and requirements. In the modern times, a highly sought-after mine manager must have a combination of qualifications, experience, knowledge, training, and skills to manage and supervise the mining operations. To be highly preferred for a mine manager position, candidates should possess the following: Bachelor of mining engineering, 10 – 15 years of experience in the mining industry and ability to manage a mining operation efficiently through meeting or surpassing production targets, strong financial results, top health and safety record, development of employees, standards, and procedures; and enforcement of mining regulations and environmental laws. Incorporating machine learning capabilities for hiring prediction to reduce uncertainties, will automate the hiring process and lower costs associated with high level management recruitment and retention. While the research team believes that the main objectives of this paper have been met, it also recognises that it would be beneficial to find additional data associated with the period ranging from 2000 to 2018 to understand better the changes in the mine manager's job profile. Standardising or harmonising the mine manager's qualifications, and responsibilities can facilitate the increasing mobility of mining professionals to work in the mining industry not only among the countries with similar mining regulations but also globally.

ACKNOWLEDGEMENTS

This work was supported by the department of Mineral Exploration and Mining at British Columbia Institute of Technology in Canada. A vote of thanks also goes to various fourth year mining students for providing job samples used in class discussions and assignments. Thanks to several job banks including careermine.com and Indeed and many mining companies for making job postings accessible to the general public.

REFERENCES

- Cavender, B, 2001. Leadership vs. management: Observations on the successes and failures of cost-reduction programs, *Mining Engineering*, vol. 53, no. 8, pp. 45.
- Fiscor, S, 2013. Education, Empowerment and Exposure: Engineering, Geology, Mineralogy, Metallurgy, Chemistry, etc., *Engineering and Mining Journal*, vol. 214, no. 6, pp. 4.
- Government of British Columbia, Canada. Certifications. <<https://www2.gov.bc.ca/gov/content/industry/mineral-exploration-mining/health-safety/certifications>> [Accessed: 24 November 2021].

- Government of South Australia, SafeWork SA, 2020. Mine Manager Competencies. <https://www.safework.sa.gov.au/industry/mining-and-quarrying/mine-manager-competencies> [Accessed: 24 March 2021]
- Manyuchi, M M, Mbohwa, C and Muzenda, E, 2020. The importance of the mine manager and the appraisal system in the mining sector. In *Proceedings of the International Conference on Industrial Engineering and Operations Management*. IEOM Society, pp 2697–2701. <http://ieomsociety.org/ieom2020/proceedings/> [Accessed: 22 March 2021].
- Musgrave, K. 1985, Participative mine management, *CIM Bulletin*, vol. 78, no. 875, pp. 131–132.
- Ottawa Citizen, 1993. Westray Mine; Mine managers charged in deaths lose legal funding: [Final Edition] 1993, Ottawa, Ont.

An AI-based personalised evaluation and training system for displaced workers in mining industry

H Soydan¹, H Ş Duzgun², J Brune³ and X Zhang⁴

1. Post-doc Researcher, Colorado School of Mines, Golden CO 80401. Email: soydan@mines.edu
2. Professor, Colorado School of Mines, Golden CO 80401. Email: duzgun@mines.edu
3. Professor, Colorado School of Mines, Golden CO 80401. Email: brune@mines.edu
4. Associate Professor, Colorado School of Mines, Golden CO 80401. Email: xlzhang@mines.edu

INTRODUCTION

Industry 4.0 is redefining and transforming the division and definition of labour by introducing a fusion of technologies on the shoulders of technological advances and digital revolution since the midst of the last-century. As a significant part of global economy, mining industry has been embarking on these ongoing operational transformation; therefore with an emerging need to manage mining workforce. Given this ongoing transformation and emerging change, retraining the workers where the new knowledge builds upon their expertise is critical, especially in mining industry where workers have significant knowledge of ongoing physical and chemical processes. Benefiting from their current know-how in their working environment, displaced workers can be quickly retrained and transitioned for jobs that require extensive digital technology skills.

Data-driven technologies, automation and autonomous operation cause a paradigm shift among today's industrial operators and engineers. Process automation will displace workers and engineers as the mining, manufacturing and metallurgical industries implement data-driven technologies. The research objective is to develop a proactive artificial intelligence (AI)-enabled tool that will assess workers' existing skill sets and knowledge to generate individualised retraining plans to prepare them for jobs of the future as their existing jobs become obsolete. The research framework that builds a bridge between the workers and their future work is given in Figure 1.

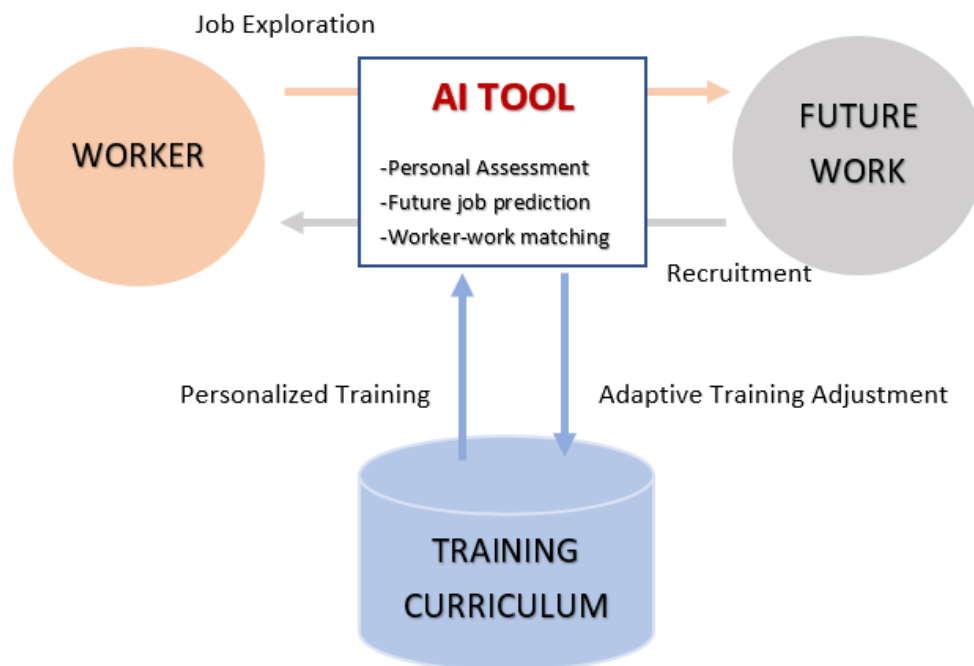


FIG 1 – The research framework.

Objectives of the research

The aim of this study is to build a human-centred Artificial Intelligence (AI) system that will assess individual workers' personal skills, abilities, knowledge, interests etc to quantify the gap between their desired job requirements and their current know-how. Towards this goal, at first, interviews are conducted with industry professionals in the US to identify the evolving needs and prospects in the

mining sector, the changing expectations on employer's end, current vision of the workforce as well as the room of development they envision in mining sector. The preliminary results show that data analytics and autonomous operations will be much more prevalent in the near future (3–5 years), particularly effecting the workforce in the technical-operational area.

In addition, the specific research objective of this research is to create a human-centred AI for personalised workforce transition that is optimised for mining industry; however might be adaptable across other sectors. This personalised AI system will conduct comprehensive personal analyses; produce explainable job recommendations with transition probabilities with the help of a semi-supervised learning and active learning methods; and adaptive training adjustments with human-in-the-loop reinforcement learning (RL) to ensure retraining success for validation. The working process of the envisioned interactive system is given in Figure 2.

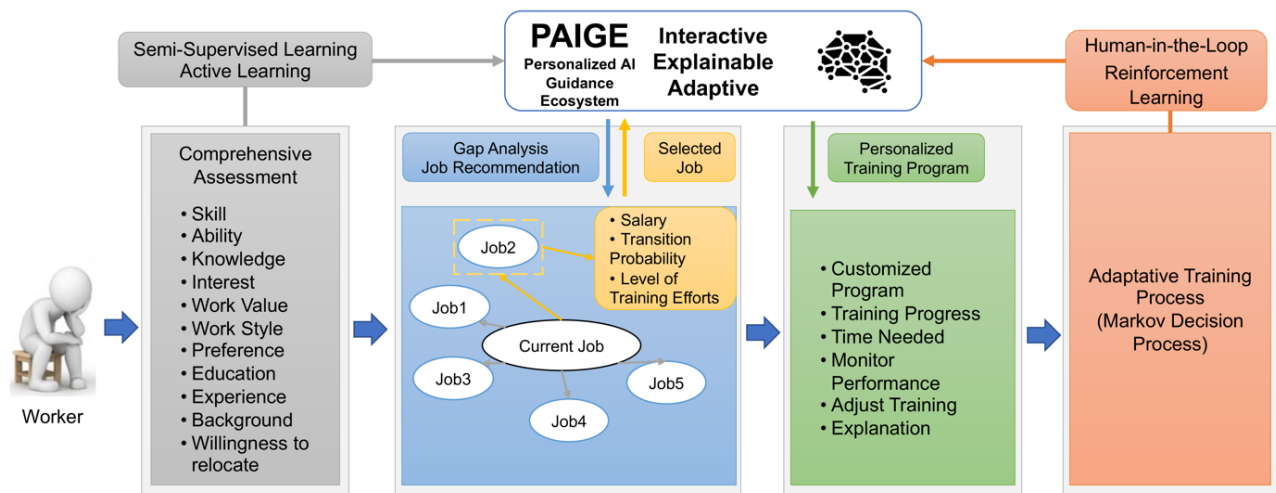


FIG 2 – The working process of the PAIGE tool. The comprehensive assessment of workers will be used for gap analysis and personalised training recommendation.

This implementation will enable scalable and sustainable workforce transition with a modular design using a Graph Neural Network, consisting of 'job-specific' and 'worker-specific' modules (Zhou *et al*, 2018). The network will learn and continuously update a map of relationships and connections among the worker and job modules. This modular design will allow the model to handle unseen worker-job combinations using a mix-and-match process to support cross-domain transition. It will also reduce the search space and save computational resources.

In this stage of the research, the machine learning basis for the workforce transition tool is generated. For this purpose, featurisation of worker skills and job requirements as quantitative parameters for use as the inputs and outputs of the machine learning models, competency modelling for comprehensive gap analysis and transition probability/difficulty estimation, features selection to improve the accuracy of the competency model, and interface design for the AI tool is realised.

Powered by human-centred/scalable AI technique, the model offers an integrative approach to generate a job seeker profile that is based on technical skills, professional skills, work values, and desire, with a holistic evaluation of job-seeking individuals. Its adaptive nature offers a cross-industry job transformation pathways and the most relevant training program generation for each user. In that, the tool provides tailored training recommendations for individuals to optimise their job prospects. In addition, it also offers guidance for companies to develop targeted training programs and will predict the cost reduction for such industrial skill shift, which is a novel concept for emerging jobs.

Deployment of machine learning model

The AI-enabled human-centred job and training recommendation system automatically assesses personalised skills and gaps, then quickly generates individualised retraining plans that can be customised to each employer. In order to achieve our goal, comprehensive set of featured input,

encompassing personal skills, ability, knowledge, personality, interests or job desires will be utilised to compare with the O*NET database of US Department of Labor (O*NET Resource Center, 2020).

Our data analysis shows that when workers' backgrounds and experience are considered, training can be customised to focus only on what they need to learn and skip what they have already mastered. The developed competency model implements a gap analysis across different domains with a directional metric, namely Kullback–Leibler (KL) divergence algorithm (Kullback and Leibler, 1951). KL divergence is normalised to a similarity measure and a heatmap to visualise similarity across domains and jobs is generated in Figure 3. The transition difficulty is discretised to five categories for easier identification (Very Easy, Easy, Medium, Hard, Very Hard).

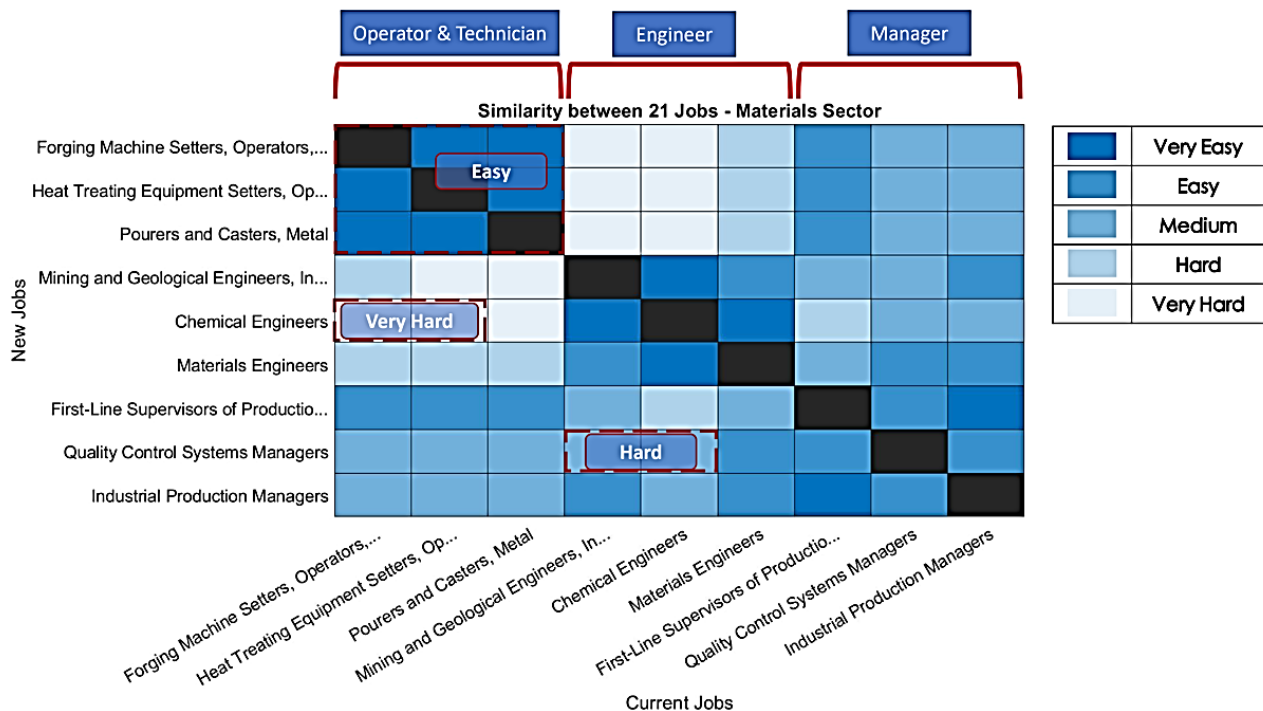


FIG 3 – Heatmap that shows the skill gaps across the domains of operator/technician, engineer, and manager.

As seen in Figure 3, jobs within a domain are close to each other and transition within the same/similar domain is easier. On the other hand, the heatmap reveals the hardship level to transition between different domains and navigates easier paths to accelerate worker transitions across different fields.

Outcomes and intellectual merit

Powered by human-centred, scalable AI techniques, the AI system offers an integrative approach to generate a job seeker profile that is based on technical skills, professional skills, work values, and desires—a holistic evaluation of job-seeking individuals. Apart from its immediate implementation in mining industry as a testbed, it is interactive, explainable, and adaptive to specific industries; that is, cross-industry job transformation analysis and training program generation. The tool will provide tailored training recommendations for individuals to optimise their job prospects.

The system will connect individual workers with jobs where periodic retraining and upskilling will be increasingly essential in the future of work. The proposed program will positively impact both job seekers and employers in the following ways:

- Skill retention and new job transformation for individual workers.
- Guidance for companies to develop training programs and find qualified workers.
- Cross-industry job transformation analysis and training program generation, such as job shifts from the conventional fossil fuel sector to the renewable energy sector.

- Prediction of training cost reduction for industrial skill shift, which is a novel concept for emerging jobs.
- Long-term, enabling data population of worker data, company data, and third-party data (eg government and industry organisational data) to forecast future gaps and demands.

The results show that our tool can facilitate the transition of ongoing job transformations by revealing shifting necessities of the evolving jobs in the mining sector and linking them to each employee in a fast and effective manner.

The developed AI technology will generate personalised job skill and training recommendation techniques for emerging jobs, which will support displaced workers and connect them to new job and training opportunities. The personalised training and assessment translates to workers from diverse backgrounds and areas. It focuses on specific individual profiles, which will allow assessing their needs as well as considering what they have already mastered. This will cut training time significantly while boosting knowledge and skills acquisition, building workers' self-awareness and self-confidence, and ensure fair treatment of workers.

For future work, once the developed tool provides personalised needs, the development of personalised training essentials will be generated. Transformation of the training process using AR/VR tools provides a great opportunity in developing personalised training materials. Furthermore, the development of personalised VR/AR-based models to assess the efficiency of the personalised training models can enable a faster transition in terms of identifying the immediate needs as well. In the long-term, the AI-enabled ecosystem will enable population of worker, company, and third-party data (eg government and industry organisational data) to forecast future gaps and demands.

ACKNOWLEDGEMENTS

This work was funded by NSF, Project Number: B6992 AI-Enabled Personalized Training for Displaced Workers in Materials Supply Chain.

REFERENCES

- Kullback, S and Leibler, R A, 1951. JSTOR: The Annals of Mathematical Statistics, Vol. 22, No. 1 (Mar., 1951), pp. 79–86, *Ann. Math. Stat.*
- O*NET Resource Center, 2020. Accessed on: May. 10, 2020. [Online]. Available: <https://www.onetcenter.org/>
- Zhou, J, Cui, G, Hu, S, Zhang, Z, Yang, C, Liu, Z, Wang, L, Li, C and Sun, M, 2018. Graph Neural Networks: A Review of Methods and Applications, doi: <https://arxiv.org/abs/1812.08434>.

IoT

Optimising blast hole loading with MWD and 3D image analysis

B Gyngell¹, T Buschjost², T Worsey³ and G Diehr⁴

1. COO, Strayos, Sydney NSW 2026. Email: brad.gyngell@strayos.com
2. Mine Engineer, Sandvik, Jefferson City MO 65101. Email: todd.buschjost@sandvik.com
3. Manager, General Drilling, Noblesville IN 46062. Email: gus.diehr@generaldrilling.com
4. Mining Engineer, Lexington KY 40508, Email: tristan.worsey@am.dynonobel.com

ABSTRACT

In recent years, Smart Drills have enabled precise GPS hole navigation along with the generation of rich Measure While Drilling (MWD) data to provide a new perspective on subsurface conditions (Sandvik, 2021). Over the same period, drones have enabled the collection of a visual, geometric, and hyperspectral geological data.

Integrating these new data types into the blast design process allows blasters to optimise fragmentation and prevent flyrock by tailoring each segment of a blast hole to its specific conditions (Epiroc Rock Drills AB, 2019). However, the application of these new technologies has not yet gained widespread adoption in day-to-day practices, largely due to the operational complexity introduced.

To address this issue, this research sought to establish a new workflow for optimising hole loading using MWD and drone data that reduced operational complexity rather than increasing it. The objective was to identify a practical and robust process that could be incorporated into everyday operations rather than just special projects.

Firstly, this paper provides an interpretation framework for MWD data and an understanding of how MWD can be used to gain unique insight into rock mass properties. A list of common MWD parameters is presented with definitions.

Next, the paper outlines a real case study demonstrating a new workflow for using MWD data to identify different strata bands and apply this to make better loading decisions. Practical techniques are described for data capture, analysis, blast design, and blast performance measurement.

This represents a collaborative effort between the site leadership, the blasting contractor, the drilling OEM and the blasting software provider to create an efficient process for achieving measured improvements in blasting outcomes.

In closing, the paper discusses how these techniques can be applied to facilitate more streamlined implementation of variable energy loading. It also presents the future opportunities that machine learning will create for automating seam detection and charging design tailored to rock conditions.

INTRODUCTION

The purpose of this research was to establish a new practical and robust process for incorporating Measure While Drilling (MWD) data into everyday blast design processes. In particular, the team focused on evaluating a method for identifying seams by combining MWD data from multiple holes with 3D contextual data. This research lays the groundwork for enabling custom hole loading by seam as well as AI-powered seam detection.

MWD INTERPRETATION FRAMEWORK

Measure While Drilling (MWD) data refers to the sensor data collected from production drill rigs during operation (Schunnesson, 1990). This is generally comprised of geospatial data (eg penetration rate), pressure data (eg feed pressure) and calculation data (eg rock hardness) (Scoble, Peck and Hendricks, 1989). It is logged at regular intervals (~every 1" or 2 cm) down the hole as the drill operates (Epiroc Rock Drills AB, 2019). Additionally, MWD-enabled drills are also often equipped with a Hole Navigation System (HNS) which captures GPS information on the hole collar position and projected path (Sandvik, 2021).

A summary of the most common output data fields can be found in Table 1.

TABLE 1
Most common data fields for MWD data.

Data field	Data type	Description
Hole depth	Geospatial (MWD)	The vector distance from the hole collar position to the current drill bit position measured in ft or m. Note: This is not just the elevation component
Penetration rate	Geospatial (MWD)	The velocity of the drill bit as it moves through the rock during drilling measured in ft/s or m/s.
Percussion pressure	Pressure (MWD)	The piston pressure used to power the hammer in Top Hammer or DTH drills
Feed pressure	Pressure (MWD)	The hydraulic pressure exerted on the drill stem to move the bit in the direction of drilling
Flush pressure	Pressure (MWD)	The compressed air pressure exerted to push the crushed rock from the drill hole up the outer annulus of the drill pipe and out of the hole
Rotation pressure	Pressure (MWD)	The hydraulic pressure applied to create torque on the drill stem and rotate it as it moves through the rock
Rock hardness	Calculation (MWD)	An estimate of the rock hardness calculated through a proprietary algorithm based on the other Data Types recorded. This may not have units.
Hole collar latitude, longitude and elevation	Geospatial (HNS)	Hole collar position determined by known GPS receiver location mounted on the drill and known displacement of the drill bit from the receiver based on control system information.
Hole toe latitude, longitude and elevation	Geospatial (HNS)	Hole toe position calculated from the known Azimuth and Inclination of the drill bit at the known Hole Collar Position.

This machine information is collected by a range of different hardware devices and control systems; however, the output structure and format are relatively standardised across all providers (Mining Editor, 2021). The main options for collecting MWD data are listed below.

- OEM MWD
- Most new drills from major OEMs come equipped with the sensors to capture MWD data. Activating the data collection from these sensors require be an additional service.
- OEM HNS
- Most major OEMs partner with GPS system providers to offer the option for an integrated HNS offering out of the box. Synchronising this system with site survey control can require an additional service.
- After-market MWD
- Older drills can be retrofitted with MWD sensors by dedicated service and hardware providers
- After-market HNS
- Most drills can be retrofitted with a HNS by the major GPS system providers

METHODOLOGY

Our research methodology followed six main steps, detailed herein.

3D photogrammetric data collection

The equipment used comprised of:

- Off-the-shelf drone with internal RTK GPS system (RTK not used for this project).
- GPS Rover connected with mine survey control system.

First, a series of five Ground Control Points were marked out on the bench surface and floor below. These points were surveyed with the GPS Rover to provide reference points for the 3D model photogrammetry process.

Next, the drone was flown over the bench to collect a set of 57 overlapping images to be used to generate the 3D survey model. These comprised of two flight modes: an autopilot flight mission taking seven passes of nadir photos of the bench surface and floor; and a manual flight mission taking two passes of oblique photos looking at the bench face. Figure 1 shows the locations of each photo taken (white circles) and Ground Control Points (orange crosses):

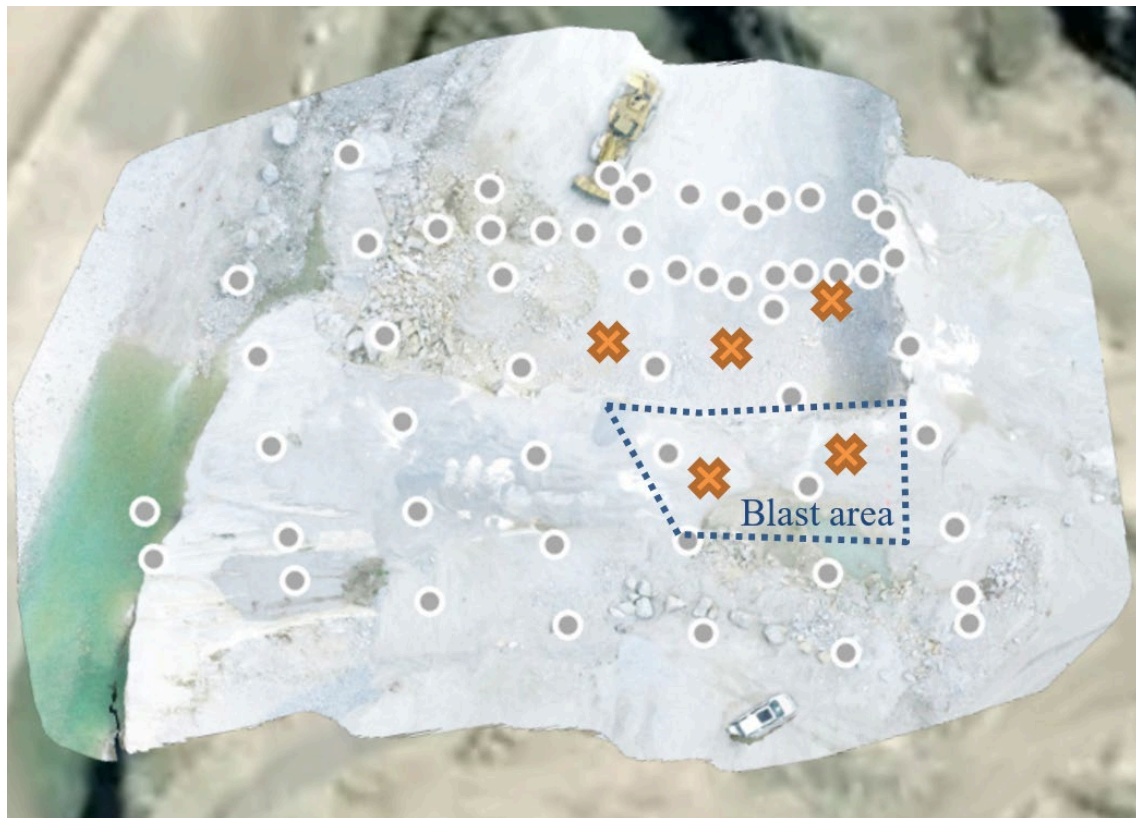


FIG 1 – Drone photo locations and ground control points.

3D photogrammetric processing and drilling design

The images and Ground Control Point data were uploaded to a cloud-based photogrammetry and blast design platform to generate a survey grade 3D photo model of the bench.

The team then used this 3D photo model to design the drill pattern with the tools built into the same software platform. The team designed an 8 ft × 9 ft (2.4 m × 2.7 m) three row staggered pattern with 29 holes, as shown in Figure 2. Front row hole locations were optimised by analysing 3D burdens.

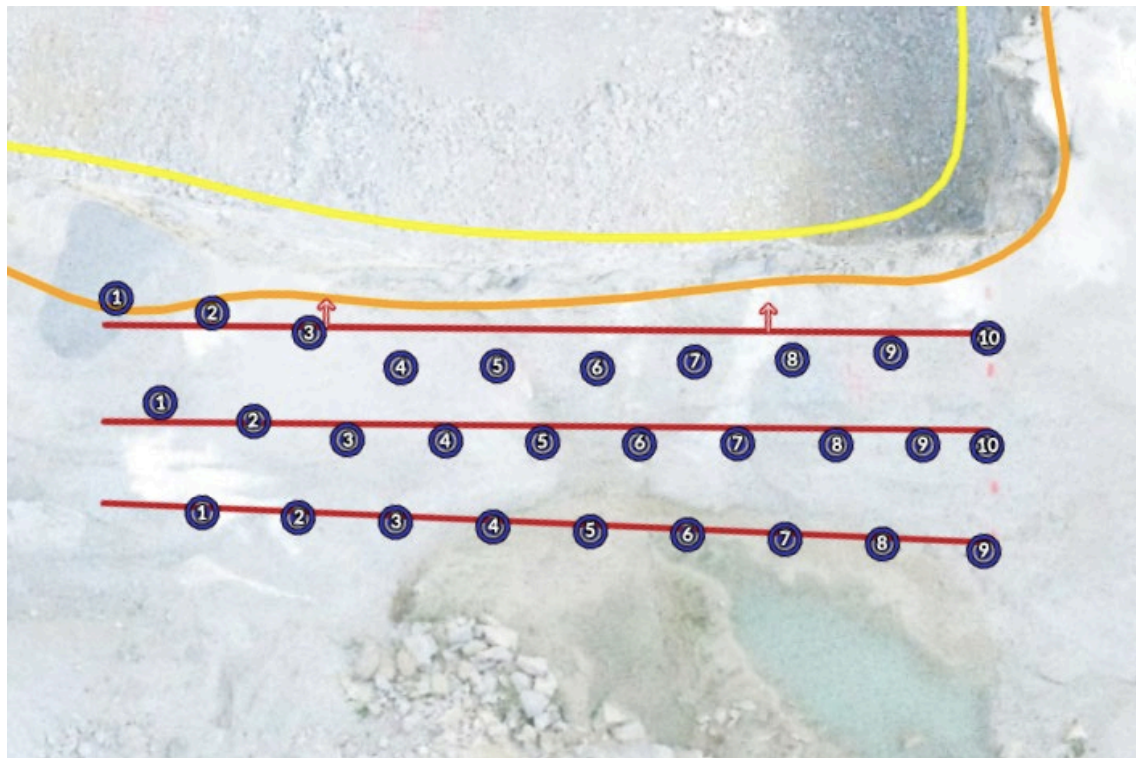


FIG 2 – Drill pattern layout.

The design was then exported directly from the cloud-based blast design platform in the OEM's IREDES file format. This was then uploaded wirelessly to the Smart Drill through the web portal provided for the OEM's communication service.

Measure while drilling data collection

The equipment used for capturing MWD data was a Smart Drill fitted out with OEM drill sensors and GPS Hole Navigation System (HNS). It was synchronised with the mine site survey control system to match the data used for the 3D model Ground Control Points.

The holes were drilled using the HNS system to ensure accurate placement on the bench. As drilled HNS hole locations were compared with the design locations in the blast design platform to ensure drilling quality control.

The MWD data fields captured were Time Tag, Depth Tag, Antijamming State, Feed Pressure, Flushing Pressure, Penetration Rate, Percussion Pressure, Rock Detect, Rotation Pressure, Rotation Speed, Stabilator Pressure, Flushing Flow State, Engine rev/min, Automatic Drilling, Flushing Level, Feed Level, Rock Contact Level, Tools Load Level.

Measure while drilling seam analysis

The MWD and HNS data were pulled wirelessly from the drill back into the cloud-based blast design platform for analysis.

The platform processed the MWD data and automatically combined it with the 3D photo model using the HNS information. Figure 3 shows the Penetration Rate extracted from MWD data visualised in the context of the 3D photo model.

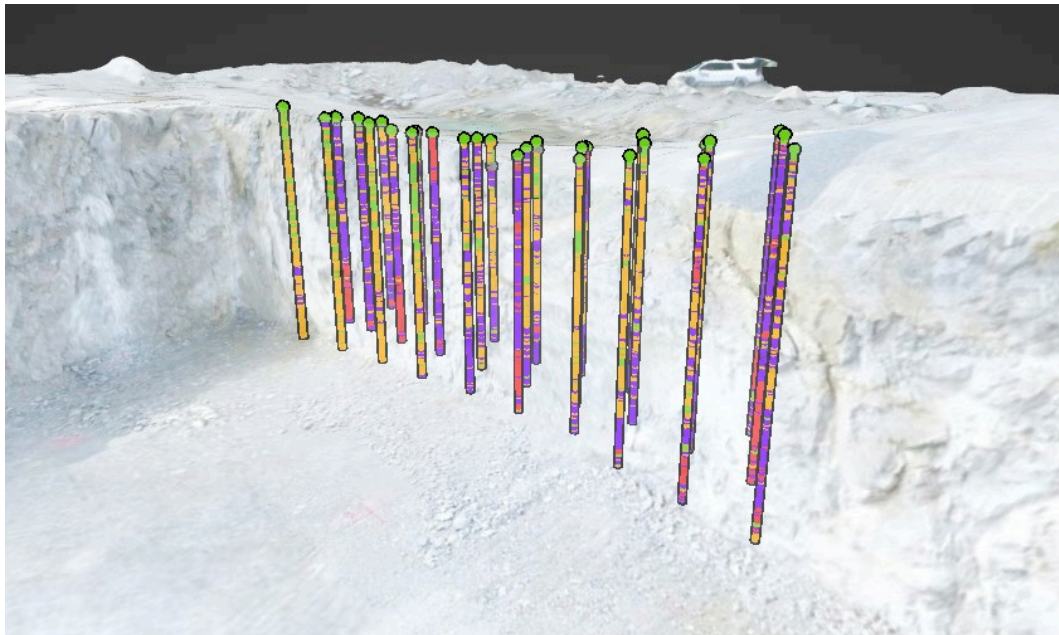


FIG 3 – MWD data (penetration rate) in context of 3D photo model.

Seam detection was also supported by quantitative analysis of the metrics at each depth interval. This was conducted using tools built into the blasting software which aggregate and analyse data from across all holes in the shot. Averages were taken across planes at each depth interval in the shot to identify trends in the bench geology.

Contextual blast loading design

The final step of the process was to integrate the MWD and 3D survey model insights into the blast loading design process.

This was achieved by visualising the MWD parameters as colour-coded bars beside the Burden Profile in the loading design module of the cloud-based blast design platform, as shown in Figure 4. For each hole, the explosive products were adjusted based on the data collected.

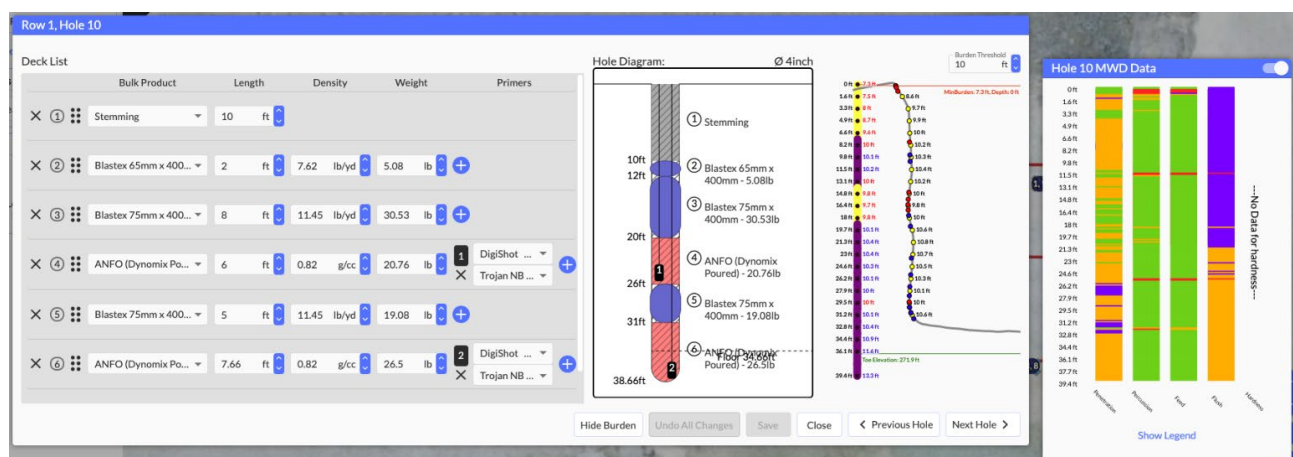


FIG 4 – Blast loading design performed in context of 3D burdens and MWD data.

Artificial intelligence post-blast analysis

After the blast was fired, the muck pile was immediately flown with the drone to capture post-blast images for blast performance analysis. These images were uploaded into the same cloud-based blast design platform to create a post-blast photogrammetric 3D model with automatically generated Fragmentation and Muck pile Movement analyses, as shown in Figure 5.

In this case, Ground Control Points were not required, and the 3D model was created using the drone's onboard GPS. To enable accurate Muck pile Movement analysis, the elevation of the post-blast model was calibrated to the pre-blast model using a common visible marker.

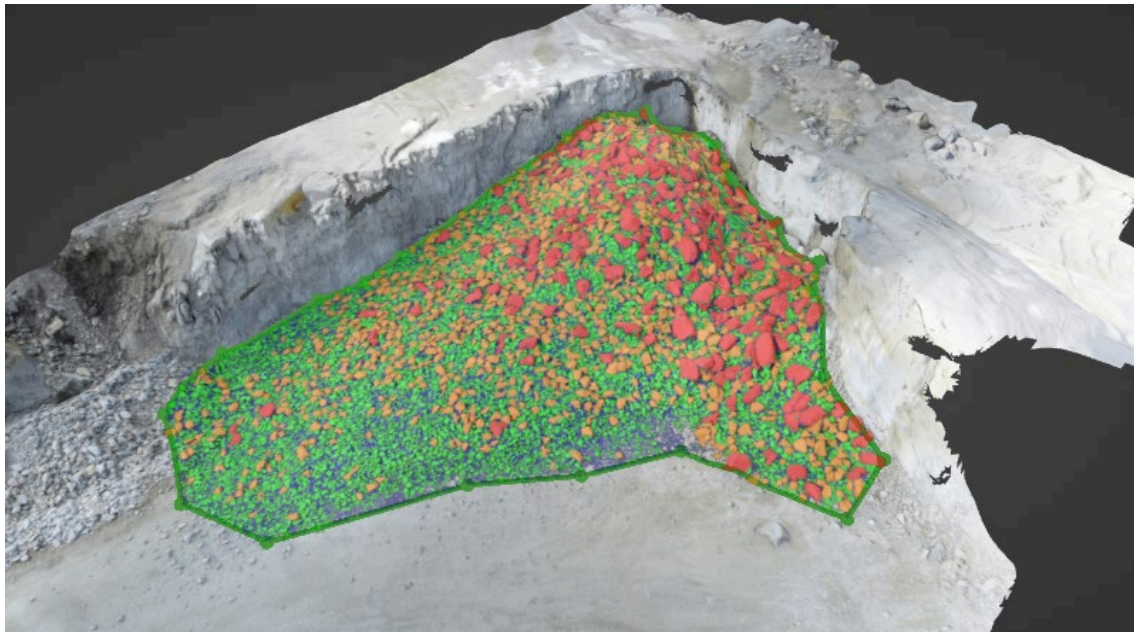


FIG 5 – 3D photogrammetric model of muck pile with fragmentation analysis.

RESULTS

The seam analysis identified two distinct seams within the bench geology:

1. A soft seam from 9.5–15 ft (2.9–4.6 m)
2. A hard seam from 25–29.5 ft (7.6–9.0 m).

All front row holes were custom loaded based on burden and MWD data as shown in Table 2.

TABLE 2

Blast hole loading determined by burden and MWD analysis.

Hole 1	Poured ANFO to 31', 3" Packaged Emulsion to 14', 2.5" Packaged Emulsion to 10', Stem
Hole 2	Poured ANFO to 28', 3" Packaged Emulsion to 12', 2.5" to 10', Stem
Hole 3	Poured ANFO to 28', 3" Packaged Emulsion to 12', 2.5" to 10', Stem
Hole 4	Poured ANFO to 10', Stem
Hole 5	Poured ANFO to 25', 3" Packaged Emulsion to 20', poured ANFO to 15', 3' Packaged Emulsion to 10', Stem
Hole 6	Poured ANFO to 18', 3" Packaged Emulsion to 10', Stem
Hole 7	Poured ANFO to 16', 3" Packaged Emulsion to 12', 2.5" Packaged Emulsion to 10', Stem
Hole 8	Poured ANFO to 10', Stem
Hole 9	Poured ANFO to 28', 3" Packaged Emulsion to 18', 2.5" Packaged Emulsion to 10', Stem
Hole 10	Poured ANFO to 31', 3" Packaged Emulsion to 26', Poured ANFO to 20', 3" Packaged Emulsion to 12', 2.5" Packaged Emulsion to 10', Stem

Tailoring the blast loading to the MWD data and 3D Burden data resulted in high quality blast outcomes. Fragmentation and Muck pile Movement analysis results are shown in Figures 6 and 7, and Table 3.

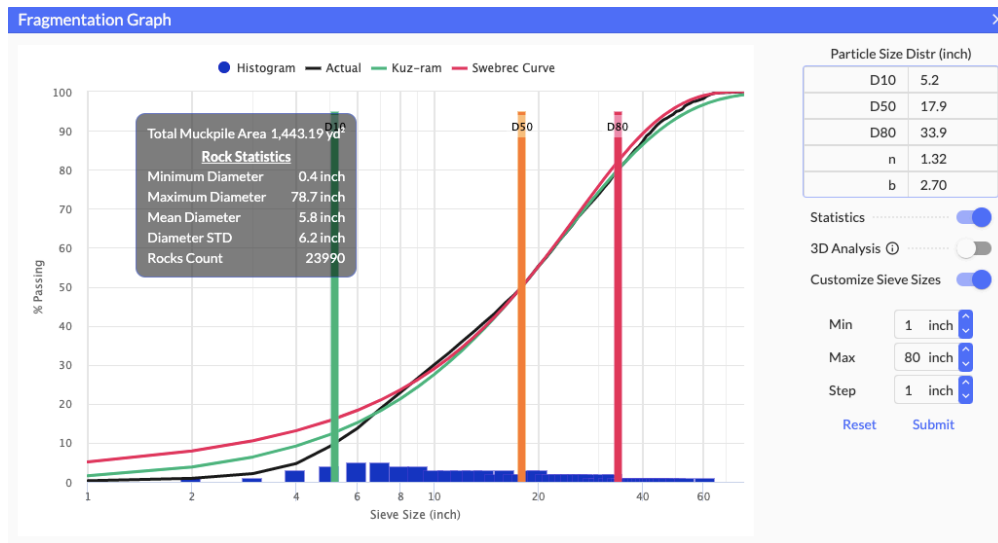


FIG 6 – Results of automated fragmentation analysis.

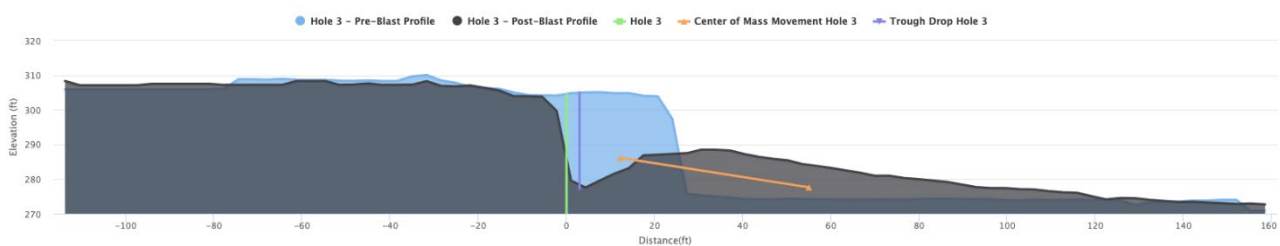


FIG 7 – Example cross-section generated by automated muck pile movement analysis.

TABLE 3

Results of automated muck pile movement analysis.

Pre-blast volume	3782 yd ³
Post-blast volume	4749 yd ³
Swell factor	1.26
Average centre of mass movement	37.8 ft
Maximum throw	51.2 ft
Average throw	164.4 ft
Average trough drop	19.8 ft

ANALYSIS

The results indicate that incorporating MWD for seam identification and blast loading optimisation can be done in a practical way for everyday drilling and blasting operations.

This workflow produced improvements in blast outcomes and increased efficiency in drilling operations by eliminating the requirement to manually measure and lay out the holes.

During this research, the team identified that the usage of Post-Processed Kinematic (PPK) drones could further streamline the field operations by removing the need to mark out Ground Control Points.

The key enablers identified throughout the research process for implementing this approach were as follows:

- Strong collaboration between site teams, drilling contractors and blasting contractors.
- Focus on quality over speed while getting processes up and running.
- Minimising data touch points and automating processes where possible.

Interestingly, tailoring the blast loading with the visualisation of MWD and 3D burden data highlighted several situations where a loading decision made purely based on burden would not have been optimal. There were parts of holes where the minimum burden threshold should have been increased due to soft ground or voids and parts where it could be decreased because of hard ground.

This concept of a 'variable minimum burden' at different depths within a hole, based on rock properties and explosives options, has the potential to bring significant safety benefits to the blasting industry in preventing flyrock and should be further explored in future research.

The approach established in this research also represents a key enabler for more widespread use of differential energy loading. If variable density gassed emulsion product was available, the team could have designed the explosives column in decks of different densities side-by-side with the MWD output as in Figure 4. This could have allowed for a more streamlined charging operation in the field by avoiding the need to switch back and forth between Poured ANFO and packaged decks within each hole.

CONCLUSIONS

This research achieved its purpose of establishing a practical and robust method for applying MWD data to optimise blast hole loading in everyday operations. This lays the groundwork for a wide scope of future work optimising efficiency and safety of blasting operations.

New research should build on this by investigating the impact that a 'variable minimum burden' based on rock properties has on flyrock and front row fragmentation.

Additionally, future research should look to establish AI algorithms for automatic seam detection from MWD data. This could use a combination of pattern recognition and clustering methods to automate that process step.

All these steps lead toward a future where highly tailored and optimised blasting is accessible across more sites. Using technology to unlock new workflows that are practical as well as powerful will be the key to lifting the industry to the next level of safety and efficiency.

ACKNOWLEDGEMENTS

We would like to sincerely thank Sam Howrigan and Shelburne Limestone Corporation for making their site and data available to conduct this research.

We would also like to thank Strayos, Inc. for making their cloud-based photogrammetry and blasting software platform available for processing the data and performing the analysis/blast design.

We would also like to express thanks to Sandvik for providing Smart Drill hardware and expert input on the details of MWD interpretation. Finally, we would like to thank Nathan Rouse, Dyno Consult and Mike Allen, Martin Marietta for their feedback and guidance for MWD data applications.

REFERENCES

- Epiroc Rock Drills AB, 2019. *Reference Book: Drilling in Surface Mining, Quarrying and Construction*, Örebro, Sweden.
- Mining Editor, 2021. Sandvik evolves drill rig to support fully autonomous operation, *Australasian Mine Safety Journal*, Retrieved August 2021 from <https://www.amsj.com.au/sandvik-evolves-drill-rig-to-support-fully-autonomous-operation/>
- Sandvik, 2021. Choosing the Right Rig for the Job, retrieved August 2021 from <https://go.rocktechnology.sandvik/490131/2020-05-01/5ryhdb>
- Schunnesson, H, 1990. Drill Process Monitoring in Percussive Drilling, Luleå University of Technology, Division of Mining Equipment Engineering.
- Scoble, M J, Peck, J and Hendricks, C, 1989. Correlation between rotary drill performance parameters and borehole geophysical logging, *Mining Science and Technology*, 8(3), 301–312.

Enabling the digital mine of the future through autonomous underground data capture

S Hrabar¹ and J Gray²

1. CEO and Co-Founder, Emesent, Brisbane Qld 4000. Email: stefan.hrabar@emesent.io
2. Mining Research Specialist, Emesent, Brisbane Qld 4000. Email: jane.gray@emesent.io

INTRODUCTION

Remote sensing data capture in the mining industry has been exponentially evolving over the last ten years. We are capturing data at an increased resolution, accuracy, and ever-shorter intervals of time, enabling a dynamic digital twin of a mine, above and below ground, and databased decision-making and planning. Furthermore, advances in data processing and analysis offer the promise of data sharing across an organisation. Intelligent remote sensing systems that reduce human involvement in data capture, georeferencing and processing help mines achieve the goals of data-driven decision-making and dynamic data models.

Mining companies are also facing new challenges. ESG policies demand increased focus on sustainable mining, however the depletion of near surface orebodies means mines are getting deeper and cut-off grades lower. Deeper mines increase hazards such as seismicity and add to the complexity of maintaining efficient extraction throughout the Life-of-mine to maintain profitability. Addressing these challenges require better data collected at ever shorter time interval. Essentially, more and detailed inspections, which paradoxically increase worker exposure to hazards.

Mining companies already use remote sensing technologies in exploration and mining. Aerial scanning typically depends on GNSS systems for operation and georeferencing, but intelligent and autonomous mapping systems, such as the Emesent Hovermap, breaks this impasse by delivering inspection and production data, above and below ground, without compromising the safety of personnel.

Addressing the challenges in underground mining with autonomous data capture

Technology has long been recognised as the key approach to managing the risks of underground mining. In an AusIMM Bulletin article, Price (2019) discussed a range of challenges that are targets for technology solutions. Here we discuss these in the context of autonomous remote sensing systems capable of operating in harsh, GPS-denied environments.

Extracting minerals from lower grades

The number of large, high-grade deposits is declining; hence, mining reserves need to include lower cut-off grades.

Technology and automation contribute to lower cut-off grades by lowering mining costs. Companies are applying automation and data analytics throughout the mining cycle. Advances in remote sensing technologies, like Hovermap also contribute by reducing the exposure risk to personnel and increasing the quality and frequency of data capture.

These mines are using Hovermap to remove the guesswork from stope operations, with accurate, timely data that helps minimise ore loss and dilution.

Evolution Mining's Mungari underground operation produces more than 125 000 ounces of gold a year. Mineralisation occurs in a zone 70 m wide by 400 m long with ore lodes two to 20 metres thick. The site uses a narrow top-down bench stoping with paste fill mining method. Hovermap replaced a traditional cavity monitoring system (CMS), which was time consuming, posed a safety risk to personnel, and produced poor data coverage and quality. Capable of autonomous flight, Hovermap is flown into stopes at frequent intervals, capturing accurate, high-resolution data that informs geotechnical conditions, fragmentation, oversize, over- or underbreak, and volume (Figure 1). Mungari's Deswik system processes and georeferences the data in less than 30 minutes, delivering data to engineering, survey, geology and geotech. By comparing final stope shape to design, the

teams can pursue continuous improvement in stope and blast design, helping to reduce dilution and ore loss, and personnel exposure to open stopes.

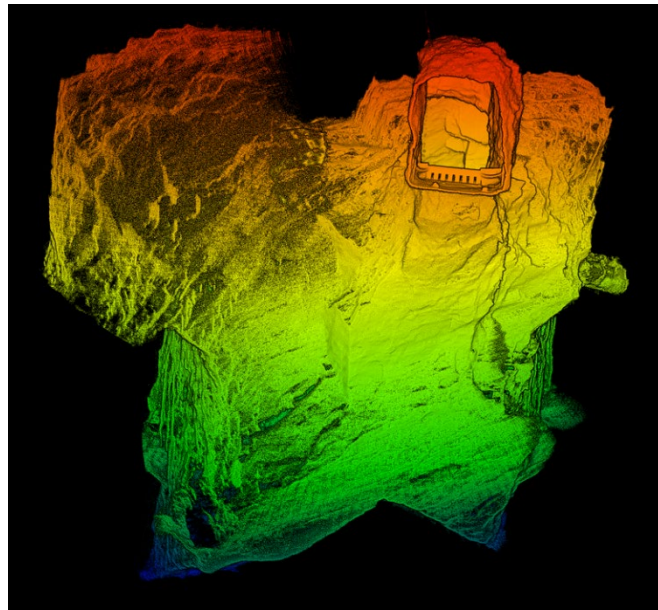


FIG 1 – Remote inspections of stopes at Evolution’s Mungari mine capture high-resolution data that improves the accuracy of stope volume, geometry and geological structures.

Extracting minerals from greater depths

With fewer large, near surface deposits being discovered, underground mines are following the lode to greater depths. Mining at depths has its challenges. High rock stresses cause extensive deformation and seismicity, making geotechnical risks the limit on the mining rate, rather than equipment capacity. The increased geotechnical risks demand more frequent and detailed inspections of production areas and access drives.

Glencore’s Kidd Operations is one of the deepest base metal mines in the world. Mining at around three kms below the surface, ground stresses cause failures that impact the operation’s mining rates or compromise access to future stopes. Seismicity is a constant issue, for both production and inspections.

The mine employs Hovermap across the operation to measure drive convergence, stope performance and re-entry to previously mined areas (Figure 2). Data is rapidly georeferenced and made available to survey, engineering, geotech and geology. A high degree of detail is extracted from each autonomous stope flight, which adds to the mine model and provides the data that inform strategies to deal with problem stopes. The mine is able to maintain safe operations and maximise output.



FIG 2 – Glencore’s Kidd Operations, an ultra-deep base metal mine located in Ontario, Canada, deploys Hovermap to remotely inspect stopes and drives throughout the mine.

Small footprint mining

With machinery automation driving down the number of on-site personnel and the increased focus on sustainable mining, an operation’s environmental footprint will continue to shrink. Intelligent remote sensing systems play an important role by removing people from the data capture process, streamlining data capture workflows and maximising development and production efficiency.

Australia’s largest mining companies use Hovermap’s autonomy capabilities to improve safety and efficiency. Surveyors now rely on remote data capture in high-risk areas such as drawpoints, stopes, old workings, vertical infrastructure, and production drives. Convergence monitoring is transitioning from manual techniques to remote sensing methods.

When a mine experiences a serious seismic event that triggers a fall-of-ground, autonomous remote sensing systems can perform inspections with minimal personnel. In 2020, LKAB’s Kiruna iron ore mine had a fall-of-ground that closed kilometres of drives. Within four days, AMKVO, a geospatial consultancy, used Hovermap to scan the affected areas and deliver detailed data that mine geotechnical engineers could use to assess the damage and plan remediation (Figure 3).

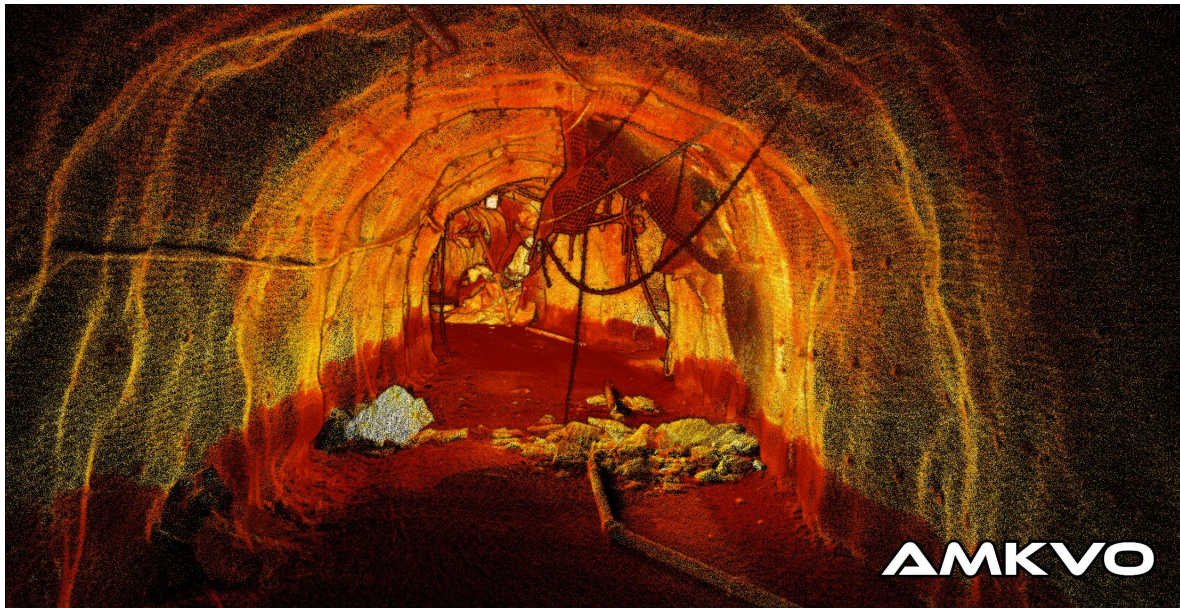


FIG 3 – At LKAB’s Kiruna mine, tens of kilometres of drives were remotely inspected using Hovermap following a seismic event. The resultant point cloud data was immediately processed, producing visuals, like this image, and baseline data sets for further geotechnical analysis.

Recent autonomy advances allow even greater levels of remote operation of the Hovermap system. At Kidd Operations, Hovermap performed an autonomous stope flight while being operated remotely from Australia. Further developments will allow take-off and landing from ground-based robots to extend flight range.

CONCLUSION

Intelligent remote sensing technologies are already used widely across mining operations to capture detailed data of critical production areas too dangerous for personnel, at an increased frequency. This technology can streamline workflows and remove personnel. Increased use will also help mining companies maximise operational efficiency and safety, enabling them to remain profitable with lower cut-off grades and mine at greater depths.

REFERENCE

Price, R, 2019. Ten mining challenges technology could solve. *AusIMM Bulletin*, (Jun 2019).

Optically powered monitoring networks

F Ladouceur¹, Y Chen² and L Silvestri³

1. Professor, UNSW, Sydney NSW 2052. Email: f.ladouceur@unsw.edu.au

2. Research Engineer, UNSW, Sydney NSW 2052. Email: yingge.chen@unsw.edu.au

3. Adjunct Fellow, UNSW, Sydney NSW 2052. Email: l.silvestri@unsw.edu.au

INTRODUCTION

Continuous monitoring of mine atmosphere is essential for the safety, health and productivity of a mine. The presence of gases like CH₄, CO₂, CO and O₂ are relevant indicators of safety risks and gas monitoring systems recording the corresponding values and trends are required especially in the most hazardous zones like return airway and longwall face. In these remote and harsh areas, electrical power delivery is not always safe nor stable, and sometimes not available. Existing gas sensors are normally powered electrically via physical connections and require an uninterruptible power supply (UPS) in case of power shortage. The increasing number of installed sensors thus raises the risk of sparks and drives up the costs of installation and cable management.

An optically powered, intrinsically safe gas monitoring system was developed to measure four essential environmental gases (CH₄, CO₂, CO and O₂), ambient temperature and pressure for underground mines (see Figure 1).



FIG 1 – Intrinsically safe, optically powered gas monitoring system. This exact system was deployed on December 17, 2020 at the BMA-operated mine of Broadmeadow.

The system consists of two gas monitoring stations designed to be installed underground and of a remote terminal unit (RTU) on the surface connected to the local network via ethernet. The gas monitoring stations are entirely powered optically by the light sent from the RTU and transmit all sensor information optically back to the RTU via the same optical path. The signal is then converted to digital electrical signal for data logging and web page display.

The system is based on two key optical technologies developed at UNSW: (1) power-over-fibre (PoF) at 1550 nm using a single industry-standard, low cost single-mode fibre (SMF) for both power delivery and information transmission, and (2) liquid-crystal-based optical transducers for optical telemetry (Brodzeli, Silvestri and Michie, 2013; Firth, Ladouceur and Brodzeli, 2016, 2017). The ultra-low power consumption design of the electronics and data transmission approach allows each gas monitoring station to operate with less than 150 MW optical power, meeting the intrinsic safety requirement (IEC60079–28).

Compared with conventional electrically powered gas sensors, this technology bypasses the usual roadblocks of underground gas monitoring where electrical power is either unsafe or unavailable.

Furthermore, using one fibre for both power delivery and data transmission enables longer distance coverage, reduces optical cabling and increases multiplexing possibilities.

FIELD WORK

A 2-month field trial at BMA's Broadmeadow underground mine proved the cabling compatibility to the mine's existing optical network and the stability of the system performance. The system was installed at two distinct locations: the two gas monitoring stations were installed side-by-side underground about 150 metres below the surface and the RTU on the surface in an air-conditioned, on-site communication room (aka Comms Hut). In the Comms Hut, the RTU's optical output channels were connected to two cores of a 250-meter long optical fibre cable running from the surface to an underground location (aka cut-through) into the marshalling cabinet and breakout box where the two cores were further connected to the ruggedised optical cable to power the two stations. The optical network configuration and installation of the system are illustrated in Figure 2(a) and Figure 2(b).

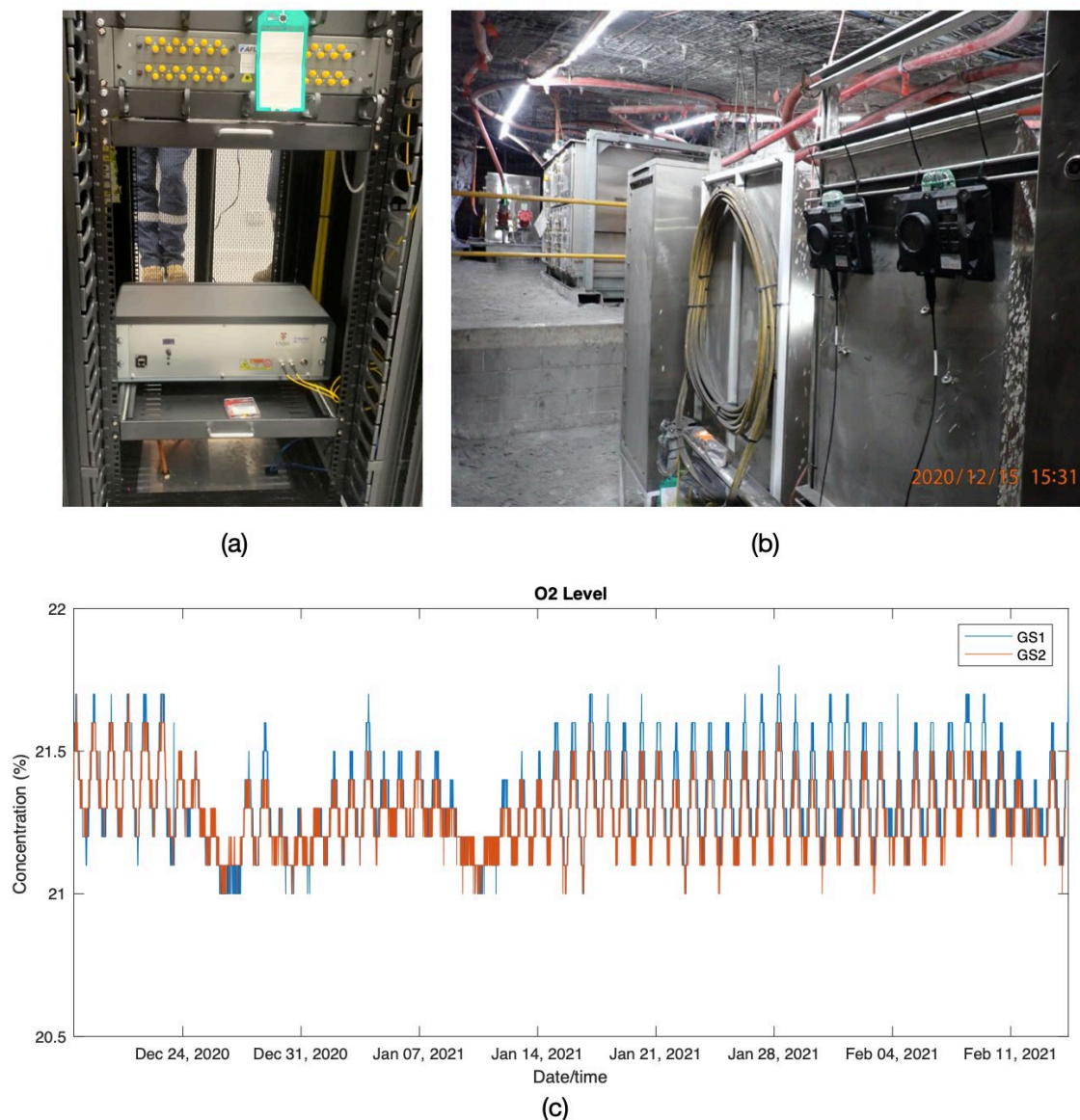


FIG 2 – Field trial of the system at Broadmeadow mine. (a) RTU is installed on the surface at the Comms hut connecting to the mine's optical fibre network. (b) Two gas monitoring stations installed 150 m underground for environmental gas detection. (c) Oxygen levels as reported by both stations over the period of the field trial.

The data collected covers the period from 17/12/2020 (at 13:04) to 14/02/2021 (09:48), in other words 59 days or 1413 consecutive hours. For the entire duration of the field trials, both monitoring

stations were placed side-by-side in a relatively clean environment and reported consistent data for all measured quantities.

All data was acquired in the Broadmeadow control room sitting on the surface and connected to RTU via ethernet. The monitoring capabilities of the stations include CO, CO₂, CH₄ and O₂. Under the conditions of the test, and except for oxygen, all gas levels are essentially zero and are within the noise of the respective sensors. Figure 2(c) illustrates the levels of O₂ as reported by both stations. The plotting scale clearly highlights the digital nature of the data as reported to the RTU on a quantified grid using integer multiple of 0.1 per cent. Please note the excellent agreement between both stations: in fact, calculating the standard deviation of the difference in concentration reported by both stations yields 0.070 per cent.

CONCLUSION

The current project aimed at delivering a fully functional, intrinsically safe, ruggedised optically powered gas sensing network and the path taken to achieve this goal has been detailed herein. Doing so, the viability of PoF technology for intrinsically safe, multi-gas monitoring station over long distance has been demonstrated.

The field trials have also successfully proven that the technology can be deployed under real-life conditions. Furthermore, the network remained in operation for almost 60 days uninterrupted and both stations reported cross-validated data (ie data sets in agreement with each other).

Although this project focused on gas monitoring, the technology presented as enables new and better monitoring approaches especially under conditions where intrinsically safe monitoring over large areas (or long distances) are required.

ACKNOWLEDGEMENTS

Our first words of gratitude go to ACARP who supported the work reported herein. More specifically, the authors would like to single out Mr Peter Bergin who acted as the ACARP liaison officer throughout the project duration. Our thanks also go to all grant monitors who provided invaluable inputs over the two years of the project: Ben McCamley, Brad Lucke, Dave Young, Greg Briggs and Bharath Belle.

REFERENCES

- Brodzeli, Z, Silvestri, L and Michie, A, 2013. Sensors at your fibre tips: a novel liquid crystal-based photonic transducer for sensing systems. *Journal of Lightwave Technology*, 31:2940–2946.
- Firth, J, Ladouceur, F and Brodzeli, Z, 2016. A novel optical telemetry system applied to flowmeter networks. *Flow Measurement and Instrumentation*, 48:15–19.
- Firth, J, Ladouceur, F and Brodzeli, Z, 2017. Liquid crystal based optical telemetry applied to 4–20 ma current loop networks. *Sensors and Actuators*, A260:124–130.

The potential of a mine-wide digital rock mass condition monitoring system

M Nöger¹, T Ladinig², P Hartlieb³, D Dendl⁴, P Moser⁵ and T Griesser⁶

1. Junior Researcher, Montanuniversitaet Leoben, Leoben Austria 8700.
Email: michael.noeger@unileoben.ac.at
2. Senior Researcher, Montanuniversitaet Leoben, Leoben Austria 8700.
Email: tobias.ladinig@unileoben.ac.at
3. Senior Researcher, Montanuniversitaet Leoben, Leoben Austria 8700.
Email: philipp.hartlieb@unileoben.ac.at
4. Technical Director, DSI Underground, Linz Austria 4061.
Email: dominik.dendl@dsiunderground.at
5. Head of Chair, Montanuniversitaet Leoben, Leoben Austria 8700.
Email: peter.moser@unileoben.ac.at
6. Group Leader, Montanuniversitaet Leoben, Leoben Austria 8700.
Email: thomas.griesser@unileoben.ac.at

INTRODUCTION

Currently rock mass monitoring programs are strongly based on observations conducted by engineering personnel on the mine as well as specific monitoring devices installed on selected locations. Shortcomings are that visual inspections of all mine openings are practically impossible on a weekly or daily basis and that documented monitoring data is mostly rather sparse and dependent on local rock mass and stress conditions. As a result, data collection, processing and analysis are rather slow and heavily dependent on experience. Judgement and interpretation are necessary in order to get an overview of ongoing rock mechanics processes, such as stress redistributions, rock fracturing, instabilities etc. Moreover, the evaluation of data needs some time. Accordingly, information and knowledge lag behind ongoing mining activities. The availability of mine wide, real time rock mass monitoring data could overcome at least some of the latter issues. Digital rock bolts providing information about the state of the bolt and deformation of the rock mass could provide this data. If such data were available, it could be used as an integral part of rock mechanical mine design and mine operation. Examples are derivation of (objective) rock mass characterisation and classification, support on demand or adoption of mining layout and mining sequence on demand. Challenges are especially related to the issue that underlying rock mass deformation and failure characteristics must be understood in order to gain benefits from mine wide, real time data. The latter aspect requires further research.

SENSOR EQUIPPED ROCK BOLTS

The list of requirements on modern monitoring systems to fulfil their defined purpose is quite extensive. For instance, information should be provided with high accuracy, spatial, rather than punctual and with small temporal intervals to track changes in ground conditions, as well as their rate, and time dependency in all areas of the mine. Moreover, to guarantee successful mine wide application, a system should be designed for easy and fast installation at low costs, which can withstand the harsh conditions of the underground environment. Additionally, efficient data handling, which includes the accumulation, transfer and automatisation in the analysis of the data, will play a key role in managing massive data sets and extracting information from them. An option to overcome many of these critical aspects is making use of rock bolts, which provide information of the bolt state and bolt deformation. Therefore, such bolts could be installed mine wide. Newly developed rock bolts could make use of methods in the application of low-cost measuring equipment, which has only insignificant influence on the price compared to 'normal' rock bolts. Furthermore, the process of handling and installing these bolts should be equivalent to current standard procedures, and, hence, no changes to procedure or equipment should disturb the mining process. For this reason, the cheap sensorised rock could contribute to monitor mine wide changes in rock mass conditions.

OPPORTUNITIES OF SENSORISED ROCK BOLTS

A considerable chance in the utilisation of such rock bolts lies in the low-cost availability as well as the easy installation of the digitalised rock support system. Due to possible mine wide application of such rock bolts, changing conditions in all areas of the mine, even in places where deformations have not been predicted or expected, may become recognisable in an early phase enabling quicker and more efficient reaction. Moreover, it is also possible observing the effectiveness of these mitigation measures in real-time.

Because of the availability of sensor equipped low-cost rock bolts could enable dense installation patterns. The vision is to detect rock mass specific deformation patterns by analysing the values of every single rock bolt installed in the mine. This enables identifying the characteristic deformation patterns, which are strongly linked to the prevailing rock mass and stress conditions, more reliably. How the different rock masses react in terms of deformation rates, magnitude and deformation distribution related to support measures and mining activities can also be analysed to gain knowledge of the rock mass behaviour and extract parameters describing its mechanical properties.

Data will be analysed to make statements in terms of bolt functionality. Hence, information of the bolt state, distinguishing between elastic, yielding or failed status, as well as the current build-up reaction force, will be extracted. That additional information can be used to evaluate the functionality of the rock support system. The continuous inspection of changing ground conditions using sensor equipped rock bolts can be beneficial for rock mechanical applications. On the one hand an improved understanding in the rock mass behaviour and an attempt to describe those with mechanical parameters will contribute to an optimisation in the mine design. On the other hand, the reaction of the rock mass related to changes in the design will be tracked, unwanted trends can be identified and according adjustments can be set easily. Furthermore, measures to control the ground conditions with rock bolt support can be checked to its functionality and statements according to the effectiveness of the support system can be taken. Consequently, optimising the support system is possible in different mining areas, which effects positively safe and economic support design. Accordingly, support design on demand becomes possible.

Finally, all this effort of extracting information regarding rock mass behaviour, support effectiveness and consistent observation can be done, to provide basic information which helps the engineer combined with individual experience to judge the regional as well as the local stability in all mining areas and to ensure safe, sustainable and economic mineral extraction. Based on the deformation data of the rock bolts, continuous areal and temporal monitoring of changing rock mass condition will be possible.

ACKNOWLEDGEMENTS

This work has been conducted within the 'illuMINEation'-project which received funding from the European Union's Horizon 2020 research and innovation programme under grant agreement No. 869379.

Optical light microscopy – a novel tool for near real time coalmine dust monitoring

N Santa¹, E Sarver², C Keles³ and J R Saylor⁴

1. Graduate Research Assistant, Virginia Tech, Blacksburg, Virginia 24061. Email: nsanta@vt.edu
2. Associate Professor, Virginia Tech, Blacksburg, Virginia 24061. Email: esarver@vt.edu
3. Senior Research Associate, Virginia Tech, Blacksburg, Virginia 24061. Email: cigdem@vt.edu
4. Professor, Clemson University, Clemson, South Carolina 29634. Email: jsaylor@clemson.edu

INTRODUCTION

As highlighted by the resurgence of occupational lung diseases among miners in the United States and Australia, respirable coalmine dust (RCMD) exposures remain a significant risk. A thorough understanding of RCMD composition and source contributions is critical to elucidating the disease factors in particular regions and improving dust controls and exposure prevention measures. To this end, there have been growing calls for new monitoring technologies.

While recent advances have enabled continuous measurements of RCMD mass concentration, capabilities for tracking specific dust constituents are still needed. In particular, real-time (or near real-time) measurement of the mineral content in RCMD would be valuable since certain mineral constituents such as crystalline silica are considered more hazardous than others.

OPTICAL MICROSCOPY AS A MONITORING TOOL

Optical microscopy (OM) has long been used for mineral identification. The advent of portable OM, image processing techniques, and rapid computation in small devices may offer a path for developing novel monitoring technologies for RCMD. Indeed, portable 'cell phone microscopy' is already being used in a range of health-related field monitoring applications (eg to diagnose blood-borne pathogen infections). Figure 1 illustrates a basic concept for an OM-based semi-continuous RCMD monitor. First, a sampling pump collects dust for a brief interval on an appropriate medium. A series of microscopic images are then acquired using a small camera device, such as a modified cell phone. These images are then processed to count particles and determine their properties. Finally, the trained models predict the mineralogy and distributions based on the particle features (Figure 1). The data collected by the monitor can be used to target specific areas or potential dust sources that need to be controlled to mitigate exposure.

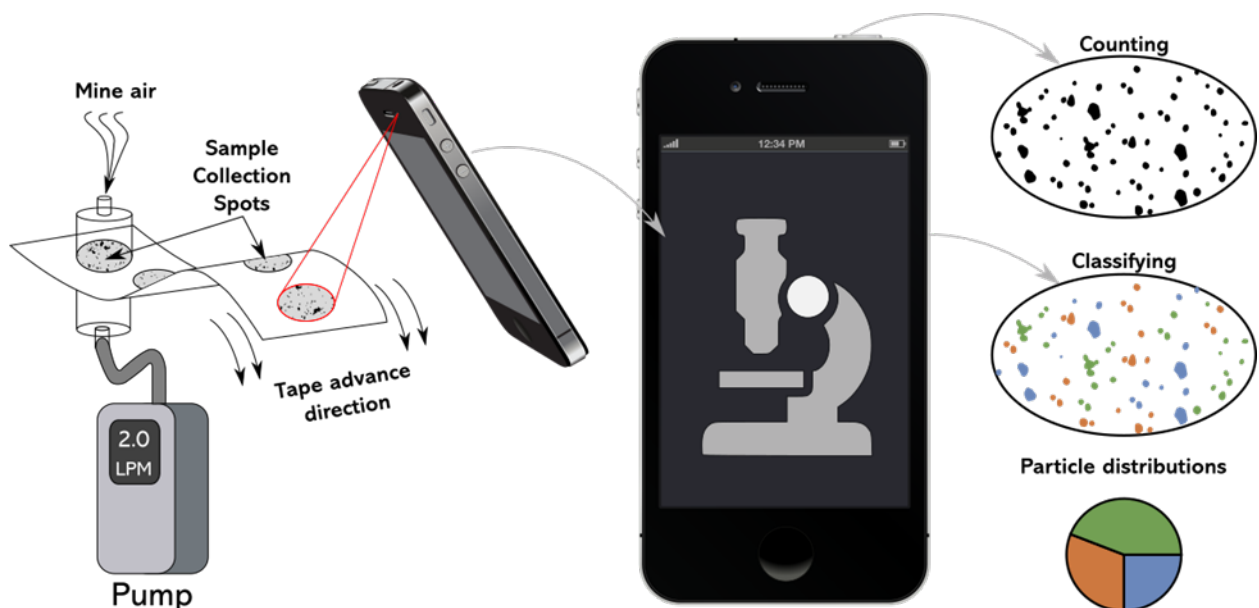


FIG 1 – Conceptual illustration of a semi-continuous coalmine dust monitor that uses an optical cell-phone microscope to count and classify particles.

RESEARCH RESULTS TO DATE

As a first step to prove the underlying OM approach, initial research was aimed at simply distinguishing coal dust from the types of mineral dust commonly expected in RCMD (ie crystalline silica, silicates, and carbonates). By exploiting the mineral particles' birefringence, which causes them to appear illuminated under polarised light, results showed that respirable-sized dust could accurately be separated into two fractions: coal and mineral. While even this simple fractionation may be quite helpful for tracking dust source contributions in specific mine locations, observed differences in the optical and topological properties of the mineral particles suggest that further classification into specific mineral types should be possible. For example, the primary mineral types show subtle differences in colour, texture, shape, and brightness.

Therefore, the current work is aimed at more thoroughly investigating those particle characteristics that could be used for mineral subclassification – with a specific focus on silica. For this, an Olympus BX53M polarising microscope and the Stream Start 2.3 imaging software are used to capture images of respirable particles representative of each of four main RCMD constituents: coal sourced from the target coal seam; crystalline silica, kaolinite (as a proxy for aluminosilicates), sourced from the rock strata in the mine; and high-purity limestone (as a proxy for rock dust products), sourced from rock dust application to mine surfaces. The dust samples are prepared by depositing respirable particles on glass coverslips using Dorr-Oliver cyclones attached to air pumps within a small chamber. The data set of OM images is processed to separate particle pixels from the background and then to locate, label, and extract particle feature information, including particle intensity values in different lighting conditions and size/shape metrics. Images of known particles (ie from single material samples) are used to quantify differences in various optical and/or topological features between the mineral types, and the most promising features are selected for modelling. Following model training, results on composite samples (ie containing multiple mineral types) are compared to those obtained by scanning electron microscopy (SEM) with energy dispersive X-ray (EDX) as a reference method.

Preliminary results on mineral subclassification suggest that using the multiplication of mean particle intensities (MMPI) in plane- and cross-polarised light might allow separating silica particles from other minerals. Using an MMPI model, the accuracy for silica classification in the model training and test data sets was 87.4 per cent and 87.5 per cent, respectively (Figure 2a). Finally, the model was challenged on composite samples containing coal (C), silica (S), and other minerals such as kaolinite (K) and rock dust (RD). A stepwise process separated the dust into three fractions (eg coal, silica, and other minerals). First, coal particles were identified via its lack of birefringence. Then, the fractions of silica and other minerals were computed using the MMPI model. The results were compared to SEM-EDX analysis (Figure 2b).

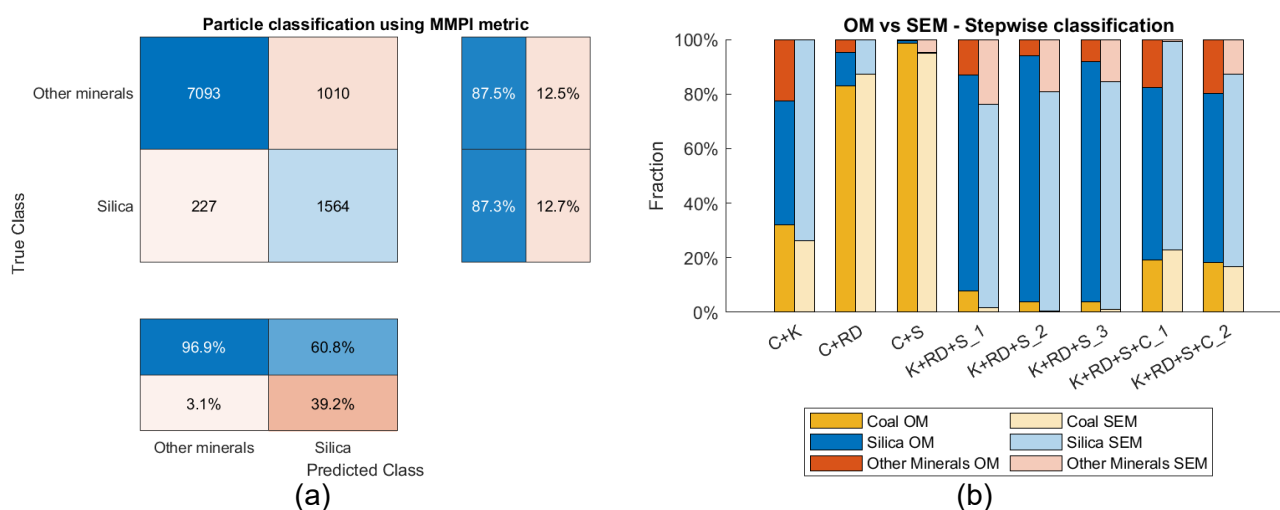


FIG 2 – Confusion matrix of the MMPI model when applied to the test set (a). Comparison between the classification results using a stepwise process and the results obtained from SEM analysis (b).

Particle loading density in the samples (eg the rate between the number of particle pixels and background pixels) has been identified as a critical factor in misclassification. To address the loading density issue, ongoing research is focused on modifying the sample collection methods to reach optimal deposition of particles on the slide. Dust samples can be generated across an array of particle loading densities and dust compositions to capture the variability of intensities and the effect of the interactions between optical signals from different particles. Moreover, as the image data set expands, efforts to identify potentially exploitable features for mineral subclassification are continuing. In future research, a 'cell phone microscope' type monitor will be built and field-tested for RCMD classification.

ACKNOWLEDGEMENTS

The authors wish to thank the *Alpha Foundation for the Improvement of Mine Safety and Health* for sponsoring this project. The authors also thank their industry partners for providing the dust materials used in this study.

Underground rock bolt identification from 3D LiDAR scanning data

S Saydam¹, B Liu², B Li³ and W Zhang⁴

1. Student, Minerals and Energy Resources, UNSW Sydney, Sydney NSW 2052; Digital Development Engineer, DSI Underground Group, Sydney NSW 2290.
Email: sarp.saydam@dsiunderground.com.au
2. Postdoc fellow, Minerals and Energy Resources, UNSW Sydney, Sydney NSW 2052.
Email: boge.liu@unsw.edu.au
3. Senior Lecturer, Minerals and Energy Resources, UNSW Sydney, Sydney NSW 2052.
Email: binghao.li@unsw.edu.au
4. Professor, Computer Science and Engineering, UNSW Sydney, Sydney NSW 2052.
Email: wenjie.jane@gmail.com

ABSTRACT

Rock reinforcement, which refers to the support that is intrusive to the rock mass, such as rock bolts (Potvin and Hadjigeorgiou, 2016), is an essential part of every tunnelling project as it consolidates the stability of the tunnel structure. Rock bolts are steel rods that are installed into a rock mass to provide geotechnical support and are an essential part of any underground operation. Rock bolts can meet a variety of geological conditions and requirements essential for a modern roof support system in an underground mine or tunnel (Morissette *et al*, 2014). The purpose of rock bolts in underground environments can be summarised as serving two key functions: suspending potentially loosened blocks together and forming a protective pressure arch around the excavated void to effectively help the ground strengthen itself.

Careful tracking of rock bolt positions is extremely significant since it allows for the modelling of stress distributions and has applications to predictive maintenance practices. If the accurate locations of installed bolts are known, then an accurate stress distribution of the excavated tunnel can be modelled. This can highlight problems with bolting pattern design and demonstrate areas with poor rock conditions that may have been overlooked. However, it is difficult to monitor rock bolts *in situ* due to the limitation of lighting and the unavailability of global navigation signals in the underground environment.

Traditionally, deformation and support conditions in underground mines are monitored through visual inspection and geotechnical instrumentation. However, the subjectivity of visual observation techniques can result in ambiguous or incomplete analyses with little quantifiable data. Monitoring displacements with conventional instrumentation can be expensive and time-consuming, and the information collected is typically limited to just a few locations (Benton *et al*, 2017). Other popular surface imaging approaches, such as photogrammetry, are subject to poor lighting environments (Singh, Raval and Banerjee, 2021).

In recent years, LiDAR, which is a special combination of 3D scanning and laser scanning, has been widely used for underground 3D mapping. With a large scanning range and being independent of lighting conditions, LiDAR offers new opportunities for underground rock bolts identification. The output of LiDAR forms a set of points with XYZ coordinates, which is called a point cloud. The point cloud represents an exact 3D replica of the scanned environment.

Identifying objects from point clouds has been widely studied in the literature. Numerous deep learning algorithms have been proposed, such as PointNet (Qi *et al*, 2017a), PointNet++ (Qi *et al*, 2017b), SO-Net (Li, Chen and Lee, 2018), etc. Although these approaches achieve impressive results for 3D object identification, almost all of them are limited to extremely small 3D point clouds or fixed input sizes (eg 4k points or 1 × 1 metre blocks) and cannot be directly extended to larger point clouds. Recently, several works have focused on extending deep learning algorithms to large point clouds, such as RandLA (Hu *et al*, 2020) and Cylinder3D (Zhou *et al*, 2020). Those methods keep downsampling the input cloud to some fixed size before feeding it to the classification network. At the same time, it tries to keep as much local structural information on the remaining points as possible by aggregating local features on sampled points during the downsampling process.

However, these algorithms are not suitable for identifying rock bolts. One tunnel scan consists of around 2 million points in this study, while one rock bolt typically accounts for 300 points. In terms of point percentage, rock bolts are tiny objects, making existing algorithms unable to be directly applied to identifying rock bolts. The reasons for this are in two folds: 1) few points from rock bolts will be preserved after the downsampling process. For example, if the downsampling rate is 1 per cent, the expected number of points for one rock bolt is only 5 after the downsampling process. Even if the sampling possibility is not uniform, the remaining number of points from rock bolts would still be too small to represent the bolt structure; 2) the feature information is lost after the downsampling process. Because rock bolts are tiny objects, the bolt features are concentrated in a small area around the rock bolts. The bolt features may be diluted with background features by repetitively aggregating local features on sampled points during the downsampling process.

A new rock bolt detection algorithm that follows a coarse-to-fine strategy is proposed in this study. The algorithm follows a two-step manner. The first step estimates possible locations of rock bolts while pruning as many non-bolt points as possible. The proportion of variance is adopted to describe how much the cloud appears at 0.1 m scale. The algorithm computes the POV for each point and uses linear discriminant analysis to label it as bolt and non-bolt. Then, a set of candidate bolts is generated by extracting a 0.2 m radius sphere from the location in which many bolt points cluster. The second step adopts an effective 3D object detection deep neural network to precisely detect rock bolts from the candidate bolts.

The experiment results, shown in Figure 1, demonstrate that the algorithm can precisely detect the location and the exact shape of rock bolts. Specifically, the algorithm achieves 89.36 per cent precision and 93.45 per cent recall.

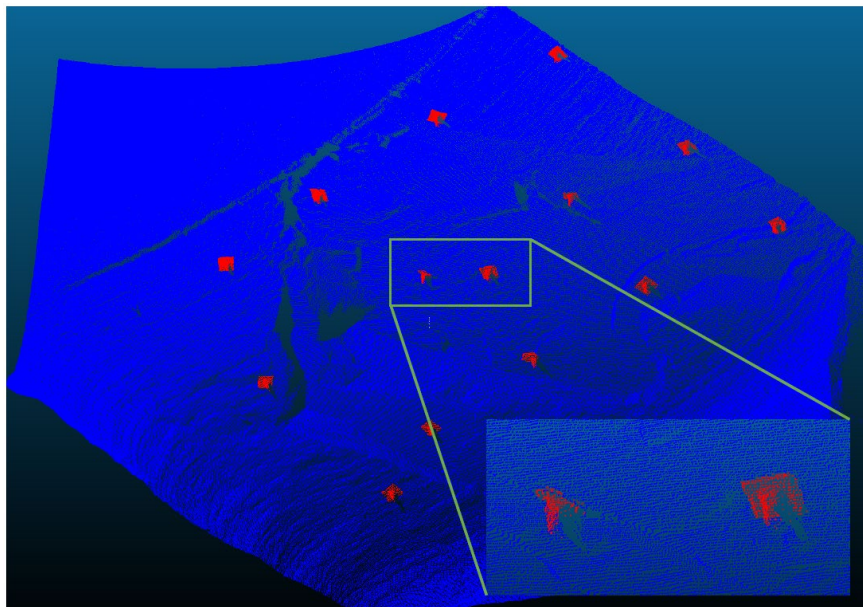


FIG 1 – The rock bolt detection results. Red points are labelled as bolt by the proposed algorithm.

ACKNOWLEDGEMENTS

The data used in this study are generously provided by 21MT and DSI.

REFERENCES

- Benton, D J, Seymour, J B, Boltz, M S, Raffaldi, M J and Finley, S A, 2017. Photogrammetry in underground mining ground control–Lucky Friday mine case study. In *Proceedings of the Eighth International Conference on Deep and High Stress Mining* (pp. 587–598). Australian Centre for Geomechanics.
- Hu, Q, Yang, B, Xie, L, Rosa, S, Guo, Y, Wang, Z and Markham, A, 2020. Randla-net: Efficient semantic segmentation of large-scale point clouds. In *Proceedings of the IEEE/CVF Conference on Computer Vision and Pattern Recognition* (pp. 11108–11117).
- Li, J, Chen, B M and Lee, G H, 2018. So-net: Self-organizing network for point cloud analysis. In *Proceedings of the IEEE conference on computer vision and pattern recognition* (pp. 9397–9406).

- Morissette, P, Hadjigeorgiou, J, Punkkinen, A R and Chinnasane, D R, 2014. The influence of change in mining and ground support practice on the frequency and severity of rockbursts. In *Proceedings of the Seventh International Conference on Deep and High Stress Mining* (pp. 165–177). Australian Centre for Geomechanics.
- Potvin, Y and Hadjigeorgiou, J, 2016. Selection of ground support for mining drives based on the Q-system. In *8th International Symposium on Ground Support in Mining and Underground Construction* (pp. 1–16). Ground Support 2016.
- Qi, C R, Su, H, Mo, K and Guibas, L J, 2017a. Pointnet: Deep learning on point sets for 3d classification and segmentation. In *Proceedings of the IEEE conference on computer vision and pattern recognition* (pp. 652–660).
- Qi, C R, Yi, L, Su, H and Guibas, L J, 2017b. Pointnet++: Deep hierarchical feature learning on point sets in a metric space. *arXiv preprint arXiv:1706.02413*.
- Singh, S K, Raval, S and Banerjee, B, 2021. A robust approach to identify roof bolts in 3D point cloud data captured from a mobile laser scanner. *International Journal of Mining Science and Technology*, 31(2), 303–312.
- Zhou, H, Zhu, X, Song, X, Ma, Y, Wang, Z, Li, H and Lin, D, 2020. Cylinder3d: An effective 3d framework for driving-scene lidar semantic segmentation. *arXiv preprint arXiv:2008.01550*.

Mobile laser scanning for automated point cloud registration, object detection and structural mapping in mining

S K Singh¹, S Raval² and B P Banerjee³

1. PhD Candidate, School of Minerals and Energy Resources Engineering, UNSW Sydney, NSW 2052. Email: sarveshkumar.singh@unsw.edu.au
2. Senior Lecturer, School of Minerals and Energy Resources Engineering, UNSW Sydney, NSW 2052. Email: simit@unsw.edu.au
3. Research Scientist, Agriculture Victoria, Grains Innovation Park, Horsham, Vic 3400. Email: bikram.banerjee@agriculture.vic.gov.au

INTRODUCTION

Light detection and ranging (LiDAR), popularly known as laser scanning has revolutionised the way of mapping and monitoring underground and open cut mine operations. Laser scanners offer the flexibility of being mounted on a mobile platform, such as drones, ground vehicles or wearable backpacks, or can be used in a static manner to produce a digital twin of the scanned environment in the form of a 3D point cloud. The obtained digital data usually has ample spatial resolution required for various mining applications; and offers the flexibility of remote data processing thereby reducing safety risks associated with the site. With recent developments in simultaneous localisation and mapping (SLAM) based mobile laser scanning, large underground mine network became possible to mapped holistically in a time-efficient manner with sufficient accuracy (Raval *et al*, 2019).

This study illustrates three important application cases of LiDAR scan in mines which include:

1. automated georeferencing and coregistration of point clouds in GNSS denied underground mines
2. automated object detection
3. automated structural discontinuity mapping.

GEOREFERENCING AND CO-REGISTRATION

Georeferencing refers to the process of conversion of point clouds from a local coordinate system to a global coordinate system whereas coregistration denotes the process of mutually aligning multi-temporal point clouds into a similar coordinate system. In a GNSS denied underground coalmine, the georeferencing and coregistration of point clouds are challenging due to inadequate distinguishable features and structurally symmetrical layouts. To this end, we have developed a three-dimensional unique identifier (3DUID), consisting of unique identity tags and 3D shape, which assist in automated effective co-registration of multi-temporal point clouds. The 3DUID tags are simple to construct, easy to decode and can be recognised in point clouds using depth information (Figure 1). An experimental study was conducted in an underground coalmine by placing 3DUID tags approximately 100 m apart in a roadway approximately 850 m long. The point cloud data was obtained from a SLAM based mobile laser scanner (ZebRevo). When compared against the previous methods, the 3DUID based approach was found accurate, robust and efficient exhibiting an accuracy of 1.76 m in georeferencing (obtained through surveyed 3DUID tags) and 0.16 m in coregistration (Singh, Banerjee and Raval, 2021). 3DUID based approach effectively overcomes conventional point picking method, which is often time-consuming, arduous and prone to bias for large scale data. The spatial frame of reference provided by 3DUID tags in underground mines facilitates applications such as automatic roadway profile extraction, guided automation, sensor calibration, convergence monitoring, change detection and deformation monitoring.

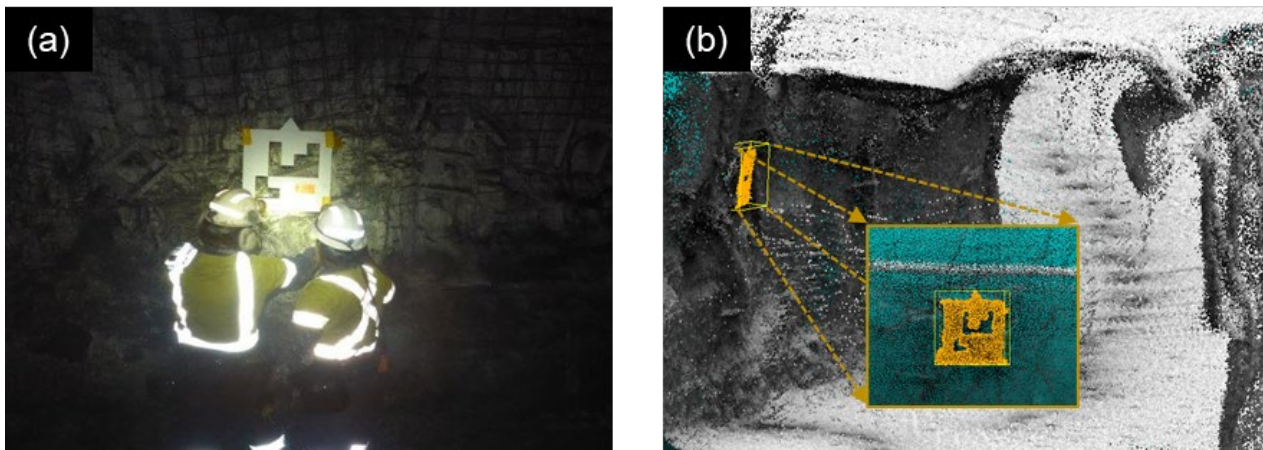


FIG 1 – (a) One of the installed 3DUID tags, (b) automatic recognition of 3DUID in point cloud (modified after Singh, Banerjee and Raval (2021)).

OBJECT DETECTION

An object such as roof bolts provide structural support in underground mines and their frequent assessment is critical to maintain roof stability and minimise safety risks. Moreover, keeping a record of the status of objects such as roof bolts, pipelines, sing boards and support elements, is often a compliant requirement in underground mines. Object detection was achieved by defining local point descriptors such as eigenvalue descriptor, radial surface descriptor and fast point feature histogram to uniquely capture the density, geometry and spatial distribution of points in a local spherical region. Henceforth, an artificial neural network (ANN) was trained on local point descriptors at multiple scales (the spherical region around query point) to identify objects in the 3D point cloud (Singh, Raval and Banerjee, 2021a, 2021b). A point cloud data, with a point density of over 15 000 points/m² and point spacing of 8 mm, was collected using a mobile laser scanner (ZebRevo) in an underground coalmine. The trained ANN was applied on an independent data set for classification (Figure 2) and accuracy was evaluated in terms of precision, recall and quality using confusion matrix. The algorithm resulted in precision, recall and quality of 89.52 per cent, 89.52 per cent and 81.03 per cent, respectively for roof bolts identification.

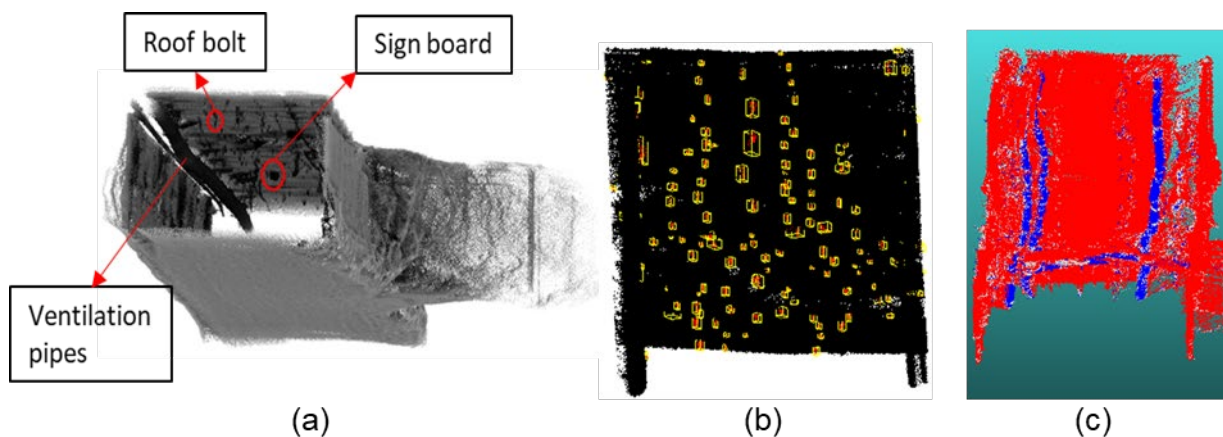


FIG 2 – (a) Visible feature in the point cloud data, (b) classified roof bolts, and (c) classified ventilation pipeline (modified after Singh, Raval and Banerjee (2021a, 2021b)).

AUTOMATED DISCONTINUITY MAPPING

Mapping of structures, such as discontinuity planes, is fundamental for slope stability analysis of a rock mass. Structural discontinuities are conventionally mapped using a magnetic compass and measurement tape in the field through direct access to the rock mass. The process is challenging due to erroneous manual measurements, missed discontinuity planes, measurements only up to human height level and associated safety risks such as rockfall. With point cloud data obtained from laser scanning, it is possible to map discontinuity planes digitally by employing manual, semi-

automated and automated approaches. Most of the existing approaches have performance challenges due to sole dependence on normal vectors and coplanarity criteria, and manually defined parameters. To address this challenge, a new point cloud processing algorithm called ‘clustering on local point descriptors (CLPD)’ was developed for automated discontinuity identification (Singh, Raval and Banerjee, 2021c). The implementation of the CLPD was demonstrated on a point cloud collected using a mobile scanner (ZebRevo) for a surface pit slope measuring approximately 120 m in length and 7.5 m in height. The CLPD method generates descriptors for individual points and then clusters them using k-Medoids clustering to identify discontinuity planes (Figure 3). Points lying on discontinuity planes can be uniquely represented through point descriptors as it captures the orientation, point association and geometry of discontinuity planes. When compared against the ground truth data, collected using a magnetic compass in the field, the CLPD method exhibited an accuracy of 3.50° and 4.32° in dip angle and dip direction, respectively.

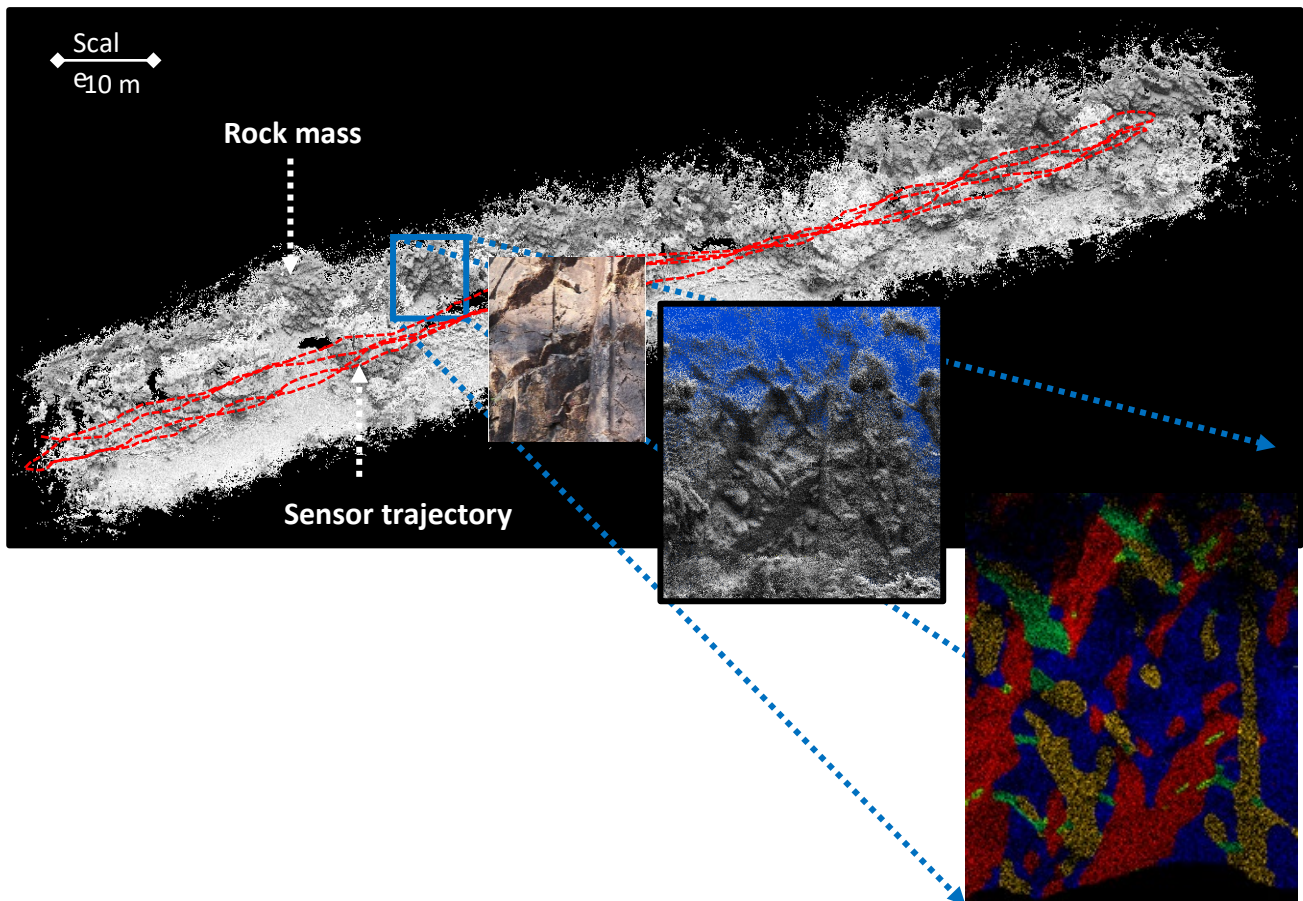


FIG 3 – Point cloud of the rock mass and automated identification of discontinuities (modified after Singh, Raval and Banerjee, (2021c).

THE FUTURE

This presentation showcased three critical applications of laser scanning in mining. The results show that all the above applications could be achieved with high accuracy using laser scanning technology. The challenging conditions present in underground mines usually renders other technologies less effective when a visual interpretation of the environment is needed. With mobile laser scanning, visualisation and monitoring of large underground space can now be done digitally in a time-efficient manner without extensively exposing mine personnel to hazards. Moreover, laser scanners can be mounted on autonomous rovers and drones which can collect the data without human intervention. Recent developments in solid-state LiDAR and computation power using graphics processing unit have caused a significant reduction in sensor cost while considerably reducing processing time for almost real-time 3D visualisation. The miniaturisation of LiDAR sensors has led to its integration in smartphone devices, which in future could substantially bring down the cost of mine site monitoring without having to compromise with the accuracy. Nevertheless, the data

still needs to be processed and application-specific algorithms need to be developed to solve various requirements of the mining industry.

ACKNOWLEDGEMENTS

This work was supported by the Australian Coal Industry's Research Program (ACARP), Project number C27057.

REFERENCES

- Raval, S, Banerjee, B P, Singh, S K and Canbulat, I, 2019. A preliminary investigation of mobile mapping technology for underground mining. In *IGARSS 2019–2019 IEEE International Geoscience and Remote Sensing Symposium* (pp. 6071–6074). IEEE.
- Singh, S K, Banerjee, B P and Raval, S, 2021. Three dimensional unique identifier based automated georeferencing and coregistration of point clouds in underground environment. *arXiv preprint arXiv:2102.10731*.
- Singh, S K, Raval, S and Banerjee, B, 2021a. Roof bolt identification in underground coal mines from 3D point cloud data using local point descriptors and artificial neural network. *International Journal of Remote Sensing*, 42(1), pp 367–377.
- Singh, S K, Raval, S and Banerjee, B, 2021b. A robust approach to identify roof bolts in 3D point cloud data captured from a mobile laser scanner. *International Journal of Mining Science and Technology*, 31(2), pp 303–312.
- Singh, S K, Raval, S and Banerjee, B P, 2021c. Automated structural discontinuity mapping in a rock face occluded by vegetation using mobile laser scanning. *Engineering Geology*, 285, 106040.

Improving interpretation of seismic data using deep generative networks

R Xu¹, V Puzyrev², C Elders³, E F Salmi⁴ and E J Sellers⁵

1. Postgraduate student, Curtin University, Curtin WA 6102. Email: rachel.xu@csiro.au
2. Senior Research Fellow, Curtin University, Curtin WA 6102.
Email: vladimir.puzyrev@curtin.edu.au
3. Professor, Curtin University, Curtin WA 6102. Email: chris.elders@curtin.edu.au
4. Research Scientist, Mining3 and CSIRO Mineral Resources, Brisbane Qld 4069.
Email: ebrahim.fathisalmi@csiro.au
5. Research Director, Mining3 and CSIRO Mineral Resources, Brisbane Qld 4069.
Email: ewan.sellers@csiro.au

ABSTRACT

The pursuit of minerals and energy resources has driven exploration and production activities into geologically complex environments. Given the geological complexity, geophysical imaging could become somewhat challenging. This lack of information, together with the repetitive, intensive, and sometimes biased interpretation and modelling of subsurface conditions, geological evaluation, and geotechnical assessment poses significant challenges to the extraction of deeply buried resources. Unlike conventional manual interpretation and physics-driven modelling techniques, the recent trend of deep learning can accelerate and automate the process of pattern discovery in data, enabling the whole learning, reasoning, and decision-making process to be efficient and accurate. In addition, deep learning methods can be used to simulate the extreme, rare, and transient scenarios where the gathering of information is difficult or dangerous. It is well known that most geoscience processes are highly complex, nonlinear, hysteretic, and coupled. Under such light, this project aims to improve interpretation and modelling techniques in geoscience. Taking the advantages of Generative Adversarial Network (GAN) and Convolutional Neural Network (CNN), this paper reports a case study that (1) quantifies and characterises the uncertainties, and (2) simulates the extreme, rare, and transient scenarios for the seismic interpretation of one of the continental shelf area surrounding Australia, namely the Northern Carnarvon Basin.

INTRODUCTION

As the deluge of the lean strategy continues to impact practically every commercial and scientific domain, the resource industry is also experiencing a transformational shift to be able to sustainably extract deeply buried resources (Löw, 2015). Extracting resources at a geographically remote environment is oftentimes accompanied by various challenges (Fairhurst, 2017). For example, the whole process of collecting exploration data, followed by the geological interpretation, could become increasingly challenging and time-consuming at an early stage of exploration. Subsequently, the geotechnical simulation also could be somewhat difficult at later stages of design, plan, and production. The existing techniques in solving these spatial problems are mainly physical-driven, meaning that domain expertise is often required in solving highly non-linear equations/derivations that are specific to their own applications. Also, the data sets used in solving these spatial problems are often interconnected or sometimes under-sampled. The conventional physical-driven modelling techniques in geoscience often suffer from validity, reliability, and generalisability issues (Drams, 2020).

With the rapid growth of computational power, new data mining techniques such as deep learning might provide an alternative. Deep learning, known for its capacity of handling multidimensional data and continuous quality improvement, has raised a significant amount of attention in almost every field of science and engineering. It also became a particular interest to the geoscience community (Lary *et al*, 2016). Deep learning allows data to be explored for consistent patterns and/or systematic relationships. It not only tracks patterns, but also learns from those patterns with minimal human intervention as the data set is growing. In the circumstances where the initial data sets could not provide enough information, as is typically the case with geological and geophysical data sets, deep

learning can also generate new synthetic data sets that preserve the utility and fidelity of the real ones and later learn from both the real and the synthetic data. The motivation of using deep learning to generate synthetic examples is to introduce more variability and enrich the data sets further. This could improve the system training process and enable deep learning algorithms to make better predictions even with limited input data.

Interpretations and modelling of geoscience problems are generally rather difficult considering that conventional manual observation and physical-driven modelling techniques in geoscience often suffer from validity, reliability, and generalisability issues, as shown in Table 1. This calls for the need to develop a framework that is sufficiently accurate, reliable, and automatic. Of great interest to the development of such a framework is the model's capacity to self-diversify if the input information is based on the motivations described above, the objective of research is to establish a systemic framework that integrates both data-driven and physics-driven approaches to improve the interpretation and modelling techniques in geoscience. In other words, the framework developed in this project aims at creating a comprehensive approach that is capable of diversifying the training sets when input data is limited.

TABLE 1

A summary of pros and cons associated with conventional manual interpretation and physical-driven modelling techniques in geoscience.

Attribute	Manual interpretation	Physical-driven
Adaptability and employability	Iterative process that is sometimes biased	Requires complex derivation, specific to application
Domain expertise reliance	Depends heavily upon domain expertise	Depends heavily upon domain expertise
Data reliance	Usually can be derived from small data	Usually can be derived from small data
Fidelity and robustness	Not quite robust	Difficult to apply on very complex systems or highly non-linear relationships

BACKGROUND

Many resources companies are searching for new methods to unlock and extract the next wave of mineral deposits. A technology proving valuable in this pursuit is seismic surveying. Seismic interpretation and analysis not only help to understand the underground mineral deposits and but also provide a tool for hazardous monitoring. For example, routine seismic monitoring in mines enables the quantification of exposure to seismicity and provides a logistical tool to guide the effort into the prevention and control of, and alerts to, potential rock mass instabilities that could result in rock bursts (Mendecki, van Aswegen and Mountfort, 1999; Mendecki, 1996; Urbancic and Trifu, 2000).

In terms of exploration activities, reflection seismic data interpretation has become an essential tool used in the oil industry in order to improve the discovery rate of oil and gas fields and to evaluate production. Seismic response can also yield information about under-compaction, hydrocarbon generation and horizontal stress (Johnston *et al*, 1998; Sena *et al*, 2011). This has enabled much more precise targeting of prospects and contributes to ensuring that drilling operations are conducted efficiently and effectively. In mineral exploration, as the focus shifts to more deeply buried resources and subsurface imaging becomes increasingly important, there is an increasing use of seismic reflection data for sediment hosted mineral deposits and in hard rock settings. In both hydrocarbon and mineral exploration, pattern recognition is an important part of understanding the geological significance of the data. A great example of this from Australia is the extensive seismic surveying and subsequent analyses conducted in the North Carnarvon Basin. The offshore portion of the basin is a gas province with minor oil sweet spots that have been discovered over a number of years. This promoted the North Carnarvon Basin to be one of the hot spots of global hydrocarbon exploration and has long been a focus for the hydrocarbon industry. Figure 1 shows an example of 3D model constructed from a seismic survey from the Northern Carnarvon Basin. The top layer shows the seabed, which has been affected by extensive slumps and submarine landslides (mass transport

complexes) and a series of layers parallel to the seabed which reveal similar structures in the subsurface.

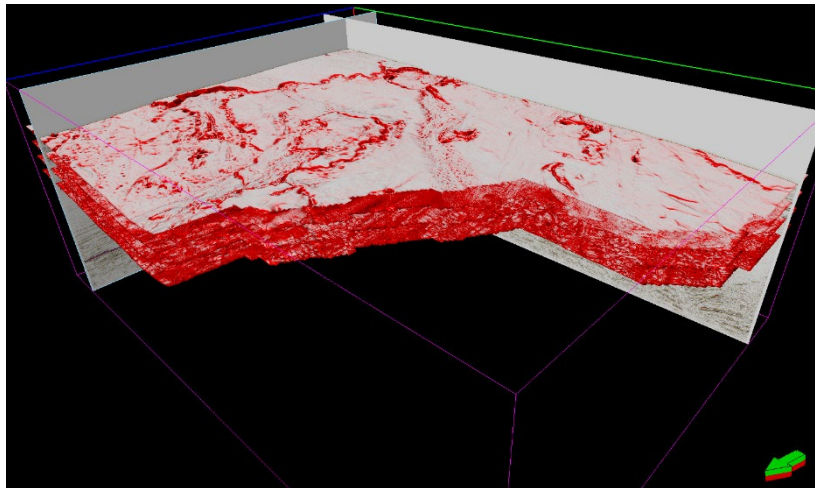


FIG 1 – 3D from the Bonaventure 3D seismic survey from the Northern Carnarvon Basin.

Knowledge of geological processes and their impacts on the terrain is important for drilling and exploration strategies. By taking slices of the 3D model parallel to the seabed as shown in Figure 1, we further derived subsurface landscapes at different depths (Figure 2), where undeformed sediments in the lower left of the image are separated from chaotically deformed sediments to the north-west by a series of irregular fault scarps that mark the headwall of the mass transport complexes. Further trimming and tiling have been applied to each horizontal slide to (1) crop out some unnecessary outer edges; (2) render and highlight the features embedded in the original picture that are hard to spot. This part of the Northern Carnarvon Basin has been affected by extensive submarine landslides (mass transport complexes, or MTC's). From this example, we identified nine types of mass movements: blocks, extensional ridges, grooves and striations, individual flow, MTC material, slump folds, scarps, polygonal faults, and undisturbed sediments. Table 2 summaries the features of those nine types of mass transport activities, together with their triggering mechanisms.

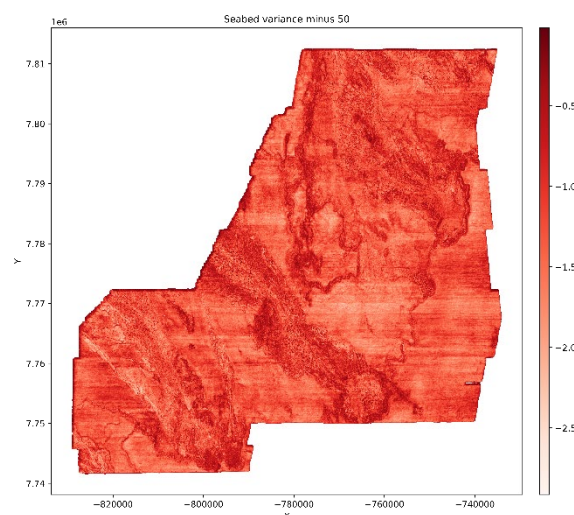
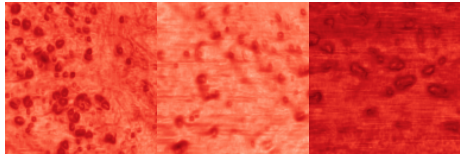
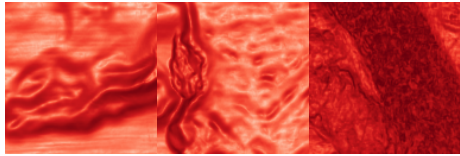
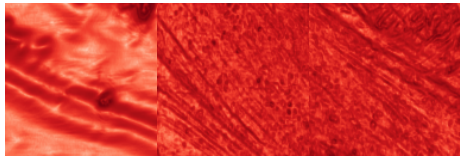
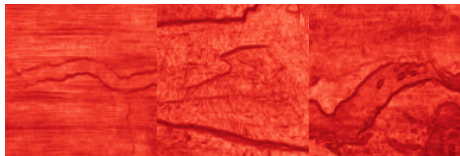
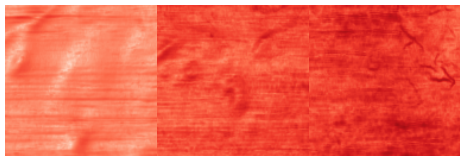
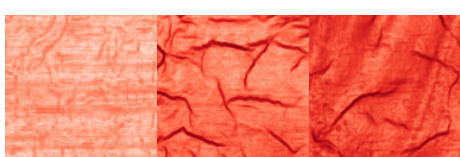
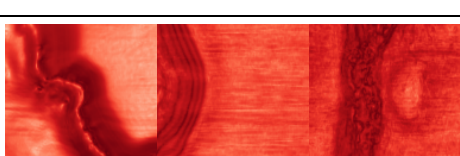
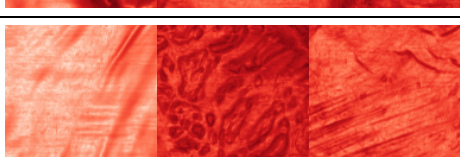



FIG 2 – Horizon slice through the Bonaventure 3D seismic survey, 50 metres below the seabed.

TABLE 2

Examples of different types of mass transport deposits – real data.

Categories	Feature	Comments
Blocks		Blocks are the detached pieces of rock that have been transported within or in front of the failed mass.
Extensional ridges		Limited translation of large-scale blocks of coherent sediment results in a series of ridges separated by extensional faults.
Grooves and striations		These features are interpreted to be the result of erosion by coherent blocks of translated material being transported at the base of a debris-like flow.
Individual flow		The late stage of a submarine landslide may be represented by individual flows formed as small-scale collapse continues.
MTC material		Most of the sediment in a mass transport complex forms a chaotic, internally deformed deposit
Polygonal faults		Polygonal faults form in fine grained sediments that are not affected by the mass transport complex. They are the result of fluid loss during burial and compaction.
Scarps		A scarp essentially represents an extensional failure surface, often found at the head of the collapse.
Slump folds		Compressional ridges and folds often form at the toe of the mass transport complex
Undisturbed		Undeformed, intact sediments, unaffected by mass transport complexes or polygonal faulting

METHODOLOGY

In this semi-supervised approach to seismic interpretation, we will use unlabelled data augmented by labelled data to train a supervised model. One particular application of this proposed semi-supervised workflow could be the understanding the geological process, triggering mechanics, and hazards associated with the submarine landslides. Figure 3 shows the streamlined process of pattern recognition and submarine landslide recognition that was proposed for this work. As shown

in Figure 2 and Table 2, pre-processing of the raw data involved depicting each horizontal slice of the subterranean landscape at different depths and identifying the different mass transport activities for each slice. From this, we obtained a training set consist of nine categories with one hundred labelled images (ie based on the dominant mass transport activity) presented in each category. To generate new samples, this work adapts the conditional style-based Generative Adversarial Networks (GAN) proposed by Oeldorf and Spanakis (2019). The reason for choosing this type of GAN lies in the fact that most GANs could potentially assist designers by either providing them with inspiration or by reducing the number of design iterations undergone with clients. A drawback concerning GAN generated content is that samples are created from an unknown noise distribution. To facilitate specification-based content generation, the user must be able to shape this latent input code in such a way that it allows for an intuitive determination of style. The basic architecture of conditional style-based GAN is shown in Figure 4.

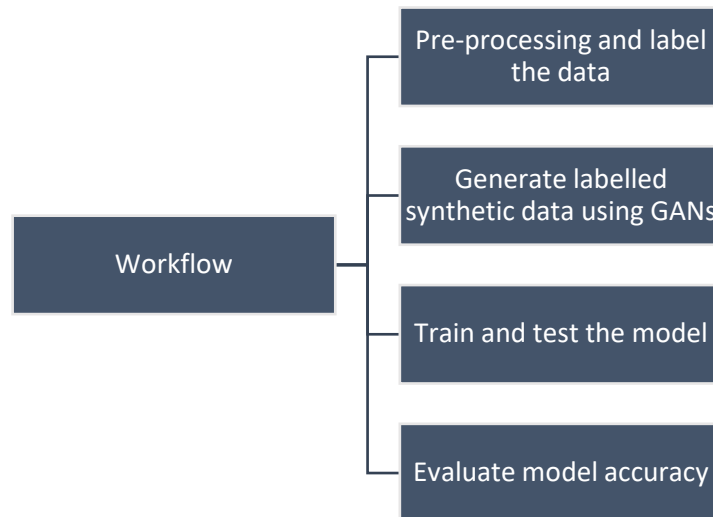


FIG 3 – Semi-supervised seismic interpretation workflow.

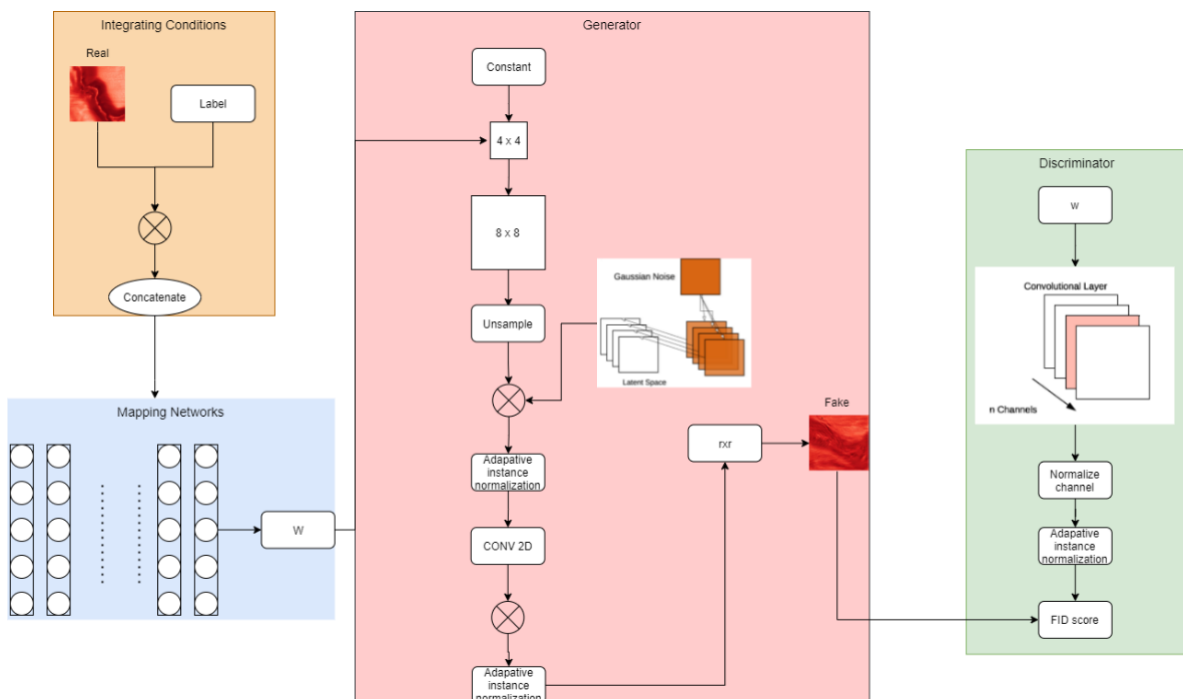


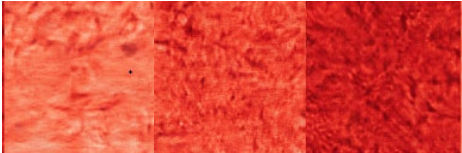

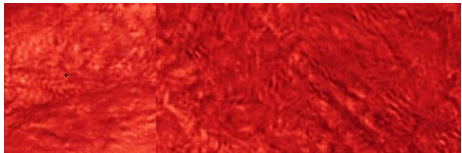
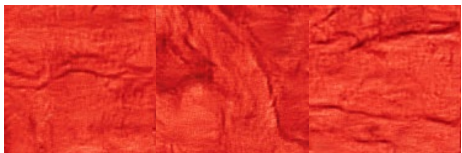
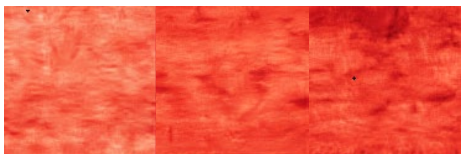
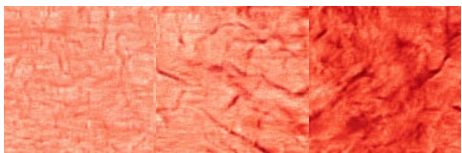

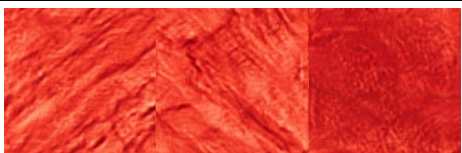
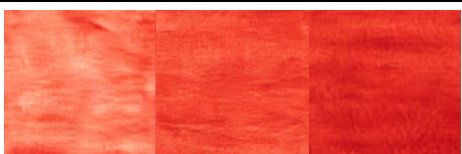
FIG 4 – The architecture of the conditional style-based GAN (Oeldorf and Spanakis, 2019).

RESULTS

After pre-processing and fine-tuning the architecture of the conditional style-based GAN, the last step is to train and evaluate the model performance. A collection of fake images produced by the

GAN is shown in Table 3, from which we can conclude that most of the artificial images resemble the real ones. For example, the fake images generated for blocks, extensional ridges, grooves and striations, polygonal faults, scarps, and undisturbed bear some striking resemblance to the real images shown in Table 2. Occasionally, such as in the cases of MTC material and slump folds, we find the model is limited as mimicking the features of the real images in those two categories.

TABLE 3
Examples of different types of mass transport activities – artificial data.

Categories	Feature	Comments
Blocks		Visual check shows high similarity
Extensional ridges		Visual check shows high similarity.
Grooves and striations		Visual check shows high similarity
Individual flow		Visual check shows high similarity
MTC material		Lower similarity compared to the real samples
Polygonal faults		Visual check shows high similarity
Scarps		Visual check shows high similarity
Slump folds		Lower similarity compared to the real samples
Undisturbed		Visual check shows high similarity

To better quantify the model performance, we employ the Frechet Inception Distance, or FID for short. FID is a metric for evaluating the quality of generated images specifically developed to evaluate the performance of generative adversarial networks (Heusel *et al*, 2017). The FID metric is the squared Wasserstein metric between two multidimensional Gaussian distributions: $\mathcal{N}(\mu, \Sigma)$, the distribution of some neural network features of the images generated by the GAN and $\mathcal{N}(\mu_w, \Sigma_w)$ and the distribution of the same neural network features from the real images used to train the GAN. As a neural network, the Inception v3 trained on the ImageNet is commonly used. As a result, it can be computed from the mean and the covariance of the activations when the synthesized and real images are fed into the Inception network as:

$$FID = \|\mu - \mu_w\|^2 + \text{tr}(\Sigma + \Sigma_w - 2(\Sigma\Sigma_w)^2) \quad (1)$$

Rather than directly comparing images pixel by pixel (for example, as done by the L2 norm), the FID compares the mean and standard deviation of one of the deeper layers in Inception v3. These layers are closer to output nodes that correspond to real-world objects such as a specific breed of dog or an airplane, and further from the shallow layers near the input image. As a result, they tend to mimic human perception of similarity in images.

Essentially, a lower FID indicates better-quality images; conversely, a higher score indicates a lower-quality image and the relationship may be linear (Brownlee, 2019). Figure 5 records the FID score for the model for all the 20 000 iterations conducted during training and testing phases. It can be seen that the FID score of the model decreases rapidly until the 2500th iteration. This means that the generator is heavily penalised by the discriminator for the poor images generated. During this process, it learns how to fool the discriminator by generating more realistic features. After that, the generator is getting better and better at mimicking the features from the real ones as the FID score decreases steadily at a lower rate. At around the 125 000 iteration, the generator reaches its limit in mimicking the features of the real images as the FID score becomes rather stable after that.

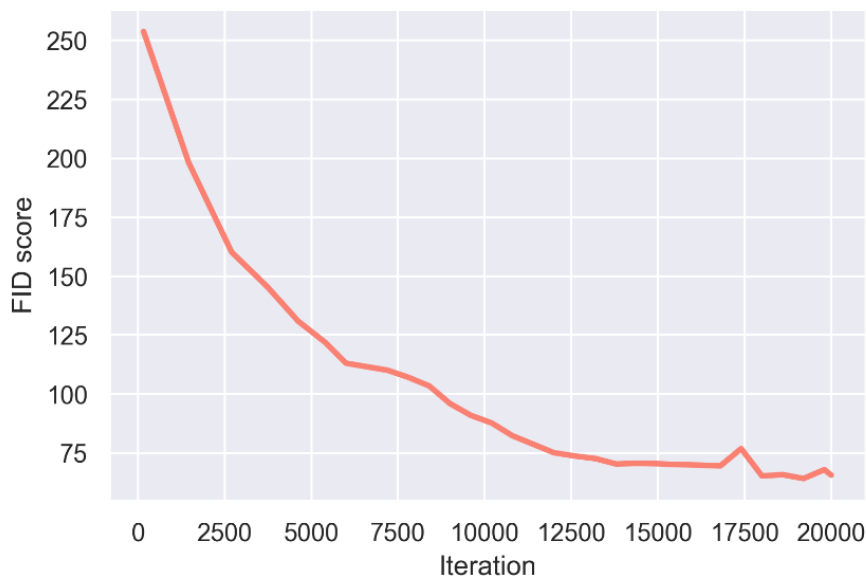


FIG 5 – The FID score for the model training and testing phases.

DISCUSSION AND FURTHER APPLICATION

Interpretations and modelling of geoscience problems are generally rather difficult considering that conventional manual observation and physical-driven modelling techniques in geoscience often suffer from validity, reliability, and generalisability issues. This calls for the need to develop a framework that is accurate, reliable, and automatic.

This paper investigates the applicability of the conditional style-based GAN for the inflation of the training sets associated with seismic reflection data. This provides an alternative, so experts do not have to spend a long time repetitively identifying specific geological features. The final stage in the project is using the extended data sets to train a convolutional neural network image classifier, a

rudimentary version of the programs employed by companies such as Tesla and Facebook in their own image recognition software.

In addition to the above application, the methodology proposed for this project shows great potential for hard rock seismic data, where coherent geological information is much more difficult to extract. The potential to define features of geological significance, use a GAN to create an artificial training data set, and then to distinguish the those features from noise, and extract them from a seismic volume has the potential to greatly enhance the interpretation of such data. For example, this proposed methodology can be used for various metalliferous mines, where a comprehensive micro seismic monitoring system is often utilised to depict the stress changes related to rock fracture during development and longwall operations. According to Gale (2018), in coalmines, significant damages such as coal bursts and caving can often be monitored and prevented through the unusual fluctuations of seismic data, as shown in Figure 6 and Figure 7. This work further provides miners with a powerful tool to achieve rapid early warning and hazard forecasting even when the initial data set is limited.

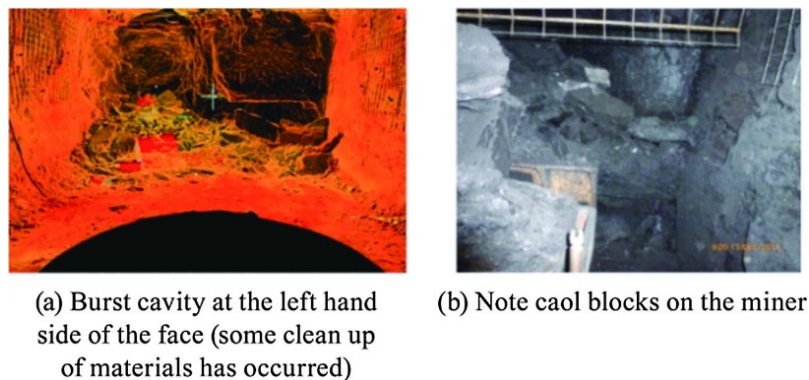


FIG 6 – Coal burst in development (Gale, 2018).

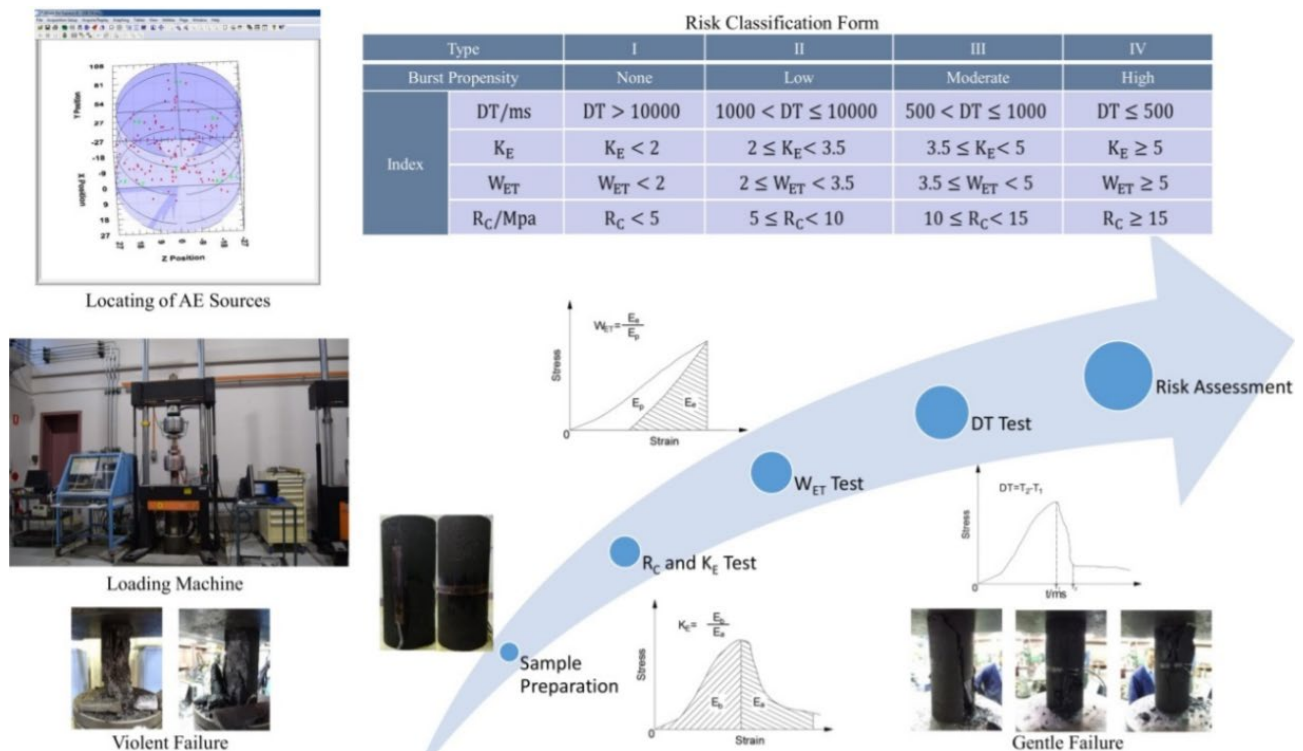


FIG 7 – Coal burst risk evaluation with coal burst propensity index (Yang *et al*, 2019).

CONCLUSION

In this paper, we experimented with a conditional extension to the popular StyleGAN architecture to control the classifications of mass transport activities. We showed that meaningful conditions can

help the model capture modes that might not be captured by an unconditional model. High-quality conditions inserted into the latent code proved to be a viable approach to controlling the output of a synthesis network. The outcomes of this study enables the seismic data to be fully labelled and inflated, which is not always feasible, due to not only the intensive labour for full-sectional seismic annotation but also the interpretational uncertainties existing in seismic sections of subsurface complexities.

Future work will focus on a convolutional neural network for predicting the different types of mass transport activities by training the mixed data sets that contain both synthetic and real seismic data. Once completed, the workflow will allow us to automate the categorisation of vast volumes of seismic data collected over the years, trends can potential hazardous then can be identified at a lower labour cost.

In addition, the proposed methodology can be used to facilitate the process of failure identification triggered by small-scale dynamic loads. For example, this method can be coupled with the micro seismic monitoring to mitigate the risks of coal burst and caving.

ACKNOWLEDGEMENTS

The first author duly acknowledges Dr. Adriel Cheng from Australia's Defence Science and Technology Group for the discussion around GANs, and Jodi Wright for the advice and suggestions along the way.

REFERENCES

- Brownlee, J, 2019. How to Implement the Frechet Inception Distance (FID) for Evaluating GANs. Accessed 3rd, Oct 2021, <https://machinelearningmastery.com/how-to-implement-the-frechet-inception-distance-fid-from-scratch/>.
- Dramsch, J S, 2020. *Advances in Geophysics*. Academic Press, Cambridge, Massachusetts.
- Fairhurst, C, 2017. Some Challenges of Deep Mining. *Engineering* 3, 527–537.
- Gale, W J, 2018. A review of energy associated with coal bursts. *International Journal of Mining Science and Technology* 28, 755–761.
- Heusel, M, Ramsauer, H, Unterthiner, T, Nessler, B and Hochreiter, S, 2017. Gans trained by a two time-scale update rule converge to a local nash equilibrium. *Advances in neural information processing systems* 30.
- Johnston, D H, McKenny, R S, Verbeek, J and Almond, J, 1998. Time-lapse seismic analysis of Fulmar Field. *The Leading Edge* 17, 1420–1428.
- Lary, D J, Alavi, A H, Gandomi, A H and Walker, A L, 2016. Machine learning in geosciences and remote sensing. *Geoscience Frontiers* 7, 3–10.
- Löw, J, 2015. *Lean Production in Mining – an overview*. PhD Thesis, Luleå University of Technology, Luleå, Sweden.
- Mendecki, A J, 1996. *Seismic monitoring in mines*. Springer Science and Business Media.
- Mendecki, A, van Aswegen, G and Mountfort, P, 1999. A guide to routine seismic monitoring in mines. A handbook on rock engineering practice for tabular hard rock mines, 35.
- Oeldorf, C and Spanakis, G, 2019. LoGANv2: Conditional style-based logo generation with generative adversarial networks. In: *2019 18th IEEE International Conference On Machine Learning And Applications (ICMLA)*, IEEE, pp. 462–468.
- Sena, A, Castillo, G, Chesser, K, Voisey, S, Estrada, J, Carcuz, J, Carmona, E and Hodgkins, P, 2011. Seismic reservoir characterization in resource shale plays: Stress analysis and sweet spot discrimination. *The Leading Edge* 30, 758–764.
- Urbancic, T I and Trifu, C-I, 2000. Recent advances in seismic monitoring technology at Canadian mines. *Journal of Applied Geophysics* 45, 225–237.
- Yang, X, Ren, T, He, X and Tan, L, 2019. A review of energy sources of coal burst in Australian coal mines.

Mineral processing frontiers

Challenges and approaches to flotation of sea floor massive sulfide ores

K Aikawa¹, I Park², N Hiroyoshi³ and M Ito⁴

1. PhD student, Hokkaido University, Sapporo Japan 060–8628.
Email: k-aikawa@frontier.hokudai.ac.jp
2. Assistant Professor, Hokkaido University, Sapporo Japan 060–8628.
Email: i-park@eng.hokudai.ac.jp
3. Professor, Hokkaido University, Sapporo Japan 060–8628. Email: hiroyosi@eng.hokudai.ac.jp
4. Associate Professor, Hokkaido University, Sapporo Japan 060–8628.
Email: itomayu@eng.hokudai.ac.jp

ABSTRACT

The demand for base and precious metals (eg copper (Cu), lead (Pb), zinc (Zn), gold (Au), silver (Ag) etc) is projected to be continuously increased in the future. To keep up with the demand, the development of new metal resources is an urgent issue for the future. Sea floor massive sulfide (SMS) deposits have gained increasing attention as one of the new metal resources. To develop SMS deposits, studies on mining technologies and environmental impacts for deep sea mining have been conducted by many researchers and in some projects (eg solwara 1 project in Papua New Guinea). However, few studies have investigated mineral processing, especially flotation of SMS ores.

SMS ores are referred to as modern analogues of volcanogenic massive sulfide (VMS) ores on land (eg Kuroko (black ore)). However, some SMS ores have distinct features different from terrestrial ores. SMS ores obtained from around Japan contain soluble minerals like anglesite, which release metal ions (eg Cu^{2+} , Pb^{2+} , Zn^{2+} , $\text{Fe}^{2+/3+}$) during flotation. Also, dissolution of metal ions was observed in SMS ores obtained from Trans-Atlantic Geotraverse active mound on the Mid-Atlantic Ridge. These soluble minerals and metal ions would affect and complicate the flotation separation of Cu-Pb-Zn sulfide minerals in SMS ores. Because of these distinct characteristics of SMS ores, the conventional flotation processes for terrestrial ores would not be applicable to SMS ores. Therefore, flotation of SMS ores is more challenging and the development of appropriate flotation processes for SMS ores is necessary. As implications to the upcoming operation of SMS ores, features of SMS ores that would affect flotation separation were reviewed and the possible flotation processes for SMS ores were discussed.

INTRODUCTION

The demand for base and precious metals (eg copper (Cu), lead (Pb), zinc (Zn), gold (Au), silver (Ag) etc) is projected to be continuously increased in the future. To keep up with the demand, techniques for new resources is required to be developed, which have not been exploited due to high mining/operation costs as well as difficulties in the processing. Sea floor massive sulfide (SMS) deposits, for example, have gained increasing attention as one of the new resources because they consist of polymetallic sulfides containing Cu, Pb, Zn, Au, Ag, etc. To develop SMS deposits, studies related to deep sea mining have been conducted from the aspects of mining technologies and environmental impacts caused by deep sea mining. However, there have been few studies for mineral processing of SMS deposits.

SMS ores are referred to as modern analogues of volcanogenic massive sulfide (VMS) ores on land (eg Kuroko (black ore)) and typically composed of Cu-Pb-Zn sulfide minerals like chalcopyrite (CuFeS_2), galena (PbS), and sphalerite (ZnS). According to the previous studies by Japan Oil, Gas and Metals National Corporation (JOGMEC), however, the flotation behaviour of SMS in mineral processing is quite different from that of Kuroko (METI and JOGMEC, 2018; Oki, Nishisu and Hoshino, 2015).

In a typical flotation method of VMS, Cu-Pb-Zn sulfide ores are processed via a two-stage flotation process whereby Cu- and Pb-sulfide minerals are recovered as froth in the first stage, followed by the recovery of Zn-sulfide minerals as froth in the second stage (Woodcock *et al*, 2007). This typical

two-stage flotation process may be difficult to be applied to SMS ores because sphalerite was activated and recovered in the froth together with Cu- and Pb-sulfide minerals in the first stage (Aikawa *et al*, 2021). In this paper, mechanisms of sphalerite activation in flotation of SMS are reviewed and a possible approach to control sphalerite floatability is introduced.

MECHANISMS OF SPHALERITE ACTIVATION IN FLOTATION OF SMS

METI and JOGMEC (2018) reported the distinct feature of SMS ores obtained from around Japan; that is, lead minerals in the SMS ores are mostly present as anglesite with a minor amount of galena. When anglesite is contained, Pb^{2+} is readily released from anglesite during flotation due to its higher solubility than that of PbS (K_{sp} of anglesite and galena are $10^{-7.79}$ and $10^{-26.77}$, respectively) (Ball and Nordstrom, 1991). In addition to Pb^{2+} , other metal ions like Cu^{2+} and Zn^{2+} can be dissolved when water-soluble minerals are contained in SMS ores, which may affect flotation behaviours of SMS ores.

For example, when Pb^{2+} is released from anglesite during flotation, lead activation of sphalerite is known to occur as illustrated in the following equation (Aikawa *et al*, 2021):



Sphalerite activation is known to increase its floatability because PbS-like compounds formed on sphalerite have higher affinities for short-chained thiol collectors like xanthate than that of sphalerite.

In a typical flotation method of VMS, Cu-Pb-Zn sulfide ores are processed via a two-stage flotation process whereby Cu- and Pb-sulfide minerals are recovered as froth in the first stage, followed by the recovery of Zn-sulfide minerals as froth in the second stage. This typical two-stage flotation process cannot be applied to SMS because sphalerite is most likely activated by Pb^{2+} dissolved from anglesite and recovered together with Cu- and Pb-sulfide minerals in the first stage (Aikawa *et al*, 2021). Therefore, the activation of sphalerite by Pb^{2+} released from anglesite makes the separation of Cu-Pb-Zn sulfides in SMS complicated, and thus suitable techniques to control sphalerite floatability in flotation of SMS are necessary to be developed.

A POSSIBLE APPROACH TO CONTROL SPHALERITE FLOATABILITY IN FLOTATION OF SMS ORES

The authors proposed a possible approach for flotation of SMS ores which contain anglesite; that is, the removal of anglesite to limit sphalerite activation prior to the first stage of flotation where Cu- and Pb-sulfides are recovered (Aikawa *et al*, 2021).

A SMS ore sample (named as sample A) obtained from around Japan was provided by JOGMEC and characterised by X-ray fluorescence spectroscopy (XRF) and X-ray powder diffraction (XRD). Based on XRF result, sample A was composed of 7.4 per cent Cu, 13.6 per cent Zn, 7.1 per cent Pb, 24.5 per cent Fe, 35.7 per cent S, 3.5 per cent Si, and 1.5 per cent Ba (mass fraction). XRD pattern of sample A showed that it contained chalcopyrite, sphalerite, galena, anglesite, barite, pyrite, and quartz (Aikawa *et al*, 2021).

Figure 1 and Table 1 show the flotation results of the SMS sample and the results of the leachability test, respectively. In flotation of sample A, sphalerite was recovered as froth together with chalcopyrite and the recovery of Pb minerals (ie anglesite and galena) was low at around 30–40 per cent, suggesting that anglesite is most likely the main Pb mineral in sample A (Figure 1). A result of leachability test showed that 38 ppm Pb^{2+} and 20 ppm Zn^{2+} were released from SMS ore sample (Table 1). These results indicate that sphalerite may be activated by Pb^{2+} , which makes the conventional flotation procedure of Cu-Pb-Zn ores not applicable for sample A. To separate Cu-Pb-Zn sulfide minerals, therefore, the effect of anglesite and Pb^{2+} on sphalerite floatability should be minimised.

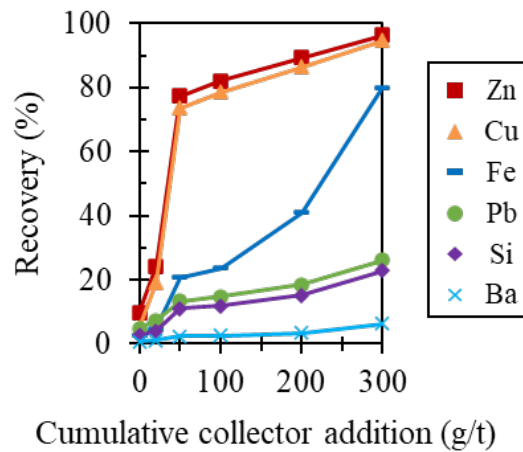


FIG 1 – Flotation result of sample A with increasing potassium amyl xanthate (KAX) dosage (conditions: 20 μ L/L Methyl Isobutyl Carbinol (MIBC, frother), 20 kg/t of sodium sulfite (pyrite depressant), pH 6.5, 25°C, pulp density 5 per cent, air introduction rate 1 L/min, impeller speed 1000 rev/min) (Aikawa *et al*, 2021).

TABLE 1

Results of leaching tests of sample A with DI water (conditions: pulp density, 1 per cent; leaching time, 10 min) (Aikawa *et al*, 2021).

Concentration (ppm)				Final pH
Cu	Zn	Pb	Fe	
–	20	38	–	5.12

Note: '–' denotes below the detection limit.

To minimise the effect of anglesite and Pb^{2+} on sphalerite floatability for the separation of chalcopyrite and sphalerite, EDTA washing prior to flotation and/or addition of zinc sulfate as a depressant for sphalerite were applied to flotation of sample A. EDTA washing was adopted to remove soluble minerals like anglesite as well as dissolved metal ions from the SMS ore sample. Zinc sulfate was added to depress lead-activated sphalerite after EDTA washing. Figure 2 shows the flotation results of sample A: (a) with EDTA washing, (b) with addition of zinc sulfate (Zn^{2+} 1000 ppm), and (c) with addition of zinc sulfate (Zn^{2+} 1000 ppm) after EDTA washing. After EDTA washing, chalcopyrite was floated first followed by sphalerite and Pb minerals. It is important to note that the recovery of Pb minerals was high (ie ~80 per cent at 100 g/t KAX) (Figure 2(a)) compared to that without EDTA washing (Figure 1), indicating that anglesite was mostly removed and the remaining galena was recovered. However, the depressive effect of EDTA washing on the floatability of sphalerite was limited. As illustrated in Figure 2(b), the effect of zinc sulfate in depressing the floatability of sphalerite was also negligible; that is, sphalerite was recovered as froth together with chalcopyrite. For the case when EDTA washing was adopted prior to the addition of zinc sulfate, although the floatability of chalcopyrite was not affected, it had a detrimental effect on the floatability of sphalerite (Figure 2(c)). These results indicate that EDTA washing followed by Zn^{2+} addition could be an effective approach to depress the floatability of lead-activated sphalerite in the flotation of SMS ores containing anglesite.

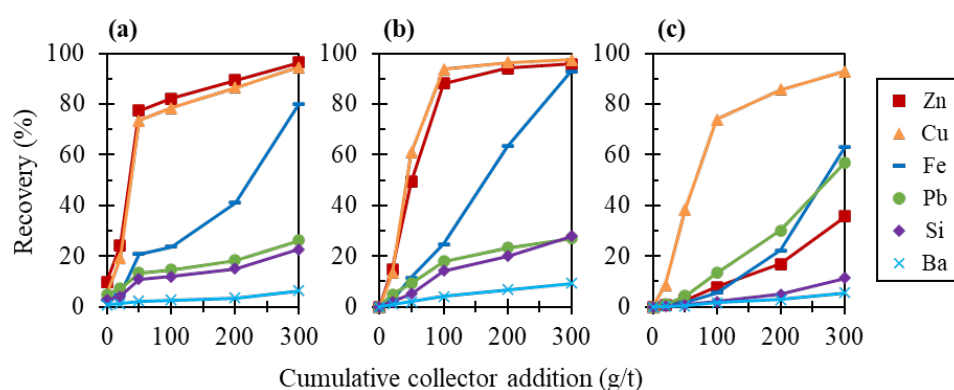


FIG 2 – Flotation results of sample A with 20 kg/t of sodium sulfite: (a) with EDTA washing, (b) with addition of zinc sulfate (Zn^{2+} 1000 ppm), and (c) with addition of zinc sulfate (Zn^{2+} 1000 ppm) after EDTA washing (conditions: 20 $\mu\text{L/L}$ MIBC (frother), 20 kg/t of sodium sulfite (pyrite depressant), pH 6.5, 25°C, pulp density 5 per cent, air introduction rate 1 L/min, impeller speed 1000 rev/min) (Aikawa *et al*, 2021).

SUMMARY

SMS ores are important sources for base metals like Cu, Pb, and Zn in the future; however, its processing remains challenging due to the presence of easily soluble minerals like anglesite that releases metal ions (eg Pb^{2+}) and activate sphalerite, making the separation of Cu-Pb-Zn sulfide minerals difficult to accomplish. To minimise the effect of anglesite and dissolved Pb on the floatability of sphalerite, EDTA washing followed by the addition of sphalerite depressant (zinc sulfate) were applied, and this approach was effective to improve the separation of Cu-Pb-Zn sulfide minerals in the flotation of SMS ores.

Apart from Pb^{2+} , other metal ions like Cu^{2+} , $\text{Fe}^{2+/3+}$ may also affect the floatabilities of minerals contained in SMS ores, so flotation of SMS ores in more complicated system is required to be further studied. In conventional mineral processing for terrestrial mines, blending/mixing of ores have been conducted to minimise the fluctuation of feed properties. In the case of SMS ores, mineral processing of excavated SMS ores would be conducted on a production support vessel (PSV) where blending/mixing of ores is impossible. Therefore, artificial intelligence (AI), internet of Things (IoT) etc could assist the smart flotation process, and its development is necessary for mineral processing of SMS ores.

ACKNOWLEDGEMENTS

This work was carried out as commissioned business by the Agency for Natural Resources and Energy, the Ministry of Economy, Trade and Industry (METI). The authors are grateful to the agency and all of the persons engaged in its duties.

REFERENCES

- Aikawa, K, Ito, M, Kusano, A, Park, I, Oki, T, Takahashi, T, Furuya, H and Hiroyoshi, N, 2021. Flotation of Sea floor Massive Sulfide Ores: Combination of Surface Cleaning and Deactivation of Lead-Activated Sphalerite to Improve the Separation Efficiency of Chalcopyrite and Sphalerite. *Metals*, 11, 253.
- Ball, J W and Nordstrom, D K, 1991. User's manual for WATEQ4F, with revised thermodynamic data base and text cases for calculating speciation of major, trace, and redox elements in natural waters, U.S. Geological Survey Water-Resources Investigations Report.
- Ministry of Economic, Trade and Industry (METI) and Japan Oil, Gas and Metals National Corporation (JOGMEC), 2018. Summary report on comprehensive evaluations of development plan of Sea floor massive sulfide deposits. Available from: <<http://www.jogmec.go.jp/content/300359550.pdf>> [accessed: 26 February.21].
- Oki, T, Nishisu, Y and Hoshino, M, 2015. Characteristics of The Existing Mineral Phases of Japanese Submarine Hydrothermal Polymetallic Sulfides and Their Influence on Respective Mineral Processing Properties. *Journal of MMIJ* 131, 619–626.
- Woodcock, J T, Sparrow, G J, Bruckard, W J, Johnson, N W and Dunne, R, 2007. Plant Practice: Sulfide Minerals and Precious Metals in Froth flotation A century of innovation (ed: Fuerstenau, M C, Jameson, G J and Yoon, R H) (Society for Mining, Metallurgy, and Exploration Inc: Colorado).

Comparative study on rougher copper recovery prediction using selected predictive algorithms

B Amankwaa-Kyeremeh¹, W Skinner² and R K Asamoah³

1. PhD student, University of South Australia, UniSA STEM, Future Industries Institute, Adelaide SA 5095. Email: bismark.amankwaa-kyeremeh@mymail.unisa.edu.au
2. Research Professor, University of South Australia, UniSA STEM, Future Industries Institute, Adelaide SA 5095. Email: william.skinner@unisa.edu.au
3. Post-Doctoral Fellow, University of South Australia, UniSA STEM, Future Industries Institute, Adelaide SA 5095. Email: richmond.asamoah@unisa.edu.au

ABSTRACT

Froth flotation is a multiphase process which exhibits inherent instability and complex dynamics. As a result of this, advances in predicting the overall performance of the process is of much significance to mineral processing engineers. In this work, we present a comparative rougher copper recovery prediction study using four predictive algorithms ie support vector machine, Gaussian process regression (GPR), artificial neural network and linear regression. Each predictive algorithm was trained and validated with 80 per cent and 20 per cent of the total data set received, respectively. Additionally, the various trained models were further assessed with an independent data set (2000 observations) collected on a later date than the training and validation data sets. Models performance assessment using correlation coefficient (r), root mean square error (RMSE), mean absolute percentage error (MAPE) and variance accounted for (VAF) indicated that GPR model performs better than all other models attaining r values >0.96 , RMSE and MAPE values <0.42 and <0.25 per cent, respectively, and VAF values >94 per cent using training, validation and testing set. The overall performance of the GPR model indicates that good rougher copper recovery prediction can be made using GPR model and relevant rougher flotation variables.

INTRODUCTION

Froth flotation is the main separation technique for the concentration of large tonnages of sulfide minerals around the globe annually (Asamoah *et al*, 2019). The process is based on the difference in the surface wettability between mineral of interest and unwanted gangue minerals (Murphy, Zimmerman and Woodburn, 1996; Urbina, 2003). The success of the process is affected by so many parameters including chemical reagents, feed particle size, airflow and agitator speed (Mathe, Harris and O'Connor, 2000). In other words, flotation can be considered as a multiphase separation technique involving so many complex subprocesses. One way to better understand froth flotation and its complex nature is through the development of comprehensive models that will look at the assessment of the various variables (Shahbazi, Chehreh Chelgani and Matin, 2017). An appropriate model should be able to predict the overall output of froth flotation in terms of recovery and grade using certain known variables as inputs. In general, inclusive flotation models based on relevant flotation variables can be used to better understand the complexity of the process variables and subsequently control the future output of the process (Quintanilla, Neethling and Brito-Parada, 2021). However, the interdependence and the complicated nature of the various factors affecting froth flotation make the development of flotation models a difficult task to carry out (Karimi, Akdogan and Bradshaw, 2014).

Over the years, froth flotation has been modelled with the use of first-order kinetic process which finds it difficult to address the complex nonlinear relationships existing among flotation variables (Polat and Chander, 2000). However, the emergence of modern day machine learning algorithms specifically supervised learning provides a way forward to better modelling of froth flotation process. These advanced computational techniques have the ability to capture the complex nonlinear relationship among flotation variables and can handle high number of input variables (Jahedsaravani *et al*, 2016). Basically, these algorithms analyse a training data, build a function that relates an input to an output and eventually make predictions from a new data set using the developed predictive function. Several machine learning algorithm including artificial neural network (ANN), GPR, support vector machine (SVM), fuzzy logic, principal component regression (PCR), decision trees and

random forest (RF) have been applied in predicting metallurgical performance of froth flotation (Ali *et al*, 2018; Amankwaa-Kyeremeh *et al*, 2021; Breiman, 2001; Feng *et al*, 2015; Jorjani, Chelgani and Mesroghli, 2007; Kettaneh *et al*, 2005; Khodakarami, Molatlhegi and Alagha, 2019; Zarie, Jahedsaravani and Massinaei, 2020). For instance Hodouin (2011) combined ANN and RF in predicting concentrate grade of platinum flotation through froth image analysis. Work done by Ali *et al* (2018) featured ANN, RF, adaptive neuro-fuzzy inference system (ANFIS), Mamdani fuzzy logic (MFL), and hybrid neural fuzzy inference system (HyFIS) in predicting froth ash content and combustible recovery of fine high ash coal (Cook *et al*, 2020).

In this work, support vector machine, Gaussian process regression, artificial neural network and linear regression algorithms have been used in a comparative study to predict rougher copper recovery with the aim of ascertaining the best predictive algorithm. The rest of the paper is organised as follows. Section 2 will highlight on methodologies, results and discussion in section 3 and finally drawing conclusions in section 4.

METHODOLOGY

Data collection and pre-processing

A total of 3200 historic data set on 15 rougher flotation variables together with their corresponding time stamped rougher recovery values were received from a typical copper processing plant in Australia. The name of the plant cannot be disclosed due to data confidentiality reasons. Table 1 gives a summary of the various input and output variables considered for this work. As a result of occasional transient operation on the plant, some of the observations in the data set were obvious outliers and were removed by visual inspection before subjecting the remaining portion to further pre-processing. The further pre-processing of the data set was to clean the difficult to detect outliers. This was carried out based on domain knowledge of steady operating bound of each rougher flotation variable. The overall cleaning of the data set resulted in 2500 useful observations for the analysis. To enhance the performance of the proposed predictive algorithms, the pre-processed data set was standardised to have the same scale using Equation 1.

TABLE 1
Summary of variables used in model development.

Rougher flotation Variable		Variable type
Feed grade (wt. %)		Input variables
Feed particle size (% passing 75 μm)		
Throughput (t/hr)		
Xanthate dosage (ml/min)	Tank cell 1	
	Tank cell 4	
Frother dosage (ml/min)	Tank cell 1	
	Tank cell 4	
Air flow rate (m³/hr)	Tank cell 1	
	Tank cell 2	
	Tank cell 3	
	Tank cell 4	
	Tank cell 5	
Froth depth (mm)	Tank cell 1	
	Tank cell 2/3*	
	Tank cell 4/5*	
Rougher copper recovery (%)		Output variable

*Froth depth of tank cell 2 and 4 also represent tank cell 3 and 5 respectively as they are kept at same level.

$$z_i = \frac{s_i - \bar{s}}{s_s}, i = 1, 2, 3.. \quad (1)$$

Where:

z_i = i th standardised observation

s_i = i th observation of sample

\bar{s} = mean of sample

s_s = standard deviation of sample

Model development

SVM, GPR, ANN and LR algorithms were used to establish relationship between the input and output variables as shown in Table 1. To generate good prediction and mimic typical plant practice, the popular hold-out cross validation approach was used to randomly divide the data set into 80 per cent (2000 observations) training data set and 20 per cent (500 observations) validation data set. In as much as there is no general rule for the partitioning ratio, the rule of thumb is that the training data set must be significantly more than the validation data set to capture the entire characteristic of the data set. Furthermore, assessing the trained models with an unseen data helps to detect whether the model is overfitting (performs good on training data set but poorly on unseen data set) or underfitting (performs poorly on both training and unseen data sets). Additionally, an independent data set made up of 2000 observations after subjecting it to the same pre-processing techniques was used as testing data set to check the robustness of the models. It must be noted that the testing data set was entirely different from the training and the validation data sets and was received at a later time. The training data set was used to train the models and fitted with the training, validation and testing data sets for performance assessment.

SVM algorithm

SVM uses an optimisation scheme to control an objective cost function (ϵ -insensitive loss function) comprising of nonlinear kernel functions (Chia *et al*, 2012). The role of the kernel functions is to estimate the conditional expectation of a random variable. The kernel functions make SVM memory efficient, versatile and effective in handling high dimensional spaces even when the number of dimensions is greater than the number of samples (Roy, Kar and Das, 2015). The Gaussian kernel function (Equation 2) was used for this work after an empirical study involving linear and polynomial kernel functions.

$$k(x, y) = 1 + x \cdot y \quad (2)$$

GPR algorithm

A Gaussian process $t(x)$ can be considered as a stochastic process such that every finite collection of the random variables comes with a joint Gaussian distribution (Amankwaa-Kyeremeh *et al*, 2021; Rasmussen, 2003). $t(x)$ is parameterised by a mean function $m(x)$ and a kernel function $k(x, x')$ expressed at points x and x' . Equations 3 and 4 have been used to express $m(x)$ and $k(x, x')$.

$$m(x) = E(t(x)) \quad (3)$$

$$k(x, x'; \theta) = (E((t(x) - m(x))(t(x') - m(x')))) \quad (4)$$

Where θ is the set of hyperparameters learned from the training data via maximum marginal likelihood.

Equation 5 has been used to express the function $t(x)$ in terms of $m(x)$ and $k(x, x')$.

$$t(x) \sim GP(m(x), k(x, x')) \quad (5)$$

GP stands for Gaussian process implying that $t(x)$ is distributed as a GP with mean $m(x)$ and a kernel function $k(x, x')$. For this work, the most commonly used kernel function (squared exponential kernel function) was used as shown Equation 6 (Snelson, 2008).

$$C(x_i, x_j | \theta) = \sigma_f^2 \exp \left[-\frac{1}{2} \frac{(x_i - x_j)'(x_i - x_j)}{\sigma_l^2} \right] \quad (6)$$

Where

θ = set of hyperparameters

σ_l = characteristic length scale

σ_f = signal standard deviation

ANN algorithm

ANN algorithm mimics the dense neurons in the human brain. Just like the neurons in the human brain, the neurons (computational elements) in ANN algorithm are also arranged in a hierarchical interconnected layers. Each neuron is responsible for receiving and processing information from the preceding neuron layer. The processed information is simplified and communicated to the next layer of neurons (Schalkoff, 1997). For this work, the ANN network structure was built with 15 input layer neurons, 30 hidden layer neurons and 1 output layer neuron. The Bayesian regularisation training algorithm was also utilised.

LR algorithm

LR models are among the most commonly used statistical methods. It is called multiple linear regression (MLR) when more than one input is used in predicting an output. The goal of (MLR) is to model the linear relationship between the input variables and the output variable. MLR is estimated using Equation 7.

$$y_i = \beta_0 + \beta_1 x_{i1} + \beta_2 x_{i2} + \beta_3 x_{i3} + \dots + \beta_p x_{ip} + \varrho_i, i = 1, 2, 3, \dots, n \quad (7)$$

Where

y_i = i th output value

β_p = p th coefficient

β_0 = constant term in the model

x_{ij} = i th observation of the j th variable, $j = 1, \dots, p$

ϱ_i = i th noise term, that is, random error

n = total number of observations

Model performance assessment

To evaluate the performance of the investigated models, correlation coefficient (r), root mean square error (RMSE), mean absolute percentage error (MAPE) and variance accounted for (VAF) performance indicators were used. The mathematical expression of these indicators are shown in Equations 8–11. For a good performing model, r should be approaching 1, RMSE and MAPE should be approaching zero with VAF close to 100 per cent as possible.

$$r = \frac{\sum_{i=1}^n (y_i - \bar{y}) - (\hat{y}_i - \bar{\hat{y}})}{\sqrt{\sum_{i=1}^n (y_i - \bar{y})^2 \times \sum_{i=1}^n (\hat{y}_i - \bar{\hat{y}})^2}} \quad (8)$$

$$\text{RMSE} = \sqrt{\left(\frac{1}{n}\right) \sum_{i=1}^n (y_i - \hat{y}_i)^2} \quad (9)$$

$$\text{MAPE} = \left(\frac{1}{n}\right) \sum_{i=1}^n \frac{|y_i - \hat{y}_i|}{y_i} \times 100\% \quad (10)$$

$$\text{VAF} = \left(1 - \frac{\text{var}(y_i - \hat{y}_i)}{\text{var}(y_i)}\right) \times 100\% \quad (11)$$

Where

y_i = i th true rougher copper recovery value

\bar{y} = mean of true rougher copper recovery values

\hat{y}_i = i th predicted rougher copper recovery value

$\bar{\hat{y}}$ = mean of predicted rougher copper recovery values

n = total number of observations

Results and discussion

This section presents comparative results and discussion on the performance of the various investigated predictive models. Using r , RMSE, MAPE and VAF, the results of model performances on training, validation and testing data sets have been summarised in Table 2. From Table 2, it can be seen that GPR had the highest r values of 0.99, 0.97 and 0.97 when its trained model was fitted with training, validation and testing data sets, respectively. This was followed by SVM and ANN which had same r value of 0.87 when their trained models were fitted with the training data set. 0.85 and 0.86 were the r values yielded when their trained models were fitted with the validation data set. Just like the r value yielded with fitting done with the training data set, their fitting with the testing data set also yielded the same r value of 0.86. LR model on the other hand had the least performance in terms of r values attaining 0.53, 0.50 and 0.51 when its trained model was fitted with the training, validation and testing data sets, respectively. The highest r values obtained by GPR model shows the unique predictive strength of the GPR model.

TABLE 2

Summary of model performance evaluation using correlation coefficient (r), root mean square error (RMSE), mean absolute percentage error (MAPE) and variance accounted for (VAF).

Model	Training data set			
	r	RMSE	MAPE (%)	VAF (%)
SVM	0.87	0.91	0.72	74.72
GPR	0.99	0.05	0.02	99.9
ANN	0.87	0.88	0.69	76.24
LR	0.53	1.52	1.32	26.56
Validation data set				
SVM	0.85	0.96	0.74	71.72
GPR	0.97	0.41	0.24	94.70
ANN	0.86	0.93	0.68	73.50
LR	0.50	1.56	1.34	24.50
Testing data set				
SVM	0.86	0.93	0.75	74.87
GPR	0.97	0.41	0.24	94.65
ANN	0.86	0.92	0.70	73.32
LR	0.51	1.54	1.32	25.62

Again as seen from Table 2, two error statistics were considered for this work (i.e.) RMSE and MAPE. In terms of RMSE, GPR model once again had the lowest values across board obtaining values of 0.05, 0.41 and 0.41 for fittings with training, validation and testing data sets, respectively. With regards to its MAPE values, 0.02 per cent, 0.24 per cent and 0.24 per cent were observed when its trained model was fitted with the training, validation and testing data sets, respectively. SVM recorded RMSE values >0.90 and MAPE values >0.70 with its training, validation and testing data sets fittings. RMSE values >0.87 and MAPE values >0.67 were recorded by ANN model across board with its training, validation and testing data sets fittings. LR model recorded the highest RMSE and MAPE values, obtaining values >1.50 and >1.30 for its RMSE and MAPE, respectively across board. These statistical results are clear indication that rougher copper recovery prediction made with GPR model deviates marginally from the true rougher copper recovery values.

VAF indicator has also been used to verify the correctness of the various predictive models and how well they approximate unseen data as shown in Table 2. From Table 2, it can thus be seen that GPR model had the highest VAF values obtaining 99.90 per cent, 94.70 per cent and 94.65 per cent for its training, validation and testing data sets fittings, respectively. All the other predictive models (SVM, ANN and LR) had VAF values <80 per cent across board with their training, validation and testing data sets fittings.

The general assessment of the predictive models indicate that GPR model makes the most precise rougher copper recovery prediction. The unique performance of the GPR could be attributed to its ability to add prior knowledge about the shape of the model by learning the hyperparameters from the training data set. For brevity, parity plots (Figure 1) on the fitting with the testing data set have been used to visualise the distribution of true and predicted rougher copper recovery values of the various investigated predictive models. From Figure 1, it can be seen that GPR model had the narrowest spread of data around its linear fit of true and predicted rougher copper recovery values confirming its superiority over the other investigated models. It must be noted that only standardised results are shown in plots for the purpose of data confidentiality.

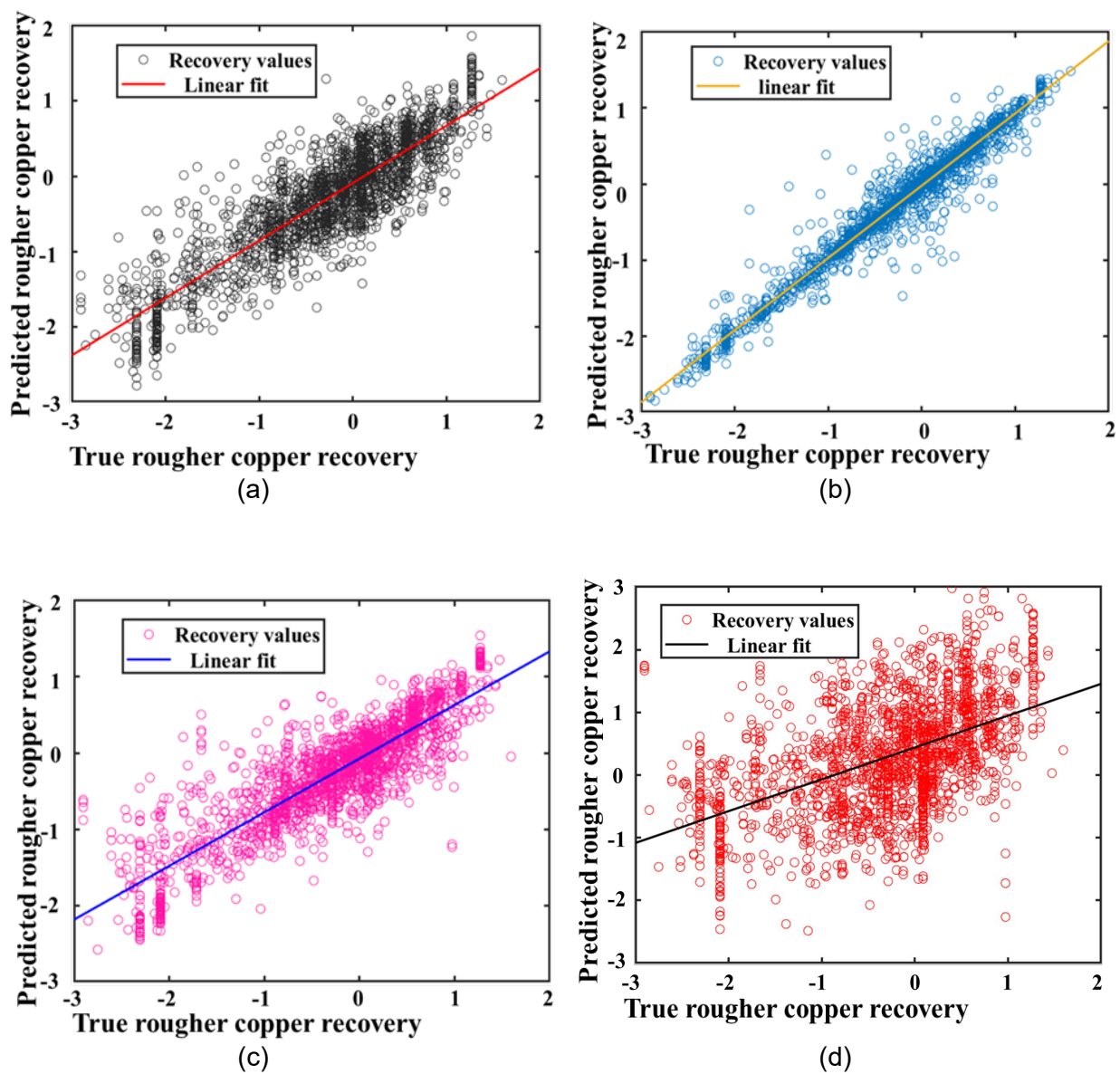


FIG 1 – Parity plot visualising the distribution of true and predicted rougher copper recovery values for: (a) SVM, (b) GPR, (c) ANN and (d) LR models using testing data set.

CONCLUSION

This research investigated the use of support vector machine, Gaussian process regression, artificial neural network and linear regression algorithms in predicting rougher copper recovery. The model performance assessment suggest that Gaussian process regression model makes the best rougher copper recovery prediction compared with other investigated models using relevant flotation variables (feed grade, feed particle size, throughput, xanthate dosage, frother dosage and froth depth).

ACKNOWLEDGEMENT

This research has been supported by the South Australian Government through the PRIF RCP Industry Consortium. The authors would also like to appreciate the tremendous support of BHP Olympic Dam and the Future Industries Institute of the University of South Australia.

REFERENCES

- Ali, D, Hayat, M B, Alagha, L and Molatlhegi, O K, 2018. An evaluation of machine learning and artificial intelligence models for predicting the flotation behavior of fine high-ash coal. *Advanced Powder Technology*, 29(12): 3493–3506.
- Amankwa-Kyeremeh, B, Zhang, J, Zanin, M, Skinner, W and Asamoah, R K, 2021. Feature selection and Gaussian process prediction of rougher copper recovery. *Minerals Engineering*, 170: 107041.
- Asamoah, R K, Zanin, M, Gascooke, J, Skinner, W and Addai-Mensah, J, 2019. Refractory gold ores and concentrates part 1: mineralogical and physico-chemical characteristics. *Mineral Processing and Extractive Metallurgy*: 1–13.
- Breiman, L, 2001. Random forests. *Machine learning*, 45(1): 5–32.
- Chia, C-C, Rubinfeld, I, Scirica, B M, Mcmillan, S, Gurm, H S and Syed, Z, 2012. Looking beyond historical patient outcomes to improve clinical models. *Science translational medicine*, 4(131): 131ra49.
- Cook, R, Monyake, K C, Hayat, M B, Kumar, A and Alagha, L, 2020. Prediction of flotation efficiency of metal sulfides using an original hybrid machine learning model. *Engineering Reports*, 2(6): e12167.
- Feng, Q, Zhang, J, Zhang, X and Wen, S, 2015. Proximate analysis based prediction of gross calorific value of coals: A comparison of support vector machine, alternating conditional expectation and artificial neural network. *Fuel Processing Technology*, 129: 120–129.
- Hodouin, D, 2011. Methods for automatic control, observation, and optimization in mineral processing plants. *Journal of Process Control*, 21(2): 211–225.
- Jahedsaravani, A, Marhaban, M, Massinaei, M, Saripan, M and Noor, S, 2016. Froth-based modeling and control of a batch flotation process. *International Journal of Mineral Processing*, 146: 90–96.
- Jorjani, E, Chelgani, S C and Mesroghli, S, 2007. Prediction of microbial desulfurization of coal using artificial neural networks. *Minerals Engineering*, 20(14): 1285–1292.
- Karimi, M, Akdogan, G and Bradshaw, S, 2014. A computational fluid dynamics model for the flotation rate constant, Part I: Model development. *Minerals Engineering*, 69: 214–222.
- Kettaneh, N, Berglund, A, Wold, S and Analysis, D, 2005. PCA and PLS with very large data sets. *Computational Statistics*, 48(1): 69–85.
- Khodakarami, M, Molatlhegi, O and Alagha, L, 2019. Evaluation of ash and coal response to hybrid polymeric nanoparticles in flotation process: Data analysis using self-learning neural network. *International Journal of Coal Preparation and Utilization*, 39(4): 199–218.
- Mathe, Z, Harris, M and O'Connor, C, 2000. A review of methods to model the froth phase in non-steady state flotation systems. *Minerals Engineering*, 13(2): 127–140.
- Murphy, D, Zimmerman, W and Woodburn, E, 1996. Kinematic model of bubble motion in a flotation froth. *Powder technology*, 87(1): 3–12.
- Polat, M and Chander, S, 2000. First-order flotation kinetics models and methods for estimation of the true distribution of flotation rate constants. *International Journal of Mineral Processing*, 58(1): 145–166.
- Quintanilla, P, Neethling, S J and Brito-Parada, P R, 2021. Modelling for froth flotation control: A review. *Minerals Engineering*, 162: 106718.
- Rasmussen, C E, 2003. *Gaussian processes in machine learning*, Summer school on machine learning. Springer, pp. 63–71.
- Roy, K, Kar, S and Das, R N, 2015. Chapter 6 – Selected Statistical Methods in QSAR. In: K Roy, S Kar and R N Das (eds), *Understanding the Basics of QSAR for Applications in Pharmaceutical Sciences and Risk Assessment*. Academic Press, Boston, pp. 191–229.

- Schalkoff, R J, 1997. *Artificial neural networks*. McGraw-Hill Higher Education.
- Shahbazi, B, Chehreh Chelgani, S and Matin, S S, 2017. Prediction of froth flotation responses based on various conditioning parameters by Random Forest method. *Colloids and Surfaces A: Physicochemical and Engineering Aspects*, 529: 936–941.
- Snelson, E L, 2008. *Flexible and efficient Gaussian process models for machine learning*. University of London, University College London (United Kingdom).
- Urbina, R H, 2003. Recent developments and advances in formulations and applications of chemical reagents used in froth flotation. *Mineral Processing and Extractive Metallurgy Review*, 24(2): 139–182.
- Zarie, M, Jahedsaravani, A and Massinaei, M, 2020. Flotation froth image classification using convolutional neural networks. *Minerals Engineering*, 155: 106443.

Correlating process mineralogy and pulp chemistry for quick ore variability diagnosis

B Amankwaa-Kyeremeh¹, C J Greet², W Skinner³ and R K Asamoah⁴

1. PhD student, University of South Australia, UniSA STEM, Future Industries Institute, Adelaide SA 5095. Email: bismark.amankwaa-kyeremeh@mymail.unisa.edu.au
2. Manager Metallurgy, Magotteaux Pty Ltd, Adelaide SA 5095. Email: christopher.greet@magotteaux.com
3. Research Professor, University of South Australia, UniSA STEM, Future Industries Institute, Adelaide SA 5095. Email: william.skinner@unisa.edu.au
4. Post-Doctoral Fellow, University of South Australia, UniSA STEM, Future Industries Institute, Adelaide SA 5095. Email: richmond.asamoah@unisa.edu.au

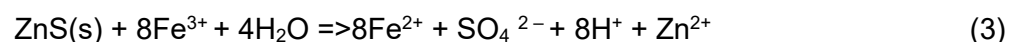
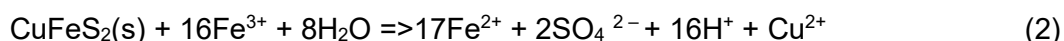
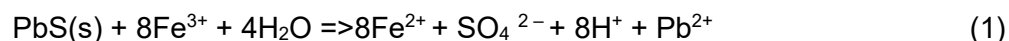
ABSTRACT

Froth flotation is a mineral separation technique that treats large tonnages of sulfide bearing ores around the globe annually. Factors such as mineralogical composition as well as galvanic interactions between minerals surfaces and grinding media are known to control and affect the selectivity efficiency of the process. To understand these interactions, pulp chemistry information such as pH, pulp potential (Eh), dissolved oxygen (DO), oxygen demand (OD), and temperature (T) could be of great use. This work focused on unravelling potential relationships between time stamped pulp chemistry data (DO, pH and Eh) and rougher feed pyritic mineral content using statistical approaches (Pearson's correlation coefficient criterion and mutual information). Furthermore, the potential prediction of rougher feed pyritic mineral content from DO, pH and Eh was also investigated using Gaussian process regression model. Results revealed some level of association (linear and nonlinear) between DO, pH, Eh and rougher feed pyritic mineral content. This results give room for improved process prediction based on pulp chemistry, a potential diagnostic tool for quick detection of ore variability.

INTRODUCTION

Froth flotation continues to be the main drive force for the sustenance of the mineral processing industry (Farrokhpay, 2011). For over a century now, the separation technique has been used to treat billions of sulfide bearing ores around the globe. In as much as the process can loosely be described as the separation of minerals based on the difference in their surface wettability, the separation efficiency is much dependent on the chemical environment in which it is carried out (Greet *et al*, 2004). It has been established that, the selectivity of valued sulfide minerals revolves around proper manipulation of pulp chemistry parameters which are generally known to be affected by the mineralogical composition of the ore as well the galvanic interactions between mineral surfaces and grinding media (Abraitis, Pattrick and Vaughan, 2004; Amankwaa-Kyeremeh *et al*, 2020; Owusu *et al*, 2013; Rimstidt and Vaughan, 2003). The main challenge is that, the flotation chemical environment is very difficult to stabilise and eventually be controlled. However, changes in flotation chemical environment can be tracked with information from pulp chemistry parameters like pH, pulp potential (Eh) dissolved oxygen (DO), oxygen demand (OD), and temperature (Sheni, Corin and Wiese, 2018).

For instance pulp potential particularly has been known to be affected by the available dissolved oxygen content in a flotation system especially when the dissolved oxygen content is not enough to consume the excess electrons produced by galvanic interactions (Rabieh, Albijan and Eksteen, 2016). As part of the work done by Greet, Kinal and Mitchell (2006), they concluded that iron sulfide content in an ore could be the main cause of redox potential depreciation in a flotation system which implies that when redox potential of a flotation system is closely monitored, variation in iron sulfide content could be detected for the necessary step to be taken. Chalcopyrite, galena or sphalerite have been reported to generate acid when their oxidation is occurring as a result of Fe(III) ions (Equations 1–3) (Alakangas, 2006). Acid generated by these sulfide minerals leads to the excessive consumption of pH modifiers and therefore the changes in pH could present a unique opportunity for predicting variation in feed characteristics towards mitigating undesirable process outcome.



Bradshaw *et al* (2006) indicated that, sulfide minerals are semiconductors in general which make them susceptible to oxidation. Oxygen content is far reduced to about less than 1 ppm when they react with reactive sulfides or when they react with ions such as chlorides and cupric ions (Kelebek and Yoruk, 2002). The higher the proportion of minerals such as pyrite and pyrrhotite, the more significant oxygen saturation becomes in enhancing mineral floatability. Early works done by researchers like Plaksin and Bessonov (1957) showed that there is strong correlation between oxygen content and sulfide minerals floatability. This therefore implies that establishing strong relationship between dissolved oxygen content and flotation feed with links to reactive component, smarter control options could be achieved.

The feasibility of predicting changes in ore mineralogy from pulp chemistry data implies that comprehensive data on flotation feed and pulp chemistry data will be required. As such, strong recent emerging machine learning algorithms such as artificial neural network (ANN), support vector machine (SVM), and Gaussian process regression (GPR) would be very useful in establishing the relationship between ore mineralogy and pulp chemistry. In this work, relationships (both linear and nonlinear) between time stamped pulp chemistry parameters (DO, pH and Eh) and rougher feed pyritic mineral content was investigated using Pearson's correlation coefficient criterion and mutual information. Pearson's correlation coefficient criterion is the most common correlation coefficient approach which has the ability to capture the linear dependence between two variables (Amankwaa-Kyeremeh *et al*, 2021). Mutual information on the other hand can capture the general dependence (including nonlinear relationships) between two random variables and therefore dependencies that do not rely on covariance can still be captured by this approach. Following this, a GPR algorithm was used to develop a predictive model for the prediction of rougher feed pyritic mineral content using DO, pH and Eh as input variables. The motivation for GPR algorithm for this work is its ability to cater for the uncertainties in a data by modelling the existing noise that comes with the data (Arthur, Temeng and Ziggah, 2020). Specifically, this work addresses the following research questions:

- Are there relationships between pulp chemistry parameters (DO, pH and Eh) and rougher feed pyritic mineral content?
- Can GPR algorithm make good rougher feed pyritic mineral content prediction using pulp chemistry parameters (DO, pH and Eh) as input variables?

The remainder of this paper is as follows. After this introduction, methodologies adopted for this work have been captured in Section 2. Section 3 highlights on the discussion of the various results that were obtained and finally drawing conclusions in Section 4.

METHODOLOGY

Data collection

This work was carried out in a typical copper processing plant in Australia. The name of the mine cannot be disclosed for the purpose of data confidentiality. The rougher bank where this study was carried out is made of five tank cells with two reagent dosing point (tank cell 1 and 4). The bank is fed from a combined stream of conditioning tank, cleaner tails and scavenger concentrate. Tails and concentrate from the roughing stage are fed to scavenger and cleaner tank cells, respectively. Unlike other flotation variables that are continuously monitored with sensors and other automatic samplers on the plant, pulp chemistry data in terms of DO, pH, and Eh had to be collected manually on the plant using a multipurpose pulp chemistry metre (TPS 90 – FLMV data logger) as shown in Figure 1.



FIG 1 – Data collection using TPS 90 – FLMV data logger.

To do this, the metre probes were first calibrated with standard calibration solutions to ensure accurate readings. About 500 ml of the rougher feed was scooped into a plastic container and continuously stirred until equilibrium readings were obtained for all the parameters. The time stamped stabilised readings were then logged in the device memory to be accessed later. The whole process was repeated at an average of four hours per day for a period of two weeks resulting in 300 observations. After this, corresponding time stamped data on rougher feed pyritic mineral content (Fe:S) was downloaded from the data historian of the plant for the analysis. It must be noted that pyritic mineral content is the amount of total iron (Fe) and sulfides (S) originating from all Fe and S bearing minerals in the ore. Table 1 gives a summary of variable types used for the analysis.

TABLE 1

Summary of variables used for the analysis.

Variable	Variable type
DO (ppm)	Input variables
pH	
Eh (mV)	
Rougher feed pyritic mineral content (%)	Output variable

Correlation analysis

Correlation analysis is a statistical evaluation technique used to investigate whether there is an association (linear or nonlinear) between two numerically measured, continuous variables. Two variables are known to be correlated when a change in the magnitude of one variable is known to affect the magnitude of the other. For this work, linear correlation analysis was carried out between two variables say a and b using Pearson's correlation coefficient criterion R as shown in Equation 4.

$$R(a, b) = \frac{1}{n-1} \sum_{i=1}^n \left(\frac{a_i - \bar{a}}{S_a} \right) \left(\frac{b_i - \bar{b}}{S_b} \right) \quad (4)$$

Where n is the total number of observations, a_i is the values of variable a , b_i is the values of variable b . \bar{a} and S_a are the mean and standard deviation of variable a , respectively. \bar{b} and S_b are the mean and standard deviation of variable b , respectively. Pearson's correlation coefficient are scaled to have values in the range of +1 and -1 such that variables with strong correlations have values approaching ± 1 depending on their directions. Variables with negligible or no correlation on the other hand have values approaching zero. Irrespective of the sign (positive or negative) of a Pearson's correlation coefficient value, the general rule of thumb for interpreting the size is such that, correlation values <0.30 have negligible correlation, 0.30–0.50 have low correlation, 0.5–0.70 indicate

moderate correlation, 0.70–0.90 shows high correlation and 0.90–1.00 is a clear indication of very high correlation (Amankwaa-Kyeremeh *et al*, 2021).

Nonlinear correlation was also investigated using mutual information. The mathematical expression of mutual information between two variables say a and b assuming a joint probability distribution is shown in Equation 5.

$$I(a; b) = D(P_{ab} || P_a \times P_b) \quad (5)$$

where

D	= Kullback–Leibler divergence
P_{ab}	= joint distribution of variables a and b
P_a	= marginal distribution of a
P_b	= marginal distribution of b

Mutual information estimates the quantity of information that can be obtained from one random variable given another random variable. Mutual information can closely be linked to the concept of entropy such that high mutual information score indicates a large reduction in uncertainty and vice versa. If the mutual information between two variables is zero, then the two random variables are independent and therefore have no correlation at all (Kraskov, Stögbauer and Grassberger, 2004; Li, 1990).

Model development

A GPR algorithm was used to build a correlation structure between the input variables and output variable as summarised in Table 1. To mimic a typical industrial practice, the hold cross validation technique was adopted for this work using a random partition of 80 per cent (240 observations) training data set and 20 per cent (60 observations) testing data set. It must be noted that there is no general rule for the partition ratio only that as a rule of thumb, the training data set should be significantly more than the testing data set to capture the entire characteristics of the data. The model was trained with training data set and fitted with both the training and testing data sets.

GPR algorithm

A Gaussian process $t(x)$ can be considered as a stochastic process such that every finite collection of the random variables comes with a joint Gaussian distribution (Amankwaa-Kyeremeh *et al*, 2021; Rasmussen, 2003). $t(x)$ is parameterised by a mean function $m(x)$ and a kernel function $k(x, x')$ expressed at points x and x' . Equations 6 and 7 have been used to express $m(x)$ and $k(x, x')$.

$$m(x) = E(t(x)) \quad (6)$$

$$k(x, x'; \theta) = (E((t(x) - m(x))(t(x') - m(x')))) \quad (7)$$

Where θ is the set of hyperparameters learned from the training data via maximum marginal likelihood.

Equation 8 has been used to express the function $t(x)$ in terms of $m(x)$ and $k(x, x')$.

$$t(x) \sim \text{GP}(m(x), k(x, x')) \quad (8)$$

GP stands for Gaussian process implying that $t(x)$ is distributed as a GP with mean $m(x)$ and a kernel function $k(x, x')$. For this work, the most commonly used kernel function (squared exponential kernel function) was used as shown Equation 9 (Snelson, 2008).

$$C(x_i, x_j | \theta) = \sigma_f^2 \exp \left[-\frac{1}{2} \frac{(x_i - x_j)'(x_i - x_j)}{\sigma_l^2} \right] \quad (9)$$

Where

θ	= set of hyperparameters
σ_l	= characteristic length scale
σ_f	= signal standard deviation

Model performance assessment criteria

To assess the performance of the developed GPR model, three performance indicators were adopted for this research. These are correlation coefficient (r), mean absolute error (MAE) and root mean square error (RMSE). The mathematical expression of these performance indicators are shown in Equations 10–12. A good predictive model should have r value approaching 1 with MAE and RMSE values approaching zero.

$$r = \frac{\sum_{i=1}^n (y_i - \bar{y}) - (\hat{y}_i - \bar{\hat{y}})}{\sum_{i=1}^n (y_i - \bar{y})^2 \times \sqrt{\sum_{i=1}^n (\hat{y}_i - \bar{\hat{y}})^2}} \quad (10)$$

$$\text{MAE} = \left(\frac{1}{n}\right) \sum_{i=1}^n |y_i - \hat{y}_i| \quad (11)$$

$$\text{RMSE} = \sqrt{\left(\frac{1}{n}\right) \sum_{i=1}^n (y_i - \hat{y}_i)^2} \quad (12)$$

where

- y_i = true rougher feed pyritic mineral content values
- \bar{y} = mean of true rougher feed pyritic mineral content values
- \hat{y}_i = predicted rougher feed pyritic mineral content values
- $\bar{\hat{y}}$ = mean of predicted rougher feed pyritic mineral content values
- n = total number of observations

RESULTS AND DISCUSSION

Results of correlation analysis

Correlation analysis has been carried out between DO, pH, Eh and rougher feed pyritic mineral content using Pearson's correlation coefficient criterion and mutual information for linear and nonlinear correlation investigations, respectively. Results from the analysis have been summarised in Table 2. From Table 2, it can be seen that DO had the highest linear correlation with rougher feed pyritic mineral content obtaining a value of -0.62. This was followed by Eh and pH which recorded linear correlations values of -0.38 and -0.20, respectively. It must be noted that the signs in front of Pearson's correlation coefficient values only indicate the direction and not the strength. With regards mutual information, DO once again had the highest mutual information score obtaining a value of 0.41 followed by pH and Eh which recorded 0.21 and 0.17, respectively. This results confirm that some level of both linear and nonlinear correlation exist between the input variables (DO, pH and Eh) and output variable (rougher feed pyritic mineral content) and therefore could be used for regression analysis.

TABLE 2
Summary of correlation analysis results.

Pulp chemistry parameter	Rougher feed pyritic mineral content	
	Pearson's correlation criterion R	Mutual information
DO (ppm)	-0.62	0.41
pH	-0.20	0.21
Eh (mV)	-0.38	0.17

Predictive model performance assessment

The prediction of rougher feed pyritic mineral content from DO, pH and Eh was investigated using a GPR algorithm. To evaluate the model performance, correlation coefficient (r), mean absolute error (MAE) and root mean square error (RMSE) indicators were used. Summary of model performance

is shown in Table 3. From Table 3, it can be observed that fitting the trained GPR model with the training data set gave a higher r value of 0.90 as compared to 0.87 when fitting was done with the testing data set. In terms of MAE indicator, 1.52 and 1.79 were the values that were recorded for fittings done with the training and testing data sets, respectively. RMSE values of 1.92 and 2.16 were recorded for fittings done with the training and testing data sets, respectively. It can generally be observed from Table 3 that the training data set performance was better than the testing data set. This is a normal trend because the training data set was already exposed to trained model unlike the testing data set which was entirely new to the model. Results from Table 3 further shows that the model is not overfitting (good training performance but bad testing performance) considering the difference in performance for fittings done with the training and testing data sets. In as much as the r values can be considered to very good (>0.80), values for the error statistics (MAE and RMSE) were not really up to expectation. This performance could be improved when more data set is collected for future work owing to the fact GPR model is data driven and therefore when high volume of data set is used for training, model would become less sensitivity to minor changes during prediction.

TABLE 3

Summary of model performance assessment using correlation coefficient (r), mean absolute error (MAE) and root mean square error (RMSE).

GPR model	Training data set	Testing data set
r	0.90	0.87
MAE	1.52	1.79
RMSE	1.92	2.16

Parity plots visualising the distribution of true and predicted rougher feed pyritic mineral values using training and testing data sets have been shown in Figure 2. For the purpose of data confidentiality, only standardised values are shown in the plots. From the Figure 2, it can be seen that fitting done with the training data set had a narrow spread as compared to fitting done with the testing data set as already discussed.

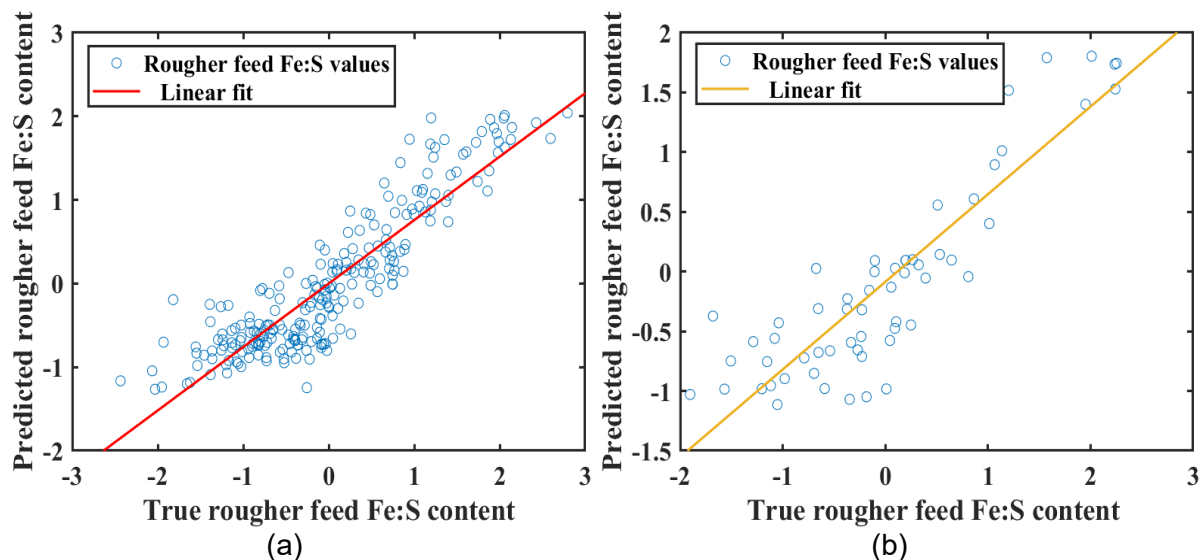


FIG 2 – Parity plots visualising the distribution of true and predicted pyritic mineral values using (a) training data set, and (b) testing data set.

CONCLUSION

This work investigated the potential relationship (both linear and nonlinear) between pulp chemistry parameters (DO, pH and Eh) and rougher feed pyritic mineral content using Pearson's correlation coefficient criterion and mutual information statistical approaches. Following this, a GPR model was

developed for the prediction of rougher feed pyritic mineral content using DO, pH and Eh as input variables. The following are the key findings:

- Correlation analysis revealed that both linear and nonlinear relationships exist between DO, pH, Eh and rougher feed pyritic mineral content.
- Assessment of GPR model using correlation coefficient (r), mean absolute error (MAE) and root mean square error (RMSE) indicators showed that GPR model can make satisfactory rougher feed pyritic mineral content prediction from DO, pH and Eh.

The significance of this work is that, an improved version of the predictive model could be used as a potential diagnostic tool for the detection of changes in ore mineralogy during froth flotation.

ACKNOWLEDGEMENT

This research has been supported by the South Australian Government through the PRIF RCP Industry Consortium. The authors would also like to appreciate the tremendous support of BHP Olympic Dam and the Future Industries Institute of the University of South Australia.

REFERENCES

- Abraitis, P K, Patrick, R A D and Vaughan, D J, 2004. Variations in the compositional, textural and electrical properties of natural pyrite: a review. *International Journal of Mineral Processing*, 74(1): 41–59.
- Alakangas, L, 2006. Sulphide oxidation, oxygen diffusion and metal mobility in sulphide-bearing mine tailings in Northern Sweden, Luleå tekniska universitet.
- Amankwaa-Kyeremeh, B, Greet, C J, Skinner, W and Asamoah, R K, 2020. A brief review of pulp chemistry parameters in relation to flotation feed variation. *International Mineral Processing Congress*, Cape town: 1909–1917.
- Amankwaa-Kyeremeh, B, Zhang, J, Zanin, M, Skinner, W and Asamoah, R K, 2021. Feature selection and Gaussian process prediction of rougher copper recovery. *Minerals Engineering*, 170: 107041.
- Arthur, C K, Temeng, V A and Ziggah, Y Y, 2020. Novel approach to predicting blast-induced ground vibration using Gaussian process regression. *Engineering with Computers*, 36(1): 29–42.
- Bradshaw, D J, Buswell, A M, Harris, P J and Ekmekci, Z, 2006. Interactive effects of the type of milling media and copper sulphate addition on the flotation performance of sulphide minerals from Merensky ore Part I: Pulp chemistry. *International Journal of Mineral Processing*, 78(3): 153–163.
- Farrokhpay, S, 2011. The significance of froth stability in mineral flotation—A review. *Advances in Colloid Interface Science*, 166(1–2): 1–7.
- Greet, C J, Small, G L, Steinier, P and Grano, S R, 2004. The Magotteaux Mill®: investigating the effect of grinding media on pulp chemistry and flotation performance. *Minerals Engineering*, 17(7): 891–896.
- Greet, C, Kinal, J and Mitchell, I, 2006. Is Measuring pH Enough? *Metallurgical Plant Design*, Perth, WA.
- Kelebek, S and Yoruk, S, 2002. Bubble contact angle variation of sulphide minerals in relation to their self-induced flotation. *Colloids Surfaces A: Physicochemical Engineering Aspects*, 196(2–3): 111–119.
- Kraskov, A, Stögbauer, H and Grassberger, P, 2004. Estimating mutual information. *Physical review E*, 69(6): 066138.
- Li, W, 1990. Mutual information functions versus correlation functions. *Journal of statistical physics*, 60(5): 823–837.
- Owusu, C, Addai-Mensah, J, Fornasiero, D and Zanin, M, 2013. Estimating the electrochemical reactivity of pyrite ores—their impact on pulp chemistry and chalcopyrite flotation behaviour. *Advanced Powder Technology*, 24(4): 801–809.
- Plaksin, I and Bessonov, S, 1957. *Role of gases in flotation reactions*.
- Rabieh, A, Albijanic, B and Eksteen, J J, 2016. A review of the effects of grinding media and chemical conditions on the flotation of pyrite in refractory gold operations. *Minerals Engineering*, 94: 21–28.
- Rasmussen, C E, 2003. *Gaussian processes in machine learning*, Summer school on machine learning. Springer, pp. 63–71.
- Rimstidt, J D and Vaughan, D J, 2003. Pyrite oxidation: a state-of-the-art assessment of the reaction mechanism. *Geochimica et Cosmochimica acta*, 67(5): 873–880.
- Sheni, N, Corin, K and Wiese, J, 2018. Considering the effect of pulp chemistry during flotation on froth stability. *Minerals Engineering*, 116: 15–23.
- Snelson, E L, 2008. *Flexible and efficient Gaussian process models for machine learning*. University of London, University College London (United Kingdom).

High density gravity separation circuits – a pathway to sustainable minerals beneficiation

M T Gill¹, R M G MacHunter² and E Raffailac³

1. AAusIMM, Senior Process Engineer, Mineral Technologies Pty Ltd, Dulwich SA 5065.
Email: matthew.gill@mineraltechnologies.com
2. Senior Principal Process Engineer, Mineral Technologies Pty Ltd, Carrara Qld 4211.
Email: dolf.machunter@mineraltechnologies.com
3. MAusIMM, Principal Process Engineer, Mineral Technologies Pty Ltd, Carrara Qld 4211.
Email: etienne.raffailac@mineraltechnologies.com

ABSTRACT

The global mining industry is facing significant challenges through declining ore grades and increased difficulty in securing required water and energy. When combined with increasing societal and shareholder pressure, it is evident that the industry must innovate to minimise the impacts of resource extraction and ensure a sustainable future.

Traditional mineral processing flow sheets, including gravity (spiral separators), magnetic and flotation, utilise significant quantities of energy and water for materials transport and to achieve optimum metallurgical performance. Consequently, these flow sheets are prime candidates to benefit from innovative approaches to lower water consumption.

Recent test work, piloting and infield trials conducted by Mineral Technologies (MT) on their new compact turbo (CT1) separator has demonstrated high recovery of valuable minerals when operating at feed densities of up to 60 per cent solids (w/w). This testing was conducted on various ores and showed comparable metallurgical performance at high feed densities compared to industry standard spiral separators fed at 35 per cent solids (w/w).

A desktop study was conducted on a low-grade, high tonnage African mineral sand wet concentration plant comparing traditional and high density three stage spiral circuits (based on tested performance curves). The simulation showed reductions of >60 per cent in total pumping volume and >70 per cent in water usage, with proportional reductions in energy consumption and equipment sizes. The high density CT1 spiral feed also leads to a high-density tailings product, which reduces tailings pumping volumes by >50 per cent.

The high-density spiral circuit presented in this paper represents a major step forward for gravity beneficiation. The demonstrated reductions in energy and water consumption and tailings volume will greatly reduce the environmental and social impacts of existing and new operations. The reduced capital and operating costs will improve the economics of lower grade marginal deposits and further increase the profitability of high-grade prospects.

INTRODUCTION

The global mining industry is facing significant challenges from declining ore grades and increased difficulty in securing the required water and energy necessary to extract and process minerals. A study into water consumption in the coal industry in New South Wales, Australia has shown that water usage per tonne of coal produced has increased from 250 litres per tonne in 2010 to 653 litres per tonne in 2019 (Overton, 2020). The impact of this water extraction, as well as water held in tailings and supply dams is often a significant concern to host communities and cannot be understated.

The combination of these factors has led to increased societal and shareholder pressure on operators to find innovative ways to minimise the impacts of their resource extraction. This paper discusses how these challenges are being met through innovations in equipment design via a heavy mineral sands example.

BACKGROUND

Traditional mineral processing flow sheets, incorporating gravity (spiral separators), magnetic and flotation separation technologies, require significant quantities of energy and water for materials transport and to achieve optimum metallurgical performance. In most cases, the feed density to these key beneficiation processes must be in the order of 20–40 per cent solids (w/w), primarily because of impaired metallurgical performance observed at higher densities. These flow sheets are prime candidates to benefit from innovative approaches to reduced water consumption.

SPIRAL SEPARATORS

Spiral separators are a selective, simple, chemical-free and low-complexity method for recovering valuable minerals. They make use of differences in specific gravities (sg) between mineral particles to achieve separation. In practice this comes about by directing a mineral slurry down an inclined, helical trough. Higher sg particles move down to the lower, inside section of the trough, whilst lower sg particles, and most of the water, are forced outwards and flow down the outer part of the trough. For the most part, depending on the particle sg, the particles follow different trajectories, and therefore, they can be diverted and kept apart via the use of splitters mounted on the trough. In mineral sands for example, the inner darker band represents the flow of the heavier minerals, typically the titanium-bearing minerals ilmenite and rutile and the zirconium silicate mineral, zircon. The wider straw-coloured band represents the passage of the lighter, silica minerals.

As a result, spiral separators have been widely accepted as one of the most flexible gravity separation devices for half a century, with benefits such as low cost, high separation efficiency and ease of operation (MacHunter, Richards and Palmer, 2003).

Shortcomings of traditional spirals

Shortcomings of traditional spiral separators include relatively low unit throughputs, the need for multi-stage processing, lack of control of product pulp density and limited acceptable feed size ranges (MacHunter, Richards and Palmer, 2003). Many of these constraints have eased through the development of newer spiral separator models, some of which are ultra-specific in their design, such as those for the beneficiation of fine mineral sand and fine coal.

Spiral circuits are typically designed and operated at feed densities in the range of 25–40 per cent solids (w/w). This feed density ensures optimal metallurgical performance and is supported by numerous laboratory and pilot testing programs as well as established mining operations. Whilst the required recoveries and product grades are achieved it does mean that large volumes of low-density tailings are produced. These tailings must be managed appropriately; usually via dewatering within the processing plant and/or at the tailings storage facility. Any water recovered through these processes is effectively 'double handled,' which further adds to the venture's operating cost.

Slime (<45 µm) material, which once emulsified follows the water balance, typically must be removed for water to be recycled in the process. This is completed via thickeners and/or settling dams. The size of the slime tailing handling facility is directly proportional to the plant (spiral) feed density and hence operating at higher feed densities will significantly reduce CAPEX and OPEX for any operation.

To reduce spiral circuit water demand, Mineral Technologies have developed the model CT1 spiral separator specifically to operate at higher slurry density feeds.

CT1 SEPARATOR

Development process

The development process of the CT1 spiral separator was novel and largely due to 'out-of-the-box' thinking by the MT research and development team. With a general trend to provide more processing power per footprint, volume hungry larger diameter mineral spirals were developed. In conjunction with traditional sized separators, these spiral models all exhibit similar constraints on feed slurry density.

In a somewhat contradictory investigation, and in conjunction with the application of 3D printed spiral troughs, an 150 mm diameter prototype spiral profile was developed. This spiral profile provided mineral recoveries close to that of a shaking table, which is unheard of with respect to any of the existing spiral separator models. This was however at a significantly reduced capacity per unit area with respect to the larger production units. Despite this, and primarily due to the order of magnitude increase in separation performance, further efforts were made to develop the smaller diameter spiral into a cost-effective process package.

The CT1 separator was developed as a small diameter, highly volume efficient gravity separator with seven starts per column/module. The final production unit utilises 250 mm diameter tooling to ensure it has the ability to pack into the same cross-sectional area as the existing flagship model, the MG12. This has minimised the changes required to existing steel spiral frames and provided seamless integration into new plant designs, as well as existing operations.

The CT1 separator is shown in Figure 1b adjacent to a conventional spiral (Figure 1a). This figure also highlights the four column design and provides a comparison in size to the MG12, refer Figure 1c.

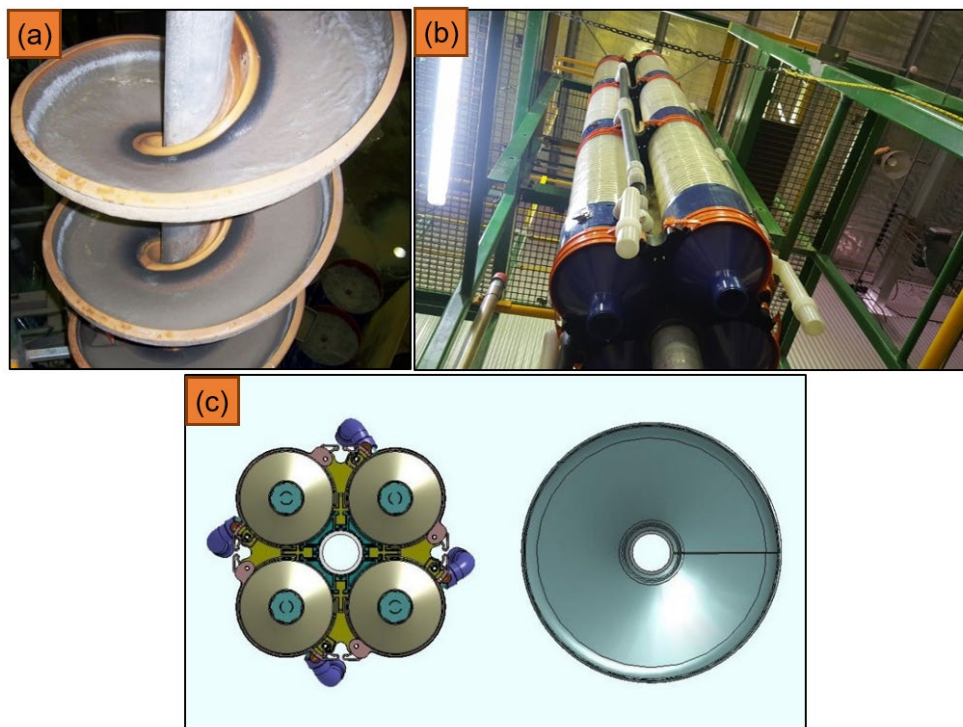


FIG 1 – CT1 separator: (a) conventional spiral separator, (b) CT1 separator, (c) CT1 versus MG12 (size comparison).

Functional description

The CT1 separator is a customisable, modular, gravity separator consisting of fully enclosed segments vertically stacked together. Strategically placed splitter segments allow extraction of high-density concentrate (super concentrate, or 'C1') as the slurry travels down the trough. The profile of the separator is designed for roughing and scavenging duties, with the primary focus on achieving high recoveries. Key features of the CT1 separator are depicted in Figure 2 and outlined below:

- The feed density to the CT1 separator is up to 60 per cent solids (w/w).
- Close coupled head distributor, feeding four × clusters (MG12 equivalent, as shown in Figure 1) or six × clusters (high-capacity model equivalent).
- Seven-way feed distribution system (transition segment) for each cluster:
 - For a typical four × cluster model, this corresponds to 28 starts per assembly.

- Adjustable concentrate splitters located within the transition segments:
 - The take-offs are optimised through test work prior to manufacture.
- Modularity and flexibility depending on the feed material:
 - As many turns as needed.
 - Typically – two, three or five module sets per assembled cluster.
 - Optimised by adding or subtracting segments.
- Optional range of highly wear-resistant polymers on all operating surfaces.

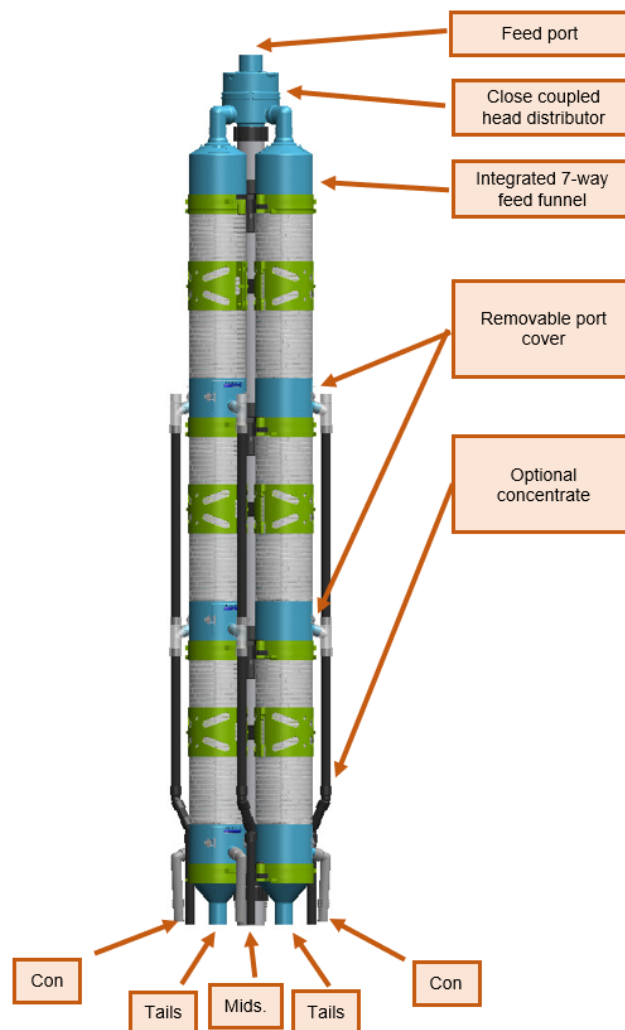


FIG 2 – CT1 separator – key features.

Test work data and performance

Mineral Technologies have conducted multiple laboratory and pilot test work campaigns to quantify the performance of the CT1 separator. Tests were conducted on a low-grade African mineral sands ore currently at the DFS level of investigation. A summary plot of separation efficiency versus feed slurry density for the MG12 spiral and CT1 separator is included in Figure 3.

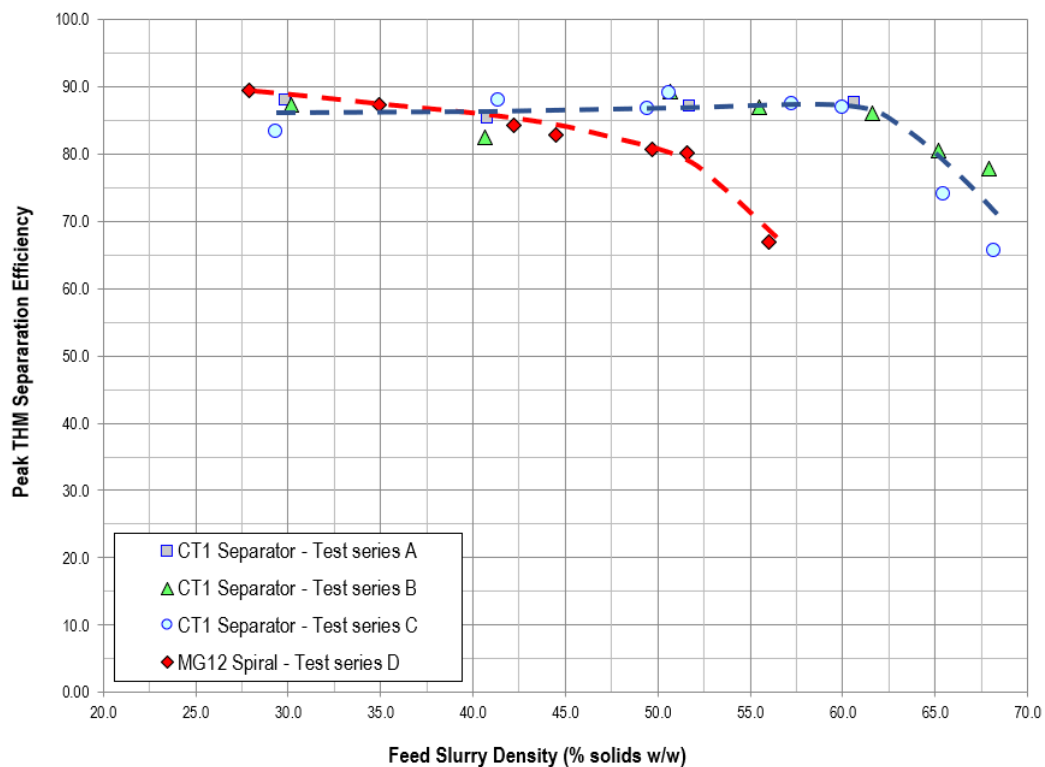


FIG 3 – CT1 spiral performance versus MG12 (various conditions).

Figure 3 demonstrates that the peak performance of the CT1 separator is comparable or slightly superior to the MG12 spiral separator at feed densities of up to 60 per cent solids (w/w). In contrast, the performance of the MG12 spiral separator falls away significantly as the feed density increases.

The CT1 separator produces concentrate, middlings and tailings densities that almost mirror the feed. That is, a CT1 separator fed at 60 per cent solids w/w will produce a tailings density like the feed density, particularly when treating low-grade feed material.

The reason the CT1 separator provides comparable performance to the MG12 spiral separator at these higher densities is not fully understood. It is believed that the CT1 separator is behaving like a 'pinched sluice' device such as a cone concentrator due to the comparatively shallower pitch and smaller diameter and profile. This leads to a reduction or elimination of cross trough circulation (secondary flow) that has been observed in larger diameter spiral separators (MacHunter, Richards and Palmer, 2003).

LFCU – ADVANTAGES AND RELEVANCE TO HIGH DENSITY SEPARATION

The mining industry, particularly in mineral sands, has been reluctant to design and operate plants which employ high density slurry lines. The cause of this hesitancy arises from plant operator and plant metallurgist belief that control of high-density slurries is problematic and unforgiving, and that even minor process upsets result in 'sanding' events that can lead to multiple-day downtimes.

The mass flow enabling design of the MT Lyons Feed Control Unit (LFCU) (Lyons *et al*, 2009), in conjunction with finely controlled dilution water, results in highly stable discharge densities of up to 70 per cent solids w/w despite variable feed inputs. This is considered a key enabler of the CT1 separator, or any other high-density gravity flow sheet.

The LFCU can be incorporated into spiral circuits to ensure consistent rougher feed densities for optimum metallurgical performance, as well as for tailings densification purposes. There are several real-world examples of LFCUs delivering densities with minimal variance, including several which are being utilised for tailings densification purposes operating well in excess of 60 per cent solids (w/w) with large pumping distances.

CASE STUDY – TRADITIONAL VERSUS HIGH DENSITY FLOW SHEET

To complement the test work result presented in Figure 3, a desktop study was conducted to highlight the significant advantages of a CT1 separator circuit. This study was centred on an African mineral sand wet concentration plant (WCP) and compared traditional and high density three-stage spiral circuits (using tested performance curves).

Flow sheet description and input criteria

For the purpose of this study, each flow sheet simulation was isolated to the spiral circuit. The circuit includes the processing stages outlined below and as depicted in the block diagram in Figure 4.

- LFCU – Surge Bin.
- Three stage gravity circuit:
 - rougher
 - mid scavenger
 - cleaner.

The rougher stage generates concentrate, middlings and tailings streams. The middlings stream reports to the mid scavenger stage for further processing, while concentrate moves forward in the circuit to the cleaner stage and the tailings to final tails. The mid-scavenger stage also generates three products, with the concentrate moving forward to the cleaner stage, middlings recirculated and tailings reporting to final tail. The cleaner stage concentrate stream reports to the final product sump, middlings recirculated and tailings to the mid scavenger stage.

The separation performance of each stage used as the basis of the simulations have been derived from physical test work data conducted on full-scale separation equipment (MG12 and VHG spiral separators and CT1 separator) on a representative sample of the expected feed material.

The traditional circuit employed industry standard MT MG12 spirals in the rougher and middlings scavenger (mid scav) duties (fed at 35 per cent solids w/w). The CT1 circuit replaced these MG12s with the CT1 separator fed at higher densities (variable). Both circuits utilised ‘very high-grade’ (VHG) spirals in a cleaning duty (fed at 35 per cent solids w/w).

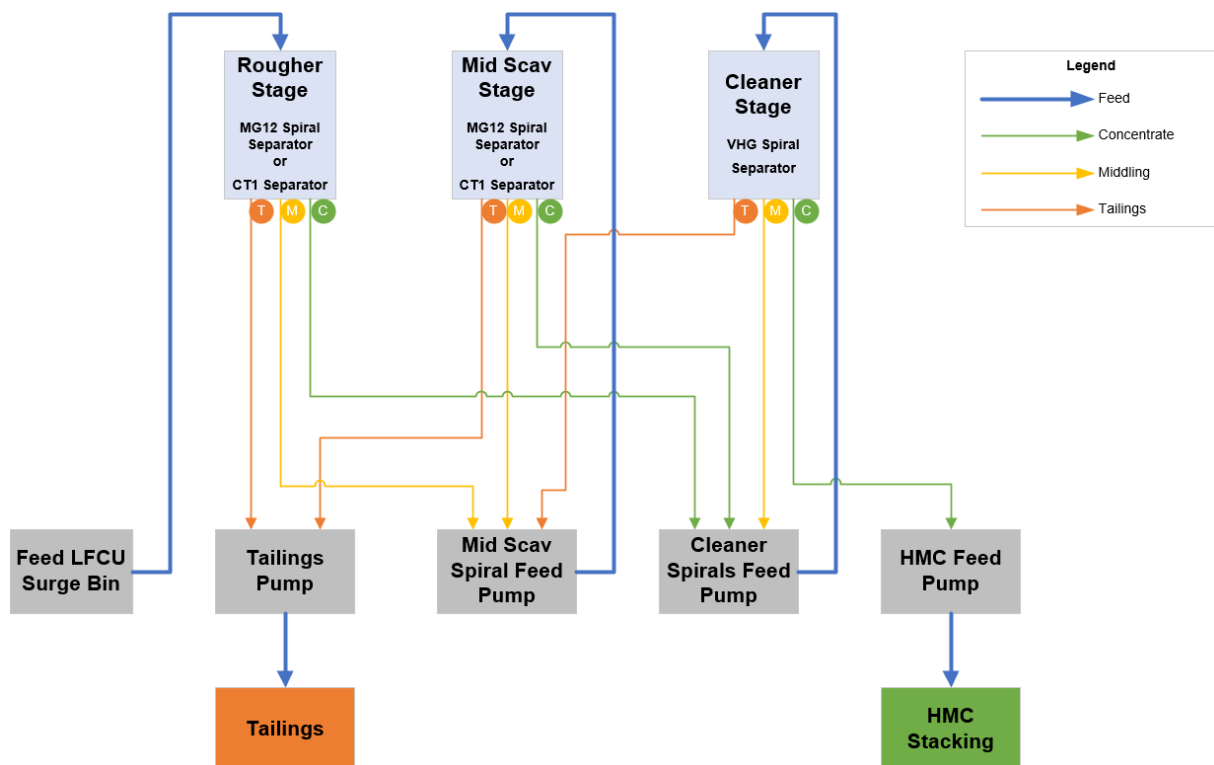


FIG 4 – Block diagram – case study.

Results and discussion

Water consumption for the gravity circuit was determined under a range of feed densities including the base case with MG12 spiral separators at 35 per cent solids (w/w), as well four × CT1 separator cases at 45, 50, 55 and 60 per cent solids (w/w) respectively. This data is presented in Figure 5 and clearly demonstrates the potential water saving in operating at the higher feed densities compared to the base case. Further results from two of the flow sheet simulations are displayed in Table 1 (MG12_35 versus CT1_60).

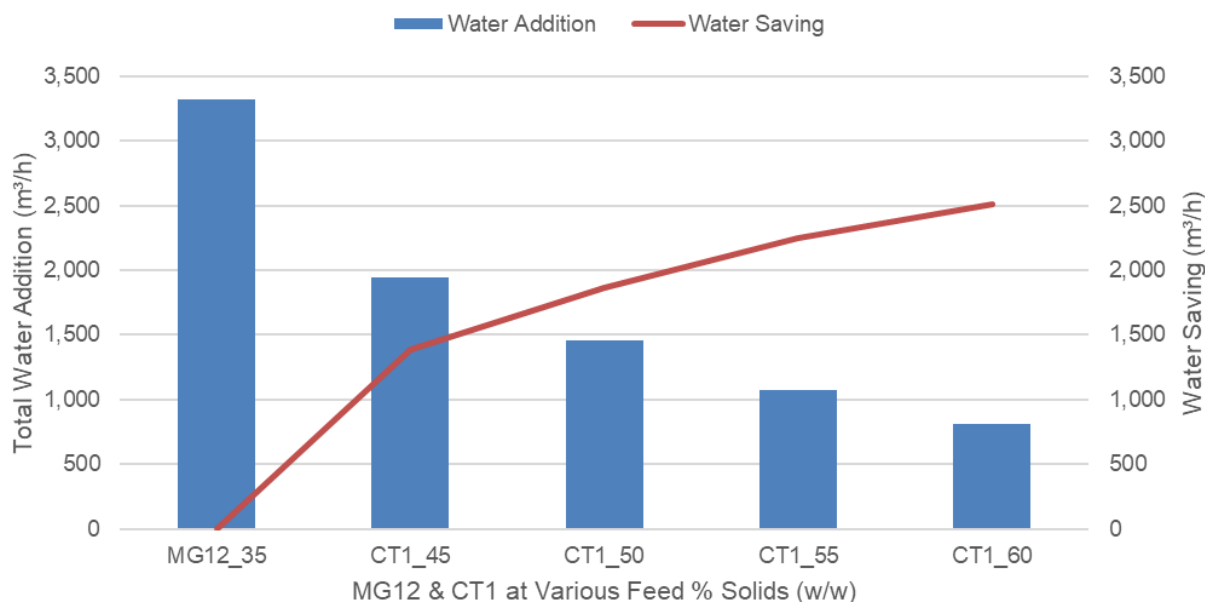


FIG 5 – Water consumption comparison – conventional spiral versus CT1 separator at varying feed per cent solids.

TABLE 1
Case study simulation – results.

Parameter	Unit	Conventional spiral separators (MG12_35)	High density separators (CT1_60)	%Reduction
Total pumped volume	m³/h	12 597	5228	69%
Total water addition	m³/h	3309	848	74%
Tailings volume	m³/h	4322	1862	57%
Final tailings density	% solids (w/w)	31.6	58.2	
Estimated pump power draw	kW	2227	1058	53%
Number of separator columns	No.	312	204	35%
Processing footprint*	m²	86	56	35%

*Footprint of separator banks only – excluding walkways and other plant items.

The desktop simulation showed reductions of >60 per cent in total pumped volume and >70 per cent water usage, with proportional reductions in energy consumption, equipment and building size. The higher density slurry fed to the CT1 separator also resulted in a higher density tailings product. It is likely that for many operators, the 58.2 per cent solids (w/w) tailings slurry would be suitable for direct deposition to a tailings storage facility without additional processing. This significant reduction in tailings volume would minimise the amount of water entering the tailings storage facility.

The total pumped volume reduction of 69 per cent leads to an estimated power reduction of 53 per cent. The annual cost saving of power for the pumps within the spiral circuit alone (assuming 0.2 c/kW) is in excess of A\$1.5 million per annum. Capital cost savings are also significant with a 35 per cent reduction in the number of spiral sticks and processing footprint required.

CONCLUSIONS

The combination of two novel technologies, the CT1 separator and Lyons Feed Control Unit has formed the basis for high density gravity beneficiation. The case study presented in this paper highlights the clear benefits of the higher density flow sheet when compared to the industry standard. The demonstrated reduction in energy (53 per cent) and water consumption (>65 per cent) and smaller tailings volume (57 per cent) would greatly reduce the environmental and social impacts of prospective operations. The demonstrated reduction in spiral footprint and pumped volumes are likely to lead to greatly reduced capital and operating costs, leading to improved economics of lower grade marginal ores and further increasing the profitability of remaining high-grade ores.

ACKNOWLEDGEMENTS

The management of Mineral Technologies is thanked for their support in publishing this paper.

REFERENCES

- Lyons, J, Hill, G, Vadeikis, C and Wiche, S, 2009. Innovative Surge Bin Design for Mineral Sands Processing Plant.
- MacHunter, D M, Richard, R G and Palmer, M K, 2003. Improved gravity separation system utilising spiral separators incorporating new design parameters and features. *Heavy Minerals 2003*, Johannesburg, South African Institute of Mining and Metallurgy, 2003.
- Overton, I, 2020. 'Aren't we in a drought? The Australian black coal industry uses enough water for over 5 million people'. Available at <<https://theconversation.com/arent-we-in-a-drought-the-australian-black-coal-industry-uses-enough-water-for-over-5-million-people-137591>> [Accessed 30 June 2021].

Mechano-activation and acid leaching of lithium from spodumene

N C Lim¹, R D Alorro², M Aylmore³, L G Dyer⁴ and H E Lim⁵

1. MPhil Student, Western Australian School of Mines: Minerals, Energy and Chemical Engineering, Curtin University, Bentley WA 6845. Email: norman.lim@postgrad.curtin.edu.au
2. MAusIMM, Senior Lecturer, Metallurgical Engineering, Western Australian School of Mines: Minerals, Energy and Chemical Engineering, Curtin University, Kalgoorlie WA 6430. Email: richard.alorro@curtin.edu.au
3. FAusIMM, Associate Professor, John de Laeter Centre, Faculty of Science and Engineering, Curtin University, Bentley WA 6845. Email: mark.aylmore@curtin.edu.au
4. Senior Lecturer, Western Australian School of Mines: Minerals, Energy and Chemical Engineering, Curtin University, Kalgoorlie WA 6430. Email: laurence.dyer@curtin.edu.au
5. MAusIMM, R&D Team Lead, Tianqi Lithium Australia, Kwinana WA 6966. Email: hazel.lim@tianqilithium.com.au

INTRODUCTION

Spodumene is becoming a significant resource in the production of lithium (Li) salt, with demand mainly driven by battery market (Kavanagh *et al*, 2018). In the conventional process of Li extraction from spodumene ($\text{LiAlSi}_2\text{O}_6$), the mineral concentrate is subjected to calcination at 1000–1100°C followed by sulfation baking at 250°C, after which Li is extracted by water leaching (Karrech *et al*, 2020). Moreover, significant amount of concentrated sulfuric acid is utilised on roasting, with the excess acid neutralised after with an alkaline medium. Thus, conventional processing of Li from spodumene is not only energy intensive but chemically demanding as well.

Mechano-activation is a technique, which relies on the use of mechanical energy to effect surface and structural changes in minerals, and results to a metastable and reactive state. A mechano-activated state is characterised by the presence of an XRD amorphous state (Klug and Alexander, 1974). The technique therefore relies significantly on the type of activator mill and the conditions of milling for activation. In the very few technical studies done on the mechano-activation of spodumene, the conditions for milling are usually not fully disclosed. In consideration of the stable nature and abrasive property of alpha spodumene, it is understandable that this technique is often receive with scepticism and thus explains why this research area has not received much attention.

The mechano-activation of a mono-mineral of alpha spodumene was reported with Li recoveries of 90–95 per cent on subsequent leaching in both acidic and alkaline conditions (Kotsupalo *et al*, 2010) but no studies can be found on the application of this technique to alpha spodumene concentrate. The M3 planetary mill used in the earlier research is patented and is not commercially available.

It is the objective of this study to investigate the mechano-activation of alpha spodumene concentrate using a commercial laboratory planetary mill. The effects of various mechano-activation variables, such as milling time, ball to concentrate ratio, dry or wet milling condition, solids density, and milling rate, were examined (see Table 1). The mechano-activated samples were then subjected to comparative leaching test using (a) 3M citric acid and (b) 50 wt. per cent sulfuric acid on 1g:20 ml solid: liquid ratio at 70+/-5°C and 1–3 hr leaching time.

TABLE 1

Experimental plan table generated from definitive screening design using Minitab 11.2

Run order	Ball: ore ratio, g/g	Solids density, %	Rev/min	Milling time, min
A	30:1	10	500	10
B	50:1	10	600	5
C	20:1	10	300	15
D	50:1	100	600	10
E	20:1	30	600	5
F	30:1	100	300	5
G	20:1	30	300	10
H	20:1	100	500	5
I	50:1	100	300	15
J	50:1	30	500	15
K	20:1	100	600	15
L	30:1	30	600	15
M	50:1	30	300	5

RESULTS

Analysis on the XRD results (Table 2) showed that only four conditions resulted to an XRD amorphous state (degree of amorphization >60 per cent) – these are the conditions used for sample D, J, K and L. These conditions are characterised by high rev/min at 500–600 rev/min and long milling times of 15 min. Sample D was milled for 10 min but the ball: charge ratio was at the highest of 50:1 (Table 1).

TABLE 2

Summary of results on XRD, PSD and Li recoveries on leaching.

Sample code	Relative degree of amorphization, %	PSD, μm , D_{80}	Sulfuric acid leaching Li recovery, %	Citric acid leaching Li recovery, %
A	47.25	23.7	6.0	2.8
B	34.90	25.4	7.6	4.2
C	18.35	30.9	2.6	1.2
D	77.27	48.3	34.1	5.1*
E	35.75	16.4	5.5	2.6
F	3.48	24.4	1.2	1.7
G	16.11	20.8	2.4	1.4
H	16.39	27.9	3.7	4.8
I	6.85	40.7	9.3	5.0
J	61.56	18.6	6.6	9.2
K	95.79	41.7	30.2	3.3**
L	82.32	16.5	16.8	4.2
M	58.47	19.2	13.7	1.7

*D-11days 10.8% D-30days 22.1% **K-11days 6.3% K-30days 17.0%

The particle size distribution of the treated samples is also shown in Table 2. From the results, there is no direct correlation of grind size with the intensity of the milling conditions. For example, a milling

condition of 20:1 g/g ball: ore ratio, 30 per cent solids density, 600 rev/min and 5 min milling time resulted in particle size of D80 of 16 μm . On the other hand, more intense milling condition of 20:1 g/g ball to ore ratio, 100 per cent solids density, 600 rev/min and 15 min milling time, resulted in particle size of D80 of 42 μm . This is an interesting result as this corrects the common notion that size can be used as a direct indication of amorphization on mechano-activation. This result emphasized the significance of the intensity of the impact forces (ball to sample, ball-sample-wall collision) during activation as opposed to other forces which results only in size reduction.

Results of the direct sulfuric acid leaching of the milled samples is provided in Table 2. From the data, it can be easily seen that the mechano-activated samples D, and K relatively have the highest Li recovery at 30–34 per cent. Sample L, which also showed an amorphous signature resulted in 17 per cent Li leaching, which is the third highest result in this investigation. This result showed that the mechano-activation resulted in distortion of the lattice and cleavage on the Li-O bonds. To note, Li-O bonds have the weakest bond strength compared to Al-O and Si-O bonds (Berger, Boldyrev and Menzheres, 1990) but in an alpha spodumene structure, the plane (110) is the exposed plane and this plane houses the Al and Si tetrahedron chain (Xu *et al*, 2016, 2017). Analysis on the leach residue for samples D and K also showed lowering of Al content but not Si, this means that these samples are mechanically activated but not to a degree of complete Li-O cleavage. This suggest that the conditions for milling will need to be intensified. In reference to the conditions used for milling samples D and K, this further suggest conditions of 600 rev/min or higher, 100 per cent solids density (dry milling) and longer milling times. Main Effects analysis done using Minitab software supports this finding to show that the order of significance of mechano-activation factors are as follows: milling speed>solids density>milling time>ball:ore ratio.

The citric acid leaching of the milled samples is also provided in Table 2. Being a weaker acid than sulfuric acid, the citric acid leaching has expectedly lower results than the sulfuric acid leaching at less than 10 per cent. However, the citric acid leaching showed consistently that samples D, J, K and J have comparatively higher results compared to the other samples. The results also showed that the Li mobilisation increased over time, as shown by the higher assays of samples D and K at 11 day and 30-day (Table 2 notes).

In summary, this study was able to define mechano-activation conditions that would result to 30–35 per cent Li mobilisation on direct sulfuric acid leaching of alpha spodumene. This study was also able to show by statistical analysis that the factors significantly affecting the mechano-activation of spodumene is milling speed. With these results, a follow-up study is highly recommended in the aim of improving Li recoveries on leaching. The direct citric acid leaching of mechano-activated samples has very poor results and will need more research.

REFERENCES

- Berger, A, Boldyrev, V and Menzheres, L, (1990). Mechanical activation of β -spodumene. *Materials Chemistry and Physics* 25(4): 339–350.
- Karrech, A, Azadi, M R, Elchalakani, M, Shahin, M A and Seibi, A C, (2020). A review on methods for liberating lithium from pegmatities. *Minerals Engineering* 145: 106085.
- Kavanagh, L, Keohane, J, Garcia Cabellos, G, Lloyd, A and Cleary, J, (2018). Global Lithium Sources—Industrial Use and Future in the Electric Vehicle Industry: A Review. *Resources (Basel)* 7(3): 57.
- Klug, H P and Alexander, L E, (1974). *X-ray diffraction procedures: for polycrystalline and amorphous materials*. New York, Wiley.
- Kotsupalo, N P, Menzheres, L T, Ryabtsev, A D and Boldyrev, V V, (2010). Mechanical activation of α -spodumene for further processing into lithium compounds. *Theoretical Foundations of Chemical Engineering* 44(4): 503–507.
- Xu, L, Hu, Y, Wu, H, Tian, J, Liu, J, Gao, Z and Wang, L, (2016). Surface crystal chemistry of spodumene with different size fractions and implications for flotation. *Separation and purification technology* 169: 33–42.
- Xu, L, Peng, T, Tian, J, Lu, Z, Hu, Y and Sun, W, (2017). Anisotropic surface physicochemical properties of spodumene and albite crystals: Implications for flotation separation. *Applied Surface Science* 426: 1005–1022.

Technospheric mining of cobalt from nickel slag – a study on complexation leaching

B Lim¹, M Aylmore², D Grimsey³ and R D Alorro⁴

1. AAusIMM, PhD Student, Western Australian School of Mines: Minerals, Energy and Chemical Engineering, Curtin University, WA 6845. Email: bona.lim@postgrad.curtin.edu.au
2. FAusIMM, Associate Professor, John de Laeter Centre, Faculty of Science and Engineering, Curtin University, WA 6845. Email: mark.aylmore@curtin.edu.au
3. MAusIMM, Principal Process Engineer, Nickel West Australia, BHP, WA 6431. Email: david.grimsey@bhp.com
4. MAusIMM, Senior Lecturer, Western Australian School of Mines: Minerals, Energy and Chemical Engineering, Curtin University, Kalgoorlie WA 6430. Email: richard.alorro@curtin.edu.au

INTRODUCTION

Metals and mineral resources have been and will always be fundamental parts of society, providing materials for the advancement and convenience of mankind. These resources are extracted from the lithosphere through mining, processed into various products, and accumulate in the technosphere. The technosphere is a material stock that has been created by anthropogenic activities. Technospheric stocks include end-of-life products and waste streams resulting from industrial, chemical or metallurgical processes. Some of these stocks contain significant amounts of valuable metals and materials, hence can be considered as important secondary sources of these materials. The extraction of values from technospheric stocks is known as technospheric mining (Johansson *et al*, 2013; Krook and Baas, 2013). The concept acknowledges all material stocks as a component of the earth rather than the wastes and promotes these by-products to be included in the material cycle through waste valourisation.

Slag is a by-product of pyrometallurgical processes and may contain significant amounts of valuable metals. Slag is getting significant attention nowadays as an important secondary source of critical and strategic metals for future mining. Slag is normally treated as waste and stored in heaps or dumps. If not managed properly, slag or slag heaps may cause serious environmental and health problems due to the release of potentially toxic elements contained in the material. Therefore, initiatives to extract metal values from waste materials through technospheric mining are not only economically beneficial but also provide several advantages for environmental protection and waste management (Kim and Azimi, 2020).

In this study, the extraction of cobalt (Co) from nickel (Ni) slag was investigated. Cobalt, as well as nickel, are both considered critical and strategic and are increasingly on-demand for high-technology applications, such as the battery, automobile, and superalloys (Gunn, 2013; Piatak, Parsons and Seal, 2015). Two types of nickel slag samples were used in this study and were collected from the flash furnace (FF) and converter (CV). The FF slag contained 0.55 wt per cent Ni and 0.15 wt per cent Co, while the CV slag consisted of 1.27 wt per cent Ni and 0.59 wt per cent Co. Considering cobalt is rarely produced as a main product and more commonly as a by-product of nickel or copper, the Co contents of the slag samples are considered significant making the slag a valuable secondary source for this metal. The major phases identified from these slag samples were fayalite (Fe_2SiO_4), magnetite (Fe_3O_4) and quartz (SiO_2).

The extraction method used in this study was complexation leaching with organic acid and complexing agents. Organic acids are weak acids but their biodegradability is considered to be highly attractive for processing. Amongst all, citric acid ($\text{C}_6\text{H}_8\text{O}_7$) is considered to be the strongest, containing three available hydrogen ions. The complexation of target metals with complexing agents increases the efficiency of leaching. Hydrogen peroxide (H_2O_2) as an oxidant and ethylenediaminetetraacetic acid (EDTA) as a complexing agent were considered. Batch leaching tests were conducted using a heating mantle with temperature control and an overhead stirrer to effect mixing. Several leaching variables were investigated, including acid concentration, temperature, time, pulp density, stirring rate, and particle size.

The recovery of cobalt from FF and CV slag with complexation leaching are presented in Figure 1. The results were generated at 1M citric acid, 60°C, 6 hr, pulp density 10 per cent (w/v), the particle size of -75 µm, and stirring rate of 250 rev/min. Leaching with 1M citric acid only showed that Co recovery decreased after 1 hr. Citric acid leaching with the addition of H₂O₂ and EDTA improved Co leaching efficiency. The effect of adding H₂O₂ was more significant in Co recovery from FF slag than CV slag. The addition of 0.3M EDTA as a complexing agent enhanced Co leaching efficiency significantly with FF slag and showed similar results with CV slag. The effect was more pronounced with lower pulp density (5 per cent). Based on these results, higher temperature and lower pulp density could increase Co recoveries from FF and CV slags using citric acid and EDTA as complexing agents. At this condition, 75 per cent of Co from FF slag and 74 per cent from CV slag were extracted. Co was also found to be associated with Fe in fayalite and a good correlation between Fe and Co dissolutions was found (89 per cent Fe from FF slag and 80 per cent from CV slag). The results indicated complexation leaching at mild conditions (atmospheric temperature and pressure) and the use of organic acids offer a very promising route to extract Co from slag materials.

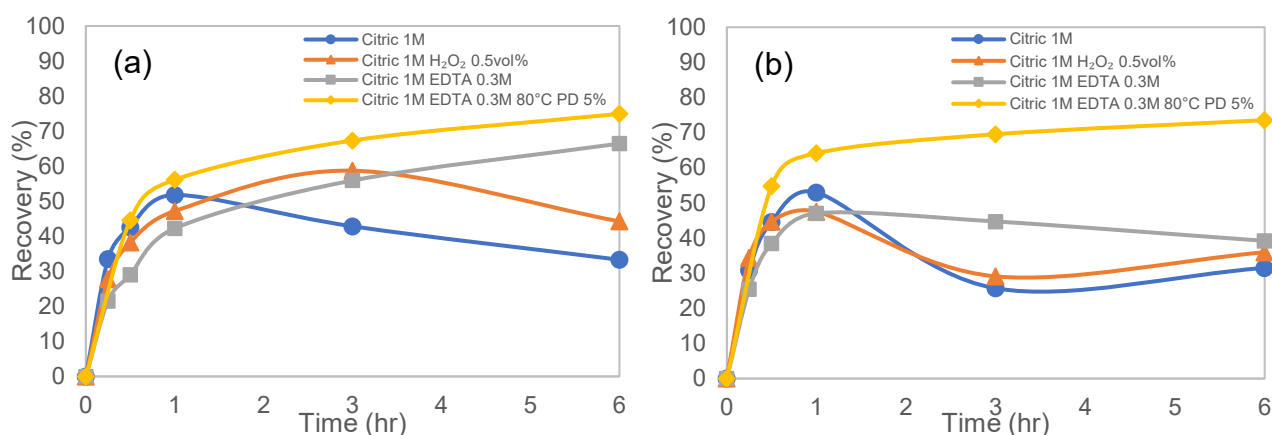


FIG 1 – Complexation leaching of cobalt from (a) FF slag and (b) CV slag (60°C and PD 10 per cent unless indicated).

ACKNOWLEDGEMENTS

The authors would like to acknowledge the financial support from Curtin University and the Science Industry PhD Fellowship by the Department of Jobs, Tourism, Science and Innovation (JTSI), Government of Western Australia. BHP Nickel West is also acknowledged for providing slag samples used in the study.

REFERENCES

- Gunn, G, 2013. *Critical Metals Handbook*, Wiley.
- Johansson, N, Krook, J, Eklund, M and Berglund, B, 2013. An integrated review of concepts and initiatives for mining the technosphere: towards a new taxonomy. *Journal of Cleaner Production*, 55, 35–44.
- Kim, J and Azimi, G, 2020. Technospheric mining of niobium and titanium from electric arc furnace slag. *Hydrometallurgy*, 191, 105203.
- Krook, J and Baas, L, 2013. Getting serious about mining the technosphere: a review of recent landfill mining and urban mining research. *Journal of Cleaner Production*, 55, 1–9.
- Piatak, N M, Parsons, M B and Seal, R R, 2015. Characteristics and environmental aspects of slag: A review. *Applied Geochemistry*, 57, 236–266.

Differentiation of AG/SAG mill feed particle size variations in batch milling process using acoustic emissions

K B Owusu¹, W Skinner² and R K Asamoah³

1. PhD student, University of South Australia, UniSA STEM, Future Industries Institute, Mawson Lakes, Adelaide SA 5095. Email: kwaku_boateng.owusu@mymail.unisa.edu.au
2. Research Professor, University of South Australia, UniSA STEM, Future Industries Institute, Mawson Lakes, Adelaide SA 5095. Email: william.skinner@unisa.edu.au
3. Research Fellow, University of South Australia, UniSA STEM, Future Industries Institute, Mawson Lakes, Adelaide SA 5095. Email: richmond.asamoah@unisa.edu.au

ABSTRACT

Variation in mill feed size distribution impacts on Autogenous/Semi-autogenous (AG/SAG) grinding mill operation, influencing mill disturbances and performance. Under batch dry and wet grinding conditions using a purpose-built laboratory-based AG/SAG mill and acoustic sensor, the present work investigates the feasibility of a real-time monitoring technique of different mono-sized ore feed fractions and binary mix ratios of distinct feed size fractions. Simple feed size variations estimation models were developed by signal root mean square analysis derived from the time-domain acoustic signal. The results obtained delineate that mill noise emissions generally increases with an increase in ore feed size. The mix ratios of relatively coarse and fine feed sizes indicated that mill acoustic response was dampened with an increase in the fine size fractions. The more suitable fit correlation plot of both mono-sized and hetero-sized feed fractions (both dry and wet grinding environment) and acoustic emissions showed a nonlinear relationship. Wet milling in the presence of steel balls and water showed a more linear correlation compared with only rock milling. The results suggest that mill acoustic emissions are sensitive to mill feed variation with a promising prospect towards real-time monitoring and optimisation of AG/SAG mill feed size.

INTRODUCTION

Comparatively, the grinding circuit (specifically AG/SAG mill) remains the most energy-intensive unit operation in large scale mineral processing plants (Ballantyne and Powell, 2014; Ballantyne, Powell and Tiang, 2012). In addition, the operation is multivariable controlled presenting optimisation challenges if not well monitored. Among the process variables such as mill speed, water flow rate, feed flow rate, slurry density, lifter profile and percentage ball loading, ore feed variability in terms of size can considerably affect the mill overall performance (Das *et al*, 2011; Morrell and Valery, 2001). Different size fractions of ore feed are characterised by the nature of ore (eg hardness) and blasting technique coupled with crushing (Pourghahramani, 2012). The introduction of varying feed sizes into the mill is known to cause fluctuations, particularly in throughput, energy usage, and product size distribution and largely affecting consistent mill operation (Behnamfard, Namaei Roudi and Veglio, 2020; Hahne, Pålsson and Samskog, 2003; Morrell and Valery, 2001; Pax and Cornish, 2016; Valery *et al*, 2007). Thus, the need to obtain homogenous size fractions is relevant to providing a successful and consistent grinding operation.

To achieve this, conventional and current procedures include modifying blasting method (first stage comminution), ROM stockpiling segregation, crushing, selective pre-screening techniques and Mine to Mill blasting concept (van Drunick and Penny, 2005; Foggatto, 2017; Morrell and Valery, 2001; Scott, Kanchibotla and Morrell, 1999). These approaches have provided some level of control for improving milling consistency in terms of feed size and efficiency. However, the available employed methods are only successful outside the mill. Further feed size monitoring on conveyor belt before reaching the mill is available (Bouajila *et al*, 2000; Pax and Cornish, 2016). Consequently, feed size monitoring outside milling operation is fairly understood. Despite that feed size control outside the mill and mill performance could be ascertained, a sudden *in situ* modification of feed size distribution could occur with time due to the operating feeders, their locations, and the distance of ore feed at different stockpile levels (Morrell and Valery, 2001; Ziming *et al*, 2019). Thus, understanding the feed size variations that are fed in AG/SAG mill in real-time is relevant to the control and possible optimisation opportunities. Owing to the hostile AG/SAG mill environment coupled with the inability

to access mill internally from outside, real-time measurement of the in-mill dynamics has become one of the most sorted out research studies (Nayak *et al*, 2020).

Capitalising on the inevitable mill acoustic emissions, promising studies have shown that mill acoustic response originating from the rock-ball-water multiple interactions alongside mill liner/lifter could be used to classify mill operating conditions, varying process parameters such as mill speed, slurry density (water flow rate), ball charge and ore charge, rock hardness (Almond and Valderrama, 2004; La Rosa *et al*, 2008; Owusu *et al*, 2020; Pax and Thornton, 2019; Spencer *et al*, 1999; Watson and Morrison, 1985, 1986). Relating to feed size, Pax and Cornish (2016) employed 12 microphone arrays to investigate feed size effect as a pathway to mitigate feed size fluctuations in a large-scale SAG mill (MMG Century SAG mill). The study reported that acoustic emission provided a promising result for identifying feed size dynamics in SAG mills. In another study, Das *et al* (2010) used a piezo-electric type tri-accelerometer positioned on a laboratory mill shell (1000 mm × 300 mm) to investigate vibration response of feed size effect. They concluded that coarse feed particles are linked with higher vibration responses than fine feed particles. However, extensive information regarding feed size variations and mill acoustics in an attempt to understand and provide real-time monitoring is limited.

To contribute to knowledge and closing the gap in this area, the present study employed a laboratory-based AG/SAG mill simulator to investigate the effect of different feed sizes using an acoustic sensor system. The study aims to provide the possibility of using mill acoustic response to distinguish different feed size classes in real-time. The following key research questions are addressed.

- Can mill acoustic emission response indicate a sudden change in ore feed size variation? Are mill noise emissions susceptible or influenced by mill feed size variations?
- What relationship exists between only rock feed variations (dry milling) or rock feed-ball-water (constant ball and water filling) and mill acoustic emissions?
- What is the effect of coarser and finer particle size mix ratios on mill acoustic emissions? What is the correlation between a binary mixture of relatively coarser and finer feed sizes and acoustic emissions?
- What is the suitable estimated model fit for feed size variations and acoustic emissions?
- What is the overall practical implication of the study?

EXPERIMENTAL WORK

Feed material and preparation

Iron ore sample sourced from SIMEC, Australia was used for the study. The as-received ore was initially fragmented through a jaw crushing unit to obtained varying size fractions. Different feed size ranges were prepared and classified as mono-size and hetero-size feed fractions and shown in Table 1 and Figure 1.

TABLE 1
Feed particle size fractions and classification.

Class	Mono-sizing (mm)	Class	Hetero-sizing (mm)
A	-2 + 0.85	-	-
B	-4 + 2	B (%)	25, 50, 75
C	-6.7 + 4	-	-
D	-8 + 6.7	-	-
E	-9.5 + 8	-	-
F	-13.2 + 9.5	F (%)	75, 50, 25
G	-16 + 13.2	-	-
H	-19 + 16	-	-
I	-26.5 + 19	-	-

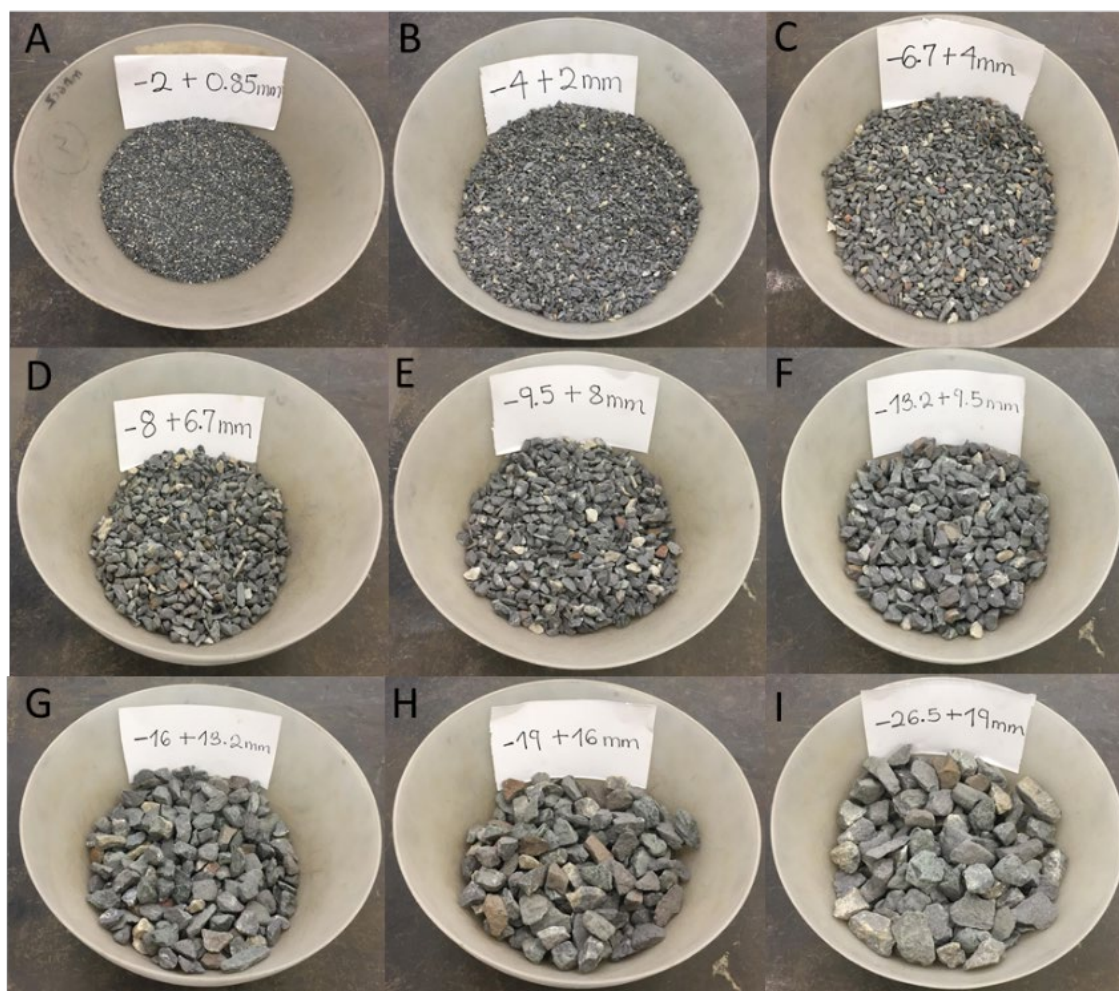
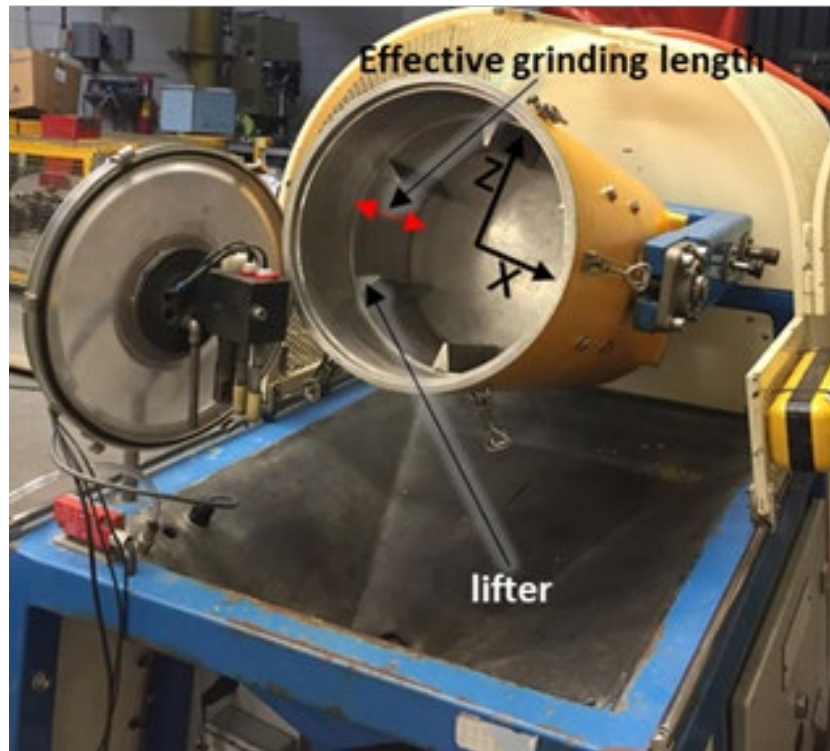


FIG 1 – Different feed size fractions.

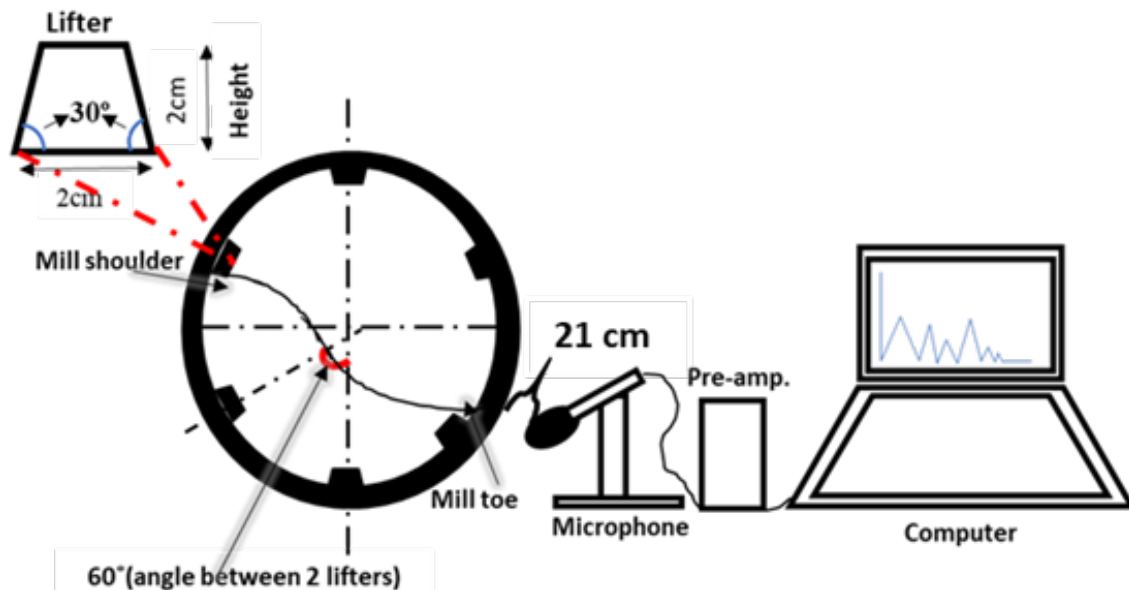
Mono-sizing describes close range of particle sizes whereas hetero-sizing refers to mix ratios of two feed classes of distinct different particle size fractions.

Experimental set-up, Grinding studies, and acoustic monitoring

A laboratory-based AG/SAG mill with size 300 mm diameter × 150 mm (length) with six equally spaced lifters was used in the experiment as shown in Figure 2. An acoustic sensor system (PreSonus iOne) consisting of a microphone and pre-amplifier connected to a laptop was used for the study. The microphone was placed close to the mill toe angle (about 21 cm) to pick up acoustic emissions during the milling operation.



(a)



(b)

FIG 2 – Grinding studies showing: (a) Laboratory-based AG/SAG mill; and (b) schematic experimental set-up.

Two kilograms (~10 vol. per cent) of feed was taken from each of the feed classes and ore only dry grinding tests were preliminary carried out for a minute at 58 rev/min (representing 75 per cent mill critical speed). Following that, wet grinding was performed with mill charge consisting of two kg ore feed, eight vol. per cent steel balls, and 857 ml water for five minutes, with the same mill speed as that of the dry milling. To gain additional insight into binary mixture of different feed classes and acoustics, feed classes F (-13.2 + 9.5 mm) and B (-4 + 2 mm) were blended in ratios of 1:3, 1:1, and 3:1. Similarly, wet grinding conditions were applied to the binary mixture. For all the wet grinding tests, the slurry product was filter pressed and allowed to dry in an electric oven (~50°C) and screened to obtain their product size distributions using the Tyler model. The mill acoustic response was recorded at a sampling frequency of 44.1 kHz for each grind test using a microphone system.

To improve the quality and noise interferences of the mill acoustic recording, a very quiet environment was ensured.

Acoustic emission data preprocessing

All data processing was carried out on MATLAB platform. Data preprocessing which includes pre-trigger and post-trigger signals removal, followed by filtering of any background noise were preliminarily undertaken to enhance signal quality. Savitzky-Golay filter was further applied to improve signal smoothness (Acharya *et al*, 2016). To appreciate the full sensitivity of rock size before substantial progressive size reduction, the analysis was highlighted on the immediate (first) 30 seconds recorded mill acoustic data. In this study, statistical root mean square (RMS) was extracted from the signal as performance indicator tool to distinguish different rock size fractions in AG/SAG mill system. RMS can be computed from the expression (Aguiar *et al*, 2012):

$$RMS_{AE} = \sqrt{\frac{1}{\Delta t} \int_0^{\Delta t} AE^2(t) dt} = \sqrt{\frac{1}{N} \sum_{i=1}^N AE^2(i)} \quad (1)$$

where AE is acoustic emission, Δt is an integral time constant, and N is number of discrete AE data set within Δt .

RESULTS AND DISCUSSION

Particle size distribution

Figure 3 shows the product size distribution (PSD) of the mono and hetero-sized feed fractions.

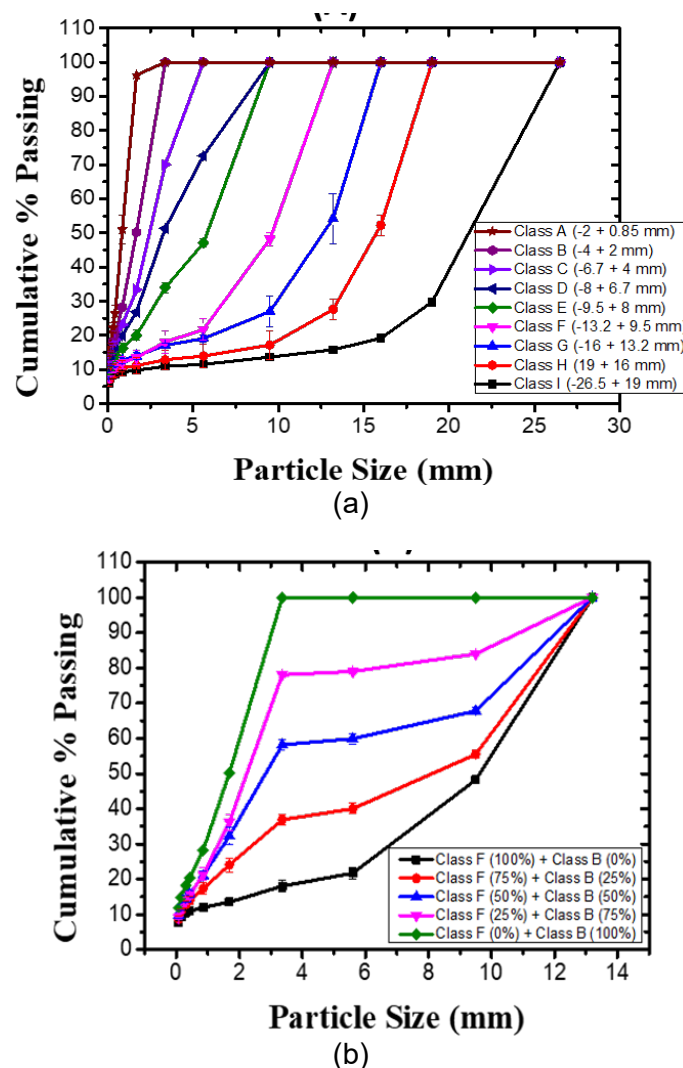


FIG 3 – Product size distribution of: (a) mono-size feed fractions; and (b) hetero-size feed fractions.

As expected, the PSD of the mono-size feed classes increased with decreasing the feed size fractions (Razani *et al*, 2018). Under the same condition (two kg ore, eight vol. per cent steel balls, and 857 ml water at 58 rev/min), smaller size fractions undergo rapid size reduction compared to coarse material. In the binary blends, it was observed that the reduction of the concentration of relatively coarser feed fraction (class F) consistently increased the size reduction process. This informs that the concentration of different feed size fractions can influence the ore breakage characteristics considerably.

SIGNAL TIME DOMAIN REPRESENTATION

The recorded mill acoustic responses in the time domain of only rock and rock-ball-water milling at 58 rev/min mill speed are illustrated in Figure 4.

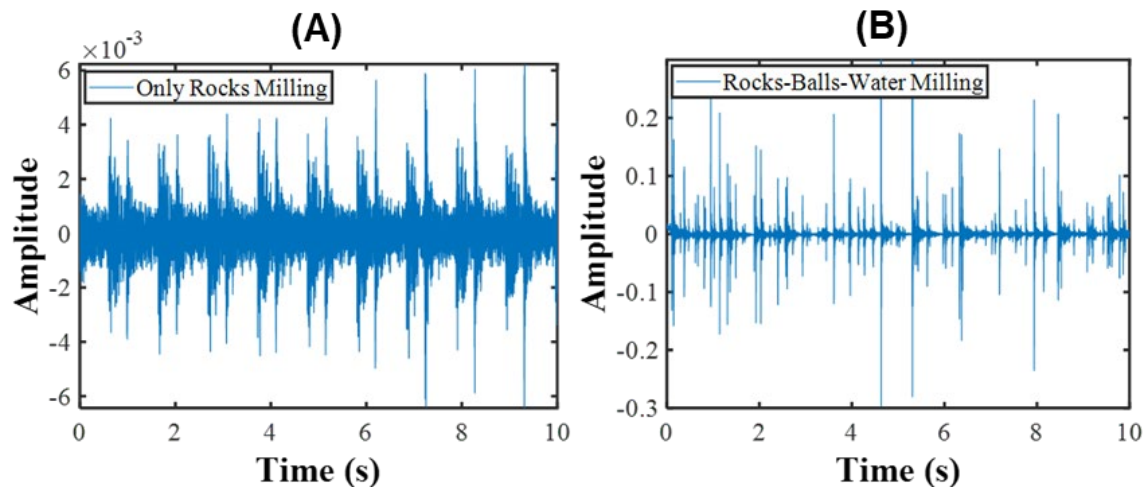


FIG 4 – Signal time domain characteristics of: (a) only rock milling; and (b) rock-ball-water mill at 58 rev/min.

From the results, it is evident that the noise emission from rock only grinding was significantly lower compared to rock-ball-water milling. Time domain signals from rock only milling also showed more periodic waveform, suggesting the sequence of falling rock charge toward the toe angle with regards to the mill revolution. In the rock-ball-water mixture, excessive noise spikes were produced with more inconsistencies. The presence of steel balls are responsible for the excessive noise emission, resulting from mainly ball-ball and ball-liner/lifter collision. Generally, limited information could be visualised for appreciable comparison in the time domain representation, hence further RMS analysis was deduced.

Statistical RMS analysis

Homo-size feed fraction

RMS values estimated for each feed fraction were correlated as plotted in Figure 5.

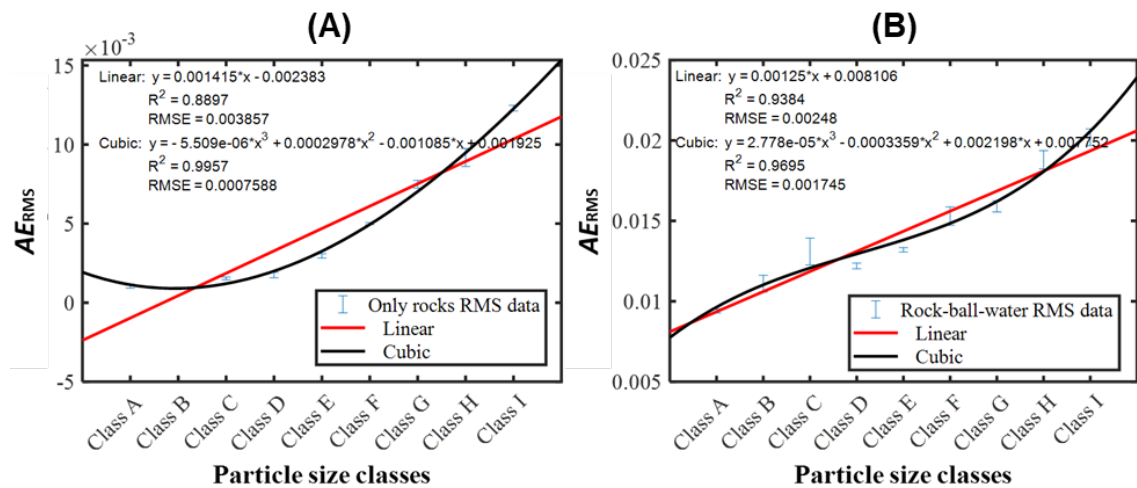


FIG 5 – Correlations between RMS: (a) only mono-sized feed fractions; and (b) mono-sized feed fractions, balls, and water.

The correlation plot of only rock grinding and their acoustic response are presented in Figure 5a. Evidently, it was observed that mill acoustic emission intensified with increasing feed size fractions. With the same ore density (ore type), this could be explained by the additional weight associated with large size fractions. Since AG/SAG mill is dominated by impact breakage of falling charge from a height to mill toe angle, large feed size could play a role in the higher noise emission than small size fraction. The plot presented linear and nonlinear (cubic) model estimations. The fitted models demonstrated that nonlinear relationship was more suitable for the estimated RMS data points and their feed size classes. From that, it appears that only rock mill is very sensitive to mill acoustic response regarding feed size variations. In the rock-ball-water mixture (Figure 5b), the linear model estimation was enhanced with $R^2 > 0.9$ compared with the only rock grinding. Also, the nonlinear relationship was marginally distorted but continued to remain stronger than the linear model. The modification of the models can be attributed to the influence of ball and water addition to the rock-ball-water grinding system. The results from both scenarios (rock only and rock-ball-water mixture) presented that ore feed size variations have a considerable impact on the mill acoustic response.

Hetero-size feed fraction

The effect and correlations of mill acoustic response for different blend ratios of coarse feed fraction (class F) and fine feed (class B) are evaluated in Figure 6. In this case, class F and class B in different ratios of 3:1, 1:1, and 1:3 were compared together with their respective 100 per cent class fractions.

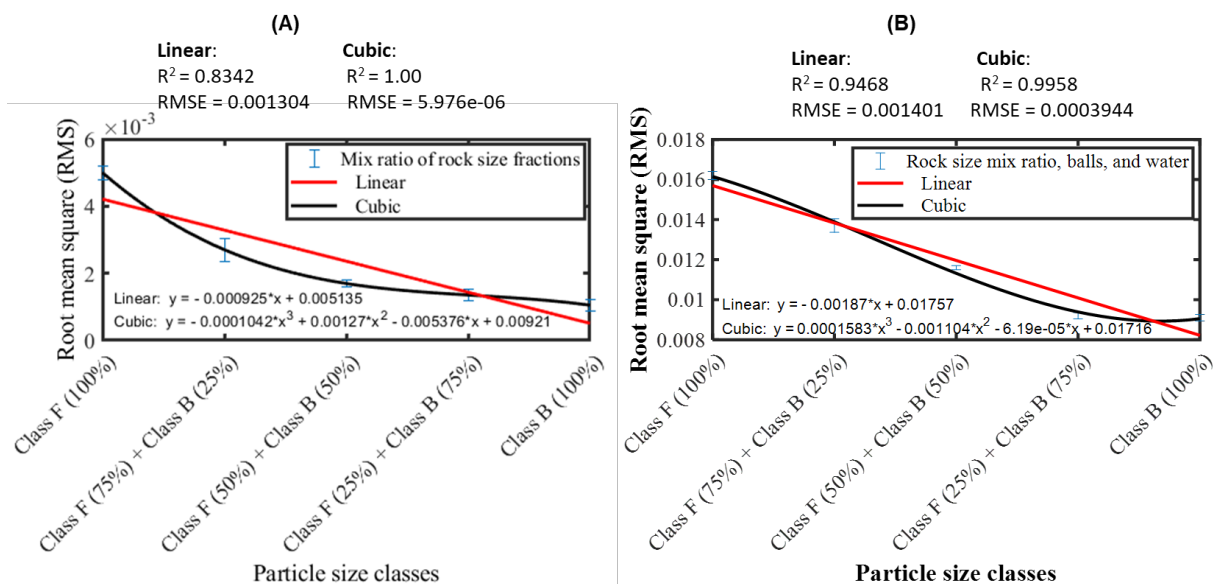


FIG 6 – Correlations between RMS (a) only hetero-sized feed fractions and (b) hetero-sized feed fractions, balls, and water.

The result showed that the highest and lowest mill noise emission corresponded to 100 per cent coarse feed size and 100 per cent fine feed size, respectively for only rock and rock-ball-water loadings. The mill acoustic response reduced continuously by decreasing the concentration of coarse feed size fraction and increasing the feed fine fraction in Figure 6a and 6b. This suggests that the presence of coarse feed promotes intense mill noise emission. Estimating for the model fitting, both linear and nonlinear relations showed good performance in the rock only and rock-ball-water mixture, however nonlinear model estimation proved more pronounced with $R^2 > 0.9$, similar to mono-size feed fraction in Figure 5.

In order to validate the estimated model for predicting the different feed size fractions, some selected theoretical predicted RMS values were plotted against the measured data (Figure 7) based on the previous model in Figure 5. In this, the feed classes (mono-size) were assigned as 1, 2, 3, 4, 5, 6, 7, 8 and 9, representing feed classes A, B, C, D, E, F, G, H and I, respectively. For simplicity, the model accuracy was tested using the linear model on rock-ball-water mixture with a suitable coefficient of determination (R^2) of more than 0.9 (Figure 5b). Generally, the plot comparison shows a good correlation between the measured and predicted theoretical values (RMS) for determining the feed size fraction and maintaining R^2 greater than 0.9. The overall promising results suggest the potential application of implementing acoustic sensors as a proxy monitoring tool for ore feed size variations.

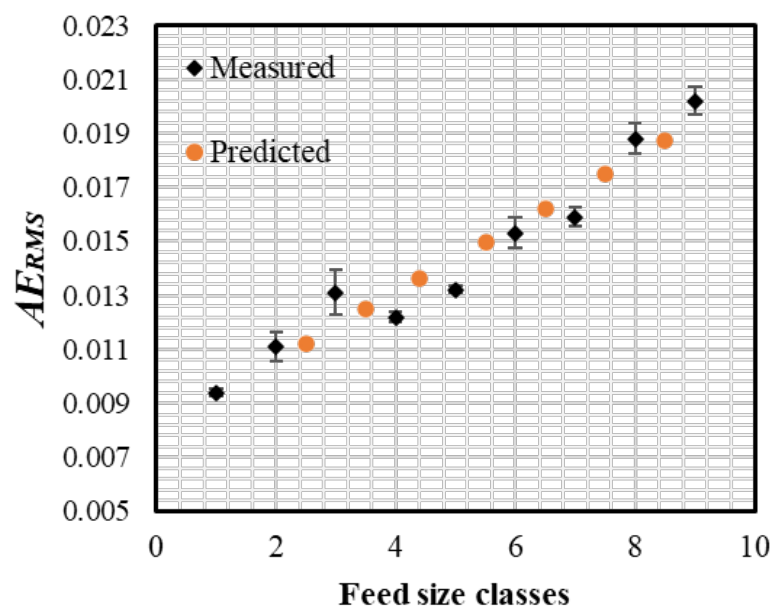


FIG 7 – Validation of model estimation for mono-sized feed variation together constant ball mass and water volume using RMS analysis.

CONCLUSIONS

The acoustic response measurements of different feed ore size fractions have been investigated in a laboratory-based AG/SAG grinding mill simulator. The acoustic emission signal was collected by a non-contact acoustic sensor positioned at the toe angle of the mill shell. Statistical root means square (RMS) values were extracted from the sampled acoustic signal data (immediate time-series signals) and used as a performance indicator. Furthermore, correlations plots were deduced from signal RMS and the feed size variations. The following conclusions were deduced from the study:

- Mill acoustic emission provided a good response indication, following the sudden change in mill feed size. Mill acoustic emission responses are sensitive to feed ore size variations as indicated by RMS analysis.
- Only rock feed size variations, as well as rock size variations with constant steel balls and water, produced a consistent increase in the mill acoustic emission with increasing feed size fraction.

- The study also indicated that the mill noise emissions are affected by the binary mix ratio of different feed classes (hetero-sized feed fractions), such that a higher concentration of relatively finer feed particle size contributes to changes in mill noise emission.
- The correlation estimation models of feed size variations deduced from the RMS shows more nonlinear relationships, especially with rock-only milling. In rock-ball-water grinding, the linear relationship is enhanced. A similar correlation model was observed for binary mixture of coarse and fine particle sizes.
- From a broader perspective, the study contributes to the public literature domain regarding the potential integration of non-contact acoustic sensors for real-time monitoring of AG/SAG mill fluctuation caused by feed ore size variations during grinding.

ACKNOWLEDGEMENT

This research has been supported by the SA Government through the PRIF RCP Industry Consortium. The authors also acknowledge the support from the Future Industries Institute (FII) University of South Australia, Australia.

REFERENCES

- Acharya, D, Rani, A, Agarwal, S and Singh, V, 2016. Application of adaptive Savitzky–Golay filter for EEG signal processing. *Perspectives in Science*, 8: 677–679.
- Aguiar, P R, Martins, C, Marchi, M and Bianchi, E C, 2012. Digital Signal Processing for Acoustic Emission. Zdravko Karakehayov (Ed), *IntechOpen*. <https://doi.org/10.5772/48557>.
- Almond, D and Valderrama, W, 2004. Performance enhancement tools for grinding mills, *International Platinum Conference 'Platinum Adding Value'*, The South African Institute of Mining and Metallurgy, pp. 103–110.
- Ballantyne, G and Powell, M, 2014. Benchmarking comminution energy consumption for the processing of copper and gold ores. *Minerals Engineering*, 65: 109–114.
- Ballantyne, G, Powell, M and Tiang, M, 2012. Proportion of energy attributable to comminution, *Proceedings of the 11th Mill Operator's Conference*, pp. 25–30 (The Australasian Institute of Mining and Metallurgy: Melbourne).
- Behnamfard, A, Namaei Roudi, D and Veglio, F, 2020. The performance improvement of a full-scale autogenous mill by setting the feed ore properties. *Journal of Cleaner Production*, 271: 122554.
- Bouajila, A, Bartolacci, G, Kock, N, Cayouette, J and Côté, C, 2000. Toward the improvement of primary grinding productivity and energy consumption efficiency. Part 1: Investigation of the feed ore size effects. *IFAC Proceedings Volumes*, 33(22): 267–272.
- Das, S P, Das, D P, Behera, S K and Mishra, B K, 2011. Interpretation of mill vibration signal via wireless sensing. *Minerals Engineering*, 24(3–4): 245–251.
- Foggiatto, B, 2017. Modelling and simulation approaches for exploiting multi-component characteristics of ores in mineral processing circuits. PhD Thesis, University of Queensland, 1–351 pp.
- Hahne, R, Pålsson, B I and Samskog, P O, 2003. Ore characterisation for—and simulation of—primary autogenous grinding. *Minerals Engineering*, 16(1): 13–19.
- La Rosa, D, Cantarutti, A, Wortley, M and Ozkocak, T, 2008. The use of acoustics to improve load estimation in the Cannington AG mill, *6th Metallurgical Plant Design and Operating Strategies (MetPlant 2008)*, pp. 105–116 (The Australasian Institute of Mining and Metallurgy: Melbourne).
- Morrell, S and Valery, W, 2001. Influence of feed size on AG/SAG mill performance. *SAG2001*, Vancouver, BC, Canada: 203–214.
- Nayak, D K, Das, D P, Behera, S K and Das, S P, 2020. Monitoring the fill level of a ball mill using vibration sensing and artificial neural network. *Neural Computing and Applications*, 32(5): 1501–1511.
- Owusu, K B, Karageorgos, J, Greet, C, Zanin, M, Skinner, W and Asamoah, W R, 2020. Variations in Mill Feed Characteristics and Acoustic Emissions, *Proceedings of 6th UMaT Biennial International Mining and Mineral Conference*, Tarkwa-Ghana, pp. 384–390.
- Pax, R A and Cornish, B, 2016. Understanding Size Effects of Semi-autogenous Grinding (SAG) Mill Operation as a Pathway to Solving Feed Disturbances – Case Study Using the MMG Century SAG Mill, *13th AusIMM Mill Operators' Conference 2016*. pp. 321–329 (The Australasian Institute of Mining and Metallurgy: Melbourne).
- Pax, R and Thornton, A, 2019. Real time measurement and fast control strategies for the optimal operation of grinding circuits, *Proceedings MetPlant Conference*, pp. 132–147 (The Australasian Institute of Mining and Metallurgy: Melbourne).

- Pourghahramani, P, 2012. Effects of ore characteristics on product shape properties and breakage mechanisms in industrial SAG mills. *Minerals Engineering*, 32: 30–37.
- Razani, M, Masoumi, A, Rezaeizadeh, M and Noaparast, M, 2018. Evaluating the effect of feed particles size and their hardness on the particle size distribution of semi-autogenous (SAG) mill's product. *Particulate Science Technology*, 36(7): 867–872.
- Scott, A, Kanchibotla, S and Morrell, S, 1999. Blasting for mine to mill optimisation, *Proceedings of the Expo'99: A Conference on Rock Breaking*. pp. 3–8 (The Australasian Institute of Mining and Metallurgy: Melbourne).
- Spencer, S, Campbell, J, Weller, K and Liu, Y, 1999. Acoustic emissions monitoring of SAG mill performance, *Proceedings of the Second International Conference on Intelligent Processing and Manufacturing of Materials. IPMM'99* (Cat. No. 99EX296). IEEE, pp. 939–946.
- Valery, W, Jankovic, A, La Rosa, D, Dance, A, Esen, S and Colacioppo, J, 2007. Process integration and optimisation from mine-to-mill, *Proceedings of the International Seminar on Mineral Processing Technology*, pp. 577–581.
- van Drunick, B and Penny, W I, 2005. Expert mill control at AngloGold Ashanti. *Journal of the Southern African Institute of Mining and Metallurgy*, 105(7): 497–506.
- Watson, J and Morrison, S, 1986. Estimation of pulp viscosity and grinding mill performance by means of mill noise measurements. *Mining, Metallurgy Exploration*, 3(4): 216–221.
- Watson, J L and Morrison, S D, 1985. Indications of grinding mill operations by mill noise parameters. *Particulate Science Technology*, 3(1–2): 49–63.
- Ziming, Y, Mohsen, Y, Marko, H and Malcolm, P, 2019. A method to evaluate the impact of stockpile size segregation on the performance of SAG mills, *SAG Conference 2019*, Vancouver, Canada.

Influence of lifter height on mill acoustics and performance

K B Owusu¹, C J Greet², W Skinner³ and R K Asamoah⁴

1. PhD student, University of South Australia, Future Industries Institute, Mawson Lakes SA 5095. Email: kwaku_boateng.owusu@mymail.unisa.edu.au
2. Manager Metallurgy, Magotteaux Pty Ltd, Wingfield SA 5013. Email: christopher.greet@magotteaux.com
3. Research Professor, University of South Australia, Future Industries Institute, Mawson Lakes SA 5095. Email: william.skinner@unisa.edu.au
4. Research Fellow, University of South Australia, Future Industries Institute, Mawson Lakes SA 5095. Email: richmond.asamoah@unisa.edu.au

ABSTRACT

Design of lifter heights and configuration are crucial for an Autogenous and Semi-autogenous (AG/SAG) grinding mill overall performance, such as power draw, charge trajectory, liner-lifter wear rate and product quality. Contributing to mill optimisation discourse through sensing technique, the present study aims to investigate the mill acoustic response and product performance of four types of lifter configurations, namely low (Lo), high (Hi), low-high (Lo-Hi) and very high (v-Hi) using a laboratory experimental AG/SAG mill (300 × 150 mm). Under similar operating conditions, the results showed that mill acoustic response measurements associated with different lifter height configurations by large produced distinct variations. The v-Hi lifters produced the maximum mill acoustic emissions, an indication of higher ball charge trajectory, followed by Hi and Lo lifters. The acoustic emission of Hi and Lo-Hi lifters were closely related to each other. In contrast, the cumulative product size distribution also reduces with increasing the lifter height configurations. Results of the mill acoustic response of different lifter heights reflect well with the size distribution, demonstrating that acoustic sensing technique could serve as a potential diagnostic tool to protect the mill liner-lifter wear rate and enhance overall mill performance.

INTRODUCTION

Owing to an increasing low ore grade in recent times, large scale Autogenous and Semi-autogenous (AG/SAG) tumbling mill (primary mill) has gained widespread application in most comminution circuits (ore size reduction and liberation process) with huge benefits in terms of large tonnage treatment and operational economics (Bueno, 2013; Morrell, 1998; Takalimane, 2014). AG/SAG mill is chiefly characterised by their large diameter to small length ratio (aspect ratio) and several internally spaced lifters. The operational ore breakage dynamics in AG/SAG mill during milling at a given mill speed is predominant by impact alongside abrasion, attrition, and nipping (Lynch, 2015; Takalimane, 2014). Among the upstream and downstream extraction processes, comminution circuit including AG/SAG mill is known to be the most energy-intensive operation (Ballantyne, Powell and Tiang, 2012; Borg, Scharfe and Kamradt, 2016). The mill performance efficiency is significantly affected by multiple processing parameters such as mill speed, feed variability, ball loading, pulp density, water flow rate, mill lifter heights and profile/configuration (Das *et al*, 2011; Nayak *et al*, 2020; Royston, 2007; Uys, 2018).

Of interest is mill lifter heights and profile/configurations among other factors, provide an integral contribution to the overall size reduction process inside AG/SAG mill. Lifter heights largely determine the mill charge trajectory and responsible for lifting the charges to assume a cataracting regime (Almond, 2005). Many research studies have reported that mill lifter profile and design along with mill speed could affect the liner-lifter wear rate, energy consumption, product size distribution, charge packing, charge slippage (Almond and Valderrama, 2004; Muhayimana *et al*, 2018; Royston, 2007; Usman, Taylor and Spiller, 2016; Yin *et al*, 2018). Depending on the mill speed, load composition, and operation over time, lifter height and profile could be deformed (accelerate wear out and change lifter height) from continuous striking of steel balls on their surfaces, including steel balls themselves (Takalimane, 2014). This can create challenges by affecting mill efficiency and wastage of energy when not quickly detected. Conventionally, mill operators have little or no response abilities to timely provide suitable control measures in real-time. Further understanding of lifter and profile in tumbling mills through simulation approaches such as discrete element methods (DEM) and positron emission

particle tracking PEPT have been reported in many studies (Mishra, 2003a, 2003b; Takalimane, 2014; Uys, 2018). Following some degree of understanding revealed by these simulations, the methods are still limited for consideration of ideal conditions. Thus, the need for an advanced instrument that could detect and inform the earliest decision-making process of mill operation and in real-time.

The in-AG/SAG mill frequent interactions of charge and liner/lifters are known to emit excessive audible noise emission and shell vibration signals (Almond and Valderrama, 2004; Almond, 2005; Das *et al*, 2011; Gugel, Rodriguez and Gutierrez, 2016; Gugel, 2015; Spencer *et al*, 1999). The mill noise and shell vibration emanate from many events such as ball-ball, rock-rock, ball-rock, ball/rock-liner/lifter collisions inside the mill corresponding to varied frequencies. Research has shown that mill noise and vibration signal could be used to distinguish mill operating conditions such as toe and shoulder position, load level, ore/rock character, slurry density, and charge dynamics (Campbell *et al*, 2003; La Rosa *et al*, 2008; Owusu *et al*, 2020a, 2020b, 2020c; Pax and Thornton, 2019; Tang *et al*, 2012; Watson, 1985; Watson and Morrison, 1985, 1986). Nevertheless, due to the harsh and hostile environment of the AG/SAG mill, on-shell vibration sensors could suffer frequent mechanical breakdown and maintenance. The acoustic sensor is a non-contact technique, rendering no sensor and mill interference (Owusu *et al*, 2020b). Employing the acoustic-based monitoring technique, Pax and Thornton (2019) reported the possibility of detecting the collision of steel ball and liner/lifter and termed it as Mill Shell Steel Hits (MSSH). Almond (2005) also classified ball falling trajectories on mill liner/lifter or rock/slurry load as critical impact or standard impact using mill noise. The critical impact produces intense acoustical levels from direct collision of ball-liner/lifter (hasten ball-liner/lifter wear rate and unnecessary energy wastage), hence must be avoided while standard impact is desirable to achieving suitable size reduction rate. However, there is a dearth of information regarding different heights and configurations and acoustic.

To close the gap in understanding mill height variations and their acoustic emission, as a potential alternative tool to inform operators on mill conditions, the present study seeks to investigate three different heights (four configurations) in a laboratory-scale AG/SAG mill simulator with an acoustic sensor placed at the toe side. The following key questions were addressed:

- What is the effect of lifter height variations and configuration on SAG mill product quality?
- Which acoustic features extraction demonstrated a suitable classification technique?
- Can mill acoustic response be used to distinguish different lifter heights and configurations? What is the effect of different lifter heights and configurations on mill acoustic response?
- What is the relationship between mill acoustic response and product size distribution of varying lifter heights?
- What is the overall implication of the study relevant to the industry?

EXPERIMENTAL STUDY

Material preparation

Pure model calcite mineral (99.95 wt. per cent) obtained from South Australia was used in this investigation. The model calcite was initially fragmented using a jaw crusher and a feed size range of $-12 + 2$ mm ($P_{80} = \sim 11$ mm) was prepared as shown in Figure 1a. Then a 1000 g calcite sample was taken as mill input rock feed. Also, 5 vol. per cent of steel ball (Figure 1b) was taken as grinding media.

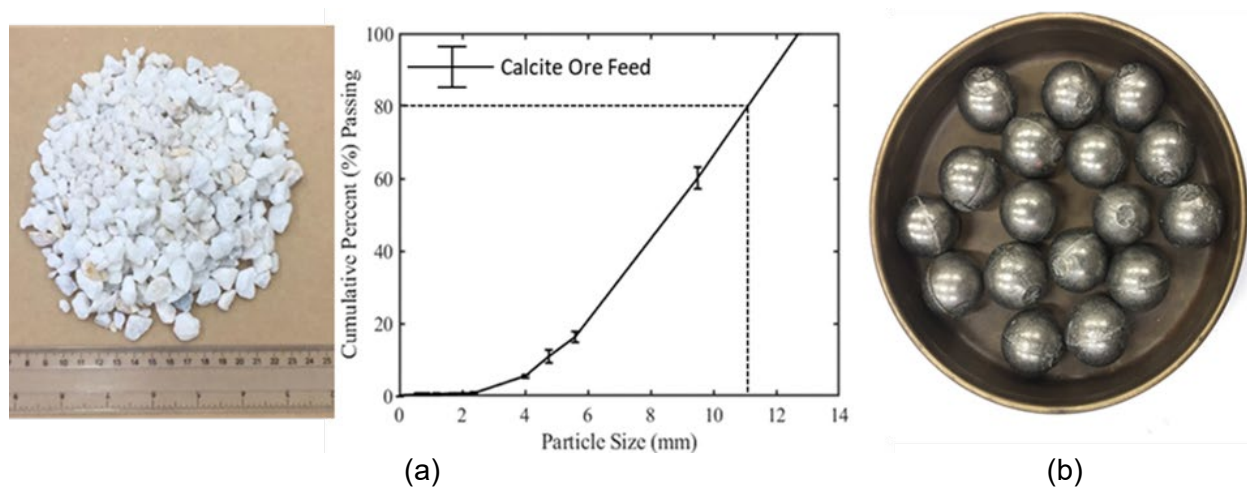


FIG 1 – (A) model calcite feed coupled with particle size distribution; and (B) steel balls (grinding media).

Lifter design and configuration

Figure 2 illustrate three different lifters that were designed as low (Lo), high (Hi), and very high (v-Hi) heights together with their configuration inside the mill.

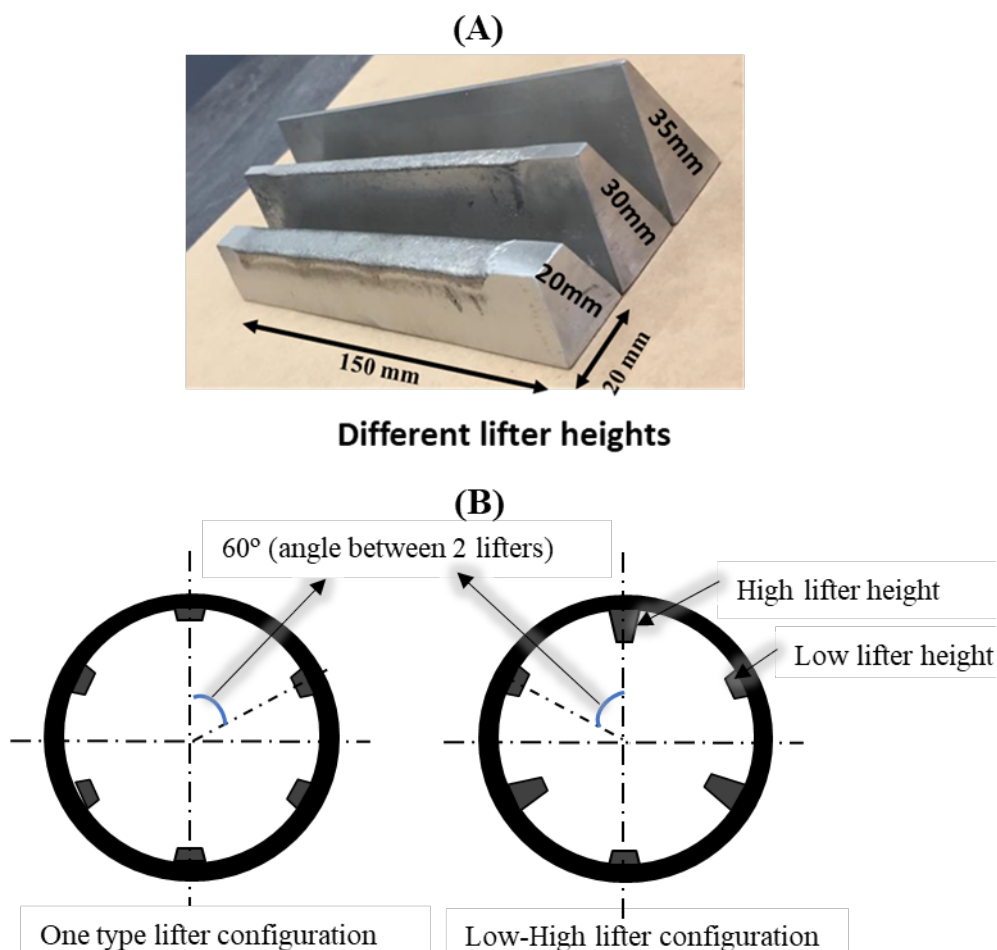


FIG 2 – (A) different lifter heights; and (B) lifter arrangement inside the mill.

As shown in Figure 2b, two different lifter configurations were used, presenting only one lifter type arrangement (either Lo, Hi or v-Hi) and mix lifters arrangement (Lo-Hi). Table 1 shows the detailed lifter design and geometry employed in the study.

TABLE 1

Geometry, dimensions, configuration of lifter designs (made of stainless steel).

No.	Lifter shape	Lifter configuration	No. of lifters	Length [mm]	Height [mm]	Top width [mm]	Bottom [mm]	Face angle [°]
1	Trapezium	Low (Lo)	6	150	20	9	20	30
2	Trapezium	High (Hi)	6	150	30	4	20	30
3	-	Lo-Hi	6	150	20–30	9–4	20	30
4	Trapezium (~ triangular)	Very High (v-Hi)	6	150	35	2	20	30

Note: Lo, Hi, and v-Hi signify only 20, 30, and 35 mm lifter height configurations, respectively. Lo-Hi means 20 mm and 30 mm lifter configuration, such that low lifters lie in-between high lifters.

Grinding study and mill acoustic monitoring

A laboratory-scale AG/SAG mill simulator (Modified Magotteaux ball mill) by size 300 mm diameter to 150 mm height with six equally spaced replaceable lifters (internal) was used for the grinding study. An acoustic sensor system made up of a microphone and pre-amplifier (AudioBox iOne – Presonus) was employed for recording mill noise emission. From preliminary study information, the microphone was positioned close to the mill toe angle. Two laptops were connected to the set-up, one for real-time acoustic visualisation and the other one for mill control. Figure 3 shows the photograph of the experimental set-up.

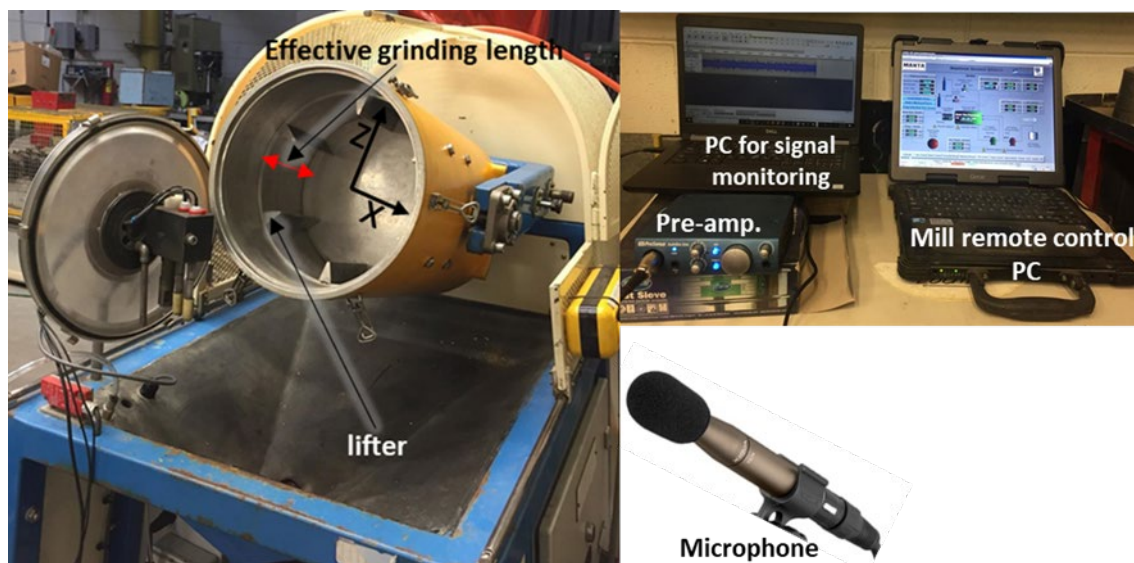


FIG 3 – Experimental set-up of laboratory-based AG/SAG mill and acoustic-based monitoring system.

In the study, the grinding performance of each lifter height arrangement (only one type) was tested alongside the combination of Lo and Hi lifters. 1000 g model calcite, 5 vol. per cent steel balls and 500 ml of water constituting mill charge were constantly used for the tested lifters and configuration. The mill revolution was maintained at 50 rev/min and a grinding time of 10 minutes. After every grinding test, wet screening was carried out to obtain -75 and +75 μm and dried in an electric oven at 50°C overnight. Following the drying process, a series of screens developed based on Tyler series to obtain the product size distribution on the +75 μm . Concurrently, the mill acoustic responses of every lifter height and configuration were recorded at a sampling rate of 44.1 kHz while milling was ongoing. All recorded signals were saved as .wave file with the right labels into a separate folder.

Acoustic signal processing

To improve signal quality by removing background noise and artefacts, acoustic signal preprocessing which is a pre-requisite step was carried out. Signal edge cutting to eliminate pre-trigger and signal tails together with designing a high-pass filter to remove background noise. Further signal smoothing using Savitzky-Golay filter (also known as digital smoothing polynomial or least square smoothing filter) was employed (Acharya *et al*, 2016). In this analysis, 30 seconds signal data points (1 323 000) were taken from the time-domain data for evaluation. Feature extractions such as wavelet decomposition (wavelet transform) and power spectral density estimate (Welch's method) coupled with root mean square (RMS) analysis as a performance indicators were used. RMS analysis was initially performed on the time-domain signal produced by each of the lifter types and arrangements. The mathematical expressions for the RMS and various transforms (WT and PSDE) used are as follow (Nayak *et al*, 2020; Nizwan *et al*, 2013; Sun *et al*, 2018):

$$RMS_{(t)} = \sqrt{\frac{1}{N} \sum_{i=0}^{N-1} [x(t+i) - \bar{x}(t)]^2} \quad (1)$$

where $x(t+i)$ is the acoustic emission signal at the time index i , N is the number of discrete data points in a specified time duration.

Wavelet transform (WT) provides the time-frequency information of a signal. WT includes continuous and discrete wavelet transform. For CWT, the original signal is convoluted with the son wavelet over the length of the signal.

$$W_x(a, b) = \int x(t) \psi_{a,b}^*(t) dt, \quad (2)$$

where $x(t)$ is original signal, $\psi_{a,b}(t)$ is son wavelet which is derived by scaling and shifting the mother wavelet $\psi(t)$ ie:

$$\psi_{a,b}(t) = \frac{1}{\sqrt{|a|}} \psi\left(\frac{t-b}{a}\right) \quad (3)$$

where a and b are scaling and translation (shifting), respectively.

For discrete wavelet transform (DWT), it is obtained from the discretisation of the CWT given as:

$$DWT(j, k) = \frac{1}{\sqrt{2^j}} \int_{-\infty}^{\infty} f(t) \psi^*\left(t - \frac{2^j k}{2^j}\right) dt \quad (4)$$

where a and b are replaced by 2^j and $2^j k$, $f(t)$ is original signal.

In DWT (decomposition analysis), the acoustic signal was filtered using high pass and low pass filters to obtain high and low-frequency components, respectively. The fourth-order Daubechies (db4) was employed to decompose the mainstream signal into approximation coefficient, cA (low-frequency component) and detailed coefficient, cD (high-frequency component) (Nizwan *et al*, 2013). Using the same db4 technique, the $cA1$ is iteratively decomposed into lower levels of $cA2$ and $cD2$ until $cA8$ and $cD8$. Following that, each decomposition level was subjected to RMS analysis. The representation of the DWT decomposition levels is shown in Figure 4.

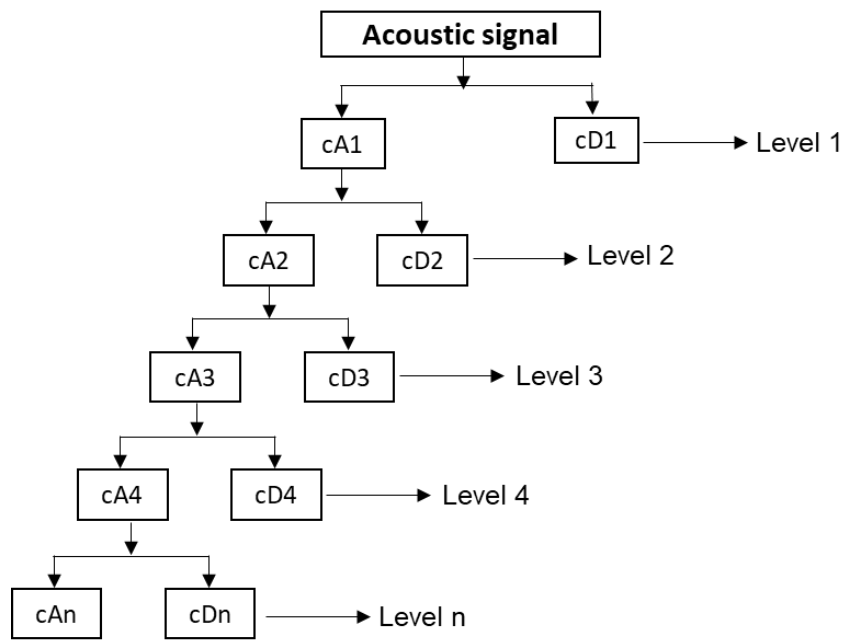


FIG 4 – DWT decomposition representation.

RESULTS AND DISCUSSIONS

Product size distribution

As a performance indicator, the product size distribution (PSD) of the different lifter heights and configurations are shown in Figure 5.

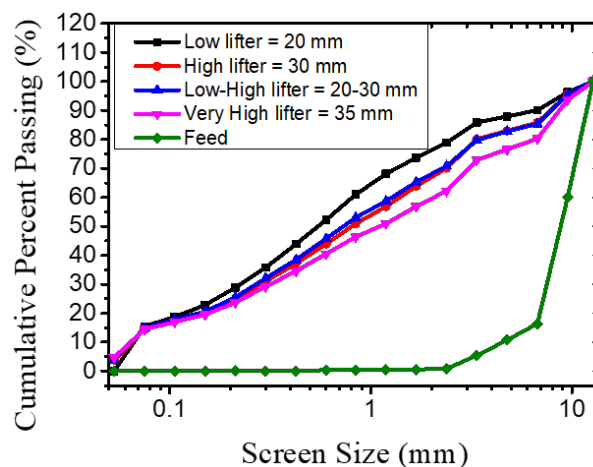


FIG 5 – Product size distribution of different lifter height configurations.

It was observed that PSD reduced with increasing lifter heights of the same type from Lo, Hi, and v-Hi configuration. Given only Hi lifters and the combination of Lo and Hi lifters, unnoticeable differences were produced. At the same mill speed, only low lifter height arrangement projected the cataracting ball charge to fall on appropriate mill toe position where sufficient rock or slurry is available to enhanced breakage. Increasing the lifter height configurations overthrow steel ball charge above mill toe angle without necessary colliding with rock material, hence less breakage rate.

Effect of lifter height/configuration and mill acoustic response

Wavelet decomposition analysis

As a preliminary analysis, RMS analysis was performed on the original acoustic signal relating to each lifter type during grinding as shown in Figure 6.

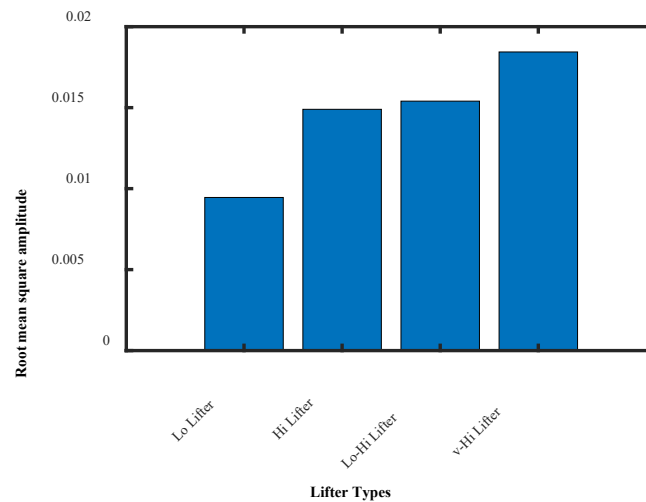


FIG 6 – Preliminary RMS analysis of different lifter heights/configuration and their mill acoustic response.

The results showed a consistent and considerable rise in the mill noise for increasing lifter height, except for only Hi and Lo-Hi that presented marginal difference. This suggests that the tested lifter arrangement inside the mill did not have significant impact on the mill acoustic response. With an increase in height, more charge material could be lifted and projected to the toe side of mill at higher velocity than a relatively shorter lifter height. Accordingly, increasing mill noise with lifter variations could be ascribed to more charge cataracting to the mill shell.

Further advanced analysis using discrete wavelet transform (DWT) was deduced, together with statistical RMS as AG/SAG mill acoustic response indicator. The original signals relating to the tested lifters were decomposed into eight decomposition levels as low-frequency components (approximation coefficients–cAs) and high-frequency (Detail coefficients–cDs) components as represented in Figure 7.

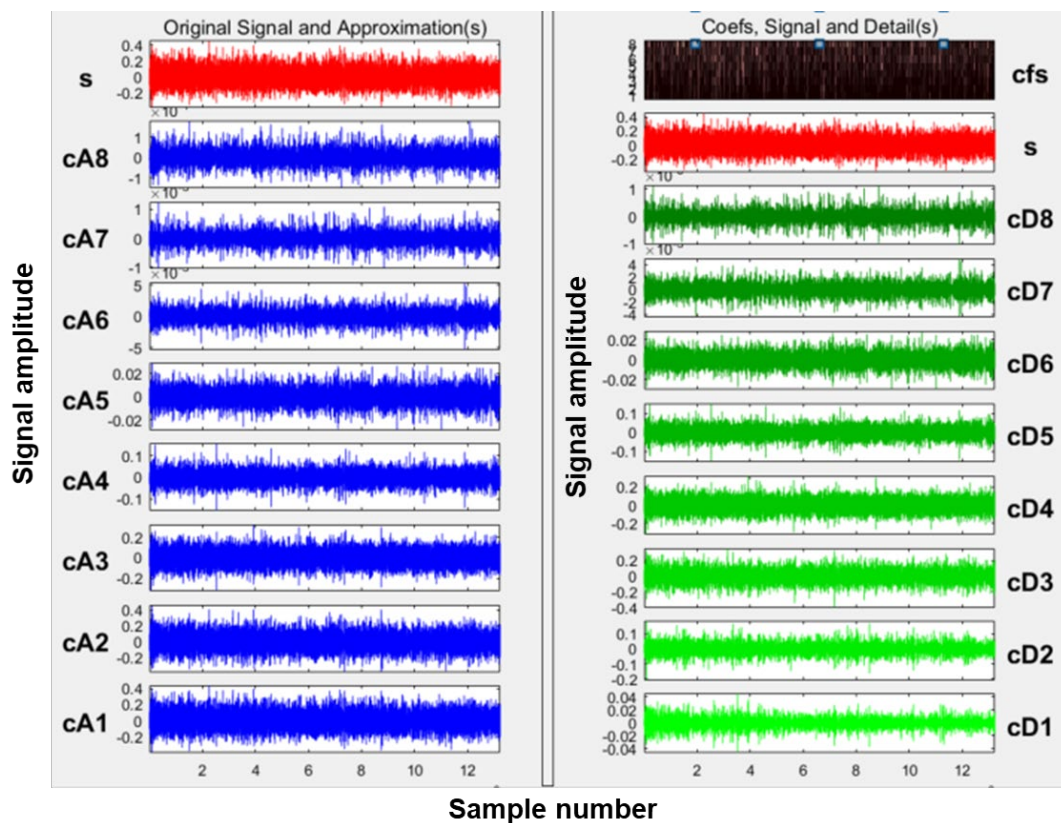


FIG 7 – DWT signal decompositions levels.

The signal energy decreased as the decomposition levels increased. By eye-balling observation, it is evident that no meaningful inferences can be obtained from only the decomposition levels. Accordingly, RMS values were extracted from each of the low and high-frequency levels for comparison purposes as demonstrated in Figure 8.

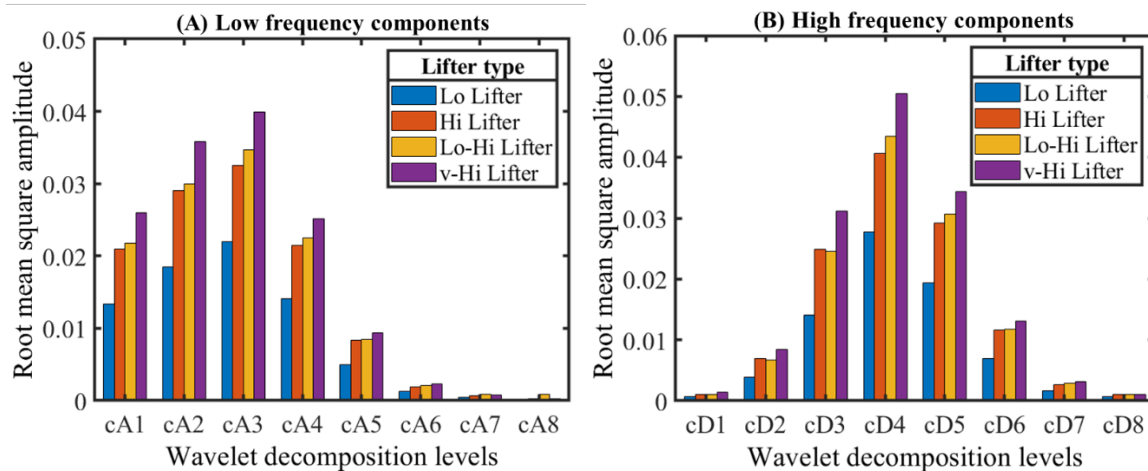


FIG 8 – Wavelet analysis coupled with RMS for different lifter heights and configuration.

Comparing the low-frequency levels of the lifter types and configuration, it was observed that almost all the decomposition levels (cA1-cA6) produced an increase in mill noise in the order of Lo<Hi<Lo-Hi<v-Hi lifter. From this analysis, it could be seen that some degree of variation existed between Lo and Lo-Hi lifter arrangement with Lo-Hi lifter being superior. In the case of high-frequency components decomposition, similar trends were produced in all the decomposition levels, except cD8 which was unclear. The consistency of the results evidently depicted that different trajectories existed for varying lifter heights, contributing to the varied mill noise emission under similar grinding conditions.

Power spectral density analysis

In terms of the frequency spectrum, power spectral density estimate (PSDE) by Welch's method was used to estimate the noise emission by each of the lifter heights and configuration as presented in Figure 9.

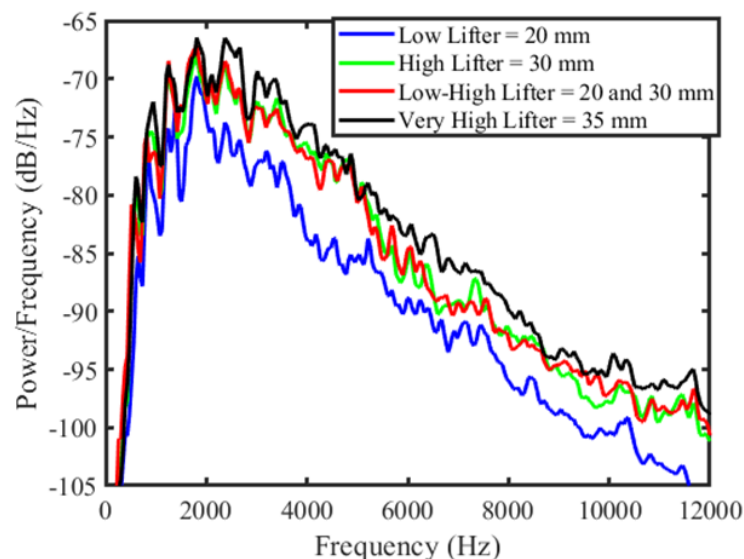


FIG 9 – PSDE analysis of different lifter heights and configuration.

As shown by PSDE, high signal energy is retained in the relatively lower frequency bands and reduces with increasing frequency bands. It was demonstrated that an increase in lifter height increases mill noise energy. The emitted mill acoustic of Lo and Lo-Hi lifters indicated closely related

results (unclear variations) which reflected very well in their PSD in Figure 4. From the result, it could also be deduced that higher lifter height allows steel balls to overthrow and strike mill shell frequently rather than rock charge. This characteristic in SAG mill is not desirable since it promotes steel ball, liner, and lifter wear rate and affects product quality, wastage of energy coupled with unnecessary production cost (Almond, 2005). To reduce the frequency of the falling balls on liner/lifter and promote maximum size reduction process in SAG mill using high lifter heights, the mill speed could be reduced (Almond, 2005; Pax and Cornish, 2015). Generally, the results obtained in PSDE and DWT coupled with RMS agree with one another.

CONCLUSIONS

An investigation has been conducted on the potential application of mill noise response sensor to understand the effect of different lifter heights (low, high and very high lifters) and configuration (single and mix arrangement) on mill performance. From the study, the following conclusions were deduced:

- Product particle size distribution considerably affected by different lifter heights and configurations. Low and very high lifter heights produced the maximum and minimum PSD, respectively. Feed size reduction of low and low-high lifter arrangements presented negligible differences.
- PSDE and DWT coupled with RMS as performance indicators presented noticeable variations from the tested lifter heights, especially DWT-RMS analysis. The extracted signal features can be used to classify the performance of different lifter heights.
- Mill acoustic response is sensitive to changes in lifter heights and configuration in that higher lifter height supported higher noise emission which reduced with decreasing the lifter height. The acoustic response between low and low-high lifter profiles presented an unclear difference in PSDE analysis. In the DWT and RMS analysis, it was identified that low-high lifter profile noise emission was slightly greater than the only low lifter configuration.
- There is a contrasting correlation between mill acoustic response and product size distribution of varying lifter heights, such that in terms of lifter heights, mill acoustic emission increases in the order of $Lo < Hi < v-Hi$ and reduces in the order of $Lo > Hi > v-Hi$ in terms of PSD.
- In general, the study implies that mill acoustic is sensitive to lifter variations which have potential application to inform a rapid decision-making process in the mill when lifter height wear over time.

ACKNOWLEDGEMENTS

This research has been supported by the SA Government through the PRIF RCP Industry Consortium. The authors also acknowledge the support from the Future Industries Institute (FII) University of South Australia, Australia.

REFERENCES

- Acharya, D, Rani, A, Agarwal, S and Singh, V, 2016. Application of adaptive Savitzky–Golay filter for EEG signal processing. *Perspectives in Science*, 8: 677–679.
- Almond, D and Valderrama, W, 2004. Performance enhancement tools for grinding mills, *International Platinum Conference 'Platinum Adding Value*, The South African Institute of Mining and Metallurgy, pp. 103–110.
- Almond, D G, 2005. Performance enhancement of semi-autogenous grinding mills through the use of instrumentation based on acoustic signals, *Canadian Mineral Processors Proceedings*, pp. 389–399.
- Ballantyne, G, Powell, M and Tiang, M, 2012. Proportion of energy attributable to comminution, *Proceedings of the 11th Mill Operator's Conference*, pp. 25–30 (The Australasian Institute of Mining and Metallurgy: Melbourne).
- Borg, G, Scharfe, F and Kamradt, A, 2016. High-velocity comminution of massive sulphide ores by the VeRo Liberator® technology for more energy efficient size reduction and particle liberation. *World of Mining–Surface and Underground*, 68(1): 45–52.
- Bueno, M d P, 2013. Development of a multi-component model structure for autogenous and semi-autogenous mills, PhD Thesis, The University of Queensland, 217 p.

- Campbell, J J, Holmes, R J, Spencer, S J, Sharp, V, Davey, K J, Barker, D G and Phillips, P L, 2003. The collection and analysis of single sensor surface vibration data to estimate operating conditions in pilot-scale and production-scale AG/SAG mills, *Proceedings: XXII International Mineral Processing Congress*, pp. 280–288.
- Das, S P, Das, D P, Behera, S K and Mishra, B K, 2011. Interpretation of mill vibration signal via wireless sensing. *Minerals Engineering*, 24(3–4): 245–251.
- Gugel, K, Rodriguez, J C and Gutierrez, L J, 2016. Automated SAG mill speed control using on-contact vibration sensor.
- Gugel, K S, 2015. Optimal SAG mill control using vibration and digital signal processing techniques, *SAG Conference*, Vancouver, Canada.
- La Rosa, D, Cantarutti, A, Wortley, M and Ozkocak, T, 2008. The use of acoustics to improve load estimation in the Cannington AG mill, *6th Metallurgical Plant Design and Operating Strategies (MetPlant 2008)*, pp. 105–116 (The Australasian Institute of Mining and Metallurgy: Melbourne).
- Lynch, A, 2015. Comminution handbook to prove highly useful for students and industry practitioners alike. *AusIMM Bulletin* (Jun 2015): 80.
- Mishra, B K, 2003a. A review of computer simulation of tumbling mills by the discrete element method: Part I—contact mechanics. *International Journal of Mineral Processing*, 71(1): 73–93.
- Mishra, B K, 2003b. A review of computer simulation of tumbling mills by the discrete element method: Part II—Practical applications. *International Journal of Mineral Processing*, 71(1): 95–112.
- Morrell, S, 1998. Recent Developments in Ag/Sag Milling in Australia, *1st Annual Crushing and Grinding in Mining Conference*, Johannesburg, South Africa.
- Muhayimana, P, Kimotho, J K, Ndeto, M K and Ndiritu, H M, 2018. Effects of Lifter Configuration on Power Consumption of Small Scale Ball Mill. *Journal of Sustainable Research in Engineering*, 4(4): 171–183.
- Nayak, D K, Das, D P, Behera, S K and Das, S P, 2020. Monitoring the fill level of a ball mill using vibration sensing and artificial neural network. *Neural Computing and Applications*, 32(5): 1501–1511.
- Nizwan, C K E, Ong, S A, Yusof, M F M and Baharom, M Z, 2013. A wavelet decomposition analysis of vibration signal for bearing fault detection. *IOP Conference Series: Materials Science and Engineering*, 50: 012026.
- Owusu, K B, Karageorgos, J, Greet, C J, Zanin, M, Skinner, W and Asamoah, R, 2020b. Non-Contact Acoustic and Vibration Sensors in Autogenous and Semi-Autogenous (AG/SAG) Mills: A Brief Review, *IMPC 2020: XXX International Mineral Processing Congress Proceedings*, Cape Town, South Africa, pp. 3292–3304.
- Owusu, K B, Karageorgos, J, Greet, C J, Zanin, M, Skinner, W and Asamoah, R, 2020c. Variations in Mill Feed Characteristics and Acoustic Emissions, *Proceedings of 6th UMaT Biennial International Mining and Mineral Conference*, Tarkwa-Ghana, pp. 384–390.
- Owusu, K B, Karageorgos, J, Greet, C J, Zanin, M and Skinner, W, 2020a. Acoustic Monitoring of Mill Pulp Densities, *Proceedings of 6th UMaT Biennial International Mining and Mineral Conference*, Tarkwa, Ghana, pp. 359–365.
- Pax, R and Thornton, A, 2019. Real time measurement and fast control strategies for the optimal operation of grinding circuits, *Proceedings MetPlant Conference*, Perth, WA, pp. 132–147 (The Australasian Institute of Mining and Metallurgy: Melbourne).
- Pax, R A and Cornish, B, 2015. A novel measurement for the internal operation of a semi-autogenous mill using acoustic sensors-A case study, *MetPlant 2015*. pp. 120–128 (The Australasian Institute of Mining and Metallurgy: Melbourne).
- Royston, D, 2007. Semi-autogenous grinding (SAG) mill liner design and development. *Mining, Metallurgy & Exploration*, 24(3): 121–132.
- Spencer, S, Campbell, J, Weller, K and Liu, Y, 1999. Acoustic emissions monitoring of SAG mill performance, *Proceedings of the Second International Conference on Intelligent Processing and Manufacturing of Materials. IPMM'99* (Cat. No. 99EX296). IEEE, pp. 939–946.
- Sun, H, Wang, J, Longstaff, A and Gu, F, 2018. Characterizing acoustic emission signals for the online monitoring of a fluid magnetic abrasives finishing process. *Proceedings of the Institution of Mechanical Engineers, Part C: Journal of Mechanical Engineering Science*, 232(11): 2079–2087.
- Takalimane, M, 2014. Evaluating the influence of lifter face angle on the trajectory of particles in a tumbling mill using PEPT, Master Thesis, Department of Chemical Engineering, University of Cape Town.
- Tang, J, Chai, T, Yu, W and Zhao, L, 2012. Feature extraction and selection based on vibration spectrum with application to estimating the load parameters of ball mill in grinding process. *Control Engineering Practice*, 20(10): 991–1004.
- Usman, H, Taylor, P and Spiller, D E, 2016. The effects of lifter configurations and mill speeds on the mill power draw and performance, *Proceedings of the 1st International Process Metallurgy Conference (IMPC)*. AIP Publishing, 2016, West Java, Indonesia, pp. 1–10.
- Uys, A M, 2018. The study of the influence of the lifter height on the charge motion, velocity profile and power draw of a laboratory tumbling mill using DEM simulations, Masters Thesis, Department of Chemical Engineering, University of Cape Town, South Africa.

- Watson, J and Morrison, S, 1986. Estimation of pulp viscosity and grinding mill performance by means of mill noise measurements. *Mining, Metallurgy Exploration*, 3(4): 216–221.
- Watson, J, 1985. An analysis of mill grinding noise. *Powder Technology*, 41(1): 83–89.
- Watson, J L and Morrison, S D, 1985. Indications of grinding mill operations by mill noise parameters. *Particulate Science Technology*, 3(1–2): 49–63.
- Yin, Z, Li, T, Peng, Y and Wu, G, 2018. Effect of Lifter Shapes on the Mill Power in a Ball Mill. *IOP Conference Series: Materials Science and Engineering*, 452: 042201.

Direct leaching of rare earth elements from circulating fluidised bed combustion coal fly ash by hydrochloric acid

M C Pacaña¹, A E Dahan², C B Tabelin³, V T Resabal⁴, R D Alorro⁵, L S Silva⁶ and R M Baute⁷

1. MS Student, Mindanao State University-Iligan Institute of Technology, Iligan City, Lanao del Norte, Philippines, 9200. Email: monalisa.pacana@g.msuiit.edu.ph
2. Process Control Metallurgist, TVI Resource Development Inc., Gold-Silver Project, Siocon, Zamboanga del Norte, Philippines, 9200. Email: almon.dahan@gmail.com
3. Lecturer, School of Minerals and Energy Resources Engineering, The University of New South Wales, Sydney NSW. Email: c.tabelin@unsw.edu.au
4. Professor, Mindanao State University-Iligan Institute of Technology, Iligan City, Lanao del Norte, Philippines, 9200. Email: vanniejoy.resabal@g.msuiit.edu.ph
5. Senior Lecturer, Western Australia School of Mines: Minerals, Energy and Chemical Engineering, Curtin University, Kalgoorlie WA. Email: richard.alorro@curtin.edu.au
6. Assistant Professor, Mindanao State University-Iligan Institute of Technology, Iligan City, Lanao del Norte, Philippines, 9200. Email: leaniel.silva@g.msuiit.edu.ph
7. Project Staff, Mindanao State University-Iligan Institute of Technology, Iligan City, Lanao del Norte, Philippines, 9200. Email: ronben.baute@g.msuiit.edu.ph

INTRODUCTION

The world is rapidly transitioning to low carbon technology such as wind turbines, solar panels and battery storage to combat climate change. However, recycling the materials that is already in circulation simply is not enough to meet the demand that is expected to rise in transforming to green energy. This require raw materials that need to be mined. And among those, rare earth elements (REE) are one of the most significant materials that will surge in demand in the following decades. The annual growth for the total REE demand is between 5 per cent and 9 per cent over the next 25 years and it is therefore projected that there will be shortages in the supply especially for the clean energy applications in the near future (Alonso *et al*, 2012). In 2014, the Raw Materials Supply Group of the European Commission (European Commission, 2014) classified REEs as critical raw materials. This projected supply shortage of REE has fuelled the quest to find alternative sources of REEs. A few studies have verified the potential of coal fly ash (CFA) as secondary resources of REEs (Franus *et al*, 2015).

Coal fly ash produced from the burning of coal in coal-fired powerplants is a fine-grained, powdery particulate material collected from flue gas. This characteristic poses a great advantage as a secondary resource of REE since it does not need intensive energy requirement for comminution. In this study, the raw coal fly ash samples are characterised to determine its potential as a REE secondary resource. Figure 1 illustrates the REE content of the raw coal fly ash sample based on economic classification. The results show that the total REE is 192.5 ppm, 36.94 per cent of which is the % critical REE. Utilising the ratio between the total relative amounts of Critical REE and Excessive REE to estimate the ore quality, the outlook coefficient is 1.03 which a strong potential for economic development according to the criteria of Seredin and Dai (2012).

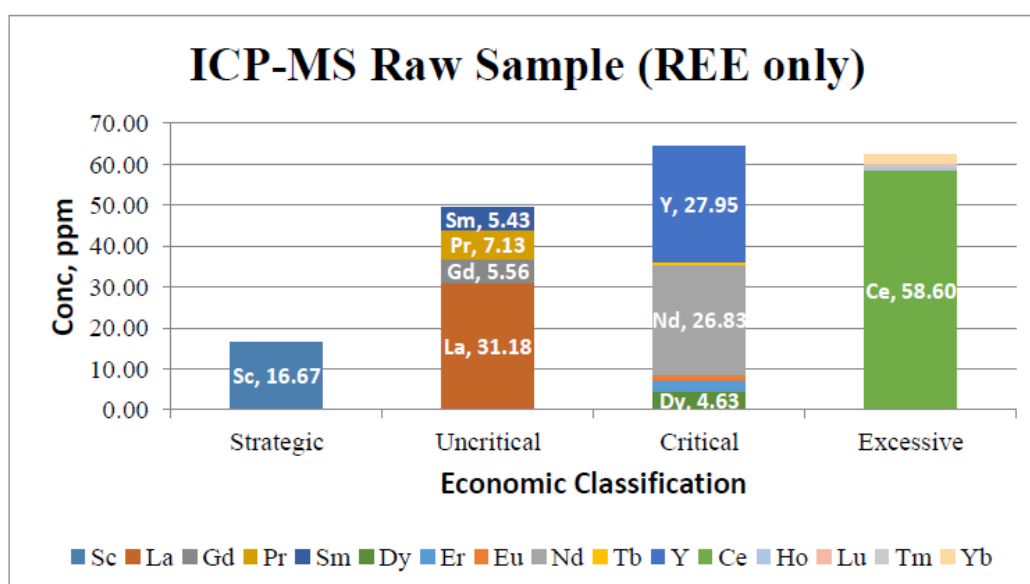


FIG 1 – REE content of coal fly ash based on economic classification.

To extract the valuable REE in the coal fly ash, direct leaching method using hydrochloric acid (HCl) is used. Initially, a screening test is done to investigate the significance of the effect of HCl acid concentration, temperature, and time on the leaching of REE from coal fly ash. A coal fly ash sample in around bottom flask with HCL solution is subjected in a heating mantle set-up with condenser, stirrer and thermometer. The following factors are studied including its levels: HCl concentration (0.25M, 0.5M, 1.0M, 3.0M); leaching temperature (25°C, 65°C); and leaching time (0.5 hrs, 1.0 hrs, 3.0 hrs, 6.0 hrs).

As shown in the Pareto chart (Figure 2), which measures the importance of the factors and its interactions, the temperature has the highest standardised effect, followed by the HCl concentration while the effect of time is almost significant as it almost reached the red border line at 2.07. The data of Nd is selected for the discussion since it has the highest concentration in the coal fly ash at 26.8 ppm for the critical REE group.

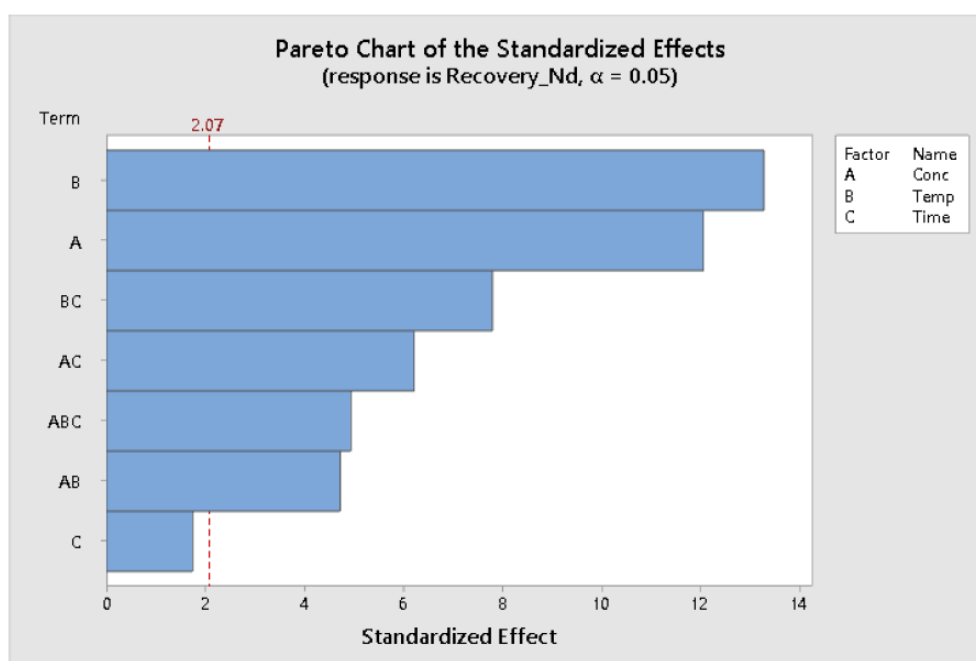


FIG 2 – Pareto chart for Nd recovery.

Response Surface Methodology (RSM) is then used to obtain the optimum parameters with the highest recovery. The result of the analysis of leaching of critical REE from coal fly ash using RSM is displayed in Table 1. The element Yttrium (Y) was not included because its concentration in the pregnant solution was not detected.

TABLE 1
Recovery of Critical REE.

Independent variable			Critical REE recovery				
Concentration (M)	Temperature (°X)	Time (mins)	Dy	Er	Eu	Nd	Tb
1	35	90	47.5	49.6	58.7	44.4	63.0
3	35	90	54.0	53.4	58.7	53.0	69.5
1	65	90	51.8	53.4	58.7	48.1	66.9
1	35	270	51.8	53.4	58.7	47.7	66.9
3	65	90	69.1	68.7	73.3	65.7	83.6
3	35	270	60.4	61.1	73.3	57.8	74.6
1	65	270	54.0	53.4	58.7	50.0	69.5
3	65	270	73.4	76.3	88.0	69.7	90.0
0	50	180	0.0	0.0	0.0	0.7	12.9
3.7	50	180	64.7	68.7	73.3	63.0	81.0
2	25	180	54.0	57.3	58.7	52.2	66.8
2	75	180	73.4	76.3	88.0	69.0	90.0
2	50	29	51.8	53.4	58.7	51.5	68.2
2	50	331	64.7	68.7	73.3	61.9	79.7
2	50	180	60.4	61.1	73.3	59.6	77.2
2	50	180	62.6	64.9	73.3	58.9	75.9
2	50	180	60.4	61.1	73.3	59.3	77.2
2	50	180	62.6	64.9	73.3	59.3	78.5

As seen in Table 1, the highest recovery can be found in the high value parameters at 3M HCl, 65°C and 270 minutes with leaching recovery of 70.8 per cent, 76.34 per cent, 88.02 per cent, 90.01 per cent and 73.38 per cent of each of the critical REEs namely Nd, Er, Eu, Tb and Dy are, respectively. Also, there is a possibility that the optimum concentration is greater than 3M especially that the HCl concentration is the most significant among the three factors. However, it is observed that increasing the HCl concentration increases the dissolution of impurities resulting to a decrease in the selectivity of the leaching process. To calculate the selectivity of the leaching of the Critical REE to major elements, this formula is used: $\text{selectivity} = \frac{\text{Critical REE recovery}}{\text{major element recovery}}$. The Critical REE recovery used for 1M and 3M is from recovery values of individual Critical REE at 1M, 65°C, 270 mins and 3M, 65°C, 270 mins. The calculated selectivity is shown in the Figure 3.

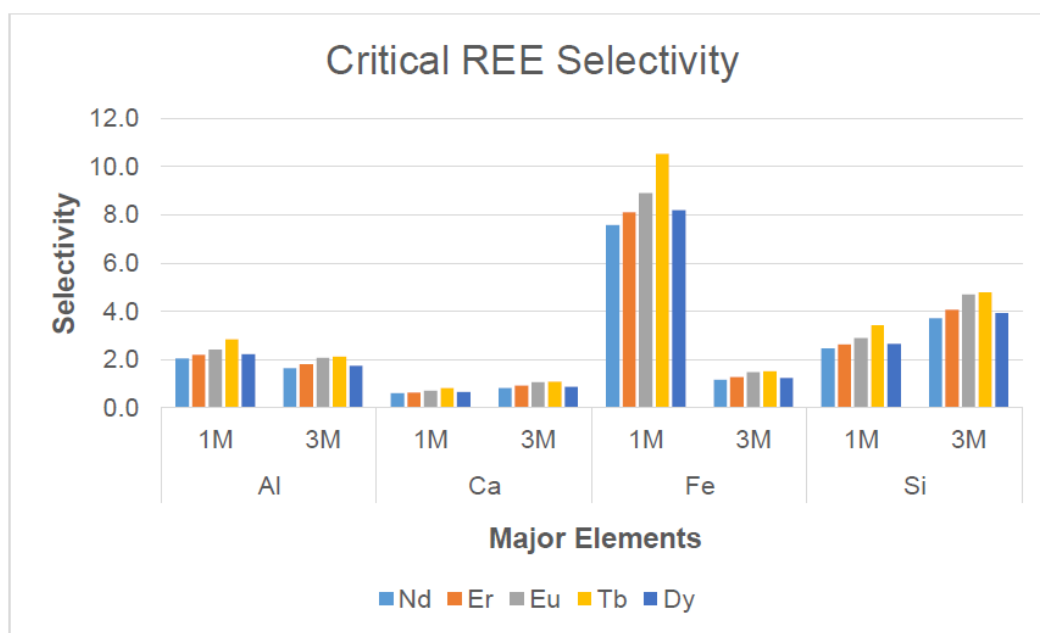


FIG 3 – Critical REE selectivity.

From the figure, the most distinguished difference in selectivity with respect to its concentration is observed in the dissolution of Fe. The selectivity of Critical REE leaching process to Fe dissolution decreases greatly as the HCl concentration was increased from 1M to 3M. There is a drop of approximately ~83 per cent in the selectivity for the individual Critical REE. The selectivity to Al dissolution slightly decreased at ~15 per cent while Ca and Si dissolution revealed slightly increased in selectivity as the HCl concentration increased. Overall, the selectivity of the Critical REE leaching process is greatly influenced by the Fe dissolution. These findings support the claim that 3M is the highest level of HCl concentration in RSM aside from the toxicity and cost of the acid. The empirical model that was established accurately predicted the dissolution of REE with accuracy of 98.20 per cent, 96.66 per cent, 97.09 per cent, 98.17 per cent, and 97.78 per cent for Nd, Er, Eu, Tb and Dy, respectively.

ACKNOWLEDGEMENTS

This work would not have been possible without the support of Dr Vannie Joy T Resabal who have been supportive of my career goals and who worked actively to provide me with the protected academic time to pursue those goals. My sincere thanks to the Engineering Research and Development for Technology (ERDT) for the scholarship. I am grateful to all of those with whom I have had the pleasure to work during this and other related projects, especially to Engr Al Mon Dahan, Engr Myra T Cabatingan, Ruth G Limbo, Wilfredo T Gatdula. I would like to thank my parents, whose love and guidance are with me in whatever I pursue. They are the ultimate role models. Above all, to my personal Lord and saviour Jesus Christ, for His unending grace that followed me all the days of my life, I am a product of His grace. To Him belongs all the glory and praise.

REFERENCES

- Alonso, E, Sherman, A M, Wallington, T J, Everson, M P, Field, F R, Roth, R and Kirchain, R E, 2012. Evaluating rare earth element availability: A case with revolutionary demand from clean technologies. *Environmental science and technology*, 46, 3406-3414. Retrieved from <http://pubs.acs.org/doi/pdf/10.1021/es203518d>
- European Commission, 2014. Report on Critical Raw Materials for the Eu.
- Franus, W, Wiatros-Motyka, M M and Wdowin, M, 2015. Coal fly ash as a resource for rare earth elements. *Environmental Science and Pollution Research*, 22(12), 9464-9474. doi:10.1007/s11356-015-4111-9
- Seredin, V V and Dai, S, 2012. Coal deposits as potential alternative sources for lanthanides and yttrium. *International Journal of Coal Geology*, 94, 67-93. doi:<http://dx.doi.org/10.1016/j.coal.2011.11.001>

Measuring charge motion from inside an operating SAG mill

P Shelley¹, E Davies², J Olivier³ and I Einav⁴

1. VP Innovation, Molycop, Global, Perth WA 6000. Email: paul.shelley@molycop.com
2. Optimisation Engineer, Molycop, Global, Perth WA 6000.
3. PhD Student, Western Australian School of Mines, Curtin University, Perth WA 6000.
4. Professor and Director, SciGEM, School of Civil Engineering, University of Sydney, Sydney NSW 2000.

INTRODUCTION

This paper reflects on how measurements from inside an operating SAG mill might be used to better understand charge motion and energy dissipation within the mill. The paper discusses how the measurements might influence and enhance approaches to energy efficient mill operation when compared with current day modelling techniques. Insights are drawn from measurement inside two operating SAG mills in Australia using sensors inserted into grinding media and sensors fixed to the rotating mill shell.

The dynamics of the operating mill are so complex that modelling and test work falls short of providing reliable actionable insight for operators and mill practitioners. We propose that a critical missing piece of the puzzle is the measurement of forces from within an operating mill as it is operating. The development of RFID sensors which are inserted into SAG grinding balls and, separately, sensors located on the rotating shell of the mill produce a digital signal which enables data analysis. A host platform allows the measured variables to be displayed in real time on a web portal. Thus, data measurement from inside an operating industrial SAG mill is now a reality and can be utilised as input into the various mill modelling software packages to track charge motion and improve energy efficient mill optimisation.

Given the status of current SAG milling models and the hindered progress toward measuring inside mills, it is reasonable to think that successfully combining real time data from inside the mill with mill optimising mathematical models might provide an industry step-change to the efficacy of energy efficient mill operation. This paper shows results of measurements inside a mill and explores the possibilities that the measures have in charge motion mill optimisation.

Measuring inside the mill

This research project, Molycop P86, involves a process control system that has a real time data tracking platform. Sensor tags are inserted into the grinding media and liner bolt sensors are fixed to the shell. The sensors send information, in parcels, as they work inside the mill to an electronic receiver via a series of antennas. Collecting the consistent flow of data enables data analysis that shows relationships between mill operating parameters and what is happening inside the mill. The system accurately measures operational defining process variables like:

- Mill Internal Slurry Temperature (found to be not a critical mill variable)
- Media Impact
- Peak G force of impact
- Impact count
- Charge Peak G (an aggregated variable)
- Peak G distributions

The system elements are represented schematically as Figure 1.

P86 SYSTEM ARCHITECTURE

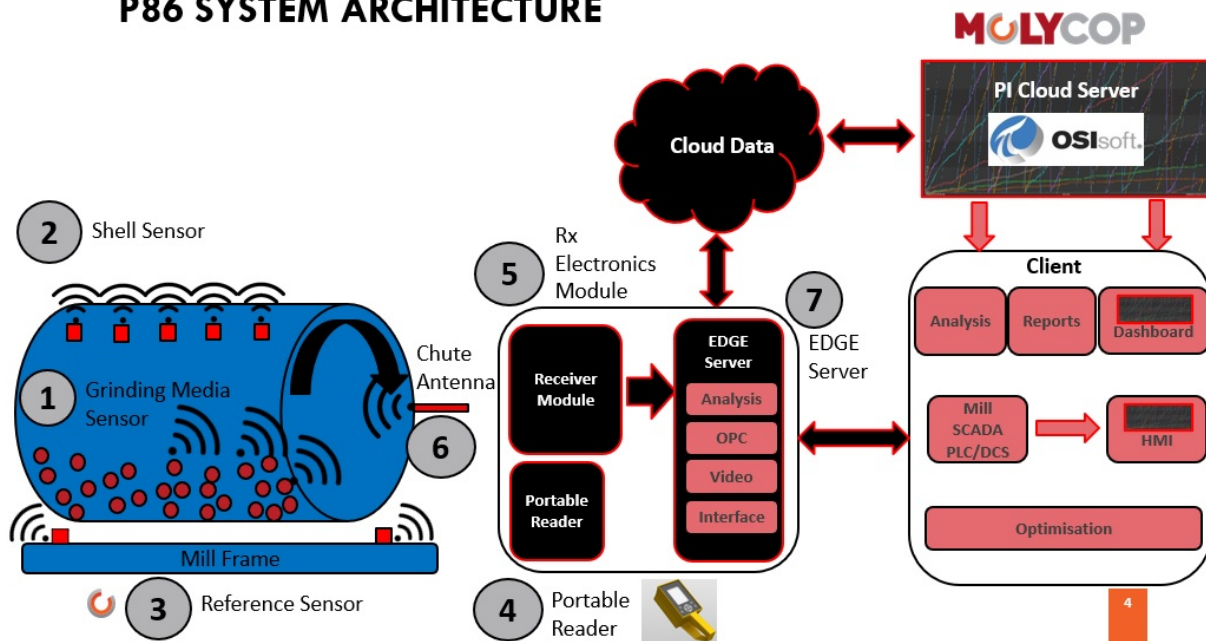


FIG 1 – P86 system elements.

The sensors provide the history of impact quanta and count of individual balls and shell impacts over a time period and in real time. To make the information meaningful, impact counts are collected in defined impact quanta; 4–7G, 7–9G, 9–11G, and beyond 11G. Sensor data are combined into single, aggregated variables. The aggregated variables provide a more holistic view of the mill charge than individual balls, provide access to variables with increased data collection frequencies, remove 'noise', while also representing the data collected more compactly for display.

The instantaneous impact value allows us to display an impact histogram over time. In this case it is necessary to aggregate the individual data of different sensors into a new variable, Charge Peak G. At times balls are buried within the charge and lost to the data capture antenna. The charge peak G media impact histogram allows us to connect impact data and the modelled behaviour of a charge within the mill, Figure 2.

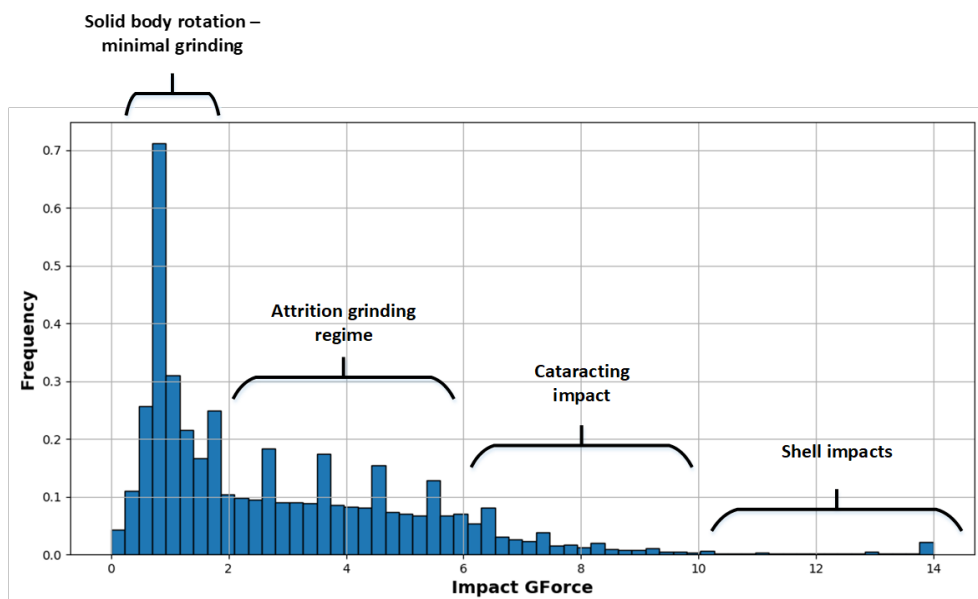


FIG 2 – Allocation of ball sensor data quanta to known mill dynamics.

Now, comparisons between comminution histograms can be analysed in time stamps where mill operating variability occurs, Figure 3.

MEDIA SENSOR IMPACT BEHAVIOUR

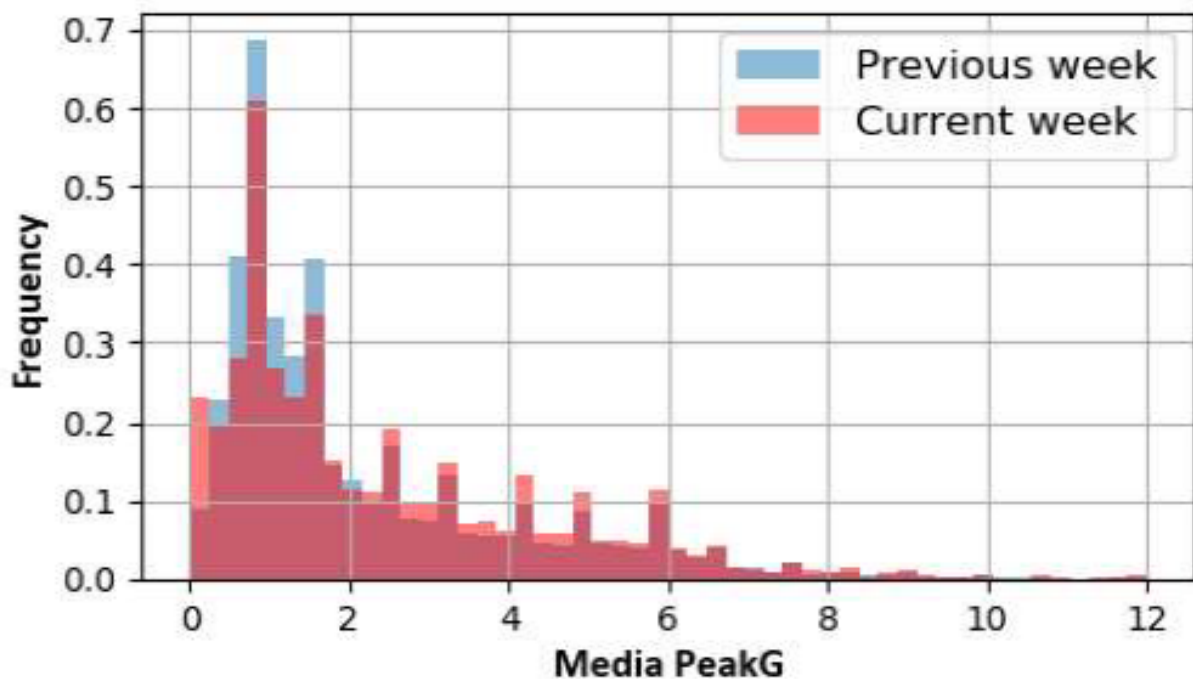


FIG 3 – Comminution profile in time steps.

Separately, we can build an evidenced based picture of mill dynamics and the operating zones within the mill and compare these to modelled mill dynamics, Figure 4.

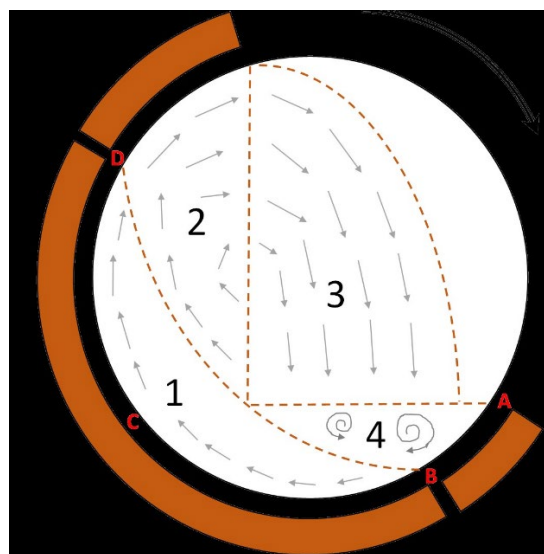


FIG 4 – Charge motion zones within a SAG mill.

Modelling mill dynamics

The best approach to date to predict the charge motion in a mill is by using Discrete Element Method (DEM) based simulations. The DEM is a way of modelling the motions and interactions of a set of individual particles and moving walls, as affected by gravity, using mathematical algorithms and Newton's Laws of Motion. Whilst DEM modelling has been a step forward for the industry, it certainly has considerable limitations. By way of specific example, the DEM model is a point in time analysis. That is, it provides insight into inter-particle behaviour at the time the relevant data is collected. The model also requires critical variable assumptions to be made to conduct the analysis. A typical analysis is very time consuming. Other constraints associated with DEM include but are not limited to; no slurry in wet applications, influence of particle shape, lacking fine particles, batch instead of

continuous operation – which includes the assumption of perfect mixing, limited ability to simulate transport through devices, ignoring the influence of the powder or slurry between the colliding elements. Given the dynamics of the system elements in the tumbling mill, one cannot say the study is typical or repetitive at another point of time. For this to be so, multiple simulations in a longitudinal study need to be undertaken. It is therefore reasonable to say that validation of models is a fundamental issue.

Combining DEM models and real time data from within a mill allows for triangulation of results. Triangulation is a powerful technique that facilitates validation of data through cross verification from two or more sources. This process might considerably improve mill optimisation in the field.

ACKNOWLEDGEMENTS

Thanks to West Gold Resources, Sydney Centre in Geomechanics and Mining, and the West Australian School of Mines

Mining system innovations

Mine floor material recovery must become part of life-of-mine plan

K Biegaj¹ and S C Dominy²

1. MAusIMM, Director/Owner, Ausvac Mining Pty Ltd, Brentwood WA 6153.
Email: ausvacmining@iinet.net.au
2. FAusIMM(CP), Camborne School of Mines University of Exeter, Penryn Cornwall TR10 9FE, UK. Email: s.dominy@e3geomet.com

ABSTRACT

The use of conventional Load Haul Dump (LHD) equipment and scrapers on uneven floors underground and surface, potentially leaves behind a significant portion of metal. During the approvals and mining process, that portion of gold, metals and precious stones included in Mineral Resource, Ore Reserve estimates and Life-of-mine Plans prior to obtaining governmental approvals and accessing capital funds for their development, continue to be included in various reconciliation factors. Up to 0.5 m of broken ore material is commonly left behind on development mine floors, which could be recovered. When using LHD equipment, due to the 'milling' effect, water and gravity, the grade of broken ore left on active mine floors for long periods increase significantly, especially in coarse-gold/nugget-type orebodies. This paper presents a solution to recover lost ore from mine floors via the application of Supersucker technology. The unit enables cost-effective reclamation of unrecoverable broken ore material left behind on mine floors. It potentially allows additional enhancement of return on invested capital and generation of additional revenue. Including generation of additional funds for rehabilitation of waste generated when accessing the ore left behind on mine floors and disposed of on surface. Apart from South Africa and few other countries, broken ore continues to be left underground never to be recovered, potentially wasting billions of dollars globally. Fundamentally, vacuum recovery of broken ore remaining on mine floors has yet to be legislated for, in Australia and in other countries, to become part of the mining cycle prior to mine closure. Mine floor material recovery should become a part of Life-of-mine Plan.

INTRODUCTION

In drill and blast underground mining methods, especially in narrow vein operations, economic quantities of broken ore can be left behind following mucking of drive and stope floors (Tuck, 2010). The mucking process itself can enhance the 'milling' of ore yielding liberated and fine ore minerals in the broken rock.

The ore left behind can have significant economic value and if not collected can be lost forever. The liberation of ore-bearing minerals (eg native gold and metal-bearing sulfides) during blasting is common. Where stope footwalls are low angle (<50°), fine metal-rich material is commonly left behind after scraping. This is likely to be particularly prevalent in coarse-gold operations but can also have an effect in sulfide-rich systems (eg gold in sulfides or other metal sulfides).

Metal -rich material can be lost in stope walls and floors, development floors, trucks and along truck routes, and on surface and underground stockpile floors (Figure 1). In extreme cases, this loss can for example, be as much as 20 per cent of the gold inventory. Metal loss in stopes and development is well-recognised and has led to the practice of sweeping and vamping using vacuum systems in some operations (Tuck, 2010).



FIG 1 – Development drive and low-angle stope floor after mucking by scraper. Remaining fines material in both the drive and stope floor contains liberated gold.

MOBILE SUPERSUCKER

Modern technology led to the development of a mobile vacuum unit or Supersucker in 2003, essentially a giant mobile vacuum cleaner. This system permits safe and efficient cleaning of development floors. Figure 2 shows the vacuumed floor on a nickel mine located near Kambalda in Western Australia with approximately 0.35 m of broken ore left on the ore drive floor where mining was performed with Flat-back Cut and Fill mining method. More commonly, the broken ore left behind on mine floors of development drives is around 0.5 m.

It has taken Ausvac Mining PL eight trials to achieve 40 t/12-hr shift with two operators.

With 85 per cent machine and working places availability and two shift continuous roster operation, up to 2074 t per month can be achieved. It is a two-person operation as the machine must vacuum continuously, and the Supersucker bin needs to empty into a Bobcat or small LHD and the recovered ore delivered to the nearest stockpile by the second operator without stopping vacuuming (Figure 3).



FIG 2 – Approximately ~0.35 m thick broken ore left behind on ore drive floor on the nickel mine located near Kambalda in WA – before and after vacuuming. Suction hose diameter 200 mm.



FIG 3 – Discharge from the bin into the Bobcat/Cat Skid Steer loader – Nickel Mine near Kambalda, WA.

The Supersucker unit best works with a skid steer/bobcat or small LHD machines to empty its 1 t capacity bin to the nearest stockpile for loading and trucking to surface or to a shaft loading bay.

In addition to a high vacuuming capability of 40 t per shift, mobility of the Supersucker is its most essential feature. The diesel-powered machine is mounted on a self-propelled steel tracked carrier that can be driven on a gradient as steep as 1 in 5.

For much longer distances and more efficient mobility, the vacuuming machine has been equipped with heavy-duty detachable wheels for towing, normally carried by an IT vehicle or a size LHD (Figure 4).



FIG 4 – Mobile vacuum unit towed out form underground nickel mine in WA.

DESIGN OF THE SUPERSUCKER

The Supersucker design is based on the late 1960s style of unit used for mining opals in Coober Pedy, South Australia.

Basic parameters of the diesel-powered vacuum unit equipped with all required safety features are: Width – 2.2 m; Height – 2.95 m/2.65 m in towing mode; Length – 5.3 m plus 3.5 m easily detachable vacuuming jib; Weight – 8.3 t; Suction Hose diameter – 200 mm, which can be easily upgraded to 250 mm to significantly improve vacuuming capabilities.

Vacuuming capabilities are up to 50 m of vertical, horizontal, or mixed vertical-horizontal vacuum lift.

The 3.5 m long vacuuming jib is easily detachable for lowering the unit down in a shaft where there is no decline access to working areas.

To reduce pollution to environment, the Supersucker can be equipped/converted to be electrically powered for vacuuming operations utilising the already installed mine electrical infrastructure and for efficient operation in mines located in high-altitude.

For vacuuming operations in open stopes (eg vacuuming of high-grade broken ore from ore pillars left for geotechnical stability), tele-remote capabilities can be installed on the unit.

Other applications of the Supersucker include:

- Underground and surface safe exploration winzings operations, the machine designed and constructed in 2000 for this purpose (Biegaj, 2000; Biegaj and Dominy, 2003).
- Alternative hoisting system for high-grade low-tonnage underground and surface deposits to reduce waste rock pollution to the environment with excavations of decline access from surface (Biegaj, 2000).
- Underground and surface sumps fast clean-down – often containing high-grade ore.
- Settling ponds and leaching mill tanks fast clean down – often containing high-grade ore.
- Civil construction work – safe and fast excavations of swimming pools located in difficult to access areas by conventional equipment.

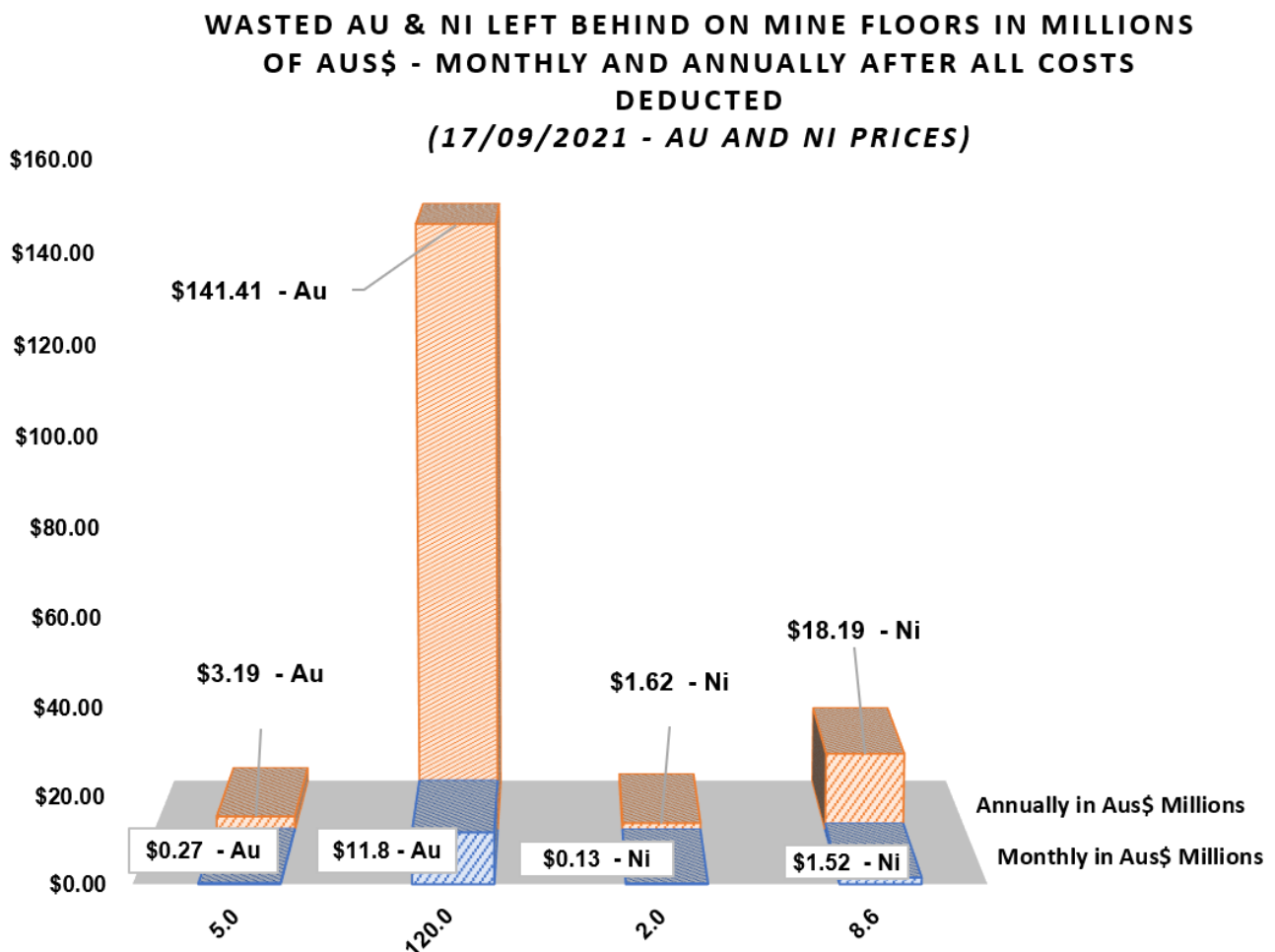
ECONOMIC VALUE OF BROKEN ORE RECOVERY

The non-recovery of broken ore stocks within a mine, results in a financial loss due to a reduction in mining recovery. Table 1 and Figure 5 show a summary of the potential financial gain by recovering broken remnant material from gold and nickel examples.

TABLE 1

Summary of potential financial metrics of broken ore recovery based on gold and nickel examples.

Recovered Gold and Nickel Left Behind on Mine Floors with 1-Shift/2-Shifts 12 Hrs Continuous Vacuuming with One (1) Machine and Two (2) Operators with 85% Working Places and Machine Availability. Productivity: 40 t/shift Thickness of mine floor material used in calculations: 0.4 m After Deduction of All Costs – including Vacuuming Costs	Gold Price/oz in US\$1,760 17/09/2021	Nickel Price/t in US\$19,530 17/09/2021
Supersucker vacuuming costs \$/t for 1/2 shift continuous roster vacuuming respectively	\$171.4/t – \$143.5/t	\$171.4/t – \$143.5/t
Vacuumed tonnes/month respectively with 1-shift/2-shifts operation	1,1216 t – 2,074 t	1,1216 t – 2,074 t
Grade Au g/t & Ni% respectively	5 g/t – 120 g/t	2.0% – 8.6%
Value of recovered normally wasted Au and Ni per month in millions of Aus\$	A\$0.27 – A\$11.78	A\$0.13 – A\$1.52
Value of recovered normally wasted Au & Ni/year in millions of Aus\$; exchange rate 0.73	A\$3.19 – A\$141.41	A\$1.62 – A\$18.19



Value of Au & Ni ore left/wasted on mine floors monthly and yearly - Au & Ni grade in g/t & % respectively

FIG 5 – Monthly and yearly summary of gold and nickel wasted on mine floors.

The above analysis shows that gold and nickel recovered from broken remnant stocks could be in the range of AU\$3.2–141M and AU\$1.6–18.2M respectively per annum. The actual yield will be highly dependent upon the individual mine case. In a case study previously undertaken by one of the authors, some 8 km of underground drives were estimated to contain c. 15 000 ounces of non-recovered gold. Based on the gold price in Table 1, this represents almost A\$25M in revenue assuming a 95 per cent metallurgical recovery. This estimate does not include broken remnant material lying on low-angle stope floors which could exceed the figure for the drives (Dominy, unpublished data).

EVALUATION OF BROKEN FLOOR STOCKS

As with any mining program, the recovery of broken floor stocks needs to be properly evaluated and costed prior to implementation. At the Feasibility stage it may be possible to make an estimate of the likely broken floor stocks that could occur during mining. It is most likely however that evaluation will need to be undertaken during mining as each drive ceases to be strategically important. Safety matters are of course paramount during any evaluation underground.

Evaluation should include the digging of pits and trenches in drive floors to determine floor stock depth and to take samples for grade determination. Application of the Theory of Sampling should be at the fore of any sampling undertaken to ensure representative and fit for purpose samples (Dominy, 2016). Knowledge of the ore type should be used to determine representative sample mass. Such sampling programs may also be important during reconciliation studies, where unaccounted lost gold needs to be identified (Dominy, 2014).

A first pass determination of the presence of gold can be undertaken by the collection of multiple small samples (eg 5–10 kg) for manual panning and identification of gold colour. Note that where gold is dominantly locked in sulfides this approach may not be optimal. For a focused sampling program, as a guide any given drive should be initially evaluated by taking 400–500 kg of material made up from eight to ten individual samples. These should be assayed via an appropriate protocol and preferably as large samples processed through a metallurgical laboratory. Evaluation must be accompanied by an appropriate QAQC program.

With surveying of the drive floor surface and base of the pits/trenches, the floor stock volume can be modelled in 3D. Grades can be interpolated into the given volume. The survey of pit/trench volumes will assist in the determination of broken rock bulk density.

The evaluation of stocks left on the floors of stopes is more problematic from a safety perspective. In a previous example, one of the authors set-up a water jet at the top of the stope to wash a down dip swath of material to the base of the stope for collection and assay. This does not necessarily produce a high quality sample due to the potential for gold loss into the uneven stope floor, but at least provides a sample for study. In the case in question, 50–100 kg washed samples yielded grades upwards of 30 g/t Au.

The results of such a program may be reported in accordance with The 2012 JORC Code (JORC, 2012). In some instances this may result in the definition of Mineral Resources and Ore Reserves. All aspects of The Code must be adhered too, including rigorous consideration of reasonable prospects for eventual economic extraction (refer Section 41 of The Code). All matters must be declared in the JORC Table 1 checklist of assessment and reporting criteria.

CONCLUSIONS

This paper presents a solution to recover lost ore from mine floors via the application of Supersucker technology. The unit enables cost-effective reclamation of unrecoverable broken ore material left behind on mine floors. It potentially allows additional enhancement of return on invested capital and generation of additional revenue. Including generation of additional funds for rehabilitation of waste generated when accessing the ore left behind on mine floors and disposed of on surface. Apart from South Africa and few other countries, broken ore continues to be left underground never to be recovered, potentially wasting billions of dollars globally. Fundamentally, vacuum recovery of broken ore remaining on mine floors has yet to be legislated for, in Australia and in other countries, to become part of the mining cycle prior to mine closure. Mine floor material recovery should be evaluated and potentially become a part of Life-of-mine Plan.

ACKNOWLEDGEMENTS

Marc Blythe and Steve Tombs of then Placer Dome Mt Pleasant Gold Mine, Kalgoorlie WA, for sponsoring the first trial of the Supersucker at their mine in 2003. Paul Maher (Maher Mining Contractors Pty Ltd) for his contribution into the design and construction of the first underground mobile Supersucker. Rob Miller (Miller Fabrications Pty Ltd) is thanked for his inventive input during the construction of the machine and subsequent modifications after the first trial in May 2003 and allowing use of his workshop in Kalgoorlie for these activities. Les Sternal is thanked for numerous discussions, practical solutions to electrical challenges and innovative ideas of making the Supersucker truly mobile machine.

REFERENCES

- Biegaj, K, 2000. Alternative access, mining and hoisting for underground deposits, in *Proceedings of the MassMin 2000 Conference*, pp 911–914 (The Australasian Institute of Mining and Metallurgy: Melbourne).
- Biegaj, K and Dominy, S C, 2003. Lowering Orebody Risk in Complex Gold Veins – Application of Underground Mobile Supersucker Winzine, in *Proceedings of the 2003 5th International Mining Geology Conference*, pp 273–278 (The Australasian Institute of Mining and Metallurgy: Melbourne).
- Dominy, S C, 2014. Predicting the unpredictable – evaluating high-nugget effect gold deposits, in *Mineral Resource and Ore Reserve Estimation*, pp 659–678 (The Australasian Institute of Mining and Metallurgy: Melbourne).
- Dominy, S C, 2016. Importance of good sampling practice throughout the gold mine value chain. *Mining Tech.*, 125, pp 129–141.

- JORC, 2012. Australasian Code for Reporting of Exploration Results, Mineral Resources and Ore Reserves, The JORC Code. Joint Ore Reserves Committee of the Australasian Institute of Mining and Metallurgy, Australian Institute of Geoscientists and Minerals Council of Australia, December 2012, 44 p.
- Tuck, M, 2010. Stope cleaning: historical methods and future developments, in *Proceedings Gravity Gold Conference 2010*, pp 25–26 (The Australasian Institute of Mining and Metallurgy: Melbourne).

Research progress towards the unlocking of *in situ* recovery

L L Kuhar¹

1. Research Team Leader, CSIRO Mineral Resources, Perth, Western Australia, 6152.
Email: laura.kuhar@csiro.au

INTRODUCTION

In situ recovery (ISR), which uses solution injection underground for metal dissolution, and further processing of the solution at the surface, has received renewed interest in the mining field, largely because of its potential economic, environmental, safety and sustainability benefits. The Commonwealth Industrial and Scientific Research Organisation (CSIRO) has focused on collaborative research with partners in industry, academia and government to unlock new applications of ISR outside of the traditional commodity of focus, namely, uranium mining. Research has focused on areas that are critical to ensure successful implementation of ISR from a technical, social and environmental perspective.

Three important technical components in ISR include: (i) containment and hydrogeological control; it is essential that fluid pumped underground be retained at the site of interest and not contaminate groundwater. (ii) Leaching; the minerals of interest should be leachable, with good *in situ* chemistry, including solution stability, dissolved metal stability and minimal gangue effects. (iii) Access creation is vital to allow for solution contact with the minerals of interest, and techniques to improve access in hard rock environments require development.

Social and environmental research is an additional critical component and underpins the technical requirements in ISR.

The CSIRO and collaborators are involved in various ISR projects, ranging from applied research to fundamental investigations aimed at unlocking the potential for application of ISR to a broader suite of commodity and deposit types. A summary and overview of some of these projects and research outcomes to date by the CSIRO together with collaborators in the three technical areas (containment, leachability and accessibility) as well as work related to social and environmental aspects of ISR are presented below.

TECHNICAL, SOCIAL AND ENVIRONMENTAL CONSIDERATIONS FOR ISR

Containment

It is vital in an ISR operation that fluid be contained within the wellfield and not contaminate groundwater systems. The CSIRO and collaborators are exploring novel strategies, including biocement, organic and inorganic options, for use as subsurface barriers for fluid containment and the mitigation of leach solution (lixiviant) loss beyond the well field. Work has also been conducted on sub-surface stirring, modelling of fluid flow and electrokinetics for flow control.

Leachability

A lixiviant for use in ISR should be able to leach the mineral of interest, be compatible with the pH of the surrounding groundwater and retain a suitable pH and solution potential (Eh) when moving from injection to recovery well to ensure that extracted metal complexes remain in solution. The CSIRO and collaborators have conducted (i) lixiviant screening tests using reagents that are not used conventionally in mining, such as ascorbic acid (vitamin C) and acetic acid (vinegar), methanesulfonic acid, which is a biodegradable alternative to sulfuric acid, and thiosulfate for gold; (ii) lixiviant stability/compatibility tests and (iii) studies to understand the interactions between lixiviant and rock to identify mineral transformations, quantify leaching rates, and understand what reaction products form and what their properties are. Furthermore, the potential for using electrokinetics, pulsed pumping and ultrasound is being explored as an option to enhance mass transfer.

Accessibility

To achieve successful ISR, fluid must be able to access the value metal. Studies involving the 3D imaging of samples pre- and post-leaching have allowed for an understanding of where fluid moves during leaching, and the abovementioned electrokinetics technology has been explored as an option to allow for fluid transfer in impermeable rock. As alternative tools to hydraulic fracturing and blasting, techniques such as microwaves, cryogenics and high voltages are being explored as access-creation approaches.

Social and environmental considerations

Earning a social licence to operate is critical in ISR. A social licence framework considers procedural fairness (whether community members feel that their voice is heard and respected in the decision-making process), distributional fairness (whether community members believe that impacts and benefits are shared equitably) and confidence in governance (whether community members believe that the regulatory and legislative arrangements will ensure responsible mining). Focus groups can be conducted with stakeholders to understand their thoughts related to ISR processing, and the inter-relationships between the factors in the social licence framework contribute to trust and acceptance.

Environmental considerations are critical for environmental protection and for contributing towards earning a social licence. An environmental scorecard approach is a useful tool that allows a focus on management and communication for the life of an ISR operation. The scorecard aims to mitigate risk during mining activity and can include operational and social aspects (if chosen targets or metrics can be monitored and evaluated). Stakeholders must be identified, indicators and indices need to be defined, scores are calculated and then results are communicated. The aim is to make no change from the baseline, and, if there is a change, clarity is required as to what the subsequent action is.

CONCLUSIONS

ISR provides an opportunity to recover previously uneconomic, lower-grade resources or resources that are constrained by conventional extraction. Provided that technical and non-technical challenges can be overcome, ISR provides a compelling economic argument and a relatively low footprint. A multi-disciplinary focus and expertise are required for ISR implementation, and required capabilities include geological and mineralogical characterisation; mining engineering; hydrogeological and reactive transport modelling; hydrometallurgy, chemistry and processing; economic modelling/evaluations; environmental science and social science.

ACKNOWLEDGEMENTS

Numerous internal CSIRO Mineral Resources, Land and Water and Energy colleagues and external collaborators (including industry, government, universities, students and other research collaborators) who have contributed to the various ISR projects are gratefully acknowledged. Funding is gratefully acknowledged, including, but not limited to that from the CSIRO; the Minerals Research Institute of Western Australia (MRIWA) Projects 0488, 0492, 0519, 0529 and 0545; the Kapunda In-Situ Copper and Gold Field Recovery Trial Cooperative Research Centres Projects (CRC-P) Grant and various industry funded projects.

Raise caving – a new cave mining method for mining at great depths

T Ladinig¹, H Wagner², J Bergström³, M Koivisto⁴ and M Wimmer⁵

1. Research Assistant, Montanuniversitaet Leoben, Leoben, Austria, 8700.
Email: tobias.ladinig@unileoben.ac.at
2. Professor, Montanuniversitaet Leoben, Leoben, Austria, 8700.
Email: horst.wagner@unileoben.ac.at
3. Senior Project Manager, LKAB, Kiruna, Sweden, 98186, Email: johan.bergstrom@lkab.com
4. Mine Planning Engineer, LKAB, Kiruna, Sweden, 98186. Email: mikko.koivisto@lkab.com
5. Manager Mining Technology, LKAB, Kiruna, Sweden, 98186.
Email: matthias.wimmer@lkab.com

ABSTRACT

Block and sublevel caving progress to greater depths associated with increasing rock mechanical and operational issues. In order to address these issues a new cave mining method called 'raise caving' was developed. A pre-study was conducted at LKABs Kiruna mine and the suitability of the new cave mining method was investigated by means of theoretical considerations, numerical simulations, field observations and mining experience. The design concept is based on de-stressing the rock mass so that vital mining infrastructure such as stope development, rock passes or footwall development can be protected from high stresses. Protective pillars are used to control stresses and seismicity. These pillars are removed in the course of subsequent stoping activities. The paper discusses the general concept and outlines considerations related to rock mechanics. Well-established design criteria and design methodologies were used to evaluate the potential of the method. A calibration of the applied design criteria based on current mining experience is the background for discussing the suitability in the prevailing rock mass condition and comparing the method with the currently applied sublevel caving in Kiruna mine. It was found that the proposed raise caving mining method is applicable from a rock mechanics perspective up to depths of 2000 m in Kiruna. Results indicate that the method would principally be applicable for depths even exceeding 2000 m. In comparison to currently applied sublevel caving raise caving offers significant improvements in the overall rock mechanical situation. These improvements comprise stability of infrastructure, encountered seismicity, productivity, potential for automation and safety. Besides the control of rock pressure, raise caving allows integrating the main steps of cave development and offers therefore a considerable alternative to block caving. Based on the promising results of the pre-study, an extensive, joint research program was launched with the objective to develop and test raise caving.

INTRODUCTION

Block, panel and sublevel caving have been progressing to greater depths and more competent rock mass conditions. Mining experience has shown that these conditions impose major challenges in cave mining. Different kind of rock mechanical issues and difficulties are reported and comprise:

- Damage of the production level, undercut level or other critical infrastructure as a result of prevailing high stress conditions (eg Gomes, Rojas and Ulloa, 2016; Shea, Sinclair and Welsh, 2018; Campbell *et al*, 2020; Holder *et al*, 2020).
- Occurrence of mining-induced seismicity and rock bursts (eg Araneda and Sougarret, 2008; Dahnér, Malmgren and Bošković, 2012; Malovichko, Cuello and Rojas, 2018; Nugraha, Bastiawarman and Edgar, 2020).
- Prohibited caveability, slow rate of cave progression and coarse fragmentation as a result of competent rock mass conditions (eg van As and Jeffrey, 2000; Ngidi and Pretorius, 2010).
- Deviation of the planned direction of cave progression (eg Parsons, Hamilton and Ludwicki, 2018).

Out of these rock mechanical issues further operational problems emerge. First of all, damage to infrastructure, rock bursts and required rehabilitation work affect safety. Furthermore, the profitability of the operation is decreased. Reasons therefore are amongst others an increased demand of

support and reinforcement, a slower production rate caused by ongoing damage repair work, a slow cave propagation rates, a need of additional pre-conditioning measures and a longer ramp-up time resulting from additional support and pre-conditioning measures and encountered damage during cave establishment. Despite the circumstance of increasing rock mechanical problems at greater depths and the associated safety and operational consequences, the mining methods, mine layouts and mining sequences have generally remained the same as in shallower depths. Far-reaching modifications or adaptations of the mine layout and mining sequence addressing the sources of the stress related problems at greater depths have principally not been made. Instead, there seems to be a trend of fighting the consequences of rock pressure problems with support passively (eg Jacobsson *et al*, 2013; Campbell *et al*, 2020). Moreover, intensive, large-scale pre-conditioning is often applied to tackle rock mechanical issues (eg Catalan, Onederra and Chitombo, 2017a, 2017b; Nugraha, Bastiawarman and Edgar, 2020; Orrego, Lowther and Newcombe, 2020).

The root of rock mechanical problems in deep sublevel, block and panel caving is often related to abutment stresses and the necessity of placing infrastructure and conducting mining activities in these highly stressed abutment areas. In block caving, undercutting generates large stress magnitudes at the boundaries of the undercut, where active undercut level infrastructure is situated, causing stress and rock burst damage. Abutment stresses increase significantly at greater depths due to higher primary stresses. Moreover, more competent rock mass conditions cause larger abutment stresses, because these conditions require larger undercut areas before cave initiation. Abutment stresses can cause further damage and rock bursting at production level infrastructure and production level pillars in a post-undercutting or advance-undercutting strategy. The latter undercutting strategies seem to be preferred over the pre-undercutting strategy, which could protect the production level from abutment stresses (Flores, 2014). The fact that the production level in block caving is principally a pillar system, which has typically an 'extraction ratio' of 40 per cent to 60 per cent and rather small pillars, aggravates the stress related problems often further. The abutment stress problematic in sublevel caving is similar. Below mined out sublevels, high abutment stresses are prevailing and mining-induced seismicity and rock bursting could be present. As mining progresses in a top-down sequence, infrastructure must be developed in these high stress areas. Furthermore, critical, long-term infrastructure, such as ore passes or access drifts, are commonly positioned near the orebody to enable distances and efficient material handling. Accordingly, this infrastructure is exposed to high abutment stresses and potential mining-induced seismicity as well.

Besides rock mechanics drawbacks, block and sublevel caving are associated with (very) long development times and high (extreme) development costs; see for example Araneda (2020) and Casten *et al* (2020). Major contributors therefore are the required, large amount of upfront infrastructure development and the necessity to conduct main steps of caving (infrastructure development, pre-conditioning, undercutting, production) in a certain part of the deposit successively. A potential option ('Single Pass Cave Establishment'), which should enable a larger cave establishment time, was recently presented by Paredes *et al* (2020). However, the Single Pass Cave Establishment does not introduce far-reaching modifications of the mine layout addressing rock pressure problems. A similar concept was proposed by Tawadrous and Preece (2015).

From a rock mechanics perspective, a distinct disadvantage of the long development times is that most of the infrastructure development is either made or its position fixed before actual production commences. Consequently, the mine layout and mining sequence must be fixed at an early stage of the project, where knowledge regarding rock mechanical conditions and rock mass behaviour is often very limited. Therefore, changes and adaptations of the mine layout and mining sequence are either not possible or associated with high cost, after development started. This inflexibility is particularly disadvantageous at great depths, because the knowledge of rock mass conditions is often more limited than at shallow depths and the high stresses impose larger constraints on the mine layout and mining sequence.

In summary, block and sublevel caving have been progressing to greater depths with mixed success. Rock mechanics issues have been causing operational and safety issues, which intensity increases with depths. Therefore, the applicability of currently applied block and sublevel caving methods at great depths is limited. Mining experience has shown that block and sublevel caving are hardly applicable at depths exceeding 1000 m to 1200 m. Major drawbacks are inherent abutment stress issues and inflexibility.

RAISE CAVING MINING METHOD

Raise caving can be implemented in different variations and it is therefore adaptable to the site-specific conditions and requirements. For example, raise caving can be applied for cave mining at great depths due to the implementation of an active stress control strategy. Another example is the application of raise caving to integrate the main steps of cave mining and therefore to accelerate the development time. Both of these variations are presented and discussed in this paper. All variations of raise caving have in common that raises are central elements utilised for the development of different kind of excavations and that host rock and/or country rock is allowed to cave. The excavations created from raises depend on the actual variation of raise caving and they comprise stopes, de-stressing slots, drawbells and the undercut. All these excavations have in common that they are developed by raise mining. Besides the development of excavations, raises can be further utilised for monitoring and controlling purposes. The rock mass formations, which are allowed to cave and the time of cave initiation and progression can be controlled by variations of the raise caving operations. Two variations are presented in this paper.

Principle of raise mining

Raises are utilised for the development of different kind of excavations and developed by means of raise boring. After raise development a hoist system is installed on top of a raise and a machine and working platform is lowered into the raise. The raise is extended by means of drilling and blasting from bottom to top. Thus, boreholes are drilled parallel to the roof of the existing excavation. The shape of the excavation below the raise is generated by the blasthole pattern and blasthole length. Then blastholes are loaded with explosives and the roof is blasted. There must be enough free volume below the roof available for the swell of the blast. During blasting the platform is lifted to the top, so that damage is avoided. Figure 1 gives an overview. Dependent on rock mass properties raises may be supported to protect remotely operated machines in raises and to allow local maintenance or repair work. However, the aim of the system is to conduct all routine work in raises remote controlled or automated. The simple, circular geometry of the raise and the possibility to position machinery through a hoist system offer considerable advantages to remote control (and automated) drilling and blasting work; compare Figure 2. There is even the possibility to parallelise drilling and blasting work. The hoist system could comprise several platforms, where the desired number of drill rigs and blasthole loading units could be installed. Summing up, the considered principle of raise mining is a modern, large-scale approach. It differs largely from raise mining conducted in the past, such as Alimak mining or Horadim mining (eg Makinen and Paganus, 1987; Ran and Mfula, 2012). A similar approach of raise mining termed ROES was shown by Gipps *et al* (2008) and Gipps and Cunningham (2011). However, the ROES approach was not implemented.

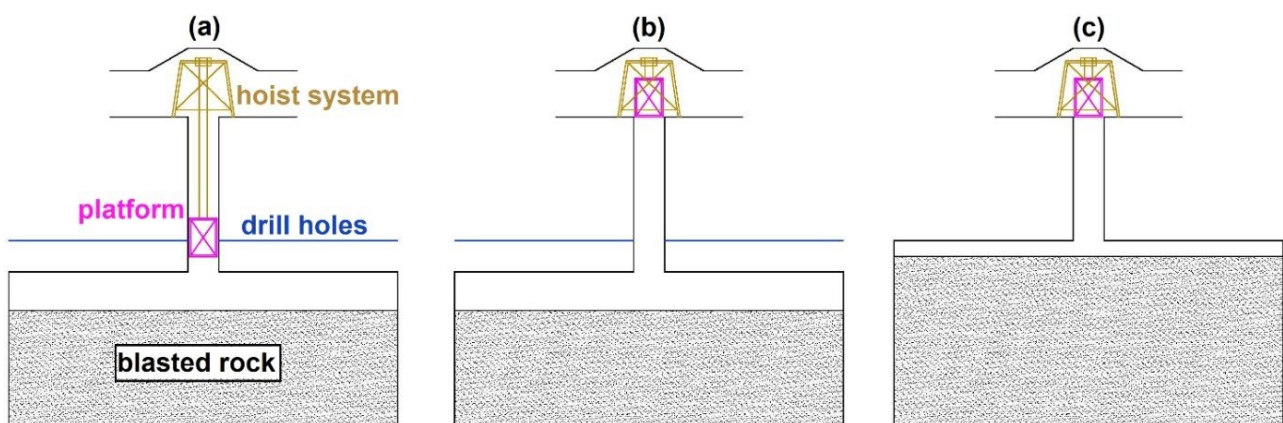


FIG 1 – Schematic overview of drilling and blasting work in a raise: (a) drilling and loading of boreholes, (b) platform lifted to top for blasting, (c) freshly blasted roof. Details of machineries are not shown. The schematic drawing shows a horizontal roof. In practice the actual roof will be an open cone the angle of which will be determined by blasting and roof stability considerations.

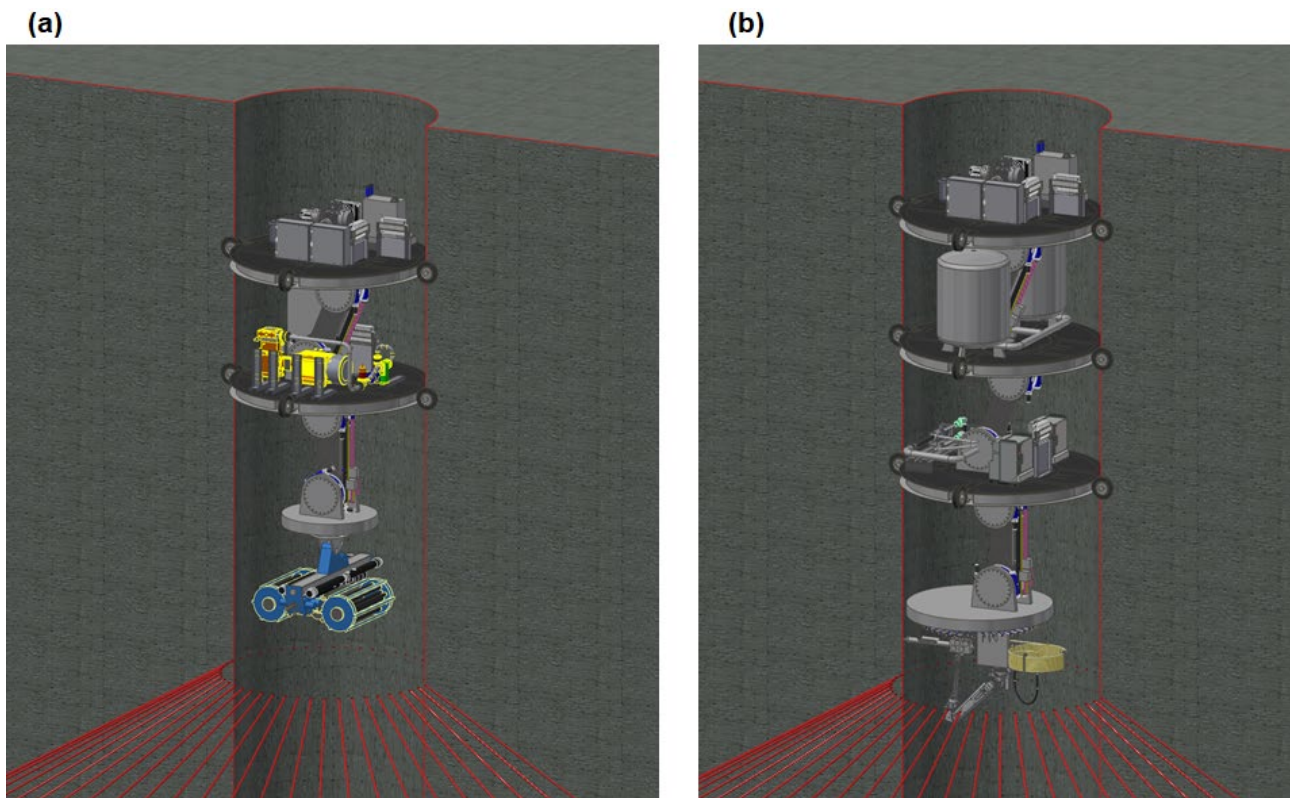


FIG 2 – Concept of an automated machinery operating on a platform inside the raise; (a) drilling; (b) charging.

Principle of active stress management

An active stress management addresses the sources of rock pressure problems. Accordingly, it is a foresighted approach and considered being superior over the passive support approach, which tackles the consequences of rock pressure problems and which is usually applied in cave mining. The key of an active stress management is an appropriate mine layout and mining sequence. Moreover, the layout and sequence must be adapted to local ground and stress conditions. A high degree of flexibility for changes in the mine layout and mining sequence is therefore advantageous.

A proven and successful strategy is to de-stress the rock mass, place infrastructure in de-stressed ground, extract ore in de-stressed ground and control the release of seismic energy (Wagner and Salamon, 1973). This concept has been widely applied in numerous deep mines for several decades, especially deep South African gold mines. In case of deep South African mines extraction of the narrow gold reefs results in the formation of extensive narrow tabular stoping excavations. In the mined-out areas the rock mass is de-stressed and as far as possible and practical the mining infrastructure is developed in the stress shadows of the stopes. Stabilising pillars, which are left between stopes, control the release of seismic energy. So far, reefs up to a depth of nearly 4000 m have been mined successfully by this methodology. In some gold mines, reefs are massive and, after the rock mass has been de-stressed by mining a narrow stope (slot) or a room and pillar system with crush/yield pillar, the remaining massive ore is extracted depending on thickness of mineral body by either sublevel stoping or room and pillar methods in de-stressed ground (Watson *et al*, 2014; Andrews, Butcher and Ekkerd, 2019).

VARIANT 1 – RAISE CAVING AT GREAT DEPTHS

In a deep mining situation, a proper rock mechanics design incorporating the implementation of an active stress management approach is considered being a key issue for a successful operation. Such an active stress control approach can be implemented with raise caving, which is therefore divided into two phases, namely a de-stressing phase and a production phase. De-stressing of the orebody is conducted in the de-stressing phase. Stress shadows are provided on required locations and minimum amount of infrastructure is used for de-stressing. Following de-stressing, stoping commences in the production phase. Corresponding infrastructure is developed in de-stressed

ground and utilised for the extraction of stopes in de-stressed ground. Ongoing stoping activities increase the extent of stress shadows further and therefore prepare other parts of the deposit for extraction. The extraction of the deposit is mainly conducted by means of drilling and blasting. The hanging wall is finally allowed to cave in the progress of mining to fill up mined out stopes.

The application of raise caving at great depths is shown in the following subsections on basis of a conceptual mine layout and mining sequence. The associated infrastructure is outlined as well. Other, central infrastructure, such as ramps, ventilation raises, hoist shafts, main haulage drifts etc are not shown. Some figures related to the geometry and size of excavations are given as well. These geometries and sizes were derived after first analyses and considerations in a study investigating the application potential of raise caving in Kiruna mine (Ladinig *et al*, 2019). Shown dimensions must therefore be considered as being preliminary and related to Kiruna mine, where a massive, inclined orebody is extracted.

De-stressing phase

Figure 3 outlines de-stressing in an initial phase schematically. First slot raises (SR) were developed between raise levels (RL). Slot raises are estimated to have a diameter of about 4 m and a length of about 100 m to 250 m. Slots (SL) and start slots (STSL) are developed from slot raises at the ore-hanging wall contact. Slots and start slots are always filled with blasted material to improve slot wall stability. After blasting, only the swell is mucked from slots and start slots through drawpoints, which are situated at the slot development level (SDL). Large, protective pillars (PI) are left between slots. These pillars are formed behind the advancing slot roof. Slots and start slots have a tabular shape and provide stress shadows for subsequent production phase. The purpose of pillars is controlling the stress magnitudes and mining-induced seismicity during de-stressing.

The position, size and orientation of slots and start slots is adapted to local conditions and required position and size of stress shadows. Slots are estimated to have a cross-section of about 50 m × 10 m and start slots of about 100 m × 10 m. Pillars have cross-section of about 50 m × 10 m. The difference between slots and start slots is that there are no pillars left between neighbouring start slots. Pillars act as stress raisers, which could damage the production level(s) (PL), which are going to be developed behind start slots. Furthermore, it can be seen that start slots start below future production level(s) at a slot development level (SDL) and they extend some distance above the future production level(s). Thereby, start slots provide a stress shadow for the production level(s). The vertical extension depends on local conditions and is estimated to be about 100 m.

Overall, Figure 3 demonstrates that de-stressing can be conducted with a minimum amount of infrastructure. Furthermore, it highlights that production infrastructure, such as production raises or production levels, have not been developed yet. Latter infrastructure can be developed delayed in the provided stress shadows.

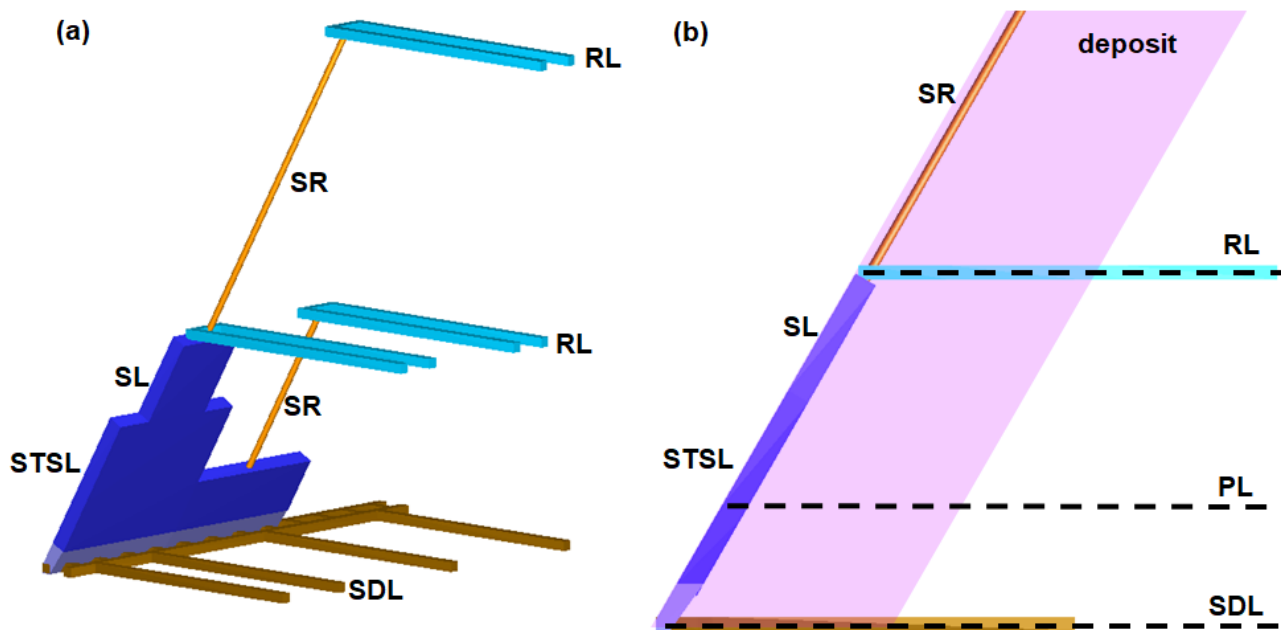


FIG 3 – Overview (a) and vertical cut perpendicular to strike (b) of de-stressing in an initial phase.

Figure 4 shows an advanced stage of de-stressing. Slot heights have been increased and additional slots and start slots are under development. Moreover, the development of production infrastructure, namely production raises (PR) and a production level (PL), has started in de-stressed ground. The production level is situated behind the start slots and is sketched as a system of small drawbells and drawpoints similar to a production level layout in block caving. However, much larger drawbells, which are shown in Figures 6 and 7, offer significant advantages regarding rock mechanical and operational aspects and are therefore considered superior over the array of small drawbells shown in Figure 4. The first production raise extends from the production level to the raise level. Additional drawpoints are developed into slots and start slots at the production level and former raise levels. For latter slots and start slots the drawpoints at the slot development level are no longer required. Accordingly, the slot development level can be abandoned in this area.

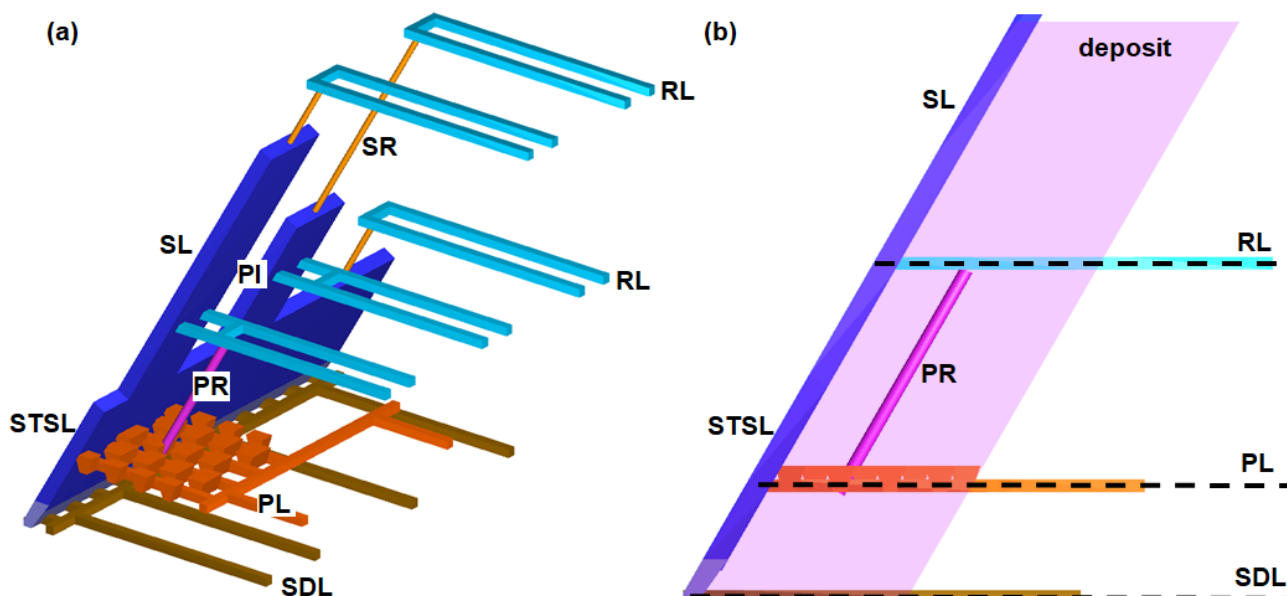


FIG 4 – Overview (a) and vertical cut perpendicular to strike (b) of de-stressing in a more advanced phase. First production infrastructure is already developed.

Production phase

After de-stressing has advanced sufficiently, stoping starts in the de-stressed areas. Production raises are placed in de-stressed ground, which is provided by the de-stressing slots and by (at a

later stage) already mined out neighbouring stopes. Rings are blasted in the production raises and stopes (ST) are successively extracted. After every blast only the swell is drawn at drawpoints at the production level, so that there is enough free volume for the swell of the successive blast. Therefore, stopes are never emptied and always filled with broken rock mass. The broken rock acts on the one hand as temporary support slowing down hanging wall caving and early dilution. Moreover, it prohibits an air gap forming on top of the stope.

Depending on the shape and ore flow characteristics, intermediate draw levels (IDL) may be necessary for ore extraction and for controlling the ore flow inside stopes. These intermediate draw levels could be either new developed or established on former raise levels. Ore passes (OP) are developed to transport the ore from intermediate draw levels to production level and the main haulage infrastructure connecting the production level with hoisting infrastructure. It is important to note that intermediate draw levels as well as ore passes are developed, after stoping passed by. Accordingly, this infrastructure can benefit from stress shadows and is protected from the abutment stresses of advancing stopes. Figure 5 shows progressing stoping schematically. Only one production raise is shown behind every de-stressing slot. If the deposit is too large to extract it with one production raise behind a slot, several production raises are required. Their position can be chosen freely under the constraint of developing them in de-stressed ground. Stope cross-sections of more than 2000 m² seem to be possible.

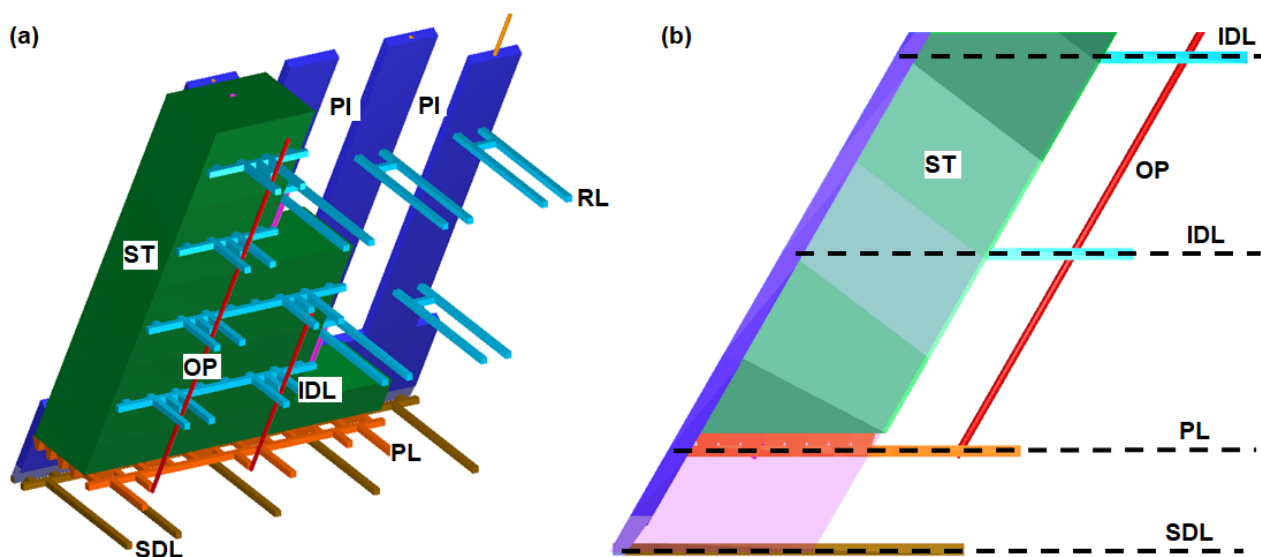


FIG 5 – Overview (a) and vertical cut perpendicular to strike (b) of raise caving during production phase.

As a consequence of stope blasting the protective pillars are weakened resulting in yielding and crushing of the pillar. Accordingly, the pillar is de-stressed and can be extracted. One possibility to extract pillars is to blast them from production raises. Another possibility is to blast only areas behind slots, but as a consequence the width-to-height ratio of pillars is decreased drastically reducing pillar strength. As a consequence, pillars would yield and de-stress, so that they can be extracted from another production raise more easily. Pillar extraction removes the temporary hanging wall support, which the pillars provide. The hanging wall caves and starts to fill up stopes. Ideally, filling of stopes with caved hanging wall commences, after stopes were completely blasted. Ongoing drawing of ore creates a void at the top of the stope, which is then filled with caved hanging wall. A good draw control strategy and practice must be set-up, which ensure that the ore pile in the stope is lowered evenly from the top. Otherwise, hanging wall could cave along the sidewall of the stope causing early dilution. Another effect of pillar yielding is the development of abutments and associated stress increases in nearby pillars. Thus, slot development must lead actual stoping by a defined number of slots.

A possible raise caving layout at great depths showing the production and de-stressing phase is shown in Figure 6. The outlined orebody is tabular, steeply-dipping and thick. De-stressing and production commence from the left to the right side. Slots are aligned along the strike direction of the orebody. De-stressing takes place some distance ahead of stoping activities. Thereby, adverse

consequences on de-stressing activities emerging from stoping and the associated regional stress and energy changes are prohibited. Stope extraction takes place first behind de-stressing slots. Extraction of stopes behind de-stressing slots reduces the pillar width-to-height ratio triggering pillar yielding and crushing. Consequently, pillars are de-stressed and extracted in stopes. Extraction of pillars follows some distance behind extraction of first stopes, because the pillar width-to-height ratio has to be reduced through stope extraction, pillars need some time to yield and crush reliably and production infrastructure has to be developed. In contrast to previous figures, large drawbells, which require drawpoints on two production levels, are established below stopes. These large drawbells improve the efficiency of drawbell and stope development as well as operational aspects, such as ore flow inside stopes and the possible production. Ore passes, additional intermediate draw levels and long-term access and hoisting infrastructure are not shown. Summarising, Figure 6 gives an example of raise caving at great depths. It illustrates that, once de-stressing was done, a high capacity extraction system can be established at great depths.

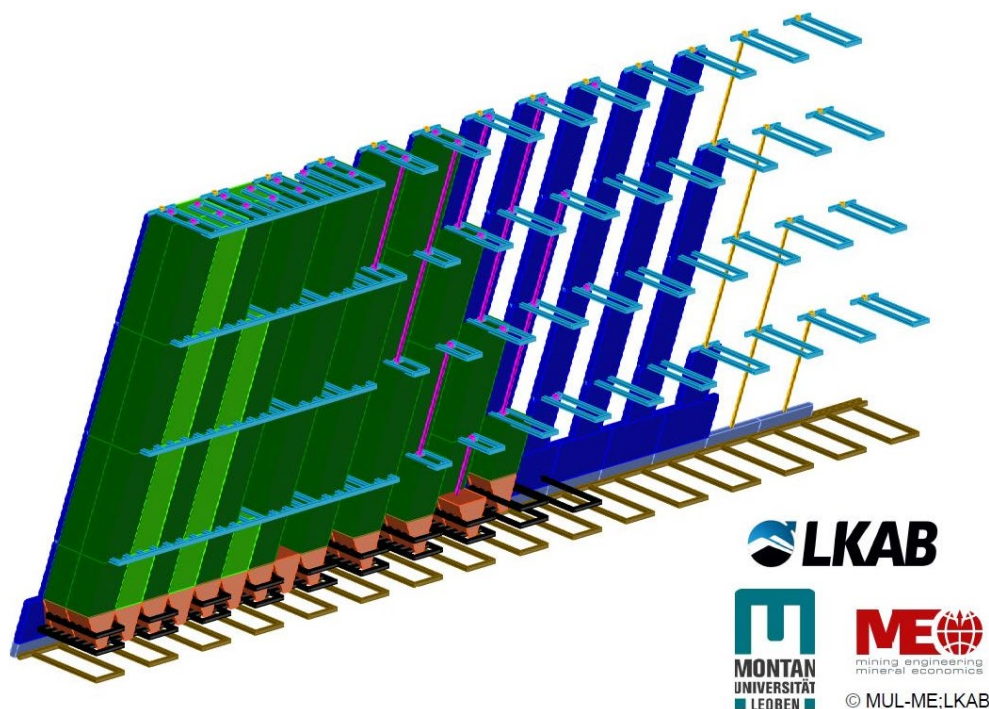


FIG 6 – A possible raise caving layout at great depths in a steeply-dipping, thick tabular deposit.

Advantages of variant 1 (raise caving at great depths)

The application of raise caving at great depths provides significant advantages compared to widely-used cave mining methods. Advantages comprise:

- Application of an active stress control approach: This approach controls the prevailing stress magnitudes and mining-induced seismicity efficiently. Thereby, active infrastructure and mining areas can be protected, as they are positioned in stress shadows and distant from released seismic energy. The active stress control approach is maintained throughout the de-stressing and production phase.
- Application of modern raise mining techniques: Raise mining enables an efficient and quick extraction of slots and stopes. Moreover, raise mining reduces the amount of levels and lateral development for the prevailing slots and stopes, which have a large vertical extension, significantly. Consequently, the productivity and safety increase. Drilling and blasting of stopes in combination with a good draw control enable further a good extraction ratio and avoid early dilution.
- Potential for automation and remote control: The relatively simple, circular cross-section of raises provides considerable potential for remote controlling or automating the work conducted inside the raise. Therefore, the exposure of personnel to highly stressed areas can be reduced.

- Potential for just-in-time infrastructure development: Raise caving enables to develop the majority of infrastructure just before its use. Accordingly, the development time and associated costs can be reduced. Another benefit is that this just-in-time infrastructure development provides considerable flexibility.
- Flexibility on short – to medium-term notice: As the majority of infrastructure is developed just before its utilisation, it is possible to react to actual ground conditions or mining experience on a short – to medium-term notice, which is a considerable benefit in a deep and high stress environment. The adaptations and modifications of the mine layout and mining sequence can be implemented within reasonable time periods and at rather low additional cost. The flexibility reduces further the risk associated with cave mining operations significantly.
- Adaptability to local conditions and requirements: The mine layout and mining sequence of raise caving can be adapted well. Raise position and correspondingly slot and stope position can be chosen according to orebody boundaries and encountered rock mass conditions. The size and geometry of slots and stopes can be adapted as well, for example by changing borehole length and orientations. Rock mechanics, ore flow and production considerations limit adaptability. For example, pillars between slots must have an appropriate geometry to fulfil their considered purpose and production raises must be situated in de-stressed ground.

Overall, the above outlined advantages outline that raise caving provides a considerable alternative for low-cost, mass mining at great depths. Raise caving can facilitate or in some cases even enable the extraction of deep mineral resources.

VARIANT 2 – INTEGRATED RAISE CAVING

Raise caving can also be utilised to integrate the main steps of cave mining, namely infrastructure development, pre-conditioning, undercutting and production and is then referred to as 'integrated raise caving'; compare Figure 7. The aims of this integration are to reduce the development times of large caving operations and to improve operational and rock mechanical aspects in cave mining. For this reason, integrated raise caving is a considerable alternative for block and panel caving. If necessary, integrated raise caving can also be applied in combination with the de-stressing approach of raise caving presented in the last sections. In this instance, the orebody would be de-stressed first and caving would be initiated in generated de-stressed zones, wherefore the below presented integrated raise caving methodology is utilised.

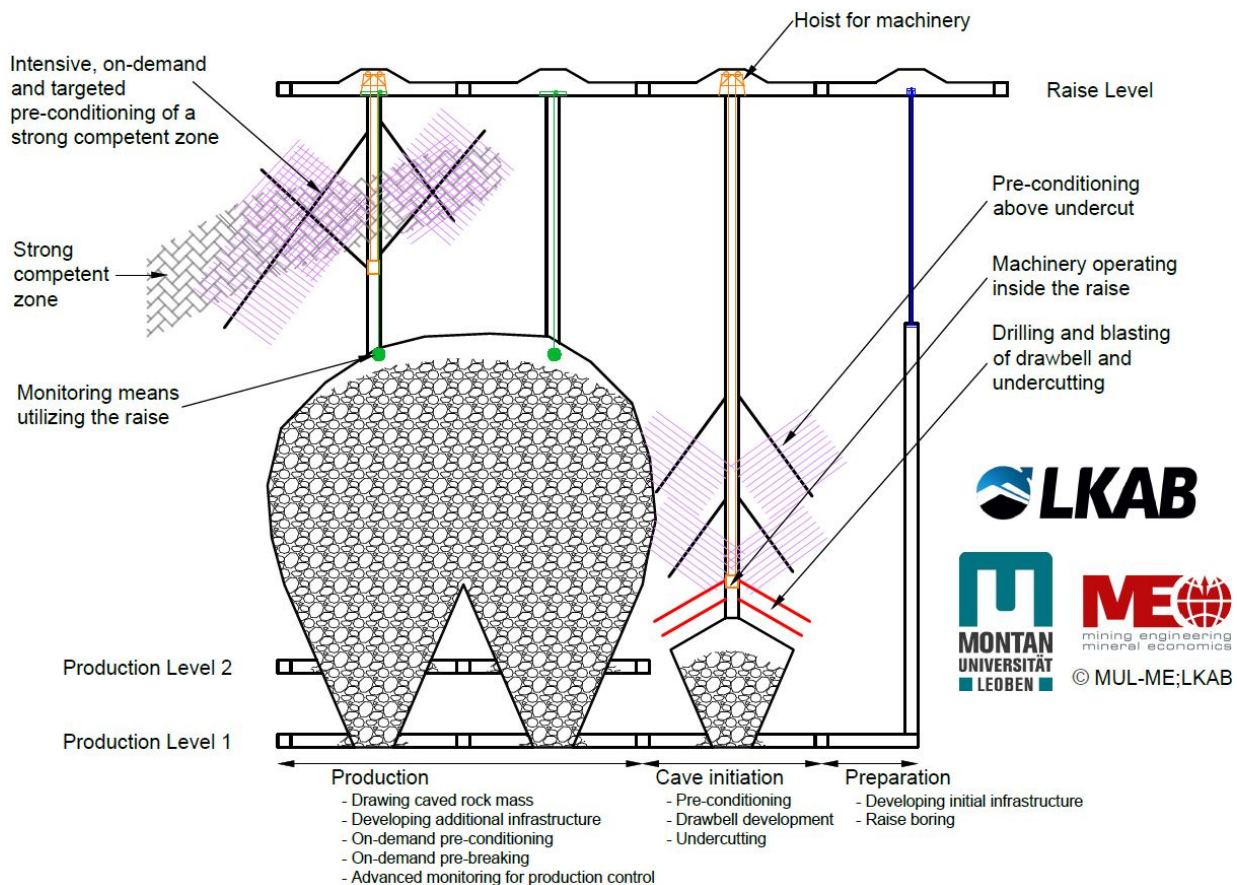


FIG 7 – Integrated raise caving as an alternative for block and panel caving.

Drawbell development and undercutting conducted from raises

The development of drawbells, which is conducted from raises, is a key aspect of integrated raise caving, because the drawbell development coincides with undercutting. In order to be efficient, the drawbell size must be rather larger. Otherwise, the required number of raises becomes excessive, blasting of small drawbells is rather constraint and undercutting takes longer. Such large drawbells require further that drawpoints must be developed on more than one production level due to ore flow considerations. Moreover, positioning drawpoints on more than one production level enables an improved and optimised drawpoint spacing and arrangement, which improves the ore flow inside the cave.

For the initiation of caving a raise a limited amount of infrastructure is developed on production level at the future bottom of the drawbell and on a raise level. Afterwards a raise is bored between these two levels; see Figure 7. Then, the drawbell is developed upwards from the production level by means of drilling and blasting. To improve stability the drawbell is always filled with blasted rock. Thus, only the swell is drawn between successive blasts. Due to the inclined sidewalls of the drawbell, drawpoints are only required at the bottom of the drawbell. This implies that the majority of drawpoints can be developed delayed, as the drawbell development comes to an end or after drawbell development was finished. The drawbell roof area is enlarged continuously during drawbell development and finally caving is initiated. Depending on the rock mass properties, stress situation and other site-specific circumstances, one drawbell could be sufficient for cave initiation or several drawbells have to be developed besides each other for cave initiation. The development of additional drawbells adjacent to an existing cave would increase the size of the caving stope and bring additional parts of the deposit into production.

In comparison with currently applied block and panel caving layouts and sequences, the development of drawbells and parallel undercutting from raises removes also the spatial and temporal dependency of the undercut level and production level. This dependency is a major reason for the experienced abutment stress problems in current block and panel caving operations.

Utilising raises for production preparation and ongoing production

Besides developing the drawbells and conducting undercutting in parallel, the use of raises offers further improvements for production preparation and ongoing production. Raises provide access to the rock mass at the position of the future caving stope. Thus, the knowledge of the geology and rock mass conditions is enhanced. Furthermore, various pre-conditioning techniques can be applied over large areas or specifically in competent areas. Pre-conditioning can thereby also be done during drawbell development and during progression of caving. In case caving stalls or in case caving direction deviates, the raises enable the application of on-demand pre-conditioning or pre-breaking. Additionally, switching from caving to drilling and blasting would be possible to address problems with cave propagation. Finally, raises offer excellent possibilities for monitoring the caving stope, the cave back and the cave progression. Monitoring from raises can be used for example for ensuring the safety of the operation by keeping the air gap below the cave back within acceptable size, providing timely information about cave progression and direction of cave progression and updating the draw strategy in real time based on the observed movement of the caved rock mass. Depending on local conditions and requirements, these raises can be developed over the full height of the caving stope or only at required positions.

Advantages of variant 2 (integrated raise caving)

Compared to currently applied block and panel caving methods, integrated raise caving provides amongst others following advantages.

- Enabling shorter development times: The integration, which is realised through the utilisation of raises, allows to conduct the main steps of cave development in parallel or within short amount of time. Moreover, the application of raise mining for drawbell development provides an efficient and fast possibility for drawbell development and undercutting.
- Reduction of required infrastructure pre-development: Upfront infrastructure development can be reduced due to the integration. This circumstance manifests itself in a faster ramp-up time and a higher flexibility.
- Improving the functionality of the undercut: The undercut is created by blasting successive slices from drawbell roofs in downwards direction. Moreover, a free surface for blasting can be provided, which reduces the constraint. Accordingly, the risk of incomplete undercutting and remnant pillars is reduced. Additionally, blasting of the undercut and drawbell is easier.
- Improving the ore flow: Due to the large drawbells, the arrangement of drawpoints can be improved. Thus, zones of slow or limited ore movement can be reduced. The risk of hang-ups in drawbells is decreased as well.
- Potential for automation and remote control: The relatively simple, circular cross-section of raises provides considerable potential for remote controlling or automating the work conducted inside the raise. Therefore, the exposure of personnel to highly stressed areas can be reduced.
- Flexibility on short – to medium-term notice: As the majority of infrastructure is developed just before its utilisation or delayed, it is possible to react to actual ground conditions or mining experience on a short – to medium-term notice. The adaptations and modifications of the mine layout and mining sequence can be implemented within reasonable time periods and at rather low additional cost. The flexibility reduces further the risk associated with cave mining operations significantly.
- Adaptability to local conditions and requirements: The position of raises and drawbells can be adapted well to prevailing ground condition and mining experience. The availability of raises above the cave allows further to adapt pre-conditioning measures easily. Strong rock mass formations could be mined-through by means of drilling and blasting as well. The provided flexibility is decisive for latter adaptability.
- Improved monitoring and controlling capabilities: Raises above the advancing cave back can be utilised for monitoring and controlling purposes. Moreover, these raises provide access for remote controlled equipment to the cave back. In combination, the latter two aspects provide improved controlling possibilities of the progressing cave. Deviations from the expected

behaviour or mine plan can be detected earlier and appropriate measures can then be implemented faster. Examples are adapting of the draw strategy on-demand through observation of the movement of the caved rock mass or influencing the cave propagation direction through targeted pre-conditioning.

- Reduction of the abutment stress issues during undercutting: The shape of the undercut (drawbell shape) generates lower abutment stresses. Moreover, there is no need to pre-develop infrastructure in these abutment areas.
- Improving the stability of production levels: Drawpoints are positioned on several production levels, which allows to leave larger pillars between neighbouring drawpoints and corresponding production level drifts.
- Possible combination with an active stress control approach: If conditions demand it, it is easily and on rather short-notice possible to combine integrated raise caving with the active stress control approach of raise caving at great depths. Slots developed from slot raises can be positioned on strategic positions to protect infrastructure from high stresses and released seismic energy.

Concluding, integrated raise caving provides several considerable advantages in cave mining, which concern mostly the safety, efficiency, flexibility and controllability. These improvements result in a considerably lower risk of cave mining. Furthermore, the range of application of efficient and low-cost cave mining is enhanced. For example, competent orebodies or narrow constraint orebodies, which are considered to be difficult to cave could be extracted with raise caving.

CASE STUDY AT KIRUNA MINE

Ongoing sublevel caving operation

Sublevel caving has been applied in Kiruna mine for several decades (Wimmer and Nordqvist, 2018). The mine layout has been optimised and upscaled continuously resulting in increased productivity, so that mining costs are kept low. Mining depth is around 900 m to 1100 m. The deposit is extracted over the full deposit strike length of about 4 km completely. Mining takes place in so-called blocks, which extent approximately 400 m in strike direction. Sublevel spacing is 25 m. Figure 8 shows a typical layout of a sublevel in a block. Longitudinal drifts, which are oriented in strike direction, are situated close to the orebody in the footwall. These longitudinal drifts are utilised as access to crosscuts. Ore passes are situated a short distance behind the longitudinal drifts. Ore passes follow the dip of the deposit and are used to transport the ore from sublevels to the main haulage level at 1365 m.

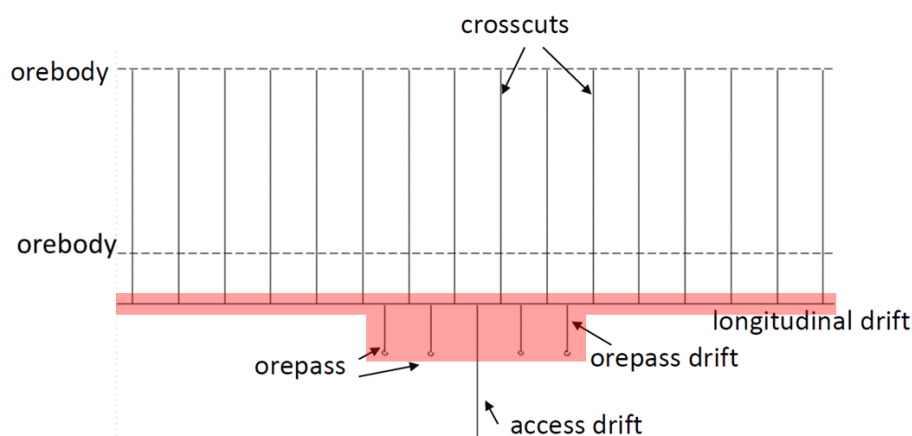


FIG 8 – Schematic horizontal cross-section showing infrastructure of a sublevel (after Quinteiro, 2018). Areas, which have been causing rock mechanics issues, are shaded in red.

Sublevel caving has been developed to a remarkably high level in Kiruna mine and has enabled an efficient, low-cost and high-tonnage production. However, increasing rock pressure problems, particularly rock bursts, have been imposing a safety risk and have been causing operational

difficulties since more than ten years (Sjöberg *et al*, 2011; Dahnér, Malmgren and Bošković, 2012; Edelbro *et al*, 2012; Dahnér and Dineva, 2020). Longitudinal drifts in the footwall and ore passes are most severely affected by rock pressure problems; compare Figure 8. High abutment stresses are considered to be a major contributor. Addressing rock pressure problems is strongly based on a passive support strategy. Heavy support and reinforcement systems are installed in vulnerable areas routinely (Jacobsson *et al*, 2013; Krekula, 2017).

Depth extension in future

Currently, a depth extension of Kiruna mine to 1800 m to 2000 m is planned. Therefore, an outlook to rock mechanics challenges in the currently applied sublevel caving layout at greater depths is made. The outlook is based on geological data (Sandström, 2003; Berglund and Andersson, 2013; Björnell *et al*, 2015; Vatcher, McKinnon and Sjöberg, 2016; Winell, Samuelsson and Andersson, 2018), mining experience at current mining depths and simple design methods. Abutment stress magnitudes are estimated by means of 3D, linear elastic, numerical simulations. Infrastructure conditions are evaluated by Wiseman's RCF-criterion (Wiseman, 1979). Mining-induced seismicity is judged by comparing the released seismic energy with the energy changes in the mine. Energy changes are approximated by a simple measure, which is tons mined multiplied by the depth of mining. Back analysis of data in the period 2014–2018 showed a reasonable fit and further that a lower than expected seismic energy release was compensated by seismic events with a large magnitude of up to 2.5. Similar, simply criteria for investigating mining-induced seismicity have been used and similar relations between lack of energy release followed by larger seismic events have been observed (Gay *et al*, 1984).

Results show that abutment stress magnitudes of about 140 MPa to 170 MPa are expected at a depth of 2000 m. These stress magnitudes already reach and exceed the (high) strength of intact rock, which is in the range of 150 MPa to 300 MPa. Furthermore, the stress magnitudes around infrastructure are significantly higher than abutment stress magnitudes. RCF analysis outline that RCF values of ore passes and longitudinal drift are larger than two at a depth of 2000 m, which implies that, even though a strong and heavy support system is installed, rather poor conditions have to be expected. Supposed the geological conditions and the yearly production stay the same, the released seismic energy will approximatively double at a depth of 2000 m compared to current mining depth of 1000 m.

Concluding, mining experience at current depths of around 1000 m outlines that rock mechanics issues affect the mining operation. The outlook to greater mining depths yields that rock mechanics problems will increase significantly in the currently applied sublevel caving layout and sequence.

Addressing high stress conditions at greater depths

LKAB investigates and studies possible mining methods for mining at greater depths below current main level very actively. Raise caving is one of the methods, which is being investigated and evaluated for deepening Kiruna operation or for extracting new orebodies. Besides raise caving other caving and stoping methods (Hoffmann, 2019) and an up-scaling of sublevel caving are analysed as well (Quinteiro, 2018, 2020).

Rock mechanics study of raise caving in Kiruna mine

The application of raise caving for a depth extension of Kiruna mine was studied (Ladinig *et al*, 2019). The aim of this study was to evaluate the application potential and possible advantage of raise caving. The investigated variation was raise caving for great depths (variant 1 in this paper), which enables an active control of rock pressure. Therefore, a system of de-stressing slots and pillars is developed at the hanging wall contact followed by stoping activities in de-stressed ground. The study focused on rock mechanics aspects and addressed identified critical areas, namely infrastructure, slot and stope stability, pillar behaviour and seismicity. Influences of sublevel caving activities at current mining depths on raise caving have not been investigated yet. The reason was to reduce complexity of investigations and determine, whether raise caving is applicable at greater depths at Kiruna. Interactions with sublevel caving are subject of further studies. For present rock mechanics analysis well-established design criteria, mainly from deep South African mining conditions, were

applied. Analysis was preliminary and thus simplified, their purpose was to outline the possible applicability of raise caving. Complex and detailed analysis were out of scope.

The results of the study supported the suitability of the basic approach of addressing the problems of high stresses and seismicity experienced with raise caving. The majority of infrastructure can be positioned in de-stressed ground and de-stressing itself requires only a minimum amount of infrastructure. Seismic energy is released distant from active infrastructure and in small steps. Stress shadows and seismicity are controlled by mine layout and mining sequence. As raise caving is a quite flexible system and does not require much infrastructure development ahead of establishment, it allows for adaption to rock mass conditions and orebody geometries on a short- and medium-term basis. However, it has to be noted that the present study is a first step in assessing the key rock mechanics issues. Further investigations are necessary to develop and implement raise caving successfully. These investigations comprise studies of critical issues in greater detail as well as incorporation of other points such as surface subsidence or transition from sublevel caving to raise caving.

Comparison of raise caving with current sublevel caving

Comparison of the initial analysis of currently experienced rock mechanics issues in sublevel caving with conducted investigations highlights the potential of raise caving from a rock mechanics point of view. Raise caving provides a considerable improvement at current mining depth and even at greater depths up to 2000 m and beyond.

Besides rock mechanics, raise caving offers operational benefits as well. Analysis of the required development effort, yield that infrastructure can be reduced by 50 per cent or even more compared to the current sublevel caving layout. Most of the infrastructure is situated in de-stressed ground reducing support effort. Additionally, infrastructure does not need to be developed years ahead freeing up a significant amount of capital. There is also additional, considerable remote control and automation potential compared to sublevel caving. This potential comprises the activities in the raise as well as loading and hauling at drawpoints, which are contrary to sublevel caving long-term and stationary. Furthermore, raise caving offers advantages in terms of ore flow and draw control. Surface subsidence in Kiruna mine is critical, because of the city being located on the hanging wall side near the mine. First considerations indicate that surface damage is most likely to be different to that of sublevel caving. Deformations may be delayed and whether the surface impact is of similar extent is yet unknown and the subject of further studies.

In summary, the study outlined considerable advantages of raise caving from a rock mechanics and operational perspective. These advantageous result in cost and safety improvements. Personnel can operate the main production equipment remotely and the majority of infrastructure is situated in de-stressed ground away from the seismic energy release areas. Due to the automation potential and decreased development and support effort, the mining costs are likely to be decreased even further.

Further development of raise caving

Due to the positive results of the study and the highlighted advantages and improvements, it was decided to develop the raise caving method further. A joint research and development project between LKAB and Montanuniversitaet Leoben was initiated in spring 2020. The project aims are to deepen the understanding of key issues and to develop the raise caving method further towards its implementation. Therefore, an emphasis is put on rock mechanics aspects, operational aspects and machinery development. Machinery development is therein conducted in close collaboration with LKAB subsidiaries Wassara and Kimit, NECAB North Engineering Consulting AB and ABB. Furthermore, raise caving is going to be tested in a designated test site in Kiruna mine.

CONCLUSIONS

Raise caving is a new cave mining method based on the principles of raise mining. Raise mining is therein applied in a modern, large-scale approach for various activities, such as de-stressing stope extraction and cave initiation. Furthermore, raise caving utilises a well-established, active stress management approach. Raise caving is flexible and adaptable. Thus, it can be used in different variants and tailored to local conditions and requirements. Two variants have been discussed in this

paper, namely raise caving at great depths, which makes use of a de-stressing concept and integrated raise caving, which integrates the main steps of cave mining. A comparison with currently applied cave mining methods highlights numerous advantages and improvements of raise caving. Overall, major drawbacks of currently applied cave mining methods are tackled. Therefore, raise caving facilitates or enables the application a safe, efficient, low-cost and high capacity mineral extraction, especially at great depths or in strong, competent rock mass conditions. A study focusing on the application of raise caving for a depth extension in Kiruna mine punctuates the potential of raise caving. However, raise caving is novel and current investigations and analysis have been preliminary. Further investigations and studies are therefore necessary. For this reason, an extensive research and development program including an *in situ* test of raise caving was launched recently.

ACKNOWLEDGEMENTS

The authors acknowledge the close and joint collaboration as well as the interdisciplinary approach followed by the Institute of Mining Engineering at Montanuniversitaet Leoben and Mining Technology Group at LKAB. This close collaboration will become highly important in future studies, which address the development of the novel raise caving method.

REFERENCES

- Andrews, P G, Butcher, R J and Ekkerd, J, 2019. The geotechnical evolution of deep level mechanized distress mining at South Deep, in *Proceedings of the Ninth International Conference on Deep and High Stress Mining*, (ed: W Joughin), pp 15–28 (The Southern African Institute of Mining and Metallurgy: Johannesburg).
- Araneda, O and Sougarret, A, 2008. Lessons learned in cave mining at the El Teniente mine over the period 1997–2007, in *Proceedings of the Fifth International Conference and Exhibition on Mass Mining*, (eds: H Schunnesson and E Nordlund), pp 43–52 (Luleå University of Technology).
- Araneda, O, 2020. Codelco: present, future and excellence in projects, in *Proceedings of the Eighth International Conference and Exhibition on Mass Mining*, (eds: R Castro, F Báez and K Suzuki), pp 1–9 (University of Chile).
- Berglund, J and Andersson, U B, 2013. Kinematic analysis of geological structures in Block 34, Kiirunavaara, LKAB internal report no. 13–746.
- Björnell, T, Andersson, U B, Eriksson, P, Faber, M and Larsson, C F, 2015. Structural mapping and 3-D photographing, in and around block 34, levels 1079–1137, in the Kiirunavaara mine, LKAB internal report no. 15–820.
- Campbell, R, Mardiansyah, F, Banda, H, Tshisens, J, Griffiths, C and Beck, D, 2020. Early experiences from the Grasberg block cave: A rock mechanics perspective, in *Proceedings of the Eighth International Conference and Exhibition on Mass Mining*, (eds: R Castro, F Báez and K Suzuki), pp 115–126 (University of Chile).
- Casten, T, Johnson, M, Zimmer, C and Mahayasa, M, 2020. PT Freeport Indonesia – The transition to underground production, in *Proceedings of the Eighth International Conference and Exhibition on Mass Mining*, (eds: R Castro, F Báez and K Suzuki), pp 23–38 (University of Chile).
- Catalan, A, Onederra, I and Chitombo, G, 2017a. Evaluation of intensive preconditioning in block and panel caving – Part I, quantifying the effect on intact rock, *Mining Technology*, 126(4):209–220.
- Catalan, A, Onederra, I and Chitombo, G, 2017b. Evaluation of intensive preconditioning in block and panel caving – part II, quantifying the effect on seismicity and draw rates, *Mining Technology*, 126(4):221–239.
- Dahnér, C and Dineva, S, 2020. Small-scale variations in mining-induced stresses, monitored in a seismically active underground mine, in *Proceedings of the Second International Conference on Underground Mining Technology*, (ed: J Wesseloo), pp 233–246 (Australian Centre for Geomechanics).
- Dahnér, C, Malmgren, L and Bošković, M, 2012. Transition from Non-seismic Mine to a Seismically Active Mine: Kiirunavaara Mine, Paper presented at the ISRM International Symposium – EUROCK 2012, Stockholm.
- Edelbro, C, Sjöberg, J, Malmgren, L and Dahnér-Lindqvist, C, 2012. Prediction and follow-up of failure and fallouts in footwall drifts in the Kiirunavaara mine, *Canadian geotechnical journal*, 49(5):546–559.
- Flores, G, 2014. Future Challenges and Why Cave Mining Must Change, in *Proceedings of the Third International Symposium on Block and Sublevel Caving*, (ed: R Castro), pp 23–52 (Universidad de Chile).
- Gay, N C, Spencer, D, van Wyk, J J and van der Heever, P K, 1984. The control of geological and mining parameters in the Klerksdorp gold mining district, in *Proceedings of the 1st International Congress on Rockbursts and Seismicity in Mines*, (eds: N C Gay and H Wainright), pp 107–120 (The South African Institute of Mining and Metallurgy).
- Gipps, I and Cunningham, J, 2011. ROES® – Automated Rock Extraction, in *Proceedings Second International Future Mining Conference*, pp 35–39 (The Australasian Institute of Mining and Metallurgy: Melbourne).

- Gipps, I, Cunningham, J, Cavanough, G, Kochanek, M and Castleden, A, 2008. ROES® – A Low-Cost, Remotely Operated Mining Method, in *Proceedings Tenth Underground Operator's Conference*, pp 147–156 (The Australasian Institute of Mining and Metallurgy: Melbourne).
- Gomes, A R A, Rojas, E and Ulloa, J C, 2016. Severe rock mass damage of undercut and extraction level pillars at El Teniente Mine, *Geomechanics and Tunnelling*, 9(5):529–533.
- Hoffmann, M, 2019. Technical and Economic Evaluation of Cave Mining Methods for Future Kiruna Iron Ore Mines, Master Thesis, European Mining Course (EMC), Aalto University, Delft University of Technology and RWTH Aachen University.
- Holder, A, Wolmarans, A, Mzimela, B, Beck, D, Tukker, H, Boshoff, P, Matoba, T and Phahla, T, 2020. A block cave construction process realigned to minimise predicted deformation in a weak mining zone, in *Proceedings of the Eighth International Conference and Exhibition on Mass Mining*, (eds: R Castro, F Báez and K Suzuki), pp 140–154 (University of Chile).
- Jacobsson, L, Töyrä, J, Woldemedhin, B and Krekula, S, 2013. Rock support in the Kiirunavaara Mine, in *Proceedings of the Seventh International Symposium on Ground Support in Mining and Underground Construction*, (eds: Y Potvin and B Brady), pp 401–409, (Australian Centre for Geomechanics: Perth).
- Krekula, S, 2017. Evaluation of the rock support system subjected to dynamic loads in Kiirunavaara, Master Thesis, Luleå University of Technology.
- Ladinig, T, Daborer, A, Wagner, H and Maier, T, 2019. Improved caving systems in LKAB's Kiruna mine, internal report.
- Makinen, I and Paganus, T, 1987. Stability of Hanging Walls At the Viscaria Copper Mine, Paper presented at the 6th ISRM Congress, Montreal.
- Malovichko, D, Cuello, D and Rojas, E, 2018. Analysis of damaging seismic event on 24 December 2011 in the Pilar Norte sector of El Teniente mine, in *Proceedings of the Fourth International Symposium on Block and Sublevel Caving*, (eds: Y Potvin and J Jakubec), pp 637–650 (Australian Centre for Geomechanics: Perth).
- Ngidi, S N and Pretorius, D D, 2010. Impact of poor fragmentation on cave management, in *Proceedings of the Second International Symposium on Block and Sublevel Caving*, (ed: Y Potvin), pp 593–601 (Australian Centre for Geomechanics: Perth).
- Nugraha, N, Bastiawarman, R and Edgar, I, 2020. Initial setup of hydraulic fracturing in Deep Mill Level Zone (DMLZ) underground mine, PT Freeport Indonesia, Papua, Indonesia, in *Proceedings of the Ninth International Conference on Deep and High Stress Mining*, (ed: W Joughin), pp 239–248 (The Southern African Institute of Mining and Metallurgy: Johannesburg).
- Orrego, C, Lowther, R and Newcombe, G, 2020. Undercutting method selection at Cadia East PC2–3 extension, in *Proceedings of the Eighth International Conference and Exhibition on Mass Mining*, (eds: R Castro, F Báez and K Suzuki), pp 370–384 (University of Chile).
- Paredes, P, Popa, I L, Kline, P R and Sykes, M J, 2020. Undercutless caving at Newcrest: towards the next generation of cave mining, in *Proceedings of the Eighth International Conference and Exhibition on Mass Mining*, (eds: R Castro, F Báez and K Suzuki), pp 166–181 (University of Chile).
- Parsons, J, Hamilton, D and Ludwicki, C, 2018. Non-vertical cave and dilution modelling at New Gold's New Afton Mine, in *Proceedings of the Fourth International Symposium on Block and Sublevel Caving*, (eds: Y Potvin and J Jakubec), pp 323–334 (Australian Centre for Geomechanics: Perth).
- Quinteiro, C, 2018. Design of a new layout for sublevel caving at depth, in *Proceedings of the Fourth International Symposium on Block and Sublevel Caving*, (eds: Y Potvin and J Jakubec), pp 433–442 (Australian Centre for Geomechanics: Perth).
- Quinteiro, C, 2020. Increasing sublevel height from 30 m to 50 m at LKAB, in *Proceedings of the Eighth International Conference and Exhibition on Mass Mining*, (eds: R Castro, F Báez and K Suzuki), pp 936–945 (University of Chile).
- Ran, J and Mfula, C, 2012. Geomechanical aspects in Alimak stoping at Barrick's Bulyanhulu Mine, *Mining Technology*, 121(1):1–10.
- Sandström, D, 2003. Analysis of the Virgin State of Stress at the Kiirunavaara Mine, Licenciata thesis, Luleå University of Technology.
- Shea, N A, Sinclair, R W and Welsh, T M, 2018. Safely re-opening a collapsed extraction level drive in a resource-limited environment, in *Proceedings of the Fourth International Symposium on Block and Sublevel Caving*, (eds: Y Potvin and J Jakubec), pp 45–56 (Australian Centre for Geomechanics: Perth).
- Sjöberg, J, Dahnér, C, Malmgren, L and Perman, F, 2011. Forensic analysis of a rock burst event at the Kiirunavaara Mine – results and implications for the future, in *Proceedings of the 2nd International FLAC/DEM Symposium*, (eds: D Sainsbury, R Hart, C Detournay and M Nelson), pp 67–74 (Itasca International Inc.).
- Tawadrous, A and Preece, D, 2015. A novel blasting technique to create drawbells and eliminate the undercut level in block cave mining, in *Proceedings 11th International Symposium on Rock Fragmentation by Blasting*, (eds: A T Spathis, D P Gribble, A C Torrance and T N Little), pp 617–624 (The Australasian Institute of Mining and Metallurgy: Melbourne).

- van As, A and Jeffrey, R G, 2000. Caving Induced by Hydraulic Fracturing at Northparkes Mines, in *Pacific Rocks 2000*, (eds: J Girard, M Liebman, C Breeds and T Doe), pp 353–360 (Balkema).
- Vatcher, J, McKinnon, S D and Sjöberg, J, 2016. Developing 3-D mine-scale geomechanical models in complex geological environments, as applied to the Kiirunavaara mine, *Engineering Geology*, 203(2016):140–150.
- Wagner, H and Salamon, M D G, 1973. Strata Control Techniques in Shafts and Large Excavations, in *Association of Mine Managers of South Africa Papers and Discussions*, pp 123–140.
- Watson, B P, Pretorius, W, Mpunzi, P, du Plooy, M, Matthysen, K and Kuijpers, J S, 2014. Design and positive financial impact of crush pillars on mechanized deep-level mining at South Deep Gold Mine, *Journal of the Southern African Institute of Mining and Metallurgy*, 114(10):863–873.
- Wimmer, M and Nordqvist, A, 2018. Present-day sublevel caving functionality uncovered – what’s next?, in *Proceedings of the 12th International Symposium on Rock Fragmentation by Blasting*, (eds: H Schunnesson and D Johansson), pp 469–480 (Luleå University of Technology).
- Winell, S, Samuelsson, E and Andersson, U B, 2018. Kartering och karaktärisering av kärnborrhål KUJ7262, LKAB internal report LKAB no. 18–931E (in Swedish).
- Wiseman, N, 1979. Factors effecting the design and conditions of mine tunnels, Chamber of Mines Research Organization, Research Report No. G01G10.

Sleep/wake up system for underground mines

J Peiris¹, K Zhao², B Li², H Gong³ and A Seneviratne²

1. University of NSW, Kensington NSW. Email: v.peiris@unsw.edu.au

2. University of NSW, Kensington NSW.

3. Roobuck (Australia) Pty Ltd, Brookvale NSW.

INTRODUCTION

Positioning is used in mining industry to ensure the safety of the mine workers. However, the environmental constraints in the underground mines immensely influence in designing and installation of such automated systems. It is a well-known that systems relying on widely used global positioning systems (GPS) are unsuitable for indoor positioning due to low GPS signal coverage caused by attenuation as they travel through walls, roofs, and buildings. The indoor positioning systems (IPS) that has been developed to overcome the limitations of GPS, such as Infra-red IPS, acoustic systems and video-based systems are also unsuitable for positioning in mines because of the hazardous operating environments and environmental conditions. In fact, environmental constraints create many trade-offs when designing wireless systems in underground mines. Henceforth, it is the responsibility of system designers to be vigilant on the possible consequences and drawbacks architectures. The design selections should be prioritised solely to fulfil the aims of system installation. The authors of this paper propose a wireless positioning system that comprises of tags and stationary anchors installed in the underground tunnels. In such system measurements are collected by the stationary anchors. The received signal strengths are then forwarded to the centre server for calibration and validation.

Regardless of the techniques and technologies used in positioning systems, powering above mentioned underground stationary devices is a major issue due to the difficulty in accessing the underground mines. Therefore, the stationary devices used in underground mines are battery powered. However, frequent battery replacement is an issue due to limited access. There is a range of low power advanced wireless technologies commonly used in IoT. But the existence of power limitations in underground mines, necessitates the ubiquitous need of a power optimisation mechanisms for mine-IoT. Besides communication to the destination nodes should be arranged power efficiently. This paper presents power efficient designing of positioning systems using a wake-up sleep mechanism of the devices.

The research classifies the operation of the underground positioning system (UPS) into three subsystems. Detection system (DS) enables human operator interaction and collaboration for decision-making by providing the raw data. The operational environments of underground mines need to satisfy special communication requirements to send the information from the DS to Decision-making and Data Management System (DM and DMS). Fundamentally, due to the cost and inconvenience of drawing cables through a mine, wireless medium is preferable over wireline medium for communication purpose of UPS in mines. A low power communication system suitable for the mine environment is proposed in the paper. The systematic study of a wake-up system for a wireless UPS presented in the paper is novel as there's not up to date study available on such a system.

METHODOLOGY

The RF range measurement based IPS technologies extract the positioning information from time of arrival (TOA) (2020), time difference of arrival (TDOA) (Mackensen, Lai and Wendt, 2012), angle of arrival (AOA) (Manpreet and Malhotra, 2015), received signal strength indicator (RSSI) (Rahayu *et al*, 2008) detection systems. Due to the environmental constraints found in mine environment the RSSI distance model is considered as the positioning technology for the DS (Li *et al*, 2018). The CS design consists of two parts namely, tag to anchor and anchor to server. The tag – anchor communication belongs to DS. The CS design of this paper rely mainly on low power consumed wireless technologies such as BLE and LoRa (Mekki *et al*, 2019)

The power optimisation techniques considered in this paper are periodic wake up and a system that wakes up only when a worker enters the communication range of the devices. The reference design

will be the continuous scanning operation mode. The systematic study is done through using Texas instrument bluetooth low energy (BLE) modules known as TI CC 2650 evaluation board and TI 2652 launchpad. The power consumption for different BLE link layer states can be measured, and the hardware related random time variable of each state can be experimentally validated through statistical approach as in Figure 1. Besides the power consumption of connectable and non-connectable modes are calculated using the above results.

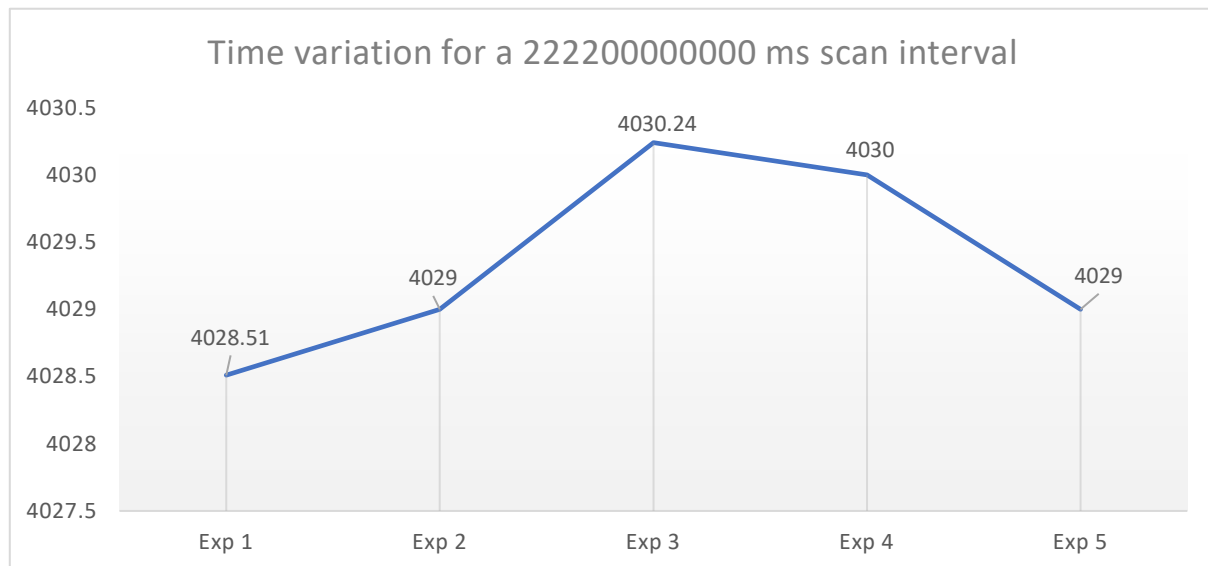


FIG 1 – Variation of scanning interval for 4000 ms scan interval through repeated experiments.

FINDINGS AND DISCUSSION

The power consumption to wake up the UPS for scanning at each worker arrival and the power consumption for periodic and continuous scanning operations are compared using experimental results obtained from the CC2652RI development kit for link layer discovery state. TI C2652 uses BLE 5 wireless protocol. The results are shown in Table 1 and the graphical representation of average energy, power and current can be seen in the Figure 2. Accordingly periodic scanning saves 78.97 per cent for 20 per cent duty cycle scanning interval of 3000 ms and 79.06 per cent for 20 per cent duty cycle scanning interval of 2000 ms than continuous scanning. Scanning duration should be configured more than the scanning interval. Therefore, for both intervals used in the continuous scanning measurements, 10 ms extra was added to the interval. The measurements were taken for 3000 ms and 2000 ms respectively. Using non-connectable BLE will extend the battery lifetime by 51 per cent due to the unavailability of a connection establishment state which consumes high power. These can be seen in results obtained using Smart RF06 evaluation board which comprises CC2650 evaluation module with BLE 4.2. However non-connectable operation might not be an option for a UPS where the same tags are available in the anchor communication range continuously and repeated scanning and reestablishment of connection are unnecessary. In such cases it is possible to update the parameters through establishing connection once and repeated power consumption for discovery and connection establishment state henceforth is omitted. The power measurements of different gap states of BLE will be used in the research to analyse the system based on a worker environmental model which will be developed in the future.

A wake-up integrated power optimisation technique can be used in any battery powered stationary system that can be triggered through a mobile device or a locomotion of a person. The 3000 ms interval consists of three scanning intervals. For a wake-up system when availability of a worker is notified the main MCU will be triggered henceforth the radio front end will switch to the discovery state. In such a system above three scanning intervals would limit to one scan interval while system will remain in standby state for rest of the time where it consumes an average current of 0.09 mA for CC2652 module and negligible current and energy consumption (0.03 mA and 0.02 μAh). Based on the experimental results of scanning intervals and assumptions approximately an average consumption of 0.39 μAh energy, 1.52 mW power and 0.47 mA current can be estimated to a trigger followed scanning operation for three seconds. This will save up to 92.93 per cent power compared

to continuous scanning operation. However, developing such a wake-up mechanism will trade-off low power consumption for system simplicity while adding hardware latency and complexity to the overall system. Considering the non-critical latency requirement of the UPS system, a wake-up system will be a solution to the above discussed power issue which exists in the underground mines.

TABLE 1

Experimental measurements for continuous and periodic scanning operation using TI CC2652R.

Operational Mode	Scanning Interval (ms)	Scanning Window (ms)	Scanning Duration (ms)	Tested Duration	Experiment Number	Energy consumed (uAh)	Average Power (mW)	Average Current (mA)	
Continuous Scanning	3000	3000	3010	3000	1	5.61	21.56	6.67	
					2	5.59	21.48	6.65	
					3	5.59	21.45	6.63	
					Mean Value	5.60	21.50	6.65	
	2000	2000	2010	2000	1	3.73	21.52	6.66	
					2	3.73	21.52	6.66	
					3	3.71	21.42	6.63	
					Mean Value	3.72	21.49	6.65	
	Periodic Scanning	1000	200	3000	3000	1	1.15	4.48	1.39
						2	1.18	4.55	1.41
3						1.17	4.54	1.41	
Mean Value						1.17	4.52	1.40	
1000		200	2000	2000	1	0.77	4.48	1.39	
					2	0.79	4.57	1.42	
					3	0.77	4.46	1.38	
					Mean Value	0.78	4.50	1.40	

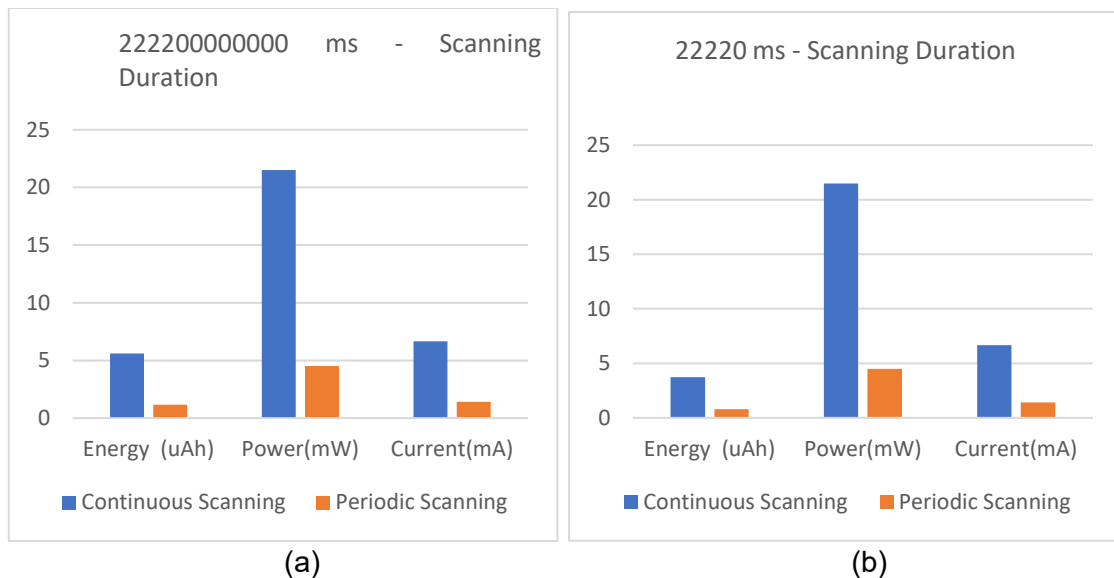


FIG 2 – Graphical representation of periodic and continuous scanning power consumption for: (a) 3000 ms scanning duration; (b) 2000 ms scanning duration.

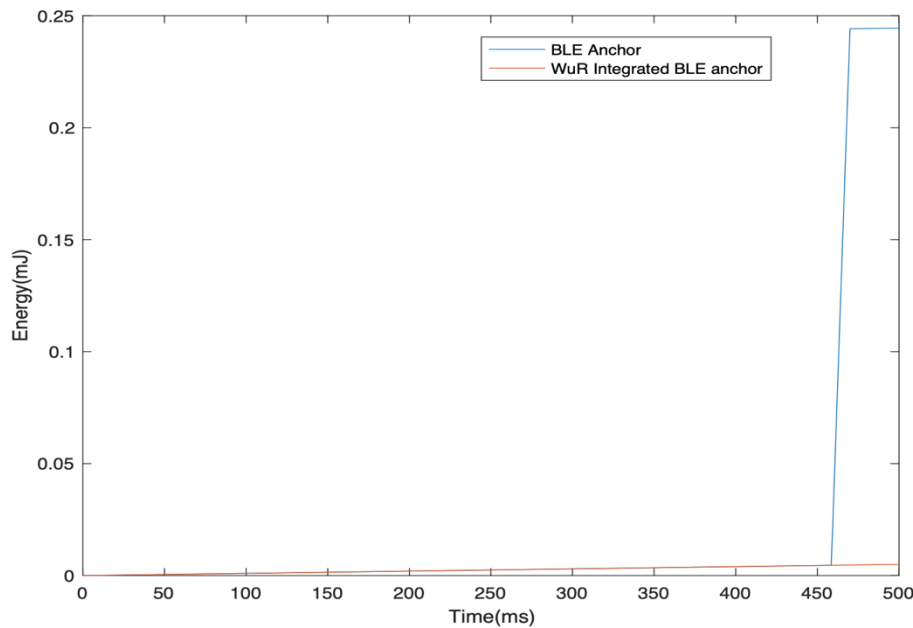


FIG 3 – Power consumption of power optimised and continuously operated BLE (Ti CC2640 BLE module).

REFERENCES

- IEEE Standard, 2020. IEEE Standard for Low-Rate Wireless Networks--Amendment 1: Enhanced Ultra Wideband (UWB) Physical Layers (PHYs) and Associated Ranging Techniques. *IEEE Std 802.15.4z-2020 (Amendment to IEEE Std 802.15.4-2020)*, 1–174.
- Li, B, Zhao, K, Saydam, S, Rizos, C, Wang, Q and Wang, J, 2018. Positioning Technologies For Underground Mines. *Far East Journal of Electronics and Communications*, 18, 871–893.
- Mackensen, E, Lai, M and Wendt, T M, 2012. Bluetooth Low Energy (BLE) based wireless sensors. *SENSORS*, 2012 *IEEE*, 28–31 Oct 2012. 1–4.
- Manpreet and Malhotra, J, 2015. ZigBee technology: Current status and future scope. *2015 International Conference on Computer and Computational Sciences (ICCCS)*, 27–29 Jan 2015. 163–169.
- Mekki, K, Bajic, E, Chaxel, F and Meyer, F, 2019. A comparative study of LPWAN technologies for large-scale IoT deployment. 5, 1–7.
- Rahayu, Y, Rahman, T A, Ngah, R and Hall, P S, 2008. Ultra wideband technology and its applications. *2008 5th IFIP International Conference on Wireless and Optical Communications Networks (WOCN '08)*, 5–7 May 2008. 1–5.

BHP WAIO Mine Planning Integration from 5YP to execution

L Talavera¹

1. Principal Engineer, BHP, Perth WA 6000. Email: luis.talavera@bhp.com

INTRODUCTION

One of the main objectives of a mining company is to create long-term value through the maximisation of net present value (NPV), a tool commonly used to estimate the value generated from cash flows over the life-of-mine (LOM), and to test if the project investments today are worth the expected returns tomorrow (Elkington, 2019). This objective can be achieved thanks to the implementation of optimal strategies that enable sustainable ore supply at an acceptable level of risk (Otto and Musingwini, 2019).

To align with the long-term goals, the mining companies cascade the long-term strategy through the generation of multiple plans at different granularity to provide guidance and targets for mining execution; also, to optimise the supply chain to maximise system capability and deliver ore to port at the right time and cost. Mining in the wrong areas has the potential to affect the business from the volume and quality point of view; unplanned changes in the mining sequence delay the ore exposition, affecting the blending strategy and therefore putting the quality of the product at risk. Hence the importance of the mine planning alignment and correct execution to ensure that the mining sequence can deliver the expected financial returns.

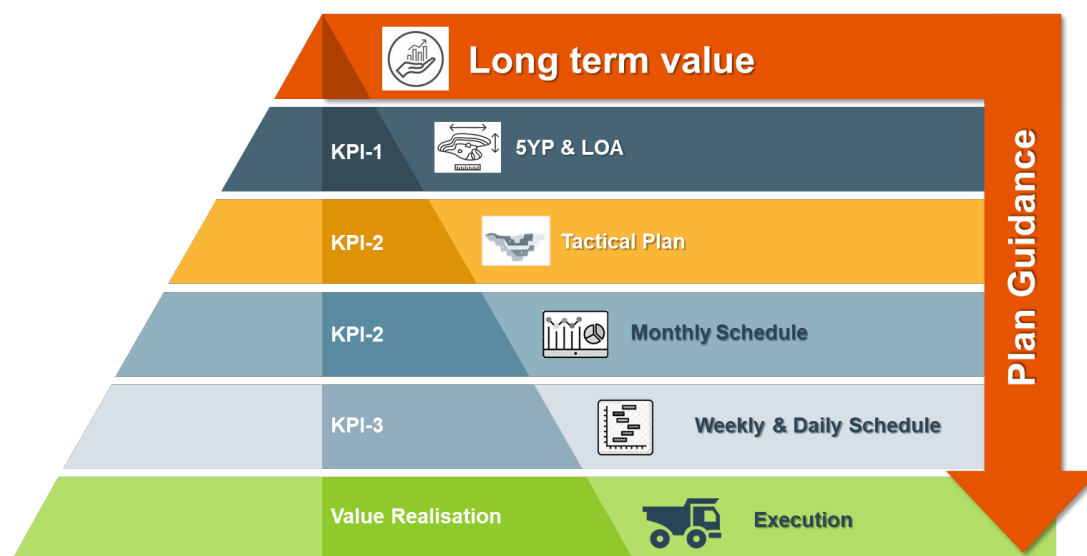


FIG 1 – Mine planning alignment.

Two components are the key enablers for this process, one is the supply chain optimisation and the second is the robustness of the mine planning alignment process. The productivity and efficiency along the mining supply chain are driven by disciplined execution, optimal resource management, and integrated systems. On the other hand, a mature mine planning alignment process requires dynamic, smart systems and applications; also, consistency in the mine planning routines, strong governance, and procedures to guarantee that guidance is properly cascaded from long-term planning to execution. Therefore, the focus of the E2E project was to address the gaps in the mine planning alignment process by introducing innovative tools, systems, and routines to enable a better plan-to-plan alignment and execution compliance.

E2E PROJECT

Contributing factors for plan-to-plan deviation

Before the implementation of the E2E project, the set-up of the *mine planning model* (set of inputs, parameters, and rules built-in in the mine planning software to create a mine plan) was a very

complex task at any planning horizon. The creation of inputs files and parameters required numerous transformations and adjustments to complete the desired outcome. During the scheduling process, the capability to create sensitivity analysis or comparison between scenarios required a complete model change and external data processing in spreadsheets, making the process extremely complex and demanding. Another major issue was the compatibility of formats between planning horizons, the different file extensions and formats made the handover between long-term and short-term planners very time-consuming and manual. At the end of the planning cycle, the generation of the output files, the integration process, and the mine plan compliance suffered from the same issues and restrictions.

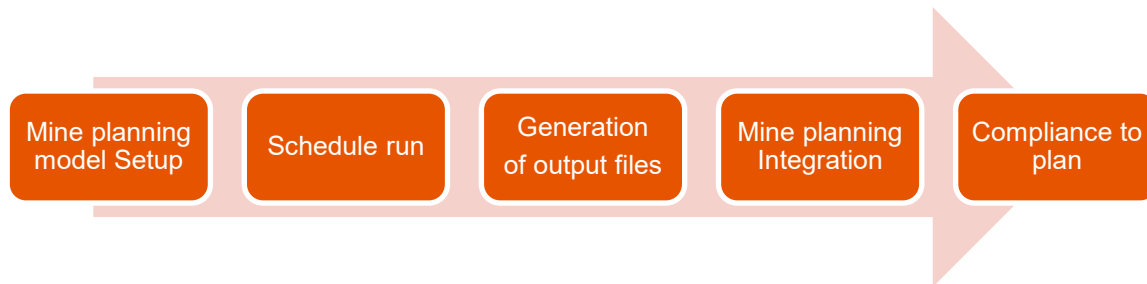


FIG 2 – High level mine planning cycle.

To determine the real contributing factors and the actions required to improve the process, the mine planning team performed a series of workshops and brainstorming sessions to capture pain points, gaps in the current process, and technology-related issues that affected the overall planning cycle. The main contributing factors are:

- The reserving process was not embedded in the planning software for most of mine planning horizons, creating the necessity to use external applications to generate the reserves. The files were generated in different formats, causing compatibility issues during the handover process; multiple conversions were required to amalgamate the variables to make them transferrable between different software, thus creating the risk of errors or file corruption during the transformation process.
- The haul network was not embedded in the planning software for most of the planning horizons, the format also made impossible the file share between applications. The lack of calibration and validation process against actuals from the fleet management system created issues such as cycle time misalignments and potential errors when forecasting fleet requirements. The haul networks were difficult to share mainly due to the different functionalities between applications.
- The naming conventions for pits, stockpiles, and dumps didn't follow a standard naming convention from long-term planning to execution. The different names for sources and destinations created issues during the cycle time reconciliation process. They also created difficulties during the alignment and reconciliation of the dumping and stockpiling strategy. To mitigate the issues related to the naming convention, multiple systems had to implement data transformations and mappings to enable the source and destination compliance process.
- The drill and blast (D&B) capability were only enabled in the short-term schedules, the long-term planning software did not incorporate a module to enable the D&B activities. Also, the D&B metrics were manually calculated, making the explosive and drill forecasting process rigid and difficult to identify bottlenecks.
- The mine planning output files were created using multiple formats, difficult to share, compare and reconcile between planning horizons. Solids, polygons from the mining, and dumping sequence required transformation before they could be used in different planning horizons. The issue also created difficulties during the reporting systems downstream. The general reporting process required the use of spreadsheets or external reporting platforms to create reports, communicate and socialise the mine plans.

TABLE 1
Mine planning integration capability – Pre-E2E.

	5 Year Plan	2 Year Plan	3 Month Schedule	Weekly Schedule
Haul Network	Not integrated	Integrated	No	No
Reserving Tool	Not integrated	Integrated	Not integrated	Not integrated
Drilling capability	Not Required	Not integrated	Integrated	Integrated
Schedule guidance	Manual	Manual	Manual	Manual
Naming convention Source	Non standard	Non standard	Non standard	Non standard
Naming convention Destination (4 Plan Horizons)	Non standard	Non standard	Non standard	Non standard
Standard Output file (4 Plan Horizons)	Not Required	Non standard	Semi-standard	Semi-standard

Baseline

The intent was to create a baseline or starting point to assess the performance of the project over time. The project baseline will be based on the current plan to plan spatial compliance metric, which compares the latest two-year plan against the monthly schedule, creating a link between long-term strategy and short-term operational guidance to execution.

According to Hall (2015), spatial compliance is extremely important to identify how well the mine plan is executed and where the materials have been mined to facilitate thorough reconciliation. Strong spatial compliance helps to ensure that pit progression enables access to future ore sources, therefore maximising the expected cumulative Discounted Cash Flows (DCF) and minimising the total cost of uncertainty associated with deviations from long-term strategic targets. If a mine operation fails to adhere to spatial execution, means that mining activities are not occurring in the correct areas at the correct time, which means that some areas were mined in the plan as expected, some areas were mined out of the plan and some other areas were planned but not mined.

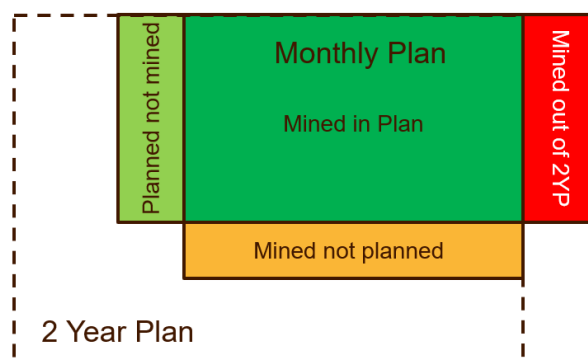


FIG 3 – Compliance measurement per category (Otto and Musingwini, 2019).

As a key performance indicator, the compliance to plan has proved to be very effective at tracking and assessing the correlation between what is planned at different planning horizons and what has been mined in a specific period (Maepa, 2021). The plan to plan (P2P) and compliance to plan (C2P) are effective KPIs when tracking and measuring operational performance and the robustness of the plan alignment process.

One of the major project risks is the plan-to-plan deviation, driven by short-term objectives such as cost reduction, cycle time minimisation, ore prioritisation against waste among others. While productivity and efficiency improvements may be the best way to reduce costs in the short-term, those initiatives should not compromise the mine planning alignment in the long-term; therefore, was

important to track short-term deviations to plan during the implementation process to ensure that the project benefit can deliver the expected benefits.

Methodology

The first step was to perform a benchmarking study for different mine planning and scheduling applications, the study included market research, review of documentation, and handbooks to capture the features and capabilities to fulfill the requirements for the long and short-term planning processes. The requirements included the introduction of improved mine planning integration solutions along with options for simplification and automation. The review was performed by a group of subject matter experts (SMEs) from multiple departments that collectively shortlisted and narrowed down all the available options to two applications for further testing. The testing criteria included the following steps:

- **Set-up Process:** The expectation was to enable a fast, comprehensive, and reliable set-up process, with the capability to verify the status of the different tasks to complete before running the plan, including the option to import inputs simply and systematically, without prior transformation.
- **Reserving tools:** The expectation was to embed the reserving process in the planning software, including the capability to import multiple pit designs, generate blast patterns, dynamic block model review, and automated reserves reporting. The end goal was to share the reserves file between different planning horizons to reduce rework and improve the alignment at the bench and pattern level.
- **Haul network and trucking:** The expectation was to introduce the capability to model the mining fleet following the same logic across all the mine planning horizons, that included the asset naming convention, time usage model, fleet parameters, truck balancing, and load and haul (L&H) logic. Other features such as dynamic haulage (dynamic control for ramps and roads based on conditions), destination constraint (constraint of destination based on design specifications), and calibration capability, were also included in the testing checklist. The end goal was to share the haul network between different planning horizons to reduce rework and improve alignment.
- **The planning and scheduling logic:** The expectation was to introduce an application with the capability to automate and optimise the crusher feed and ore blending process based on priorities and incentives. The application should be fast and intuitive enough to enable a fluent schedule, straightforward troubleshooting process, and provide the option to create multiple scenarios to compare the outcome of every iteration in a simple and systematic platform.
- **Automated reporting:** The expectation was to introduce an application with the capability to report the key metrics relevant to the mine plan built-in in the software, providing quick feedback to the user about the effect on model changes and adjustments. The end goal was to reduce rework by removing the reliance on spreadsheets to produce the graphs required to communicate the outcome of the mine plan.

Managing Reserves Files

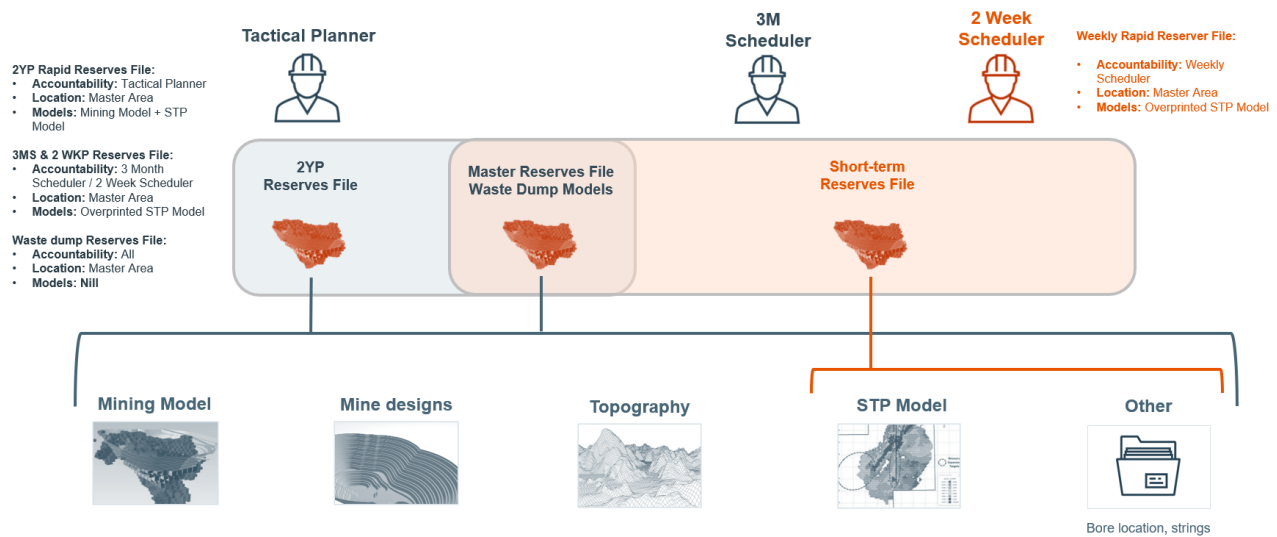


FIG 4 – New reserves file management and handover.

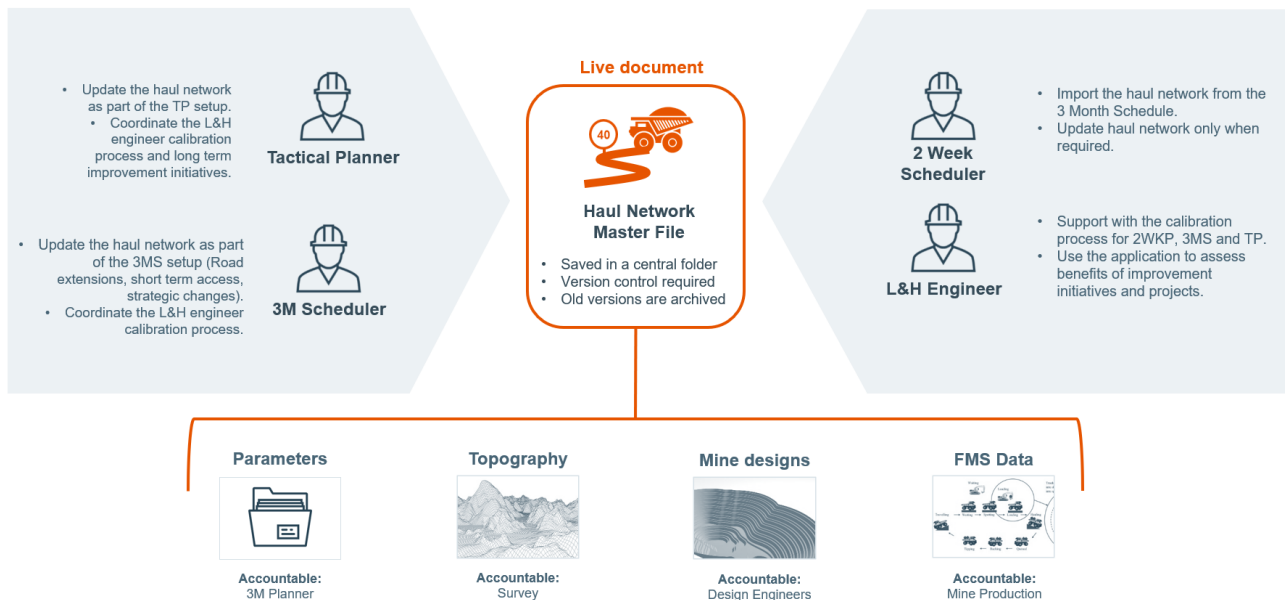


FIG 5 – Haul network file management and handover.

The selection process concluded with the generation of a cost-benefit matrix to compare the pros and cons of the two new applications versus the one currently in use, including the licensing and set-up cost. The selection criteria also considered the voice of the customer, estimated learning curve, and the training requirements, extremely relevant for dynamic teams with high turnover ratios. To complete the process, SMEs performed a voting session on which the most optimal application was selected for rollout and deployment.

Rollout

The project rollout process was split into two different activities to speed up the project execution and to align with the yearly planning cycle:

- Process implementation:** A management of change was generated to capture all the potential impacts and risks related to the implementation, including the introduction of new tools, processes, and routines into the business. The following sub-processes and projects were generated and delivered to enable a smooth implementation:

- Multiple cyber-security tests and risk assessments to guarantee system stability and controls in place to run the application in line with business expectations.
- The creation of a new central data repository to save the new mine planning models and output files (Mine Planning models,.csv files, power points, animations, solids, triangulations, .dxf files among others). The aim was to create links to the central data repository to source all the key stakeholders. To complement the project, a new data upload engine was introduced to enable better version control for the published mine plans to the new data warehouse.
- The implementation of a new software allowed the opportunity to introduce a new naming convention for source and destination for WAIO, the new naming convention included a systematic approach to name pits, pushbacks, stages, benches, and blast names from the five-year plan to execution. The same approach was taken to create a new naming convention for destinations, including waste dumps and stockpiles based on destination location, dump staging, and the material type to storage.
- The implementation of a universal physicals output file from five-year plan to weekly schedule, the new physicals output file contains and standard reporting structure with the same number of columns, headers, and formats; making the reporting process systematic, easy to audit and compare across all the horizons.
- With the introduction of new naming conventions, standard output files and cloud-based central data repositories, we had the opportunity to create automated dashboards and tools to standardise the way we report. The project included the creation of a new set of tools:
 - **Digital mine planning and grade consolidation tool:** Application to consolidate the mine plans and grades for all the WAIO operations from two-year plan to the weekly schedule, including the capability to perform sensitivity analysis and integrated reporting of shut schedule and processing capability.
 - **Explosive forecasting tool:** Application to consolidate and forecast the explosive requirements for all the WAIO operations, including the capability to perform sensitivity analysis and adjustments.
 - **Mine planning dashboards:** Set of intuitive dashboards to report mine plans and schedules for the two-year plan, three month and weekly schedule. The main goal is to provide a self-service platform for the stakeholders to access the mine planning output files in a visually reach and intuitive central dashboard.
- **Technology deployment:** The deployment process covered multiple planning horizons, considering minimal disruption in the submission deadlines but also avoiding disruptions with the business general reporting requirements. The implementation process started in August 2019 for the monthly schedule, followed by the two-year plan in October 2019 and the weekly schedule in July 2020. Multiple training sessions were scheduled during the deployment process to cover a total of 40 team members in multiple departments.

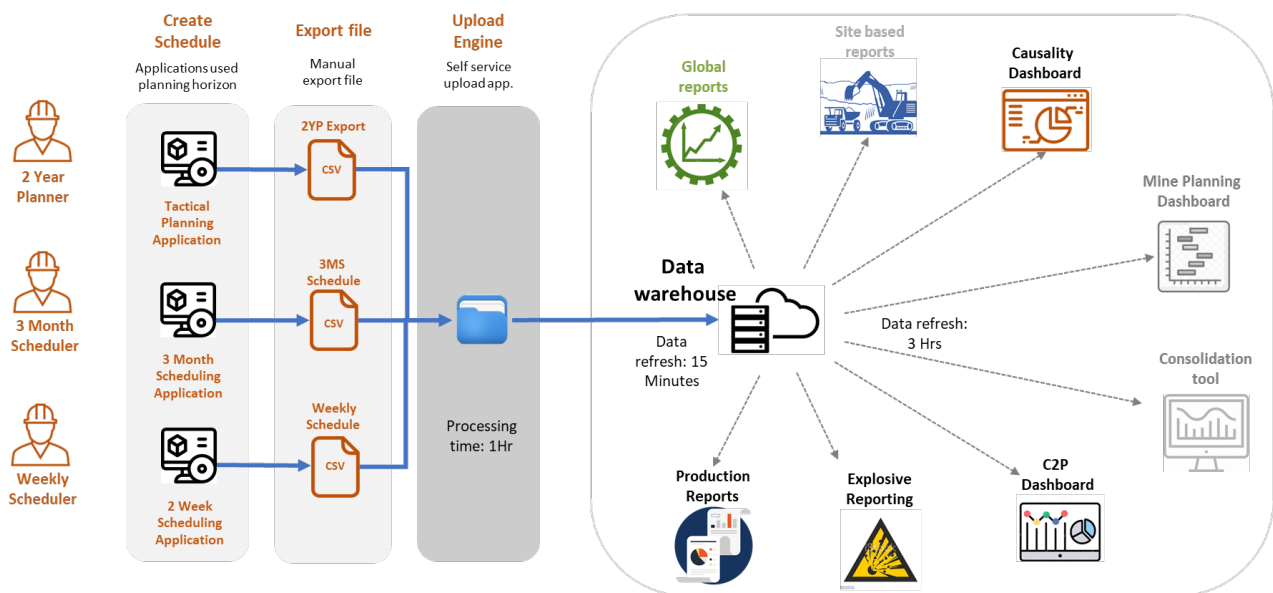
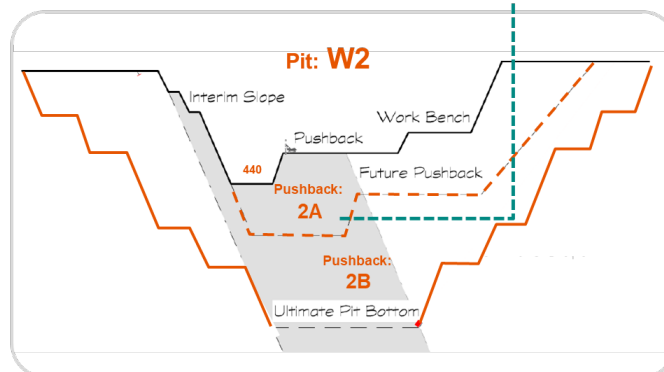


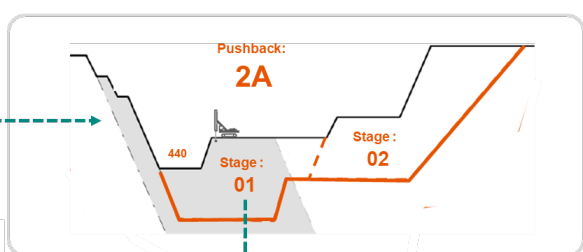
FIG 6 – New WAIO mine planning reporting process.

Component	Pit	Pushback	Stage	-	Bench/RL	-	Blast	-	Block
Convention	2	2	2	1	4	1	4	1	3
Example	W2	2A	01	-	0440	-	2027	-	001
Result	W22A01-0440-2027-001								

W22A01-0440-2027-001



W22A01-0440-2027-001



W22A01-0440-2027-001

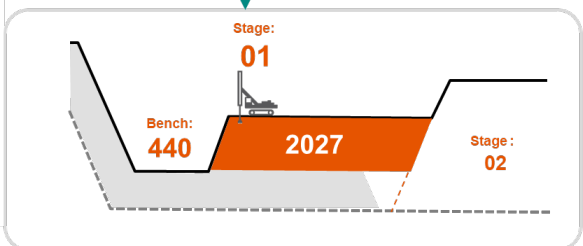


FIG 7 – New mine planning naming convention.

CONCLUSIONS AND RESULTS

The project objective was achieved with the implementation of the new set of applications and processes across all the mine planning horizons.

- The mine planning and scheduling models were set-up following a systematic approach on which version control, naming conventions, and calibrations are controlled and tracked on a monthly and quarterly basis. Exist governance over the model handover process and the release of new versions.
- The set-up process includes an embedded checklist to help the users with the tracking of changes in the model; therefore, reducing the rework during the set-up process. The hauling and reserving processes are now fully embedded in the planning software, proving flexibility during the set-up and scheduling process, also reducing the rework and non-productive time related to the external reserving process.
- The haul networks can be calibrated and validated to improve the accuracy of the cycle time and fleet hours estimation. The process includes the collection of actuals from the fleet management system, data analytics to assess truck speed per segment and the adjustment

of the haul network. The new process reduces the exposition and risk to the capital expenditure and the operational costs by improving the accuracy of the fleet forecasting requirements.

- The output files are compatible from five-year plan to the weekly schedule, they also can be easily shared and customised for guidance. The introduction of an automated and centralised upload system for the mine plans has helped to achieve the desired 'single source of the truth' when reporting.
- The project managed to achieve the complete standardisation of the source and destination naming conventions from five-year plan to execution, creating substantial benefits related to cycle time alignment, dumping compliance, and improved spatial compliance. The historical P2P compliance from 2019 to 2021 reported a 13 per cent of improvement pre versus post-E2E implementation (2YP versus 3MS).

TABLE 2

Mine planning integration capability – Post-E2E.

	5 Year Plan	2 Year Plan	3 Month Schedule	Weekly Schedule
Haul Network	Integrated	Integrated	Integrated	Integrated
Reserving Tool	Integrated	Integrated	Integrated	Integrated
Drilling capability	Not Required	Integrated	Integrated	Integrated
Schedule guidance	Automated	Automated	Automated	Automated
Naming convention Source	Implemented	Implemented	Implemented	Implemented
Naming convention Destination (4 Plan Horizons)	Implemented	Implemented	Implemented	Implemented
Standard Output file (4 Plan Horizons)	Not Required	Standard Output	Standard Output	Standard Output

P2P Tactical Plan vs Monthly Schedule - WAIO

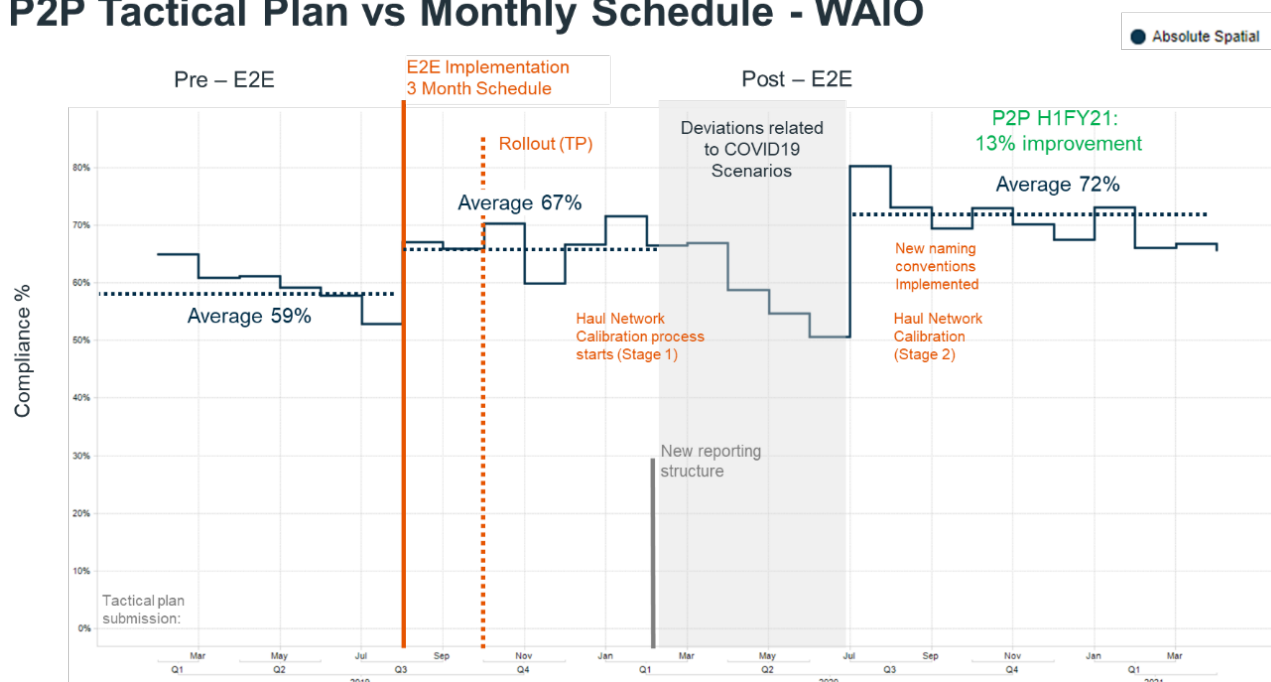


FIG 8 – Plan to Plan compliance Pre versus Post E2E Implementation.

The introduction of rigorous compliance to plan process will often lead to improved operational discipline and reduced variability. The compliance to plan process should be regularly measured and

monitored, non-compliances should be investigated to identify the contributing factors deviation and actions should be taken to avoid future deviations. Internal audits orientated to review the naming conventions and version control must be organised on a monthly and quarterly basis to guarantee the multi-planning alignment and to help with the sustainability of the project in time.

REFERENCES

Elkington, T, 2019. The secrets of mine plan optimisation have been known for at least 97 years. *LinkedIn Pulse*.

Hall, A, 2015. The role of mine planning in high performance. *AusIMM Bulletin*.

Maepa, T, 2021. Compliance to Plan in Open Pit Mining. *LinkedIn Pulse*.

Otto, T and Musingwini, C, 2019. A spatial mine-to-plan compliance approach to improve alignment of short and long-term mine planning at open pit mines. *The Journal of the Southern African Institute of Mining and Metallurgy*, 119(3).

Image-based recognition of withdrawn coal and automatic control of drawing opening in longwall top-coal caving faces

J Wang¹, L Li², S Yang³ and W Pan⁴

1. Professor/Vice President, China University of Mining and Technology-Beijing, Beijing, China, 100083. Email: wangjiachen@vip.sina.com
2. PhD candidate, China University of Mining and Technology-Beijing, Beijing, China, 100083. Email: lilianghui@cumt.cn
3. Professor, China University of Mining and Technology-Beijing, Beijing, China, 100083. Email: yslcumtb@163.com
4. Associate Professor, China University of Mining and Technology-Beijing, Beijing, China. 100083, Email: pwd@cumtb.edu.cn

INTRODUCTION

Longwall top-coal caving (LTCC) mining is one of main technology used for thick or extra thick seams in China. This method enjoys its own benefits, such as high-efficiency and low-costs. But the equipment, such as shearer, support and conveyor, are controlled by human, which is high labour intensity. With the development of deep learning and big data, intelligent LTCC mining is the shape of things to come. The automatic control of drawing opening of supports is bottleneck for realising intelligent LTCC mining. Our group proposed a solution, ie image-based method, to recognise the withdrawn coal and then output a signal to control the drawing opening. Withdrawn coal is the top-coal drawn from drawing opening of support. Key issues related to image-based recognition of withdrawn coal and automatic control of drawing opening were proposed and discussed as following.

GREY SCALE FEATURES OF WITHDRAWN COAL UNDER DIFFERENT ILLUMINANCE

In traditional LTCC face, miners can judge whether rock is mixed in the withdrawn coal stream by observing the apparent colour. In some cases, the method is effective. For example, when the rock is sandstone and the coal is dark coal, the rock mixed in coal can be clearly recognised by naked eyes, because there were obvious differences in visual between sandstone and dark coal.

Image-based recognition is an alternative strategy to recognise withdrawn coal and withdrawn rock. As mentioned above, in some cases, miners can recognise withdrawn coal and withdrawn rock well by colour difference only with naked eyes. Therefore, we can also use machines and algorithms to recognise withdrawn coal and withdrawn rock by calculating grey scale features or texture features. Grey scale and texture features are two of the most classic indexes for image recognition. Specifically, grey scale features represented the grey scale distribution of image, mainly including mean, variance, skewness, kurtosis, energy, entropy, etc. While texture features described the periodicity of grey scale distribution of image, mainly including contrast, correlation, angular second moment and homogeneity, etc. This method was widely used in image-based sorting, and the reliability has been verified.

In previous studies, our group found that illuminance has an impact on grey scale features and texture features. Coal and rock show different features under the same illuminance. The features also change with the illuminance, and coal and rock have different characteristics. Under different illumination conditions, the grey scale and texture characteristics of coal or rock are different. It is not that any features of coal and rock are obviously different under any illuminance. If the illuminance is set randomly or the features are selected randomly, the recognition performance will be greatly affected. Therefore, the grey scale features and/or texture features of coal can be accurately expressed by selecting appropriate illuminance. And the grey scale feature and/or texture features differences between coal and rock can be moderately enlarged under appropriate illuminance.

IMAGE SEGMENTATION AND ROCK MIXING RATIO RECOGNITION

Rock mixing ratio recognition was of great significance for judging the caving states and improving the coal recovery rate. Previous studies found that when the rock mixing ratio was 10 per cent

~15 per cent, the recovery rate of top coal in LTCC face can be maximised, which requires that the rock mixing ratio should be quantitatively and accurately judged and controlled when recognising withdrawn coal and withdrawn rock, otherwise, it will cause greater coal loss. Accurate image segmentation was the premise to calculate rock mixing ratio.

For image-based sorting in the fields of mineral processing, the coal and rock were placed on conveyor without overlapping each other. Coal and rock passed through the camera in turn at constant speed, and their images were collected and processed in real time. Hence, coal and rock can be easily segmented from the background, ie the conveyor.

However, in LTCC face, with the drawing of the top-coal, the rock was gradually mixed into and drawn out to the rear armoured face conveyor (RAFC). Rock mixing ratio was the ratio of projection area/surface area/volume area of rock to the sum of coal and rock, which was an important index to judge the caving state. Therefore, accurate picture segmentation was the premise of realising the recognition of rock mixing ratio in LTCC face.

The marker-controlled watershed algorithm was used to segment images of coal and rock touching or overlapping each other. The marker-controlled watershed algorithm mainly contains the following parts: segmentation function computing, foreground objects marking, background marking computing, segmentation function modifying, watershed transform computing. The rock, which has higher grey scale, was regarded as foreground, while the coal was regarded background. Several sub-images were generated by image segmentation. And those sub-images can be classified and the rock mixing ratio can be calculated.

BINOCULAR STEREO VISION BASED ILLUMINANCE MEASUREMENT USED FOR INTELLIGENT LIGHTING

As mentioned above, illuminance is a significant factor for image-based recognition of withdrawn coal, because withdrawn coal and withdrawn rock have different responses to light due to their different physical and chemical properties. Therefore, accurate measurement and control of illuminance is the prerequisite for obtaining high quality images and realising high precision recognition. Illuminometer is a special equipment used to measure the level of light intensity. The premise of using the illuminometer to measure the illuminance is to place the illuminometer on the surface of the object to be measured.

In the process of coal mining in longwall top-coal caving face, the withdrawn coal and/or withdrawn rock move rapidly on RAFC. However, there is no way to place the illuminometer on the rapidly moving withdrawn coal and/or withdrawn rock, resulting in difficulty in measuring and then controlling the illuminance. Therefore, our group proposed a novel method for estimate illuminance using depth measurement technology by binocular stereo vision.

The value of illuminance of the surface of withdrawn coal was related to the power of light source, as well as the image depth, ie the distance between light source and withdrawn coal. The power can be measured by power metres. There are many depth measurement methods, such as infrared ranging, laser ranging, ultrasonic ranging, etc. However, the accuracy of infrared ranging is low and the measurement distance is close. Laser ranging has high accuracy, but its cost is high. Ultrasonic ranging has high environmental adaptability, but low accuracy and high cost. In addition, the grey scale, colour or texture features of objects cannot be directly obtained by laser ranging and ultrasonic ranging.

Depth measurement technology of binocular stereo vision develops rapidly and has been widely used in recent years. For instance, it helped people to make more accurate movements to step over obstacles and gaps in virtual locomotion. Binocular stereo vision technology has clear advantages in-depth measuring, such as lower cost than laser ranging or ultrasonic ranging and higher accuracy than single visual ranging. More importantly, binocular stereo vision-based depth measurement can extract the grey scale, colour or texture features of objects and further realise semantic segmentation.

Therefore, our group proposed a binocular stereo vision-based illuminance measurement method to provide optimal illuminance for image-based recognition of withdrawn coal. In intelligence LTCC face, the stereo camera and the light source were fixed on support, and the power of light source

was measured by the power metre in time. The optimal illuminance can be obtained by power management, and then the images can be segmented and recognised under optimal illuminance.

In addition, other methods, such as ultrasonic-based, laser-based, infrared-based, and microwave-based sensing, can be combined with binocular stereo vision-based method to improve the measurement accuracy and save energy consumption. Quantities of dust or/and water mist were filled in the rear of support of LTCC working face, especially in the initial of caving stage. Therefore, if only the method based on binocular stereo vision was used, it may be difficult to obtain a clear image, so that it was difficult to calculate the depth and further measure the illuminance. In these cases, ultrasonic sensors can be used as an auxiliary means for depth measurement. When the images with high-resolution cannot be obtained by camera due to the influence of dust or water mist, ultrasonic sensors can be used to measure depth temporarily. Near the end of the caving stage, it is the stage where withdrawn rock will be mixed in, and it is also the key period for recognition. On-site investigation found that the dust concentration in the environment at this stage was usually lower than that at the initial stage of caving. Therefore, the binocular stereo vision-based method can still be used as the main tool for accurate illumination measurement and dynamic control of illuminance in LTCC working face.

DRAWING MECHANICS OF TOP-COAL AND PACKING MECHANICS OF WITHDRAWN COAL

In LTCC working face, the top-coal was drawn gradually with the opening of drawing opening. BBR research system was one of the commonly used system for analysing drawing mechanics of top-coal, which investigated the internal relationship between the drawing body, boundary of top-coal, recovery and rock mixing ratio in LTCC face.

The drawing mechanics of top-coal can guide the timing of image acquisition to ensure the long-term cleaning of the camera. The quantity of top-coal withdrawn can be calculated by analysing the shape of drawing body. Therefore, the duration of drawing can be roughly estimated, and the timing of opening camera lens can be guided. It is important to turn on the camera at the right time to keep the lens clean. That is to say, only a period of time before the rock was drawn, the camera was turned on for image recognition. The results of field investigation show that the drawing time of each support was mostly less than five minutes, and the rock drawing time does not exceed 20 per cent of the whole process. Therefore, choosing the right time to open the camera based on drawing mechanics of top-coal can reduce the exposure time of the lens in the high-concentration dust environment. This was helpful to improve the robustness of the system and provide high-quality images for a long time for intelligent recognition.

The packing mechanics of withdrawn coal were helpful to reveal the spatial accumulation features of withdrawn coal and withdrawn coal rock on RAFC, so as to correct the result of image recognition. As we all know, traditional image recognition was based on 2D image analysis, so the rock mixing ratio was the projection area ratio between withdrawn rock in the image to the sum of withdrawn coal and withdrawn rock. However, in fact, withdrawn coal and withdrawn rock were not 2D objects, nor were they laid flat on RAFC separately. They were not only 3D blocks, but also overlapped on each other. Therefore, there may be a great error in evaluating the caving state by analysing the projection area. To solve this problem, the relationship between the projected area ratio and the surface area ratio/volume ratio can be further obtained by the analysis of packing mechanics. On the basis of the surface area ratio/volume ratio corrected by the 2D image, the drawing state can be described more accurately.

SHAPE CHARACTERISATION AND ROUGH RECONSTRUCTION OF WITHDRAWN COAL BLOCKS BASED ON 2D IMAGES

The shape characteristics, mainly including geometry and morphological characteristics, affect the drawing and packing mechanics of withdrawn coal blocks. However, the non-spherical coal blocks were always simplified as disks in 2D or sphere in 3D. A shape descriptors control method was proposed to roughly reconstruct the withdrawn coal blocks. The descriptors that can be directly measured were geometry descriptors, mainly including area, perimeter, maximum (minimum) ferret diameter, minimum length (width) of bounding rectangle, martin's diameter, major (minor) axis length, equivalent diameter, and so on. Morphological descriptors were calculated by geometry

descriptors to give a more comprehensive description of shape, such as aspect ratio, length width ratio, roundness, blaschke index, modified blaschke index, convexity, and so on.

These descriptors describe the shapes of blocks projected in 2D images. More than one projection image with different viewing angles was used, which can be more helpful to describe the shape of the block. The weighted average of descriptors in three projected views was calculated in previous studies. In addition, there may be significant shape differences between images with different projected views. The weighted average and standard deviation of descriptors in three projected views together constitute the shape index.

Based on the shape descriptors obtained by image analysing, the numerical model can be established by voxelisation processing. The number of pebbles constituting the voxelised model was related to the resolution selecting. Higher resolution selected, better reconstructed performance can be obtained, but more pebbles were used to reconstruct the voxelised model. Excessive redundant pebbles reduced the efficiency of numerical simulation. Therefore, our group proposed a robust and efficient method to simplify the voxelised model, ie bubble burst method (BBM). The pebble in the voxelised model was regarded as bubble, and busted one by one. Cavity was detected in the process of bust bubble. If cavity was generated because of the bust of a certain bubble, the corresponding pebble cannot be simplified, otherwise it can be simplified. The results show that over 50 per cent pebbles can be simplified under resolution of $20 \times 20 \times 20$ by using BBM.

3D RECONSTRUCTION AND VOLUME ESTIMATION OF WITHDRAWN COAL BLOCKS BASED ON SEQUENCES OF 2D IMAGES

As described above, the withdrawn coal blocks can be roughly reconstructed by shape descriptor control method, which was an efficient procedure of generating a large number of blocks. The reconstructed model with rough shape can be used for top-coal caving numerical simulation by using discrete element method. However, higher-accuracy reconstruction method was also significant for revealing the shape-related properties of blocks, such as analysing the drawing and packing mechanics, as well as measuring the rock mixing ratio with irregular rock blocks.

From the respective of contact mode, there were two ways to obtain the 3D shape information of block, ie contact method and non-contact method. According to different measurement processes, contact methods can be further divided into manual measurement method and 3D digitiser based automatic measurement method. Among them, the manual collection method mainly uses naked eye observation, and measures the block shape with the aid of tape measure, protractor and other tools, which is not only labour intensive, but also inaccurate.

3D digitiser based automatic measurement methods mainly used the equipment including coordinate measuring machine and mechanical arm 3D scanner, and measured the position of probe in 3D space to realise the digitalisation of block. Compared with manual measurement method, the measurement efficiency of 3D digitiser based automatic measurement method was relatively high, but there were still a series of problems, such as relatively complex operation, slow storage speed of measurement results, and inability to obtain block surface texture information.

In recent years, with the rapid development of computer and sensor technology, the non-contact 3D information measurement method has been widely used. There were mainly two types of non-contact measurement methods, ie activeness method and passive method. The activeness method was to use controllable radiation emitted by equipment, such as laser, ultrasonic wave etc, and then obtain the 3D shape characteristics of the block by analysing the reflection characteristics of the block to the controllable radiation. Pulse distance measurement method, structured light method, coded light method, computed tomography (CT) method and magnetic resonance imaging (MRI) method were commonly used activeness method.

Compared with the activeness method, the principle of block reconstruction by passive method was simpler. The passive method does not need to emit laser or ultrasonic waves to the block, so expensive experimental equipment and complicated experimental operations were not needed. By analysing the photos of the block and extracting the shape information, the reconstruction of the block 3D model can be realised. Single image method, stereo vision method, silhouette-based method, motion image-based method and slice recovery method were widely used passive method.

Therefore, our group proposed a withdrawn coal block reconstruction method based on silhouette. The performance of 3D reconstruction was significantly affected by the quality of image obtained. In order to obtain high-quality images, our laboratory developed an image acquisition system. The system mainly contained CMOS camera, professional photo light box, aluminium alloy tripod, light source, intelligent turntable, wireless remote-control, stainless-steel bracket, and so on.

Coal block was placed on standing tray and rotated with the turntable. The camera was at an elevation of around 20° relative to the base of the coal blocks. Every time the turntable rotated 10° , the camera automatically shot a photo and saved it. Hence, a sequence of images with 36 multiple views were obtained. Then, the camera was lifted at an elevation of around 30° and shot a sequence of images at a rotation interval of 20° . Therefore, another 18 images were obtained for block reconstruction. The sequences of images with multiple views were further analysed by the silhouette-based reconstruction method. The result showed that the shape of blocks was recovered with high accuracy and the texture was also obtained.

Furthermore, in LTCC face, sequence images of the withdrawn coal block on RAFC can be captured by camera, and block can be reconstructed by image analysing. And the volume of block can be measured based on reconstructed model, which was an important factor to estimate the output of coal and the rock volume mixing ratio.

THE RELATIONSHIP BETWEEN 3D MORPHOLOGICAL PROPERTIES AND 2D MORPHOLOGICAL PROPERTIES

Both 2D morphological properties and 3D morphological properties of blocks were important index to characterise the shape of irregular withdrawn coal blocks. 2D morphological properties were easy to obtain from 2D images, but it cannot fully characterise the block shape. 3D morphological properties contained many data, but it was hard to measure. Therefore, it was a significant topic to estimate 3D morphological properties quickly and directly from 2D images. Based on laboratory experiment and numerical simulation, our group revealed the relationship between 3D morphological properties and 2D morphological properties of withdrawn coal blocks.

The 2D morphological descriptors mainly contain area, convex hull area, perimeter, inscribed diameter, 2D sphericity. The 3D morphological descriptors mainly contain volume, convex hull volume, largest ferret diameter, and 3D sphericity.

2D morphological properties was related to the viewing of image acquisition, that is, the 2D morphological properties was different under different viewing. In LTCC face, the withdrawn coal blocks observed on conveyor always tend to accumulate in a preferred orientation. Therefore, it was necessary to consider just some certain viewings of withdrawn coal blocks on conveyor, rather than random viewings. Based on this assumption, our group carried out the freefall numerical experiment was conducted with the discrete element method. Silhouette-based reconstruction method was used to reconstruct withdrawn coal block. 2D morphological descriptors and 3D morphological descriptors of blocks under preferred orientation were calculated, respectively. The correlation analysis of 2D morphological descriptors and 3D morphological descriptors was conducted to reveal the relationship between the morphological descriptors. Result showed that some 2D morphological descriptors had relatively high correlation with 3D morphological descriptors. It was possible to estimate the 3D morphological descriptor of the withdrawn coal blocks by analysing 2D images. Therefore, the rock mixing ratio can be modified based on high-accuracy shape analysing.

IDENTIFICATION OF ROCK-PARTING MIXING AND ABNORMAL TOP-COAL CAVING

It is of great significance to judge the caving state of the top coal by analysing the sequences images of withdrawn coal. In fact, even if the correct image recognition result was obtained, the coal caving state may not be judged correctly. This was because there were many special situations in the mining process, such as the existence of rock-parting.

It was relatively difficult to recognise rock-parting with high accuracy, because in most cases, the appearance of rock-parting was very similar to that of coal. In LTCC face, it was sometimes difficult to distinguish rock-parting from withdrawn coal only by naked eyes. However, the workers can distinguish the rock-parting from the coal by the difference of the sound of hitting the tail beam and

RAFC. Therefore, some other recognition methods, such as voice recognition and vibration recognition, can be integrated with image recognition to distinguish the rock-parting more accurately.

How to distinguish the rock-parting from the immediate roof accurately was also a difficult problem when the lithology of the rock-parting was similar to that of the immediate roof. In LTCC face without rock-parting, instantaneous rock mixing ratio can be obtained by image recognition and directly used for controlling drawing opening, while in LTCC face with rock-parting were not. Because if instantaneous rock mixing ratio was used as the index to close the drawing opening of support, the rock-parting may be mistaken for the immediate roof and wrong instructions will be given. Therefore, our group put forward the concept of interval rock mixing ratio instead of instantaneous rock mixing ratio to control the drawing opening of support. Interval rock mixing ratio, that was, the average value of rock mixing ratio in a period of time. By analysing the average value of rock mixing ratio in a period of time, rather than rock mixing ratio at a specific moment, it can effectively avoid the premature closure of the drawing opening caused by the release of rock-parting.

HIGH-QUALITY IMAGES OBTAINED ON-SITE

In LTCC face, there was high-concentration coal dust, rock dust or/and water mist, which can scatter and absorb light. The target objects (ie coal and rock) in the image can be degraded in contrast and clarity, colour distortion etc, which not only affected the subjective visual perception of workers, but also was not conducive to the automatic recognition of coal and rock in the image by computers. Therefore, the high-quality image acquisition under the harsh environment with high concentration dust or water mist in LTCC face was the premier to realise high-accuracy image recognition.

On the one hand, dust or water mist suspended in the air affected the brightness, contrast, and clarity of images, which affected the accuracy of image recognition. Many attempts were conducted to remove dust, water mist and noise from photos. Image processing based dehazing technology and optics based dehazing technology were two main types of technology to remove the dust or/and water mist in image.

Image processing based dehazing technology was to enhance or restore the collected images to improve the image quality. The classic image processing based dehazing technology was relatively mature and widely used, such as median filtering, wiener filtering, non-local mean filtering, wavelet transform, empirical mode decomposition, variational mode decomposition, 2D-variational mode decomposition, Gaussian mixed model, retinex theory, and so on. In recent years, with the development of deep learning, some more intelligent algorithms have been proposed and achieved better dust and/or water mist removal performance.

Optics based dehazing technology needs to reform the optical imaging system, and then use the algorithm to restore the collected images. Visible light-near infrared fusion dehazing and polarimetric dehazing were two representative methods to remove dust or/and water mist. Among them, the polarimetric dehazing method had some obvious advantages, such as strong adaptability, low cost and fast processing speed. At present, this technology was rarely used in the intelligent top-coal caving face, and it has broad prospects to develop polarimetric dehazing technology which is suitable for the harsh environment of high concentration coal dust, rock dust or water mist.

On the other hand, dust or water mist suspended in the air will fall and accumulate on the camera lens, affecting the image quality and even damaging the lens. Therefore, it was very important to develop an intelligent high-definition camera with automatic dust sensing and removal, so as to adapt to the harsh environment of underground mining and obtain high-quality images that can meet the recognition requirements. 'Insight-I', an intelligent camera with automatic dust sensing and dust removal, was developed by our groups in 2020. In the following research, more attention should be paid to the development of image-based intelligent caving equipment based on edge AI.

ACKNOWLEDGEMENTS

The research work described in this paper was supported by National Natural Science Foundation of China (51934008, 52121003), Natural Science Foundation of Hebei Province of China (E2020402041).

New mining frontiers

Leveraging virtual reality for mine accident investigations

H C Grobler¹, H Thomas² and J van Dalen³

1. Head of Department, University of Johannesburg, Gauteng, South Africa.
Email: hgrobler@uj.ac.za
2. Senior Lecturer, University of the Witwatersrand, Gauteng, South Africa.
Email: huw.thomas@wits.ac.za
3. Senior Surveyor, Harmony Gold, Gauteng, South Africa. Email: jacovandalen@gmail.com

ABSTRACT

The aim to achieve zero harm in mining activities is the primary focus of all responsible mining companies. The quality, focus and method of recording evidence from mine incident investigations are not standardised in most cases. This paper aims to investigate methods of improving the quality of evidence collection and more specifically, the visualisation and recording of the site of a mine incident. It is argued that accurate recording and visualisation will provide more informed decisions to be made and will ultimately lead to a greater understanding of the factors leading to incidents from the perspective of first responders, mining personnel and investigating teams. The combination of lidar scanning and virtual reality visualisation tools are discussed in an underground mining environment and how these technologies can contribute to the improvement of mine safety.

INTRODUCTION

The mining industry has adopted the 'Zero Harm' philosophy (Johnson, 2018; Hinze, 2002; Adams, 2011; Jusko, 2019) to reduce mining accidents to a minimum. Hinze (2002) investigated interviews from the 1990s by the US Construction Institute, which at the time established a 'Making Zero Accidents a Reality' project team. A current example of the 'Zero Harm Culture' approach to safety undertaken by Siemens (Jusko, 2019). All evidence points to a high level of focus on safety yet, accidents and deaths are still reported by the building, manufacturing and mining industries. In 2014, there was a combined figure of 380 500 deaths in the workplace globally (Hämäläinen, Takala and Kiat, 2017). Unfortunately, even if the 'zero harm' policy is widely adopted and implemented, leading to a significant reduction in incidents, there was still a combined total of 161 fatalities in the mining industry from 2016 to 2017 (Department of Mineral Resources, 2018).

A review of current literature shows a correlation between the quality of accident investigations and the safety performance of large-scale mining operations in Ghana (Stemn *et al*, 2019). To successfully mitigate the recurrence of accidents and deaths in the workplace, there must be a deep understanding of the factors leading to the incident. The most accepted manner of understanding these factors is an in-loco investigation followed by an accident investigation (Health and Safety Executive, 2004). The aim of an accident investigation is to formulate and implement safety improvements that would mitigate the recurrence of the accident (Stemn *et al*, 2019). Stemn *et al* (2019) identified an increased research interest in the field of incident investigations and learning from incidents; a process called Learning From Incidents (LFI) (Leistikow *et al*, 2017). Stemn *et al* (2019) further elaborated that an LFI aims to improve organisational safety, his findings based on investigations of five large scale mining operations in Ghana which had similar characteristics such as ownership and several factors that might have contributed to their accident rates. The main finding indicated that there is a direct correlation between the quality of the findings of incident investigations and safety performance. Stemn *et al* (2019) research argued that a rudimentary investigation fails to provide value to prevent or mitigate the reoccurrence of a similar event in future.

The aim of investigating an accident is to add value to safety (Stemn *et al*, 2019) through the recreation of the factors leading to the incident, identify the critical contributing factors and establish or reinforce preventative and mitigating controls (Morrish, 2017). Both Morrish (2017) and Stemn *et al* (2019), found that the quality of the controls developed is directly dependant on the quality of the investigation.

This paper is focused specifically on the mining industry, but some of the case studies (Buck *et al*, 2006, 2013; Martin, Lardy and Laumon, 2011) discussed are based on a crime scene and accident investigations that provide examples of the application of lidar and VR technology in the mapping,

presentation and interpretation of incidents. Mine surveyors in South African mines make use of 3D scanners for significant accidents (Webber-Youngman *et al*, 2019) where there was a serious injury to a person or a loss of life. The authors would like to present a case for the widespread adoption of modern surveying and visualisation tools to improve the capture of data during an incident investigation and proposes that such improvements will improve the quality of investigations, provide realistic feedback and lead to improved safety performance driven by a better understanding of the underlying factors.

It is planned to conduct a further Proof of Concept (PoC) study in a controlled environment in a training mine in order to investigate the results and identify shortcomings in current forensic surveying and in-loco investigation procedures.

FORENSIC INVESTIGATION TECHNIQUES IN OTHER SECTORS

In the case of law enforcement, crime scene investigators will typically make use of two-dimensional (2D) photos, videos, and spherical photographs, but this system is still flawed and still present challenges in describing and documenting a crime scene (Tung *et al*, 2015). In many cases, it is a challenge to represent the scene completely unbiased. Eyre *et al* (2017) argues that a three-dimensional (3D) presentation of a crime scene allows for a better representation of the event and environment during the incident reconstruction. A detailed 'reality capture' of an incident will provide a full record of the scene, reduce the time that the scene must remain secure for investigations and can when represented correctly, provide investigators unlimited virtual access to the scene to conduct further investigations (Ren *et al*, 2018).

Laser scanning can provide a 'rapid collection of highly accurate information' (Laing and Scott, 2011) (Webber-Youngman *et al*, 2019). In the context of a mining incident where accident scenes cannot remain undisturbed for long due to production reasons or become inaccessible due to safety considerations, it is critical to capture the entire scene in as much detail as possible, as soon as possible after an incident.

Case study 1 – fatal vehicle accident

In this case study, a cyclist was fatally injured when struck by a motor vehicle. The use of 3D scene capture and reconstruction methods using high-resolution laser scanning of the incident, vehicle and Multi-slice Computer Tomography (MSCT) combined with Magnetic Resonance Imaging (MRI) scanning provided the basis to reconstruct the incident in an animation based on the facts obtained in the investigation (Buck *et al*, 2006). A significant correlation could be drawn between specific areas on the vehicle and the fatal injuries sustained by the cyclist. A hand-held scanner was used to scan the incident including the vehicle, bicycle and the deceased at the scene of the incident.

Buck *et al* (2006) describes the process of converting the physical and medical evidence into accurate 3D models which were used by the investigation team to link evidence of the damage sustained by the vehicle to the injuries sustained by the cyclist as indicated by the MRI scans. Figure 1 shows: (a) Recording the damage sustained on the bicycle with a three-dimensional scanner; (b) Scanning of the damaged car; (c) 3D surface model of the body of the deceased young male that shows the injuries in true colour.

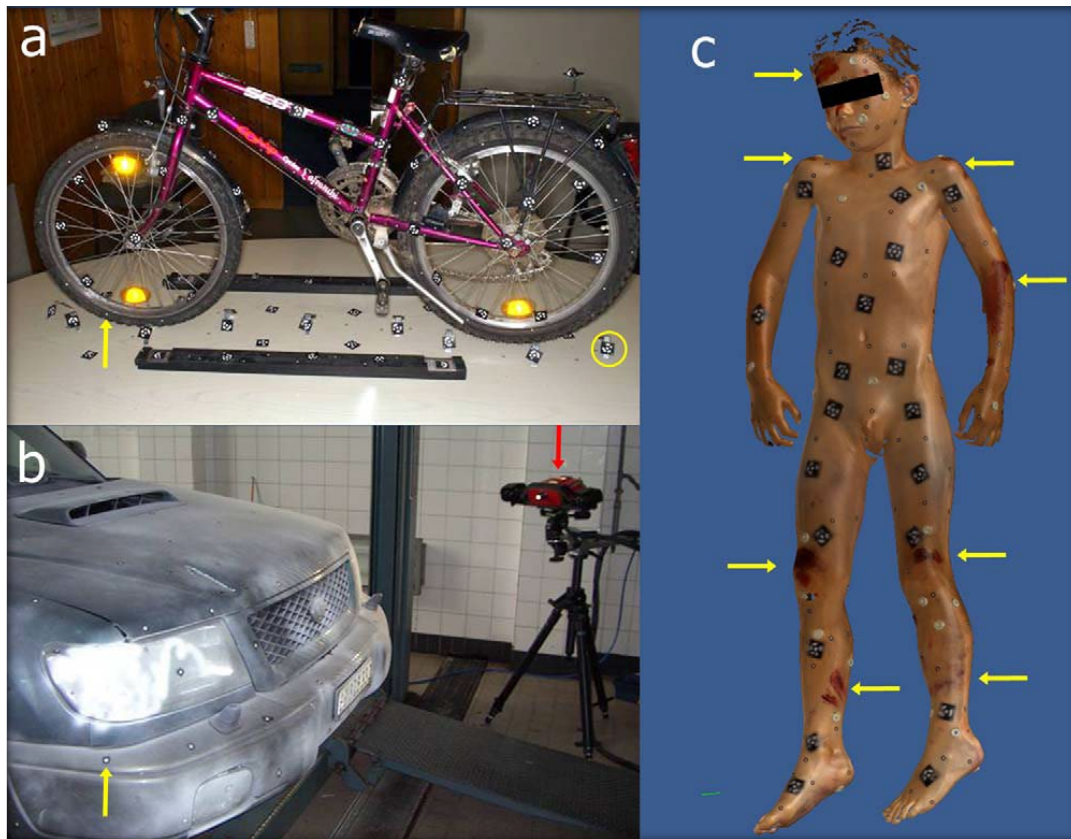


FIG 1 – 3D scanning of evidence (Buck *et al*, 2006).

Case study 2 – fatal shooting incident

During an argument, it is alleged that one person shot and fatally wounded another. The investigation needed to prove if the shooting was to be ruled an accident or a homicide (Buck *et al*, 2013). The investigation team had the statement of the accused, the bullet wound of the deceased, bullet casing, the firearm and the scene where the shooting occurred (Buck *et al*, 2013). The District Attorney in charge of the case ordered that the scene of the shooting needed to be scanned and reconstructed as a 3D virtual environment.

The data from the 3D scene capture was combined with medical reports and the trajectory of the bullets could be reconstructed from the witness report provided by the accused. The trajectory investigation and medical evidence did not support the witness statement. The evidence proved that someone did indeed commit a murder, but the same methodology could equally be used to prove if someone was innocent (Buck *et al*, 2013).

FORENSIC INVESTIGATION IN MINING

The process of measuring a lost-time or fatal incident is initiated as soon as the initial patient recovery process begins. In instances where the patient can be recovered safely without the assistance of a proto team, the surveyor will only become involved at a later stage. In the event where a rescue or recovery process must be initiated by a mines rescue service unit, the surveyor will provide rescue plans and detailed plans of the area. Once the rescue or recovery has been successfully completed the Inspector of mines is notified of the incident. At the earliest possible time, an in-loco inspection is arranged to the undisturbed incident scene. During this in-loco inspection, the inspector of mines, mine manager, production members, union representatives and the mine surveyor visits the scene. After the initial in-loco interviews, the inspector then requests the surveyor to 'pick up' specific features including the position of the patient(s) and important features and indicates specific sections views. This is then left to the surveyor to execute. Measurement can take hours depending on the level of detail required and the complexity of the incident. Once completed the surveyor presents an incident plan that consists of a title block, a plan view and one or more section views. This is normally labelled 'Exhibit B' for the official investigation. In many cases, there are cultural ceremonies to be conducted and protocols to be observed after a fatal incident.

The use of 3D laser scanners to record significant injuries and fatality scenes (Webber-Youngman *et al*, 2019) are becoming more commonplace but is still not widely accepted or insisted upon by investigation teams and the DMR. Webber-Youngman *et al* (2019) highlighted that the advantages of 3D laser scanners for accident investigations over the inadequate level of detail captured by conventional survey methods.

The standard method of tachymetric observation using a total station to specific points of interest, traditional offsetting of features using tapes and scene capture using conventional photography is time-consuming and to a great extent limited by the time available to measure the scene and the level of detail observed by the surveyor and the investigation team, in an underground environment, this method of scene capture is compromised by prevailing dangerous conditions that may have been a root cause to the incident occurring in the first place, poor or no lighting and a tendency to focus on the direct area where the person was injured rather than capturing a holistic view of the surrounding area. This method of measuring is time-consuming and prone to observational and booking errors in the field and the further error introduced in the interpretation of field notes, the plotting of observations and the draughting of the incident scene plan and sections. The final plan and cross-sections rarely have sufficient detail recorded and provides a record of the incident rather than providing solid, irrefutable evidence of the prevailing conditions at the incident site during the in-loco investigation. It is argued that evidence may be missed or misrepresented using this method of surveying. Subsequently, a re-visit of the accident scene is often impossible and the only record that remains is the photographic evidence which may be poorly lit, improperly focused and biased in the sense that only specific items and areas were photographed. The official accident plan becomes a document for the record and is normally labelled as an exhibit for the official investigation. The surveyor tasked with measuring the scene and constructing the accident plan may be asked during the investigation to explain why certain elements which may become important during the examination of witnesses was not measured or recorded. In some cases, a specific area of the scene might only become relevant at a much later stage of the investigation and by that time the scene is no longer accessible to retrieve evidence or has changed (Ren *et al*, 2018). A 3D scan of the environment would enable the mine surveyor to extract critical data after the scene is no longer available should new questions arise that were not relevant during the initial stages of the investigation. Technology is changing at a rapid rate (Morrison, 2017) and this applies to 3D laser scanners as well as point cloud data. Point cloud data sets consist of individual points that have a specific geospatial location (x, y, z) and each point can be allocated a Red, Green and Blue (RGB) colour space. A single point cloud scan can contain millions of points and a raw pointcloud file is exceptionally large (Brennan *et al*, 2015). Point clouds are difficult to navigate and there is a need to enhance the visualisation. The ability of a laser scanner to record a scene in grey scale under zero light conditions allows the full recording of a scene even in areas where no lighting is available or where areas are inaccessible due to geotechnical or environmental hazards. The exposure of the surveyor to risks are significantly reduced as most of the survey is done remotely and no direct contact with any object or excavation is required.

THE APPLICATION OF PHOTOGRAMMETRIC SCANNING, CASE TEST 1

It is argued by the authors that the combination of laser scanning, 3D photogrammetry techniques and Virtual Reality systems will add value to mine safety both in training and safety improvements (Webber-Youngman and van Wyk, 2013). A test was conducted to evaluate technology in a controlled environment similar to that of an underground mine through a Proof of Concept (PoC) study at the DigiMine mock mine at the University of the Witwatersrand, Johannesburg. The PoC study entailed that the identified working areas in the mock mine would be captured in VR. It is expected that this test would prove that a user will be able to navigate the VR environment using a mobile phone, tablet, laptop or computer. The VR experience would have to be of high quality and enable the user to observe the environment as if the user was there in the physical environment.

A VR scan was done in August 2019 using a lightweight, tripod-mounted Matterport Pro 3D Camera. To capture the identified areas, it was required that the camera be moved from one area to the next to ensure that there was sufficient overlap between each scan. The entire scan was done in sixty minutes and it included the tunnel and the stope area in the mock mine. There was a challenge to manoeuvre the camera and the tripod in the confined spaces of the stope but it was possible to capture all the desired areas. During the scanning, it was observed that there are concerns regarding

the quality of the scan due to lack of illumination in the areas where there was little to no lighting. This issue highlights the most critical shortcoming of most purely photogrammetric systems currently available to consumers. The camera systems require a good, multidirectional light source to effectively capture the scene. In surface applications, it has been found that bright sunshine or directional lighting may also reduce the efficiency of data capture.

To illustrate this challenge, the image labelled 'A' and 'B' in Figure 2 illustrates the difference between two consecutive scans. 'A' was scanned with little to no lighting and 'B' was scanned in an area that was well illuminated. The amount of detail that is lost due to bad illumination adversely affects the quality of the VR experience and unless compensated for, may lead to a significant loss in data captured.

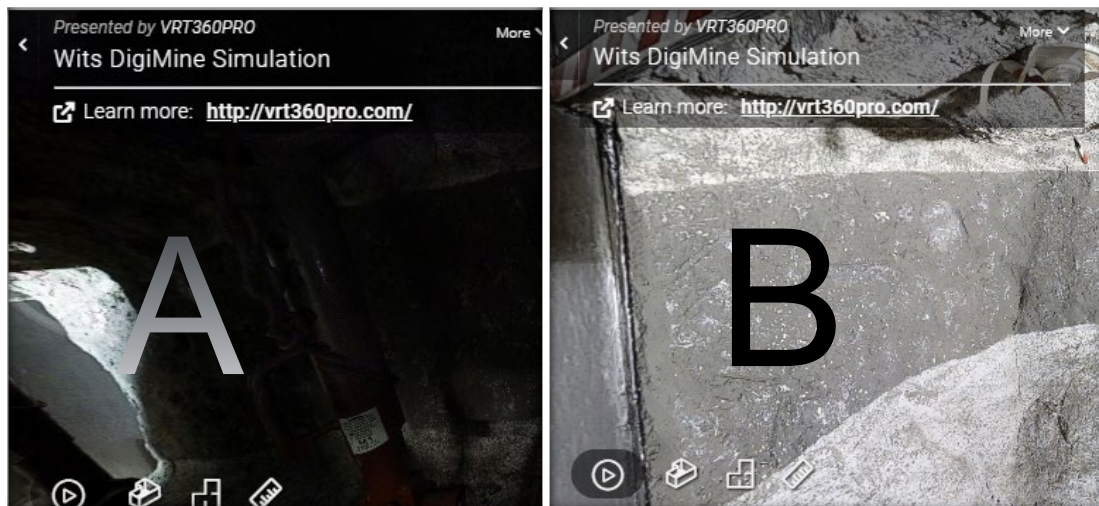


FIG 2 – Screenshots of two scans. A – Unilluminated scan versus B – Illuminated scan where the geology was identifiable on the sidewall (my.matterport.com).

Suitably well-illuminated areas provided data of high quality and it was sufficient to prove that it was possible to capture an environment such as an underground mine. The VR tour of the DigiMine mock mine is accessible through a cloud-based program. The user can access the environment through an internet connection and a hyperlink that would automatically divert to the specific VR tour as illustrated in Figure 3.

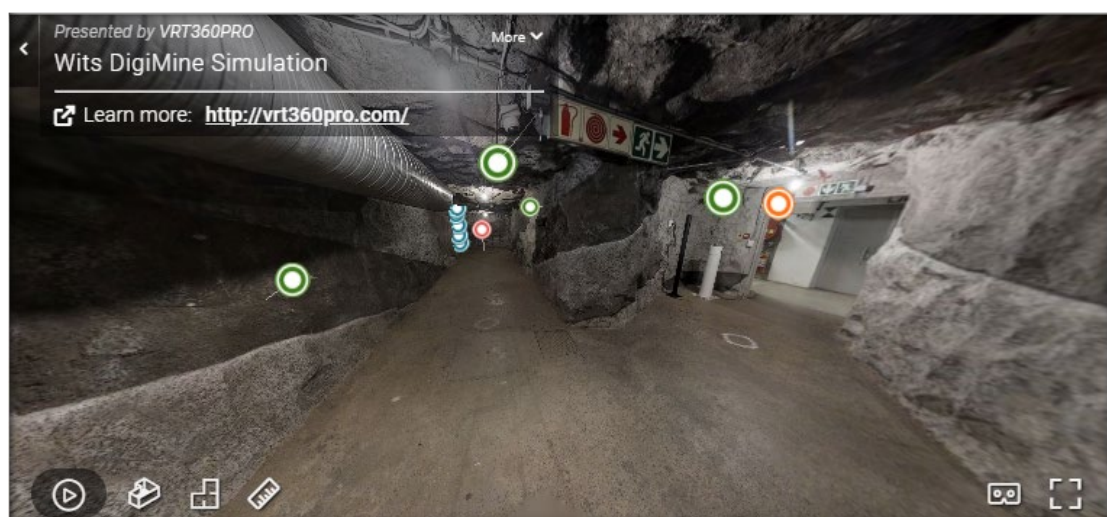


FIG 3 – Screenshot of the VR Tour on a web browser (my.matterport.com).

The VR tour created from the #D scan enables the user to rotate and manipulate the view of the scanned area to visualise the environment from any viewpoint. The user can choose between different visualisation options such as plan view, side views and rotational views. The user can observe the environment from a bird's-eye view and zoom in and out as required. Once the user

accesses the environment, the user is effortlessly placed in the environment and observations can be made as if the user was standing in the physical environment.

This specific VR tour has been made available to the University of the Witwatersrand and used as part of the Geological Modelling course. The students make use of the VR environment to access the tunnel for mapping purposes while they are busy modelling the geological structures in the mock mine. This method saves time because the students can access the environment from the comfort of their homes, office, class or any other location where they might be working. The VR tour is also used as part of the introduction for the students to explain what they are going to observe in the DigiMine mock mine and what is important during the physical visit in the tunnel. The VR tour can also be used as part of the induction and safety briefing process as the experience indicate the location of emergency exits and fire extinguishers.

THE APPLICATION OF PHOTOGRAMMETRIC SCANNING, CASE TEST 2

A scan of a tunnel boring project on a platinum mine was undertaken to test the efficiency of the scanner under realistic mining conditions. The challenges of lighting highlighted during the proof of concept study required an immediate solution in order to complete this work. Although the site assured the surveyor at the time of preparation was that the working place was well illuminated it was decided to develop a lighting system to pre-empt any potential complications on-site. It is necessary to provide the 3D scanner with a lightweight, compatible, and portable solution that could be attached to the camera and provide enough light to mitigate the effect of poor illumination while at the same time not affecting the rotation capability of the camera. It was decided to use two light-emitting diode (LED) flashlights and attach them above and below the lenses of the camera. It required the lights to be stripped down to their essential components. Due to the increased power demand of the system, it was decided to supplement the onboard batteries with an external USB power supply.

The camera was taken underground and set-up with the modified lighting solution. The environment was well illuminated but certain sections of the tunnel did not have adequate illumination. The LED lights were switched on throughout the entire duration of the scan that lasted approximately ninety minutes.

The expectations of the VR experience were very high and although the environment was similar to that of the DigiMine mock mine one could not replicate the environmental conditions such as water, humidity, dust and ventilation that did affect the set-up of the camera. The environmental conditions prolonged the set-up process but ultimately did not affect the quality of the VR experience as indicated in Figure 4.



FIG 4 – Rotated section view of VR experience (my.matterport.com).

The acquisition of the scans proved to be challenging due to the environmental conditions because the water and moisture making it slippery underfoot to set-up. During the scan, there were power failures that caused the ventilation to change and that affected the visibility due to dust in the tunnel. The operator could not prepare or mitigate the effect of the dust except to wait until the power was

restored and the effect of the dust had subsided. The scanning was concluded even though there were minor challenges but nothing that had a significant impact on the quality of the VR experience of the tunnel.

EXAMPLES OF THE APPLICATION OF LASER SCANNING

Due to the sensitive nature of incident investigations, this case study is based on images and documentation obtained from non-related incidents investigated over several years. In Figure 5, an example of a trackless mining machine involved in an accident is illustrated. The low roof height and significant damage to the equipment make the identification of contributing evidence difficult. In this example, the final output from the investigation was a two-dimensional plan and cross-section based on CAD drawings of the OEM equipment involved in the incident.



FIG 5 – An example of a vehicle damaged in a blast.

The accuracy of laser scanners is in most cases within 1 mm, although this is dependent on the type and range of the specific instrument. (Colombo & Marana, 2010). The accuracy of laser scanning can be influenced by wet surfaces, highly absorbent features such as coal seams. The advantage of an accurate point cloud is that distances can be measured between any of the objects scanned. Laser scanning on its own does not require illumination to measure and can therefore be used in poor lighting conditions. Because the measurement does not require physical contact with the objects surveyed, the scanning of an object will not affect the stability or integrity of an object. These measurements combine to form a grey scale point cloud. Although lighting will improve the quality of data, a very accurate image can be obtained in low to no lighting conditions. The penetration of the laser can provide some evidence of blast damage and sockets as indicated in the image of a scan below. In addition, the scan data can be compared to the mine design that in turn may provide better insight to contributing factors leading to the incident amount of over and underbreak in the excavation. The condition of the hanging wall and sockets are visible in the excavation. Figure 6 indicates a LiDAR pointcloud of an excavation compared to the plan view of the excavation.

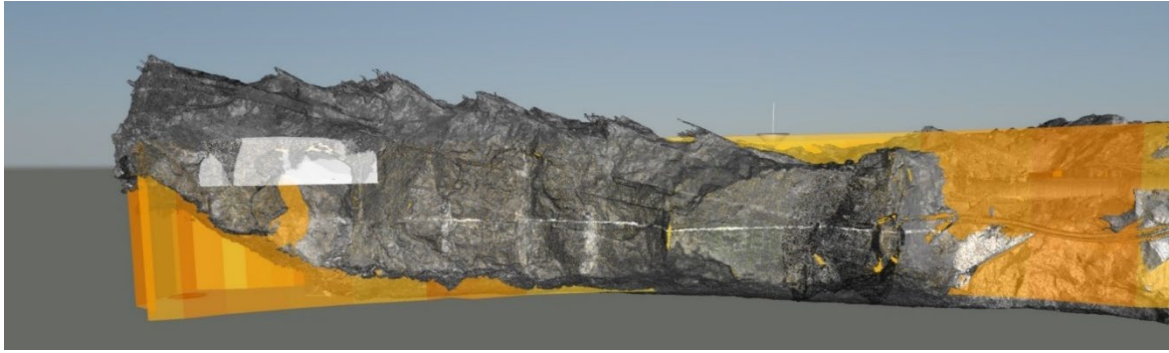


FIG 6 – Hanging wall conditions and the mine design.

In the next example, the hanging wall conditions can be observed by moving ‘outside skin’ of the scan and looking at the scan from an external perspective. Although cross-sections may have been able to document some of the shapes of the excavation, this point cloud represents the entire excavation in a 3D visual of an excavation as indicated in Figure 7.

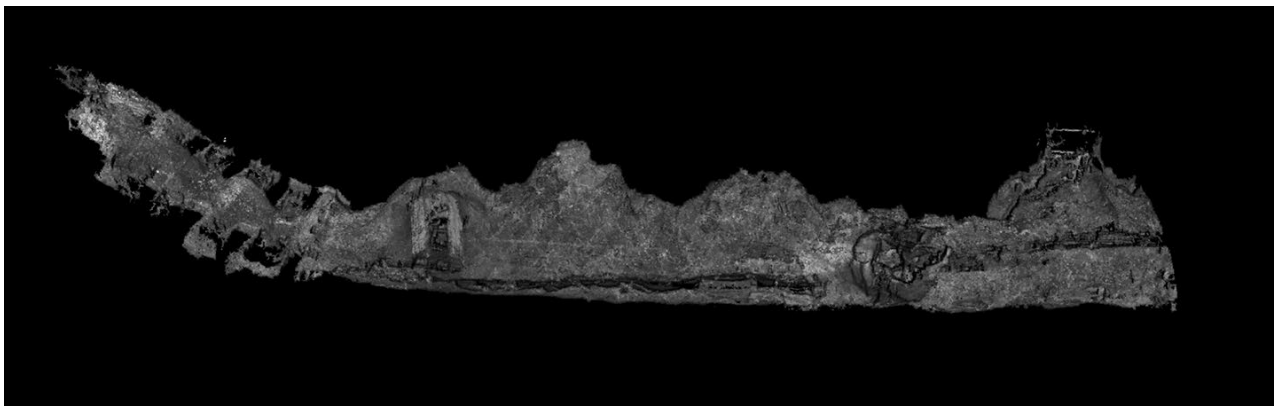


FIG 7 – Cross-section of a point cloud.

Figure 8 shows a greyscale image of the cross-section shown in Figure 7. The complexity and clutter of material and equipment in this very restricted environment would not be adequately captured by a sequence of photographs or conventional surveying methods.



FIG 8 – A typical complex cross-cut environment.

Laser scanning with HDMI photographs can present a more detailed and realistic picture than plain grey scale images. Figure 9 shows a 360-degree panoramic image of a face of a 1.7 m high platinum

stope scanned to map the position of ground penetrating radar points and geology. An external view of the same panel in a pointcloud view shows the presence of drill holes and blasting damage as well as prominent jointing in the hanging wall of the excavation. The paint lines from the production crew can be clearly seen in the scan.

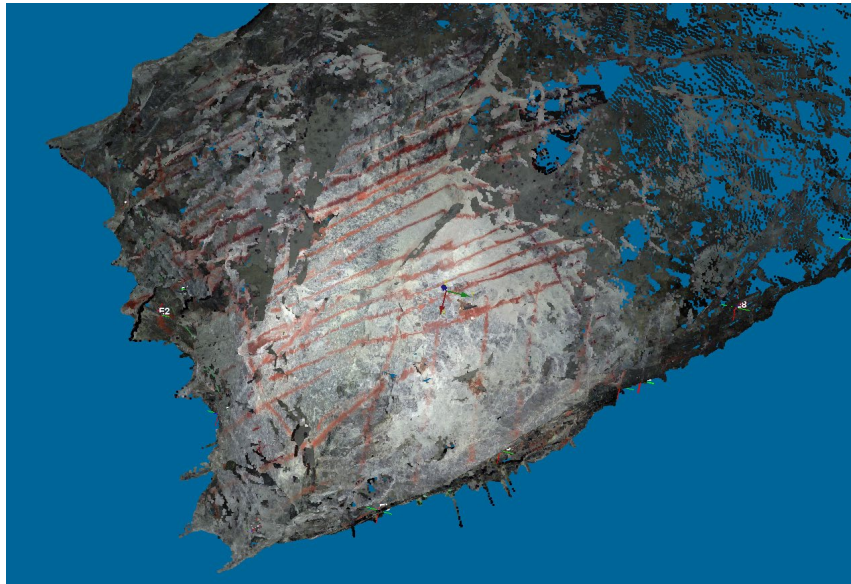


FIG 9 – Top view of the hanging wall of the excavation.

A cross-sectional view of the panel indicated in Figure 10 shows the geology clearly and the profile of the hanging wall and footwall.

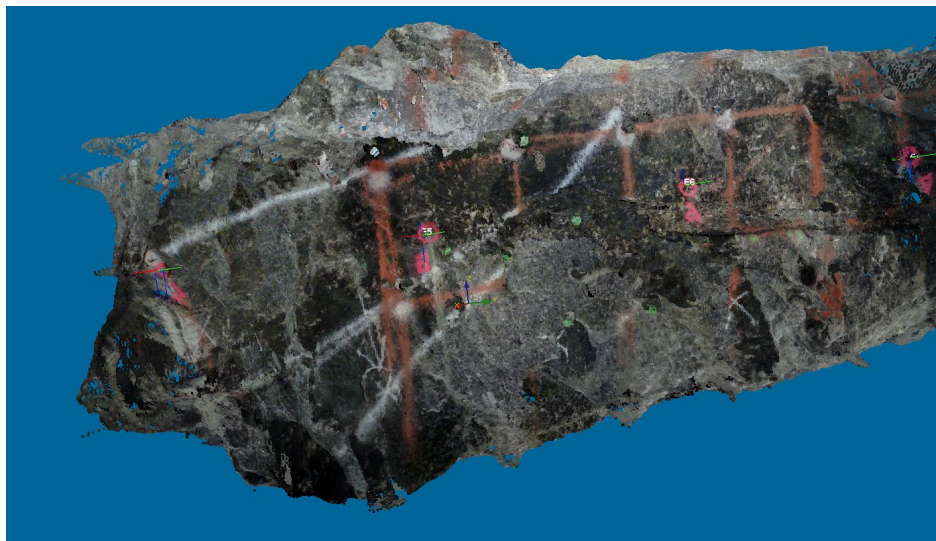


FIG 10 – Cross-sectional view with geology and blast damage.

In the scan of an orepass development, the point cloud can be used to identify the safety sling installed at the bottom of the excavation while at the same time providing the point of view of a person at the face of the orepass excavation looking down into the haulage. Figure 11 shows a pointcloud view of the safety net and the excavation face behind the net from a single scanner set-up.

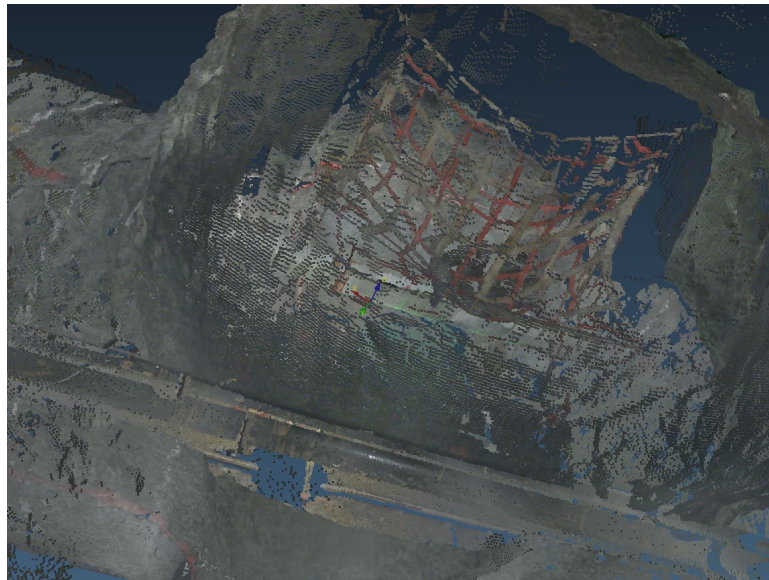


FIG 11 – Orepass view from the face into the cross-cut.

FINDINGS AND ANALYSIS

The foregoing case studies proved that it is possible to capture an underground mining environment in 3D and make it available in a VR environment. The effect of the illumination on the quality of the VR experience must be addressed to ensure that the VR experience remains of high quality. It was proven that external and additional lighting will improve the quality of the VR experience, but environmental conditions such as water, humidity, dust and ventilation will create additional challenges and may affect the quality of the data captured.

The purpose of the study was to investigate whether VR will improve the quality of investigations when an accident or fatalities occur in the mining industry. It is critical to improve the current investigation methods because this will directly influence the safety performance of the mine (Stemn *et al*, 2019).

Mine surveyors are increasingly making use of 3D scanners to record significant injuries and fatality scenes (Webber-Youngman *et al*, 2019) in the mining industry. 3D scans provide a point cloud with large amounts of data that is significantly more than the traditional 2D plans and photographs (Webber-Youngman *et al*, 2019). The use of 3D laser scanners mitigates the shortfalls of the traditional methods.

The point clouds that are generated by the 3D laser scanners can be difficult to navigate. There is a need to enhance the visualisation of the recorded scenes. VR will not only improve the visualisation but will also allow the user to be immersed in the scene (Mures *et al*, 2016). It was found that the VR experience was enhanced due to the ability to manipulate the view of the scanned environment and visualise the environment according to the preference of the user. The added benefit of the VR scan is that the user is capturing the scene with a high level of accuracy and a very high level of detail.

3D documentation and geometric reconstruction methods enable the investigators to prove correlations between the injury-causing object and the injuries caused to a victim (Buck *et al*, 2006). This enables the investigating team to link injuries sustained to an injury-causing object.

It is argued that in an incident where a person sustains injuries when encountering a scraper winch in a raise, the spatial data obtained from the proximity warning system on the scraper winch can be used in conjunction with the MRI scan and the scene scan to critically investigate and reconstruct the incident as illustrated by the cyclist case study described by (Buck *et al*, 2013). The VR scan would provide a digital copy of the entire scene in the condition it was during the investigation and safeguard the evidence in the form of a VR tour of the scene (Eyre *et al*, 2017).

The application of post-incident scanning and scanning for structure monitoring for prevention is well-established in law enforcement and industrial applications. Laser scanning data and VR representation can provide first-responders with a valuable tool for understanding the environment

in which a rescue operation must be performed. The advantage of a scanning device on a mobile platform would be that an incident scene may be surveyed and mapped in a short time by the initial response team. In a complex rescue scenario a 3D image could provide response teams with a better understanding of the positioning of patients as well as the safety conditions, access routes and risk areas to be avoided (Grobler, 2018).

CONCLUSIONS AND RECOMMENDATIONS

The research clearly illustrates that the use of VR will improve the quality of investigations when accidents or fatalities occur in the mining industry. It can be accepted that a further improvement in the safety performance in the mining industry is needed. The literature has proven that the safety performance of a mine is directly dependent on the quality of the accident investigations.

The application of reality capture systems such as photogrammetric systems and LIDAR scanning systems highlight some of the challenges and shortcomings in technology. Photogrammetric systems require excellent lighting conditions and reasonable environmental conditions to operate effectively. Lidar systems can provide a detailed point cloud of the area of interest in zero light conditions but may require additional lighting when combined with panoramic camera systems should a coloured point cloud be required.

Both types of systems can capture a high level of detail that is not possible with conventional tacheometric and tape surveying methods. The level of three-dimensional detail provides the end-user with a realistic sense of immersion into the captured scene and enables the user to inspect and analyse the scene as if the user was actually on the scene. The data integrity of laser scanning and images reduces the potential corruption, misrepresentation or intentional tampering with evidence and safeguards the evidence for future analysis and investigation. This is sometimes seen as a double-edged sword as the unbiased capture of the facts in a point cloud may prove innocence or guilt where conventional investigative techniques may have missed evidence. In many, it may be difficult or impossible to re-visit the scene of an incident or access the surrounding area for follow up investigations. 3D point clouds and VR allow the opportunity to capture the scene in one visit and the remainder of the investigation can be done in a virtual environment. The method of capture and digital representation allows for the easy manipulation of images to a specific witness's viewpoint and extract measurements and dimensions from the data.

The use of VR to capture incidents and safety hazards can be used effectively to document, investigate and analyse conditions to inform training and mitigating actions in the mining industry. It is argued that the drive to 'zero-harm' can be informed through improved forensic investigation techniques and documentation. The cost of 3D lidar and photogrammetric VR systems may be considered to be high but as these systems have a multitude of value-adding benefits in engineering, mining, and geology capture, these start-up costs can be written off against the tremendous value that is created by VR. This methodology could be leveraged by the mining houses to show their commitment to safety and use the VR to take the inspectors of the DMR directly to the scene in a virtual environment and remove any misconceptions an investigation team may be labouring under.

The fundamental reason for an investigation is to prevent a reoccurrence, mitigate any contributing factors that may have led to an incident or accident and identifying the root causes of the incident. Any such investigation must be above any suspicion of bias and requires irrefutable, accurate facts in order to be conducted objectively. Unfortunately, some of the current methods of investigative data capture methodologies are not accurate enough and may not correctly be identifying the real factors that led to an incident. Consequently, identifications of controls that have failed, or that must be introduced, cannot be identified with a high level of confidence. To improve the identification of these factors, one must be able to understand what happened during the event and use that knowledge to cross-examine the witnesses to either accept or disregard their version of the event.

By making use of 3D SLAM scanners and possibly a VR camera, one can combine the data for an accurate and true representation of the scene and the creation of a digital twin (DT). The DT is a virtual model that is a precise representation of the physical environment.

The DT model is used as the main component to accurately reconstruct the incident that is being investigated. Any device that has timestamp data can be added to the model. The internet of things can now allow the combination of a DT model and 'timestamped' spatial data such as the data that

are increasingly being collected by proximity monitoring systems, equipment in the vicinity of the incident, camera and other operating systems to more accurately reconstruct the sequence of events leading up to an incident.

The methodology may enable the animation of events and the chain of evidence with the help of avatars (the representation of a human in digital space) of the witnesses in the DT. Such technology will enable an investigation team to develop a clearer understanding of individual points of view of the incident. A comprehensive DT should be able to provide corroboration of witness reports or provide data to refute the evidence provided and inform the conclusions and recommendations reached by the investigation. The repercussions of identifying the incorrect cause of the incident may have further fatal consequences if it goes unidentified. In the case where a similar incident re-occurs, blame may be shifted to the management team for taking inappropriate or ineffective preventative measures to prevent such an incident. The cost of implementing new controls and retraining of staff will have a significant impact on the financial status of the operation. If these measures are based on incorrect conclusions drawn from a poorly or incorrectly documented incident investigation. Controls will, directly and indirectly, have a financial effect on the operations. When controls are introduced, the mine must have a high degree of confidence in their findings. The level of confidence provided by 3D scanning and reality capture should be adopted by an industry that is serious about a culture of 'zero harm'.

REFERENCES

- Adams, G, November 2011. Business Leader' Health and Safety Forum. <https://www.zeroharm.org.nz/assets/docs/case-studies/Coca-Cola-Case-Study.pdf> (accessed 27 March 2020).
- Brennan, P F, Ponto, K, Casper, G, Tredinnick, R and Broecke, M, 2015. Virtualizing living and working spaces: Proof of concept for a biomedical space-replication methodology. *Journal of Biomedical Informatics*, vol 57, 2015: 53–61. <https://www.sciencedirect.com/science/article/pii/S1532046415001471> (accessed 24 April 2020).
- Buck, U, Naether, S, Braun, M, Bolliger, S, Friedrich, H, Jackowski, C, Aghayev, E, Christe, A, Vock, P, Dirnhofer, R and Thali, M, 2006. Application of 3D documentation and geometric reconstruction methods in traffic accident analysis: With high-resolution surface scanning, radiological SC T?MRI scanning and real data based animation. *Forensic Science International*, 2006: 1 – 9. <https://europepmc.org/article/med/16997523> (accessed 14 April 2020).
- Buck, U, Naether, S, Räss, B, Jackowski, C and Thali, M, 2013. Accident or homicide – Virtual crime scene reconstruction using 3D methods. *Forensic Science International* vol: 225, 2013: 75 – 84. <https://www.sciencedirect.com/science/article/pii/S0379073812002587> (accessed 10 March 2020).
- Department of Mineral Resources, 2018. Annual Report. 2017/2018. https://www.gov.za/sites/default/files/gcis_document/201810/mineral-resources-annual-report-20172018.pdf. (accessed 11 April 2020).
- Eyre, M, Foster, P, Speake, G and Coggan, J, 2017. Integration of Laser Scanning and Three-dimensional Models in the Legal Process Following an Industrial Accident. *Safety and Health at Work*, Vol 8, Issue 3, 2017: 306–314. (accessed 19 March 2020).
- Hämäläinen, P, Takala, J and Kiat, T, 2017. Global estimates of occupational accidents and work-related illnesses 2017. *Singapore: Workplace Safety and Health Institute*, 2017. <http://www.icohweb.org/site/images/news/pdf/Report%20Global%20Estimates%20of%20Occupational%20Accidents%20and%20Work-related%20Illnesses%202017%20rev1.pdf> (accessed 05 April 2020).
- Health and Safety Executive, 2004. *Investigating accidents and incidents*. HSE Books, HSG245, 2004. <https://www.hse.gov.uk/pubns/hsg245.pdf> (accessed 25 May, 2020).
- Hinze, J, 2002. Safety plus: Making zero injuries a reality. Research Report 160–11. March 2002, University of Texas at Austin, Austin, Texas. Gainesville, pp. 110.
- Johnson, D, 2018. Tesla's journey to be the world's safest factory — 10 takeaways, *Industrial Safety and Hygiene News*. <https://www.ishn.com/articles/109463-the-journey-to-be-the-worlds-safest-factory-10-takeaways> (accessed 07 April, 2020).
- Jusko, J, 2019. Siemens Takes a 'Zero Harm Culture' Approach to Safety, *Industry Week*. <https://www.industryweek.com/operations/article/22028630/siemens-takes-a-zero-harm-culture-approach-to-safety> (accessed 24 March 2020).
- Laing, R and Scott, J, 2011. 3D high-definition scanning: Data recording and virtual modelling of the built heritage. *Journal of Building Appraisal*, 6, 2011: 201–211. (accessed 21 April 2020).
- Leistikow, I, Mulder, S, Vesseur, J and Robben, P, 2017. Learning from incidents in healthcare: The journey, not the arrival, matters. *BMJ Quality and Safety*, 2017: 252–256. (accessed 11 March 2020).

- Martin, J, Lardy, A and Laumon, B, 2011. Pedestrian Injury Patterns According to Car and Casualty Characteristics in France. *Association for the Advancement of Automotive Medicine vol: 55*, 2011: 137 – 146. (accessed 01 April 2020).
- Morrish, C, 2017. Incident prevention tools—incident investigations and pre-job safety analyses. *International Journal of Mining Science and Technology, Vol 27, issue 4*, July 2017: 635–640. (accessed 10 April 2020).
- Morrison, N, 2017. Donald Trump is not the biggest threat to global business. *Forbes*. <https://www.forbes.com/sites/nickmorrison/2017/02/09/donald-trump-is-not-the-biggest-threat-to-global-business/#5a620c641b73> (accessed 14 April 2020).
- Mures, O, Jaspe, A, Padrón, E and Rabuñal, J, 2016. Virtual Reality and Point-Based Rendering in Architecture and Heritage. In *Handbook of Research on Visual Computing and Emerging Geometrical Design Tools*, by Guiseppe Amoroso, 549–565. IGI Global, 2016. http://publications.crs4.it/pubdocs/2016/MJPR16a/vcegd2016-pbr_architecture_heritage.pdf (accessed 19 April 2020).
- Ren, P, Shui, W, Liu, J and Fan, Y, 2018. A Sketch-based Rapid Modelling Method for Crime Scene. *Journal of Digital Forensics, Security and Law: Vol. 13: No. 1, Article 8*, 2018: 43–58. <https://commons.erau.edu/cgi/viewcontent.cgi?article=1484&context=jdfsl> (accessed 29 March 2020).
- Stemn, E, Bofinger, C, Cliff, D and Hassall, M, 2019. Investigating the Maturity of Incident Investigations. *Safety*, 5 (1), 2019: 30. <https://www.mdpi.com/2313-576X/5/1/3> (accessed 15 April 2020).
- Tung, N, Sheppard, D, Elliot, D, Tottey, L and Walsh, K, 2015. Spherical Photography and Virtual Tours for Presenting Crime Scenes and Forensic Evidence in New Zealand Courtrooms. *Journal of forensic science*, 60, 2015: 753–758. (accessed 05 April 2020).
- Webber-Youngman, R, Grobler, H, Gazi, T, Stroh, F and van der Vyver, A, 2019. The impact of forensic laser scanning. *The Journal of the Southern African Institute of Mining and Metallurgy, Vol 119*, 2019: 817–824 (accessed 15 April 2020).
- Webber-Youngman, R and van Wyk, E, 2013. Incident reconstruction simulations—potential impact on the prevention of future mine incidents. *The Journal of The Southern African Institute of Mining and Metallurgy, vol 113*, 2013: 519–528. (accessed 12 April 2020).

Space mining

Picturing the future – assessment of mining systems needed for lunar volatiles excavation

M Bates¹, A Williams², P Siribalamurali³, J M Chua⁴, Z Li⁵ and C Zhang⁶

1. School of Mechanical and Manufacturing Engineering, UNSW, Sydney NSW 2033.
Email: m.bates@student.unsw.edu.au
2. School of Mechanical and Manufacturing Engineering, UNSW, Sydney NSW 2033.
Email: anjelica.williams@student.unsw.edu.au
3. School of Mechanical and Manufacturing Engineering, UNSW, Sydney NSW 2033.
Email: p.siribalamurali@student.unsw.edu.au
4. School of Mechanical and Manufacturing Engineering, UNSW, Sydney NSW 2033.
Email: j.chua@student.unsw.edu.au
5. School of Materials Science and Engineering, UNSW, Sydney NSW 2033.
Email: zihao.li2@student.unsw.edu.au
6. School of Minerals and Energy Resources Engineering, UNSW, Sydney NSW 2033.
Email: chenggou.zhang@student.unsw.edu.au

INTRODUCTION

As humanity looks to move into a new frontier, the frontier of space, the need for resources off of Earth will only increase with time. Resources collected off-Earth on moons and asteroids will be used for construction of larger spacecraft and colonies; they will fuel transportation throughout the solar system, and provide life support for crews. Of particular interest to this investigation are resources that will assist in the early phases of off-Earth mining operations, resources like ice, which allow for the production of drinking water, breathable air, and rocket fuel. This extended abstract will mainly cover the following topics: past research into complete mining systems, realistic mass constraints for the next decade, specifics of the lunar environment, and an overview of the proposed mining system, that are considered include excavation, control, power, and resource transportation. The outcome of this paper will provide insights into the feasible off-Earth resources extractions.

BACKGROUND

Research into how lunar mining colonies could optimally operate suggest that a multi-phased approach is ideal. The approach looks to build out each component of the system in succinct phases, allowing for comprehensive testing and validation of each systems integrity before moving on the next. Systems like power and maintenance are the first systems to be deployed while the mass excavation systems are the final phase of deployment. Another aspect of off-earth mining to be considered are the constraints of mass and volume imposed by the available launch vehicles. Any building components for early to mid-stage mining colonies will need to come from Earth via rockets, which can only lift so much mass per launch and are traditionally expensive. In the next decade, this upper limit appears to be around 100 tonne per launch while component dimensions must fit in a 9 m diameter by 18 m long cylinder (SpaceX, 2021). However, the costs of launching are expected to rapidly decline as modern heavy lift vehicles come online in the early 20's, allowing for launch frequency to increase.

LUNAR ENVIRONMENT

Off-Earth mining encompasses mining asteroids, moons, and other planets; however, The Moon is the body of choice for this study due to its accessibility, non-negligible gravity, and confirmed presence of ice. The lunar environment is unique and imposes a range of novel technical challenges. The regolith is a fine, abrasive dust with characteristics like wet sand. It is electrostatically charged causing it to 'stick' to machinery. These properties of the dust cause significant wear and tear on moving parts, increasing the maintenance needed. Due to the inaccessibility of the moon, traditional maintenance will not be possible. Therefore, designs will be heavily constrained in the number of moving parts that are used, and will need to accommodate means of operation that work without maintenance.

Other environmental aspects include the day-night cycles on The Moon, at 28 days they cause surface temperatures to fluctuate 100s of degrees either side of 0° Celsius (Hauser, 2020). The gravity on the surface is 1/6th of Earth's gravity, reducing the feasibility of excavation methods that rely on gravity to stay grounded while pushing against orebodies. Not to mention the lack of atmosphere, eliminating thermal convection and natural pressurisation of gas systems. All together, these contextual aspects of operating a lunar mining colony will affect the design of the system. As indicated by the orange outlines in Figure 1, the South pole of the moon contains many permanently shadowed regions. These regions are believed to contain the highest concentrations of ice due to the absence of sunlight (Tabor, 2018). Conversely, there exist regions shown in the left figure that are permanently lit, ideal for power generation.

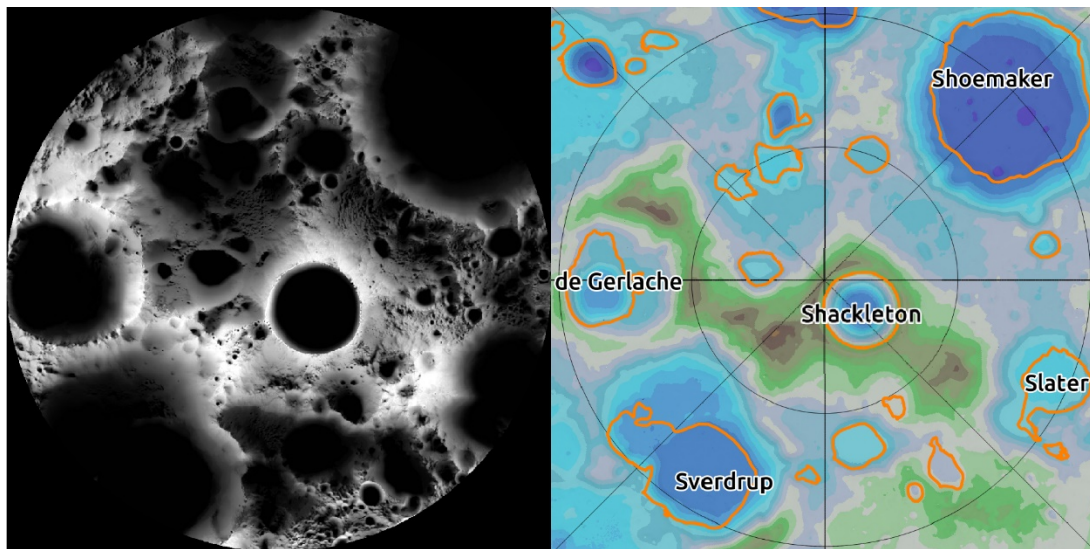


FIG 1 – Lunar light (left) (NASA Science, 2019) and topographic (right) (LROC, 2021) profiles.

MINING SYSTEMS

The respective mining systems considered in the lunar environment are the excavation, control, power, and resource transportation systems. These systems are chosen due to the differences in design compared to traditional systems due to Lunar constraints. There is no need to re-invent the wheel so where possible designs have adapted traditional methods. For the excavation system, a hollow bucket drum design is opted to collect and store regolith. The drum will then counter-rotate to unload material. This allows for a reduced part count with a single motor and solid drum piece. Two drums on either end of the excavator will rotate in opposite directions, partially anchoring the vehicle during excavation and alleviating the challenges of low gravity. Due to the maintenance requirements and mass constraints the system will utilise a fleet of smaller, vehicles rather than fewer larger vehicles. This provides redundancy for component failure in that the loss of a vehicle will not significantly impact the mining operation.

The power system will not be able to utilise existing infrastructure and will be a closed-loop design. Energy requirements of the system will be determined by the scale of operation, however scaling up the system will be easier than setting it up due to the self-perpetuating nature of power; existing energy can be used to produce facilities that produce more energy but the initial production will start from scratch. For power generation solar is the optimal source, with nuclear facing political challenges and fuel cells requiring hydrogen to be brought from Earth. Power storage will be needed for eclipse periods with batteries used for short-term storage and hydrogen generation used for long-term storage. Batteries allow for instantaneous power distribution but linearly increase in mass as storage capacity increases. Hydrogen storage however require hydrolysis, fuel tanks, and fuel cells. The storage itself is in the form of tanks, which can be scaled more efficiently than batteries due to the ratio of scaling surface area to volume. Lastly, the design incorporates a conveyor-belt-like material transport system with no touching moving parts. Ore will be placed in trays that passively levitate on lightweight electromagnetic tracks. Similar to a Maglev train, the trays can be moved frictionlessly from the collection site to a processing part. This system is scalable over large distances, requires little to no maintenance, and consumes minimal power.

ACKNOWLEDGEMENTS

The authors would like to acknowledge the UNSW School of Minerals and Energy Resources Engineering for access to facilities and resources.

REFERENCES

- Hauser, A. (2020) 'CRADLE-California Research Analog for DeepSpace and Lunar Environments', in *ASCEND 2020*. American Institute of Aeronautics and Astronautics (ASCEND). doi: 10.2514/6.2020-4186.
- LROC (2021) *Permanently Shadowed Regions | Lunar Reconnaissance Orbiter Camera*. Available at: http://lroc.sese.asu.edu/psr/SP_830760_0866010 (Accessed: 21 April 2021).
- NASA Science (2019) *Illumination Map of the Moon's South Pole*, *NASA Solar System Exploration*. Available at: <https://solarsystem.nasa.gov/resources/2329/illumination-map-of-the-moons-south-pole> (Accessed: 25 July 2021).
- SpaceX (2021) *SpaceX Starship*, *SpaceX*. Available at: <http://www.spacex.com> (Accessed: 25 July 2021).
- Tabor, A. (2018) *Ice Confirmed at the Moon's Poles*, *NASA*. Available at: <http://www.nasa.gov/feature/ames/ice-confirmed-at-the-moon-s-poles> (Accessed: 6 July 2021).

Off Earth mining? Watch this space...

N J Bennett¹ and A G Dempster²

1. PhD Candidate, Australian Centre for Space Engineering Research, UNSW, Sydney NSW 2052. Email: nicholas.j.bennett@student.unsw.edu.au
2. Director, Australian Centre for Space Engineering Research, School of Electrical Engineering and Telecommunications, UNSW, Sydney NSW 2052. Email: a.dempster@unsw.edu.au

ABSTRACT

Is the profitable exploitation of space resources like fusion technology? Only 20 years out, and always will be. The authors think not! Space resources viability could change rapidly with modest improvements to the certainty and disposition of resources and to the required technologies.

The first connection between Space Resources and the terrestrial economy will be by contributing to the existing space operations economy. All the current lifting of geostationary equatorial orbit satellites could be performed using propellant derived from water ice at the lunar poles. Lunar derived propellants could also supply the developing market for satellite servicing and station keeping, or orbit modification, propellants in sun synchronous and geostationary equatorial orbits. Safely removing dangerous orbital debris will require substantial amounts of propellant. Lunar propellants could contribute to the sustainability of the US Artemis and other mooted international lunar and Mars exploration programs. There is the potential for even larger propellant markets lifting space based solar power stations. Supplying the SpaceX Mars program would require a million tons of lunar propellant in low Earth orbit every 26 months.

For a mining style cash flow pattern, large initial investments followed by ongoing positive revenue, the time horizon to achieve an internal rate of return (IRR) hurdle can be very sensitive to changes in the ratio of the initial cost to ongoing revenues. Modest changes can pull the time to achieving a viable IRR from forty years down to a decade. Ongoing public investments in lunar scientific exploration, resource utilisation proofs of concept, and pilot plants will prepay initial costs and reduce uncertainty. The authors' work focuses on understanding uncertainty, reducing production costs, and increasing revenues per ton mined on the Moon.

Off Earth mining has many layers: choice of resource, excavation, beneficiation, extraction, power, transportation, logistics, products, markets, and the players. In many cases, improvements on one layer multiply with those of another. By doubling the market price, the efficiency of extraction, and transportation efficiency, one achieves an eight times improvement in recoverable value.

INTRODUCTION

Figure 1 plots the time to reach a 20 per cent internal rate of return (IRR) against the ratio of initial costs to ongoing revenue, generated from a simple mine-like idealised cash flow model with a single large initial cost and a series of subsequent annual revenues. Reducing the ratio from four to five reduces the time to viability by thirty years. Informed by results from their research the authors contend that at some point space resources business cases will approach an inflection point like the one illustrated, and that cost to revenue reductions on the scale required to significantly affect the viability horizon are likely.

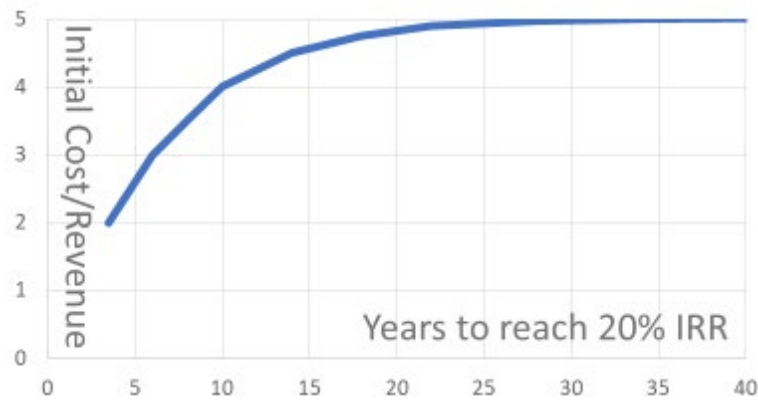


FIG 1 – Time to reach a viable IRR versus the ratio of initial cost to ongoing revenue, illustrating the sensitivity.

The authors present some examples from their research into the use of rocket propellant derived from water ice that is present at the lunar poles. This propellant may be transported, thus consuming some production output, and sold or used to provide services directly. Depositing GEO satellites in their beginning of life orbits is an example where the customer only wants a transportation service, in contrast the SpaceX Mars program could only use oxygen as oxidiser as part of their methalox (CH₄LOX) propellant.

The so-called tyranny of the rocket equation, that there are diminishing returns from adding propellant to solve a transportation problem, is also an opportunity; one can engineer large reductions in transport cost by breaking the problem into smaller chunks. In the space domain movement is denominated in delta-v, change of velocity, to move between orbits or change their shape and orientation one must invest delta-v by expending propellant. Any orbital change costs propellant, and most is expended in moving propellant will be needed later in the trip. Moving mass around cislunar space, the area around the Moon and the Earth, is very propellant expensive, the image to keep in mind is using a petrol tanker to deliver a briefcase.

It is clear that finding a lower propellant cost transportation pattern will increase the revenues of a lunar propellant producer, since more of the propellant produced on the Moon is available as delivered product, but similar kinds of opportunities occur throughout the production chain from extraction through to delivery. These opportunities often multiply their effects through the chain and can have non-linear pay-offs as the rocket equation does.

A fruitful research method used by the authors is to take a published proposal and deconstruct the underlying model and assumptions, then rearchitect using the same building blocks. The existing proposals embodies significant effort in determining underlying geophysics and space systems properties, and so provide high quality building blocks, rearranging them can often deliver improvements to key metrics while retaining the solid foundation provided by the original proposals.

SPACE RESOURCES EXAMPLES

The examples show a range of techniques that deliver internal rate of return improvements to other published proposals, these can simultaneously reduce costs and increase recoverable revenue, reducing the cost to revenue ratio and reducing the time to viability.

The chicken and egg problem

The lunar propellant chicken and egg problem is that neither miners nor customers will invest before the other. Satellite operators will not invest in being lunar propellant ready until lunar propellant is available, and no one will invest in lunar propellant production without customers able to take delivery of the product. Satellite orbit raising from Low Earth Orbit (LEO) to geostationary equatorial orbit (GEO) is a common use case for lunar water derived hydrolox rocket propellant (LH₂LOX) (Kornuta *et al*, 2019). The GEO satellites that currently lift themselves from Geostationary Transfer Orbit (GTO) to GEO using onboard propulsion are unable to make use of hydrolox, but they would be customers for a 'lift' service, which one could provide using tugs filled with lunar propellant.

When inserted into a published financial model, shifting from supplying rocket fuel in LEO to a satellite raising service in GTOs increased IRR from 5 per cent to 50 per cent. This is possible because GTOs are costly to get into from Earth, and thus any mass you deliver there has high value, and cheap to get into from the Moon (Bennett and Dempster, 2020). In comparison with a business selling lunar propellant in LEO to support GEO lift; the GTO tug business needed a mine about 10 per cent the size and could recover at least five times the revenue per ton of water extracted.

Every year about 20 GEO satellites are left in a GTO; they subsequently burn half their mass or spend months before they can begin earning in GEO. Satellite operators spend, or forgo, from one-half to two billion dollars per annum on this segment of GEO launch, which could be provided by a lunar-based tug using propellant manufactured on the Moon, as illustrated in Figure 2. The authors performed further elaboration of the GTO tug work as part of *Aqua Factorem*, a NASA Innovative Advanced Concepts (NIAC) project (Metzger, 2020). This showed one could supply the current market with about 200 tons of water per annum, which means one could recover between 2.5 to 10 million dollars per ton for lunar water extracted.

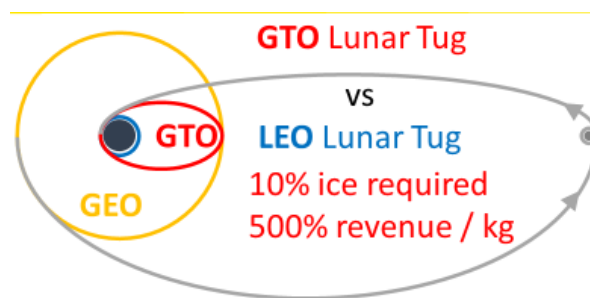


FIG 2 – GEO satellite orbit raising with lunar tugs, from LEO versus from GTO.

These GTOs are also ideal for pushing mass around cislunar space, the lift service can expand as the markets do. From a suitably oriented GTO it costs about the same delta-v to get to Low Lunar Orbit (LLO) as to get to GEO, so lunar propellant could contribute to moving mass to the Moon in support of the US Artemis or European Moon Village programs. Moving mass in this kind of 'bucket relay' uses substantially less propellant than either Earth or Moon taking sole responsibility. Similar GTO-like orbits are useful for interplanetary transfers, either for science payloads or for something like the SpaceX Mars project.

Expect the unexpected...

On occasion, unanticipated effects can reveal a novel opportunity. The authors' analysis of vehicle propellant efficiency shows that a market for lunar propellants in LEO is, in effect, a market for lunar manufactured propellant tanks. This is surprising since lunar metals are not usually anticipated to be useful until long after propellant production becomes viable.

A tanker that leaves the propellant in tanks at LEO and is only large enough to return its engines to the Moon can deliver 30 per cent more propellant to LEO than a roundtrip tanker. In the petrol tanker analogy, one can deliver more petrol if one leaves the whole trailer and just drives the cab back to the refinery.

This strategy requires manufacturing propellant tanks on the Moon. Propellant tanks are the simplest and cheapest part of rocket manufacture. Some propellant manufacturing techniques produce metals as a by-product, lunar soil yields about 1 per cent by weight unoxidised metals, about the right amount for tanks to hold the extracted propellant. Relativity Space's is developing additive manufacturing techniques to print propellant tanks, these techniques could be used on the Moon. If the manufacture is cheap enough, this strategy will deliver an IRR bump (Metzger, 2020).

An important caveat here is that the authors' model was for propulsive (propellant burning) transfer. There are opportunities to have the tanker perform aerobraking into LEO, a sort of partial reentry to use the atmosphere to slow down, thus providing delta-v with reduced propellant consumption. In the long-term the lunar propellant tank market concept might have only novelty value, but it is an indication that the unexpected can pop out of research.

Multiproduct mines

The canonical use case for lunar water is to produce hydrolox and sell it in Low Earth Orbit (LEO) (Kornuta *et al*, 2019). The authors found that when servicing a LEO market, supplying oxygen produces 50 per cent more revenue than hydrolox (Bennett and Dempster, 2020, 2021). Water contains 8:1 oxygen to hydrogen by mass, regular hydrolox rocket propellant contains 5.5:1, so the canonical use case discards about 30 per cent of the extracted and processed water. Since water extraction and processing dominate production costs, this is in effect discarding 30 per cent of the initial capital expenditure (Kornuta *et al*, 2019). However, one could burn all the lunar hydrolox produced to enable one to deliver the oxygen by-product. Oxygen alone is useful because both hydrolox and methalox are about 80 per cent oxygen, in fact oxygen is the only lunar product a methalox transportation system like SpaceX Starship could use. Water (H_2O) and hydrogen peroxide (H_2O_2) both contain a higher proportion of oxygen than regular hydrolox, and so can help reduce output waste. They are ideal propellants within their niches, station keeping and smaller orbit transformations in sun synchronous (SSO) and geostationary equatorial orbits (GEO). Figure 3 plots output utilisation against normalised revenue for a range of products and markets.

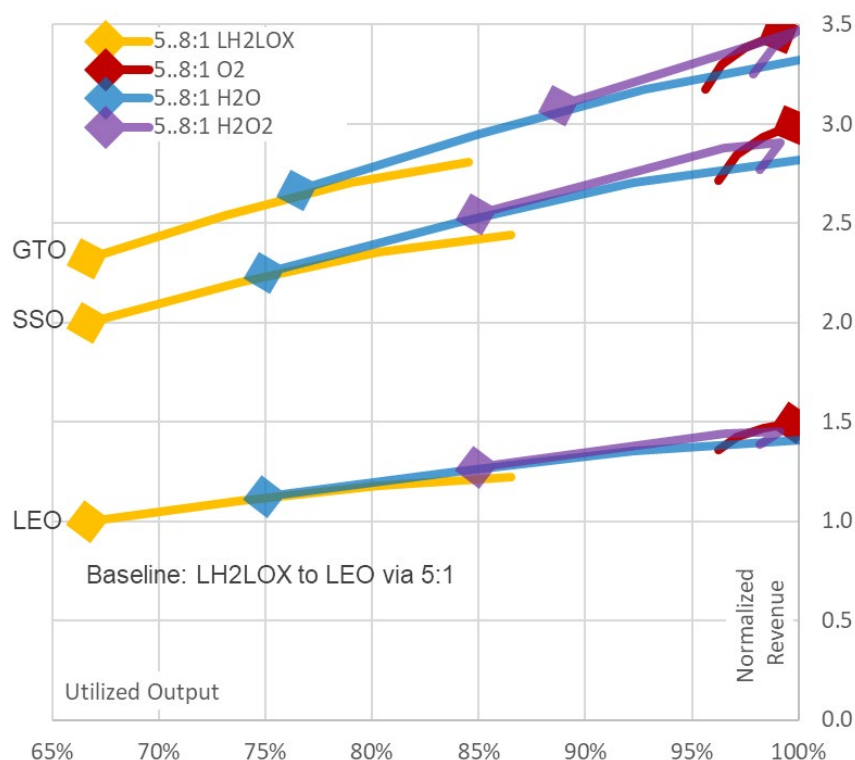


FIG 3 – Output Utilisation versus Normalised Revenue for a range of propellant products and markets.

Figure 3 shows how a lunar ice mine's products, markets, and transportation determine revenue and opportunity losses from discarded oxygen by-product. The diamonds represent product delivery by lunar hydrolox, at a 5:1 oxygen to hydrogen ratio. The x-axis shows how much mine output can be used as transportation propellant or product. The y-axis is revenue, normalised to the baseline case of selling hydrolox in LEO, the lower left yellow diamond sitting at two thirds utilised output. The lower red diamond shows that switching to oxygen as a product in LEO turns a one third opportunity loss into a 50 per cent revenue bump. Geostationary Transfer Orbits (GTOs) have lower transport costs. An Earth transport parity argument gives Sun Synchronous Orbits and GTOs higher value. The final feature is the smearing of the diamonds; rocket engines can burn 'oxygen rich' which increases the available transportation propellant but reduces its efficiency. As one moves away from the diamond more oxygen is included in the propellant, up to the 8:1 oxygen to hydrogen ratio of water. The difference between the red oxygen diamond and the best, blue, water delivery shows the impact of the reduced efficiency of high oxygen hydrolox. The purple series are the high-test peroxides that OrbitFab are planning to use in SSOs, and one can see it is a product a water mine would like to sell. A mine operator has a strong incentive to sell out of LEO, to sell oxygen, and to use variable

oxygen ratio engines to maximise deliverable product. Customers also have an incentive to use 8:1 propellant, because that gives the producer a lower cost base.

A systematic examination of products, markets, and transportation reveals a rich trade space. The simplest strategy is just to deliver oxygen. A significant opportunity revealed here is the increased flexibility pay-off for developing rocket engines that can burn oxygen rich propellant mixtures, turning oxygen by-product into useful transportation propellant. There are engineering challenges in dealing with hotter combustion, but since available heat is one of the factors limiting the scale of expander style hydrolox engines, there is reason to hope the challenges can be overcome. Producers can increase revenue by up to 50 per cent by altering transportation propellant oxygen to hydrogen ratio or delivered product, they can increase revenue by 350 per cent by also delivering to out of LEO markets.

Integrating propellant and cargo

Delivering services rather than commodity propellant also pays off when the goal is landing mass on the Moon from low lunar orbit (LLO). A recent proposal derived a viable commercial surface price of 27 M\$/t for lunar propellant, the operation could earn around 20 per cent IRR at that price (Charania and DePasquale, 2007). Using that vehicle model, one could compete with Earth sourced propellant in low lunar orbit, available at 20 M\$/t, and recover about 9 M\$/t. The authors modelled a cargo landing service that begins full of lunar propellant on the surface, flies to orbit, stacks cargo, and lands empty. The surface-based cargo landing strategy is the red (right hand) section of Figure 4, the blue (left hand) section is the more usual 'from LLO' strategy. The figure is to scale, and one can see that the surface-based strategy lands more cargo for less propellant, it delivers more value for less cost. Where the baseline strategy can recover 9 M\$/t of lunar propellant the alternate can recover 18 M\$/t, this bridges half the commercial viability gap. Burning an oxygen rich 8:1 propellant mixture, as outlined above in the Multiproduct Mines section above, probably spans the rest. With just a change of strategy it looks like one can triple the recoverable revenue from water by burning all of it and operating from the surface.

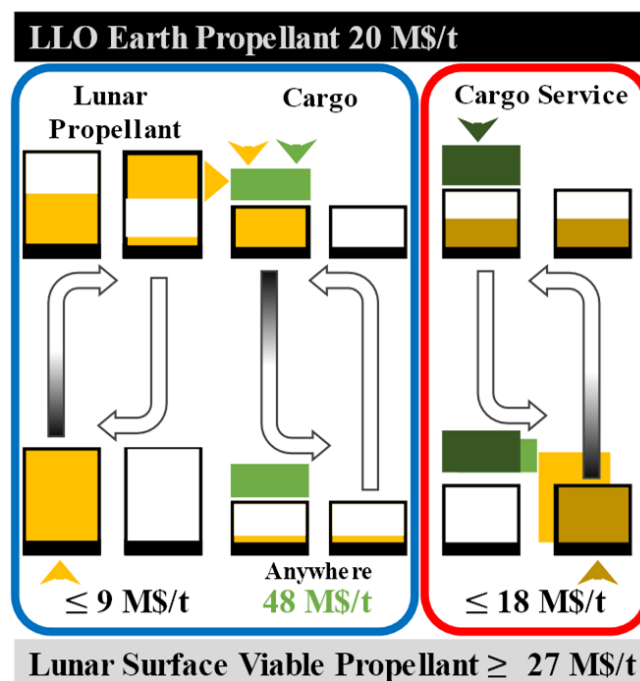


FIG 4 – LLO to lunar surface cargo, two CONOPs with different recoverable revenue.

The importance of scale

Scale and constraints can have unexpectedly large impacts. Launch to LEO costs are currently at least 2 M\$/t, with some payload's costs at much higher levels. SpaceX aims to reduce this by a factor of 200, which will undermine lunar propellant revenues, but one might be able to make it up in volume.

In some cases, outputs can scale up more rapidly than another metric like mass or geometry. For example, for nuclear reactors, as one increases the total power output the kg/kWe falls. A published lunar propellant analysis took the usual, conservative, approach of integrating a complete power and mineral processing system on Earth and launching many copies to meet their posited demand (Jones *et al*, 2019). The scale of nuclear reactor selected forced high kg/kWe and limited the scale of the mineral extraction plant that could be bundled in one launch, forcing 16 copies, each launched on an SLS. The extraction plant, based on molten regolith electrolysis, became more mass and power efficient as its diameter increased. Relaxing the constraint that both power and mineral processing must be integrated into one delivery allowed the authors to increase the scale of both. Rather than launch many copies of an integrated system one launches the largest possible nuclear reactor and mineral processing units, each on their own launcher, and plugs in a power cable on the lunar surface. The mineral extraction plant was scaled up to the maximum diameter that will fit in an SLS fairing, and a sufficiently powerful historically costed space reactor design was selected. This reduced the required SLS launches from 16 down to 2. However, the selected reactor could power two mineral extraction plants so one can double output by adding an additional launch of the relatively cheaper mineral processing unit. This rescaling of production elements and demand reduced production costs to 7 per cent of the original analysis (Bennett, Ellender and Dempster, 2020).

The reactor the authors chose was a significant part of the cost base and an historical design that had been cancelled, at least in part, because there was no compelling use case for its level of power output. One could land even larger reactors by applying the same assembly concept, landing modular components, and assembling on the lunar surface, for example a reactor core with power generation and a separate cooling/heat rejection system. The main constraint to lowering production cost further is having a limited market for product. Figure 5 illustrates the source of the effects and the magnitude of the compounded impact.

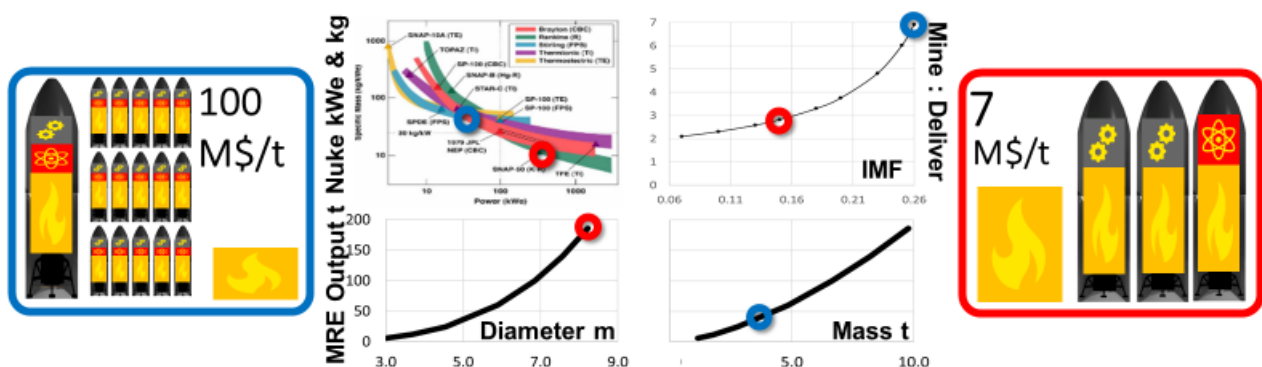


FIG 5 – The effect of compounding nonlinearities as scale increases.

The SpaceX Mars Project would require a million tons of oxygen in Low Earth Orbit (LEO) every 26 months. If the Mars Project begins when they have achieved a factor of 20 reduction in LEO launch cost, then the LEO market for oxygen will be bigger than Australian coal. If they achieve a factor of 100 reduction in launch costs this market will still be around 10 billion dollars annually. Supplying this market would require 1.4 million tons of lunar water annually, so there would be from 700 000 to 7000 dollar per ton of recoverable value.

CONCLUSIONS

The authors have presented an argument for why, although space resources might seem a distant prospect, they could rapidly transition to being viable business opportunities. The viability horizon of a business with the cash flow pattern of a space resource proposal can be very sensitive to the ratio of initial investment to ongoing revenues. There are many links in the production and delivery chain that multiply together and many where small changes yield large pay-offs. Government programs are reducing the scale of initial investment required by funding lunar science and resource utilisation proof of concepts and pilot plants (Linne *et al*, 2019). Taken together this means seemingly modest changes to processes or proposal structure can bring viability forward by decades.

The authors provided a selection of research results that showed large pay-offs for relatively small interventions to, or rearrangements of, published space resource proposals and analyses. Geostationary Transfer Orbit (GTO) orbit raising using lunar propellant demonstrates that there is no chicken and egg problem, there are some customers ready to take advantage of space resources, a vertically integrated services company only needs to be cost competitive, though the relatively small market poses a challenge. The unexpected identification of an ‘in effect’ market for lunar manufactured propellant tanks points to the potential for other unidentified space resource use cases. Expanding the perception of what the lunar propellant product is and where it can be sold delivered small multiples of recoverable value and revealed a rich tradespace with a diverse mix of recoverable value, products, and markets. As lunar propellant production costs come down, more markets become viable, this provides an arena for competition to drive down costs. Finally, the authors demonstrated an example scaling up production elements and the size of the market to deliver a factor 14 reduction in costs. One can see that there is scope for further improvements in this direction indicating that space resources could retain utility even in the face of large falls in the cost of Earth launch. Somewhat paradoxically one of the drivers of falling Earth launch costs is also a huge potential market for lunar propellant.

Given the sensitivity of the viability horizon to the ratio of initial costs to ongoing revenues, and the demonstrated scope for both reducing costs and increasing revenue per ton produced, the viability of off Earth mining could undergo rapid transformation.

ACKNOWLEDGEMENTS

The authors would like to acknowledge the authors of all the academic works we have drawn on, especially those who have been keeping the space resources flame alive since before the Apollo program.

REFERENCES

- Bennett, N and Dempster, A, 2021. Off-Earth Propellant to leverage our activities in space; Looking deeper than water. *43rd COSPAR Scientific Assembly. Held 28 January-4 February*, 43, 179.
- Bennett, N J and Dempster, A G, 2020. Geosynchronous transfer orbits as a market for impulse delivered by lunar sourced propellant. *Planetary and Space Science*, 182, 104843.
- Bennett, N J, Ellender, D and Dempster, A G, 2020. Commercial viability of lunar In-Situ Resource Utilization (ISRU). *Planetary and Space Science*, 182, 104842.
- Charania, A and Depasquale, D, 2007. Economic Analysis of a Lunar In-Situ Resource Utilization (ISRU) Propellant Services Market. SpaceWorks Engineering Inc., International Astronautical Congress, India.
- Jones, C A, Klovstad, J, Komar, D and Judd, E, 2019. Cost Breakeven Analysis of Cis-lunar ISRU for Propellant.. *AIAA Scitech 2019 Forum. American Institute of Aeronautics and Astronautics*.
- Kornuta, D, Abbud-Madrid, A, Atkinson, J, Barr, J, Barnhard, G, Bienhoff, D, Blair, B, Clark, V, Cyrus, J, Dewitt, B, Dreyer, C, Finger, B, Goff, J, Ho, K, Kelsey, L, Keravala, J, Kutter, B, Metzger, P, Montgomery, L, Morrison, P, Neal, C, Otto, E, Roesler, G, Schier, J, Seifert, B, Sowers, G, Spudis, P, Sundahl, M, Zacny, K & Zhu, G, 2019. Commercial Lunar Propellant Architecture: A Collaborative Study of Lunar Propellant Production. *REACH*, 100026.
- Linne, D, Sanders, G, Kleinhenz, J and Moore, L, 2019. Current NASA In-Situ Resource Utilization (ISRU) Strategic Vision.
- Metzger, P T, 2020. *Aqua Factorem: Ultra Low-Energy Lunar Water Extraction* [Online]. Available: https://www.nasa.gov/directorates/spacetech/niac/2020_Phase_I_Phase_II/Aqua_Factorem/ [Accessed 20200927 2020].

Regulating space mining – use a system that works

A J Cannon¹

1. Principal, ACannonconsulting, Adelaide SA 5000. Email: acannonconsulting@gmail.com

ABSTRACT

Space mining will require legal certainty over rights to prospect, explore and mine space resources, which under existing treaty agreements cannot be subject to nation state sovereignty. The Hayabusa2 probe was launched in December 2014 and it took six years to recover samples from asteroid Ryugu and return them to Woomera. No investor will undertake an expense like that without enforceable legal rights to exploit a valuable resource that its probe identifies.

Analogues from the attempt to have a treaty regime for mining in Antarctica, which failed, and the UNCLOS III treaties for Deep Seabed mining, where an international authority regulates any mining have not been workable solutions. An individual nation state regime cannot provide the legal certainty investors will require without the backing of an international agreement. The best analogue for space mining is good nation state regulation of mining on Earth, backed by international agreement to provide clear titles to prospect, mine and explore in return for compliance with internationally agreed standards of regulation and payment of royalty to an internationally administered fund to satisfy the benefit to all mankind.

The very large investments needed to prospect, explore and mine space resources require a clear title and regulatory system. There are profound benefits for the whole of mankind in unlocking and sharing the value of space resource. But inadequate regulation risks disputes over mine sites and ownership of resources which might involve nation state conflicts and the risk of poorly skilled and resourced miners causing a major accident such as a catastrophic collision of an asteroid with Earth.

INTRODUCTION

There will be space mining. As soon as resources are needed in space and it is cheaper to use resources found in space than to deliver them from Earth, the resources in space will be used. That will involve mining. The first is likely to be water. The USA Artemis project aims to establish a moon base populated by humans by 2024 (NASA, 2021). Once that occurs the humans will need water, to support life, as a radiation shield and as fuel for shuttle rockets when the water is broken down into its constituent Hydrogen and Oxygen by electrolysis from solar or nuclear generated electricity. Water is heavy. A cubic metre weighs a tonne and each kilogram using the cheaper SpaceX Falcon delivery system (Cobb, 2019) costs US\$2720 to deliver into Low Earth Orbit (LEO), so each tonne of water has a supply cost to LEO from Earth of US\$2.7 million and maybe ten times that to deliver it to the moon. The delivery itself comes with difficulties because in the low gravity of the Moon. A descending rocket displaces surface gravels like bullets and the lack of atmosphere does not slow them. Deliveries will necessarily be a long way from the base. There is water on the moon so prospectors will seek it out and if they can collect and deliver it to the base at a lesser cost than a delivery from Earth, they will: both for the adventure and the profit.

The Japanese Aerospace Exploration Authority (JAXA) probe Hayabusa2 collected samples from Near Earth Orbit (NEO) Asteroid 162173 Ryugu and returned them to Earth at Woomera Range in South Australia (JAXA, 2020). This establishes that mining asteroids is now just a matter of scale and expense. Asteroids have been studied by telescopes, flybys and by probes returning samples to Earth (Physics World, 2018). There is evidence of the presence of valuable resources in asteroids in large quantities and concentrations much higher than on Earth (NASA, 2019). For example, platinum has been identified at 100 ppm compared to 5–10 ppm in open cut mines in South Africa (Sonter, 2006). As more people populate Earth and expect a higher standard of living, then resources on Earth will become more difficult to extract and more expensive. Prospectors will explore NEO asteroids and eventually the cost of extraction and delivery will be competitive with resource extraction on Earth (Brak, 2006) (Johnson, 2011). Another possibility is Helium-3, which has been identified on the Moon (Hepeng, 2006) and it has potential to generate more power by fusion than Deuterium Tritium fusion with less radioactive contamination (Santarius, 1992; Schmitt, 2005). However, since fusion power has yet to be harnessed on Earth this is a long-term speculation.

Although much work has been done to develop a framework for the mining of space resources such as the Hague Building Blocks 2019 and the Vancouver Recommendations 2020, the present legal regime in space is not ready for this speculative interest in prospecting for resources in space because there is no clarity about the ownership of resources in outer space (Cannon, 2020). To attract the large investments that mining space resources will require, it will be necessary to have legal certainty over prospecting rights, exclusive rights to explore and mine an identified valuable resource, ownership of recovered resources and regulatory clarity. There will be no investment in a venture without clear legal rights to investigate and sell the recovered resource. No regulation, for investors, is worse than over regulation. One can allocate costs for regulatory compliance, but not with any confidence for uncertainty.

THE UNRESOLVED ISSUE OF THE OWNERSHIP OF SPACE RESOURCES

Our present understanding of ownership on Earth is founded on the principle of nation state sovereignty. The German sociologist Max Weber put it this way (Weber, 1918):

'Every State is founded on force' said Trotsky at Brest-Litovsk. That is indeed right. ...Today, however, we have to say that a State is a human community that (successfully) claims the monopoly of the legitimate use of physical force within a given territory.

Ownership of property is usually recognised and enforceable under the sovereign power of nation states. It is their capacity to exercise power over the property that provides the enforceability of the notion of a title of ownership. Without that power the control over an asset depends on all other comers respecting it. There are examples where collective intention is sufficient to enforce ownership rights within a small group without the need for external power (Cannon, 2020). The author gives examples of a small mining camp in a remote area of South Australia where individuals rights to camps were respected and to the sub Arctic island of Spitzbergen (renamed Svalbard in 1925) which until 1920 was *terra nullius* but occupied by various individuals for mainly mining purposes. But in the first instance a degree of external state control was provided by mining regulation and in the latter competing claims were eventually resolved by *The Spitzbergen Treaty* which granted sovereignty over the island to Norway on the basis that it recognised the established rights of occupiers. The establishment of nation state sovereignty was necessary to provide the power of enforcement necessary to protect property rights against outsiders. It is clear that any rights of collective intention depend upon a cohesive community so that mutual accountability to community members ensures respect for each other's rights. Even then there is no protection against an intruder who does not respect that locally enforced comity.

As technology permitted access to valuable resources in unclaimed areas of Earth such as Antarctica, the deep seabed, and now outer space, a contest of ideas has developed over the right to exploit those resources. There are more than 90 nations newly independent from the colonial era in the United Nations General Assembly (UNGA). These developing nations passed a resolution (UNGA res 1803) to claim sovereignty over their national resources and the right to reclaim them on the payment of compensation (Ng'ambi, 2015) and in 1974 UNGA announced a New International Economic Order for a redistribution of resources to relieve poverty and stated that there would be co-operation among all States to (UNGA res 3021):

... correct inequalities and redress existing injustices, make it possible to eliminate the widening gap between the developed and the developing countries and ensure steadily accelerating economic and social development and peace and justice for present and future generations.

In parts of Earth where nation states have not already asserted sovereignty developing nations want to prevent the richer nations from appropriating these unclaimed areas and the resources in them. Under Roman Law principles property that is not subject to sovereignty by any nation state is divided into *res nullius* which can be claimed by anyone and *res communis omnius* also described as *res extra commercium* or *res publica* (Nicholson, 2002) which cannot be subject to individual ownership and is available to all on a non-exclusive basis. These notions were developed by the Venezuelan scholar Andrés Bello who proposed that this property was an 'indivisible common patrimony' and only available for shared regulated use (Nicholson, 2002, pp 177–178). The UNGA majority of

developing nations have proposed that the deep seabed, Antarctica and outer space should be treated as the Common Heritage of Mankind (CHM), also referred to as a global commons (Frakes, 2003). These areas are not subject to nation state sovereignty and any property interests should be managed by an international authority and, if exploited at all, the resources must be equitably shared, peacefully used, and protected and preserved for the benefit of all mankind (Johnson, 2011). Depending on how they are expressed in practice, these notions can discourage private enterprise investment that sensibly wants a return on the funds ventured on what will be a difficult endeavour. This conflict of ideas underpins the question of who will control and benefit from the exploitation of resources in areas not subject to national sovereignty and has prevented the development of a working regulatory regime. The problem has been the conflation of the notion of regulatory control with the acquisition of ownership. This article suggests that the regulatory control over exploration and mining is best managed by nation state regimes operating in accordance with internationally agreed standards while the title to any resources that are recovered is purchased from the international community by the payment of a royalty to an internationally administered fund. There will be other benefits in development of technology and transfer of knowledge. There is no particular benefit to the developing world to be had from administering a regulatory system, as long as regulatory systems meet a required set of internationally agreed standards.

The existing treaty regime for outer space

The *Outer Space Treaty 1967* (OST 1967) is the primary treaty presently governing outer space.¹ Article I states:

The exploration and use of outer space, including the Moon and other celestial bodies, shall be carried out for the benefit and in the interests of all countries, irrespective of their degree of economic or scientific development, and shall be the province of all mankind. Outer space, including the Moon and other celestial bodies, shall be free for exploration and use by all States without discrimination of any kind, on a basis of equality and in accordance with international law, and there shall be free access to all areas of celestial bodies. ...

The OST 1967 continues in Article II by stating: 'Outer space, including the Moon and other celestial bodies, is not subject to national appropriation by claim of sovereignty, by means of use or occupation, or by any other means.' It is a widely held view that this only precludes claims of sovereignty and is silent about the mining of resources (von der Dunk, 2018). The *Agreement Governing the Activities of States on the Moon and other Celestial Bodies 1979* ('Moon Treaty 1979') was an attempt to make clear that outer space was the Common Heritage of Mankind. Article 1 provides that the treaty applies to all celestial bodies in the solar system other than Earth. Article 4.1 provides that 'The exploration and use of the Moon shall be the province of all mankind and shall be carried out for the benefit and in the interests of all countries, irrespective of their degree of economic or scientific development'. Article 6.2 provides that minerals and other substances can be used to support missions, but Article 11.3 of the Treaty makes clear that outer space resources cannot become the property of any State, body or natural person:

Neither the surface nor the subsurface of the moon, nor any part thereof or natural resources in place, shall become property of any State, international intergovernmental or non-governmental organization, national organization or non-governmental entity or of any natural person. The placement of personnel, space vehicles, equipment, facilities, stations and installations on or below the surface of the moon, including structures connected with its surface or subsurface, shall not create a right of ownership over the surface or the subsurface of the moon or any areas

¹ There are other treaties in place dealing with the consequences of space activities, namely *The Agreement on the Rescue of Astronauts, the Return of Astronauts and the Return of Objects Launched into Outer Space 1968*, Consensus Agreement of the General Assembly, resolution 2345 XXII (entered into force December 1968), which as its name implies expands on the duty to render assistance in Arts IV and VIII of the OST 1967 and to return space objects to their launching states; the *Convention on International Liability for Damage Caused by Space Objects 1972*, opened for signature on 29 March 1972, 961 UNTS 187 (entered into force 1 September 1972), which regulates the responsibility and liability of nation states for space objects launched by them or their citizens; and the *Convention on Registration of Objects Launched into Outer Space*, opened for signature 14 January 1975, 1023 UNTS 15 (entered into force 15 September 1976), which establishes a registration system for all space objects.

thereof. The foregoing provisions are without prejudice to the international regime referred to in paragraph 5 of this article.

Articles 11.5 and 18 anticipate the establishment of an international system to govern the exploitation of space resources, which has not occurred. This adoption of the CHM principle has resulted in this so far being a failed treaty with only 18 State Parties (including Australia), none of whom are major participants in outer space activities. Art 11.5 of this treaty may yet provide a process to reach an international regime but the USA has made it clear for now that the treaty is of no effect. Sec 2 of the Executive Order issued by the President of the USA on 6 April 2020 declared that: (Executive Order 13914, 2020)

... the United States does not consider the Moon Agreement to be an effective or necessary instrument to guide nation states regarding the promotion of commercial participation in the long-term exploration, scientific discovery, and use of the Moon, Mars, or other celestial bodies. Accordingly, the Secretary of State shall object to any attempt by any other state or international organization to treat the Moon Agreement as reflecting or otherwise expressing customary international law.

For now, that leaves the OST 1967 as the only the legal framework for space mining. The preamble to the OST 1967 states:

Inspired by the great prospects opening up before mankind as a result of man's entry into outer space,

Recognizing the common interest of all mankind in the progress of the exploration and use of outer space for peaceful purposes,

Believing that the exploration and use of outer space should be carried on for the benefit of all peoples irrespective of the degree of their economic or scientific development ...

Under the *Vienna Convention 1980* a treaty must be interpreted in good faith in the context of its object and purpose. An object and purpose of the OST 1967 is to progress 'the exploration and use of outer space for peaceful purposes.' So long as there is no claim of national sovereignty over a space object the permission in Article I of the OST 1967 that 'Outer Space, including the Moon and other celestial bodies shall be free for exploration *and use* by all States without discrimination of any kind ...' (author's emphasis) leaves open the right to extract resources, firstly to sustain and assist exploration (which is also expressly permitted by Article 6.2 of the *Moon Treaty 1979*) and secondly to sell them to a space station for a profit, or to deliver them to Earth (Johnson, 2015). Article VI of the OST 1967 provides that States Parties have international responsibility for the activities of their governmental and non-governmental entities in outer space and discussed below are examples where nation states have established regulatory regimes to manage outer space activities undertaken under their authority. Article VIII of the OST 1967 provides that a State Party retains jurisdiction over items launched into outer space and in particular:

Ownership of objects launched into outer space, including objects landed or constructed on a celestial body, and of their component parts, is not affected by their presence in outer space or on a celestial body or by their return to the Earth.

Some commentators argue that once a space resource is in the hold of a space ship it is protected and upon its return to Earth then the nation state can recognise title to it like the wild 'fish in the net' of an ocean trawler (von der Dunk, 2018). A fishing trawler on the sea has clear nation state sovereignty and once possessory title is taken over the wild fish by catching them in the net and taking them aboard, the nation state sovereignty of the ship recognises the ownership title over the fish. It is not clear that wild fish in an Earth ocean caught by a fishing trawler are a proper parallel with a space ship exploring an inanimate resource in outer space. No possessory title is gained over a resource in a space object just by exploring it *in situ*, save over any samples taken. Presumably another explorer might come and take it. This metaphor ignores the complexity of prospecting, exploration and mining itself, before any resource is finally recovered, refined and delivered to market. Multiple rights must be provided against all other comers on that journey before there will be investment in mining.

Space mining rights will need international agreement

The Hayabusa2 probe was launched in December 2014 and it took until June 2018 to reach NEO asteroid Ryugu. It spent eighteen months surveying the asteroid and collecting samples and then it took a year to return the samples to Earth (JAXA, 2020). That is more than four years of travel time and six years overall. If this were a prospecting expedition the mining company would need to be clear that if the substantial expense of the expedition established a physically and economically promising resource project to mine the asteroid, it would retain the exclusive and enforceable right to mine it within a realistic time frame. Otherwise, a competitor might take the resource with legal impunity. Some proposals to address security over the sites of mining activities are 'safety zones', 'first presence rights' or a 'zone of non-interference'². These might be effective on a co-operative basis to protect exploration bases, as Article IX of the *OST 1967* provides that 'States Parties to the treaty shall be guided by the principle of cooperation and mutual assistance...[and will conduct all their activities] with due regard to the corresponding interests of all other States Parties to the Treaty'. But it is likely to be a prohibited act of sovereignty if such notions purport to grant an exclusive mining right over an asteroid for several years enforceable against all comers. The inability of nation states to provide legal title in outer space was demonstrated by the example where eight equatorial States signed the *Bogotá Declaration* in 1976 to claim ownership over the valuable geostationary equatorial telecommunication satellite slots 36 000 km above their territorial location on Earth. However, the United Nations International Telecommunications Union (ITU) with 193 member States has continued to allocate slots in disregard of the Declaration in accordance with the international norms and Article II in the *OST 1967* which prevents any national claim of appropriation of that area because it is in outer space. This absence of nation state sovereignty in outer space will make an international agreement necessary to provide a clear legal basis for the grant of an exclusive exploration and mining rights.

After prospecting to find a potential resource it will be necessary to explore it to establish that it is commercially viable. Experience of mining on Earth suggests that there will be legal transfers, joint ventures and mortgaging of the mining rights to fund the mounting expenses of developing a detailed mining plan and then to fund the actual mining, refining and transport of the space resource to the end purchaser. Many of these legal transfers and mortgages will be of rights over space objects but will need to be enforceable under legal regimes on Earth. Legal uncertainty over the right to control exploration sites and ownership of mined space resources will deter investors. Every investment decision must weigh the potential return of an investment against the risk of financial loss and other negative outcomes. If there are not clear legal frameworks in place to define rights of ownership over space-mined assets it would expose potential investors to prohibitive regulatory and legal risk, outweighing potential returns. This limits potential investors to a small risk-seeking group with attendant likelihood they may ignore good practices, or there may be no investors at all.

A project to return an asteroid or a large quantity of material from it to market to a space station on the Moon, or to Earth, will come with dangers of contamination or of a disastrous collision. There needs to be regulation to ensure the competence of any prospectors and miners of space resources. Without regulatory control insurers will not be able to make an actuarial calculation of risk so the necessary insurance of the activity will not be available. This compounds the investment problems flowing from the lack of legal certainty over rights to prospect, develop potential mines sites, and to mine and sell space resources.

The Hague International Space Resources Governance Working Group, established in 2014, developed set of Building Blocks as a basis for international co-operation in managing the recovery of space resources in accordance with existing treaty obligations. They discuss the following topics:

- Definitions
- An international framework to provide for State or international organisation responsibility for space resource activities
- States to have jurisdiction and control over space made products

² Proposals to assure security over an exploration site suggested in the Hague Building Blocks and the USA *Space Resource Exploration and Utilization Act of 2015*, where § 51302 (a)(3) entitles US citizens to acquire space resources 'free from harmful interference' which implies a protection over the area of their recovery.

- Allocation of time limited priority rights
- Recognition of property rights in acquired material
- Avoidance of harmful impacts to space and earth
- Benefit to all mankind and developing States
- Safety zones as a way of avoiding conflict over areas without offending the *OST 1967* non-appropriation clause in Art II.
- Monitoring and remedying harmful effects
- Registration and sharing of information
- Assistance in the case of distress, liability for damage, inspection
- An international registry
- Adaptive regulation
- Dispute resolution

The Vancouver Recommendations for Space Mining have urged that multilateral agreement is necessary rather than unilateral adoption of national legislation. This is necessary to provide clear and transparent oversight to manage the dangers of space mining. They also propose the retention and sharing of the results of exploration and mining, mandatory monetary and other benefit sharing, monitoring and accountability of operators, recognition and protection of biota in space and investigating the need to establish planetary boundaries. No doubt both these guidelines will inform the ultimate regulations, but regulation is only effective if it is enforceable and workable.

The regime for space mining will need to provide legal certainty to explorers and miners over exploration areas, mines and recovered space resources in space and on Earth. There will need to be a clear regulatory regime and incentives to encourage compliance and sanctions for non-compliance. The aspirations of the developing nations will need to be satisfied at the same time as sufficient incentives to encourage investment remain. The key to unlock the present impasse over these objectives is how to manage the power to grant enforceable rights to explore and mine and title to recovered resources. Under the *OST 1967* nation states cannot do it by extending their sovereignty to space. An international agreement will be necessary to trade clarity over rights to explore and mine and title to space resources in return for regulatory compliance and a benefit to the whole international community. This agreement will be informed by an existing regime. What is the best analogue from which to develop a regime to regulate space mining?

Analogues that might be used to regulate space mining

The two existing regimes that have considered mining on Earth in areas which are not subject to national sovereignty are the Antarctic Treaty and Deep Sea Mining. Neither has been successful, in part as a result of the unresolved CHM issue. The ice cover over most of Antarctica has made mining difficult (Zumberge, 1979). Although seven States have territorial claims over Antarctica, these have all been put into abeyance by the *Antarctic Treaty* in 1959. Further agreements now comprise the Antarctic Treaty System³. One of them, the *Protocol on Environmental Protection to the Antarctic Treaty* (the *Madrid Protocol*) in Art 7 provided that 'Any activity relating to mineral resources, other than scientific research, shall be prohibited.' The protocol will be open for review in 2048. It avoided references to the Common Heritage of Mankind. For example in the preamble it stated:

Convinced that the development of a comprehensive regime for the protection of the Antarctic environment and dependent and associated ecosystems is in the interest of mankind as a whole.

³ The *Convention for the Conservation of Antarctic Seals*, opened for signature 1 June 1972, 29 UST 441 (entered into force on 11 March 1978); The *Convention on the Conservation of Antarctic Marine Living Resources*, opened for signature 1 August 1980, 33 UST 3476 (entered into force on 7 April 1982); The *Protocol on Environmental Protection to the Antarctic Treaty* (the *Madrid Protocol*), opened for signature on 4 October 1991, 30 I.L.M. 1455 (entered into force 14 January 1998).

Whether Antarctica is part of the CHM is contested. In later negotiations 'wilderness park' is preferred to 'world park' (Heim, 1990) but some commentators hold that Antarctica is a global commons (Frakes, 2003). The *Madrid Protocol* was in part a response to the *Antarctic Mineral Convention*, which was negotiated outside of the United Nations between industrialised nations (Starke, 1988) intending to provide a basis to regulate mining while protecting the environment. Under its terms mining is not permitted until it comes into force. It is not in force. Australia and France withdrew their support for the convention and no parties have ratified it. It provides for a Commission to oversee any mining with a Scientific, Technical and Environmental Committee, Regulatory Committees, and Secretariat. Any party would have a right to veto an application to mine. This structure has not resolved the tension over CHM and importantly it does not deal with sharing the benefits of mining.

Following claims by some nations after WWII to resources to the edge of their continental shelf the United Nations Conference on the Law of the Sea was convened in 1956 leading to four United Nations Conventions on the Law of the Sea (UNCLOS I) in 1958. The UNCLOS II convention in 1960 did not result in a treaty but when the mining of manganese nodules which also contain nickel, copper, cobalt, gold and other minerals excited the possibility of deep sea mining (Viikari, 2002) the UNCLOS III convention was negotiated between 1973–1982 (Koh, 1993). This achieved an accepted state practice to claim an Exclusive Economic Zone (EEZ) of 200 nautical miles (300 km) from the low water line of coastal nation states but preserving freedom of passage in that zone (Warne, 2007). It established the International Seabed Authority (ISA) to regulate the management of resources in the deep sea zone and, to satisfy the CHM principle, part XI of the treaty mandated technology transfers from developed to developing nations and established an international mining company (the Enterprise) to compete with private enterprise licences over the deep sea area (Heim, 1990). Uncertainty over access rights and dissatisfaction with mandated technology transfers resulted in most developed nations refusing to sign the treaty (Matte, 1987) and in turn to the negotiation of the 1994 New York Agreement which was adopted as a binding international convention. By that agreement the limitations on seabed production and mandatory technology transfers did not apply, the USA was guaranteed a seat at the ISA, a modification of voting and the establishment of a finance committee where the largest donors were members and decisions had to be by consensus. The USA still has not ratified UNCLOS III but abides with all except Part XI. The ISA is developing a mining code to regulate exploration and mining (ISA, *Mining Code*) but the fact the USA still refuses to accept Part XI is a strong indication that it will not accept a regulatory regime that is administered by an international body. This treaty is one analogue to regulate space mining, and the *Moon Treaty* 1979 anticipated this approach in Arts 11.5 and 18, but the trenchant rejection of that approach by the USA means it is unlikely to succeed in its present form. Each of these analogues highlights the unresolved tension between the poorly defined CHM which grants a majority poorer nation control over unexplored resources and a market orientated economy where risk taking entrepreneurs need certainty of rights to retain enough profits to justify what will necessarily be an expensive and risky investment. Entrepreneurs will be reluctant to gift expensively gained technological expertise to others which can then be used to reduce their profits by informed competition which will reduce prices by flooding the market.

Existing nation state regimes

In the meantime, some nation states have been developing their own regimes for space exploration including provisions in relation to space resources, but without any detail of what mining regulation might look like. The United States of America has passed *US Commercial Space Launch Competitiveness Act of 2015* with the clear intent stated in Title 1 encourage private entrepreneurial drive into space mining (Tronchetti, 2016). It permits US citizens to acquire possessory and ownership title to space resources obtained under the legislation. However, to comply with the OST 1967, s 403 makes clear that the USA does not make any claim of state sovereignty:

SEC. 403. DISCLAIMER OF EXTRATERRITORIAL SOVEREIGNTY.

It is the sense of Congress that by the enactment of this Act, the United States does not thereby assert sovereignty or sovereign or exclusive rights or jurisdiction over, or the ownership of, any celestial body.

The Executive Order of 6 April 2020 repeats the encouragement and right of private recovery of space resources and the rejection of the notion of a global commons:

Americans should have the right to engage in commercial exploration, recovery, and use of resources in outer space, consistent with applicable law. Outer space is a legally and physically unique domain of human activity, and the United States does not view it as a global commons. Accordingly, it shall be the policy of the United States to encourage international support for the public and private recovery and use of resources in outer space, consistent with applicable law.

Luxembourg has passed the *Law of 20 July 2017 on the Exploration and Uses of Space Resources* which also provides that ownership of space resources can be recognised in Luxembourg Law but again the law makes no claim of sovereignty over any space body. The United Arab Emirates (UAE) established a space agency in 2014 and has legislation (UAE Federal Law no. 12) which provides regulation for 'space resource exploration or extraction activities'. France has a *Space Operations Act* to licence commercial space activities. India introduced a draft *Space Activities Bill 2017* and continues a process to legislate it. Although some of these regimes recognise title to resources that are recovered, they do not clarify the key issues identified above: legal certainty over exploration areas and mine sites in outer space, clear title over recovered resources, a clear and enforceable regulatory regime and sharing of the benefits with developing nations while leaving sufficient incentives to encourage the necessary investment.

The USA announced the Artemis program in 2020 with the intention to establish a base for humans on the moon by 2024 and to 'establish sustainable exploration by the end of the decade' and to send an astronaut to Mars (NASA, 2021). NASA 'will collaborate with our commercial and international partners' but on condition that they agree to the 'Artemis Accords' (NASA, 2021) which include undertakings that operations are to be for peaceful purposes, transparency, interoperability, emergency assistance, registration, release of scientific data, protecting heritage, space resources, deconfliction of activities, ensuring no orbital debris and spacecraft disposal. 'Deconfliction' would be achieved by the parties agreeing 'safety zones.' This is a major attempt to move the discussion forward (Borgen, 2020) but the unilateral approach may encounter resistance. Dmitry Rogozin, the head of the Roscosmos, the Russian Space agency has already accused the USA of attempting to circumvent the UN (Clark, 2020). Although using space resources to sustain exploratory bases and for fuel for further space flights is unlikely to offend the *OST 1967* this is very different to commercial mining for profit. It is unlikely that a small multinational group can deliver the clear regulatory environment and legal certainty over exploration areas and title to resources that can be traded in outer space that will be necessary to encourage the large investments and insurance against risks that will be needed for successful mining of space resources. Nation State regimes that comply with internationally agreed standards may be a sensible way to regulate space mining but they will need the backing of an international agreement to deliver the necessary regulatory and legal certainty.

CONCLUSION

This article argues that the most appropriate analogue to regulate space mining will be based on the way that mining is managed in good nation state regimes on Earth. These can be adapted to space mining by the factors identified in the work already done in the Hague Building blocks, Vancouver Recommendations, Artemis Accords and other like international endeavours. The international community can agree a set of minimum regulatory standards with which any nation state regulating space resource mining must comply. If a nation state regime complies with those internationally agreed standards, then it will be empowered to grant prospecting, exploration and mining rights which will be mutually recognised by all the nation state parties to those internationally agreed standards. As occurs here on Earth any mining company must comply with the regulatory regime to keep its right to explore and mine.

Mining of space resources will require several levels of legal rights which will need to be legally enforceable in Earth based international law and nation state legal regimes. The first is the right to prospect: a licence to roam the realms of outer space looking for valuable resources, responsibly and without interfering with others. The second is a right to exclusive exploration of an object or a part of it for a finite period and on conditions of work being done to identify and evaluate the resource. The next is a right to mine an object or a part of it to extract and refine resources. The last is the ultimate aim: a title of ownership of the mined resource, a title which protects possession and gives the right to sell. Nothing less will provide the legal certainty that investors and their insurers will

require to make it happen at all. The international community could agree to confer those rights conditional upon payment of fees to cover the expense of monitoring regulatory compliance and satisfy the need to provide a benefit for all mankind by making the mining company purchase a good title to the extracted resources by payment of a royalty to an internationally administered fund. That will be the primary benefit to the international community from the extraction of resources from the unowned or common property of outer space. Other benefits of education, employment and the knowledge gained can be included in the internationally agreed regulatory standards. Payment of royalty is a well-established practice on Earth. It is a cost of business to obtain legal certainty and can be calculated in the costings to determine whether a project is financially viable. It will be cheaper than the increased cost of finance and insurance that legal and regulatory uncertainty would cause.

The author has discussed how experience from nation state mining regimes on Earth can inform the regulation of space mining (Cannon, 2020, pp 5–9). Key elements will include licensing and monitoring to make sure that explorers and miners act responsibly, transparency of exploration results to save repeating expensive exploration efforts, collecting sufficient fees to fund the regulation systems and dispute resolution and enforcement processes to manage conflict and sanction bad actors. That is detail that will need to be agreed later. The argument here is to separate the issue of how to acquire good title to resources from the issue of how space mining is regulated. There should be agreement to allow title to be purchased from the international community upon compliance with internationally agreed standards. Nation state experience in regulating mining should be used as the analogue for mining in outer space rather than constructing an international body that does the regulating. The existing attempts to do that on Earth have not been promising.

Australia is a leading mining regulator and its companies have highly developed skills in remote operating machinery. It has recently established the Australian Space Agency (DIIS, 2019). Australia has a co-operative arrangement with a key player in the race to develop space resources, the USA. This background puts Australia in a good position to assist in the process of developing international regulatory standards for space mining. The international community may agree to review the *Moon Treaty 1979* in a constructive way so that it can gain the necessary States Parties to provide under Article 11.5 for minimum standards for nation state regulatory regimes or there may be negotiations for the development of a new separate treaty regime. Either way it is important that space mining is managed in a way that avoids conflict and encourages orderly investment so that it can create wealth and contribute to the benefit of all on Earth.

ACKNOWLEDGEMENTS

I gratefully acknowledge advice from Professor Melissa de Zwart, previously Dean of the Law School, Adelaide University, now Professor at the Jeff Bleich Centre for the US Alliance in Digital Technology, Security and Governance and Matthew Anibal Fuentes-Jiménez for his very helpful research assistance regarding the current state of space mining law.

REFERENCES

- Antarctic Mineral Convention: Convention on the Regulation of Antarctic Mineral Resource Activities, opened for signature 2 June 1988 (not in force).
- Antarctic Treaty, opened for signature 1 December 1959, 402 UNTS 71 (entered into force June 23, 1961).
- Bogotá Declaration: The Declaration of the first meeting of equatorial countries (adopted 3 December 1976) https://www.jaxa.jp/library/space_law/chapter_2/2-2-1-2_e.html signed by Colombia, Republic of Congo, Ecuador, Indonesia, Kenya, Uganda, Zaire with Brazil as an observer. Gabon and Somalia joined later.
- Borgen, C, 2020. 'The Artemis Accords: one small step for space law?', *OpinioJuris* (online), 8 May 2020 <<http://opiniojuris.org/2020/05/08/the-artemis-accords-one-small-step-for-space-law/>>
- Brak, R. 2006. 'The Great Asteroid Mining Con', on Ronald Brak, Because not everyone can be normal <<http://ronaldbak.blogspot.com/2006/02/>>.
- Cannon, A, 2020. 'The Great Space Rush: Regulating Space Mining', 39(1) *Australian Resource and Energy Law Journal*, 1–17.
- Clark, S, 2020. 'NASA space treaty to allow for the establishment of lunar 'safety zones'', *The Guardian* (online), 21 May 2020 <<https://www.theguardian.com/science/2020/may/20/nasa-new-space-treaty-artemis-accords-moon-mission-lunar-safety-zones?CMP=>>.

- Cobb, W, 2019. 'How SpaceX lowered costs and reduced barriers to space', *The Conversation*, 1 March 2019 <<https://theconversation.com/how-spacex-lowered-costs-and-reduced-barriers-to-space-112586>>.
- Department of Industry, Innovation and Science (DIIS), 2019. Australian Space Agency, <<https://www.industry.gov.au/strategies-for-the-future/australian-space-agency>>.
- Executive Order, 13914, 85(70) Fed Reg 20381, April 2020. Encouraging International Support for the Recovery and Use of Space Resources.
- Frakes, J, 2003. 'The Common Heritage of Mankind Principle and Deep Seabed, Outer Space, and Antarctica: Will Developed and Developing Nations Reach a Compromise', 21(2) *Wisconsin International Law Journal* 409.
- France Space Operations Act 2008. République française, Légifrance, LOI n° 2008–518 du 3 juin 2008 relative aux opérations spatiales <<https://www.legifrance.gouv.fr/affichTexte.do?cidTexte=JORFTEXT000018931380>>.
- Heim, B, 1990. 'Exploring the Last Frontiers for Mineral Resources: A Comparison of International Law Regarding the Deep Seabed, Outer Space, and Antarctica' 23 *Vanderbilt Journal of Transnational Law* 819, at p. 842 n 179.
- Hepeng, J, 2006 'He asked for the moon-and got it', *China Daily* (online), <http://www.chinadaily.com.cn/cndy/2006-07/26/content_649325.htm>.
- India: Department of Space, Indian Space Research Organisation, Seeking comments on Draft 'Space Activities Bill 2017' (1 November 2017) <<https://www.isro.gov.in/update/21-nov-2017/seeking-comments-draft-space-activities-bill-2017-stake-holders-public-regarding>>.
- International Seabed Authority, Mining Code, <<https://www.isa.org.jm/mining-code>>.
- JAXA, 2020. 'Confirmation of the sample collected during the first touchdown on asteroid Ryugu by asteroid explorer, Hayabusa2' 15 December 2020, <https://global.jaxa.jp/press/2020/12/20201215-3_e.html>, JAXA, Hayabusa2 Project <<https://www.hayabusa2.jaxa.jp/en/>>.
- Johnson, D, 2011. 'Limits on the giant leap for mankind: Legal ambiguities of extraterrestrial resource extraction', 26(5) *American University International Law Review*, 1477 <<https://digitalcommons.wcl.american.edu/auilr/vol26/iss5/8/>>.
- Johnson, D, 2015. Reality and Clarity in Understanding the prohibition on National Appropriation in Article II of the Outer Space Treaty 2–3 <<https://swfound.org/media/205288/reality-and-clarity-in-understanding-the-prohibition-on-national.pdf>>. 66th International Aeronautical Association Congress IAC-15, Jerusalem.
- Koh, T, 1993. 'The Third United Nations Conference on the Law of the Sea: What Was Accomplished?', 46 *Law & Contemporary Problems* 5.
- Luxembourg space resources Act 2017: Loi du 20 juillet 2017 sur l'exploration et l'utilisation des ressources de l'espace <<http://data.legilux.public.lu/file/eli-etat-leg-loi-2017-07-20-a674-jo-fr-pdf.pdf>>.
- Madrid Protocol: The Protocol on Environmental Protection to the Antarctic Treaty, opened for signature on 4 October 1991, 30 I.L.M. 1455 (entered into force 14 January 1998).
- Matte, N, 1987. 'The Common Heritage of Mankind and Outer Space: Toward a New International Order for Survival', 12 *Annals of Air & Space Law* 313, 316–317.
- NASA, 2019. Science, Solar System Exploration: Asteroids <<https://solarsystem.nasa.gov/asteroids-comets-and-meteors/asteroids/in-depth/>>.
- NASA, 2021. Artemis, humanity's return to the moon, <https://www.nasa.gov/specials/artemis/>
- New York Agreement: Agreement relating to the Implementation of Part XI of the United National Convention on the Law of the Sea of 10 December 1982, opened for signature 28 July 1994, UN Res 48/263 (entered into force on 28 July 1996).
- Ng'ambi, S, 2015. 'Permanent Sovereignty Over Natural Resources and the Sanctity of Contracts, from the Angle of Lucrum Cessans' 12(2) *Loyola University Chicago International Law Review* 153, at p 156.
- Nicholson, G, 2002. 'The Common Heritage of Mankind and Mining: An Analysis of the Law as to the High Seas, Outer Space, the Antarctic, and World Heritage', 6 *New Zealand Journal of Environmental Law* 177.
- OST 1967: Treaty on Principles Governing the Activities of States in the Exploration and Use of Outer Space, including the Moon and Other Celestial Bodies, opened for signature on 27 January 1967, 610 UNTS 205 (entered into force on 10 October 1967).
- Physics World, 2018. The Asteroid Trillionaires <<https://physicsworld.com/a/the-asteroid-trillionaires/>>.
- Santarius, J, 1992, 'Lunar He-3, fusion propulsion, and space development', NASA. Johnson Space Center, *The Second Conference on Lunar Bases and Space Activities of the 21st Century*, Volume 1 p 75–81.
- Schmitt H. 2005. *Return to the Moon: Exploration, Enterprise, and Energy in the Human Settlement of Space*. Springer.
- Sonter, M, 2006. 'Asteroid Mining: Key to the Space Economy', Space.com (online), <<https://www.space.com/2032-asteroid-mining-key-space-economy.html>>.
- Starke, J, 1988. 'International Legal Notes', 62 *Australian Law Journal* 956.

- The Hague International Space Resources Governance Working Group, 2019. Building Blocks for the Development of an International Framework on Space Resource Activities (November 2019) <<https://www.universiteitleiden.nl/binaries/content/assets/rechtsgeleerdheid/instituut-voor-publiekrecht/lucht--en-ruimte-recht/space-resources/bb-thisssrwwg--cover.pdf>>.
- The Outer Space Institute, 2020. The Vancouver Recommendations on Space Mining, <http://www.outerspaceinstitute.ca/docs/Vancouver_Recommendations_on_Space_Mining.pdf>.
- Tronchetti, F, 2016. 'Title IV – Space Resource Exploration and Utilization of the US Commercial Space Launch Competitiveness Act: A Legal and Political Assessment' 41(2) *Air & Space Law* 143.
- UAE Federal Law no 12 of 2019 (n 21) art 4.1(i).
- UNCLOS I: The Convention on the Territorial Sea and the Contiguous Zone, 1958, 516 UNTS 205 (entered into force on 10 September 1964); The Convention on the High Seas, 1958, 450 UNTS 82 (entered into force 30 September 1962); The Convention on the Continental Shelf, 1958, UNTS 311 (entered into force on 10 June 1964); and The Convention on Fishing and Conservation of Living Resources of the High Seas, 1958, 559 UNTS 285 (entered into force on 20 March 1966).
- UNCLOS III: The United Nations Convention on the Law of the Sea, opened for signature Dec. 10, 1982, U.N. Doc. A/CONF. 62/122 (entered into force on 16 November 1994).
- UNGA Res 1803 (XVII), at 15, U.N. Doc. A/5344 (Dec. 14, 1962) asserted the sovereign rights of all states over their national resources and the right to nationalise them upon payment of compensation.
- UNGA Res. 3021, U.N. Doc. A/RES/ S-6 (May 1, 1974).
- US Commercial Space Launch Competitiveness Act, Public L No 114–90.
- US Commercial Space Launch Competitiveness Act, Title 1: The Space Resources Exploration and Utilisation Act of 2015, 51 USC § 51301.
- Vienna Convention on the Law of Treaties, opened for signature 23 May 1969, 1155 UNTS 331 (entered into force 27 January 1980) arts 31 and 32.
- Viikari, L, 2002. From Manganese Nodules to Lunar Regolith; A Comparative Legal Study of the Utilization of Natural Resources in the Deepseabed and Outer Space, University of Lapland.
- von der Dunk, F, 2018. 'Asteroid Mining: International and National Legal Aspects', 26 *Michigan State International Law Review* 83–102, p 93 <<https://digitalcommons.law.msu.edu/ilr/vol26/iss1/3/>>
- Warne, P, 2007. 'Arctic Scramble: International Law and the Continental Shelf' 1 *Aberdeen Press and Journal* 24.
- Weber, M, 1918. 'On Politics: selected passages from a series of lectures given by Max Weber at the end of 1918 to the Free Students Union of Munich University and published the following year' *Panarchy* <<https://www.panarchy.org/weber/politics.html#:~:text=Today%2C%20however%2C%20we%20have%20to,the%20characteristics%20of%20the%20state>>.
- Zumberge, 1979. 'Mineral Resources and Geopolitics in Antarctica' 67 *American Scientist* 68.

Development of a Martian water resource project management system

S Casanova^{1,2}, R C Anderson³ and S Saydam^{2,4}

1. The School of Minerals and Energy Resources Engineering, UNSW, Sydney NSW 2052.
Email: s.casanova@unsw.edu
2. The Australian Centre for Space Engineering Research, School of Electrical Engineering, UNSW, Sydney NSW 2052.
3. Jet Propulsion Laboratory/California Institute of Technology, Pasadena, CA, USA.
4. Professor, School of Minerals and Energy Resources Engineering, UNSW, Sydney NSW 2052.

INTRODUCTION

In situ resource utilisation (ISRU) refers to operational practices to extract natural resources locally on a non-terrestrial body (ie the Moon, Mars, or asteroids) and transform them into useable products to support in-space activities. Viewed as a means to dramatically reduce overall mission cost and reliance on Earth for the supply of critical resources, ISRU forms an integral part of both the US National Aeronautics and Space Administration's (NASA; Moore, 2016) and the company SpaceX's (Musk, 2018) current plans to accomplish human missions to Mars. Locating a source of extractable water has been identified as a near term priority, with interest growing in the potential use of Mars's mid-latitude (~30–60°) buried ice deposits (Abbud-Madrid *et al*, 2016; McEwen *et al*, 2020).

Incorporating the use of locally acquired water into the design of a human exploration mission to Mars will require a high degree of confidence in the capability to locate, access, extract, and produce required quantities to meet human mission demands. At present, there are significant knowledge gaps in our understanding of the physical characteristics of Mars' buried ice deposits, particularly at the spatial scales required to assess the viability of a proposed water production project. This work presents a project management system to guide resource exploration and evaluation of Martian water ice resources. Application of the recommended practices will assist mission planners, operators, scientists, and other stakeholders planning to conduct water production projects on Mars.

Martian water resource project management system – an overview

The Martian water resource project management system is comprised of two key components: 1) a framework for the classification and categorisation of Martian water resource projects; and 2) a Martian water ice resource assessment framework. Together, these elements provide operators and evaluators of Martian ISRU water production projects a standardised approach to estimate quantities of recoverable product, assess a project's technical feasibility and development viability, and convey important information clearly and consistently.

Classification framework for martian water ice resources – specifications on the application of UNFC-2019

Resource classification systems provide a framework for comparable and consistent categorisation of a resource project based on the degree of confidence in recorded estimates of producible resource and the status of a project towards development and operation. This work has selected 'The United Nations Classification Framework for Resources' (UNFC, 2019) as the template for classifying Martian water ice resources. UNFC-2019 was designed to be universally applicable to all sources of resource product (ie energy, mineral, nuclear fuels, renewable and anthropogenic sources), to all types of resource assessments (ie assessment of resources for commercial projects, non-sale/direct-use projects and national/international resource endowment surveys) and for all stages of project development maturity (ie from early concept design through to currently producing projects). Specifications for its application to Martian water resource projects and its integration with NASA mission project management systems (ie Hirshorn, Voss and Bromley, 2017) are devised. This work demonstrates that UNFC-2019 provides a simple but powerful tool for communicating important information to ISRU project operators, investors, governments, and other stakeholders in space resource projects.

Another benefit of UNFC-2019 is the inclusion of bridging documents to aligned systems that map linkages in classification between UNFC-2019 with widely used and industry endorsed reserve

reporting standards such as the Committee for Mineral Reserves International Reporting Standards (CRIRSCO, 2019) and the Petroleum Resource Management System (PRMS; SPE, 2018). The availability of these bridging documents allows evaluators to compare earth-based resource assessments prepared using different classification systems/standards to assessments of Martian resource projects conducted using UNFC-2019. It also provides a means, if necessary, to convert the UNFC-2019 classification of a Martian project to another aligned resource classification system allowing greater comparability and transparency in recording and reporting on resource quantities.

Resource assessment framework for martian water ice production projects

A key limitation of the UNFC-2019 scheme is that it lacks detailed guidance on requirements for resource assessment and specific data-gathering/result benchmark criteria to justify assigning a project a certain classification. Just as there are notable differences in the approaches used by the petroleum, mineral mining, and other resource production industries (ie nuclear fuels, geothermal, renewables, bulk rock) to conduct resource assessments, operators of Martian water ice resource projects will require advice tailored to the unique geology, technology, economic, environmental, legal and political conditions. Consequently, the resource assessment framework for Martian water ice production projects outlines non-mandatory guidance on data-gathering, resource modelling and technical study activities along with workflows and decision criteria.

CONCLUSION AND BROADER APPLICATION

Good decision-making requires a clear and transparent means for information to be gathered, recorded and communicated. This work serves as an initial step in providing a standardised approach to Martian water ice resource project management. While the work presented in this study is primarily driven to address research gaps in communicating the degree of confidence in the quantity of Martian water ice resources and the likelihood of project development, the presented advice can be expanded to guide the management of other space resource projects both on Mars and on other celestial objects such as asteroids and the Moon. Ultimately it is envisioned that by incorporating a harmonised resource classification framework, such as UNFC-2019, with space resource reporting standards which outline mandatory resource assessment guidelines, a single unified framework to manage all space resource projects can be devised.

REFERENCES

- Abbud-Madrid, A, Beaty, D, Boucher, D, Bussey, B, Davis, R, Gertsch, L, Hays, L, Kleinhenz, J, Meyer, M and Moats, 2016. Mars water in-situ resource utilisation (ISRU) planning (M-WIP) study, 90.
- CRIRSCO, 2019. Committee for Mineral Reserves International Reporting Standards (CRIRSCO) – International Reporting Template for the Public Reporting of Exploration Results, Mineral Resources and Mineral Reserves (2019), Available online: http://www.crirSCO.com/templates/CRIRSCO_International_Reporting_Template_November_2019.pdf.
- Hirshorn, S R, Voss, L D and Bromley, L K, 2017. NASA Systems Engineering Handbook.
- McEwen, A, Sutton, S, Bramson, A, Byrne, S, Petersen, E, Levy, J, Golombek, M, Williams, N and Putzig, N, 2020. Phlegra Montes: Candidate Landing Site with Shallow Ice for Human Exploration. LPI, 2099: 6008.
- Moore, C, 2016. The Evolvable Mars Campaign, NAC Research Sub Committee pp. 2.
- Musk, E, 2018. Making Life Interplanetary, 2017.
- Society of Petroleum Engineers (SPE), 2018. Petroleum Resources Management System (PRMS). Society of Petroleum Engineers, <http://www.spe.org>.
- United Nations Framework Classification (UNFC), 2019. United Nations Framework Classification for Resources, United Nations, Geneva.

Integrating the approaches to space and mining project life cycles

A G Dempster¹

1. Director, Australian Centre for Space Engineering Research, School of Electrical Engineering and Telecommunications, UNSW, Sydney NSW 2052. Email: a.dempster@unsw.edu.au

ABSTRACT

This paper examines the different approaches to project life cycle taken by the space and mining industries and finds them to be somewhat incompatible, primarily due to the criteria for decision-making in the life cycle processes. Whereas the space industry uses system engineering ideas, the decisions in a mining life cycle are all commercial. This is because the space sector thinks in terms of developing *products*, and the mining industry develops *businesses*. The paper does not propose solutions to the difficulties in communication between these two sectors, rather it aims to define the problem and highlight some aspects of the industries which are *not* yet solutions.

INTRODUCTION

The space industry and the mining industry are both very large, led by sizable multinational corporations and have a very well established way of doing business. In 2019, the global space industry had revenues of USD424 billion (Mazareanu, 2020) while the top 40 mining companies had revenues of 692 billion in 2019 (Garside, 2021), led by Glencore (\$178 billion), BHP (\$42.9 billion) and Rio Tinto (\$41.8 billion) (Johnston, 2020). The top aerospace companies are Airbus (\$78.9 billion), Boeing (\$76.6 billion) and Lockheed Martin (\$59.8 billion) (Morrison, 2020), but that revenue is also shared with defence and aviation.

With the advent of space resources, possibly for the first time, the two industries are being forced to consider working together. However, their long-established methods of going about their business are not necessarily compatible with each other and there are ample opportunities for miscommunication at several levels. A simple example is the use of the word 'exploration', which to miners means prospecting and for space people means expanding knowledge of extra-terrestrial bodies and space more generally. Each does what they call exploration for completely different, possibly incompatible, reasons.

Anecdotal evidence from space resources events is strong that the two sides are not yet able to talk to each other unambiguously. This is largely because such events are still dominated by space people, and the miners are the ones scratching their heads. A simple example of the communication problem was the representative of a large mining company who came away from Space Resources Week in Luxembourg in 2019 with the opinion that after the entire event there was not a single thing that they could take to their company's board to discuss (pers. comm, 2019). After consideration of the different approaches to life cycles recorded later in this paper, it turns out that this triggering comment identified what turned out to be a critical insight: how decision makers are informed is not just important to how a life cycle develops, but it is also the key difference between the approaches taken in these industries.

The breakdown of attendees at that Luxembourg event was not available in a 'space versus mining' sense, but an analysis done by the author of first presenter's affiliation at a different event, Lunar ISRU 2019 (July 15–17, 2019, Columbia, Maryland – www.hou.usra.edu/meetings/lunarisru2019, tagline: Developing a New Space Economy Through Lunar Resources and Their Utilisation) gave the results in Table 1: 92 per cent space-related, and only 4 per cent mining-related. This seems to be typical of such events. If anything, the Luxembourg event was more skewed towards space, and the attendees perhaps even more so than the presenters. As a group, these people are relatively comfortable speaking to each other, as they tend to overwhelmingly come from a single discipline.

TABLE 1

Affiliations of the first named presenter on presentations at Lunar ISRU2019.

Affiliation	Space agency	Space company	University (space)	University (mining)	Agency (mining)	Other
	38	28	41	2	3	4

The team at UNSW led by the author and Professor Serkan Saydam has for some time been working on an approach to space resources research that ‘reduces the risk perceived by an investor in a space resources venture’. One of the key assumptions on which that work has been based is that such an investor will need to be a very large company, and because of the nature of the business to be pursued, that company is likely to be an existing mining company. Regardless of whether this assumption proves accurate, there is undoubted value in pursuing research with it as a motivator. If these risks and barriers are not addressed, the opportunity to engage such an investor will be lost.

Some preliminary work has been carried out. For instance, in (Hadler *et al*, 2020), the authors start to address some issues of language, and propose a ‘framework’, but because the authors only address how agencies would pursue resource utilisation, it does not progress the problem of communicating with resources companies.

This paper examines one element of the communication disconnect: the high-level approach to project life cycle, sometimes described by the space industry as Systems Engineering. The two industries have very well established approaches to the development of projects and these are contrasted with each other, with the ultimate aim of extracting a common approach, though this goal is out of scope of this paper.

EXISTING LIFE CYCLE APPROACHES

Space

The approach to life cycle by NASA is contained in its Systems Engineering Handbook (NASA, 2016) that is summarised in Figure 1. Phases A to F are separated by key decision points associated with specific reviews.

Key Decision Points ... are the events at which the decision authority determines the readiness of a program/project to progress to the next phase of the life cycle (or to the next KDP). Phase boundaries are defined so that they provide natural points for ‘go’ or ‘no-go’ decisions. (NASA, 2016)

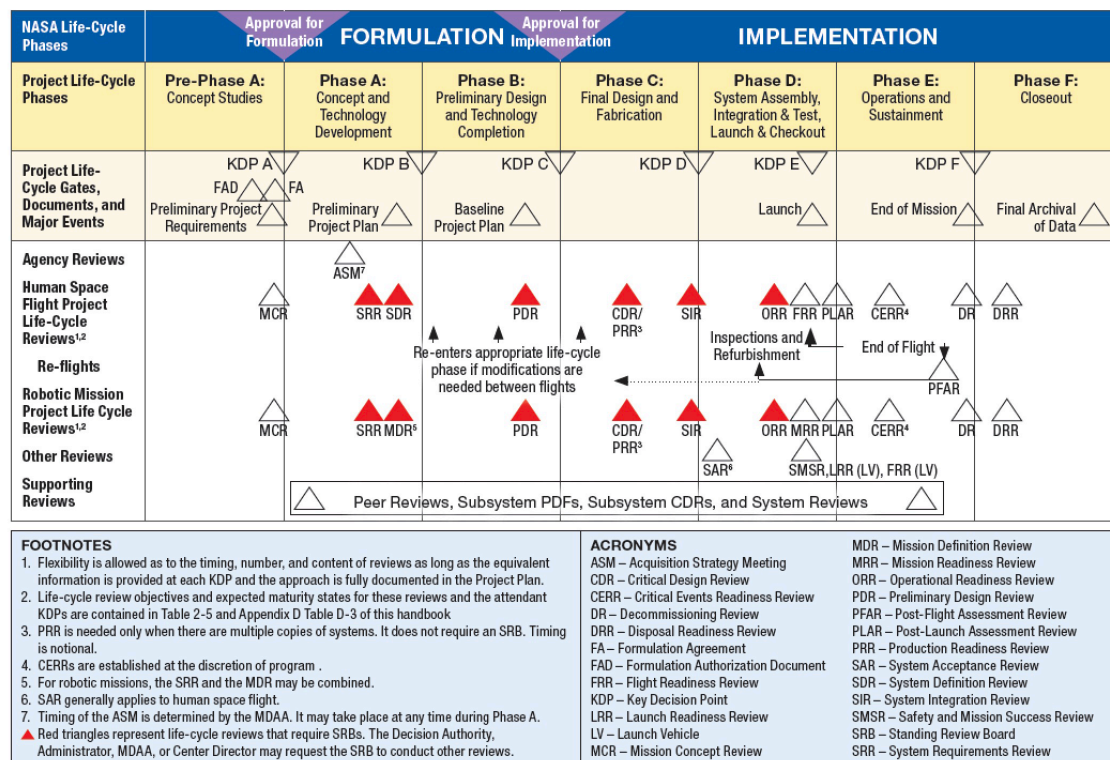


FIG 1 – Project life cycle from NASA Systems Engineering Handbook (NASA, 2016).

As can be seen in Figure 2, the phases identified in Figure 1 are nearly identical to those used by the European Space Agency (ECSS, 2009), with the minor modification that pre-phase A is called phase 0. This close convergence in approaches is an example of effective standardisation of the sector across international borders, which allows companies of different nationalities to work together, and for clients in different countries. This represents great *coherence*, ie the ability for cooperation within the industry, but not great *adherence*, the ability to work with industries that have different but similarly well developed and entrenched life cycle approaches.

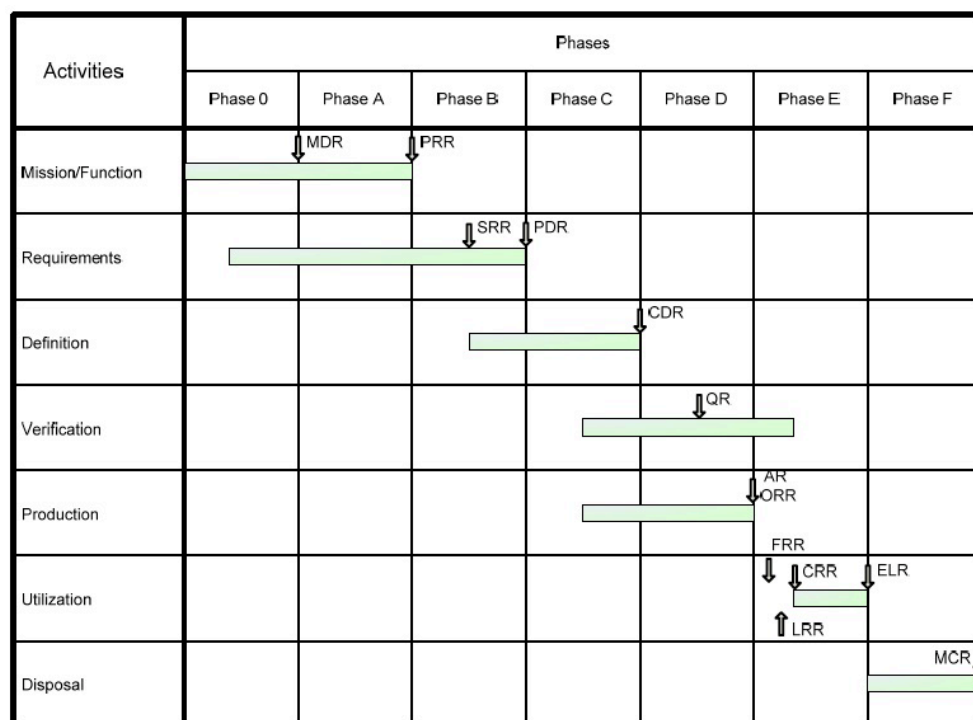


FIG 2 – Project life cycle as defined by ESA (ECSS, 2009).

These agency-driven approaches are very *design-oriented*, eg (NASA, 2016), on p 72, states ‘Most of the major system decisions (goals, architecture, acceptable life cycle cost etc) are made during the early phases of the project’. Note that delivering stakeholder outcomes, and how that is to be achieved are listed before cost is mentioned.

Key decisions points in Figure 1 follow reviews, of which there are many. To take the first, the Mission Concept Review, as an example, its purpose is ‘The MCR will affirm the mission need and evaluates the proposed objectives and the concept for meeting those objectives’ (NASA, 2016, p 161).

The life cycle as described in Figure 1 and Figure 2 maps very readily onto the classic system engineering ‘V-model’ (Forsberg and Mooz,1990) as shown in Figure 3. Phase A and B are in the descending, design arm of the V, C is along the bottom and D and E are in the ascending arm. So the management of life cycles as understood for space systems is very closely aligned with system engineering approaches.

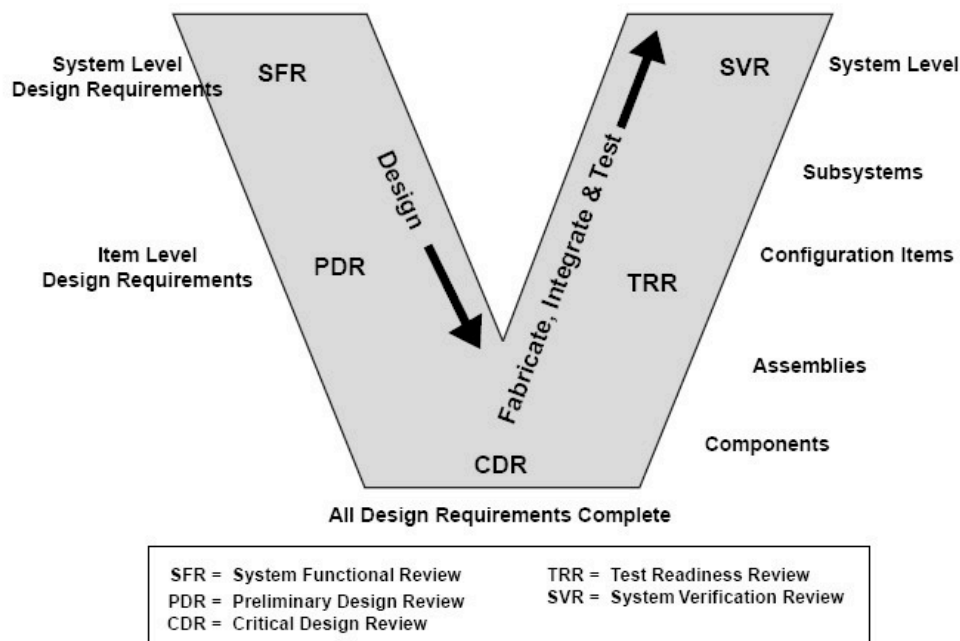


FIG 3 – Classic V model originally introduced in (Forsberg and Mooz,1990) (Wikimedia commons).

Mining

The comparable life cycle process in mining is less well documented. The process is relatively well agreed and ‘standardised’ but there is no real ‘standard’. In fact ‘there is no ready-made recipe that applies in all situations’ (Scott and Whateley, 2008). The key decision points in the life cycle of a mine relate to feasibility studies, and are based on commercial considerations. One of the few documents that addresses the life cycle directly uses the term ‘study management spectrum’, highlighting this importance of these studies (AusIMM, 2012). Some of the relevant terminology is shown in Figure 4, but (AusIMM, 2012) also notes that there is not an agreed term describing each phase. For instance, the term used for the scoping study can also be a ‘concept’, ‘order of magnitude’, or ‘identification study’.

The role of each study is to improve the degree of certainty about the cost and viability of the opportunity, as shown in Figure 5. As more money is spent on each study, more knowledge and certainty are gained. The term ‘bankable’ has been used for the Feasibility Study phase but as noted in (AusIMM, 2012), ‘[it] is the character of the investment, the sponsor and the lender who decides whether the project can be ‘banked’ or not, and in that sense, no engineer can contract to deliver a Bankable Study.’ An interesting requirement of these studies is that they must be performed by a ‘competent person’ (Scott and Whateley, 2008).

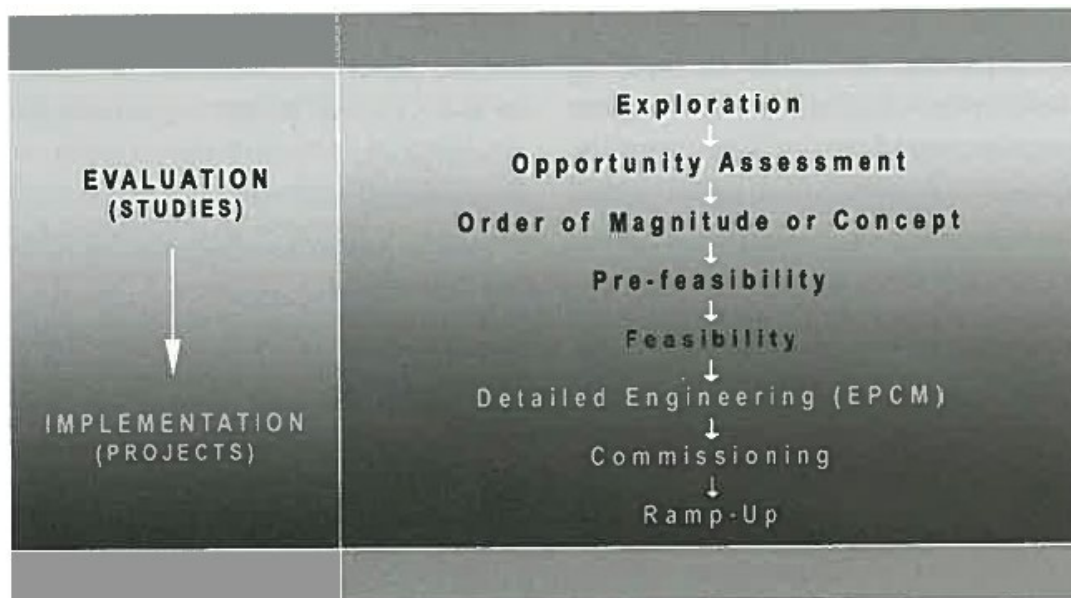


FIG 4 – The study management spectrum from (AusIMM, 2012).

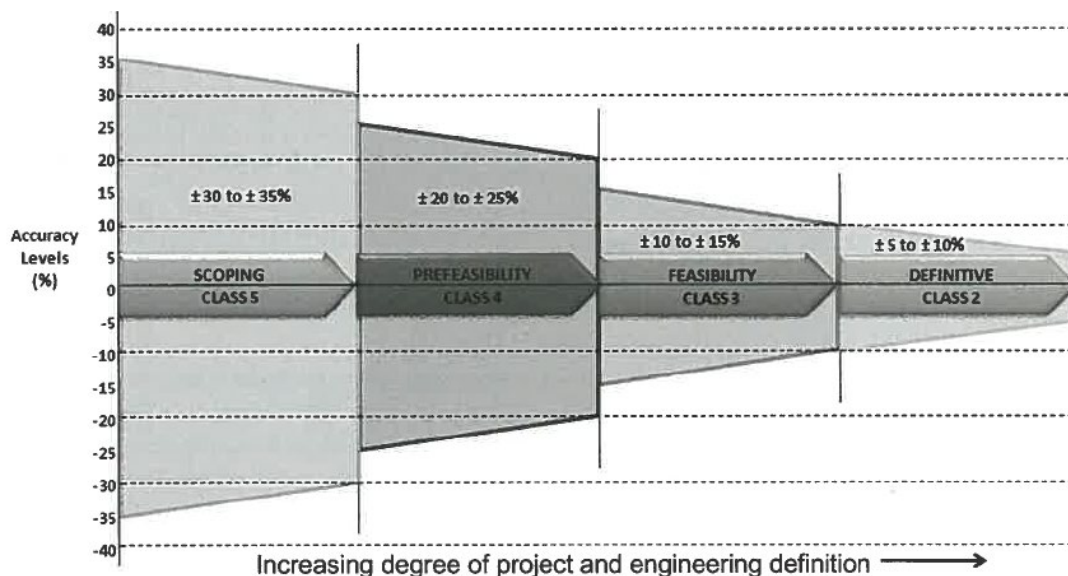


FIG 5 – Concept of increasing certainty with progress through the feasibility study process (AusIMM, 2012).

A simplistic role for each study can be assigned via individual questions as in Figure 6. One similarity can now be discerned with Figure 1 – that of operations. The final phase, 'Remediation' after operations for a mine, also has the analogy with 'close-out' in Figure 1, but there is not a clear mapping for the other project phases. Note there is only one key decision point in this figure – the investment decision after the Feasibility Study. However, it makes sense that 'study stages are defined by a set of objectives at the start, a set of work programs designed to achieve these objectives, and a decision point at which the project may progress to the next stage' (Scott and Whateley, 2008). A decision tree that does not cover the whole life cycle but the early study phases is shown in Figure 7 (Scott and Whateley, 2008). There are decision points after each phase and there is only one criterion: net present value (NPV). This is a simplification – other valuation methods are used as well, but all are investment-based decisions (Scott and Whateley, 2008).

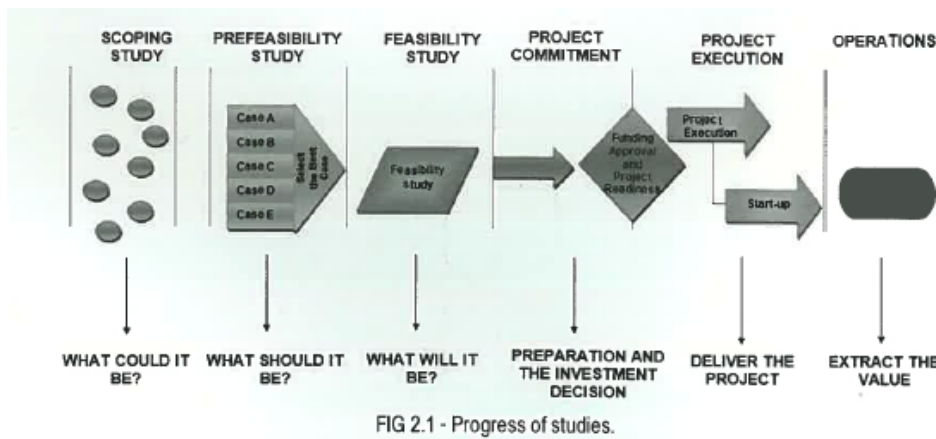


FIG 6 – Simple questions identify the role of each study (AusIMM, 2012).

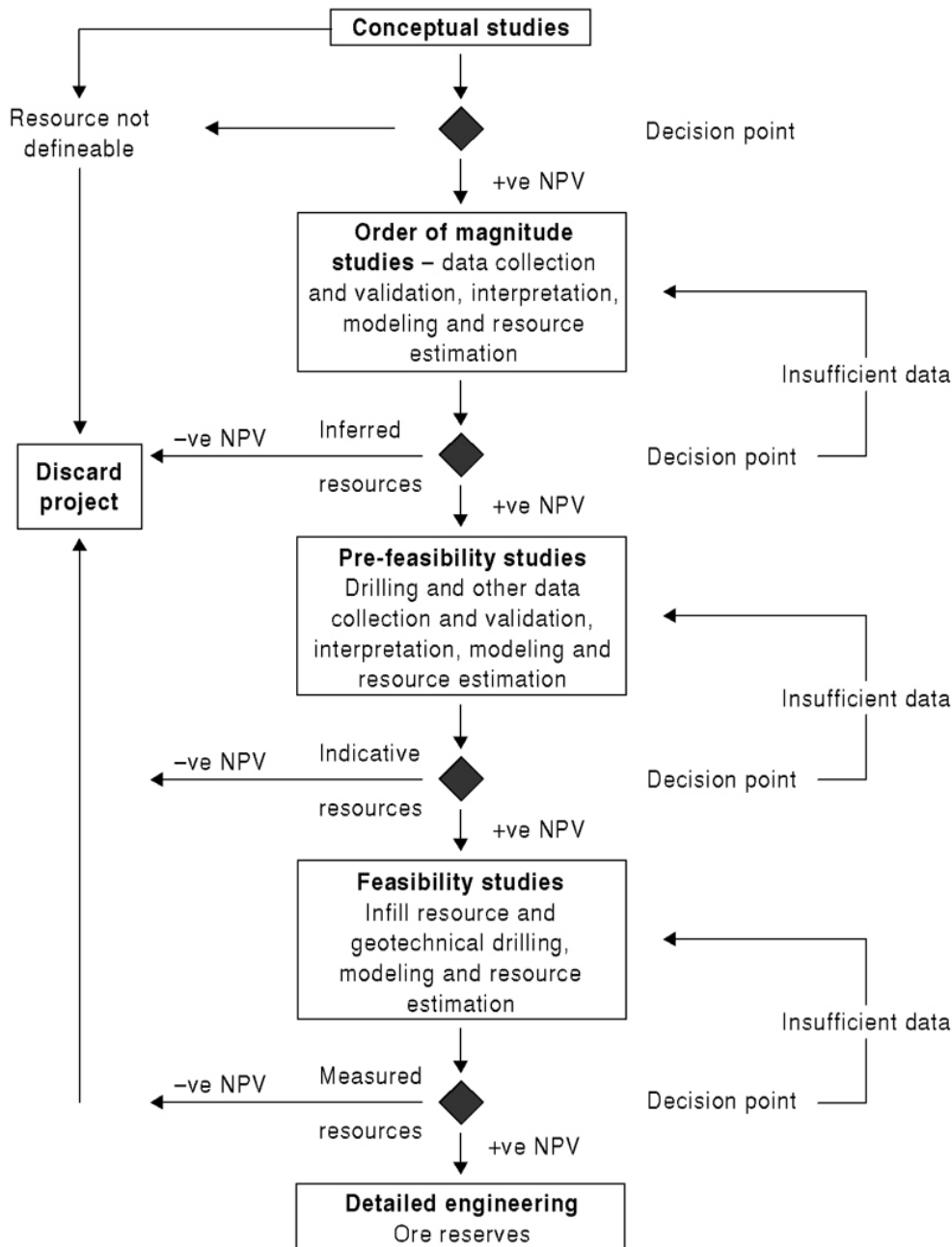


FIG 7 – More detailed decision-making tree for early study phases (Scott and Whateley, 2008) (artwork from https://media.wiley.com/product_ancillary/70/14051131/DOWNLOAD/Ch11.zip).

The phases progress through inferred to indicated to measured resources as defined by the JORC Code (JORC, 2012) and shown in Figure 8. The JORC Code is primarily concerned with standards of reporting about the state of a mineral deposit to regulatory bodies such as the Australian Securities Exchange or the New Zealand Stock Exchange. It also relies on the ‘Competent Person’ to provide those reports, and restricts the language to that used in Figure 8 as a standardisation measure.

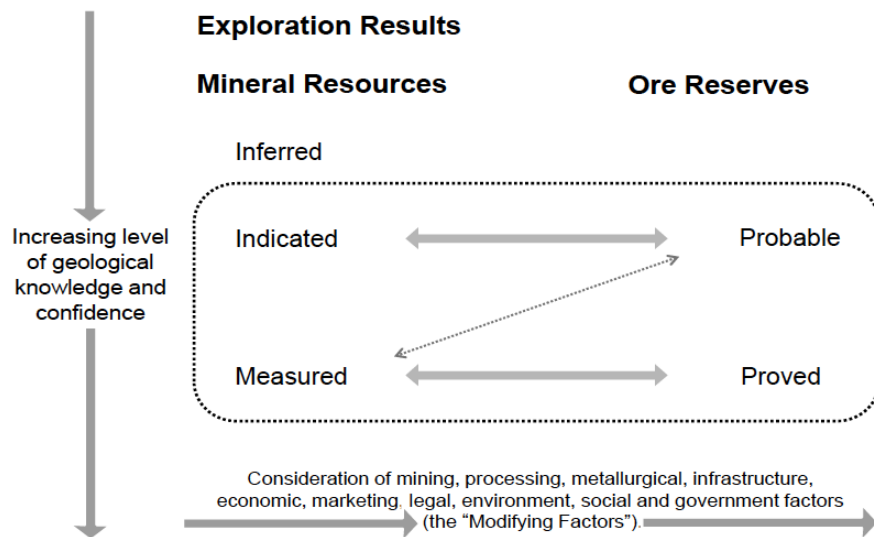


FIG 8 – Progression of a project as perceived under the JORC Code (JORC, 2012).

The processes of Figure 4 to Figure 7 improve knowledge (what is the state of the geology?) in the vertical dimension of Figure 8, but each study also examines the ‘modifying factors’ (how can that geology be exploited, all things being considered?) in the horizontal. The aim is to arrive at the bottom right of the diagram.

The JORC definition: ‘A ‘Mineral Resource’ is a concentration or occurrence of solid material of economic interest in or on the Earth’s crust in such form, grade (or quality), and quantity that there are reasonable prospects for eventual economic extraction’ seems directly transferable to Off-Earth locations, as do the other JORC definitions, including: ‘An ‘Ore Reserve’ is the economically mineable part of a Measured and/or Indicated Mineral Resource’. The latter definition has the important emphasis on knowledge (measured/indicated) and finance (economically), ie using both axes of Figure 8. There is also a comprehensive listing in (JORC, 2012) of the types of content required in the feasibility study process.

There has been recent interest within NASA in the creation of a different definition of ‘reserve’ for off-earth resources (Kleinhenz *et al*, 2020). This approach is acceptable if the aim is only to communicate with the space sector, but the mining sector is unlikely to see the need for a new definition given these are already embedded in standards. Encouragingly, although the NASA study included no mining sector contributors, it stated ‘There are enough differences between how the term ‘reserve’ is used on Earth, and how it might be used on the Moon (and on Mars) that a consensus definition should be developed.’ The author of this paper suggests that the original definition be kept (with removal of the reference to the Earth’s crust) and if that is insufficient for early stages of what occurs in space, the term ‘reserve’ should not be used, rather something modified (such as ‘life-support reserve’, where the replacement for profitability is embedded in the definition) or something altogether new.

The JORC Code does not deal with life cycle issues such as decision criteria arising from those feasibility studies.

The UN Framework (UN, 2020) provides a very useful way of categorising projects using three criteria: technical feasibility, degree of confidence, and environmental-socio-economic viability: see Figure 9. In other words the ‘modifying factors’ axis of Figure 8 is split into two axes: technical and environmental feasibility. The feasibility study approach to project life cycle navigates between these categories, but the framework itself does not define such life cycle activity.

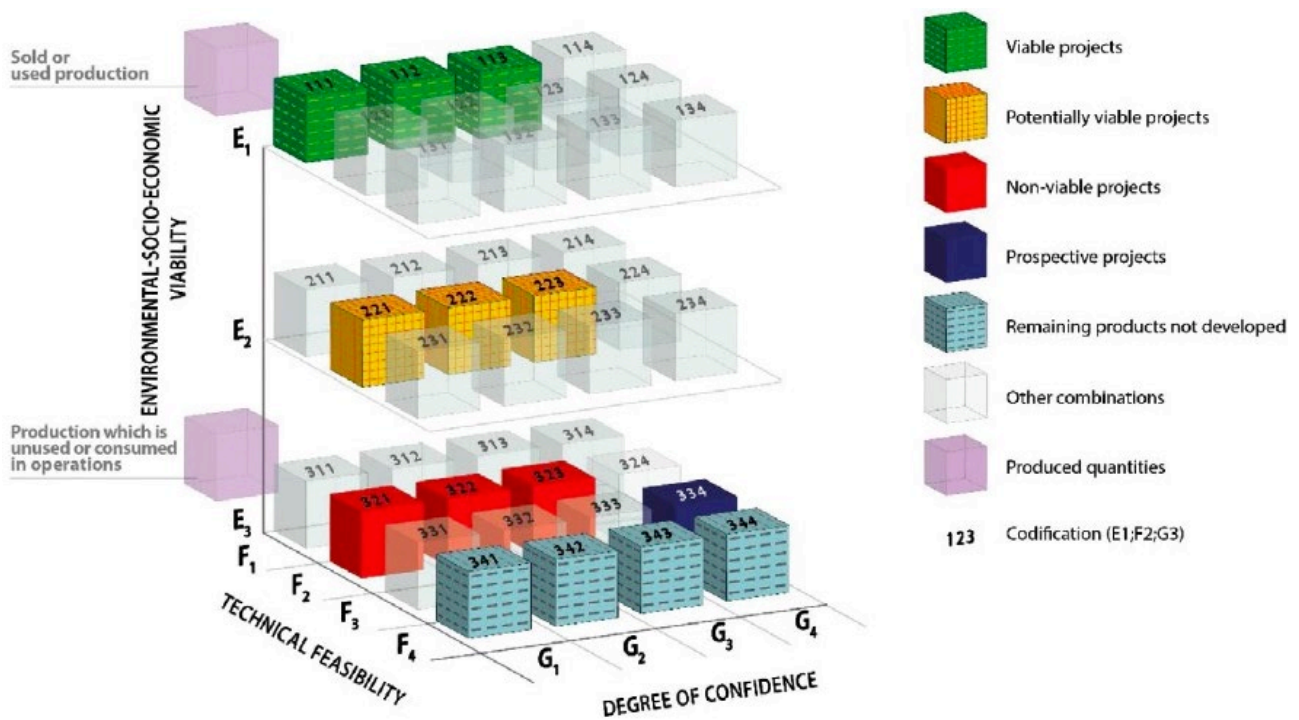


FIG 9 – Categories under the UN framework (UN, 2020).

Oil and gas

A more formal structure that has very explicit decision points has been used to describe the life cycle of oil and gas projects, as shown in Figure 10. Note the clear decision gate process, and the division into the ‘choose the right project’ and ‘do the project right’ phases. In a similar way to the space life cycle relating closely to the system engineering V-model, this methodology (stage gates or phase gates) is also well-established (Muiño and Akselrad, 2009), and used more in oil and gas than mining.

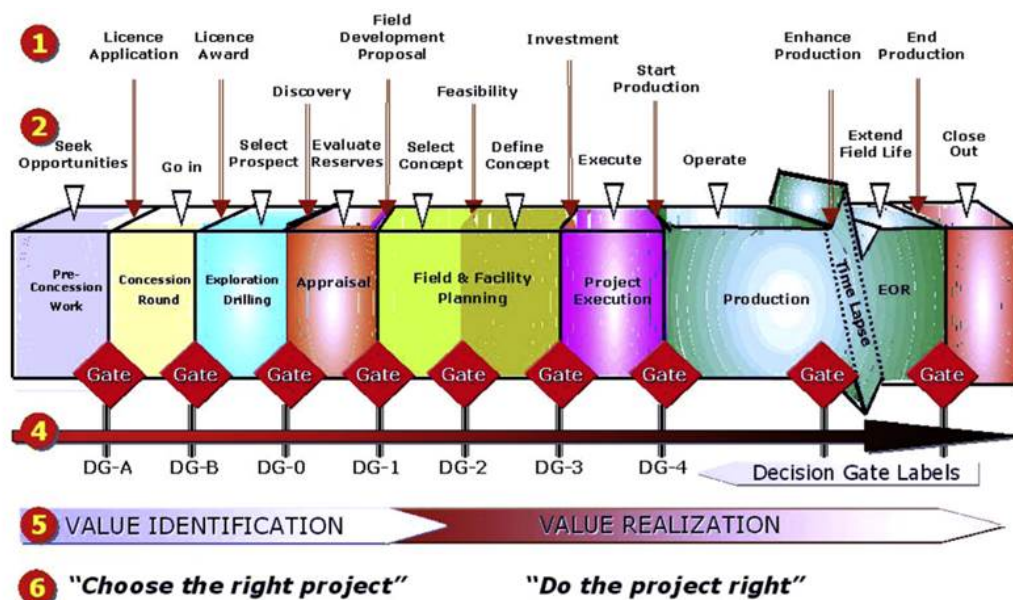


FIG 10 – Project life cycle illustration for an oil and gas project (Weijermars, 2009) with clear decision gates.

DISCUSSION

Similarities and differences

The high-level difference between the approaches of the two industries is that the mining (and oil and gas) decision points are all and always commercial, whereas the agency-driven space projects have more technical 'system engineering' decision criteria.

The high-level 'shape' of a project life cycle could be considered to be similar, given each could be divided into two halves. The space project can be divided as in Figure 3 into 'Design' and 'Fabricate, Integrate and Test' halves, whereas the resources project of Figure 10 divides into 'choose the right project' and 'do the project right'. However, the roles of those halves do not map well onto each other, particularly the first half. In both second halves, 'operations' and 'closeout' phases occur and are genuine analogues of each other. The different stakeholders and their objectives dictate that what occurs before these phases is different.

At each decision point, documentation is presented and that documentation for one industry would not look familiar to those at a similar stage in the other industry. However, there are chapters of the documents that correspond. In AusIMM (2012), the suggested chapters in each of the mining industry feasibility studies are:

1. Summary and Recommendations
2. Development Approach and Business Case(s)
3. Risk
4. Health, Safety and Security
5. Environment
6. Geology and Mineral Resource
7. Mining and Ore Reserves
8. Mineral Processing
9. Waste and Water Management
10. Infrastructure and Services
11. Human Resources, Industrial and Employee Relations
12. Technology and Information Systems
13. Project Execution
14. Operations
15. External and Community Relations
16. Capital Costs
17. Operating Costs
18. Marketing
19. Ownership and Legal Aspects
20. Commercial
21. Financial Analysis
22. Status of Studies
23. Work Plan
24. Bibliography and References
25. Appendices

Note the importance of points 2 and 18–21, the commercial aspects. Aspects specific to the type of engineering, ie mining, are given prominence (6–8). There are similarities and differences with the criteria for success at a space project review, all of which are listed in (NASA, 2020). The critical review that separates the two halves of the mining life cycle is the ‘Feasibility Study’ so comparison is probably best made with the review that plays that role in Figure 3, ie the Critical Design Review (CDR). Its list of success criteria is presented in (NASA, 2020, p 90):

1. The detailed design is expected to meet the requirements with adequate margins.
2. Interface control documents are sufficiently mature to proceed with fabrication, assembly, integration, and test, and plans are in place to manage any open items.
3. The program/project cost and schedule estimates are credible and within program/project constraints.
4. High confidence exists in the product baseline, and adequate documentation exists or will exist in a timely manner to allow proceeding with fabrication, assembly, integration, and test.
5. The product verification and product validation requirements and plans are complete.
6. The testing approach is comprehensive, and the planning for system assembly, integration, test, and launch site and mission operations is sufficient to progress into the next phase.
7. Adequate technical and programmatic margins (eg mass, power, memory) and resources exist to complete the development within budget, schedule, and known risks.
8. Risks to safety and mission success are understood and credibly assessed and plans and resources exist to effectively manage them.
9. Safety and mission assurance (eg safety, reliability, maintainability, quality controls, SCRM, QA, and EEE parts) have been adequately addressed in system and operational designs, and any applicable SandMA products (eg PRA, system safety analysis, and failure modes and effects analysis) meet requirements, are at the appropriate maturity level for this phase of the program/project life cycle, and indicate that the program/project safety/reliability residual risks will be at an acceptable level.
10. The program/project has demonstrated compliance with applicable NASA and implementing Center requirements, standards, processes, and procedures.
11. TBD and TBR items are clearly identified with acceptable plans and schedule for their disposition.
12. Engineering test units, life test units, and/or modelling and simulations have been developed and tested per plan.
13. Material properties tests are completed along with analyses of loads, stress, fracture control, contamination generation, and other analyses.
14. EEE parts have been selected, and planned testing and delivery will support build schedules.
15. The operational concept has matured, is at a CDR level of detail, and has been considered in test planning.
16. Manufacturability has been adequately included in design.
17. Software components meet the success criteria defined in NASA-HDBK-2203.
18. Concurrence by the responsible Center spectrum manager that the program/project has provided requisite RF system data.
19. Procurement and supply chain risk management execution is complementary with the technical development schedule.

Comparing these two lists leads to a fundamental observation about the difference between mining engineering and the space engineering disciplines (electrical, electronic, software, mechanical) in terms of the problem being examined here. The latter designs a *product* (as in CDR points 4 and 5) while the former designs a *business* (Feasibility points 2, 18–21). It appears this is the fundamental disconnect that has been sought.

Going through each of the above lists point by point, in general an analogue can be found in the other list but these analogues are not obvious. For instance, CDR point 1 'meet the requirements' follows similar points in earlier reviews that refer to meeting 'stakeholder expectations', which aligns to some degree with feasibility study point 18 'Marketing'.

So similar types of information could be gathered in each process, but it is differently presented to support arguments for the decision points. For example, Mission Concept Review (MCR) success criterion 9 (NASA, 2020, p 76) is 'Alternative concepts have adequately considered the use of existing assets or products that could satisfy the mission or parts of the mission.' Similarly, (Scott and Whateley, 2008) states 'The role of the Pre-Feasibility Study is to evaluate the various options and possible combinations of technical and business issues ... and to rank the various scenarios prior to selecting the most likely for further, more detailed, study.' In other words, both life cycle approaches consider multiple technical solutions, but the role that consideration plays in decision-making is different.

Other life cycle options

The current study is premised on the importance of communicating to mining executives, so it would appear that it is the space 'system engineering' approach that needs to be modified in order to facilitate that communication.

Communications satellites

The space agency approach of NASA (2016, 2020) and ECSS (2009) is not necessarily geared to commercial outcomes, so examination of commercial space activity may seem a good place to seek an approach that can be leveraged. One highly lucrative business has developed in space, that of satellite communications. Remote sensing has also become a more commercial application in recent years. Comparing commercial spacecraft to science and defence spacecraft in Figure 11 shows that costs can be reduced and schedule stabilised by following a modified version of the system engineering approach (Hertzfeld, 2017).

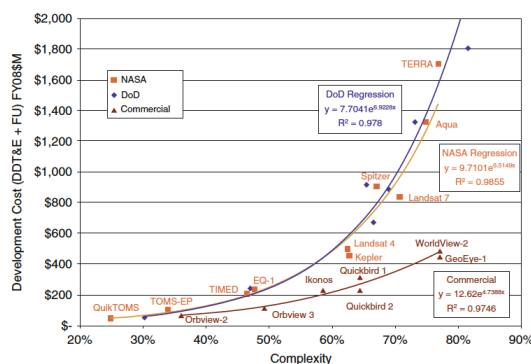


Fig. 2 Efficiencies in DoD and NASA production are similar but less than commercial

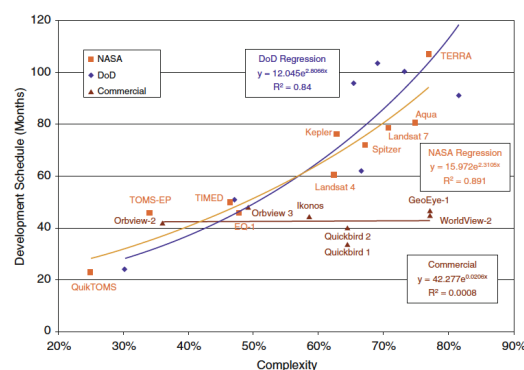


Fig. 3 Schedule increases with complexity for government systems

FIG 11 – Comparison of costs (left) and schedule (right) versus complexity for three types of satellite: agency-driven science, defence, and commercial (from Hertzfeld, 2017).

The differences in approach were summarised (Hertzfeld, 2017) as in Table 2. This is encouraging but it still does not face head-on the problem of communicating with the mining industry, in that the space system engineering approach is still used, but applied more efficiently. The commercial approaches in the table are appropriate but they don't represent a different high-level life cycle approach.

TABLE 2

Summary of differences in approach for government and commercial satellites, from (Hertzfeld, 2017).

Category	Commercial	Government
Development trend	Evolutionary	Revolutionary
Production	Standardization and reuse of building blocks. Build multiple units	Unique designs. Build one of a kind
Requirement definition	Well understood before project start	Not well understood at project start
Requirement stability	Stable	Unstable
Stakeholders	Single customer/stakeholder	Many stakeholders
Performance specification	Specifies only performance requirements	Specifies performance requirements and methods
Design incentive	Profit driven	Science driven
Design approach	Satellite buses viewed as product line and are a known entity	Changes, especially after the start of the project, drives the design of the satellite bus
Cost and schedule	Based on known similar historical data (buy mode)	Cost and schedule estimates are optimistic (sell mode)
Funding stability	Stable	Potential annual changes (often a result of budget pressures)
Portfolio management	If a project gets into trouble, it typically gets canceled	Projects allowed to continue and usually cause collateral damage to the portfolio (a very inefficient outcome)
Procurement process	Streamlined	Long and complicated
Contract type	Incentives for early delivery and late delivery penalties	Cost-plus-type contracts
Oversight and reporting	Minimal oversight of subcontractors	Extensive oversight of primes and subcontractors
Test philosophy	Deletes non-value-added processes (profit driven)	Tends to avoid seeking waivers. Success valued on success of mission, not cost or schedule overruns

Concurrent design

Concurrent design (Finger *et al*, 1992) takes a more holistic approach to design, assessing each design decision using as many consequences as possible. However, when applied to space systems, in general it simply replaces early stages within the overall system engineering framework, without replacing that framework (Bandecchi *et al*, 2000).

Space 2.0

'Space 2.0', or 'Newspace', is a philosophical change in the way space projects are pursued, moving from large, expensive satellites developed by governments via large agencies, to a more dynamic paradigm, featuring new technologies, very small satellites, low cost access to space and a more commercial focus (Pelton, 2019).

Embracing space 2.0 philosophies has also led to some re-evaluation of the system engineering approach inherited from 'Space 1.0', but the newly proposed life cycle approach is still recognisably 'system engineering' (da Motta Silva and Perondi, 2021).

An advantage that space 2.0 may appear to have in this discussion is that the idea of designing the business is inseparable from designing the product, ie a start-up company is formed purely to deliver one type of service via satellite. This has to some extent been characterised in (Hertzfeld and Pelton, 2020) where examples used included SPIRE, OneWeb, Skybox, and Planet Labs. The life cycle approach and go/no-go decisions are not really discussed, the main focus being the advantages of mass production and new investments sources. Even large successful disruptive space 2.0 companies such as SpaceX, Blue Origin and Virgin Galactic are still producing a recognisable product, heavily based on hardware (the ‘rocket’) (Madry, 2020). Some lessons can be learned from space 2.0, but the solution does not yet lie there, as a development approach seems not to have been formalised.

CONCLUSION

Key takeaways:

- The work here is premised on the assumption that large resources companies will be the eventual investors in space resources enterprises.
- To communicate with these companies, a new approach needs to be taken to life cycle design by the space industry (rather than the mining industry). Presently, there seems to be no real effort being applied to that communication.
- Historically, space industry engineers have designed products, where mining engineers design businesses. Even where space people design businesses, that approach seems not yet to be applicable to space resource extraction.
- There seems at present not to be a life cycle approach that can address the space resources project problem. How best to combine the approaches of the two industries remains important future work. This paper acts only as problem definition.

ACKNOWLEDGEMENTS

The author acknowledges the helpful contributions of sources by Serkan Saydam, Ben McKeown, Damon Ellender, Ruud Weijermars, Jason Held, Lily Qiao, and the copyright holders of the images used.

REFERENCES

- AusIMM, 2012. *Cost Estimation Handbook, Monograph 27*.
- Bandecchi, M, Melton, B, Gardini, B and Ongaro, F, 2000. The ESA/ESTEC Concurrent Design Facility, Proc EuSEC 2000.
- da Motta Silva, F and Perondi, L F, 2021. A Proposal of a Life-Cycle for the Development of Sounding Rockets Missions, *Journal of Aerospace Technology Management*, São José dos Campos, v13, 2021, doi.org/10.1590/jatm.v13.1193
- ECSS Secretariat, 2020. Space project management: Project planning and implementation, ECSS-M-ST-10C Rev. 1, 6 March 2009.
- Finger, S, Fox, M S, Prinz, F B and Rinderle, J R, 1992. Concurrent Design, *Applied Artificial Intelligence an International Journal*, vol 6 no3, pp257–283, 1992, DOI: 10.1080/08839519208949955
- Forsberg, K and Mooz, H, 1990. *Proceedings of the First Annual NCOSE Conference*.
- Forsberg, K, Mooz, H and Cotterman, H, 2000. *Visualizing Project Management*, John Wiley and Sons.
- Garside, M, 2021. Combined revenue of the top mining companies 2005–2019, Statista.com, accessed 24 March 2021.
- Hadler, K, Martin, D J P, Carpenter, J, Cilliers, J J, Morse, A, Starr, S, Rasera, J N, Seweryn, K, Reiss, P and Meurisse, A, 2020. A universal framework for Space Resource Utilisation (SRU), *Planetary and Space Science*, vol 182, March 2020, doi.org/10.1016/j.pss.2019.104811
- Hertzfeld, H R and Pelton, J N, 2020. Financial Models and Economic Analysis for Small Satellites Systems, in J N Pelton (ed), *Handbook of Small satellites*, Springer Nature, 2020.
- Hertzfeld, H R, 2017. Economics and Financing of Communications Satellites, in *Handbook of Satellite Applications*, J N Pelton, S Madry, Sergio Camacho-Lara (eds), 2nd ed, pp 305–324.
- Johnston, M, 2021. 10 Biggest Mining Companies, *Investopedia*, accessed 14 September 2020.

- Joint Ore Reserves Committee of The Australasian Institute of Mining and Metallurgy, Australian Institute of Geoscientists and Minerals Council of Australia (JORC), 2012. Australasian Code for Reporting of Exploration Results, Mineral Resources and Ore Reserves' (The JORC Code), 2012 edition, 20 Dec 2012.
- Kleinhenz, J, McAdam, A, Colaprete, A, Beaty, D, Cohen, B, Clark, P, Gruener, J, Schuler, J and Young, K, 2020. 'Lunar Water ISRU Measurement Study (LWIMS): Establishing a Measurement Plan for Identification and Characterization of a Water Resource', NASA/TM-20205008626, October 2020.
- Madry, S, 2020. *Disruptive Space Technologies and Innovations*, Springer Nature, 2020.
- Mazareanu, E 2020. Space industry worldwide – statistics and facts, Statista.com, accessed 23 September 2020.
- Morrison, M, 2021. Top 100 aerospace companies ranked by revenue, *FlightGlobal*, accessed 15 September 2020.
- Muiño, A and Akselrad, F, 2009. Gates to Success: Ensuring the Quality of the Planning, *PMI Global Congress 2009*, EMEA, Amsterdam, The Netherlands.
- NASA, 2016. NASA Systems Engineering Handbook, NASA/SP-2016–6105 rev 2, 2016.
- NASA, 2020. NASA Procedural Requirements: NASA Systems Engineering Processes and Requirements, NPR 7123.1C, Effective Date: February 14, 2020.
- Pelton, J N, 2019. *Space 2.0: Revolutionary Advances in the Space Industry*, Springer Nature.
- Scott, B C and Whateley, M K G, 2008. Project Evaluation, in C J Moon, M K G Whateley, A M Evans (eds), *Introduction to Mineral Exploration*, 2nd ed, pp 253–277, Blackwell.
- UN, 2019. United Nations Economic Commission For Europe, United Nations Framework Classification For Resources: Update 2019, Geneva 2020.
- Weijermars, R, 2009. Accelerating the three dimensions of E&P clock speed – A novel strategy for optimizing utility in the Oil and Gas industry, *Applied Energy*, vol 86, 2009, pp 2222–2243.

Facilitating commercial lunar water ice extraction – a terrestrial mining perspective on governance

B McKeown¹, S Saydam² and A G Dempster³

1. PhD Student, Australian Centre for Space Engineering Research, UNSW, Sydney NSW 2052. Email: b.mckeown@unsw.edu.au
2. Professor, Australian Centre for Space Engineering Research, UNSW, Sydney NSW 2052. Email: s.saydam@unsw.edu.au
3. Director, Australian Centre for Space Engineering Research, School of Electrical Engineering and Telecommunications, UNSW, Sydney NSW 2052. Email: a.dempster@unsw.edu.au

INTRODUCTION

Resources sourced off-earth will be vital for the eventual development of a space economy. The most immediate resource need will be for water sourced from lunar water ice for life support purposes, and later potentially for propellant production. The production of water derived from lunar ice is at a nascent stage, with current research focused on technical feasibility rather than commercial viability. It is recognised however, that if an off-earth economy is to ultimately become a reality, the involvement of the commercial sector will be imperative.

The development of a fit for purpose governance framework will be critical for the long-term sustainable development of commercial lunar resource extraction, acting as an ‘enabler’ of commercial activity and providing the ground rules and oversight required.

Recent initiatives to address this include the US led Artemis Accords whose focus has been on developing mechanisms to enable lunar resource extraction whilst not breaching the non-appropriation principle of the Outer Space Treaty. Whilst a useful step forward, the Accords do not appear to have considered the perspective of the entities likely to undertake possible commercial lunar resource activities – entities similar to today’s terrestrial mining companies. If there is real intent to facilitate commercial lunar resource extraction, the requirements of these entities (and the financing behind these entities) will need to be addressed. The international mining industry has substantial experience in addressing the governance requirements for resource projects, and this experience could help with the development of appropriate governance frameworks for a commercial lunar resource sector.

Considerations for terrestrial mining activities relevant to potential lunar resource activities include:

- The requirement for secure title to in-ground assets with the right to extract and own minerals, together with the ability to monetise exploration success.
- Competition based primarily on being a ‘price taker’, leading to competitive advantage accruing to companies with low cost, high quality assets.
- The ability to access to financing throughout the development cycle of a resource project.
- Legal/regulatory certainty over the long-term.

Taking these factors into account, governance for commercial lunar water ice activities should be considered in the context of factors including the following.

The geological context

- Estimates of lunar water resources range from >500 Mt to several billion tonnes (Rubanenko, Venkatraman and Paige, 2019) existing as water ice located in the Permanently Shadowed Regions (PSRs) at the lunar poles. It is estimated that there are >2300 PSRs (Mazarico *et al*, 2011), however only a fraction are anticipated to contain ice (Li *et al*, 2018).
- Characteristics of this water ice are uncertain, with the only physical data point to date being the LCROSS mission indicating a water ice concentration of 5.6 per cent +/- 2.9 per cent at the impact site in the Cabeus crater (Colaprete *et al*, 2010). Some modelling indicates that the

highest concentration of ice may occur in the top 1 m of regolith in the PSRs (Cannon and Britt, 2020), and that 'cut-off' grade considerations may be appreciable (Sowers and Dreyer, 2019).

- Potential ice resources located proximal to sites suitable for infrastructure (power and communications) and access could be very limited (eg Elvis, Krolikowski and Milligan, 2021).

Potential implications include that lunar water ice deposits of economic size and grade, and suitable location may be relatively scarce, thereby requiring significant exploration/appraisal programs to identify and delineate to a sufficient level of confidence. Additionally, the area required for a commercial operation could be substantial, a function of a relatively low ice concentration contained within a limited vertical extent.

Current legal context

Existing law/governance relevant to lunar resources includes:

- 1967 Outer Space Treaty (OST) providing principles on what is permissible in space. Resource extraction was not anticipated at the time of negotiation, leading to substantial ambiguity. Articles relevant to resources include Article I – freedom of use and benefit of mankind principles, and Article II – prohibition of national appropriation.
- 2015 US Commercial Space Launch Competitiveness (SPACE) Act recognising right of US entities to own space resources once extracted on a first come first served basis (Luxembourg and UAE have enacted comparable legislation).
- Artemis Accords signed by US and 10 other countries (including Australia) in 2020 introducing the concept of 'Safety Zones' to prevent interference and for their use in the extraction of space resources. Messaging around the Artemis Accords includes the aspiration that the Accords could set precedent for future commercial activity.

In addition, the 1979 Moon Agreement attempted to provide clarity on the extraction and ownership of space resources. However, most States, including all spacefaring States, declined to sign the Agreement. In 2020, the Hague Working Group in an advisory capacity proposed Building Blocks to inform a future governance framework for space resource activity.

DISCUSSION

Assuming commercial space resource entities could have similar requirements to terrestrial resource companies one could ask the question, would a legal/regulatory toolbox comprising the OST, the US SPACE Act (or equivalent) and the Safety Zones detailed in the Artemis Accords be sufficient for the private sector to invest billions of dollars in exploring for and developing a lunar resource project?

Reasons why such a governance toolbox may not be sufficient from the perspective of a commercial lunar water ice resource developer include the fact that economic deposits may need to cover a large surface area and possibly encompass multiple locations for an individual operation to be commercially viable. This in turn could require extensive exploration activity to identify and delineate. Additionally, the potentially heterogeneous nature of lunar ice deposits could result in significant competition for the highest quality assets. For these reasons, and others, lunar resource entities would require confidence that they have the exclusive right to extract resources from these areas over lengthy development and operational periods, including during periods when there is no actual activity at the resource location.

Unfortunately, neither the OST nor the US SPACE Act address the issue of exclusive rights, and the Safety Zones in the Artemis Accords are a concept aimed at preventing short-term third-party interference at a particular lunar location, rather than providing long-term exclusive access. Additionally, the ambiguity in the OST regarding space resource activities in general and non-appropriation more specifically remains, and it is difficult to see how this suite of legal instruments would provide the long-term certainty required for resource financing and development. In order to encourage such activities, an appropriate governance framework will need to be developed. Perhaps Australia, with its vibrant resource industries, and as the only State party to both the Artemis Accords and the Moon Agreement, could be uniquely positioned to take a lead role in such a development?

REFERENCES

- Cannon, K M and Britt, D T, 2020. A Geologic Model for Lunar Ice Deposits at Mining Scales, *Icarus*.
- Colaprete, A, Schultz, P, Heldmann, J, Wooden, D, Shirley, M, Ennico, K, Hermalyn, B, Marshall, W, Ricco, A, Elphic, R C, Goldstein, D, Summy, D, Bart, G D, Asphaug, E, Korycansky, D, Landis, D and Sollitt, L, 2010. Detection of Water in the LCROSS Ejecta Plume, *Science*, 330(6003): p. 463–468.
- Elvis, M, Krolkowski, M A and Milligan, T, 2021. Concentrated lunar resources: imminent implications for governance and justice, *Philosophical Transactions of the Royal Society A: Mathematical, Physical and Engineering Sciences*, 379(2188): p. 20190563.
- Li, S, Lucey, P G, Milliken, R E, Hayne, P O, Fisher, E, Williams, J-P, Hurley, D M and Elphic, R C, 2018. Direct evidence of surface exposed water ice in the lunar polar regions, *Proc Natl Acad Sci U S A*, 115(36): p. 8907–8912.
- Mazarico, E, Neumann, G A, Smith, D E, Zuber, M T and Torrence, M H, 2011. Illumination conditions of the lunar polar regions using LOLA topography, *Icarus*, 211(2): p. 1066–1081.
- Rubanenko, L, Venkatraman, J and Paige, D A, 2019. Thick ice deposits in shallow simple craters on the Moon and Mercury, *Nature Geoscience*, 12(8): p. 597–601.
- Sowers, G and Dreyer, C, 2019. Ice Mining in Lunar Permanently Shadowed Regions, *New Space* 7(4): p. 235–244.

Determination of the stability of microtunnel opening in lunar regolith and low gravity conditions

T Pelech¹, M Dello-Iacovo², N Barnett³, J Oh⁴ and S Saydam⁵

1. PhD student, School of Minerals and Energy Resources Engineering, UNSW, Sydney NSW 2052. Email: t.pelech@unsw.edu.au
2. PhD student, School of Minerals and Energy Resources Engineering, UNSW, Sydney NSW 2052. Email: m.dello-iacovo@student.unsw.edu.au
3. PhD student, School of Minerals and Energy Resources Engineering, UNSW, Sydney NSW 2052. Email: nicholas.barnett@unsw.edu.au
4. Senior Lecturer, School of Minerals and Energy Resources Engineering, UNSW, Sydney NSW 2052. Email: joungh.oh@unsw.edu.au
5. Professor, School of Minerals and Energy Resources Engineering, UNSW, Sydney NSW 2052. Email: s.saydam@unsw.edu.au

INTRODUCTION

In situ resource utilisation and off-Earth mining require novel methods and models to test capabilities at a low cost prior to committing to expensive experiments on-site. This research aims to determine the stability of tunnels in lunar regolith and conditions using the capability of the Discrete Element Method (DEM). The YADE DEM program will be used for the experiments in this paper. Calibration and validation of the lunar regolith samples will be carried out using various published data and simulated triaxial testing.

The DEM has been developed for modelling granular materials where Newtonian calculations are carried out on discrete particles in each iterative timestep (Zhao, 2017). The open source YADE code has been used in this research.

DEM has been favoured for Off-Earth soil mechanics modelling due to the difficulty in obtaining realistic samples and experimental set-ups on Earth. Lane, Metzger and Wilkinson (2010) conducted a review of the appropriate DEM particle shapes and size distributions for simulating lunar regolith. Jiang, Shen and Thornton (2013) have further developed a contact model used in DEM for lunar regolith which includes the van der Waals force originating from a very thin layer of adsorbed gas on the particles in the vacuum of space. It has been found that the van der Waals is an important component of cohesion in lunar conditions. In terms of tunnelling, a terrestrial tunnel and ground support study has been conducted using YADE by Boon, Houlsby and Utili (2015). This study focuses on terrestrial hard rock tunnelling and with failure caused by discontinuities in the rock. Some of the methods and experimental set-ups used for the hard rock study can also be applied to lunar regolith tunnelling as in this paper.

MODELLING METHOD

Physical laws and interactions

The YADE Discrete element program runs an iterative loop carrying out interaction detection and physics integration along with other supplementary functions on each timestep. The loop used for the simulations in this paper is shown in Figure 1. Further details on the working of each of the functions in this loop are available in the YADE Documentation (Šmilauer *et al*, 2015).

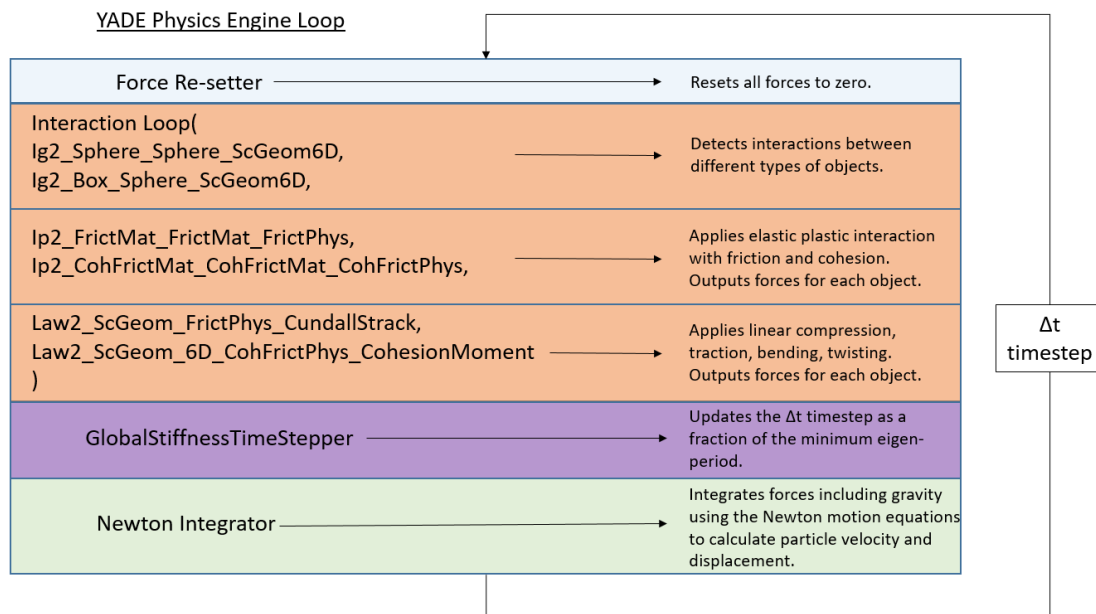


FIG 1 – YADE interaction and physics loop used in this research.

To ensure the physics and interaction loop is working as desired, some checks should be conducted prior to beginning calibration and experimental trials. Confirmation of successful interactions and cohesive laws can be made by counting the number of cohesive interactions at the start of the simulation compared to the end of the simulation. The experiment will only run until initial failure of the tunnel begins, or a steady state is reached. At this time, there will not be enough kinetic energy developed in the sample to break 100 per cent of all cohesion bonds. Results showing otherwise indicate problems with the interaction or cohesive laws.

The frictional laws are easily checked via triaxial test, applying 0 confining pressure to a test sample shows a weak sample and the same test conducted at a higher confining pressure should show a stronger sample. This demonstrates the functioning of the frictional bonds.

Material parameter calibration

The Mohr Coulomb failure criterion is used to validate the model using a triaxial test set-up. Triaxial tests have been performed at four different confining stresses ($\sigma_{min} = 0 Pa, 100 Pa, 1000 Pa, 10000 Pa$) to derive the macro-sample cohesion and friction angles. DEM parameters (mean particle size and damping coefficient) have been iteratively adjusted to reconcile the input friction angle and cohesion values derived from the Mohr Coulomb failure envelope.

Figure 2 shows the YADE set-up for the triaxial test. A cylindrical sample surrounded by facets that provide confining pressure (σ_{min}). The green and the red spheres at each end of the sample are constrained to move toward each other at a constant strain rate. The stress-strain relationship for the sample is recorded and used to derive the Mohr Coulomb failure envelope. An example of the stress-strain curve for a single test is shown in Figure 2. The overall results of DEM particle parameter calibration are shown in Table 1.

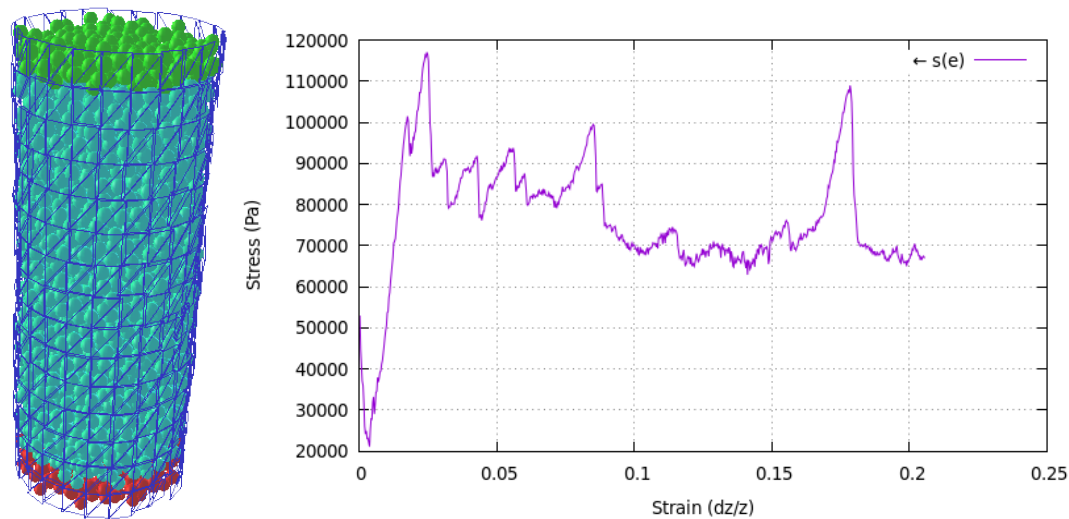


FIG 2 – Triaxial test DEM set-up and normal stress/strain chart for sample with 5 mm mean particle radius, 50° friction angle, 3 kPa cohesion, 10 kPa confining pressure.

TABLE 1
Final sample calibration results.

	Particle radius	Damping	Input	Target	Output
Cohesion	0.0025 m	0.25	3 kPa	3 kPa	3 kPa
	0.005 m	0.2	3 kPa	3 kPa	3 kPa
	0.0125 m	0.2	3 kPa	3 kPa	4 kPa
Friction angle	0.0025 m	0.25	54°	54°	54°
	0.005 m	0.2	50°	54°	54°
	0.0125 m	0.2	50°	54°	56°

MODELLING RESULTS

As presented in Figure 3, the Tunnel Stability chart shows a pattern of stability, where stability increases with depth or confinement pressure and decreases significantly with an increase in tunnel diameter. The stable tunnel at 4 m depth and 160 mm diameter (Index D) shown in Figure 3 has been selected for an additional lunar seismic test in YADE. A vibration of amplitude 2 mm and period 10 Hz has been applied to the right-hand wall to observe the effects. The results of seismicity tests indicate that the tunnel becomes unstable under the lower range of dynamic loading recorded on the lunar surface (under a 2 mm amplitude quake). This indicates that this tunnel in lunar regolith is unlikely to be stable over longer time periods and under non-static conditions. This finding may also be problematic for the tunnel during excavation or with nearby vibrating machinery and rockets.

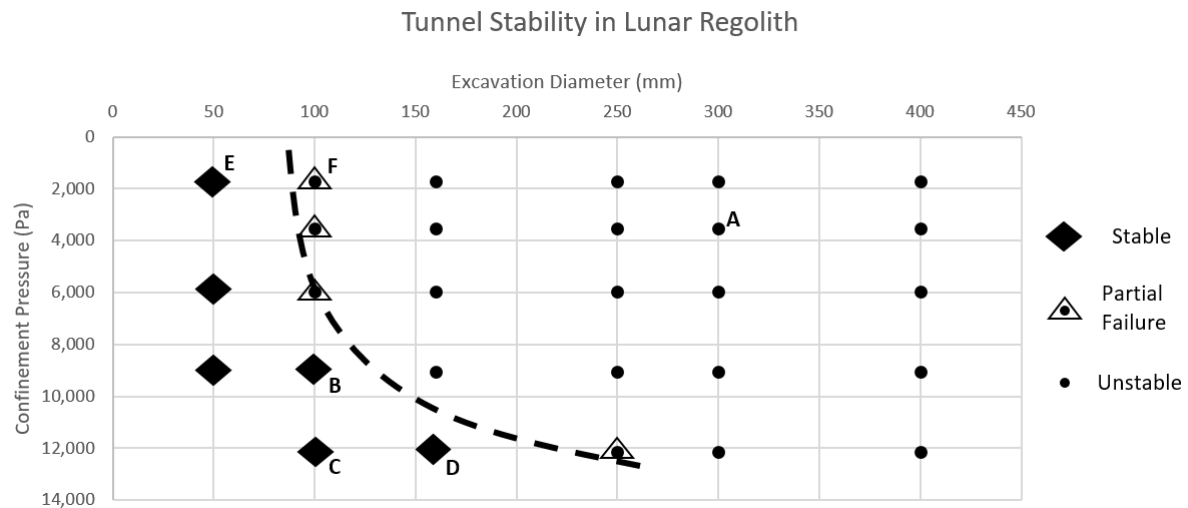


FIG 3 – Experimental results for tunnel stability in lunar regolith.

REFERENCES

- Boon, C, Housby, G and Utili, S, 2015. Designing tunnel support in jointed rock masses via the DEM, *Rock mechanics and rock engineering*, 48:603–632.
- Jiang, M, Shen, Z and Thornton, C, 2013. Microscopic contact model of lunar regolith for high efficiency discrete element analyses, *Computers and Geotechnics*, 54:104–116.
- Lane, J E, Metzger, P T and Wilkinson, R A, 2010. A review of discrete element method (DEM) particle shapes and size distributions for lunar soil, NASA TM 2010-216257, *NASA Technical Reports Server*, NASA Glenn Research Center, Cleveland, Ohio.
- Šmilauer, V, Catalano, E, Chareyre, B, Dorofeenko, S, Duriez, J, Dyck, N, Eliáš, J, Er, B, Eulitz, A, Gladky, A, Guo, N, Jakob, C, Kneib, F, Kozicki, J, Marzougui, D, Maurin, R, Modenese, C, Scholtès, L, Sibille, L, Stránský, J, Sweijen, T, Thoeni, K and Yuan, C, 2015. Yade Documentation 2nd ed. Zenodo. <https://doi.org/10.5281/zenodo.34073>.
- Zhao, T, 2017. Introduction to Discrete Element Method, in: *Coupled DEM-CFD Analyses of Landslide-Induced Debris Flows*, Springer, pp 25–45.

High vacuum metallurgy – opportunities in lunar resource processing

M G Shaw¹, G A Brooks², M A Rhamdhani³, A R Duffy⁴ and M I Pownceby⁵

1. PhD Candidate, Swinburne University of Technology, Melbourne Vic 3122.
Email: mgshaw@swin.edu.au
2. Professor, Swinburne University of Technology, Melbourne Vic 3122.
Email: gbrooks@swin.edu.au
3. Professor, Swinburne University of Technology, Melbourne Vic 3122.
Email: arhamdhani@swin.edu.au
4. Professor, Swinburne University of Technology, Melbourne Vic 3122.
Email: aduffy@swin.edu.au
5. Senior Principal Research Scientist, CSIRO Mineral Resources, Melbourne Vic 3168.
Email: mark.pownceby@csiro.au

ABSTRACT

The effect of low-pressure environments on metal compound stability is a well-known but rarely utilised phenomenon, even though reduction processes operating at subatmospheric pressures offer significant benefits in terms of the energy requirements for metal compound reduction. At industrial scales, some vacuum metallurgical processes such as silicothermic reduction to produce magnesium metal via the Pidgeon process, routinely operate under low vacuum conditions ($\sim 10^{-5}$ atm). However, more often in terrestrial industry, the benefits of these vacuum conditions are counteracted by equipment availability, production rates, and higher operational costs. The use of high vacuum conditions ($< 10^{-10}$ atm) to promote the production of metals at significantly lower temperatures is rendered unviable by the lack of industrial scale vacuum pumping apparatus capable of attaining these pressures. The difficulty in obtaining ultra-low pressures at industrial scales combined with the seeming lack of need to focus on the reduction of energy requirements for metal compound reduction, results in vacuum metallurgical processes being overlooked for terrestrial applications. In contrast however, the challenge presented by the likely need for metal production in space for supplying future off-Earth activities has the opposite requirements. In space, and specifically on the Moon, access to electrical energy is significantly limited and extremely costly, and instead of high vacuum conditions requiring specialised pumping equipment, these conditions represent the natural ambient conditions found on the lunar surface. We predict that the development of low-pressure metal production technologies for use in space will heavily favour the field of vacuum metallurgy. In the current work we present a set of calculated Ellingham diagrams that demonstrate the effects of vacuum conditions on oxide stability at elevated temperatures and highlight the significant advantages these vacuum conditions can provide in the field of astrometallurgy.

INTRODUCTION

The use of vacuum conditions in processing operations has been a topic of study for many decades. However, despite the initial enthusiasm for the potential presented by vacuum metallurgy, very few current industrial processes use such conditions. The current interest in extra-terrestrial resource processing is driving a renewed interest in such implementations. Access to space, and the natural vacuum conditions found there, inherently lead to a much simpler implementation of vacuum metallurgy processes in this environment.

The current work will briefly review vacuum metallurgy, relevant history and uses, as well as explore some of the significant limitations that have led to its lack of application in modern industry. We will cover Ellingham diagram theory as a foundation to then present a novel set of Ellingham diagrams generated at vacuum conditions. The effect of such vacuum conditions on the stability of oxides and subsequent energy requirements for reduction will be explored. Finally, we comment on some of the limitations of high-vacuum metallurgy, on how the access to the vacuum of space will help promote research addressing these issues, and how terrestrial vacuum metallurgical applications will benefit from research in this area.

VACUUM METALLURGY

The beneficial effects of low pressure environments on some metallurgical processes is well documented (Browne, 1971; Kroll, 1951). Vacuum can be used as a replacement for an inert atmosphere; to promote the separation of product material via fractional distillation; to facilitate the degassing of molten metals to improve physical characteristics, and; to reduce the temperature requirement of reactions with gaseous products (Browne, 1971). Despite these benefits, very few large-scale processing operations utilise vacuum metallurgy. One of the few processes used industrially is the Pidgeon process, the silicothermic reduction of magnesium under vacuum.

The Pidgeon process, developed in the 1940s (Pidgeon and Alexander, 1944), saw a large rise in application especially within China since the first industrial application in 1978 (Zang and Ding, 2016). The silicothermic reduction of magnesium is undertaken at 1200 to 1500°C at pressures of 10^{-4} to 10^{-5} atm (Halmann, Frei and Steinfeld, 2008). Magnesium metal produced during this reduction is in a gaseous form which is then condensed to form a high purity (~99.97 per cent) magnesium 'crown'. This magnesium crown is then re-melted under inert atmosphere into ingots (Halmann, Frei and Steinfeld, 2008).

The silicothermic reduction of magnesium, is not thermodynamically favoured at 1 atm pressure and instead would require temperature conditions in excess of 2000°C. However, under vacuum conditions, reaction temperatures as low as 1000°C have been achieved (Wada *et al*, 2017). The use of low pressure in this manner, to reduce the thermal requirements of metallurgical reactors has also been explored for many other applications. For example, the carbothermic reduction of Al_2O_3 , BeO , MgO , SiO_2 , Fe_2O_3 , TiO_2 , ZrO_2 , HfO_2 , and GeO_2 are all favoured under vacuum conditions. The use of vacuum in these reactions lowers the required reaction temperature and has the added benefit of minimising complications due to carbide and oxycarbide formation (Halmann, Frei and Steinfeld, 2011).

Despite these demonstrated benefits of vacuum metallurgy, on Earth, the reduction in the thermal energy requirements of a process due to a vacuum environment is insufficient to counteract the increase in energy (ie cost) required by pumping apparatus' to maintain that low pressure environment (Balomenos, Panias and Paspaliaris, 2012). This means that unless there are other factors involved, for example highly reactive product materials which require a lack of air, the reduction of reactor temperatures in metallurgical operations due to vacuum conditions will not be viable as it results in a net increase in energy use. This is further amplified if pressures even lower than typical 'industrial vacuum' conditions were to be considered.

The term industrial vacuum is often used to refer to the pressure reached by traditional industrial sized rotary vacuum pumps, typically in the realm of between 1 to 10^{-5} atm (Roth, 1990; O'Hanlon, 2005). However pumping systems such as turbomolecular vacuum pumps can reach pressures of 10^{-10} atm (O'Hanlon, 2005). This raises the question as to what sorts of thermal energy savings could be made at such pressures. While industrial operation at these pressures would similarly result in a net increase in energy cost, turbomolecular pumping systems being significantly less efficient than rotary vacuum pumps (O'Hanlon, 2005), the potential thermal energy savings are at least intellectually intriguing.

Beyond the energy inefficiency of operating metallurgical reactors at high vacuum conditions, there are also other factors that make this sort of operation unlikely. The cost of such systems, the scalability, maintenance requirements, considerably lower pumping rates, and requirement for much more efficient sealing technology on any reactor, make the implementation of these systems doubtful in the near future with current pumping technologies. However, in the interest of better understanding the potential benefits of high-vacuum metallurgy, we will examine the thermodynamic effects of these low-pressure conditions in the current work with the use of Ellingham diagrams. This work however, is aimed at a future where high vacuum pumping systems are made more efficient and applicable to industrial application. Or, when free access to high and even ultra-high vacuum environments is made considerably easier, such as in the field of astrometallurgy, when operating reduction processes in space or on other celestial bodies.

ELLINGHAM DIAGRAMS

A common tool for the extractive metallurgist when examining the thermodynamic viability of any given proposed process involving chemical reactions is the Ellingham diagram. An Ellingham diagram is a graph showing the temperature dependence of the stability of compounds. This analysis is usually used to evaluate the ease of reduction of metal oxides and sulfides. In the current work we will briefly review some theory around Ellingham diagrams and then we will discuss the implications of pressure on oxide reduction mechanisms with reference to Ellingham diagrams generated at alternate total pressure conditions.

Ellingham diagram theory

The specific principles involved with most thermodynamic calculations when it comes to determining equilibrium states are the free energy functions, Gibbs free energy and Helmholtz free energy. These two functions calculate the free energy within a system at isothermal and isobaric conditions (Gibbs) and isothermal and isochoric conditions (Helmholtz) (Rosenqvist, 2004). In most thermodynamic calculations a constant pressure is assumed for all systems, and as such, Gibbs free energy is used most often. The function for Gibbs free energy can be seen in Equation 1 where G is the Gibbs free energy (J), H is enthalpy (J), T is temperature (K), and S is entropy (J/K).

$$G = H - TS \quad (1)$$

In an isothermal system, the ΔG of a reaction $A \rightarrow B$ is equal to $G_B - G_A$. There is no absolute value for G in this case however the ΔG can also be calculated as per Equation 2.

$$\Delta G = \Delta H - T\Delta S \quad (2)$$

In an isobaric and isothermal system, and in the absence of work beyond volume work, ΔG is negative for spontaneous reactions and zero for fully reversible processes. A reaction with a positive ΔG value will not proceed forwards in an isolated system (Rosenqvist, 2004). It is important to note that the ΔG of a reaction is not directly related to the kinetics of that reaction, a spontaneous reaction, especially at lower temperatures, may take a long time to occur (Rankin, 2011).

First constructed by Harold Ellingham in 1944 (Ellingham, 1944), the Ellingham Diagram is a visual representation of the changes in ΔG for the formation of a compound with respect to temperature. The most common Ellingham diagram is for oxide formation which is shown in Figure 1. The diagram is predicated on the idea that Equation 2 can be represented as a linear equation with ΔH being the intercept and $-\Delta S$ being the slope. After plotting a number of oxide reactions, Ellingham (1944) found that whilst changes in ΔH and ΔS do occur with temperature, the changes are small enough that they can be considered constants for the purpose of graphing. A change in ΔS will occur at phase transition points which are also marked on the diagram.

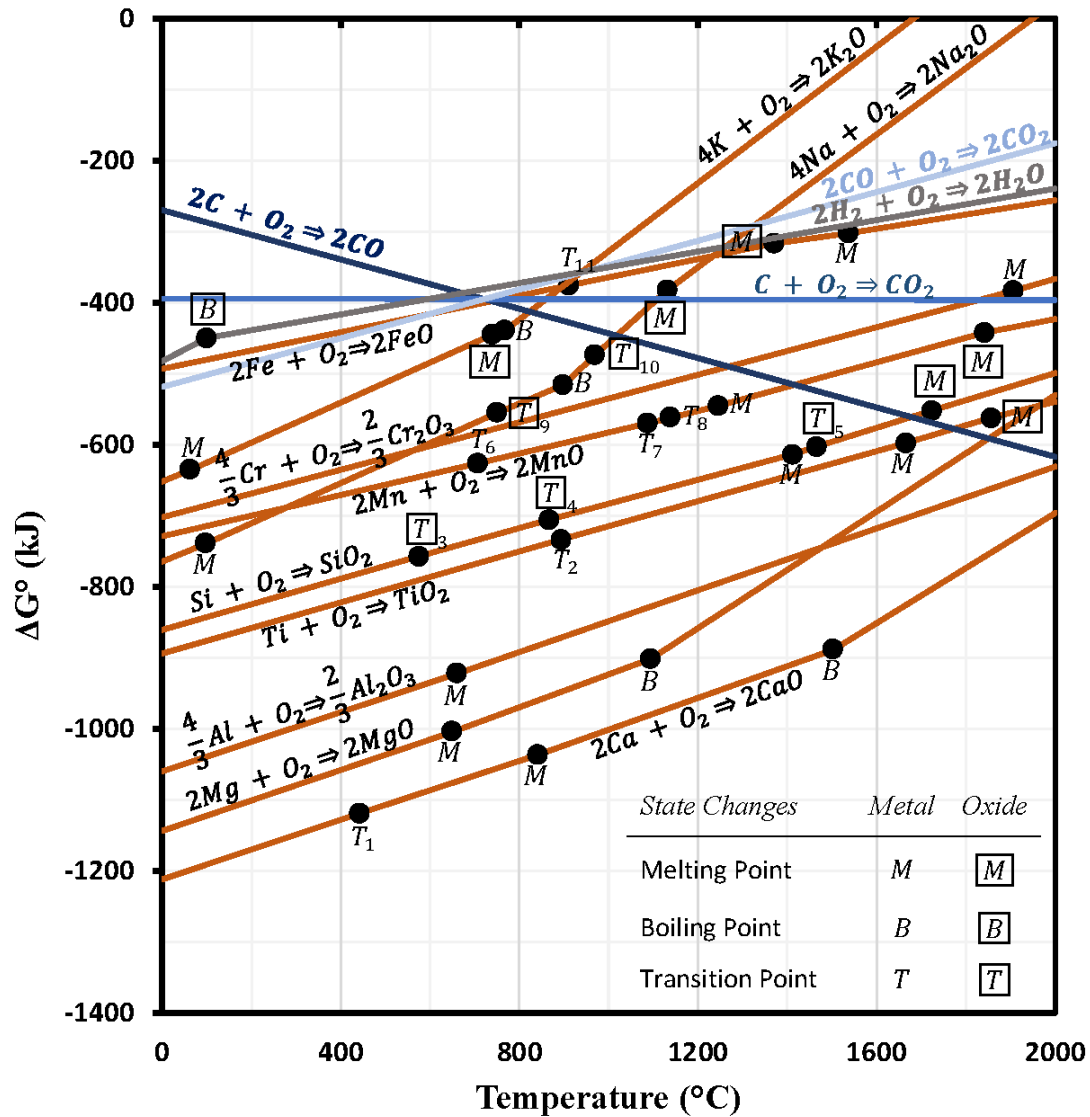
When considering the reduction of a metal oxide by another metal, any metal that is found lower on the diagram at the desired temperature can act as a reductant. The lower a reaction occurs on the diagram the more stable the product is, meaning that the metal reactant has a higher affinity for oxidation. With an increase in temperature, the ΔG of these oxide reactions also increases. This means that the oxide products are less stable at higher temperatures. If a plotted equation extends above zero, spontaneous thermal dissociation of this oxide into oxygen and metal is thermodynamically favoured in an isolated system (Rosenqvist, 2004).

The calculation of Gibbs free energy presumes constant temperature and pressure. Therefore, for the generation of an Ellingham diagram where temperature is used as the x-axis variable, the pressure is assumed to be constant. To see the effect of pressure on the ΔG it is necessary to consider enthalpy in more detail. Expanding the enthalpy function in Equation 2 gives Equation 3 where U is internal energy (J), V is volume (m^3), and P is pressure (Pa).

$$\Delta G = \Delta U + P\Delta V - T\Delta S \quad (3)$$

Ellingham Diagram

Modelled at 1atm absolute ambient pressure



Transitions:

T_1	Ca FCC to BCC
T_2	Ti HCP to BCC
$[T]_3$	SiO ₂ α-Quartz to β-Quartz
$[T]_4$	SiO ₂ β-Quartz to β-Tridymite
$[T]_5$	SiO ₂ β-Tridymite to β-Cristobalite

FCC = Face Centred Cubic
 BCC = Body Centred Cubic
 CBCC = Complex Body Centred Cubic
 HCP = Hexagonal Close-Packed
 SC = Simple Cubic

Transitions:

T_6	Mn CBCC to SC
T_7	Mn SC to FCC
T_8	Mn FCC to BCC
$[T]_9$	Na ₂ O S1 to S2
$[T]_{10}$	Na ₂ O S2 to S3
T_{11}	Fe BCC to FCC

Modelling completed in the FactSage 7.2 thermochemical software package.

FIG 1 – Ellingham diagram for the formation of various common lunar oxides at 1 atm pressure

In theory, the magnitude of the constant pressure can be anything, however, in practice, all readily available Ellingham diagrams are calculated at 1 atm pressure. For terrestrial industry and practical metallurgy the 1 atm Ellingham diagram makes sense. However, for an investigation into the effects of high-vacuum on metallurgical processes, and especially in the context of space exploration and materials processing, the assumed constant pressure of 1 atm is completely arbitrary. The generation of basic Ellingham diagrams for some common oxide species at varying pressures allows for an easy way to visualise the effect of pressure on the stability of these oxide species. The oxides chosen in the current work are all common oxides found on the lunar surface (Papike, Simon and Laul, 1982; McKay *et al*, 1991). Some common reductants such as C, CO, and H₂ have also been included.

Low pressure Ellingham diagrams

In order to investigate the practical effects of pressure on oxide stability, a series of ‘standard’ Ellingham diagrams were created at four distinct pressures. The four chosen pressures represent the four rough tiers of vacuum, these tiers and their significance, are described in Table 1. The colloquial designation of the vacuum tiers varies significantly depending on source, each level is often associated with a range of pressures. The pressures chosen here to represent the different tiers are therefore rough generalisations.

TABLE 1

The pressures used for Ellingham diagram generation and their significance.

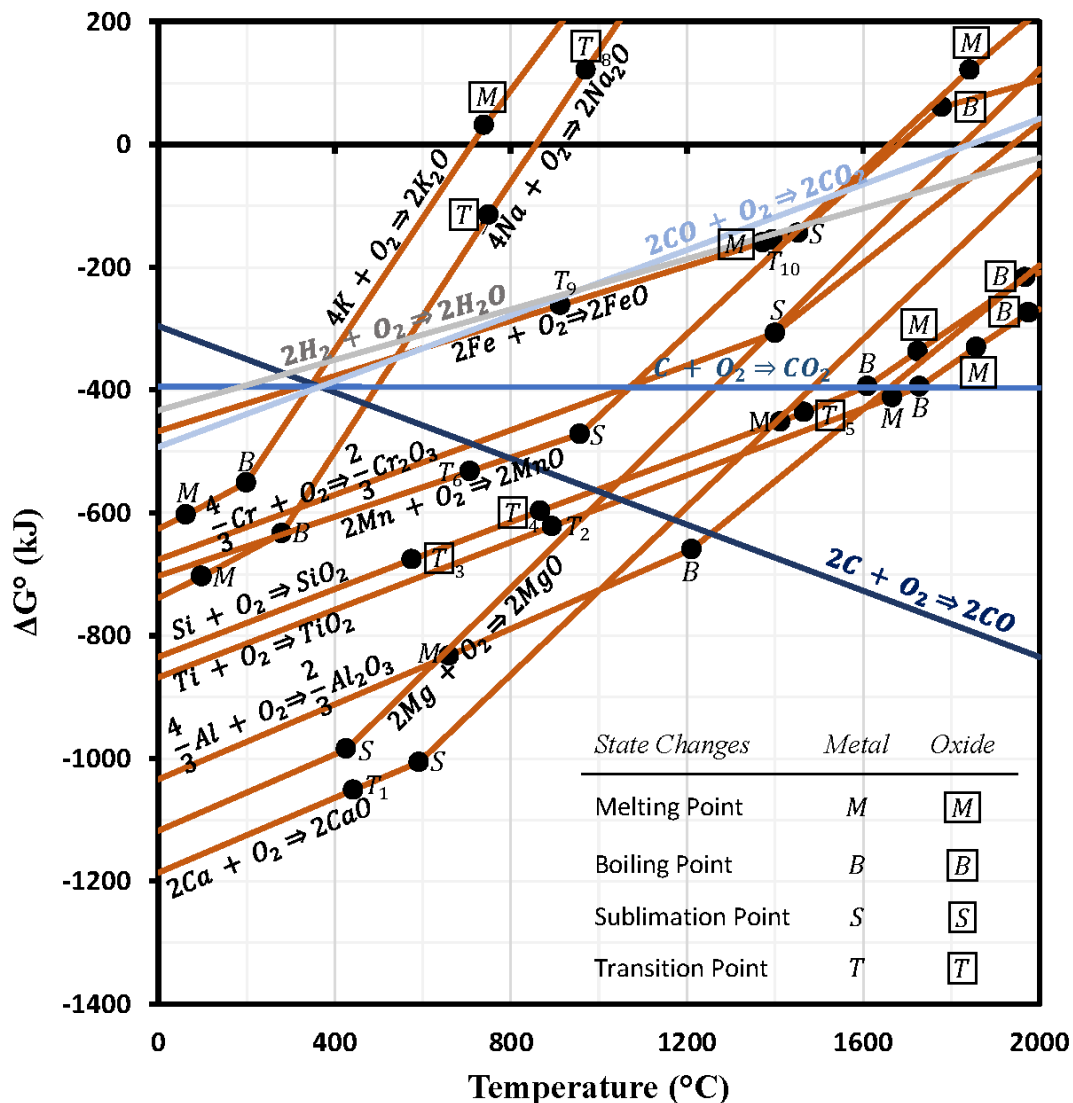
Colloquial designation	Pressure	Significance
No vacuum	1 atm	Normal operation on Earth’s surface.
Low vacuum	10 ⁻⁵ atm	The pressure reasonably attainable in terrestrial industry with mechanical pumps.
High vacuum	10 ⁻¹⁰ atm	The pressure attainable in industry and labs using specialised pumping equipment.
Ultra-high vacuum	3 × 10 ⁻¹⁵ atm	The ambient pressure measured on the lunar surface at night; attainable in labs using very specialised pumping equipment.

Ellingham diagrams generated at 1 atm, 10⁻⁵ atm, 10⁻¹⁰ atm, and 3 × 10⁻¹⁵ atm are shown in Figures 1, 2, 3 and 4 respectively. The data for these diagrams was obtained using the reaction module in the FactSage 7.2 thermochemical modelling software. The databases used for the modelling were FactPS and FTOxid. All phase changes and transition points have been marked. Lines for the carbon and hydrogen reduction steps have been added for reference as per the standard Ellingham diagram. Further detail on the FactSage modelling package can be found elsewhere (Bale *et al*, 2002, 2009, 2016; CRCT-PC).

In the standard 1 atm Ellingham diagram, Figure 1, the majority of the oxides are found well below the C to CO₂ line with only Cr₂O₃, FeO, K₂O, and Na₂O being viable options for reduction with C. The diagram has a y-axis maximum of 0 with only Na and K able to be spontaneously thermally reduced in the 0 to 2000°C temperature range. The majority of the plotted oxides trend towards a positive ΔG^0 with extrapolated intersects well above 3000°C. This diagram differs from the common oxide Ellingham diagram only in that the oxides plotted represent those 10 major oxides found on the lunar surface omitting for example Fe₂O₃ which, whilst common on Earth, is not seen in high concentrations on the lunar surface (Papike, Simon and Laul, 1982; McKay *et al*, 1991).

Ellingham Diagram

Modelled at 1×10^{-5} atm absolute ambient pressure



Transitions:

T_1	Ca FCC to BCC
T_2	Ti HCP to BCC
$[T]_3$	SiO ₂ α-Quartz to β-Quartz
$[T]_4$	SiO ₂ β-Quartz to β-Tridymite
$[T]_5$	SiO ₂ β-Tridymite to β-Cristobalite

Transitions:

T_6	Mn CBCC to SC
$[T]_7$	Na ₂ O S1 to S2
$[T]_8$	Na ₂ O S2 to S3
T_9	Fe BCC to FCC
T_{10}	Fe FCC to BCC

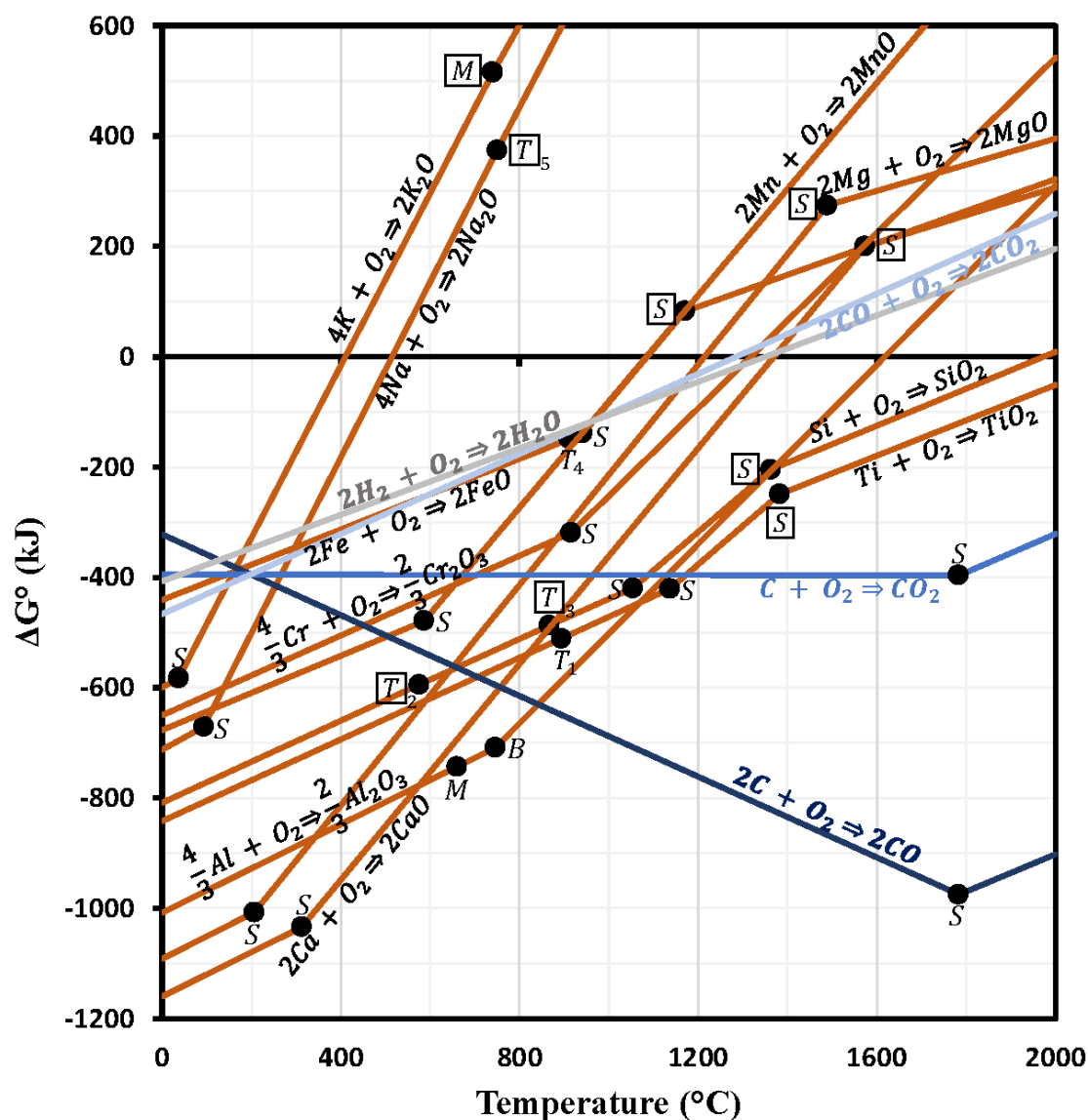
FCC = Face Centred Cubic
 BCC = Body Centred Cubic
 CBCC = Complex Body Centred Cubic
 HCP = Hexagonal Close-Packed
 SC = Simple Cubic

Modelling completed in the FactSage 7.2 thermochemical software package.

FIG 2 – Ellingham diagram for the formation of various common lunar oxides at 10^{-5} atm pressure.

Ellingham Diagram

Modelled at 1×10^{-10} atm absolute ambient pressure



Transitions:

T_1	Ti HCP to BCC
T_2	SiO_2 α -Quartz to β -Quartz
T_3	SiO_2 β -Quartz to β -Tridymite
T_4	Fe BCC to FCC
T_5	Na_2O S1 to S2

State Changes

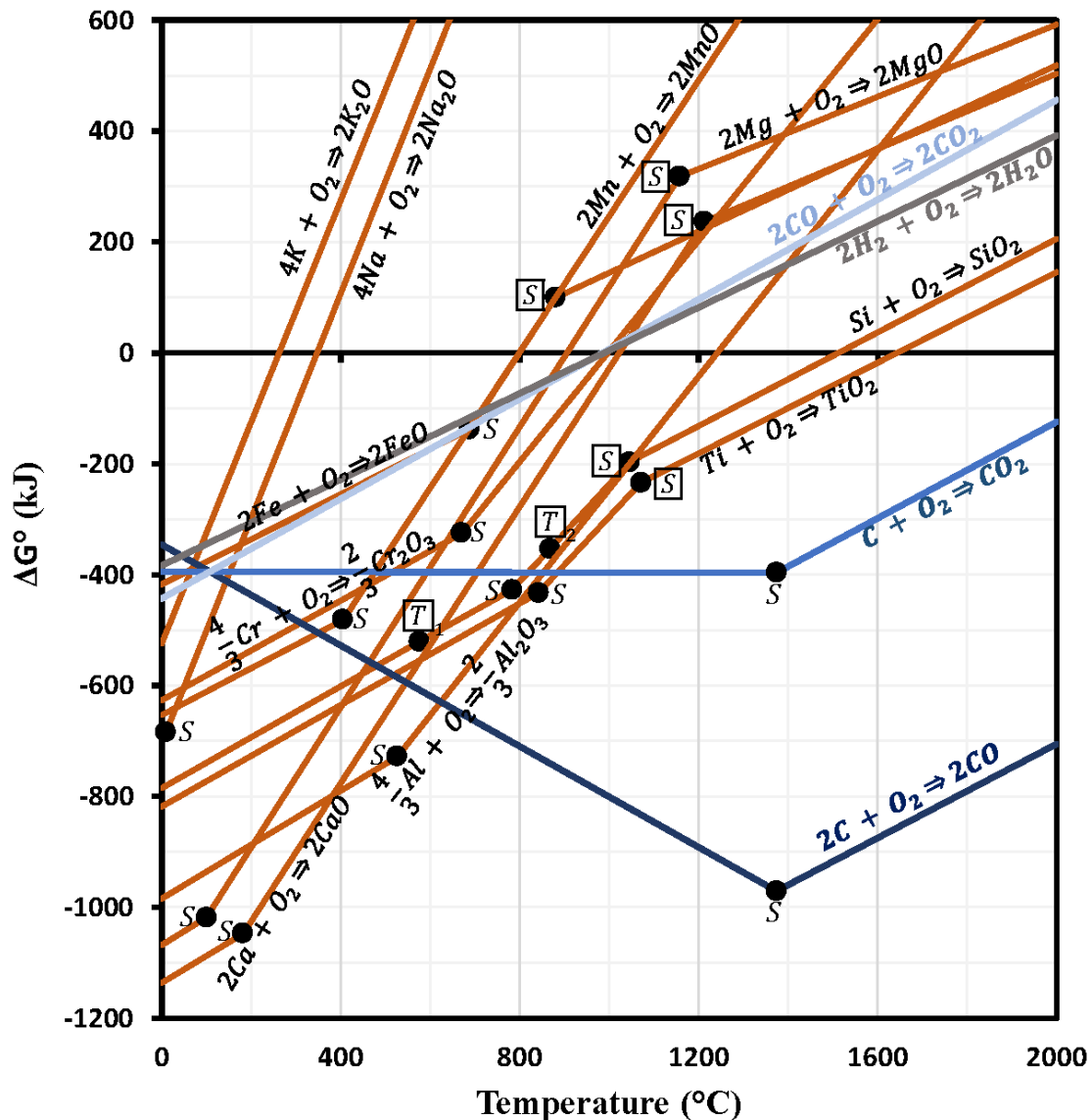
State Changes	Metal	Oxide
Melting Point	M	M
Boiling Point	B	B
Sublimation Point	S	S
Transition Point	T	T

Modelling completed in the FactSage 7.2 thermochemical software package.

FIG 3 – Ellingham diagram for the formation of various common lunar oxides at 10^{-10} atm pressure.

Ellingham Diagram

Modelled at 3×10^{-15} atm absolute ambient pressure



Transitions:		State Changes	Metal	Oxide
$[T]_1$	SiO ₂ α-Quartz to β-Quartz	Melting Point	M	$[M]$
		Boiling Point	B	$[B]$
$[T]_2$	SiO ₂ β-Quartz to β-Tridymite	Sublimation Point	S	$[S]$
		Transition Point	T	$[T]$

Modelling completed in the FactSage 7.2 thermochemical software package.

FIG 4 – Ellingham diagram for the formation of various common lunar oxides at 3×10^{-15} atm pressure.

Moving to a total pressure of 10^{-5} atm, Figure 2 shows some small but significant changes when compared to the standard 1 atm Ellingham diagram. The thermal dissociation of Cr, Mg, Fe, Mn, along with Na and K, is now thermodynamically favoured below 2000°C. Notice also that due to the change in ΔS in the Mg reaction line by the sublimation of Mg at ~430°C, the Mg and Si reaction

lines now cross at $\sim 1050^{\circ}\text{C}$. This means that at 10^{-5} atm, and above 1050°C , MgO will spontaneously be reduced by Si metal, which, as discussed above, is known as the Pidgeon process. The reason we point this out is that when looking at a normal Ellingham diagram, reconciliation of the data provided therein with the industrially used Pidgeon process can be somewhat confusing, this is one of the benefits of generating entire Ellingham diagrams at differing pressures. Also of note within Figure 2, all plotted oxides are able to be reduced by solid carbon below 2000°C . It is important to observe at this point that the diagrams depicted here are intended as a visual representation of the effect of vacuum on oxide stability. The Ellingham diagram is limited in the sense that it cannot be relied upon to accurately predict a reaction sequence without the inclusion of all relevant reactions. The oxide version found in Figures 1–4 ignores, for example, the formation of carbides which may result in an even lower Gibbs free energy for the system. Ellingham diagrams of sulfides, chlorides, fluorides, carbides, carbonates, silicates, aluminates etc at 1 atm pressure can be found elsewhere (Rosenqvist, 2004), although diagrams at reduced pressures have not been generated to date in the manner presented here.

Figure 3, generated at 10^{-10} atm, represents high-vacuum conditions. These conditions are theoretically attainable on Earth using complicated pumping systems but are readily available in space. Some interesting trends when compared to the higher-pressure diagrams can be seen. All plotted oxides barring TiO_2 , CO_2 , and CO spontaneously thermally dissociate below 2000°C . A number of the metals and oxides now undergo sublimation rather than melting and boiling, and significantly fewer transitions (described below the diagram) take place. Carbothermal reduction of most of the oxides is now predicted to be feasible below 800°C . The y-axis maximum has been moved to 600°C in this figure to show more information.

The final diagram, Figure 4, at 3×10^{-15} atm pressure, moves into the realm of the theoretically pristine lunar environment. Of all the diagrams presented in the current work this one is considered the most theoretical as the operation of a reactor under these conditions, considering the inherent gas generation, would be rendered kinetically impossible. However, in the interest of presenting extreme, but theoretically attainable conditions, it has been included. At this pressure, carbon is predicted to sublime before 1400°C and all plotted oxides apart from CO_2 and CO are predicted to be unstable above 1650°C with Cr_2O_3 , MnO, MgO, FeO, H_2O , CO_2 , K_2O , and Na_2O all being unstable above 1000°C . Only SiO_2 is predicted to undergo any phase transitions (from α -quartz to β -quartz and then to β -tridymite) at this temperature. Note the lack of liquid phases as direct sublimation is favoured for all products and reactants at this pressure.

SPACE AS A PLATFORM FOR HIGH VACUUM METALLURGY

While pumping equipment and the increased process complexity of operating vacuum processes on Earth are limiting, the field of astrometallurgy does not suffer from these restrictions. High (10^{-10} atm) and even ultra-high ($<<10^{-10}$ atm) vacuum conditions are readily available in space just as 1 atm conditions are readily available on Earth. Similarly, whereas on Earth energy is relatively cheap, access to electrical energy on the Moon will be significantly more limited, therefore the design of astrometallurgical processes will favour low energy consumption more so than in designs for terrestrial application.

With access to what could be considered 'industrial quantities' of high vacuum, the feasibility of using vacuum metallurgy is no longer restricted by acquisition and instead more technical concerns come into play. Issues such as reaction kinetics at low temperatures, mass transport within the reactants, rapid removal of product gases, evaporation and sublimation rates, and efficient condensing apparatus' that do not lose product to the natural vacuum, will play larger roles. Historically, little research has been done in these areas as the access to vacuum has been a significant enough limiting factor that the rest are not considered important. However, with an expansion of operations into space, and more importantly the easier access to such vacuum conditions for research purposes, a deeper understanding of these specific limiting mechanisms within vacuum metallurgical operations will become possible. While this targeted research will almost certainly be aimed at the development of astrometallurgical processes, the knowledge gained will be extremely applicable to terrestrial vacuum metallurgy technologies and may increase the viability of using vacuum in a wider variety of areas on Earth.

The exciting prospect of access to essentially infinite ultra-high vacuum conditions aside, when it comes to industrial resource processing in space, the 'contamination' of the natural vacuum should be considered. Whilst any short-term artificial 'atmosphere' created by the venting of gases in space will eventually dissipate, the continual discharge of gaseous species as part of an industrial process could lead to a semi-permanent 'contamination', or increase in pressure, of the ambient vacuum. This should ideally be avoided, both in terms of maintaining the clean environment of space, but also to avoid the deposition of miscellaneous materials on the outside of equipment and sensors in the local area. Large pressure spikes on the Moon as a result of human activity have been reported; with such low natural pressures on the Moon it is estimated that the act of launching the return stage of the Apollo missions *doubled* the total mass of the *entire* lunar atmosphere (Vondrak, 1992). This added gas naturally dissipated over time, however, herein lies the source of the reasoning mentioned previously of the active lunar pressure during prolonged human or robotic presence on the Moon. A constant pressure of 3×10^{-15} atm is not expected during industrial activities and human presence on the Moon, the ambient pressure will have to be monitored and balanced with activities (both industrial and other) resulting in gas discharge. The careful control of ambient pressures will be important for prolonged industrial activity on the lunar surface both in terms of detrimental process inhibiting effects and societal license to operate.

CONCLUSIONS

Vacuum metallurgy is understood to be beneficial in some circumstances on Earth but is severely limited by pumping technology. Some industrial processes do operate at low pressures using mechanical vacuum pumps, such as the Pidgeon process for magnesium production, however high vacuum conditions (10^{-10} atm) have to date not been used in large scale metal reduction processes on Earth.

Despite the issues inherent in the application of high vacuum conditions to terrestrial resource processing, an understanding of the potential benefits of these conditions is still relevant. The current work has aimed to highlight the significant thermodynamic effects of vacuum conditions on the stability of oxides. Four Ellingham diagrams modelled using the FactSage thermochemical software at pressures of 1, 10^{-5} , 10^{-10} , and 3×10^{-15} atm have been presented and described here. Analysis of these diagrams shows that oxides under vacuum conditions require significantly less energy for reduction to take place. It is also noted that the use of Ellingham diagrams to display the effect of vacuum on a system can remove some confusion when analysing processes such as the Pidgeon process which, when analysed using a standard Ellingham diagram, generated at 1 atm pressure, is not thermodynamically viable at the temperatures used in industry.

Space provides us with an excuse and a platform to further explore vacuum metallurgy as an area of research. The potential benefits of high-vacuum conditions on industrial processing operations are known but have been hindered historically by our lack of access to these vacuum conditions. The application of high vacuum metallurgy in astrometallurgical processes, ie resource processing in space, has significant merit. It will lead both to the development of metal extraction techniques that simply aren't feasible on Earth, but also to a deeper understanding of the vacuum metallurgical applications that can be used on Earth.

In 1951, Kroll stated that 'In the course of time it [vacuum metallurgy] will firmly entrench itself in the front line of a steadily advancing metallurgy' (Kroll, 1951). Over 70 years later this statement is more relevant than ever.

ACKNOWLEDGEMENTS

This research is supported by an Australian Government Research Training Program Scholarship (RTPS) and a CSIRO top-up scholarship.

REFERENCES

- Bale, C W, Bélisle, E, Chartrand, P, Decterov, S, Eriksson, G, Gheribi, A, Hack, K, Jung, I-H, Kang, Y-B and Melançon, J, 2016. Reprint of: FactSage thermochemical software and databases, 2010–2016. *Calphad*, 55, 1–19.
- Bale, C W, Chartrand, P, Decterov, S, Eriksson, G, Hack, K, Mahfoud, R B, Melançon, J, Pelton, A and Petersen, S, 2002. FactSage thermochemical software and databases. *Calphad*, 26, 189–228.

- Bale, C, Bélisle, E, Chartrand, P, Decterov, S, Eriksson, G, Hack, K, Jung, I-H, Kang, Y-B, Melançon, J and Pelton, A, 2009. FactSage thermochemical software and databases—recent developments. *Calphad*, 33, 295–311.
- Balomenos, E, Panias, D and Paspaliaris, I, 2012. Exergy Analysis of Metal Oxide Carbothermic Reduction under Vacuum—Sustainability prospects. *International Journal of Thermodynamics*, 15, 141–148.
- Browne, J R, 1971. A review of the fundamentals of vacuum metallurgy. *Vacuum*, 21, 13–16.
- CRCT-PC. *FactSage Database Documentation* [Online]. Available: <http://www.crct.polymtl.ca/fact/documentation/> [Accessed 15/09/2019].
- Ellingham, H J T, 1944. Reducibility of oxides and sulfides in metallurgical processes. *J Soc Chem Ind*, 63, 125–133.
- Halmann, M, Frei, A and Steinfeld, A, 2008. Magnesium production by the pidgeon process involving dolomite calcination and MgO silicothermic reduction: thermodynamic and environmental analyses. *Industrial and Engineering Chemistry Research*, 47, 2146–2154.
- Halmann, M, Frei, A and Steinfeld, A, 2011. Vacuum Carbothermic Reduction of Al_2O_3 , BeO , MgO-CaO , TiO_2 , ZrO_2 , $\text{HfO}_2 + \text{ZrO}_2$, SiO_2 , $\text{SiO}_2 + \text{Fe}_2\text{O}_3$, and GeO_2 to the Metals. A Thermodynamic Study. *Mineral Processing and Extractive Metallurgy Review*, 32, 247–266.
- Kroll, W, 1951. Vacuum metallurgy: its characteristics and its scope. *Vacuum*, 1, 163–184.
- Mckay, D S, Heiken, G, Basu, A, Blanford, G, Simon, S, Reedy, R, French, B M and Papike, J, 1991. The lunar regolith. *Lunar sourcebook*, 285–356.
- O'Hanlon, J F, 2005. *A user's guide to vacuum technology*, John Wiley and Sons.
- Papike, J, Simon, S B and Laul, J, 1982. The lunar regolith: Chemistry, mineralogy, and petrology. *Reviews of Geophysics*, 20, 761–826.
- Pidgeon, L and Alexander, W, 1944. Thermal production of magnesium-pilot plant studies on the retort ferrosilicon process. *Transactions AIME*, 159, 315–352.
- Rankin, W J, 2011. *Minerals, Metals and Sustainability: Meeting Future Material Needs*, CSIRO publishing.
- Rosenqvist, T, 2004. *Principles of Extractive Metallurgy*, Trondheim, Norway: Tapir Academic Press.
- Roth, A, 1990. *Vacuum technology*, Amsterdam/New York.
- Vondrak, R R, 1992. Lunar base activities and the lunar environment. NASA Conference Publication. NASA, 337–337.
- Wada, Y, Fujii, S, Suzuki, E, Maitani, M M, Tsubaki, S, Chonan, S, Fukui, M and Inazu, N, 2017. Smelting magnesium metal using a microwave Pidgeon method. *Scientific Reports*, 7, 1–7.
- Zang, J C and Ding, W, 2016. The Pidgeon process in China and its future. *Essential Readings in Magnesium Technology*. Springer.

Design and application of swarm robotics system using ABCO method for off-Earth mining

J Tan¹, N Melkounian², R Akmeliawati³ and D Harvey⁴

1. PhD student, The University of Adelaide, Adelaide SA 5000.
Email: joven.tan@student.adelaide.edu.au
2. Senior Lecturer, The University of Adelaide, Adelaide SA 5000.
Email: noune.melkounian@adelaide.edu.au
3. Associate Professor, The University of Adelaide, Adelaide SA 5000.
Email: rini.akmeliawati@adelaide.edu.au
4. Senior Lecturer, The University of Adelaide, Adelaide SA 5000.
Email: david.harvey@adelaide.edu.au

ABSTRACT

The concept of *in situ* resource utilisation (ISRU) was proposed by the USA National Aeronautics and Space Administration (NASA) to extract off-Earth resources from the Moon, asteroids, and Mars to maintain successful long-term manned space missions. The focus of this paper is to develop an optimal swarm robotics system in terms of its design and operation strategy, and to consider its application for extracting water from the super frozen craters at the Moon's poles. The optimisation of swarm robotics system has been conducted in terms of fleet size, collision avoidance and convergence time. Analytical research, numerical modelling and simulation have been applied to design and evaluate the performance of swarm robot fleets for off-Earth mining. This involved determining the optimal number and dynamic interaction of robots in the fleet to achieve the best swarm performance for the considered task. The proposed swarm robotics system has been designed based on the behaviour and autonomy of swarm insects. Its performance has been evaluated using swarm intelligence (SI) classification, ie natural and artificial swarm intelligence using numerical simulations. To study the swarm robotic system design, the behaviour of two different insect colonies, namely the ant colony and the bee colony, has been studied. After comparative evaluation of these methods, the artificial bee colony (ABC) optimisation method has been used to construct a swarm robotics system, as it has been deemed more suitable for the considered task because it does not require the feature for pheromone tracking. Based on the collision and signal error analysis for different size swarm robot fleets, the characteristics of swarm robotics systems (eg scalability, robustness, and flexibility) have been evaluated. Assuming that the maximum robot signal coverage is 300 m, and the maximum movement speed of the robot is 150 m/h, the swarm fleet size of 10 robots with 0 per cent signal and collision error has been identified as the most optimal. The convergence time for 10 robots is 150 seconds, and for 15 and 20 robots is 200 seconds and 275 seconds, respectively. The findings presented in this paper can also be utilised and beneficial for on-Earth mining and other geotechnical engineering activities.

INTRODUCTION

Over the decades, the NASA Planetary Science Program had aimed to achieve a better understanding on the structure of the solar system and has further innovated and applied engineering knowledge to spacecraft and swarm robotics technologies for this. Hoffman and Kaplan, (1997) pointed out that the purpose of planetary exploration is to find life beyond the Earth, study the geological conditions and climate of other planets and provide convenience for human exploration. In September 2019, Australian Prime Minister Scott Morrison announced the provision of A\$150 million to the Australian Space Agency for innovative technology that will be utilised in the US mission to land space explorer on the Moon by 2024 (Crowe, 2020).

The concept of *In situ* Resource Utilisation (ISRU) was proposed by the USA National Aeronautics and Space Administration (NASA), and it recommends extracting and using off-Earth resources for long-term manned space missions (Linne *et al*, 2017). The motivation behind planetary exploration via off-Earth mining includes the scientific knowledge and information about space, the proliferation of progress, the establishment of the global business market, and requires understanding between countries involved in space exploration. Space mining provides new opportunities for extracting

valuable resources, such as minerals, water and gas on other planets, asteroids and the Moon. At the same time, it poses challenges related to various stages of mining and unique environmental conditions on the Moon and other planets and asteroids, which must be addressed in order to implement mining practices in space successfully. The complexity of space mining requires innovation, and more targeted and effective problem-solving methods.

Water is one of the most valuable and widely used resources both on Earth and for long-term manned missions. It is very expensive to ship water to the Moon, and also there is shortage of this resource on Earth. Hence, extracting water from super frozen ice present in the craters of the Moon poles will allow to provide the necessary water for long-term manned missions, and related activities on the Moon and other planets. Considering the specificities of the off-Earth environment, as well as extremely high costs of moving heavy mining machinery used on Earth and the need for their regular maintenance, new methods and strategies must be considered for off-Earth mining.

This paper proposes an off-Earth mining method for extracting water on the Moon by using the methods and models of biomimicry (nature-inspired designs). For this swarm robotics application is being proposed. The swarm robotics system has been designed based on insect swarm behaviour models, namely artificial bee colony (ABC) optimisation and ant colony optimisation (ACO) proposed by Dorigo *et al* (2016) have been used. The ABC optimisation has been deemed better suited for off-Earth mining since it does not involve unrelated features, eg pheromone tracking present in the ACO models. Analytical studies, and numerical modelling and simulation have been conducted to design and evaluate the performance of swarm robots, that is to determine the required number and dynamic interaction of robots in the swarm to achieve the best possible swarm robot fleet performance for the considered environment and task.

The focus of this paper is to develop and propose a new more efficient bio-inspired method for off-Earth mining and ISRU. The findings from this research can also be utilised for other off-Earth mining activities such as building underground habitants or other excavations for civil applications on the Moon, as well as will be beneficial to the mining industry on Earth since they will help to reduce the environmental footprint of mining by allowing to carry out more targeted mining activities and will contribute to the automation and application of robotics in mining.

METHODOLOGY

The swarm robotics system's features and performance have been designed and optimised by implementing methods and models of biomimicry and by adopting nature-inspired solutions such as behaviours observed in swarms of insects to improve the extraction efficiency of the lunar water.

Swarm robotic system

This section focuses on the design of swarm robotics system for off-Earth mining using analytical and numerical studies, and biomimicry. The performance of the swarm robotics system has been evaluated through the taxonomy of swarm intelligence: natural swarm intelligence and artificial swarm intelligence, via numerical simulations, and by implementing methods and models of biomimicry to achieve nature-inspired solutions. MATLAB has been used to design the swarm robotics system. According to Alers *et al* (2011), biomimicry and nature-inspired systems (such as ant foraging or bee-inspired foraging) have received more attention in data clustering, exploration, and exploitation. Considering that the capabilities of individual insects are very limited, the phenomenon of interaction between each individual insect is very simple, robust and effective in solving complex tasks. In this study for the swarm robotics system design two insect swarm behaviour models, namely artificial bee colony (ABC) optimisation and ant colony optimisation (ACO) proposed by Dorigo *et al* (2016) have been considered.

Ants foraging involves the use of pheromone for decentralised simulation (Dorigo, Birattari and Stutzle, 2006). If the physical means fail, the pheromone tracking needs to be re-established by another robot or centralised component, which will increase the computational burden of the distributed system, thereby reducing scalability and adaptability. In the bee foraging inspired model, direct communication with the navigation path integration and recruitment mechanisms are used, which result in the mechanism being completely decentralised in nature and very suited for implementation in imbedded systems. By comparing both ABC optimisation and ACO foraging

algorithms, it has been concluded that bee-foraging has higher scalability, adaptability and is more effective in an unknown environment (Lemmens *et al*, 2005; Lemmens and Tuyls, 2010). Therefore, bee foraging has been identified as a suitable nature inspired model for designing the swarm robotics system's behaviour for application in lunar water extraction. For this, insect swarm behavioural models, namely ABC optimisation proposed by Dorigo *et al* (2016) has been applied. The bee-inspired algorithm has been modified using a 5×5 matrix with a total of 25 robots via MATLAB with the accessed of GitHub Library (Ahmadzadeh, 2015). The bee foraging system is characterised by the use of three different behaviours: (1) hive behaviour, (2) food source behaviour, and (3) foraging behaviour. The behaviour of the MATLAB simulation has been studied and issues related to collision avoidance have been identified.

Swarm robotics systems play an important role in considering mutual communication, sensing capabilities and computational resource constraints, thus the collision avoidance in a group of robots needs to be more emphasised. The open-source GitHub library simulation package (Michael and Kumar, 2009) has been accessed, and the collision avoidance simulation has been further implemented in the MATLAB simulation software. Collision avoidance simulation provides interaction between individual robots with anti-collision detection capabilities. The collision avoidance simulation was carried out through MATLAB simulation, and the simulation model was optimised and modified to match off-Earth mining application, such as the internal specification of NASA's BTIC lunar lander (eg robot size, length, weight, and fleet size). In the collision avoidance equation proposed by Michael and Kumar (2009), the separation distance (ϵ) between robots can be calculated using Equation 1.

$$\epsilon = 2\rho + \epsilon_s. \quad (1)$$

Based on the motion planning technique proposed by Michael and Kumar (2009), simulations of 10, 15 and 20 robots with a safety distance of 0.1 m has been conducted and has shown that there is no collision in the experiment with a real robot with a robot radius of 0.25 m. According to NASA's Break The Ice Challenge (BTIC) lunar lander specifications, the hypothetical mass and volume specifications of the lunar lander's main section with the assumed dimensions of length: 10.45 m, diameter: 6.35 m, volume: 331 m³, and the nose section with the assumed dimensions of length: 7.15 m, diameter: 6.35 m, volume: 127 m³, have been considered in order to align with the rocket capacity (NASA's Break the Ice Lunar Challenge, 2021). In the collision avoidance simulation of swarm robots, the robot size (ρ) and the safety distance (ϵ_s) are assumed to be 2 m and 0.1 m respectively as shown in Figure 1. Since the maximum robot radius of the internal specification is specified as 3.18 m from NASA's BTIC, the robot radius used in this simulation is considered to be within the specification.

```

=====
%% Separation Distance for Swarm Robot (ε) %%
r = 0.15;           % Robot Radius %
l = 0.05;           % Robot Nose Length %
εs = 0.1;         % Safety Distance %
ε = 2(r + l) + εs % Separation Distance – Collision avoidance equation %
=====

```

FIG 1 – Collision avoidance simulation.

Based on the information from the Science Museum in Boston radio waves have been used by NASA satellites and spacecraft for communication purposes (Mos.org., 2021). Radio waves are an electromagnetic spectrum that can travel at the speed of light, with wavelengths from 1 mm to 100 km. According to Gorostiza *et al* (2011), a sensorial system to measure the transmitted signal from a robotic experiment was conducted to compare the local positioning systems with the detection techniques using received signal strength indicator (RSSI) detects the location precision of various transmitters. The evaluation results show that GSM and Bluetooth perform well on local positioning in the range of 2 m to 3 m, whereas RFIS and wi-fi are kept between 1 m to 2 m. Exploration missions are mainly focused on huge lunar craters near the lunar poles, such as Shackleton Crater (20 km),

Faustini Crater (39 km), and Shoemaker Crater (51 km). In order to cover the entire crater for exploration, the signal transmission must be more advanced. According to Rappaport, Roh and Cheun (2014), extensive research and testing of the behaviour of millimetre waves has been conducted in New York City, one of the toughest radio environments in the world. The test was carried out on a busy street in Manhattan, using a prototype operating at 28 GHz and a small 5 mm patch antenna. The signal was successfully connected to a transmitter 200 m away. By arranging a dozen of 28 GHz patch antennas in a grid pattern, coverage could be extended to more than 300 m. This set of antennas has been used for radar and space communications for a long time. The exploration trajectory (shown in the red circle in Figure 4) has been modified to the maximum transmission signal range to achieve the maximum water detection range, thus the diameter of the exploration trajectory ($S1D$) is set to be 300 m (0.3 km). When lunar water is detected, the robot will locate its position, construct an exploitation trajectory (shown in blue circle in Figure 4), and send a signal to the group through swarm intelligence system for assembly.

The exploitation trajectory has been modified based on the distance between the extraction location and the water extraction plant at the centre of the exploitation trajectory. The water extraction plant has been placed in the centre, which has been set in the X-Y coordinates ($uCentroidD$). According to Sasiadek (2013), the current travel speeds of two unmanned rovers named Curiosity and Opportunity are 0.14 km/h and 0.18 km/h, respectively. To date, the other three rovers travelling on the surface of distant celestial bodies are Yutu, Spirit and Sejourner, with speeds of 0.2 km/h, 0.18 km/h and 0.024 km/h (Malenkov and Volov, 2019). The fastest unmanned mobile landers in history are the Soviet Lunokhod 1 and 2, which have a speed of 2 km/h. Based on all rover vehicles, it can be assumed that the maximum speed of the robot ($Rspeed$) is 0.15 km/h on average.

This paper focuses on the design of the swarm robotics system and considering its application for mining, namely water extraction on the Moon. Investigation and development of mining operations, such as drilling methods, mining strategies, and mine is outside the scope of this paper. The detection of lunar water at specified coordinates [3,3] which are also taken as the water extraction plant coordinates in the MATLAB simulation are based on the design specifications proposed by Battsengel and Tan (2021). Considering unique geological conditions, full automation, and 24-hour continuous operation, the extraction operation time per shift is 10.2 hours, which includes drilling holes to 1 m depth (80 min), time to move back and forth from the water extraction plant (80 min) and discharge time (10 min). Assume, the duration of the movement from the water extraction plant to the blue outermost periphery ($Ttravel$) is 40 min. Therefore, the maximum diameter of the exploitation trajectory can be calculated using Equation 2.

$$S2D = Rspeed \times Ttravel. \quad (2)$$

The movement duration from the water extraction plant to the blue outermost trajectory is 40 minutes, which allows the robot to move 100 m at a speed of 0.15 km/h. Therefore, the exploration trajectory ($S1D$) and exploitation trajectory ($S2D$) have been set to 0.3 km and 0.1 km respectively as shown in Figure 2.

```
=====
%% Initializing Exploration and Exploitation Trajectory %%
uCentroidD = [3,3];      % Water Extraction Plant Coordinates %
s1D = 0.3;               % Exploration Diameter %
s2D = 0.1;               % Exploitation Diameter %
thetaD = 1.0.
=====
```

FIG 2 – Initialising the exploration search trajectory and lunar extraction area.

Swarm robot evaluation

This section evaluates the swarm robot performance using numerical simulations. After fully modelling and simulating the robots for the swarm, the robot performance has been evaluated. Considering the scalability, robustness and flexibility features for swarm robotics system given below

(Kassabalidis *et al*, 2001; Brambilla *et al*, 2013; Hecker and Moses, 2015), the spatial distribution configuration of the robots for each fleet size has been investigated and observed. According to En.linkfang.org. (2020), the effective payload of existing and operating orbital space vehicles is very limited, with a weight ranging from 6000 kg (Dragon cargo) to 12 600 kg (TKS cargo), as shown in Table 1.

TABLE 1
Orbital space vehicles cargo payload.

Spacecraft	Origin	Manufacturer	Payload (kg)
TKS	Soviet Union	TsKBM	12 600
ATV	Europe	EADS	7667
Tianzhou	China	CAST	6500
Dragon	USA	Space X	6000
Dragon 2 cargo	USA	Space X	6000

Based on Battsengel and Tan (2021), the design of the lunar water extraction robot considering the appropriate size of equipment and robots, the overall weight has been determined to be 600 kg. Then by using the maximum payload of 12 600 kg and the minimum payload of 6000 kg to determine the size of the swarm fleet, it can be assumed that the swarm robot fleet size ranges from the smallest of 10 robot to the largest of 20 robot fleet sizes. The proposed swarm robotics system has been compared for different robot fleet sizes, namely for 10 robot fleet, 15 robot fleet and 20 robot fleet, and the best option has been identified for swarm mining/extraction of water on the Moon.

$$\text{Scalability} = \alpha = \frac{u_i}{-\nabla_{q_i} \phi_i(q)}, \phi_i(q) = \frac{\gamma_i(q)}{\gamma_i(q)^k + \beta_i(q)^{1/k}} \quad (3)$$

The scalability of the swarm robotics system can be determined by calculating the scaling factor (α) with both goal function ($\phi_i(q): F \rightarrow R$), obstacle function ($\beta_i(q): F \rightarrow [0, 1]$) and a tuning parameter (k). $\phi_i(q)$ is achieved when the distance between the agent i and the neighbour is ideal, where $\beta_i(q)$ is achieved when the agent i doesn't come into collision with any hurdle or another agent.

$$\text{Robustness} = \frac{RE2 - RE1}{RE1} \times 100\%. \quad (4)$$

The robustness of the swarm robotics system can be determined by observing the average error percentage developed presuming absence of error ($RE2$) and presence of error ($RE1$). As for the flexibility of the swarm robotics system, it can be determined by investigating the efficiency of the finest approach contrary to specific assets allocation ($FE1$), and the efficiency of an alternative approach examined contrary to different assets allocations ($FE2$) as shown below:

$$\text{Flexibility} = \frac{FE2}{FE1} \times 100\%. \quad (5)$$

Also, the most optimal robot fleet size for swarm mining has been investigated from continues and uninterrupted mining/water extraction production point of view, and the best suited mining strategy has been identified. This study demonstrates that swarm mining can be successfully applied in ISRU and can be one of the best suited options for off-Earth mining.

RESULTS AND DISCUSSION

Swarm robotics system

ABC optimisation solves complex optimisation problems (Karaboga, 2005) by using three different phases of methods (eg employed bees, onlooker bees and scout bees). Since space mining on the Moon for ISRU applications requires maximum water extraction, rather than searching for high-quality water sources for exploration and extraction, employed bees have been considered only for lunar water extraction applications. The simulated behaviour of the swarm robots shown in Figure 3 follows the bee foraging system, which is inspired by hive behaviour and food source behaviour.

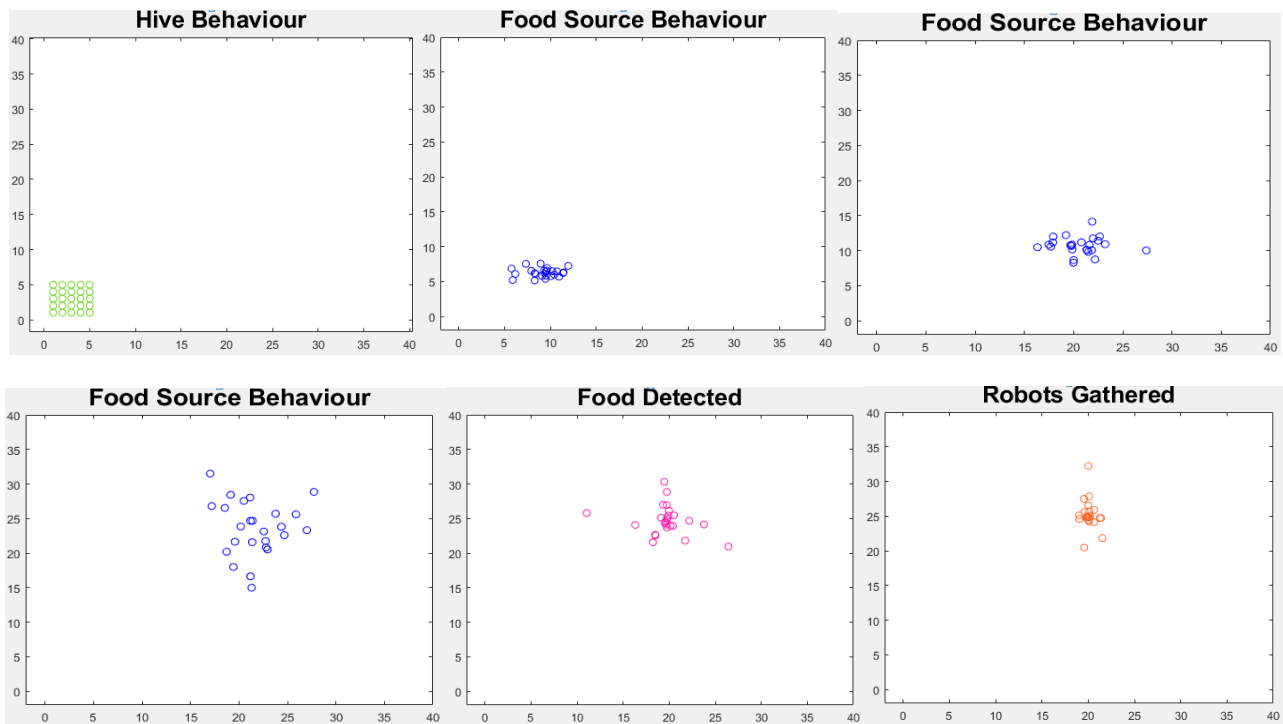


FIG 3 – Bee-inspired algorithm for exploration.

The bee algorithm implemented in MATLAB simulation shows a trend similar to the honey bee foraging behaviour mentioned above, where the hive bees will search for the nearest food sources around the hive and gather for honey collection when honey is detected. The natural behaviour of foraging bees is a good practice for navigation and self-assembly in swarm robot applications. Applying this approach to real-life swarm robot applications for lunar water extraction will encounter several problems, such as robot collision, signal transmission and positioning accuracy limitations, and the maximum exploration distance away from the hive. To bolster the MATLAB simulation above, more advanced simulations were further studied, including changing the trajectory coverage of signal transmission and positioning, separation distance between robot for collision avoidance, and swarm convergence time, making it more effective and suitable for automated space mining swarm robot navigation.

These parameters have been implemented into the advanced simulations and include collision avoidance, trajectory coverage, and convergence time. The simulation has run for two hours, of which three simulations have been run for 10 robot size swarm fleets to achieve the average convergence time. Figure 4 shows the entire process of lunar water exploration and extraction.

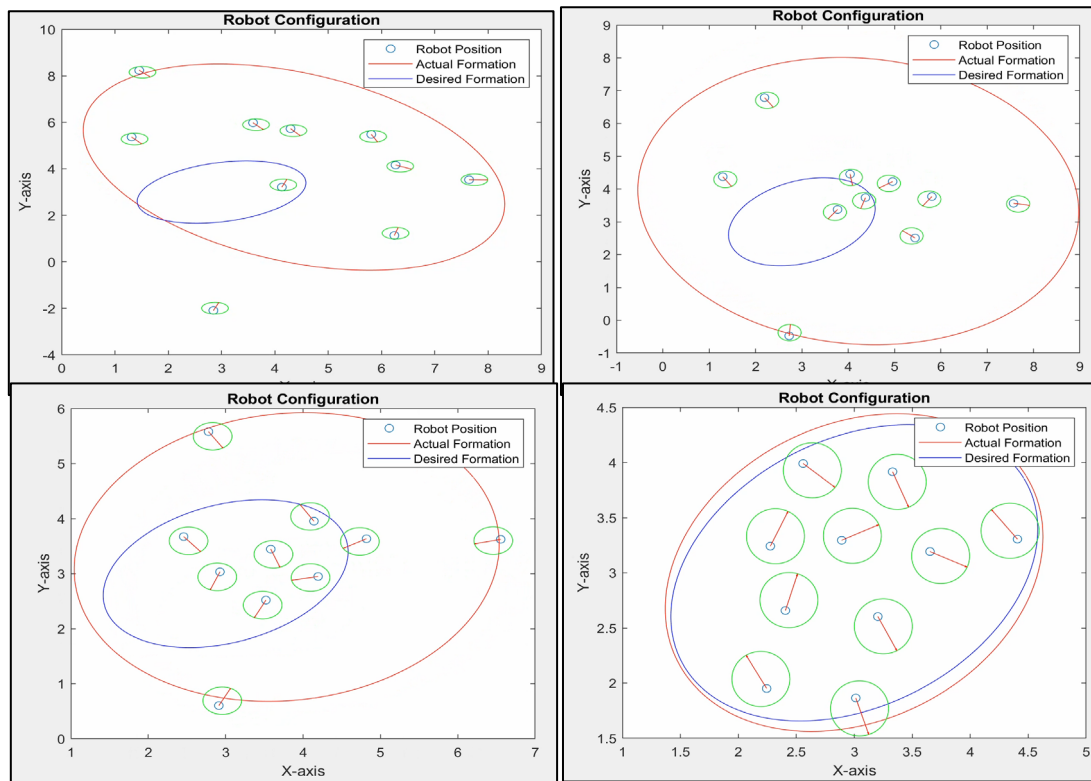


FIG 4 – Advanced modified simulation of the entire process of lunar water exploration and extraction.

The robot will be dispatched to a random location, and once it detects water, it will send a signal to the group and locate the coordinates in the blue trajectory for assembly. All robots will receive a signal and move towards the blue trajectory. At the same time, when the robot moves to the blue trajectory, the separation distance (ϵ) will be implemented for each robot. Advanced simulations show good results for extracting water on the Moon. as can be seen from Figure 4, the spatial distribution configuration of robots with a fleet size of 10 robots has been evaluated and executed in the advanced simulation. The swarm fleet size of 10 robots meets the collision avoidance conditions, and all the robots are successfully assembled in the blue trajectory without collision or overlap. In terms of positioning accuracy, 10 robots showed high localisation precision when there were no robots located outside of the blue trajectory. Assuming that the safety distance is equal to 0.1 m, it is reasonable to avoid collisions for 10 robots, and the signal coverage of 300 m is suitable for receiving signals from 10 robots. The average convergence time of 10 robots running three simulations is 150 seconds, as is shown in Figure 6.

Swarm robot evaluation

This section evaluates the spatial distribution configuration of different size robot fleets namely, of 10, 15 and 20 robots, and further investigates the characteristics of the swarm robotics systems, ie its flexibility, robustness, and scalability. The sizes of different robot fleets executed in the advanced simulation are shown in Table 2. The three main key assessments that will be evaluated are robot collision, positioning accuracy and convergence time.

TABLE 2
Swarm robot simulation for fleets of 10, 15 and 20 robots.

No. robot	Swarm robot simulation	
	Exploration	Extraction
10		
15		
20		

According to Table 2, the spatial distribution configuration of robots within the swarm fleets of the size of 10, 15 and 20 robots has been evaluated. The swarm fleet size of 10 robots satisfied the collision avoidance conditions meaning that all robots entered the blue trajectory without overlapping. The 15 and 20 robot fleet sizes didn't satisfy the collision avoidance conditions, and there were

multiple robots overlapping, with four robots overlapping for the 15-robot fleet and eight robots overlapping for 20 robot fleet. Due to the insufficient overlap avoidance function in advanced simulation, the results on overlapping for the 15 and 20 robot fleets can be explained. When the robot enters the blue trajectory, the robots tend to merge and overlap to achieve no collision, thus reduce the collision avoidance efficiency. In terms of positioning accuracy, the swarm fleet size of 10 robots allows all robots to successfully enter the blue trajectory for positioning with the highest positioning accuracy. The larger size swarm fleets with 15 and 20 robots showed low positioning accuracy, with multiple robots being located outside of the blue trajectory, with four off-track robots for the 15-robot fleet and seven off-track robots for the 20 robot fleets being observed. As for the localisation precision, the robot often uses the required coordinates sent by the signal to calculate the distance to enter the blue trajectory which involves problems with uncertainty and distance calculation, since due to the orientations of the robots they have different waypoints.

The corresponding swarm intelligence system (bees' algorithm for swarm robotics) has been evaluated on the characteristics of swarm system ie its scalability, flexibility and robustness to assess the swarm behaviour and swarm performance. Since the robots have been assigned to the swarm to perform specific water extraction task, considering Equation 5 it has be evaluated that the flexibility of the swarm robotic system's performance is at 100 per cent. Due to the specific task assigned, there are no alternative tasks to be considered in the flexibility equation. The scalability equation (Equation 3) is not applicable for the evaluation on swarm robot performance in this case due to the specific task allocation and robot size is limited by the ease of transportation through space. The robustness (Equation 4) has been evaluated based on the collision avoidance efficiency and the positioning accuracy with different size robot fleets and have been summarised in Table 3. The average swarm robotics system error for different size swarm fleets is as follows: for 10 robot fleet – no error: 0 per cent, for 15 and 20 robot fleets there was an error and it has been calculated as being at 27 per cent and 38 per cent respectively, as shown in Figure 5.

TABLE 3
Swarm robotic system robustness evaluation.

No. of robot	Off-track robot	Overlap robot	Localisation error %	Collision error %
10	0	0	0%	0%
15	4	4	27%	27%
20	7	8	35%	40%

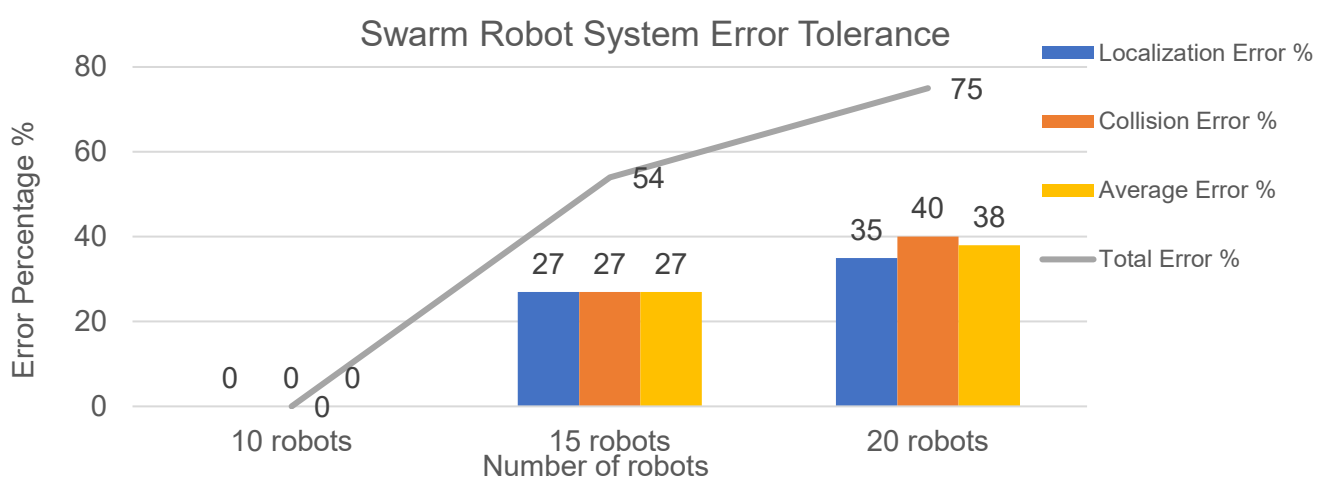


FIG 5 – Error tolerance per cent for 10, 15 and 20 robots.

As the number of robots in the swarm increases, signal transmission becomes more complicated, and collisions between the robots are more likely to occur, resulting in an increase in the percentage of error. When dealing with a large number of robots performing specific tasks in dynamic

environments, the convergence time is very important for evaluating the effectiveness of the simulation solution. The convergence time of 10, 15 and 20 robot fleets were further studied, and three simulation runs were performed to obtain the average convergence time of each fleet size. The minimum convergence time for 10 robot swarm fleets is 150 seconds, whereas the convergence times for 15 robot and 20 robot swarm fleets are 200 seconds and 275 seconds, respectively as shown in Figure 6. As the size of the swarm robot fleet increases, the local interaction and communication between robots in a dynamic environment increases, which also increases the autonomy of the individual robot. The response of individual robot to environmental changes becomes more complex, thereby prolonging the process of convergence.

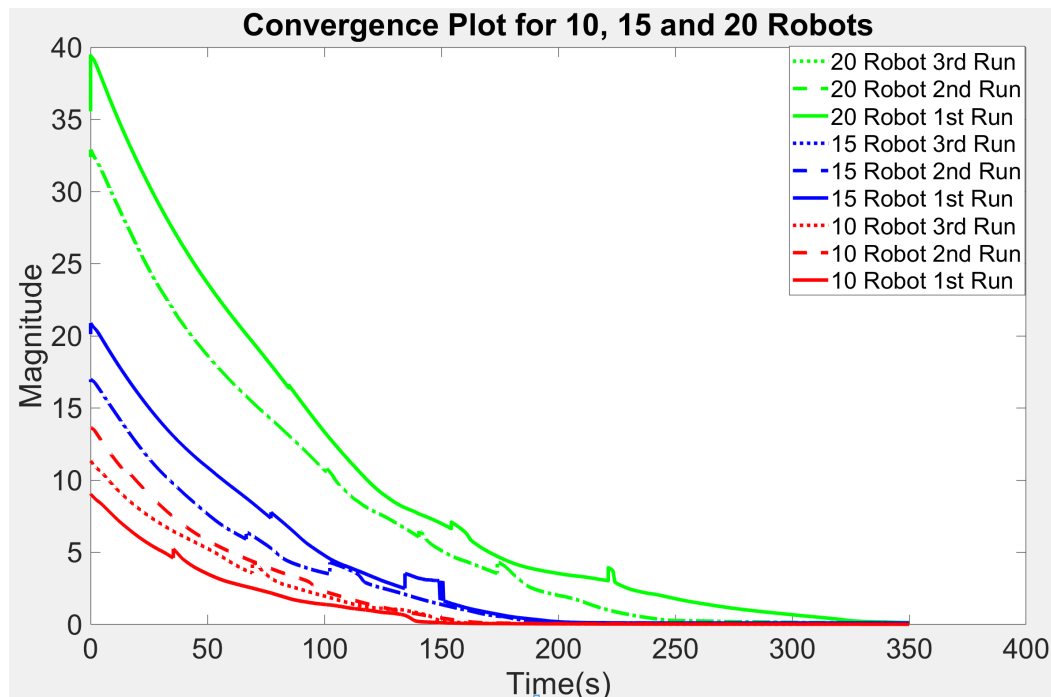


FIG 6 – Convergence Plot for 10, 15 and 20 Robots.

The evaluation of the error tolerance of the swarm robot performance shows that, 10 robot fleet has the most outstanding swarm robot performance compared with 15 and 20 robot fleets. The 10-robot fleet has been chosen for swarm mining of the super frozen ice on the Moon, since the 10-robot fleet size is the best suited one for the desired exploration size under the limit of 100 m extraction trajectory and robots can fit and operate in that area without collision. Compared with 15 and 20 robot fleets, the convergence time for the 10 robot swarm fleet is faster, because the robots have less local communication and interaction, and the solution is more efficient.

CONCLUSIONS

In this paper, a bio-inspired new method for off-Earth mining operations has been proposed, designed and performance efficiency evaluated based on the behaviour of foraging ants and bees. The swarm mining method has been proposed and studied with the focus on lunar water extraction from superfrozen regolith. Since the foraging behaviour of ants requires pheromone feature, it has been deemed unsuitable for the swarm robotics system design for lunar water extraction. Instead, the bee colony foraging behaviour algorithm has been applied in the design of the mining swarm robotics system, which has proven to be highly flexible, scalable, and adaptable as have been observed from the numerical simulations. The first simulation followed the algorithm of bees eg., hive behaviour, food source behaviour and foraging behaviour, but the main problem faced in this simulation was the collision between the robots, localisation accuracy and maximum exploration distance, which needed to be addressed. The collision avoidance simulation for various size swarm robots' fleets has been studied, and 10 robot swarm fleets showed to be best suited, hence they were further simulated and modified. The second modified simulation showed better results. Due to the limitations of the group robot signal coverage and robot movement speed, search trajectory and extraction trajectory have been limited to 300 metres and 100 metres respectively.

Using flexibility, scalability and robustness equations, the fleets of 10 robots, 15 robots and 20 robots have been investigated and evaluated for swarm robot performance. The studies have shown, that the 10 robots fleet has no localisation errors, and this has been deemed as the most optimal robot fleet size for the considered swarm mining, whereas 15 robot and 20 robot swarm fleets both had signal errors of 27 per cent and 35 per cent, respectively. As for the collision within the design trajectory, 10 robot swarm fleet again has shown the best result with a collision error of 0 per cent, whereas both 15 robot and 20 robot swarm fleets resulted in a collision error of 27 per cent and 40 per cent, respectively. The average error tolerance for 10, 15 and 20 robot swarm fleets are 0 per cent, 27 per cent and 38 per cent, respectively. The convergence time for 10 robot fleet is 150 seconds, which is shorter compared with that for 15 robot fleet being at 200 seconds and for 20 robot fleet being 275 seconds, due to less local interaction and communication between individual robots, less complex environmental changes and more efficient solution. As can be observed from the results, with the increase of the number of robots in the swarm fleet also increases the occurrence of errors and a prolonged convergence time is being observed. The 10 robot swarm fleet has been selected as the most optimal swarm robot fleet size for the given task. The ease and cost-effectiveness of shipment of the robot fleet to the Moon was also investigated and it has been demonstrated that the cargo weight of a fleet of 10 swarm robots is within the limits of the average cargo size of 6000 kg to 12 600 kg per shipment. It can be stated that the flexibility of the proposed swarm robotics system is at 100 per cent, and because a specific task is being assigned, there is no comparison task to choose from.

It is recommended that future research be conducted on the efficiency of other swarm robotics systems for mining applications, on developing details on exploration and extraction using swarm robots, and on improving the convergence speed and performance of individual robots in the swarm fleet.

ACKNOWLEDGEMENTS

The authors would like to thank Mr Gal-Erdene Battengel for his contributions to this study and participation in this project.

REFERENCES

- Ahmadzadeh, R, 2015. zeeshanahmad10809/particle-swarm-optimization. [online] *GitHub*. Available at: <<https://github.com/zeeshanahmad10809/particle-swarm-optimization>> [Accessed 15 July 2021].
- Alers, S, Bloembergen, D, Hennes, D, De Jong, S, Kaisers, M, Lemmens, N, Tuyls, K and Weiss, G, 2011, May. Bee-inspired foraging in an embodied swarm. In *The 10th International Conference on Autonomous Agents and Multiagent Systems*, Vol 3 (pp. 1311–1312).
- Battengel, G and Tan, J, 2021. Biomimicry for lunar water extraction: an evaluation of swarm robotics applications. Master's Thesis. The University of Adelaide, Adelaide.
- Brambilla, M, Ferrante, E, Birattari, M and Dorigo, M, 2013. Swarm robotics: a review from the swarm engineering perspective. *Swarm Intelligence*, 7(1), pp.1–41.
- Crowe, D, 2020. Australia To Sign MOU With NASA For Moon Mission By 2024. [online] *The Sydney Morning Herald*. Available at: <<https://www.smh.com.au/politics/federal/australia-to-sign-mou-with-nasa-for-moon-mission-by-2024-20190920-p52tax.html>> [Accessed 20 May 2020].
- Dorigo, M, Birattari, M and Stutzle, T, 2006. Ant colony optimization. *IEEE Computational Intelligence Magazine*, 1(4), pp. 28–39.
- Dorigo, M, Birattari, M, Li, X, López-Ibáñez, M, Ohkura, K, Pinciroli, C and Stützle, T (eds), 2016. *Swarm Intelligence: 10th International Conference, ANTS 2016*, Proceedings (Vol. 9882). Springer.
- En.linkfang.org. 2020. Comparison of space station cargo vehicles – en.LinkFang.org. [online] Available at: <https://en.linkfang.org/wiki/Comparison_of_space_station_cargo_vehicles> [Accessed 15 July 2021].
- Gorostiza, E M, Lázaro Galilea, J L, Meca Meca, F J, Salido Monzú, D, Espinosa Zapata, F and Pallarés Puerto, L, 2011. Infrared sensor system for mobile-robot positioning in intelligent spaces. *Sensors*, 11(5), pp.5416–5438.
- Hecker, J P and Moses, M E, 2015. Beyond pheromones: evolving error-tolerant, flexible, and scalable ant-inspired robot swarms. *Swarm Intelligence*, 9(1), pp.43–70.
- Hoffman, S J and Kaplan, D I, 1997. Human exploration of Mars: the reference mission of the NASA Mars exploration study team (Vol. 6107). *National Aeronautics and Space Administration*, Lyndon B. Johnson Space Center.

- Karaboga, D, 2005. An idea based on honey bee swarm for numerical optimization (Vol. 200, pp. 1–10). Technical report-tr06, Erciyes University, Engineering Faculty, Computer Engineering Department.
- Kassabalidis, I, El-Sharkawi, M A, Marks, R J, Arabshahi, P and Gray, A A, 2001, November. Swarm intelligence for routing in communication networks. In *GLOBECOM'01. IEEE Global Telecommunications Conference* (Cat. No. 01CH37270) (Vol. 6, pp. 3613–3617). IEEE.
- Lemmens, N and Tuyls, K, 2010, July. Stigmergic landmark routing: a routing algorithm for wireless mobile ad-hoc networks. In *Proceedings of the 12th Annual Conference on Genetic and Evolutionary Computation* (pp. 47–54).
- Lemmens, N, De Jong, S, Tuyls, K and Nowé, A, 2005. Bee behaviour in multi-agent systems. In *Adaptive agents and multi-agent systems III. Adaptation and multi-agent learning* (pp. 145–156). Springer, Berlin, Heidelberg.
- Linne, D L, Sanders, G B, Starr, S O, Eisenman, D J, Suzuki, N H, Anderson, M S, O'Malley, T F and Araghi, K R, 2017. Overview of NASA technology development for in-situ resource utilization (ISRU).
- Malenkov, M I and Volov, V A, 2019. Comparative Analysis and Synthesis of Schemes of Balanced Suspension of Planetary Rovers with Autonomous Control. *Russian Engineering Research*, 39(3), pp.211–219.
- Michael, N and Kumar, V, 2009. Planning and control of ensembles of robots with non-holonomic constraints. *The International Journal of Robotics Research*, 28(8), pp.962–975.
- Mos.org. 2021. [online] Available at: <https://www.mos.org/sites/dev-elvis.mos.org/files/docs/offerings/mos_educator-guide_nasa_waves-and-information-transfer.pdf> [Accessed 12 July 2021].
- NASA's Break the Ice Lunar Challenge. 2021. Mission Scenario – NASA's Break the Ice Lunar Challenge. [online] Available at: <<https://breaktheicechallenge.com/mission-scenario/>> [Accessed 8 July 2021].
- Rappaport, T S, Roh, W and Cheun, K, 2014. Mobile's millimeter-wave makeover. *IEEE Spectrum*, 51(9), pp.34–58.
- Sąsiadek, J, 2013. Space robotics and its challenges. *Aerospace Robotics*, pp.1–8.

AUTHOR INDEX

Abbo, E	77	Casanova, S	440
Abrahamsson, L	238	Chen, Y	271
Agioutantis, Z	81, 128	Chua, J M	419
Aguey-Zinsou, F	162	Clausen, E	156
Aikawa, K	296	Dahan, A E	349
Akmeliawati, R	474	Danko, G L	4
Alapfy, B	205	Davies, E	353
Alonzo, D	223	Dello-Iacovo, M	459
Alorro, R D	323, 326, 349	Dempster, A G	422, 442, 456
Amankwaa-Kyeremeh, B	300, 308	Dendl, D	274
Anderson, R C	440	Dias, T	4
Androulakis, V	81	Diehr, G	259
Asamoah, R K	300, 308, 328, 338	Dominy, S C	358
Ashifa, M	165	Dowd, P A	140
Aylmore, M	323, 326	Duffy, A R	463
Bacich, S	179	Duzgun, H Ş	24, 254
Bagai, Z B	33	Dyer, L G	323
Banerjee, B P	282	Einav, I	353
Barnett, N	459	Elders, C	286
Bates, M	419	Feldmann, Y	205
Baute, R M	349	Gill, M T	315
Belle, B	4	Gong, H	385
Bennett, N J	422	Goto, Y	112
Bergström, J	368	Gray, J	267
Berner, M	98	Greet, C J	308, 338
Biegaj, K	358	Griesser, T	274
Blauermel, G	205	Grimsey, D	326
Blunck, S	211	Grobler, H C	46, 230, 405
Bonci, G	248	Gyngell, B	69, 259
Bowes, S	226	Hartlieb, P	274
Bridgwater, H	2	Harvey, D	474
Brooks, G A	463	Heiertz, A	211
Brune, J	254	Hillig, T	205
Buschjost, T	259	Hiroyoshi, N	223, 296
Cannon, A J	429	Hobbs, K	145

Hrabar, S	267	Mugebe, P	149
Hyongdoo, J	33	Nehring, M	121
Isleyen, E	24	Nikolaidis, S	128
Ito, M	223, 296	Nöger, M	274
Iwanow, G	145	Oching, W E	248
Jeon, S	223	Oh, J	459
Johansson, J	238	Olivier, J	353
Karadjian, G K	241	Owada, N	33
Kawamura, Y	33, 112	Owusu, K B	328, 338
Keles, C	276	Pacaña, M C	349
Kitahara, I	112	Pan, W	398
Kizil, M S	121, 149, 153	Park, I	223, 296
Knights, P	121, 153	Peiris, J	385
Koivisto, M	368	Pelech, T	459
Kubat, B	244	Phengsaart, T	223
Kuhar, L L	366	Phillips, T	121
Kuroki, H	112	Pienaar, M	46
Ladinig, T	274, 368	Pokrajcic, Z	28
Ladouceur, F	271	Poller, D	77
Lam, K Y	207	Pownceby, M I	463
Lehnen, F	156	Puzyrev, V	286
Li, B	279, 385	Qu, J	153
Li, H M	101	Radzhabov, O	69
Li, L	398	Raffaillac, E	315
Li, Z	419	Raval, S	282
Lim, B	326	Reilly, P	207
Lim, H E	323	Resabal, V T	349
Lim, N C	323	Reznichenko, S	159
Liu, B	279	Rhamdhani, M A	463
Löow, J	238	Roth, M	205
Lottermoser, B G	205	Saadat, M	112
Low, R	149	Salmi, E F	286
MacHunter, R M G	315	Santa, N	276
Mant, K	145	Sarver, E	276
McKeown, B	456	Sato, T	112
Melkounian, N	474	Saydam, Sa	279
Mitra, R	156	Saydam, S	440, 456, 459
Monastyrov, V	159	Saylor, J R	276
Moser, P	274	Sbravati, A	207

Schafrik, S	81, 128	Toriya, H	112
Schmid, M	211	Uth, F	156
Schwarze, B	156	Utsuki, S	33
Sellers, E J	286	van Dalen, J	405
Seneviratne, A	385	Villacorte-Tabelin, M	223
Shaw, M G	463	Vorobyov, B	159
Shelley, P	353	Wagner, H	368
Shemang, E	33	Wang, J	398
Sifferlinger, N A	98	Wang, S R	101
Silva, L S	349	Wang, W	101
Silvestri, L	271	Wang, Z G	101
Sinaice, B B	33	Williams, A	419
Singh, S K	282	Wimmer, M	368
Siribalamurali, P	419	Worsey, T	259
Skinner, W	300, 308, 328, 338	Xenaki, A	128
Sörensen, A	156	Xu, R	286
Sottile, J	81	Yahyaei, M	149, 153
Soydan, H	254	Yang, S	398
Stewart, P	28	Yoo, K	223
Sullivan, S	43	Yoshino, K	112
Tabelin, C B	223, 349	Zhang, C	419
Takanohashi, Y	33	Zhang, H	128
Talavera, L	389	Zhang, W	279
Tan, J	207, 474	Zhang, X	254
Thomas, H	405	Zhao, K	385
Tong, W X	121		